STUDIES IN INTERFACE SCIENCE

13

SERIES EDITORS:
D. MÖBIUS
R. MILLER

Surfactants: Chemistry, Interfacial Properties, Applications

V.B. Fainerman, D. Möbius and R. Miller, editors

ELSEVIER

STUDIES IN INTERFACE SCIENCE

Surfactants: Chemistry, Interfacial Properties, Applications

STUDIES IN INTERFACE SCIENCE

SERIES EDITORS

D. Möbius and R. Miller

Vol. 1
Dynamics of Adsorption at Liquid Interfaces
Theory, Experiment, Application
by S.S. Dukhin, G. Kretzschmar and R. Miller

Vol. 2
An Introduction to Dynamics of Colloids
by J.K.G. Dhont

Vol. 3
Interfacial Tensiometry
by A.I. Rusanov and V.A. Prokhorov

Vol. 4
New Developments in Construction and Functions of Organic Thin Films
edited by T. Kajiyama and M. Aizawa

Vol. 5
Foam and Foam Films
by D. Exerowa and P.M. Kruglyakov

Vol. 6
Drops and Bubbles in Interfacial Research
edited by D. Möbius and R. Miller

Vol. 7
Proteins at Liquid Interfaces
edited by D. Möbius and R. Miller

Vol. 8
Dynamic Surface Tensiometry in Medicine
by V.N. Kazakov, O.V. Sinyachenko, V.B. Fainerman, U. Pison and R. Miller

Vol. 9
Hydrophile-Lilophile Balance of Surfactants and Solid Particles
Physicochemical Aspects and Applications
by P. M. Kruglyakov

Vol. 10
Particles at Fluid Interfaces and Membranes
Attachment of Colloid Particles and Proteins to Interfaces and Formation of Two-Dimensional Arrays
by P.A. Kralchevsky and K. Nagayama

Vol. 11
Novel Methods to Study Interfacial Layers
by D. Möbius and R. Miller

Vol. 12
Colloid and Surface Chemistry
by E.D. Shchukin, A.V. Pertsov, E.A. Amelina and A.S. Zelenev

Vol. 13
Surfactants: Chemistry, Interfacial Properties, Applications
edited by V.B. Fainerman, D. Möbius and R. Miller

Surfactants: Chemistry, Interfacial Properties, Applications

Edited by

V.B. Fainerman

International Medical Physicochemical Centre
Donetsk Medical University, 16 Ilych Av., Donetsk 83003, Ukraine

D. Möbius

Max-Planck Institut für Biophysikalische Chemie
P.O. Box 2841, 37077 Göttingen, Germany

R. Miller

Max-Planck Institut für Kolloid- und Grenzflächenforschung
Am Mühlenberg 1, 14476 Potsdam/Golm, Germany

2001
ELSEVIER
Amsterdam – London – New York – Oxford – Paris – Shannon – Tokyo

ELSEVIER SCIENCE B.V.
Sara Burgerhartstraat 25
P.O. Box 211, 1000 AE Amsterdam, The Netherlands

First edition 2001

Library of Congress Cataloging in Publication Data
A catalog record from the Library of Congress has been applied for.

ISBN: 0 444 50962 3
ISSN: 1383 7303

♾ The paper used in this publication meets the requirements of ANSI/NISO Z39.48-1992 (Permanence of Paper).
Printed in The Netherlands.

FOREWORD

Surfactants are amphiphilic substances of synthetic or natural origin, able to adsorb at interfaces, thus reducing the surface or interfacial tension. The large number and wide range of technologies in which surfactants could be applied to increase the efficiency of wetting agents, detergents, micelle formation promoters, foam or emulsion stabilisers etc. had stimulated the interest in this class of substances, especially during the last fifty years. After the fundamental monograph by Schwartz and Perry (1949) who first summarised the chemical, physicochemical and technological properties of surfactants, a number of monographs and data books were followed, and some excellent books dealing with various classes of surfactants or particular physicochemical aspects of the problem had been published in the Surfactant Science Series (Marcel Dekker, New York).

Progress in this field is stipulated by simultaneous developments in all branches which constitute surfactant science. On one hand side, new classes of surfactants are emerging brought by the synthesis or extraction from biologic objects. On the other hand, new experimental and theoretical physicochemical studies constantly add to the understanding of properties of traditional and new surfactants. Also, the area of scientific studies and technologic applications of amphiphiles is constantly enlarged. Here the biologic membranes comprised of proteins, lipids and ordinary surfactants is a good example.

In the present book we attempt to summarise the current problems in the field, with particular emphasis on the interrelations between the chemical structure, physicochemical properties and the efficiency of technologic application, where the final aim is to provide tools for the prognostication of principal physicochemical properties and even the technologic applicability from the structure of a surfactant.

Chapter 1 gives a systematic view of different classes of surface active substances: non-ionic, anionic, cationic, amphoteric and zwitter-ionic surfactants. For each class, the synthesis of a surfactant from different initial substances (including the reaction mechanisms, main production routes, conditions for the best performance etc.), and the chemical analysis of the product properties are summarised. Reference information about manufacturers, nomenclature

and product properties is also given. The list of literature references is very extensive and provides a good data base for the reader. The chapter is finalised with a short review of the interrelation between basic physicochemical properties of surfactants (adsorption and micelle formation) and the structure of the compounds.

In Chapter 2 the theoretical analysis of the equilibrium adsorption behaviour of surfactants at liquid interfaces is presented. In addition to the classical models proposed by Langmuir and Frumkin, recently developed new concepts are presented and analysed, which assume molecular processes taking place in the adsorption layer, in particular, the reorientation and cluster formation (aggregation). The examples presented in the Chapter clearly demonstrate the advantages of the new models as compared to the traditional ones. A detailed analysis of the adsorption behaviour for surfactant mixtures is made. Possibly, for the first time, equations are derived which account for some specific features of surfactant mixtures, in particular, the difference in the molecular areas and the non-additivity of attractive interactions. Also the adsorption behaviour of proteins assuming interfacial reconformation, and protein/surfactant mixtures are analysed. A theoretical treatment of the penetration of soluble surfactant into insoluble monolayers is presented in the framework of different approaches. Here, for the first time, systems are considered in which the penetration process stimulates a two-dimensional condensation of the insoluble component of the monolayer. The thermodynamic characteristics of adsorption are analysed and rigorous relationships for the increments of the adsorption free energy of ionic surfactants are given.

Chapter 3 summarises experimental data for the equilibrium surface tension for 14 homologous series of various (non-ionic and ionic) surfactants. The results were processed using the theoretical models developed in Chapter 2. New important results are obtained which reveal interrelations between the structure and properties of substances. In particular, it is shown that the behaviour of the surfactant molecules in the adsorption layer can be described by ideal, Frumkin, reorientation or aggregation models, depending on the structure of the surfactant molecule. It is shown that, irrespectively of the nature of a linear surfactant and addition of electrolyte, the free energy increment per methylene group is constant, while the increments which correspond to the polar group depend on the nature of the group. In particular, for

oxyethylated surfactants a certain dependence exists between the increment and the number of oxyethylene groups. Therefore, a basis is developed for the estimation of the adsorption characteristics of a surfactant from its structure. The Chapter also includes extensive experimental data concerning the surface tension of surfactant mixtures, showing perfect agreement between the experimental data and a rigorous theory, and a simple additivity-based model developed for mixtures recently.

In Chapter 4 the adsorption dynamics of surface active molecules at liquid interfaces is systematically treated. The physical phenomena that govern the transport of surfactants from the solution to the surface layer are summarised. The molecular processes (reorientation and aggregation) which can take place in surface layers are incorporated into the theoretical analysis. It is shown, in particular, that in the framework of the diffusion model the aggregation at interfaces leads to the retardation of the rate of surface tension decrease. This effect was so far ascribed to the presence of an adsorption barrier. Assuming adsorbed molecules undergo reorientations in the surface layer, one obtains more options for the analytical treatment: both more rapid (for the quasi-equilibrium case) and slower adsorption (for a finite rate of transition between the states of the adsorbed molecules), as compared with the traditional diffusion model, can be explained. Therefore, the surfactant structure determines not only the equilibrium properties, but also the dynamic adsorption characteristics. Much attention is paid to theoretical aspects of the kinetics of adsorption from mixed solutions, adsorption at the surface deformed in various ways, mass transfer into a second adjacent liquid phase, the effect of surfactant charge and electrolyte additions, the dynamics of penetration of a soluble surfactant into an insoluble monolayer. In Chapter 4 a summary of experimental data is also presented, with particular emphasis on the progress achieved in the application of relaxation method. A number of examples is presented of experimental studies of the dynamics of systems characterised by ideal surface behaviour, aggregation or two-dimensional condensation in the adsorption layer, for solutions of ionised surfactants, mixtures of surfactants and proteins, penetration, slow and fast adsorption experiments. These examples demonstrate not only the options provided by enhanced experimental technique, but lead in

many cases to a perfect agreement between experimental data and modern theoretical approaches.

The equilibrium and dynamics of adsorption processes from micellar surfactant solutions are considered in Chapter 5. Different approaches (quasichemical and pseudophase) used to describe the micelle formation in equilibrium conditions are analysed. From this analysis relations are derived for the description of the micelle characteristics and equilibrium surface and interfacial tension of micellar solutions. Large attention is paid to the complicated problem, the micellation in surfactant mixtures. It is shown that in the transcritical concentration region the behaviour of surface tension can be quite diverse. The adsorption process in micellar systems is accompanied by the dissolution or formation of micelles. Therefore the kinetics of micelle formation and dissociation is analysed in detail. The considered models assume a fast process of monomer exchange and a slow variation of the micelle size. Examples of experimental dynamic surface tension and interface elasticity studies of micellar solutions are presented. It is shown that from these results one can conclude about the kinetics of dissociation of micelles. The problems and goals of capillary wave spectroscopy of micellar solutions are extensively discussed. This method is very efficient in the analysis of micellar systems, because the characteristic micellisation frequency is quite close to the frequency of capillary waves.

Chapter 6 summarises various technologic applications of surfactants. The action of surfactants in many processes is determined by the ability to be adsorbed, to wet solid surface or to spread over a liquid surface, to disperse, form and stabilise foams and emulsions. Therefore it seems possible, at least in principle, to formulate certain general approaches for the optimum application of a surfactant, based on the interrelation between structure and properties of the substance. This approach was successfully implemented in Chapter 6, where the mechanism of the surfactants' action as foam formation agents and emulsifiers is considered in details. Impressive results are presented in respect to the application of surfactants and their compositions in the preparation of detergents and cleaning agents, food products, drugs, in the textile, paper, construction and other industries. Large attention is paid to surfactant control and prevention of their penetration into the environment.

The theoretical models proposed in Chapters 2-4 for the description of equilibrium and dynamics of individual and mixed solutions are by part rather complicated. The application of these models to experimental data, with the final aim to reveal the molecular mechanism of the adsorption process, to determine the adsorption characteristics of the individual surfactant or non-additive contributions in case of mixtures, requires the development of a problem-oriented software. In Chapter 7 four programs are presented, which deal with the equilibrium adsorption from individual solutions, mixtures of non-ionic surfactants, mixtures of ionic surfactants and adsorption kinetics. Here the mathematics used in solving the problems is presented for particular models, along with the principles of the optimisation of model parameters, and input/output data conventions. For each program, examples are given based on experimental data for systems considered in the previous chapters. This Chapter can be regarded as an introduction into the problem software which is supplied with the book an a CD.

The team of authors express its gratefulness to many colleagues who provided experimental data to be displayed and analysed in the present book. Most of all they want to thank Ludmila Makievski and Sabine Siegmund for their invaluable support in gaining data from various sources of literature, preparing the graphs in this book, and checking the final text, a significant piece of the tremendous work to be done to compile this manuscript.

This Page Intentionally Left Blank

List of contents

1. CHEMISTRY OF SURFACTANTS

Michael Y. Pletnev

Chair of Organic Chemistry, Belgorod State University, 12 Studencheskaya Street, Belgorod 308007, Russia

1.1. An Introductory Overview

Surface active substances or surfactants are amphiphilic compounds having a lyophilic, in particular hydrophilic, part (polar group) and a lyophobic, in particular hydrophobic, part (often hydrocarbon chain). The amphiphilic structure of surfactants is responsible for their tendency to concentrate at interfaces and to aggregate in solutions into various supramolecular structures, such as micelles and bilayers. According to the nature of the polar group, surfactants can be classified into nonionics and ionic, which may be of anionic, cationic, and amphoteric or zwitterionic nature.

Surfactants are important ingredients in a great number of formulations and processes. Practically any human activity deals with surfactants. So, the weight of surfactants in present-day detergent products accounts for around 15-25 % of the total production. Their world production approaches 9 million tons* plus the same number of soap, and about half of the quantity is the share of West Europe and North America [1].

Figure 1.1 presents the consumption of the major surfactants in the world market in 1996. Along with soap, linear alkylbenzene sulphonates (LAS) remain the most bulky and cost-effective anionic surfactants. LAS will continue to be the workhorse of the detergents industry on a global basis. However, the LAS share decreases gradually: their recess is occupied by alcohol-derived surfactants, first of all alcohol sulphates (AS), alcohol ethoxylates (AE) and alcohol ether sulphates (AES). In West Europe alkylphenol ethoxylates (APE) have been removed over the last two decades from a large number of household applications in view of

environmental impact and legislative limitations. The same tendency, perhaps, will continue to be gradually including institutional detergents and industrial uses. Consumption of soap has remained essentially stable since 1980. The weight of soap within detergent products has fallen from 63 % in 1960 to 20 % today [1b], but the trend of its rising is observed again.

Fig. 1.1 Global use patterns of major surfactants in 1996 [*1a*]

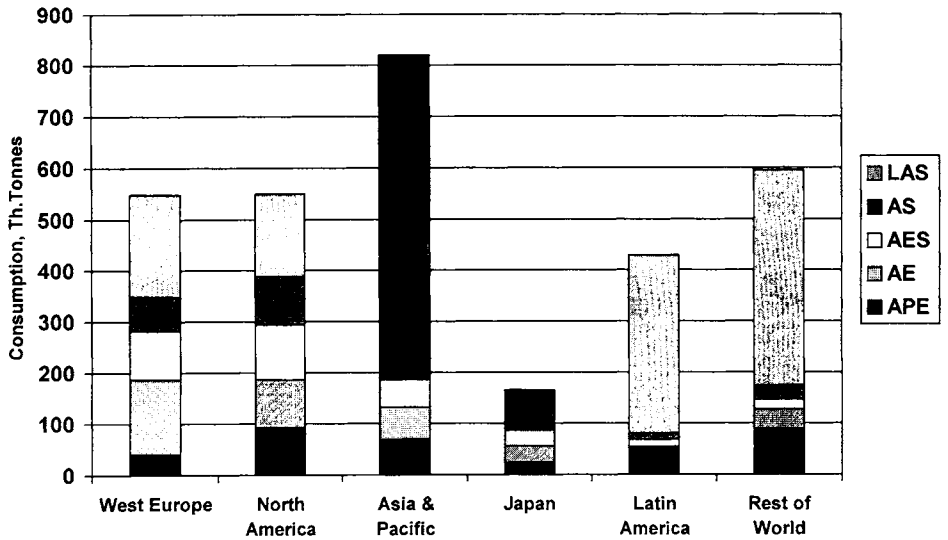

The concept of the sustainable development declared by the United Nations at the beginning of the 90th claim beneficial technologies and products which require use of essentially renewable resources or are able to shorten the energy and resource consumption. All leading producers of chemicals, particularly surfactants, demonstrate adherence to this concept. Several tendencies have an impact on surfactant production and use towards the end of the 2nd millennium, and the most important among them concern also the detergent industry [1, 2]: 1) the growing emphasis on environmental acceptability, safety and mildness; 2) the gradual refusal of powder detergent producers from the spray tower technology towards the energy-saving technologies of

---

* According to the recent report of W. Dolkemeyer (*Condea*) at the 5th World Surfactant Congress CESIO 2000, Florence, Italy, the annual world production of surfactants has reached some 11million tons.

laundry formulation; 3) wide adoption of low-temperature laundering and new washing machines; 4) increasing use of enzyme- and cationic-compatible (AE, AES and amphoteric) surfactants; 5) introducing, among others, new criteria in particular concerning the sustainability concept and the environmental assessment of detergents. Recent introduction of N-methylacylamino-D-glucitols [3] and alkyl polyglycosides [4-6] tailored from renewable sources is the most impressive example of these tendencies. All these tendencies work objectively on the increasing use of nonionic surfactants, apart from APE, over the past few years and in the future.

Vegetable oils and natural fats are traditional raw materials for the production of soaps and other surfactants. Coconut oil, palm and palm kernel oil, rape oil, cotton oil, tall oil, as well as the fats of animal origin (tallow oil, wool wax), present renewable raw sources. Linear paraffins and olefins (with terminal or internal double bond), higher synthetic alcohols, and benzene are fossil sources for surfactant production which are obtained from oil, natural gas and coal. Other auxiliary materials are required to construct amphiphilic surfactant structure, such as ethylene oxide, sulphur trioxide, phosphorous pentaoxide, chloroacetic acid, maleic anhydride, ethanolamine, and others.

1.2. Nonionic Surfactants

Nonionic surfactants are amphiphilic compounds the lyophilic (in particular hydrophilic) part of which does not dissociate into ions and hence has no charge. However, there are nonionics, for example such as tertiary amine oxides, which are able to acquire a charge depending on the pH value. Even polyethers, such as polyethylene oxides, are protonated under acidic conditions and exist in cationic form. Long-chain carboxylic acids are nonionic under neutral and acidic conditions whereas they are anionics under basic conditions. So, the more accurate definition is as follows: nonionics are surfactants that have no charge in the predominant working range of pH. The main part of nonionics can be classified into alcohols, polyethers, esters, or their combinations.

The importance of nonionics is that their total world production reaches two million tons per year and they occupy up to a quarter of the total surfactant production. In addition, this is the most diverse type of surfactants with respect to properties, structure and fractional composition.

At least three quite comprehensive books on the chemistry of nonionic surfactants can be recommended [7-9].

1.2.1. Alcohols

Alcohols are hydrocarbon derivatives with hydroxy groups. Primary long-chain C_{10}-C_{18} alcohols are the most interesting compounds as surfactants. They exhibit all the properties of nonionics with the exception of micelle formation in aqueous solution. Higher aliphatic alcohols are better soluble in oils than in water. They are widely used as co-surfactants/ emulsifiers and foam stabilizers in aqueous solutions of anionic surfactants. Furthermore, alcohols serve as an intermediate raw material in manufacturing water-soluble surfactants, such as ethoxylated products and ether sulphates [7-11].

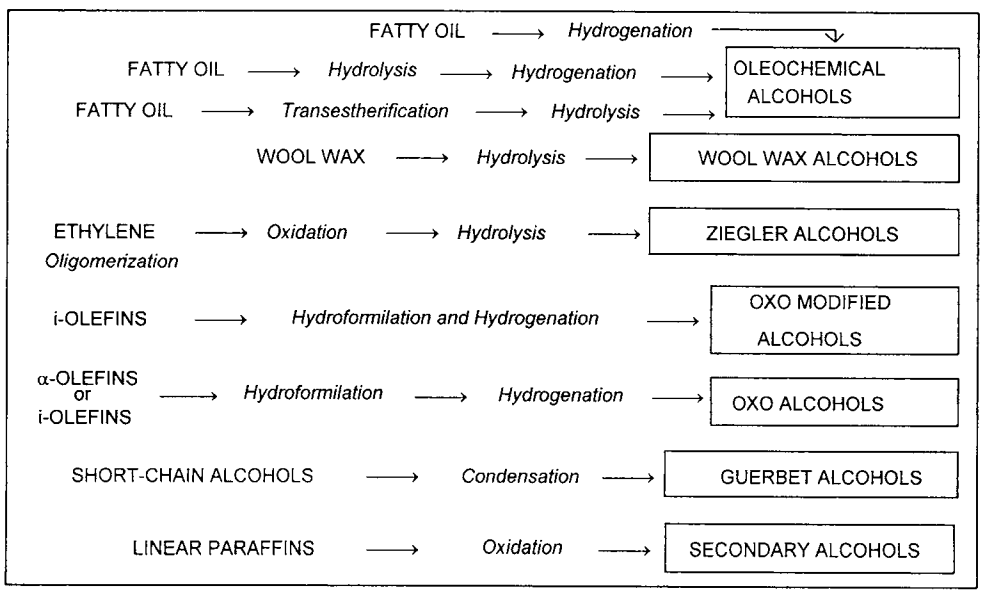

Fig. 1.2 Long-chain alcohols: process schemes

Natural oils and fats are traditional sources for the production of alcohols [12, 13]. Even long-chain alcohols (I) are produced by hydrogenation of methyl esters and glycerides of fatty acids as well as free fatty acids (cf. Fig. 1.2). The part of synthetic alcohols amounts to ca. 60 % of the total C_9-C_{18} alcohol production. The main ways of alcohol synthesis are α-olefins

hydroformilation, Ziegler's synthesis and catalytic oxidation of linear paraffins. Partially branched odd and even alcohols (II) are obtained by hydroformilation ("oxo process") [14]. Primary odd-chain alcohols (III) are produced by Ziegler's method. Oxydation of normal paraffins in the presence of boric acid results mainly in secondary odd and even alcohols [15].

Branched long-chain alcohols (IV) obtained by condensation of lower alcohols (Guerbet synthesis) have some importance as lipophilic surfactants, emollients, and surfactant intermediates. Alcohols and sterols derived by saponification of wool wax, such as "Amerchol 400" (*Amerchol*), "Argowax" (*Westbrook Lanolin*), "Super Hartolan" and "Lanethyl" (*Croda*), sterols from vegetable waxes and oils, diols (such as 2,4,7,9-tetramethyl-decyne-5-diol-4,7 (V) that is known as wetting agent) as well as long-chain epoxy hydrolysates (1,2-diols) are also of some importance.

Trade names of some long-chain alcohols are: (I) "Adol" (*Witco*), "Hydrenol D", Lanette", "Lorol" and unsaturated series "HD-Ocenol" (*Cognis/Henkel*); (II)"Alfanol" (*Condea*), "Neodol" and "Dobanol" (*Shell Chemicals*); (III) "Alfol" (*Condea*), "Crodacol CS" (*Croda*), the "Kalcol" series (*Kao*), "Laurex CS" (*Albright & Wilson*, aquired recently by *Rhodia*), "Stenol 1618" and "Lorol 1214S" (*Henkel*); (IV) "Ceraphyl CA" (*ISP*), "Guerbitol 16/20", "Eutanol G" (*Henkel*); (V) "Surfynol 104" (*Air Products & Chemicals*).

1.2.2. Nonionic ethers

The most extensive group of ether surfactants is that of polyethoxylated long-chain alcohols and related ethoxylated products considered, in view of their practical importance, in a separate section. Other ether nonionics of importance are polypropylene glycols, propoxylated alcohols, block-copolymers of ethylene oxide and propylene oxide, block-copolymers of ethylene oxide and butylene oxide [8, 16-20], block-copolymers having a hydrophobic polydimethylsiloxane moiety [19, 21], as well as alkyl polyglycerides, alkyl polyglycosides, derivatives of maltose and other saccarides.

Addition of propylene oxide to 1,2-propylene glycol results in polypropylene glycol (PPG):

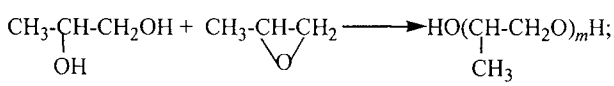

The propoxylation is carried out at 110-130 °C in a batch reactor in presence of alkali or alcoxide as catalyst.

The feature of propylene oxide group as part of the polyether chain of PPG is to show hydrophobic character. So, as the average molecular weight increases, the surface activity of PPG rises and its solubility in water drops. On the other hand, when added to hydrocarbon tail of alcohol or alkylphenol, the propylene oxide group plays the role of weak hydrophilic group. This group does not render a remarkable rise in solubility to the compound as a whole, even though it improves its dispersibility in water. Water solubility and micelle formation are reached by the ethoxylation leading to low-foaming nonionics (I) such as REP or RPE depending on the sequence of ethoxylation and propoxylation [9, 17].

Addition of ethylene oxide to PPG results in surface active block-copolymers of EPE type, named "Poloxamers" (II). The PPG chain acts as hydrophobic part while the ethylene oxide chains offer the hydrophilic part here. Usually, the weight percentage of EO groups is from 10 to 80 % when the total molecular weight of block-copolymer amounts to 20 000. Apart from PPG, other compounds having mobile hydrogen atoms, such as ethylenediamine, glycerol, sorbitol and glucose, can be subjected to propoxylation followed by ethoxylation. Block-copolymers such as EBE (III) are known where the hydrophobic part is formed by butylene oxide polymerisation product [16c, 18-20]. In comparison with EPE products, polyoxybutylene/ polyoxyethylene block-copolymers exhibit lower surface and interfacial tensions and enhanced wetting of cotton [16d, 20]. All these polyethers find use for example in pharmacy, cosmetics, microbiology, detergents, adhesives, polyurethan elastomers, and in oil recovery as demulsificators. Propoxylated lanolin alcohols are useful in personal care products.

Silicone surfactants (IV) have linear, branched or comb-like hydrophobic polydimethylsiloxane backbone and PEG or/and PPG as hydrophilic part. Silicone block-copolymers and monoalkyl ethers are referred to polyether nonionics as well. Usually silicones with mobile halogen, hydroxy- or epoxy-groups are subjected to modification [21]. The polydimethylsiloxane part of silicone surfactants show both hydrophobic and oleophobic nature. Owing to the high surface activity, silicone surfactants are used in elastomer manufacturing, cosmetics, domestic and agricultural chemicals, photography, and paints. Organofunctional lyophobic silicones themselves and as components of fine dispersions are rather effective as defoamers in varnish

and paint coatings, fuels, low-foaming detergents, fermentation, pulp and paper industry [19, 21, 22a, 22d].

Trade names of some polyether block-copolymer surfactants are: (I) "Dehypon LS/LT" (*Henkel*), "Antarox BL/FM" and "Miravon B" (*Rhodia*, former *Rhône Poulenc*), "Empilan PF/KCM0703/F" (*Albright & Wilson*), "Imbentin SG/PPF" (*Kolb*), "Marlowet 5001" (*Condea*, former *Hüls*), "Synperonic LF" (*Uniqema/ICI*); (II) "Caradol ED/MD/SC" series (*Shell*), "Empilan P/P7062/P7087" (*Albright & Wilson*), "Fluid AP" (*Union Carbide/Dow Chemical*), "Genapol PA/PF/PL" (*Clariant*), "Ifralan P8020" (*IfraChem*), "Pluronic F/L/P" (*BASF*), "Synperonic PE" (*ICI*); (III) "Butronic L/R" (*BASF*); (IV) "DC" series (*Dow Corning*) and "Abil B/EM" series (*Goldschmidt*), "Addid 100/320", "DMC" series (both of *Wacker-Chemie*) , "LK-Methicone" (*Elkay Silicones*), "Penoregulator KEP-2" (*Silan*), "Silicon DC 193" (*Shell*), "Skinotan S 10" (*Zschimmer & Schwarz*).

Addition of glycidol (2,3-epoxypropanol-1) to long-chain alcohols in the presence of alkaline catalyst results in monoglycerine and polyglycerine ethers:

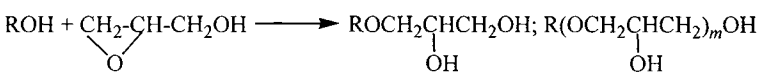

To obtain water-soluble products it is sufficient to add three or four glycerol groups depending on the alkyl chain length. One glycerol group is a hydrophilic equivalent of about three ethoxy groups [23]. Aqueous solutions of alkyl polyglycerine ethers do not show cloud points unlike solutions of polyethoxylated nonionics. In contrast to esters of glycerol, they are more hydrolytically stable in acidic and alkaline media. Monoglycerine ethers, e.g. monoisostearylglycerine ether, and polyglycerine ethers of long-chain alcohols are also obtained by transetherification of lower ethers. Surfactants of this type are mainly recommended for cosmeceuticals, particularly by *Kao Corp* and *Nikko*.

A present-day boom of interest to alkyl polyglycosides APG, known however for hundred years, is caused by several reasons: finding of technologically acceptable and cost-effective ways of their synthesis, availability of renewable resources (starch, treacle and alcohols of natural origin), environmental compatibility, high surface activity, excellent usage and dermatological properties [4-6; 24].

Oligoglycosides used for the APG production are manufactured from starch by hydrolysis. Reactions of direct heterofacial alkylation of carbohydrate by long-chain alcohol are carried out at 100-120 °C in presence of sulfuric acid. The average degree of oligomerisation of the glucoside part is 1.0-1.5. Another practically evaluated process leading to the same result has two stages. First butanolysis of wet starch in autoclave yields butylpolyglycosides. APG of the general formula $R(Gluc)_m$ ($R \sim C_8$-C_{12}) are produced by transetherification of butylpolyglycosides in presence of sulphuric acid [5].

Properties and applications of APG depend on the average degree of polymerisation of the glucose chain and the length of the aliphatic alcohol tail. Just as other nonionics, APG are almost insensitive to electrolytes and stable in a wide pH range. Some of them foam and wash well in aqueous solutions. In combination with biodegradability, mildness and low toxicity, these properties open a promising outlook for their wide use in cosmetic products, domestic and institutional detergents. APG show especially good performance in household cleansers and dish washing liquids.

Large-scale production of APG has been introduced recently by *Henkel* in Cincinnati, Ohio, and Düsseldorf, Germany. Their trademarks are: "Plantcare 818 UP" and "Plantcare 1200 UP" ("Coco Glucoside" and "Lauryl Glucoside" are *INCI/CTFA* names); "Plantaren 1200 UP/ 2000" (Lauryl Polyglucose and Decyl Polyglucose) - all products of cosmetic grade. "Agrimul PG", "Disponil AP215/AP600", "Glucopon 225 CSUP/ 600 CSUP/ 600 EC/ 650 EC" (*Henkel*), "Lutensol GD 70" (*BASF*) and "Triton BG-10/ GG-110" (*Rohm & Haas*) are surfactants for agricultural, industrial and domestic aids, while "Emulgade" and "Texapon GL 20UP" are APG containing commercial concentrates (both of *Henkel*). Recently *Wacker-Chemie* launched to market silicone polyglucoside "Belsil SPG" useful in cosmetics.

Other types of saccharide -derived nonionic surfactants of synthetic or microbiological origin can be classified as polymers [25-28]. Methylcellulose is a foaming water-soluble surface active polymer showing a cloud point. Hydrophobic modification of methylcellulose, hydroxyethylcellulose, hydroxypropylcellulose or other polysaccharides leads to interesting polymeric surfactants [29, 30]. Cetyl hydroxyethylcellulose, "PolySurf" of *Aqualon/Hercules*, and $C_{12\text{-}16}$ alkyl hydroxyethyl/ethylcellulose, "Elfacos CDHM" of *Akzo*, are typical examples. Many surfactants of microbiological origin can be specified as mono-, di-, or polysaccharides

[28, 31-33]. Some of them are nonionic surfactants, trehalolipids for example. Taking into account the sustainability concept, their role is growing.

1.2.3. Ethoxylated nonionic surfactants

The most abundant products among nonionics are ethoxylated alcohols and alkylphenols, polyglycol esters of fatty acids and related compounds having polyoxyethylene chain as hydrophilic group.

Alcohol ethoxylates are obtained by addition of ethylene oxide to alcohol under pressure and heating [7-9]:

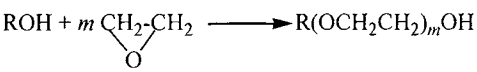

$$ROH + m\,CH_2\text{-}CH_2 \longrightarrow R(OCH_2CH_2)_mOH$$

This synthesis is usually carried out in the presence of alkaline catalysts. The catalyst is neutralized and at least partially remains in the final product. Primary C_8-C_{18} long-chain alcohols are generally used for ethoxylation. The alcohols may be of synthetic (Ziegler or oxo alcohols), vegetable and animal origin. Other hydroxo compounds can be subjected to ethoxylation, for example diols, such as 2,4,7,9- tetramethyl-5-decyne-4,7-diol ("Surfinol"), vegetable sterols, lanoline fractions enriched by sterols and fatty alcohols [34]. Ethoxylated alcohols and mercaptanes modified by a subsequent addition of propylene oxide or ethoxylated and propoxylated alcohols mentioned before (section 1.2.2) are of some industrial importance.

Along with the desired main product, industrial ethoxylated alcohols contain some quantity of initial alcohol as impurity, especially at low *m*, and free PEG the amount of which increases with *m*. Ethoxylated alcohols represent mixtures of oligomer-homologues with a wide ethylene oxide chain length distribution. Hence *m* is always some average value.

One of the modern technological trends consists in the production of ethoxylated alcohols having a rather narrow molecular weight distribution [9, 35-37]. It can be achieved by an intermediate distillation of the initial and low-ethoxylated products or by using more selective ethoxylation catalysts. Narrow-range ethoxylates present a new formulation potential, particularly in modern low-temperature detergents for automatic machines [38].

Individual polyethylene glycol ether derivatives of long-chain alcohols are supplied as fine chemicals for scientific use. They can be separated, for example, by preparative column

chromatography from technical-grade oligomer-homologues or by condensation of alkyl halide with individual PEG followed by a molecular distillation of the reaction product.

Depending on the source alcohol and the mean degree of ethoxylation, ethoxylated alcohols differ in their physicochemical properties and under normal conditions they can be liquid, paste or solid wax. The assigned hydrophile-lipophile balance (HLB) value varies generally from 3 to 16 and more [39]. Biodegradability of ethoxylated alcohols depends essentially on the ethoxylation degree: when $m < 12$ the biodegradability as a rule exceeds 90 % [40, 41]. The biodegradability goes down as the hydrocarbon chain length and branching rise.

Ethoxylated alcohols are ingredients of detergents, particularly low-temperature laundry aids, and cleaners, ancillary agents in textile industry, wetting agents, dispersants, and solubilisers of lipophilic materials. The main applications of ethoxylated nonionics correlate with the HLB and the mean ethylene oxide content as shown in the Table 1.1.

Table 1.1 HLB range of ethoxylated nonionics and their application

HLB value	EO content, %	Application
3-6	20-30	W/O emulsifiers
7-11	35-55	Wetting agents
8-18	40-90	O/W emulsifiers
10-15	50-75	Detergents
10-18	50-90	Solubilizers

The large variety of ethoxylated alcohols is available as 100 % products or with co-solvent under the following trade-names: "Akyporox RLM 22/40/80V" and "Findet1214N/1618A/1816/18-27" (*Kao*), "Alfonic" (*Conoco Chemicals*), "Brij" and "Synperonic A/BD/K" (*ICI*), "Cremophor A", "Lutensol A" and "Plurafac" (*BASF*), "Elfapur LM/LP" (*Akzo Nobel*), "Genapol C/L/OA/OX/OXD/SE/T/UD/ZDM/X" (*Clariant,* previously *Hoehst*), "Emulgen", "Akyporox" (*Kao*), "Imbetin-AG/AGS/C/KIB/L/T" (*Kolb*), "Marlipal" and "Marlowet" (*Condea*), "Neodol" and "Dobanol" (*Shell Chemicals*), "Rewopal", "Lauropal" and "Witconol" (*Witco*), "Rhodasurf" (*Rhodia*), "Tergitol 12/15" (*Union Carbide*),

"Sintanol" (*Kaprolaktam*), and many other products. Ethoxylated secondary alcohols are known for example as "Gardinol C" (*Albright & Wilson*) and "Softanol" (*Nippon Shokubai*). Individual polyoxyethylene ethers of dodecanol and other alcohols with $m \leq 8$ are supplied by *Nikko Chemical Co.* and *Sigma-Aldrich.*

The ethoxylated Guerbet alcohols with 2-8 EO mole are useful as defoaming and emulsifying agents, for example "Dehydol G 162/205" (*Henkel*). A similar nonionic surfactant but end-blocked with butyl groups show enhanced stability in acidic and basic conditions (product "Dehypon G 2084"). "Ethoxylated lanolin" and lanolin alcohols may be applied for a solubilisation of substances in water, such as oils, vitamins, fragrances, UV-filters, as well as ingredients of detergents, dispersing, wetting and thickening agents. Ethoxylated lanolin derivatives are: "Atlas G 1790/1795" (*ICI Specialties*), "Crodalan AWS/C34" and "Polychol 5/10/15/20/40" (*Croda*), "Findet LN/8750" and "Findet FF/8750" (*Kao*), "Lanoxyl 30" and "Rewolan ASW" (*Witco*), and "Solulan C" (*Amerchol*).

Alkylphenol ethoxylates are important kinds of nonionic surfactants. A characteristic feature of the catalytic ethoxylation of alkylphenols is the enhanced reactivity of phenol hydroxyl for ethylene oxide in comparison with alcohols. Esters of ethylene glycol and alkylphenol behave already as an alcohol. Therefore di-, tri-, and *m*-mers are allowed to form only after the complete consumption of the starting material. All commercial ethoxylated alkylphenols are mixtures of oligomer-homologues having a Poisson-like distribution with some PEG and catalyst as impurities. Both alkylphenols and dialkylphenols are useful for ethoxylation as a hydrophobic moiety. Among the alkylphenols, isooctylphenol and isononylphenol are most widely used. They are synthesized by the Friedel-Crafts alkylation of phenol with butene dimer and mixture of propene trimers, respectively.

Commercial alkylphenol ethoxylates come with almost 100 % surfactant content or with rheological modifiers. Their consistency changes from liquid via paste to solid wax as ethoxylation number rises. Isooctylphenol and isononylphenol ethoxylates with $m \leq 4$ are oil-soluble, those with m = 4-5 form emulsions in water, and products with $m \geq 5$ form clear aqueous solution.

Applications of alkylphenol ethoxylates are nearly the same as those of alcohol ethoxylates with stronger emphasis on technical needs. The production of alkylphenol ethoxylates is reduced gradually in view of their worse biodegradability and the established aquatic toxicity of their intermediates [40, 41].

Ethoxylated alkylphenols are known under the following trade names: "Baymol A/LN" (*Bayer*), "Empilan NP" (*Albright & Wilson*), "Hostapal CV/B" (*Clariant*), "Lutensol AP/TO" (*BASF*), "Makon" and "Polystep" series (*Stepan*), "Mulsifan RT 18/37" (*Zschimmer & Schwarz*), "Neonol AF" (*Nizhnekamskneftekhim*), "Nonipol" (*Sanyo*), "Renex" (*Uniqema/ICI*), "Rewopal HV" (*Witco*), "Tergitol NP" and "Triton X" series (*Union Carbide*), and so on.

Ethoxylated amides of the general formula $RCONHCH_2CH_2(OCH_2CH_2)_mOH$ or $RCON[CH_2CH_2(OCH_2CH_2)_mOH]_2$ are produced, like ethoxylated alcohols, by reacting alkyl amide, mono- or diethanolamide (section 1.2.5) with ethylene oxide. Most of them are viscous, waxy or solid products. Amides/ alkanolamides of lauric, coconut, oleic, tallow, and ricinoleic acids are often used as raw material. In contrast to ethoxylated alcohols and alkylphenols, the ethoxylated amides are less stable to hydrolysis, especially in alkaline media. Ethoxylated amides are characterized by mild detergency, decent emulsifying action at $pH < 7$, and low to moderate foaming, but they work as foam boosters and thickeners in combination with anionic surfactants. Some representatives can be useful as solubilisers and antistatics.

Typical examples of commercial ethoxylated amides are: "Amadol" and "Ethomid" series (*Akzo Nobel*), "Amidox C/L" (*Stepan*), "Aminol N" (*Kao*), "Lutensol FSA" (*BASF*), and "Rewopal C/O" (*Witco*).

Ethoxylated carboxylic acid esters are widely used in drug and cosmetics production, wetting and ancillary agents in textile, agriculture, machine and metal-processing industry. This is quite diverse group of very mild nonionic surfactants. The ethoxylated carboxylic acid esters are produced by reacting ethylene oxide and free hydroxyl of polyol, carbohydrate, or the hydroxyl group of carboxylic acid, such as ricinoleic acid. Typical chemical structures of ethoxylated carboxylic acid esters are presented below. Such as glycerol (I) and sorbitol (II) derivatives, one can produce ethoxylated esters of carboxylic acids and 1,2-propylene glycol, pentaerythritol, xylitol, mannose, methylglucose, and other carbohydrates.

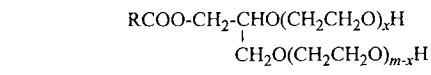

Ethoxylated monoglyceride (I)

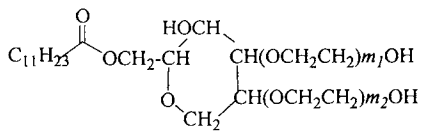

$m = m_1 + m_2$

Polyoxyethylene sorbitan monolaurate (II)

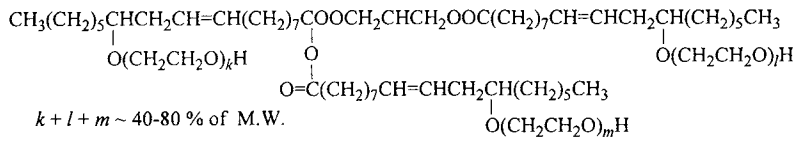

$k + l + m \sim$ 40-80 % of M.W.

Ethoxylate of glycerol triricinoleate - ethoxylated castor oil (III)

Sometimes it has been found advantageous to prepare first ethoxylated polyole or carbohydrate and than to react it with carboxylic acid at 110-130 °C in presence of toluene sulphonic acid or other catalysts. This is may be the simplest reaction between carboxylic acid and PEG:

$$RCOOH + H(OCH_2CH_2)_m OH \rightarrow \underset{(IV)}{RCO(OCH_2CH_2)_m OH} + \underset{(V)}{RCO(OCH_2CH_2)_m OOCR}$$

Depending on the reagent ratio, the reaction gives predominantly monoacyl or diacyl derivatives. Reaction with acid chloride and the ethyl ester transesterification brings the same result. To produce solely monoester, end-blocked PEG may be used but it should be remembered that the product will be worse soluble in water at the same polyoxyethylene chain length.

POE monoesters can be produced by direct interaction of carboxylic acid and ethylene oxide but they contain a large quantity of PEG as by-product [7, 8]. Principally, the carboxylic acid alkoxylation is applied for the monoester production such as glycol stearate and propylene glycol stearate (VI) that show good performance as oil-soluble emulsifiers, emollients and opacifiers in cosmetics.

Glycol diesters of carboxylic acids can be produced at a mole ratio acid: glycol of 2:1 with an almost quantitative yield. Glycol distearate (VII) is the conventional pearl-forming ingredient in recent personal care products.

Some of the most commonly used trade-marks of the ethoxylated carboxylic acid esters are: (I) "Arosurf 66" and "Rewoderm ES/LI" series (*Witco*), "Cetiol HE", "Cutina E 24" (*Henkel*), "Glycerox L" series (*Croda*), "Levenol C/V/H&B" (*Kao*), "Oxypon 2145" (*Zschimmer & Schwarz*), "Tagat L/S/O/TO" and "Tegosoft GC/GMC6" (*Goldschmidt*); (II) "Arlatone G 285/289/983", "Atlox 1045/1086/1256/1285" and "Tween" series (*ICI*), "Armotan PM" series (*Akzo*), "Kaopan TW-L/O/P/S" (*Kao*), "Kotilen L/O/P/S" (*Kolb*), "Lonzest SMS-20" (*Lonza*), "Sorgen TW" series (*Dai-Ichi Kogyo Seiyaku*), and so on; (III) "Arlatone" (*ICI*), "Cremophor EL/RH" (*BASF*), "Emulpon EL 33/40" (*Witco*), "Findet AR/52" (*Kao*), "Hedipin RH", "Sympatens TRH" (*Kolb*), "Mulsifan RT 7/163" (*Zschimmer & Schwarz*), "Stepanex CO" and "Toximul 8240/8244" (*Stepan*), "Tagat R 40/60" (*Goldschmidt*); (IV) "Cerasynt 616/660/840" (*ISP*), "Empilan AQ/BQ" (*Albright & Wilson*), "Mulsifan RT 1/2/113" (*Zschimmer & Schwarz*), "Rewopal EO70/M365" (*Witco*); (V) "Emerest 2712" (*Emery Industries*), "Rewopal PEG 6000 DS" (*Witco*), and "Kessco PEG 200DS/6000DS" (*Akzo Nobel, Stepan*); (VI) "Cerasynt MN/PA/PN" (*ISP*), "Cithrol EG/PG" (*Croda*), "Empilan EGMC" (*Albright & Wilson*) and "Kessco EGMS/PGMS" (*Akzo Nobel, Stepan*); (VII) "Emerest 2355" (*Emery*), "Kessco EGDS" (*Akzo Nobel, Stepan*) and "Tegin EGS /G 1100" (*Goldschmidt*). Ethoxylated lanolin acids, such as "Lanpol 5/10/20" of *Croda*, are used as emulsifiers in cosmetics. "Atlox 4914" of *ICI* presents polymeric surfactant of agricultural use in which the hydrophilic portion is PEG and the hydrophobic portion is alkyd resin. Alkyl-polyoxyethylene alkanoates, where alkyl is C_{12}-C_{18}, and rosin acid ethoxylates, as abietic acid ethoxylates (products "Scurol C" and "Soprophor 64/C" of *Rhodia*), are of some practical importance too.

1.2.4. Esters as nonionic surfactants

Obviously, esters between long-chain carboxylic acids and glycerol (acyl glycerols, or glycerides) are the most widespread lipophilic surfactants in food industry [42, 43] and cosmetics [44-46]. Glycerides are prepared from naturally occurring oils, fats and hydrogenated oils by alkaline, high-temperature (220 °C or more) glycerolysis, or by reesterification of methyl esters and a direct esterification of fatty acids and acyl chlorides with glycerol:

$$RCOCl + HOCH_2\text{-}\underset{\displaystyle OH}{\underset{|}{CH}}\text{-}CH_2OH \rightarrow RCOOCH_2\text{-}\underset{\displaystyle OH}{\underset{|}{CH}}\text{-}CH_2OH + RCOOCH_2\text{-}\underset{\displaystyle OH}{\underset{|}{CH}}\text{-}CH_2OOCR \quad \text{(II)}$$

Recently, lipase-induced low-temperature (42 °C) glycerolysis with a yield of 70-90 % monoglycerides has been developed [31b]. Monoglycerides and diglycerides of C_{12}-C_{18} fatty acids, oleic and linoleic acids are applied as food emulsifying agents and consistency modifiers in margarines, shortenings, and confectionery, as thickeners, co-emulsifiers, foam stabilizers, opacifying and emollient ingredients in cosmetics and detergents, as ingredients under leather finishing. Monoglyceride of undecylenic acids show fungicidal and antiseborrheic action [47]. Fatty acyl polyglycerols (III) are used as emulsifiers and skin humectants.

Glycerine stearate, other fatty acids glycerides are produced under the following trade names: (I) "Cerasynt GMS/Q/SD" (*ISP*), "Cutina EGMS/KD16/MD/GMS" and "Monomuls" series (*Henkel*), "Kessco GML/GMS" (*Stepan, Akzo Nobel*), "Quest GMS/GMLO" (*Quest/ICI*), "Rewomul MGSE" (*Witco*), "Tegomuls" and "Tegin 90/4100/ISO/M/O/V" series (*Goldschmidt*); (II) "Cerasynt 847" (*ISP*), "Cremophor WO-A" (*BASF*), "Monomuls 60" (*Henkel*); (III) "Admul WOL 1403/1405/1411" (*Food Industries*), "Dehymuls PGPH" (*Henkel*), "Drewpol" series (*Stepan*), "Isolan GI34/GO33" (*Goldschmidt*), "Quest PGO/PGS/PGPR" (*ICI*), "Witconol 14 F"(*Witco*), and other products.

Among other surface active esters, polyglycol esters of fatty acids, alkanoyl glycerol acetates and lactates, alkyl lactates, esters of fatty acids and pentaerythritol, glucose, methylglucose, mannose, sucrose, and, especially, sorbitol are often exploited. The latter, sorbitan acylates, are particularly known as "Spans", "Arlacels", and "Arlamol ISML" - all of *ICI* production. These mild and low-toxic emulsifiers are widely applied in food, pharmaceutical, personal care and other consumer and industrial products.

The structure of sucrose monoesters can be seen below:

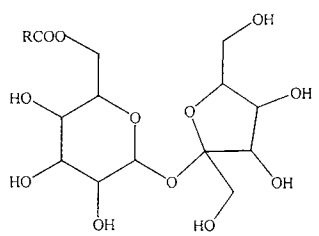

As can be seen, several additional hydroxyl groups are available for esterification. Thus, a variety of economically attractive sugar esters with a wide range of HLB may be prepared on a synthetic or enzymatic way. This very mild sucrose acylates are useful as edible emulsifiers and food-grade cleaners. When used in breadmaking, sucrose monoesters and diesters improve the

volume and crumb grain and reduce the dough mixing time up to 20 % [43]. They can be exemplified by the "Sucro Ester WE 7/11/15" (*Gattefosse*), "Ryoto Sugar Ester LWA/OWA/P/S" (*Ryoto*) and "DK Ester F-20/50/70/160B..." (*Dai-Ichi Kogyo Seiyaku*).

1.2.5. Alkanolamides and other amide-group containing nonionics

These practically important nonionic surfactants are produced by interaction of a fatty acid, its methyl ester, or another derivative and aminoalcohol. Thus, about equal mole fraction of lauric acid and 2-aminoethanol at 150 °C yield lauric ethanolamide:

$C_{11}H_{23}COOH + H_2NCH_2CH_2OH \rightarrow C_{11}H_{23}CONHCH_2CH_2OH$

The final substance contains aminoester of the formula $C_{11}H_{23}COOCH_2CH_2NH_2$ and amidoester $C_{11}H_{23}CONHCH_2CH_2OOCC_{11}H_{23}$ as by-products. In addition, alkanolamides may contain some alkanolamine soaps as well. The reaction between the methyl ester of a fatty acid and alkanolamine proceeds under milder conditions and gives higher yield of the final products.

Along with monoethanolamides (I), isopropanolamides (II) and diethanolamides (III), synthesized analogously, have a practical importance. Purer fatty acid mono- and diethanolamides containing some ethoxylated amides could be prepared by the reaction of fatty acid amides with controlled amounts of ethylene oxide. Ethoxylation of fatty acid amides results in mixtures of mono- and diethanolamides as well as polyethoxylated alkanolamides.

Fatty acid ethanolamides and isopropanolamides are solid or waxy products insoluble in water. Diethanolamides are usually pastes or liquids and show better dispersibility in water. In institutional and household formulations, shampoos, bath and shower preparations, fatty alkanolamides play the role of foam stabiliser, thickener, corrosion inhibitor, and ancillary agent that improves the skin compatibility of anionic surfactants. Undecylenic ethanolamide and undecylenic diethanolamide act as fungicides also [47]. Use of diethanolamine derivatives has legislative limitations today in some countries (but not its amides) because they are proved to be precursors of carcinogenic nitrosoamines. The probability of the nitrosoamine formation is assumed to increase in the presence of formaldehyde and formaldehyde-releasing preservatives [44-46].

Among ethanolamine -derived amides, alkylethoxyglycolic acid ethanolamide of the formula:

$R(OCH_2CH_2)_mOCH_2CONHCH_2CH_2OH$ (IV)

exhibits good water dispersibility in view of liquid consistency, foam stabilisation and viscosity increase over a wide range of temperatures, especially in shampoos [48].

Fatty acid alkanolamides are widely known as a secondary surfactant, namely: as foam and detergency booster, co-emulsifier, viscosity modifier, hair and skin conditioner, corrosion inhibitor, and moderate antistatic [2, 22]. Some trade names of alkanolamides are as follows: (I) "Amidet A-111" (*Kao*), "Comperlan 100/LM" (*Henkel*), "Empilan CME" (*Albright & Wilson*), "Lauridit KM" (*Akzo Nobel*), "Monamid MEA" (*Uniqema*), "Rewomid C/L/S/U" (*Witco*); (II) "Empilan CIS/LIS" (*Albright & Wilson*), "Ninol M-10" (*Stepan*), "Rewomid IPE/IPL/IPP" and "Witcamide SPA" (all of *Witco*); (III) "Alkamide KD" (*Rhodia*), "Aminol KDE" (*Kao*), "Comperlan COD/KD/LD/OD/VOD" and "Texamin PD1" (all of *Henkel*), "Empilan CDE/CDX/ 2502/LDE" (*Albright & Wilson*), "Lauridit KDG" (*Akzo Nobel*), "Mackamide CS/LLM" (*McIntyre*); "Purton CFD/SFD" (*Zschimmer & Schwarz*), "Rewomid DC/ DO/F", "Rewocid DU 185 SE" and "Witcamide LDT/S" (all of *Witco*); (IV) "Aminol A15" (*Kao*).

Some enzymatically prepared glycolipids and polymeric biosurfactants, such as trehalolipids and emulsan [*31b, 32b*], as well as acylated proteins (see Section 5) are mainly of nonoinic nature.

Along with APGs, commercial interest in other carbohydrate-derived surfactants of "green" environmental image has been rise sharply in recent years. Glucose amides are typical examples, especially, N-lauroyl-N-methylglucamine or N-dodecanoyl-N-methyl-1-amino-1-deoxy-D-glucitol, commercialised by *Procter & Gamble* and *Clariant.* This glucose amide is synthesised from glucose (obtained from cornstarch), methylamine, hydrogen, and methyl laurate in two steps [3]:

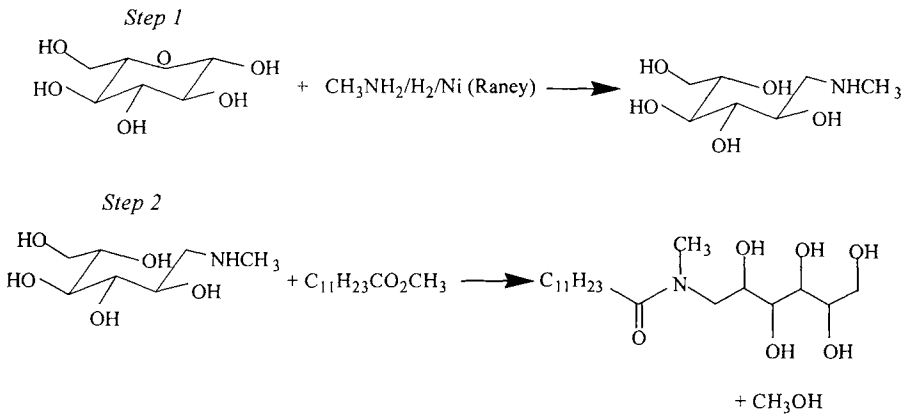

The first reaction is the reductive alkylation of methylamine with glucose, performed using glucose syrup and nickel hydrogenation (Raney) catalyst. The subsequent reaction is acylation of the secondary amine by methyl laurate with distilled off methanol as a by-product. The N-lauroyl-N-methylglucamine has mildness, excellent dispersing, foam and cleansing characteristics. From an economical point of view, this compound, along with anionic surfactants, is quite attractive for use in light-duty detergents and personal care products.

1.2.6. Pseudocationic nonionic surfactants

Addition of ethylene oxide and propylene oxide to fatty amines prepared from naturally occurring fatty acids encounters no difficulties. The reaction results in surfactants of mainly nonionic character those are characterised by better compatibility with anionics and moderate toxicity in comparison to initial amines. The ethoxylated fatty amines found application in textile finishing, acidic cleaners and cosmetics. Commercial ethoxylated fatty amines are known, for example, as "Ethomeen", "Genamin C/O/S/T", "Imbentin-CAM/OTM", "Marlazin", and "Rhodameen/Cemulcat" series of *Akzo Nobel*, *Clariant*, *Kolb*, *Condea*, and *Rhodia*, respectively.

There are some nonionics that turn, under certain conditions at least partially, into cationic surfactants, which provides them the specific behaviour. Typical representatives of pseudocationic nonionic surfactants are long-chain tertiary amine oxides prepared by oxidation of tertiary amines, aliphatic, as N-lauryldimethylamine, or cyclic, as N-alkyl piperidine, by hydrogen peroxide:

$$C_{12}H_{25}N(CH_3)_2 + H_2O_2 \rightarrow \underset{\underset{O}{|}}{C_{12}H_{25}N(CH_3)_2} \quad (I)$$

Commercial amine oxide contains some amount of unoxidised tertiary amine that may account for some of the cationic behaviour of the product, particularly at low pH. The formation of semipolar N–O bonds both rises affinity to water and highly reduces the basic character of the amine so that the transition into a salt becomes possible at low pH only or as a result of mixed micelle formation with an anionic surfactant at neutral pH [49, 50]:

$$\underset{\underset{O}{|}}{C_{12}H_{25}N(CH_3)_2} + C_{12}H_{25}OSO_3^- + \bar{H}_2O \rightarrow \underset{\underset{OH}{|}}{C_{12}H_{25}N^+(CH_3)_2} \cdot C_{12}H_{25}OSO_3^- + OH^-$$

Amine oxides of the same kind are manufactured by reaction of alkanoic acids and their esters with N,N-dimethyl-1,3-propanediamine and subsequent oxidation of the amino amide by hydrogen peroxide [9]:

$$RCONHCH_2CH_2CH_2N(CH_3)_2 + H_2O_2 \rightarrow \underset{\underset{O}{|}}{RCONHCH_2CH_2CH_2N(CH_3)_2} \quad (II)$$

Mild amine oxide with hydroxyethyl groups in the polar moiety can be also produced by oxidation of ethoxylated fatty amine.

Tertiary phosphine oxides, alkylmethyl sulphoxides, and alkylhydroxyethyl sulphoxides produced in the same way from trialkyl phosphines and thioethers, as well as N-alkyl-pyrrolidones (III) [51] and some long-chain imidazoline derivatives (IV) [52] should be considered as pseudo-cationic nonionic surfactants.

The relatively good stability of amine oxides in oxidising, acid, and alkali media makes them useful emulsifiers, foam and viscosity boosters, antistatics, dispersants, and cleansers in a wide range of household, cosmetic, and special aids. Imidazolines are known as corrosion inhibitors, emulsifiers, and agents facilitated in electrochemical and acid-etching processes.

Examples of commercial pseudocationic surfactants are given below. Amine oxide-type surfactants are: (I) "Aromox L/D/T" (*Akzo Nobel*), "Empigen OB/OH/OY" (*Albright & Wilson*), "Euroxide CPO/LO/M25" (*EOC*), "Genaminox C5/CST/LA" (*Clariant*), "Oxidet L-75/DM-246" (*Kao*), "Rewominox L 408" (*Witco*), "Rhodamox LO" (*Rhodia*), "Synprolan 35 DMO" (*ICI*); (II) "Aminoxid WS 35" (*Goldschmidt*), "Empigen OS" (*Albright & Wilson*), "Rewominox B 204" (*Witco*), "Oxidet DMC-LD" (*Kao*); N-alkyl-pyrrolidones (III) are

"Surfadone LP 100" and "Surfadone LP 300" of *ISP*; (IV) imidazoline derivatives – "Rewopon IM AN/OA" of *Witco*.

In a chapter of limited volume it is rather difficult to cover all versatility and characteristic properties of nonionic surfactants. Immense opportunities of organic synthesis and microbiology as well as scientific and technological needs cause the great scope of amphiphilic compounds with unique structures and properties. There are, e.g., surfactants containing chromophores and reactive groups. Surface active macrocyclic polyethers are of great particular interest [53]. These compounds are able to complex selectively metal cations turning them into associated cationic form and changing dramatically their behaviour and properties. A complete volume of the *Surfactant Science Series* [54] and later chapters of this book are devoted to the physicochemical properties of nonionics.

1.3. Anionic Surfactants

Anionic surfactants are amphiphilic substances that include an anionic group as an obligatory component attached directly or through intermediates to a long hydrocarbon chain. The most commercial anionic surfactants are generally inhomogeneous mixtures with respect to both the composition and hydrocarbon chain length since the purity is often not crucial for their performance. With soap their portion reaches about 75 % of the world market [11]. Anionics are often named "detergents" to emphasise their significance in cleaning products. Dispersing ability, high foaming, sensitivity to water hardness and protein denaturation are among the most characteristic properties of anionic surfactants.

Dissociating in water, anionic surfactants form the surface-active anions and hydrated cations, for example, cations of alkali metals or ammonium:

$$C_{12}H_{25}OSO_3Na + aq \longrightarrow C_{12}H_{25}OSO_3^- + Na^+$$

The hydrocarbon part of the surfactant can be a straight-chain aliphatic radical, as in the case of sodium dodecyl sulphate given above, as well as a branched-chain, unsaturated radical, and can involve benzene or phenolic residues and polar groups:

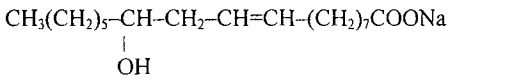

Sodium ricinoleate

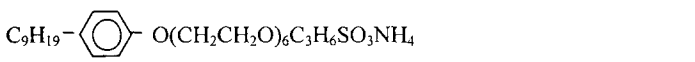

Ammonium *iso*-nonylphenol hexa(ethoxy)propanesulphonate

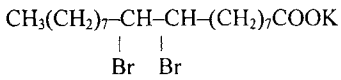

Potassium 9,10-dibromostearate

About 75 % of anionic surfactants (other than soaps) in the world are based on synthetic raw materials. Recent tendencies however let expect that in the 3rd millennium renewable materials of biological and botanical origin will be more and more preferred.

1.3.1. Raw materials for anionic surfactants

The most important starting materials for the production of the anionic surfactants are:

- alkyl benzene and other alkylated aromatics,
- linear paraffins,
- linear olefins (with terminal or internal double bond) and branched olefins,
- long-chain alcohols, their ethoxylates and alkylphenol ethoxylates,
- fatty acids and their derivatives (methyl esters, glycerides, alkanolamides).

These materials form the hydrophobic part of anionic surfactants. Many other raw materials are required for modifying a hydrophobe to render the amphiphilic structure required. They include, for example: sulphation/sulphonation agents, phosphorylation agents (such as $ClSO_3H$, SO_3, Na_2SO_3, P_4O_{10} and $POCl_3$), ethylene oxide, maleic anhydride, sodium chloroacetate, sodium isethionate, N-methylglycine, 1,3-propane sultone, sodium hydroxide, ammonium hydroxide, triethanolamine, and many other compounds. Moreover, formulation chemists are often faced with a problem of quality of the final product, particularly concerned their dark colour, turbidity and off-odour. This requires many other auxiliaries to the surfactant concentrate finishing, namely: bleachers, diluents, hydrotropes, preservatives, and so on.

With some nuances all anionic surfactants can be characterised by the same set of parameters determining the quality, including toxicological and environmental safety, application. The parameters and their test methods are compiled in Table 1.3.

Table1.3 Parameters to characterise anionic surfactants and their test methods

Parameter of importance	Test method
Appearance at 20 °C or another temperature	Visual assessment: (clear/ cloudy, thin/ viscous) liquid, paste or solid, colour, odour
Active matter (%)	Two-phase titration, column chromatography
Solid and moisture content (%)	Gravimetry, Fischer titration
Average molecular weight	Titration/gravimetric analysis, vapour pressure osmometry
Molecular weight or alkyl chain length distribution	Gas chromatography, hydrolysis and GC, pyrolysis GC, HPLC, ion chromatography
Unmodified (f. e., unsulphated) material (%)	Extraction, column chromatography
Alcohol-soluble matter (%)	Extraction
Coupling agent (co-solvent, hydro-trope or solubiliser) (%)	GC, HPLC or column chromatography
Unsaturation (g I_2 per 100 g of organic matter)	Iodine value titration
pH value	Potentiometry
Colour (scores)	Gardner or Klett test
Other specific parameters	Solubility, density, viscosity, hydroxyl value, carbonyl value, salts, toxicity, biodegradation ability, and so on

1.3.2. Alkylarylsulphonates, alkanesulphonates, olefinsulphonates, ether sulphonates and other sulphonates

A large body of modern anionic surfactants constitutes alkylbenzenesulphonates and other sulphonates based on alkylarenes. Among other synthetic detergents, their technology is one of

the oldest and underwent an evolution since the late 1920s [2, 56-59]. The hydrocarbon sources for the surfactants are of fossil origin: petroleum, natural gas and coal.

The Friedel-Crafts acidic alkylation with n-olefins and n-chloroparaffins has been developed in different configurations. Feedstocks for arene alkylation are generally *n*-paraffins derived from paraffin-rich oil cuts obtained by distillation and molecular sieves (zeolites). By dehydrogenation over platinum catalyst the C_{8-18} paraffins are converted to olefins. Linear monoolefins (α-olefins and internal olefins) other than branched olefins are preferable for arene alkylation [58, 59]. Another industrially meaningful source of *n*-olefins is the process of ethylene oligomerisation developed by *Shell*. The alkylation process is generally carried out in column reactors at 40-135 °C with some excess pressure and recirculation of unreacted benzene and heavy alkylates. Including the recycled polyalkylates, the molar benzene/olefin ratio is 3.0-3.5. All reaction parameters depend strongly on each other and influence the alkylate output and composition. The polyalkylates formed as by-products can be readily subjected to the subsequent transalkylation with benzene or separated for further conversion into higher sulphonates and dopes as well.

The alkylation with chlorinated paraffin is used as before for the production of LAB, higher benzene alkylates and other alkylaromatics. To avoid the formation of many by-products a high excess of aromatics to chloroparaffin (ca. 10 : 1) is generally chosen. Unreacted benzene, di- and trialkylates are returned into the process. The ratio between $AlCl_3$ used as an alkylation catalyst and chloroparaffin is critical too. The reaction takes place at 35-90 °C and pressures of ca. 3 bar where the residence time is 5 to 60 minutes [56].

Both (olefin and chloroparaffin) electrophilic reagents have insufficient reactivity to interact with the weakly nucleophilic aromatic ring. To enhance the electrophilicity of the reagents it is necessary to use catalysts such as HF and Lewis acids. Some kind of zeolites as heterogeneous acidic alkylation catalyst is advantageous in some respects (such as high selectivity, low corrosion, complete regeneration, appreciable savings in raw materials, technical and safety facilities) [58-60].

The Friedel-Crafts acid alkylation with strait-chain olefins and chloroparaffins give rise to mixtures of alkylarenes the composition of which is a function of the process configuration and

parameters. Dealing with benzene alkylation, mixtures of alkylbenzenes are formed with predominance of secondary alkylbenzenes (2-phenylalkane), if α-olefins were used. Under normal alkylation conditions primary alkyl benzenes are not formed.

The double-alkylated arenes, as dibutylnaphthalene, have some importance also as starting materials for alkylarylsulphonates. So, dibutylnaphthalene can be obtained by a reaction between naphthalene and butanol at 25-35 °C catalysed by sulphuric acid. Another raw material source for alkylarylsulphonates ("petroleum" sulphonates) are the oil cuts enriched with alkylarenes.

For different hydrocarbons, sulphonation methods are to a large extent of the same kind. Equally with other stages and techniques of surfactant production, the methods experience an impressive progress both in implementation and technological innovations from the sulphonation with sulphuric acid and related agents [61, 62] to the present-day SO_3 sulphonation processes [59, 62-65].

In the detergent industry sulphonation processes with sulphuric acid, oleum and SO_3-complexes are essentially of historical significance, and are not any longer used in developed countries. In the production of white oils, however, sulphonation with concentrated sulphuric acid and oleum is still used. The sulphuric acid treatment of selected petroleum fractions lead to petroleum sulphonates the sodium or ammonium salts of which are used in tertiary oil recovery, metallurgy, froth flotation and concrete industry, while the magnesium, calcium and barium salts are used as dopes in fuels and lubricants. The sulphonation with chlorosulphonic acid continue to remain useful in batch processes, typically on a relatively small scale:

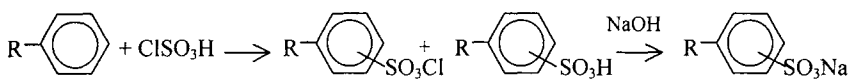

Accompanying HCl is absorbed with water to recover in hydrochloric acid. The quality of alkylbenzenesulphonic acid (ABSA) depends on the contact time, temperature, molar ratio and humidity of the reagents. Disulphonic acid and split-up products accompany the reaction as main associates.

To attain the quality and high conversion required, the sulphonation is performed now with gaseous sulphur trioxide in reactors summarised in Table 1.4.

Table 1.4 Sulphonation Reactors [62]

Producer	Reactor type
Ballestra-Sulfurex system	Continuous stirred tank cascade
Ballestra-Mazzoni MTFF reactor	Multitube falling film reactor
Chemithon impact jet reactor	Atomises organic feed in SO_3/air
Chemithon falling film reactor	Falling film reactor
Lion Corporation TO reactor system	Falling film reactor
Mecchaniche Moderne falling film reactor	Concentric tube falling film reactor

The sulphonation of alkylarenes with SO_3 is a quite exothermic process: for linear alkylbenzene (LAB) the reaction enthalpy ΔH_R = -170 kJ per mole at 5-7 % (v/v) SO_3 in air. Thus, to control temperature and colour any construction of the reactors quoted above has well designed contact surface where SO_3 is diluted with air or SO_2. The range of the optimal alkylate/SO_3 ratio is equal to 1.02-1.05. When we deal with a detergent-grade LAS synthesis, the main chemical reactions can be written as follows [62, 64]:

$$RC_6H_5 + 2SO_3 \longrightarrow \underset{\text{Pyrosulphonic acid}}{2RC_6H_4SO_2OSO_3H} \text{ (fast)}$$

$$RC_6H_4SO_2OSO_3H + RC_6H_5 \longrightarrow 2RC_6H_4SO_3H \text{ (slow)}$$

In consequence of the slow second reaction some ageing is required to convert the pyrosulphonic acid and alkylate to ABSA. Four main side reactions accompany the sulphonation where two of them lead also to the desired product:

$$RC_6H_4SO_2OSO_3H + RC_6H_4SO_3H \longrightarrow \underset{\text{Sulphonic anhydride}}{RC_6H_4SO_2OSO_2C_6H_4R} + H_2SO_4$$

$$RC_6H_4SO_2OSO_2C_6H_4R + H_2SO_4 + RC_6H_5 \longrightarrow 3RC_6H_4SO_3H \text{ (ageing)}$$

$$RC_6H_4SO_2OSO_2C_6H_4R + H_2O \xrightarrow{H^+} 2RC_6H_4SO_3H \text{ (in the presence of water)}$$

$$RC_6H_4SO_2OSO_3H + RC_6H_5 \longrightarrow \underset{\text{Sulphone}}{(RC_6H_4)_2SO_2} + H_2SO_4$$

The undesirable sulphone formation is assumed to arise from the elevated temperature and concentration of H^+ ions.

The third step of LAS synthesis is the batch or continuous neutralisation of ABSA. It can be performed in the same production unit or at any other detergent plant before further use of the surfactant. Aqueous sodium hydroxide, ammonia and triethanolamine are the most convenient neutralising agents. Commercial LAS come as ~40-50 % aqueous concentrates (or up to 70 % with hydrotropes and viscosity modifiers). Sodium salts of LAS can be subjected to drying for manufacture of solid product. Ca, Ba, Na and Li alkylarenesulphonates have some importance also as technical-grade emulsifiers, corrosion inhibitors, grease and flotation agents. The short-chain alkylarenesulphonates, as cumene- and xylenesulphonates, increase the solubility of LAS, higher alkylsulphates and sulphonates in aqueous formulations (act as hydrotropes).

Among alkylarenesulphonates, LAS is the most important usage- and cost-effective, toxicologically and environmentally safe surfactant that constitutes a great variety of recent domestic and institutional detergents. Its world production is estimated to over 2 million tonnes and continues to rise. The performance of LAS is not highly affected in the presence of hard water. Depending on the structure, alkylarylsulphonates can show efficient wetting, dispersing ability, and solubilisation. LAS are available as the following commercial products: "Bio-Soft D/N-300", "Nacconol 40G/90G", "Polystep A7/A15/LAS-50" (all of *Stepan*), "Hexaryl D 60L" (*Witco*), "Lumo WW 75" (*Zschimmer & Schwarz*), "Maranil Paste A55/A75" and "Maranil Pulver A" (*Henkel*), range of "Marlon A/ADS/AMX/ARL/AS/AT" products (*Condea*), "Meliosol 65R" (*Kao*), "Nansa SBA/SSA/HS/SB/SS/TS" series (*Albright & Wilson*), "Petresul" series (*Petresa*), "Soft Detergent 60" (*Lion*), "Sulfonol LABS A/B" (*Kinef*), "Ufasan 65/TEA" and "Ufaryl DL85" (*Unger*). Contrary to LAS, alkylbenzenesulphonates on the base of branched tetrapropylene alkylate lost their importance gradually in view of the bad biodegradability [2, 40, 41].

Alkanesulphonates, or alkylsulphonates, are produced since the 40's by photochemical sulphochlorination of linear $C_{10\text{-}18}$ paraffins with gaseous SO_2 and Cl_2 at 25-40 °C with a subsequent neutralisation by aqueous sodium hydroxide [2, 10, 11, 56, 66]:

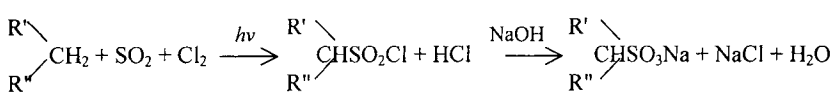

The sulphochlorination is a radical chain reaction, initiated by vis./UV light (λ < 480 nm, quantum yield of ~2000). The reagents must contain O_2 and H_2O in very limited quantities. As a result, complex mixtures of isomeric alkanesulphonates are formed comprising di- and polysulphonates, paraffins, chloroparaffins and salts as well. Other stages allow for alkanesulphonate manufacturing of a sufficiently high quality.

The sulphoxidation is a more recent technical rout to manufacture alkanesulphonates as commercialised by *Hoehst* and *Hüls*. It is a radical chain reaction too, excited by UV light. The reaction mechanism, modifications and technical features of the process are described elsewhere [11, p. 146 ff; 66, 67]. The sulphoxidation results in mainly secondary alkanesulphonates of a decent quality. Sodium alkanesulphonates are safe enough for humans and environment.

The world alkanesulphonate production is rated to ca. 300 000 tonnes per year (Germany, Eastern Europe, Russia and China). Their properties and uses are essentially similar to LAS. They are known as: "Emulsifier E30" (*Leuna*), "Hostapur SAS 30/60/93" (*Clariant*), "Levapon ME", "Emulgator K30", "Mersolate H" (*Bayer*), "Lutensit A-PS" and "Golpanol ALS" (*BASF*), "Marlon PS 30/60/65" (*Condea*), "Volgonat" (*Volgogradskoye AO Sintez*).

The chemistry of olefinsulphonates (AOS) has undergone a strong evolution in the 60th and 70th. Perhaps, their production procedures and techniques are most complex among other anionic surfactants consisting of four stages: sulphonation, ageing, neutralisation, and hydrolysis [68, 69]. Even C_{12}-C_{18} α-olefins are of major importance as raw material for the olefinsulphonate synthesis. The process scheme is shown in Fig. 1.3.

The olefin sulphonation with gaseous SO_3 is a highly exothermic process (ΔH_R = - 210 kJ·mol^{-1}) generally performed in falling olefin-film reactors with counterflow of the air-diluted SO_3 at 25-30 °C. As a first step, very fast addition of SO_3 to α-olefin yields highly reactive, unstable 1,2-sultone or zwitter-ion R-$^{+}$CH-CH$_2$-SO$_3^{-}$ that rearranges to isomeric alkene sulphonic acids and 1,3- and 1,4-sultones. Coupled reactions take place leading particularly to sultones with broader ring, pyrosultone, and alkenedisulphonic acids (not shown in Fig. 1.3). To manufacture high-quality products, mild operating conditions for the α–olefin sulphonation are required [64] as presented in the Table 1.5.

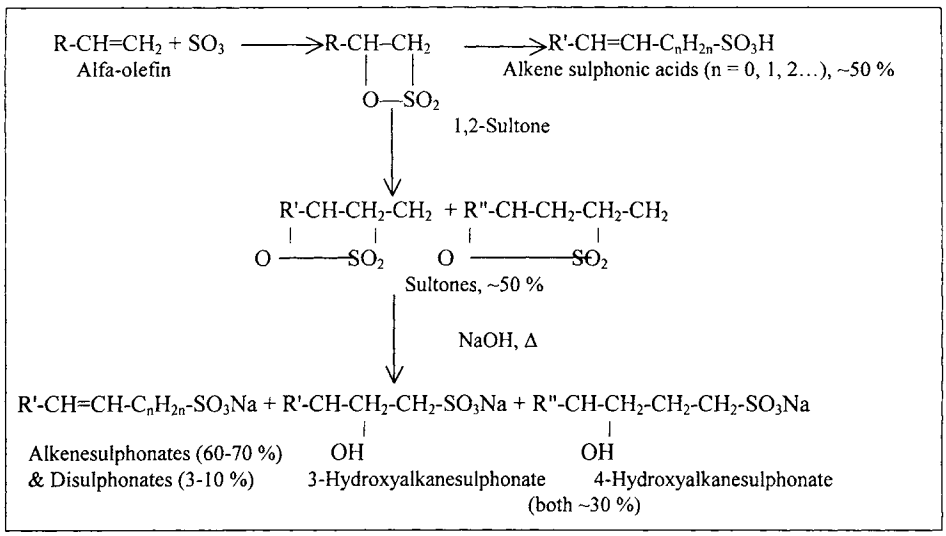

Fig. 1.3 The synthesis of α-olefinsulphonates

Table 1.5 Thin-film sulphonation techniques with gaseous SO_3

SO_3/ olefin mole ratio	1.06-1.08
SO_3 concentration, vol. %	2.5-4.0
Optimum reaction temperature, °C	15
Digestion time before neutralisation/ hydrolysis, min	5-10
Digestion temperature, °C	30-35

Some modification of the sulphonation is required when we deal with internal olefins [62, 69]. The β-branched olefins give rise to alkenesulphonates only because in the sulphonation no sultones are formed.

The subsequent neutralisation performed at 30-40 °C converts sultones principally to alkenesulphonates and hydroxyalkanesulphonates. The presence of irritant and allergic sultones is highly undesirable in the final product. Therefore it should be subjected to ageing for a limited time at 140-160 °C and pressure.

Recent AOS synthesis leads to multifunctional surfactants that are less sensitive to water hardness than most anionics, and are better biodegradable than LAS. The C_{10-16} α-olefin-

sulphonates are used in liquid soaps, foaming and LDL compositions whereas internal AOS are more known as wetting agents. $C_{14\text{-}20}$ α-olefinsulphonates are used in powdered spray-dried detergents. The total worldwide production of AOS approaches 100 000 tonnes and one-third or more accounts for Japan. AOS are manufactured in powdered form and as aqueous concentrates with active matter of 35-40 % under the following trade names: "Bio Terge AS-40/90", "Polystep A-18", "Stepantan AS-12/40" (all of *Stepan*), "Elfan OS 46" (*Akzo Nobel*), and "Hostapur OS" (*Clariant*), "Lipolan AO/AOL/G/327F/ 440/1400" (*Lion*), "Nansa LSS38/AS" and "Nansa LSS480" (*Albright & Wilson*), "Nikkol OS-14" (*Nikko*), and "Witconate AOS 38" (*Witco*).

The sulphonates derived from fatty acid alkyl esters (mainly, as sodium salts of α-sulphomonocarboxylic esters or, in other words, methyl ester sulphonates) become more and more attractive in view of their renewable raw material sources, such as triglycerides of animal and vegetable origin. Fatty acid alkyl esters are produced via a direct transesterification of triglycerides with alcohol, typically methanol, or via direct esterification of fatty acids. The same thin-film sulphonation techniques (see Table 1.5) with gaseous SO_3 are used today to manufacture these surfactants [62, 70]. The two-step sulphonation can be represented by the sequential reactions [70, 71] shown in Fig. 1.4.

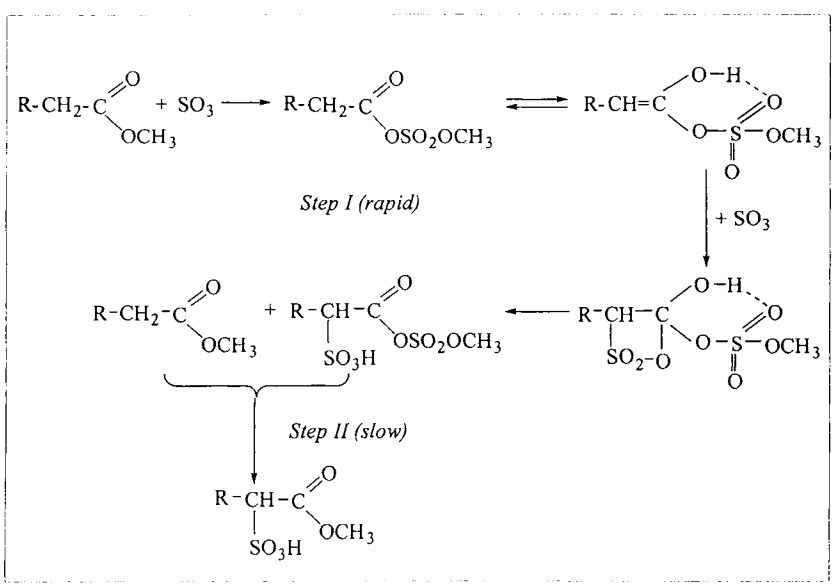

Fig. 1.4 Mechanism of fatty acid ester sulphonation

In the first step, an SO_3 molecule is implanted in the ester bond to form a mixed anhydride that exists in a very fast equilibrium with its enolic form. Then fast electrophilic addition of a second SO_3 molecule occurs to the enolic double bond, and the α-sulphonated anhydride is formed. In the second (slower) step, the intermediate reacts with other fatty acid ester molecules by releasing SO_3 that serve in new reaction cycles. The sulphonation goes with air-diluted SO_3 at 80-90 °C followed by ca. 30 min ageing at 90-95 °C. The neutralisation gives rise to sodium salt of the α-sulphocarboxylic acid ester and disodium salt of the α-sulpho-carboxylic acid as a by-product. Before neutralisation, reesterification of the semifinished item has been proposed in consequence of the bad detergency of α-sulphocarboxylates.

A major disadvantage of this process is the formation of dark brown impurities that create aesthetic and odour issues in the final product. Consequently, bleaching of acid and/or neutralised product is required for which hydrogen peroxide is conveniently adopted [70]. It is worth to note that no bleach processes are needed for the purification of the potassium palm $C_{16\text{-}18}$ methyl ester sulphonates based on recrystallisation from water [72]. If the quality problems were solved well, the methyl ester sulphonates may be possible candidates to replace LAS in detergents and as low-cost lime soap dispersants. Sodium alkyl α-sulphoalkanoates with comparable lengthes of the alkyl and acyl chain show high wetting and foaming ability and other properties resembling "Aerosol OT" (see sulphosuccinate-type surfactants).

Acyl isethionates are ester-type anionic surfactants formed by monocarboxylic acids and isethionic acid $HOCH_2CH_2SO_3H$. The latter is formed by reaction of 30 % aqueous sodium bisulphite and ethylene oxide at 70 °C [66]. All commercial isethionates (as sodium "cocoyl" isethionate) are esters derived from natural carboxylic acids by esterification of the acids or acyl chlorides with sodium isethionate:

$$RCOOH + HOCH_2CH_2SO_3Na \xrightarrow{170\text{-}190\ ^\circ C} RCOOCH_2CH_2SO_3Na$$

For a better colour it is advantageous to curry out the esterification for up to ~90 % conversion and under some excess of sodium isethionate [73]. Acyl isethionates derived from acyl chloride are formed under milder conditions but contain NaCl.

Acyl isethionates are surprisingly mild surfactants having excellent biodegradability. As most other esters, they are hydrolytically unstable and generally marketed as powders or flakes. Acyl isethionates are particularly useful for combo bar soaps [45, 46]. They are known as: "Arlatone SCI" (*ICI*), "Elfan AT 84/84 G" (*Akzo Nobel*), "Geropon AS 200" (*Rhodia*), "Hostapon SCI65/SI" (*Clariant*), "Igepon AC-78" (former *GAF*), "Metaupon SCI" (*Leuna*).

The hydrolytic stability of a surfactant can be enhanced critically if the condensation is carried out with sodium methyltaurate instead sodium isethionate, for example [10, 56, 74]:

$$CH_3(CH_2)_7CH{=}CH(CH_2)_7COCl + CH_3NHCH_2CH_2SO_3Na \longrightarrow$$

$$\longrightarrow CH_3(CH_2)_7CH{=}CH(CH_2)_7CONH(CH_3)CH_2CH_2SO_3Na + NaCl$$

Sodium N,N-oleoylmethyltaurate (Igepon T)

The fatty acid N-methyltaurides are used in textile treatment aids and personal care detergents, particularly in toilet combo bars and shampoos.

Sulphosuccinic acid esters should be grouped into mono- and diesters. The first step of the monoester sulphosuccinate synthesis is the esterification of a hydroxyl-bearing stock material by maleic acid anhydride. As stock materials, long-chain primary alcohols, ethoxylated alcohols, ethoxylated alkylphenols, alkanolamides, ethoxylated alkanolamides, or monoglycerides are generally used [10, p. 405 ff; 75, 76].

The group of monoester sulphosuccinates is synthesized in two steps. In the first step, the hydroxyl-carrying molecule and maleic anhydride form the monoester of maleic acid:

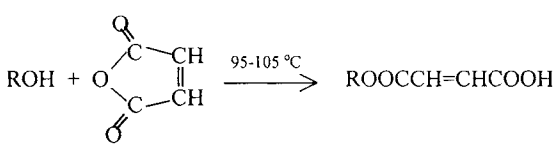

(where R = C_nH_{2n-1}-, $C_nH_{2n+1}(OCH_2CH_2)_m$-, $C_nH_{2n+1}CONHCH_2CH_2$-, ...)

An excess of maleic anhydride (up to 5 % wt.) is generally used. Unreacted ROH, diester, and maleic acid/anhydride are formed as by-products. Note, monoalkylethoxymaleates are of interest as polymerisable surfactants in the emulsion polymerisation [77].

After 20-30 min ageing the maleic acid monoester is sulphonated at 75-90 °C by aqueous sodium sulphite (or other salts of sulphurous acid) taken in 0-5 % excess:

$$\underset{\text{(Second step)}}{ROOCCH{=}CHCOOH} + Na_2SO_3 \longrightarrow ROOCCH(SO_3Na)CH_2COONa$$

Water content is adjusted to the total surfactant concentration of 30-42 % wt. The residual sulphite in the product may be oxidised to sulphate. The sulphonation proceeds also well when using partially hydrated crystalline sodium sulphite in a jacketed shear-stress reactor. This process modification is especially appropriate for manufacturing concentrated sulphosuccinate monoesters as flakes or vermicelli (often with plasticisers and fillers added in situ) suitable in mild synthetic soap bars [78]. The $C_{12\text{-}18}$ alcohols (I), ethoxylated (×2-4 mole EO) alcohols (II), and fatty monoethanolamides (III) esters of sulphosuccinic acid, mainly as sodium and alkanolamine salts, are of most practical importance as very mild high-foaming surfactants useful for personal care products and in wool, fur, and leather treatment. Very mild disodium PEG-5 laurylcitrate sulphosuccinate (in combination with sodium lauryl ethersulphate) serve for cosmetics produced by *Witco* as "Rewopol SB CS 50".

The sulphosuccinate monoester surfactants are known as the following commercial products: (I) "Empimin MH/MK" (*Albright & Wilson*), "Rewopol SBF 12" (*Witco*), "Tensuccin" (*ICI*), "Texin 128 P" (*Henkel*), (II) "Anionyx 12 EO" (*Onyx*), "Emery 5320" (*Emery*), "Empicol SDD" (*Albright & Wilson*), "Genapol SBE" (*Clariant*), "Mackanate EL/L-2" (*McIntyre*), "Preparat NMS-243" (*DPO Sintez*), "Rewopol SB FA 30" (*Witco*), "Setacin F/103" (*Zschimmer & Schwarz*), "Surfagene S 30" (*Kao*), "Texapon SB 3" (*Henkel*), (III) "Alconate CPA" (*Witco*), "Emery 5325" (*Emery*), "Mackanate CM-100/CP/OM/UM" (*McIntyre*), "Rewoderm S 1333", "Rewopol SB L 203/SB C 212", "Rewocid SB U 185" (all of *Witco*), and many others.

Dealing with the sulphosuccinate diester synthesis, the esterification procedure is performed very similar to that described above for monoesters but the feed of hydroxyl-bearing material (generally $C_{6\text{-}18}$ alcohols) should be twice more with respect to maleic anhydride. The first step is performed under a gradually increasing temperature to 120-150 °C and with continuous vacuum distillation of water from esterification. At that step esterification catalyst may be used, such as *p*-toluenesulphonic acid or ABSA. The sulphonation with sodium bisulphite proceeds as described above. A representative example of diesters is sodium bis(2-ethylhexyl) sulphosuccinate known as "Aerosol OT" of the formula:

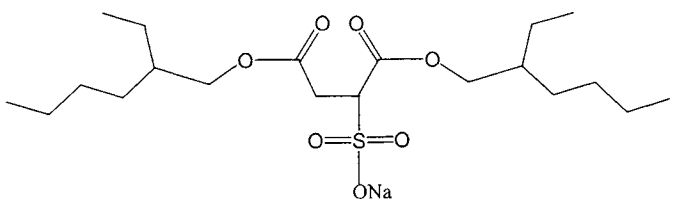

Among conventional hydrocarbon-derived anionics, the diesters rank as an optimal surfactant with respect to surface tension reduction and wetting in aqueous systems. Remarkably, the diesters are soluble in most nonpolar solvents too. At NTP only the short-chain ($\leq C_8$) homologues are able to form micelles in aqueous media. Similarly to monoesters, sulfosuccinate diesters are mild and readily biodegradable surfactants more known as excellent wetting and dispersing agents. Sodium bis(2-ethylhexyl)sulphosuccinate may be exemplified by the set of the following liquid, paste or solid products: "Aerosol OT-B/GPG/75/100" (*American Cyanamid*), "Emcol 4500" (*Witco*), "Empimin OP70/OT/OT75" (*Albright & Wilson*), "Geropon DOS" (*Rhodia*), "Lutensit A-BO" (*BASF*), "Nikkol OTP" (*Nikko*), "Rewopol SB DO" (*Witco*), "Texin DOS 75" (*Henkel*), "Triton GR-5M/7M" (*Rohm & Haas, Union Carbide*), "Triumphnetzer ZSG" (*Zschimmer & Schwarz*). Diesters with longer chains are used in textile industry, froth flotation and extraction of rare earth elements.

Alkylamines of petrochemical, vegetable or tallow origin react with maleic anhydride at a temperature below 100 °C forming maleic monoalkyl- or dialkylamides followed by sulphonation with aqueous sodium bisulphite in the same manner as of maleic esters [10, 79]. The long-chain sulphosuccinamates obtained have enhanced hydrolytical stability (but more expensive) in comparison to sulfosuccinates that offer ample scope for their use in soaps bars, carpet cleaning, textile and wool finishing, and some other specialties.

As accessible and safe sulphonation agents, sulphites are used for a long time in the manufacturing of many other anionic surfactants derived from unsaturated oleochemicals, such as sodium sulphooleate, sulphonated castor ("turkey-red") oil, alkylacetosulphonates, and other sulphonated esters. Concentrated H_2SO_4, oleum, $ClSO_3H$ are more severe agents leading to deeper sulphonation that may have some importance in small-scale productions as well.

More recently $NaHSO_3$ become useful for the ether sulphonate synthesis [22c, 80a]:

$$\underset{\text{Allyl chloride}}{ROH + CH_2{=}CHCH_2Cl} + NaOH \xrightarrow{100\text{-}120\ ^\circ C} \underset{\text{Allyl ether}}{ROCH_2CH{=}CH_2} + NaCl + H_2O$$

$$ROCH_2CH{=}CH_2 + NaHSO_3 \longrightarrow \underset{\text{Sodium ether propanesulphonate}}{ROCH_2CH_2CH_2SO_3Na}$$

where R is $R'(OCH_2CH_2)_m$- or $R''Ph(OCH_2CH_2)_m$-.

In the first step, the allyl ether synthesis occurs either with alkali metal hydroxides and at a pressure < 0.2 MPa, as shown here, or with a preliminary hydroxyl-carrying reagent conversion into the alcoholate followed by refluxing with allyl ether in toluene solution. In the final step other factors may affect the conversion, such as thinning of the reaction mixture and the presence of final products (ether propanesulphonate) seemingly acting as a phase-transfer catalyst. Another root for the ether sulphonate synthesis is known for a long time to be 1,3-propane sultone but it has lesser usage in view of higher prices and carcinogenic properties.

Ether sulphonates are insensitive to Ca^{++} ions and water salinity, they are hydrolytically stable, skin-friendly surfactants that are of interest for tertiary oil recovery, cosmetics and chemical specialities [22c, 80]. Particularly, sodium alkylarylethoxypropanesulphonates were supplied by *Rohm & Haas* as "Triton X-200" and "Triton X-202".

1.3.3. Alcohol sulphates and ether sulphates

The salts of monoesters of sulphuric acid (mainly known as alkyl sulphates, alcohol sulphates or sulphated higher alcohols and ether sulphates or sulphated ethoxylated alcohols) have been proceeded for tens of years through the competition with alkylbenzenesulphonates and other anionic and nonionic surfactants with respect to the consumer's merits and cost performance. Among other surfactants, the today's world consumption share of alcohol sulphates and ether sulphates is ca. 25 % in household and laundry aids and ca. 20 % in personal care products [81]. The formers are mostly based on sulphates of petrochemical origin whereas the least are more oriented to sulphates from oleochemicals.

The preferred hydrophobes for the alkyl sulphate production are the C_{8-20} primary alcohols although reaction of α-olefins yielding secondary alkylsulphates is possible too. Most of the recent alkylsulphates are derived from synthetic alcohols or alcohols of renewable raw materials (for more details see Section 1.2.1). The sulphation of primary alcohols with air- or nitrogen-diluted SO_3 bear a strong resemblance to the sulphonation of LAB. At first, two molecules of SO_3 add rapidly to an alcohol forming metastable monoalkylpyrosulphate [62, 64, 82]:

$ROH + 2SO_3 \longrightarrow ROSO_2OSO_3H$

The alkylpyrosulphate takes the function of a sulphating agent for the second molecule of alcohol (the slower step):

$ROSO_2OSO_3H + ROH \longrightarrow 2ROSO_3H$

It should be avoid to raise the reaction temperature above 35-40 °C (ΔH_R = -150 kJ·mol^{-1}) because side reactions may be significant and deteriorate product's quality. For long-chain (C_{16}+) alcohols the reaction temperature should be somewhat higher than their melting point. The optimal parameters for sulphation of long-chain alcohols is summarised in Table 1.6 [62].

Table 1.6 Optimal parameters for sulphation of long-chain alcohols

Sulphation apparatus	See Table 4
SO_3/ alcohol mole ratio	1.02-1.03
SO_3 concentration, vol. %	3-5
Optimum reaction temperature, °C	30-40 (C_{12-14}) 60-65 (C_{16-18})
Neutralisation step	Just after sulphation

Essentially the same mechanism and parameters are valid in the case of sulphation of alcohol ethoxylates. Among other impurities, 1,4-dioxane may be formed in alkylethoxysulphates when the ethoxylation degree m > 2 [62, 82]. The sulphation of alkylphenol ethoxylates requires a higher SO_3/ ethoxylate ratio due to the accompanying sulphonation into aromatic rings. This sulphonation can be prevented by choosing of proper milder sulphating agent, such as sulphamic acid H_2NSO_3H [61, 82].

Unlike LABs, hydrogen alkylsulphate (and hydrogen alkylethoxysulphate too) is not stable enough to be kept or transported but requires immediate neutralisation. The neutralisation agents, as caustic soda (predominantly), ammonia, MgO, triethanolamine (TEA), and monoethanolamine (MEA), are of most practical importance. The typical reaction equations are as follows:

$ROSO_3H + NaOH \longrightarrow ROSO_3Na + H_2O$

$2R(OCH_2CH_2)_mOSO_3H + MgO \longrightarrow [R(OCH_2CH_2)_mOSO_3]_2Mg + H_2O$

where *m* is generally from 1 to 6 (more often 2-3).

Under neutralisation of the sulphation/sulphonation product of ethoxylated alkylphenols with SO_3, the use of moderately concentrated caustic soda yields sodium sulphate-sulphonates while the desulphation reaction proceeds smoothly when the acids are reacted with concentrated alkali [83].

The resulting conversion of hydroxyl-bearing matter into alkylsulphate and/or ethersulphate is equal and amounts to 94-98 %. It is a function of the initial moisture content, alkyl chain length, carbonyl value, iodine value, EO chain length, free PEG content, and other specification properties. The final product is prepared as a clear viscous aqueous concentrate with pH ~ 9 and 25-30 % or 60-70 % of active matter (for sodium or ammonium salts, respectively). Within this concentration interval highly viscous hexagonal mesophases are formed which should be taken into account under the neutralisation/ dilution operations. The viscosity problem may be overcome using hydrotropes and cosolvents, such as carbitols. The long-chain sodium alkyl sulphates can be subjected to drying for further use in detergent powders or dentifrices.

Another way having major industrial importance as far ten years back is the sulphation of alcohols and ethoxylated alcohols with chlorosulphonic acid. The reaction is best carried out at 25-30 °C in batch or flow reactors according to the equation:

$$ROH + ClSO_3H \longrightarrow ROSO_3H + HCl$$

The reaction yield is nearly quantitative but to make a high-quality product, the heat-transfer characteristics should be carfully regulated. Other problems (corrosion, foaming and high level of chloride as a by-product) are caused by the evolved hydrogen chloride. The sulphoester should be well degassed to minimise the chloride content in the end product [61, 62, 82].

In spite of low conversion, the sulphation with concentrated H_2SO_4 has some advantage in the laboratory synthesis of individual sodium alkylsulphates: unsulphated alcohol is removed readily by continuous Soxhlet extraction whereas Na_2SO_4 is separated by repeated crystallisation.

Sodium or TEA laurylsulphate (I), both of synthetic and coconut sources, is a micelle-forming, high-foaming surfactant that has a great scope of practical applications, particularly in detergents, cleaners, personal care products, "synthetic" fire-fighting foams, and industrial

chemicals. The purified sodium dodecyl sulphate (SDS) is assumed to be one of the most popular anionic surfactants in colloid-chemical and biological studies. SDS is taken as standard in some skin and mucous membrane compatibility studies and all other products are compared with its reference results. Long-chain (C_{16}+) alkylsulphates (II) have deficient solubility in water and they found use in high-temperature detergent compositions and ore flotation. Short-chain alkylsulphates, such as sodium 2-ethyl-hexylsulphate, are used as wetting and etching agents, hydrotropes for aqueous formulations. All alkylsulphates are a weak oral toxicants and moderate-to-severe skin irritants depending on the chain length, counterion and concentration [2, 10, 44, 82]. Alkylsulphates as well as ethersulphates have little environmental impact at any stage in their life cycle [41, 82] and fully break down under normal aerobic conditions [40, 41].

Physicochemical and usage properties of ether sulphates depend on the ethoxylation degree *m*, along with the counterion and carbon chain length. As *m* increases, the colloidal solubility of alkylethoxysulphate in cold water is highly improved. The nature of the counterion is not so critical for ether sulphates as for alkylsulphates: the calcium, strontium and barium salts are even quite well soluble and form micelles in water [84]. The insertion of the EO group between the alkyl and $-SO_4M$ groups gives rise to a strong CMC lowering. The increase of the ethoxylation degree gains mildness. So, combining C_{12-18} alkyl with six (in average) EO units, and magnesium plus sodium as counterions, specialists of *Henkel* designed the ultra-mild and high-foaming product known as "Texapon ASV" that is especially useful as a basic ingredient for the "no more tears" shampoos [45, p. 146]. The most of the ordinary European shampoos, bath and douche products comprise sodium alkyl[ethoxy×(2÷3)]sulphate (II) where alkyl are of vegetable (lauryl, coconut, palm-kernel) or synthetic (even carbon number straight C_{12-14} alcohos) origin. Excellent detergency and foaming in hard water along with personal and environmental safety are among of the most valuable properties of alkylethersulphates. Of some importane are secondary alcohol ethersulphates the stability of which to hydrolysis is much higher than the stability of secondary alkylsulphates.

Commercial alkylsulphates and alkylethersulphates are known as follows: (I) "Elfan 240 S/240T" (*Akzo Nobel*), "Emal 10N/10P-HD" (*Kao*), "Empicol LB40/AL70/AL30/LQ33/LX/ TL40/0758/0775" (*Albright & Wilson*), "Rewopol NLS 28/NLS 90/MLS 30/NEHS 40", "Neopon LAM/LSNF/LTNF" (both series of *Witco*), "Sulfetal

AF/C38/CJOT60/FA40/KT400/MF/TC50/4069/4105/4187" (*Zschimmer & Schwarz*), "Sulfopon 101Spec/1218GF/K35/T55/TP" and "Texapon K12/K1296/ALS/MLS//T42/TH/V/Z/ZHK" (both series of *Henkel*), "Ufarol TCL92/TA40" (*Unger*); (II) "Elfan NS 242/243S/243S Mg/NS 252 S" (*Akzo Nobel*), "Emal 270D" (*Kao*), "Empicol ESA/ESB3/ESB70/ESC70/EAA25/EAB/EAC/BSD/ BSD52/ETB/ETIB90" and "Empimin KSN27KSN70/LSM30" (all of *Albright & Wilson*), "Genapol LRO/ZRO" (*Clariant*, former branch of *Clariant*), "Neodol 25-3S-70E/25-3A-60E" (*Shell*), "Neopon LOA/LOSNF/LOSH/LOS2N70" (*Witco*), "Rhodapex EST30" (*Rhodia*), "Tensagex" (*ICI*), "Texapon ASV70/K14S/N28/N70/ NSO" (*Henkel*), "Ungerol LES3-70/N2-70" (*Unger*), "Zetesol NL/AP/MS/856/2056" (*Zschimmer & Schwarz*).

Monocarboxylic acid PEG monoesters, monoalkanolamides, their ethoxylates, and monoglycerides can be subjected to esterification with SO_3, $ClSO_3H$, or other sulphating agents. For high-melting alkanolamides the joint sulphation with alcohols has being proposed to avoid the product's deterioration [10, 63]. Neutralisation of the hydrogen sulphoesters with proper aqueous alkali leads to mild high-foaming surfactants useful as lime soap dispersants [10, 11, 85] and components of liquid or bar detergents and personal care aids [2, 10, 45, 46]. So, the TEA amidoethersulphate (product "Genapol AMS") created by *Hoehst* in 70th was especially introduced for hair and children's cosmetics. It is characterised by moderate degreasing action, strong foaming, good dermatological and toxicological properties, and some conditioning effect. The major drawback of sulphated glycerides and sulphated PEG monoesters is their hydrolytic decomposition intrinsic for all esters.

1.3.4. Soaps, ether carboxylates and amidocarboxylates

Soaps, the sodium salts of long-chain alkanoic (or carboxylic, or fatty) acids, are the oldest surfactants that were recognized at ancient times, presumably in Egypt. The bar soap was invented later, in the Middle Ages. Now twenty percent of the ca. 90 million tons of oils and fats produced worldwide in 1996 are for technical use in the oleochemistry and feedstuff industry [86]. The target-oriented part of them is cultivated and the other part is used as a by-product of oil and meat industry. The Japanese gather and process extensively discarded cooking oil into soap flakes [87].

Fatty acids, soaps and fatty acid methyl esters are the most extensively used oleochemicals [13]. The free fatty acids are prepared by hydrolysis of oils and fats by alkalis. This procedure named saponification proceeds at high temperature and pressure and leads to crude soaps the acidification of which gives fatty acids. They are subjected to various purification procedures, and finally isolated individually or as mixtures of carboxylic acids of the general formula RCOOH or as soaps RCOOM. The carboxylic acid methyl esters can be produced in two ways: by esterification of the isolated carboxylic acid with methanol or by low-temperature transesterification between fat/oil and methanol. The methyl esters are used for the further synthesis of other oleochemicals and soaps as well. Most of the natural acids are monofunctional and possess straight even-numbered carbon chains. The chain can be aliphatic (acids with R = C_{11-17} are conventionally used as surfactants), olefinic (as in oleic and linoleic acids) or olefinic/aliphatic and hydroxyl-substituted (as in the native or hydrogenated ricinoleic acid) as exemplified below.

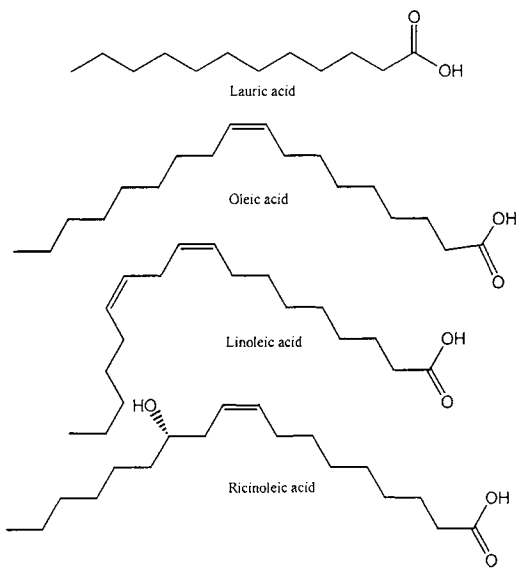

Clay-catalysed oligomerisation of unsaturated acids from oil crops leads to C_{36}-dimer, C_{54}-trimer and C_{18}-monomers. The monomeric fatty acid fraction is subjected to distillation, hydrogenation and following separation into solid stearine and liquid isostearic acids widely used as semifinished items in surfactants and emollients [88].

Long-chain alkanoic acids have a limited use as surfactants. They are very weak acids having a pH range between 5 and 6. They are soluble in most organic solvents but purely soluble in water. Alkali metals and short-chain amines as counterions yield water-soluble soaps which, as a result of hydrolysis, form with free acids the dispersible 1:1 or 1:2 association complexes, so-called "acid soaps".

The personal care industry remains traditionally the largest consumer of soaps: depending on the region, from 50 to 75 % of the total surfactant consumption accounts for soaps [81]. The increase in body shampoo consumption last decades is assumed to alter the soap market slightly. The consumption rate of soap in household and laundry aids is quite modest now and limited essentially by the "old times" detergents, foam-control additives, chlorine-containing alkali cleaners, and metal cutting oils. The sodium salts of rosin acids and wool wax acids are of some importance for technical needs and bar soaps.

Free carboxylic acids and metal soaps (other than alkali metal soaps) are water-insoluble. Along with naphthenates, the metal soaps found use in greases and as gelling agents for hydrocarbons. The zinc salt of undecylenic acid has antimycotic and antiseborrheic action [47]. Lime soap exhibits poor water solubility causing unaesthetic deposits on bath surfaces and hair. The soap deposition in hard water can be prevented by addition of lime soap dispersants (LSD) - surfactants possessing a complex polar end group, such as acyl isethionates, ether sulphates, ether sulphosuccinates, betaine-type ampholytes, ethoxylated nonionics, and many other surfactants and their synergistic mixtures [10, 11, 45, 85, 89]. The brominated olefinic acids and their derivatives are useful as weighting emulsifiers [90]. Some of the biologically and pharmacologically active compounds, such as bile acids and prostaglandines, as well as some of the microbial surfactants are surface-active carboxylic acids too.

Alkylpolyether carboxylates, or simply ether carboxylates, derived from ethoxylated alcohols are mild "cryptoanionic" surfactants of growing importance [80a, 91, 92]:

$$R(OCH_2CH_2)_mO(CH_2)_nCOOM$$

where R is preferably a linear $C_{8\text{-}18}$ alkyl or alkylamidoethyl, M is usually Na^+ or H^+, m = 1-20, and n = 1-2. Ether carboxylates of the same kind and rather similar properties (with the exception of biodegradation) can be derived from ethoxylated alkylphenol.

The modified Williamson synthesis is one of the oldest batch method for the preparation of ether carboxylates:

$$R(OCH_2CH_2)_mOH + NaOH + ClCH_2COONa \xrightarrow[+ H_2O]{60\text{-}90\,^\circ C} R(OCH_2CH_2)_mOCH_2COONa + NaCl$$

The synthesis works with some excess of NaOH and chloroacetic acid or sodium chloroacetate. The ethoxylation grade of nonionics and the water content influence the conversion and reaction rate. Along with NaCl, a certain amount of sodium glycolate and sodium diglycolate $NaOOCCH_2OCH_2COONa$ is formed.

Ether carboxylate of better quality with almost 100 % yield is formed under the mild air oxidation of nonionics under alkaline conditions and Pd/ Pt deposited on charcoal as a catalyst. In this case the ethylene oxide chain is shorten by one unit:

$$R(OCH_2CH_2)_mOH + NaOH + O_2 \xrightarrow{Pd/Pt,\ 40\text{-}100\ ^\circ C} R(OCH_2CH_2)_{m-1}OCH_2COONa + H_2O$$

The oxidation of ethoxylated alkanolamides, ethoxylated alkylphenols and 1,2-alkandiols gives similar results. Other methods of the ether carboxylate synthesis are not of practical relevance. Ether carboxylates are applicable as mild special surfactants for cosmetics, household bleachers, low-to-moderate foaming cleaners and wetting agents. In a wide range ether carboxylates are produced by *Kao* (former *Chem-Y*) under the "Akypo" trade name as well as "Empicol C" of *Albright & Wilson*, "Sandosan/ Sandopan" of *Clariant* and "Surfine WCT" of *Finetex*.

Acylated amino acids are known as anionic surfactants for a long time. Besides ether carboxylates mentioned above, sarcosinates (N-methylgycinates) is the most known type of mild "cryptoanionic" surfactants synthesised by direct reaction between saturated or unsaturated fatty acid halides and sarcosine in aqueous alkali [10, 11, 74]:

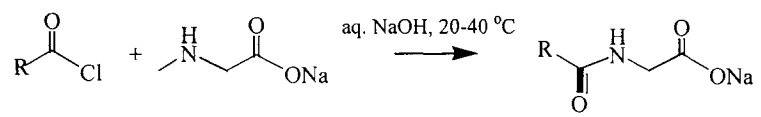

acyl chloride sodium sarcosinate sodium N-acyl sarcosinate

A convenient source of sodium sarcosinate is sodium chloroacetate and methylamine. Before the 2nd World War sarcosinates have been known as "Medialan", useful as textile chemicals with recognised lesser sensitivity (as compared to soaps) to hydrolysis, compatibility with other surfactants, and higher stability in hard water. Some antistatic, lime soap dispersing, bacteriostatic and corrosion-preventive properties are other useful properties of sarcosinates. Sodium N-lauroyl sarcosinate show moderate compatibility with a range of cationic

quaternaries. Use of sarcosinates is limited now mainly to cosmetics and toiletries [22c]. Sarcosinates are known under the following trade names: "Crodasinic LS/OS" (*Croda*), "Hamposyl C/L/M/O" (*Hampshire*, now a subsidiary of *Dow Chemical*), "Korantin SH" (*BASF*), "Medialan LD" (*Clariant*), "Nikko Sarcosinate CN/LN/MN/OH/PN" (*Nikko*).

Among other acylated amino acids, N-acylglutamates and N-acyl-N-alkylalanates have some importance, particularly in Japan [93], for the same purpose. Acylglutamates provide a soft feel to the skin, in consequence of their usage they are restricted to personal care preparations. Their sodium and TEA salts are readily soluble and foam well in hard water. Acylated amino acids possess better resistance to hydrolysis than acylated hydroxyacids. Sodium salts of another N-acyl amino acids, such as aspartates and leucinates, are less available or, as glycinates and lysinates, exhibit low solubility and bad usage properties in water [93c].

1.3.5. Phosphorous-containing anionic surfactants

Phosphate esters are usually prepared from fatty alcohols (I), alkoxylated alcohols and alkyl phenols (II). The first two have good biodegradability, whereas all phosphate esters are compatible with skin and show resistance to alkaline hydrolysis and oxidisers, such as hypochlorite. Their chemistry bears much resemblance to the chemistry of sulphate esters but resulting products are more diverse in the first case because: i) the three-basic nature of orthophosphoric acid H_3PO_4 that can give mono-, di- and triesters, and ii) the phosphoric acid polymorphism leading to esters of polyphosporic acids ($H_{n+2}P_nO_{3n+1}$ where $n > 1$). Phosphoric anhydride P_4O_{10}, phosphoryl chloride $POCl_3$, orthophosphoric acid and polyphosporic acids can be used for the phosphorylation. The reaction conditions are generally selected to maximise the monoester phosphate yield:

$$4\ R(OCH_2CH_2)_mOH + P_4O_{10} + H_2O \xrightarrow{20\text{-}60\ ^\circ C} R(OCH_2CH_2)_mOPO(OH)_2 \xrightarrow{+\ aq.NaOH} 4\ R(OCH_2CH_2)_mOPONa_2$$

In practice commercial surfactants include usually monoesters, diesters, free (ethoxylated) alcohols and other minor by-products. Using polyphosphoric acids as phosphating agents gives high-purity monoesters that have good foamability and negligible skin damage in the neutral pH range. TEA alkyl phosphates have better solubility in water as compared with sodium and

ammonium alkyl phosphates. The solubility and other properties can be widely controlled by a proper counter-ion selection, the length and kind of the hydrophobe or alkylene oxide chain. To maximise the dialkyl hydrogen phosphate formation, $POCl_3$ is preferred as phosphating agent. Temperature and water control, reagent ratio and minor additives as well can affect the properties of the final products [10, 11, 22b, 94-96].

Phosphate esters are special surfactants with multiple functions. Depending on the structure, they are dispersants, emulsifiers, hydrotropes and solubilisers, foam regulators, antistatics, corrosion inhibitors, wetting agents, reagents for actinides and lanthanides extraction, flotation reagents, inhibitors of scale deposition and crystallisation. Trade names of some phosphate esters are: (I) "Arlatone MAP" series of monoalkylphosphates (*Uniqema*), "Emcol CS/PS/TS" (*Witco*), "Empiphos TM" (*Albright & Wilson*), "Hostaphat F" series, "Flotinor SM15" (*Clariant*), "Marlophor" series (*Condea*); (II) "Celanol PS", "Soprophor PA/PS" series, "Rhodafac PC-100" (all of *Rhodia*), "Crodafos N-3/10" (*Croda*), "Empiphos DF" series (*Albright & Wilson*), "Forlanit P", "Forlanon" and "Crafol AP 261" (all of *Henkel*), "Phosfetal" series (*Zschimmer & Schwarz*).

Derivatives of phosphonic acid and phosphorous acid are of marginal importance as special P-containing anionics. Their chemistry, along with phosphates, was reviewed comprehensively by Wasow [96].

1.4. Cationic Surfactants

A surfactant is classified as cationic if its molecule can dissociate in solution forming a surface-active cation and normal anion. According to the chemical structure, cationic surfactants are subdivided into the following main classes: alkyl amines, ethoxylated amines, alkyl imidazolines, and quaternaries. Cationic surfactants do not generally provide effective cleaning and therefore, they are not used in general-purpose detergents. Nevertheless, experience over the last decades suggests that cationic surfactants may take part in soil removal when formulated with nonionic, amphoteric and cryptoanionic surfactants [45, 46, 97-100]. Thus, "two-in-one" shampoos and special "softergents" with cationics appeared relatively recently. More convenient applications of cationic surfactants are concerned with their germicidal, hydrophobisation and antistatic effects. Typical examples of cationics uses are: bactericides,

fungicides, herbicides, textile auxiliaries, fabric softeners, hair conditioners, antistatics, corrosion inhibitors, anticaking agents in fertilisers, flotation agents, adhesion promoters and dispersants for mineral fillers in hydrocarbons. Quaternaries account for ca. 90 % of the total cationics production. Some cationic surfactants serve as source materials for other surfactant synthesis.

1.4.1. Alkyl amines and ethoxylated amines

Primary amines and their salts are derived from natural fats and oils through fatty acids, acid amides and acid nitriles as intermediates:

$$RCOOH + NH_3 \xrightarrow[(-H_2O)]{>150\ ^\circ C} RCONH_2 \xrightarrow[(-H_2O)]{280\text{-}350\ ^\circ C} RCN + H_2 \xrightarrow{Ni\ (Raney),\ 120\text{-}150\ ^\circ C} RCH_2NH_2$$

All reactions are reversible and proceed at high temperatures and pressures. In fact the reactions run a multistep course with formation of a range of by-products, particularly dialkyl (secondary) amines. Addition of ammonia in the last stage would suppress the formation of secondary amines.

Amines can be produced by the catalytic reaction between ammonia and long-chain alcohols or alkyl chlorides at 100-400 °C and P = 130-180 at. The product has quite a complex composition and contains mono-, di-, and trialkylamines as well as quaternary ammonium compounds [101, 102].

There are some other opportunities for the synthesis of primary amines, such as the reaction between an alkyl halides and hexametylene tetramine:

$$RX + (CH_2)_6N_4 \longrightarrow R[(CH_2)_6N_4^+]X^- \xrightarrow{Hydrolysis} RNH_2 + NH_3 + HCHO$$

Acyl chlorides react with ethylenediamine and polyamines forming acylated polyamines that can be used in further syntheses. Just as ethylene oxide is added to alkyl amine, so ethyleneimine is added to it in the presence of $AlCl_3$ or other Lewis acids to produce polyamines. Polyamines can be prepared also by the reaction of alkyl amine with acrylonitrile with a subsequent catalytic hydrogenation.

Diamines with interesting properties can be derived from α-olefins through epoxidation [103]:

$$R\text{–}CH{=}CH_2 \xrightarrow{\text{Peroxide}} R\text{-}CH\text{-}CH_2 + NH_2CH_2CH_2NH_2 \longrightarrow R\underset{\displaystyle OH}{\underset{|}{C}}HCH_2NHCH_2CH_2NH_2$$

Aliphatic amines and polyamines are bases nearly as weak as ammonia. Alkyl amine hydrochlorides are used rarely now in view of the recognised toxicity. They are known in free or salt form as corrosion inhibitors, flotation collectors and adhesion promoters for asphalt coatings. Acylated polyamines are of interest for the amphoteric biocide synthesis.

Ethylene oxide adds easlily to an alkyl amine without catalyst forming alkyl diethanol amines or ethoxylated alkyl amines as mentioned previously (pseudocationic nonionics as discussed in Sec. 1.2.6). Primary amine and acylated polyamine ethoxylation brings forth milder and low-toxic surfactants.

The direct reaction of long-chain carboxylic acids and ethylenediamine or polyamines catalysed by sulphuric or toluenesulphonic acid gives a mixture of amidoamine, diamide and imidazoline-type compounds of the formula:

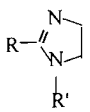

where R' = H, alkyl, 2-hydroxyalkyl or polyamine

The reaction conditions can be selected to maximise the formation of imidazoline cationics quaternised derivatives of which have some importance as cationic fabric softeners [22c, 98, 99, 102]. Surface-active tertiary amines can be formed from alkyl chlorides, acyl chlorides or fatty esters as can be illustrated by the following reactions:

$$RCl + HN(CH_3)_2 \longrightarrow RN(CH_3)_2 \cdot HCl$$

$$RCOCH_3 + H_2NCH_2CH_2CH_2N(CH_3)_2 \xrightarrow{\text{-MeOH}} RCONHCH_2CH_2CH_2N(CH_3)_2$$

Reductive alkylation of nitrile by secondary amines having the same or different alkyl chains is another alternative for tertiary amine preparation. Many other special cationics, N-alkyl monoaza crown ethers [53], for example, can be classified as tertiary amines. The surface-active tertiary amine compounds are used as such (as corrosion inhibitors, dopes, antistatics, reagents in mineral processing) or as semifinished products. Alkyldimethylamines and dialkylmethylamines were run on a commercial level, e.g., by *Albemarle* (former *Ethyl Corp.*) as "ADMA Tertiary Amines" and "DAMA Tertiary Amines", respectively.

1.4.2. Quaternary aliphatic compounds

Quaternary ammonium compounds, or simply “quaternaries” or "quats", are assumed to be the most diverse class of cationic surfactants. They contain at least one nitrogen atom that is covalently bonded to four alkyl or aryl substituents. Quaternaries may be stucturally subdivided into: two kinds of tetraalkyl derivatives (with one long-chain alkyl and two ones), compounds having mixed short-chain N-substituents (methyl, ethyl, hydroxyethyl, benzyl, halide-substituted benzyl, and so on), heterocyclic compounds, *bis*quaternary ammonium compounds or polyquaternaries in a wide sense. "Destractible" quaternaries can be now highlighted as well in which long chains are interrupted by hydrolyzed, often ester, ketal or amide, group.

The most convenient way of a quat synthesis consists in the exhaustive methylation using primary or secondary fatty amines and methyl chloride to yield $RN^+(CH_3)_3Cl^-$ (I) and $R_2N^+(CH_3)_2Cl^-$ (II), respectively [101, 102]. In order to enhance the quat yield the reaction is carried out in an aqueous or alcoholic solution of sodium carbonate at 60-95 °C. Tertiary amine quaternisation with benzyl chloride gives benzylalkyldimethylammonium, or "benzalkonium", chloride (III):

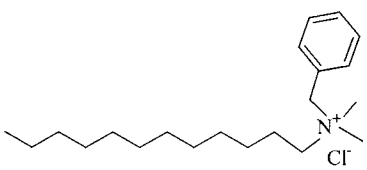

Benzyldodecyldimethylammonium chloride

Instead of alkyl halides, methyl or ethyl sulphate is often taken advantage as an alkylation agent, e.g.:

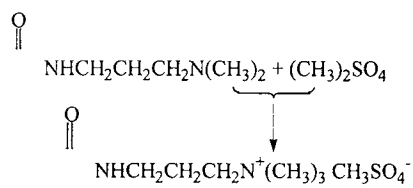

Undecenoyl-1-aminopropyl-3-trismethylammonium methosulphate

Probably, the oldest source of surface-active quaternaries with biocidal, hair-conditioning and textile-softening properties is the reaction between alkyl halide and trimethylamine:

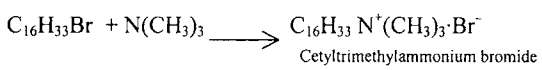

Cetyltrimethylammonium bromide

Commercial long-chain alkyl quaternaries having one alkyl chain C_{12}-C_{18} are recognised fungicides and bactericides, especially for gram-positive bacteria [101, 104]. Their germicidal activity differs widely with the alkyl chain length, chain saturation, length and nature of short-chain substituents, and the nature of the counterion. Benzylalkyldimethylammonium salts (alkyl is C_{12}-C_{14}) exhibit strong germicidal and fungicidal effects, so that these are widely used, especially as medicinal antiseptics. Additional modification of the antimicrobial action can be achieved by chlorine or other halide substitution into the phenyl ring. All quats are used as special surfactants, emusifiers and foaming agents stable in a wide pH range.

They are inactivated by most of the anionic surfactants and polyelectrolytes forming insoluble salts. Among quats having improved compatibility with anionic surfactants are: acylated (cocoyl, behenoyl, oleoyl, ...) N-oligo(ethylene glycol or propylene glycol) "trimonium" methosulphates or halides (IV), alkylamido- or alkenylamidopropyltrimonium sulphates/halides (V), related derivatives of lanoloin carboxylic acids [102, 105], quaternised ethoxylated fatty amines (VI), iso-octylphenoxyethoxy-2-ethyldimethybenzylammonium chloride ("benzethonium" chloride), and quaternised condensation products based on protein hydrolysates (VII). Note that the last products show excellent conditioning properties, compatibility and mildness with sodium lauryl ether sulphate in shampoos for daily use, in shower and foam bath preparations [106]. Most nonionics act as quats inactivators also in view of the mixed micelle formation and lowering of their effective monomer concentration. Nevertheless, synergism in germicidal action between quats and nonionic surfactants occurs sometimes in a narrow concentration range [45, 104].

Remarkable germicidal properties show C_8-C_{10}-dialkyldimethylammonium salts whereas distearyldimethylammonium salts and the similar products are high-volume cationics with pronounced conditioning and antistatic action. Amphiphiles with two moieties joined together by methylene or other spacer groups are named dimeric or "gemini" surfactants, in particular *bis* quats [107] showing original properties. As a rule the quats with two long chains are characterised by a vesicular-type aggregation in water. More than other quats, *bis*quaternaries and

diamidoamine quaternaries have affinity towards negatively charged materials, such as glass, cotton, polyester, wool and hair.

The new quats generation presents readily biodegradable surfactants the long chains of which are interrupted by ester groups, thus named "esterquats" [102, 108]. Esterquats are derived frequently from the diester of triethanolamines and the partially hydrogenated tallow or oleic acid followed by a diester quaternisation. The final product, N-methyl-N,N-di[2-(C_{16-18}-acyloxy)-ethyl]-N-(2-hydroxyethyl)ammonium methosulphate (VIII), of the formula

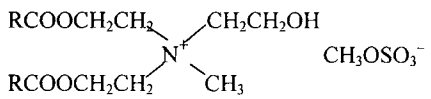

has decent fabric softening, hair conditioning, antistatic and anticorrosive properties [22, 99, 108].

The commercial quaternary ammonium compounds are: (I) "Arquad 16-50/18-50/MC-50/C-35/S-50/T-50/HT-50" (*Akzo*), "Atlas G-263/265/271" and 'Synprolam 35TMMQC/35TMQS" (*ICI*), "Empigen CM" (*Albright & Wilson*), "Incroquat CTC-30" and "Incroquat Behenyl TMC" (*Croda*), "Cetrimide BP" (*Rhodia*), "Dehyquart A" (*Henkel*), "Dodigen 55/1383/1383/2544/5594" (*Clariant*), "Quartamin 24P/86P/60L/ CPR/TPR" (*Kao*); (II) "Adogen 432CG/442/462", "Varisoft 432CG/TA" (*Witco*), "Ammonyx D34" (*Stepan*), "Arquad NF-50/2C-75/HC/2T-70/2HT-75/88" (*Akzo*), "Dodigen 1490", "Genamin DSAC" and "Präpagen WK/WKT/3445" (*Clariant*), "Quartamin DCP" (*Kao*), "Rhodaquat WR" (*Rhodia*), "Synprolam FS" (*ICI*); (III): "Ammonyx 4/4B/485/4002/KP" (*Stepan*), "Arquad B-50/DMHTB-75/DMMCB-50" (*Akzo*), "BEQ/BQ Quats" (*Albemarle*), "Dehyquart LDB 50" (*Henkel*), "Empigen BAC/BCM/BCB50" (*Albright & Wilson*), "Hyamine 2389/3500" (*Rohm & Haas*), "Protectol KLC 50" (*BASF*), "Tetranyl B-C-80L" (*Kao*), "Varisoft SDC" (*Witco*); (IV): "Akypoquat 131/132" (*Kao*), "Emcol CC9", "Rewoquat CPEM" (*Witco*), "Synprolam 35DMBQC" (*ICI*); (V): "Incroquat BES-35S/BA-85" (*Croda*), "Rewoquat RTM 50" and "Rewocid UTM 185" (*Witco*), "Tetranyl U" (*Kao*); (VI): "Ethoquad C/25' and "Ethoquad HT/25" (*Akzo*), "Dehyquart SP" (*Henkel*); (VII): "Croquat HH/L/M/S/WKP" and "Crosilkquat" - the whole range of *Croda,* "Lamequat L" and "Gluadin WQ" of *Henkel*; (VIII): "Ammonyx GA-70/90", "Stepanex UK-90/UR-90/GE-90/HR-100" (all of *Stepan*), "Dehyquart

AU 36/46/56" and the mix of the conditioning agent and fatty alcohol "Dehyquart F 75" (*Henkel*), "Rewoquat WE 18/20/28" (*Witco*), "Tetranyl AT 7590/CO 40/L190" (*Kao*).

*Bis*quaternary ammonium compounds can be exemplified by "Duoquad T-50" (N,N,N',N',N'-pentamethyl-N-tallow-1,3-propane diammonium chloride) of *Akzo* production. One- or two-chain guanido derivatives and quats based on amino acids, such as lysine and arginine, may have potential value as mild natural skin and hair conditioners. Polysiloxane with reactive alkyl halide or epoxy functional substituents can be converted by the reaction with tertiary amines or amine-containing spasers into cationic organosiloxanes. According to the *CTFA* nomenclature, such a product is known as "Quaternium-80" and commercialised by *Goldschmidt* (products "Abil Quat 3270/3272/3474"), *Uniqema* ("Monasil PDM/PLN"), *Dow Corning* and *GE*. The quaternised and tertiary amine modified silicones show excellent hair conditioning after shampooing (gloss, wet and dry combability, easy styling, resistance to charge build-up) and pleasant feeling after shower [21, 109].

1.4.3. Alkyl imidazolines and other heterocyclic cationics

Heterocyclic quats are discerned as unsaturated quaternary ammonium salts and saturated (non-aromatic) quaternary ammonium salts. Their chemistry reviewed comprehensively in the books [101, 102a] is very abundant. General feature of these cationics is that the nitrogen atom carrying the positive charge is part of a heterocyclic ring. The approaches for the synthesis of heterocyclic quats are essentially the same as for their straight-chain analogues.

Most unsaturated ring quats of industrial importance are alkylpyridinium halides (I) and substituted imidazolinium compounds (II). To prepare alkylpyridinium halide, pyridine is reacted with the equimolar amounts of alkyl halide for several hours at 100-150 °C without solvent according the reactions given above. The reaction is two orders slower in this case because the basicity of pyridine is much weaker in comparison with aliphatic tertiary amines and heterocyclic aliphatic amines, such as N-alkylpiperidine and N-alkylmorpholine, too. Typical examples of the aromatic quaternaries are given below:

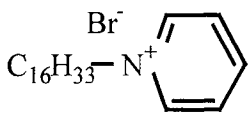

N-cetylpyridinium bromide

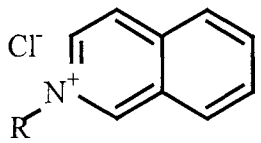

N-alkylisoquinolinium chloride

Instead of alkyl halide, short-chain dialkylsulphate can be refluxed with imidazolinium to produce quaternary imidazolinium compound [52, 101, 102a] such as shown below:

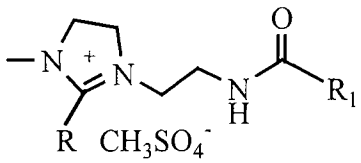

1-methyl-2-alkyl-3-(2-acylaminoethyl)imidazolynium methosulphate
were R and R_1 are hydrated tallow, soya or oleic residues

The surfactants in which the second long chain R' is interrupted by the ester or amido group show better biodegradability. Alkylethylmorpholinium ethosulphate (e.g., "Forestall" cationic series, were alkyl = tallow or soy) is used as water-soluble conditioning agent compatible with some anionic surfactants. Other heterocyclic compounds have not so much practical importance. The heterocyclic quaternaries are used as antistatics, fabric softeners, antimicrobial agents and corrosion inhibitors.

Products of industrial importance are: (I) alkylpyridinium halides known, e.g., as "Dehyquart C/D" of *Henkel* and "Emcol E 607S" of *Witco*; (II) "Accosoft 808/808HT" of *Stepan*, "Ammonyx 4080" of *Onyx*, "Rewoquat W75/W90" and "Varisoft K-75/455/475/3690" series of *Witco*.

Cationic non-nitrogeneous surfactants may be synthesized essentially in the same way as the nitrogeneous compounds. So, tertiary long-chain phosphines or arsines are quaternised with conventional alkylating agents, such as alkyl halides or alkyl sulphates [101, 102]. However, heterogeneous chain compounds other than N-containing ones are not so beneficial especially from an economical viewpoint.

1.5. Amphoteric and Zwitterionic Surfactants

An amphiphilic compound is named amphoteric surfactant if its functional group is capable of carrying both anionic and cationic charges. The term "amphoteric surfactants" or

"amphoterics" is referred generally to compounds that show pH-dependent amphoteric properties. This behaviour can be represented schematically as follows:

$$A^- \overset{+}{R}NH_2CH_2CH_2COOH \underset{H^+}{\overset{OH^-}{\rightleftharpoons}} \overset{+}{R}NH_2CH_2CH_2COO^- \underset{H^+}{\overset{OH^-}{\rightleftharpoons}} RNHCH_2CH_2COO^- \; M^+$$

Acid range (cationic properties) — Isoelectric range — Alkaline range (anionic properties)

In these structures A^- and M^+ are some kind of anions (e.g. Cl^-) and cations (e.g. Na^+).

However, there are amphiphiles containing both strongly acidic and strongly basic groups, such as the sulphonic group and quaternary ammonium group, respectively. Those amphiphiles show both anionic and cationic properties independent of the pH and they were specified as zwitter-ionic surfactants. There is a great scope for the synthesis of amphoteric and zwitter-ionic surfactants [74, 111-113], although these compounds represent less than 2 % of the world surfactant market. In order to simplify matters this type of surfactants is called "amphoterics". The majority of useful amphoterics can be subdivided into two classes: N-alkyl amino acids and N-acyl amino acids, all kinds of betaines.

1.5.1. N-Alkyl amino acids, acyl amino acids and protein-derived amphoterics

In the middle of the 20th century carboxymethylated fatty (poly)amine derivatives gain currency as relatively mild germicidal surfactants [56, 57, 103]. They are derived from linear amines, such as the alkylamidoethylenediamine, and sodium chloroacetate, as presented below:

Other alkylating agents able to convert into an anionically charged group may be: ethyl

$$RNHCH_2CH_2NHCH_2CH_2NH_2 + 2ClCH_2COONa \xrightarrow{OH^-} RNHCH_2CH_2\overset{CH_2COONa}{\overset{|}{N}}HCH_2CH_2NHCH_2COONa$$

N-$C_{10\text{-}18}$-alkyldiethylenetriamine — Disodium N-$C_{10\text{-}18}$-alkyldiethylenetriamine-N',N''-diacetate

acrylate, acrylic acid, sodium salt of 1-chloroethane-2-sulphonic acid, epichlorohydrin, acrylonitrile, vinyl chloride, 1,3-propane sultone.

For a long time some amphoterics in this group, particularly derivatives of fatty acids and aminoethylethanolamines (NH_2-CH_2CH_2-NH-CH_2CH_2OH), were treated as heterocyclic derivatives of imidazoline but they hydrolyse as a rule during alkylation. The alkylation with sodium chloroacetate or ethyl acrylate gives rise to the opening of the imidazoline ring and the

formation of secondary/tertiary amines and ether carboxylates. Typical chemical structures and their *INCI* nomenclature are listed below. As one can see, some of the compounds may contain betaine-like quaternised structures. This group of mild surfactants is supplied as salts or as free acids. Recent N-acyl amino mono-, di-... polyglycinates, β-aminopropionates and β-iminodipropionates are produced from essentially natural oils (coconut, rape, tallow, oleic, etc.). When applications dictate low salt contents, the amphoterics may be purified by redissolution, ion exchange or electrodialysis. Salt-free products are marked by the abbreviation "SF", "KSF" or "KE" (Keine Salze/ Elektrolyte). The surfactant ranges, such as "Ampholak" of *Akzo*, "Amphotensid" of *Zschimmer & Schwarz*, "Betadet" of *Kao*, "Deriphat" of *Henkel*, "Empigen CD" of *Albright & Wilson*, "Incromate" of *Croda*, "Miranol" and "Mirataine" of *Rhodia*, "Rewoterics" of *Witco*, "Librateric" of *Libra*, present the extremely mild imidazoline-derived amphoterics. Many show antistatic, ion-sequestering and deodorising properties.

Salts of alkylated ω-aminocarboxylic acids are the group of amphoteric surfactants that loose step by step their practical importance. Depending on starting material and reaction conditions, the condensation products present alkylated β-aminoacetate, β-aminopropionate or β-iminodiacetate/ dipropionate. Surfactants having more than one-two CH_2 spacers in the head group are not produced and only a few of them exhibit the structures analogous to those of the derivatives from natural α-amino acids. The foaming, emulsifying, cleansing and antistatic abilities, substantivity to hair and mildness are highly dependent on the balance of amino and carboxylic groups and on the pH.

Amphoterics with repeated amino and carboxylic groups show decent binding of polyvalent cations, such as NTA and EDTA. Relative chelating surfactants can be prepared by modifying the ethylenediamine/ chloroacetic acid reaction product with halogenated higher fatty acids, primary amines, alkyl halides or fatty alcohols [111, 114]. Combining a chelation functionality and a surfactant in a single "chelactant" molecule is advantageous in detergents, other decontamination aids, chemical analysis and medicine.

Condensation products of fatty acid halides and protein hydrolysates are produced now in a wide range as secondary surfactants for the same needs. They may be modified additionally by quaternisation to gain more cationic nature as mentioned in the previous paragraph. The number of amino acids attached varies over a wide range whereas their morphological state

depends on the source of hydrolised polypeptides. Their specific ratios are crucial for the identification of the protein and its origin. The sources of particular importance are animal proteins (collagen, elastin, keratin, casein, albumins), bacterial proteins and vegetable ones (corn, wheat, soybean, tannery proteins).

Table 1.7 Commercially prominent imidazoline-derived amphoterics [111]
R represents the residue of coconut fatty acids

Predominant structure	INCI/CTFA Designation*)
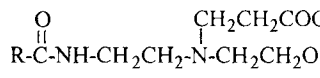	Sodium Cocoampho-propionate
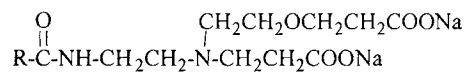	Disodium Cocoampho-carboxypropionate
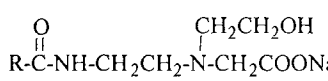	Sodium Cocoampho-(mono)acetate (or Glycinate)
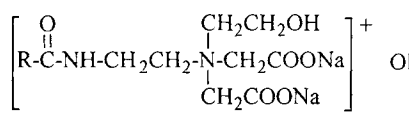	Disodium Cocoampho-carboxyglycinate (diacetate)
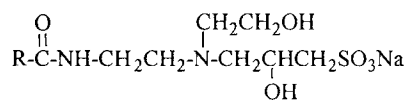	Sodium Cocoampho-hydroxypropyl Sulphonate
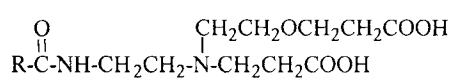	Cocoamphocarboxy-propionic Acid

*) The abbrevation "INCI" stands for International Nomenclature of Cosmetic Ingredients and was adopted as a truly international approach;the CTFA (Cosmetics, Toiletries and Fragrance Association) designation has essentialy the same meaning for USA and Canada.

Most proteins as such are water-soluble or soluble in aqueous media of moderate ionic strength, while some are insoluble under normal conditions or lose solubility due to denaturation by heating or polyvalent cation binding [115]. Soluble proteins exhibit moderate surface activity, i.e. adsorb at extremely low bulk concentrations but decrease the surface tension typically by about 20 mN/m. Emulsifying and foaming properties are highly dependent on the protein structure, pH and the composition of the solution. They give rise to stable foams that remain very persistent as the water lost proceeds in view of drainage and evaporation. So, denaturated collagen (gelatin), whose isoelectric point lies between pH 4.75 and 5.0, produces under shaking the most copious foam in the pH range 5.0-8.5 [116].

Table 1.8 Commercial protein derivatives of *Henkel* [117]

Trade name	Chemical name	Active substance %	Function/ application
Collagen hydrolysates (INCI/ CTFA: Hydrolyzed Collagen)			
Nutrilan H	Partial (low-iron) protein hydrolysate	35-36	Improves hair quality, the skin and mucous membrane compatibility. Surfactant preparations, cold waves
Nutrilan I/I-50/I Powder	Partial collagen hydrolysate pH 4.0-5.0	38-40, 50-52 and 94-97	Care additive in surfactant preparations, hair after-treatment aids and after-sun preparations
Nutrilan L/ L-Powder	Partial collagen hydrolysate pH 5.5-6.5	35-36 and 94-97	
Condensates of fatty acids and collagen hydrolysates			
Lamepon LPO/ LPO-Powder	Protein oleic acid condensate (Oleoyl Hydrolyzed Collagen)	30-32 min. 97	Alcohol- and oil-soluble, film-forming properties. Decorative and skin care cosmetic preparations
Lamepon S/ S-TR and Lamepon ST 40	Protein coconut-fatty acid condensate, potassium and TEA salts	31.5-32.5 39.5-40.5	Very mild secondary surfactants in cosmetic skin cleansing preparations
Lamepon PA-K/ PA-TR	Condensate with abietic acid, potassium and TEA salts	30-32	Retards refatting on scalp. Shampoos for oily hair, hair aftertreatment preparations
Lamepon UD	Protein undecylenic acid condensate, potass. salt (Potassium Undecylenoyl Hydrolyzed Collagen)	31.5-32.5	In combination with active agents to support anti-dandruff action through mild fungicidal effect of the undecylenic acid
Other protein hydrolysates			
Nutrilan Keratin W and Nutrilan Cashmere W	Keratin hydrolysates (Hydrolysed Keratin)	ca. 20	Strengthening and nutrition of natural keratine structure. Cysteine-rich additive in skin and hair care preparations and decorative cosmetics
Nutrilan Elastin E 20 and Nutrilan Elastin P	Elastin hydrolysates (Hydrolyzed Elastin)	30-32 min.94	Provides elasticity of cutaneous tissue. Skin and hair care preparations
Gluadin AGP	Partial wheat protein hydrolysate (Hydrolysed Wheat Protein and Hydrolysed Wheat Gluten)	min. 94	Active ingredient, care and protective additive. Emulsions and surfactant preparations
Gluadin Almond	Partial protein hydrolysate from almond (Hydrolysed Sweet Almond Protein)	ca 20	Active ingredient, additive. Emulsions and surfactant preparations, additive for alcoholic/ aqueous preparations
Gluadin R	Partial protein hydrolysate from rice and vegetables	ca 20	Improves hair quality, skin and mucous membrane compatibility. Surfactant preparations, hair care products and emulsions
Gluadin W 20 and Gluadin W 40	Wheat protein hydrolysate and hydrolysed wheat gluten	min. 20 min. 40	Care additive, active ingredient. Surfactant preparations, hair care products and emulsions
Gluadin WK	Wheat protein/ coco fatty acid condensate, sodium salt	ca. 30	Very mild surfactant for shampoos, shower and bath preparations, particularly for babies and children

A general property of collagen and other water-soluble proteins consists in protecting the skin from the harsh effects of various detergents [45, 46]. Solution and consumer characteristics of the protein hydrolysate depend on the kind, time and temperature of hydrolysis. Leather scraps, feathers and fish skillets can be autoclaved with caustic lime for 1-5 hrs at 110-130 °C in the presence of water or steam followed by neutralisation of the product with acid. Traditionally protein foams are used in fire-fighting, civil engineering and food industry. In cosmetics protein derivatives are usually combined with alkyl ether sulphates and other anionics providing foam creaminess, conditioning effects to hair, eye and skin compatibility. Renewed interest in protein-based surfactants is attributed to their role in protein-bearing waste disposal and utilisation of industrial by-products. Microbial proteins and amino acids serve as another promising source for the production of amphoteric surfactants [31-33, 93b, 109, 117]. Encountered N-acylated proteins may be exemplified by some lipoproteins, such as surfactin [32].

The "Crotein" and "Nutrilan" products present the wide scope of animal protein hydrolysates produced by *Croda* and *Henkel,* respectively, for cosmetic use. Preserved protein hydrolysates, protein condensation products and special protein products of the *Chemische Fabrik Grünau* (*Henkel Group*) compiled from [106] are presented in Table 1.8.

1.5.2. Carboxybetaines and other betaine-type surfactants

Betaine-type surfactants do not show anionic character in alkaline solutions or reduced water solubility close to the isoelectric point as other amphoterics do. These surface-active betaines generally exhibit excellent solubility in water and compatibility with anionics over a wide pH range. So, the betaines are often specified as zwitter-ionic surfactants.
The oldest and most convenient synthesis of betaine-type amphiphiles is the quaternisation of higher tertiary amines with aqueous sodium chloroacetate at 70-90 °C [74, 111]:

$$RN(CH_3)_2 + ClCH_2COONa \longrightarrow R\overset{+}{N}(CH_3)_2CH_2COO^- + NaCl$$

To produce related betaine structures the ammonium can be replaced by phosphonium (III) or sulphonium (II) as illustrated below:

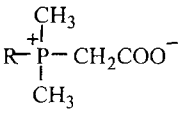

Phosphoniocarboxybetaine

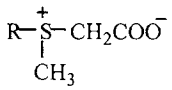

Sulphoniocarboxybetaine

As long-chain intermediates fatty acids are often advantageously used, their methyl esters or triglyceride followed by a conversion into the acid aminoamide using dimethylaminopropylamine and further into the carboxybetaine:

$$RCOOH + NH_2CH_2CH_2CH_2N(CH_3)_2 \rightarrow RCONHCH_2CH_2CH_2N(CH_3)_2 + H_2O$$

$$RCONHCH_2CH_2CH_2N(CH_3)_2 + ClCH_2COONa \rightarrow RCONHCH_2CH_2CH_2N(CH_3)_2CH_2COO^- + NaCl$$

Here the alkyl part originates generally of coconut or tallow fatty acids. If methyl fatty acids or glycerides are the precursors, the liberated methanol is separated whereas glycerol is generally retained in the final product. Similar betainic structures, along with imidazoline-type amphoterics, occur as condensation products of fatty imidazolines and chloroacetic acid, as mentioned above.

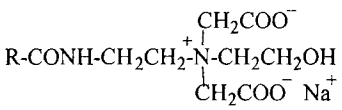

Surface-active betaines can be synthesized also by quaternisation of long-chain tertiary amines with acrylic acid or β-propiolactone and from partially acylated dibasic amino acids and alkyl halides.

As 30-50 % active matter concentrates, laurylcarboxybetaine (I) and cocoamidopropyl-carboxybetaine (II) are offered widely as secondary or first surfactants in personal care, household and drycleaning formulations. Carboxybetaines are used as intermediaries for anionics and cationic constituents in conditioning and hair-colouring shampoos and in "softergents". They exhibit excellent foaming, mildness, antielectrostatic performance, proper cleansing and insensitivity to water hardness. As it follows from their biocidal activity [74, 118], carboxybetaines show dominating cationic character.

Similar to the carboxybetaines, sulphobetaines and sulphatobetaines belong to mild zwitter-ionic surfactants. Two main synthetic approaches for the production of sulphobetaines are

carried out: quaternisation of long-chain tertiary amine with ω-halogenated sodium C_{2-3}-alkanesulphonate or 1,3-propane sultone; modification of quaternary compound by proper sulphonating agent as seen below.

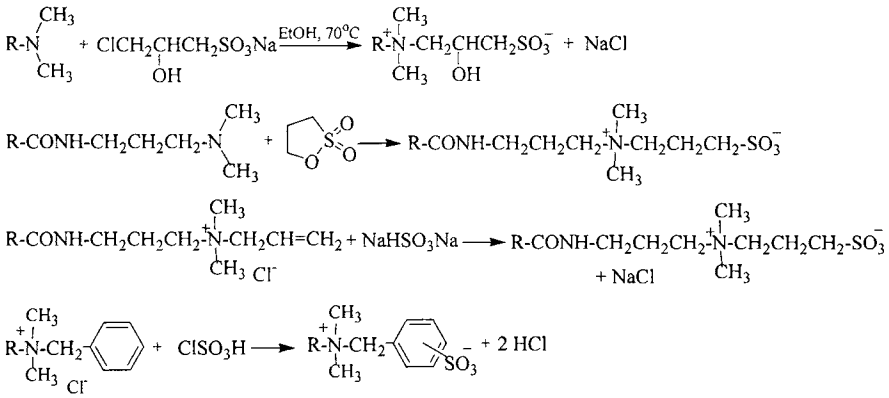

Sulphobetaines may also be synthesized with worth yield through nucleophilic addition of tertiary amines to unsaturated sulphoacids such as ethenesulphonic acid [111, 112]. Using low-ethoxylated fatty amines and allyl chlorides for the quaternisation followed by the addition of sodium bisulphite results in sulphobetaines with hydroxyethyl substituents in the head group. The reaction product of alkylmethyldiallylammonium chloride and sodium bisulphite depends on the catalyst and pH control, so the typical sulphobetaine structure incorporates 4-sulphopyrrolidinium or 3,4-disulphopyrrolidinium rings [119]. Now sulphobetaine-type surfactants of commercial importance contain a propane or 2-hydroxypropane spacer group between the nitrogen and sulfonic acid group (III).

Convenient reactants, such as $ClSO_3H$ and gaseous SO_3, may be used for the preparation of sulphatobetaines. The reaction is illustrated by the equation:

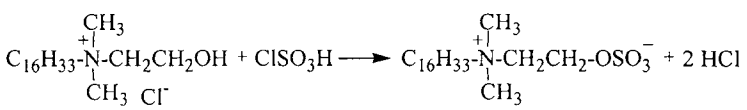

Monoester of sulfuric acid and 3-chloro-1,2-propanediol (as a result of $NaHSO_4$ addition to epichlorohydrin) can also be used for the preparation of sulphatobetaine through the reaction with tertiary amines. The same reaction of the monoester of phosphoric acid gives rise to

phosphatobetaine whereas phosphonation of the quaternary compound with N-allyl group leads to a phosphobetaine-type zwitter-ionic surfactant.

Taking into account the unsurpassed mildness of all these surfactants, promising sphere of their application is "no-more-tears" child shampoos and products for intimate hygiene. In various combinations phosphobetaines and phosphatobetaines are patented in a range of personal care products by *Johnson & Johnson* [44, 45, 111]. Zwitter-ionic 3-amidopropyldimethylammonio-1-propane-3-sulphonate derived from cholic acid (ChAPS) has been used as selective membrane protein solubiliser in the biochemical practice. All surface-active betaines are compared favourably with quaternary ammonium compounds in respect to their moderate toxicity, low mucous membrane irritation and better biodegradation.

Commercial betaine-type surfactants are known as follows:

Alkylbetaines: "Amphoteen 24" (*Akzo*), "Dehyton AB 30" (*Henkel*), "Empigen BB" (*Albright & Wilson*), "Miratаine D40" (*Rhodia*).

Cocoamidopropylcarboxybetaines: "Amphoteen BCA-30" (*Akzo*), "Amphotensid B4" (*Zschimmer & Schwarz*), "Betadet HR-50K" (*Kao*), "Dehyton K/PK45/3016B" (*Henkel*), "Empigen BS" series (*Albright & Wilson*), "Genagen CAB" (*Clariant*), "Lexaine C" (*Inolex*), "Lonzaine C" (*Lonza*), "Maprolyt C" (*Onyx*), "Rewoteric AMB/ AMR" series (*Witco*), "Tego Betain" series (*Goldschmidt*). Cocoamidopropylsulphobetaines are: "Betadet SH-R" (*Kao*), "Crosultaine C-50" (*Croda*), "Lonzaine CS" (*Lonza*), "Miratаine CBS" (*Rhodia*), "Rewoteric AM CAS" (*Witco*).

Phosphatides that occur in a great variety of vegetables, oil crops, living organisms and egg yolk are well-known natural zwitter-ionic surfactants. Their complex mixtures are known also as "lecithin". The lecithin constituents can be illustrated by phospholipids and sphingolipids as exemplified by α-phosphatidylcholine (A) and sphingomyelin (B), respectively:

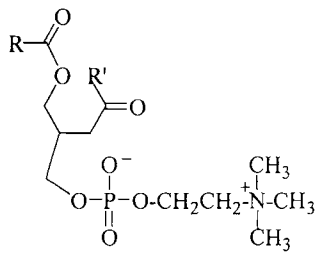

A

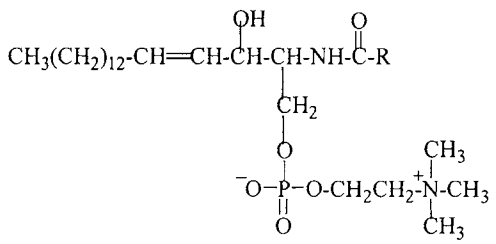

B

Besides choline, the cationic character of phosphatides is created also by 2-aminoethanol, sphingosine and other aminoalcohols. Phosphatides with two hydrocarbon chains attached to the same head group are more lipophilic amphiphiles characterised by vesicular (liposomal) aggregation in water contrary to single-chain surfactants that typically form micelles. Synthetic monoalkylphosphorylcholines are essentially water-soluble zwitter-ionic surfactants [120] the distinction of which consist in the hindered compatibility with anionics in view of the end position of the cationic betaine group.

Lecithins, mainly from soy-beans and egg yolk, are convenient emulsifiers and wide-range supplements in food industry [42, 43]. In cosmetics and pharmaceuticals they act as emulsifiers, emollients and liposomal carriers for unstable active ingredients [44, 46, 121, 122].

1.6. Fluorinated Surfactants

The surfaces of fluorocarbons and, in particular, perfluoroalkyl chains of surfactants have extremely low surface free energies (in average 10-20 $mJ \cdot m^{-2}$ lower than for ordinary hydrocarbons). Perfluoroalkyl chains tend much less to intermolecular interactions than aliphatic chains. This is due to the high symmetry and low polarisability of C–F bonds. Depending on neighbour atoms, the energy of the bonds is 451-583 kJ per mole in contrast with 356-431 kJ per mole for the C–H bonds. Carbon and fluorine atoms are similar in their parameters, so, in spite of the polarity, their covalent bonds are characterised by high symmetry and density of electron clouds. As compared with hydrogen atoms, fluorine atoms are bigger in diameter and screen a carbon chain more effectively, that provides for the latter unique chemical and biological inertness and thermal shock resistance. These properties along with high surface activity are the most valuable ones of fluorinated surfactants. These surfactants are useful for very special applications.

At low concentrations fluorinated surfactants are capable of lowering effectively the surface tension of aqueous solutions and non-aqueous liquids and work well in acidic, alkaline and electrochemical media as well as at elevated temperatures. Their destruction may be bound up just with the decomposition of polar groups, e.g. polyoxyethylene chain. Adsorbing with the

head group on a solid surface, fluorinated surfactants can provide water- and oil-repellence and resistance to soiling. Reducing the surface tension of aqueous solutions down to 15-22 mN/m, fluorosurfactants are able to provide the spontaneous spreading on low-energy surfaces of hydrocarbons and other combustible materials. This is an important feature, for instance, in connection with problems of fire-fighting and evaporation reduction of volatile or toxic liquids.

1.6.1. Technology of lyophobic moiety

The amphiphilic nature is the indispensable attribute of the structure of any surfactant. The nonpolar, "solvophobic" part of fluorosurfactants constitutes usually with perfluoroalkyl, ω-hydroperfluoroalkyl or perfluoroether chain of normal or branched structure. Surfactants with semifluorinated carbon chains are not quite effective as the ones with completely fluorinated carbon chains. Usually the optimum perfluorocarbon chain length is from 6 to 10 carbon atoms. Three industrially important methods of fluorosurfactants synthesis are known [123-126]:

(1) Electrochemical fluorination of carboxylic acid fluoride and chloride or alkylsulphonic acid fluoride/ chloride is carried out in anhydrous hydrofluoric acid medium at $t < 19\ ^{\circ}C$ (or $t < 35\ ^{\circ}C$ for n-$C_8H_{15}SO_2F$) at a voltage of 5-12 V and electric current density of $\approx 0.02\ A/m^2$:

$$C_nH_{2n+1}COCl + (2n+2)HF \rightarrow C_nF_{2n+1}COF + HCl + (2n+1)H_2 + \text{by-products}$$

The Simons process of electrochemical fluorination can be operated batchwise or continuously [126, 127]. By-products of the process are mixtures resulting from the CC bond cleavage and chain cyclisation. The yield usually does not exceed 65 % when $n = 3$ and highly decreases as n rises. This process was brought into commercial practice by *3M, BASF, Bayer, Dainippon Ink & Chemicals, GIPKh* (Russia) and *Tohoku Hiryo.*

(2) The process of telomerisation of tetrafluoroethylene with trifluoromethyl iodide or pentafluoroethyl iodide is initiated by UV irradiation or by a catalyst. In the latter case the reaction is carried out under pressure and at $t = 80\text{-}220\ ^{\circ}C$:

$$C_2H_5I + n\,C_2F_4 \longrightarrow C_2H_5(C_2F_4)_nI$$

The advantage of the telomerisation process is the high yield of perfluoroalkyl iodides, although the telomer distribution is wide (n is generally from 2 to 6). Numerous modifications

of this process have been patented, which concern either catalytic systems or the choice of telogen and methods of its preparation [124-126]. Thus perfluoroisopropyl iodide and perfluoroacetone can be used as starting telogens, as illustrated here:

$$(CF_3)_2C{=}O + KF \longrightarrow (CF_3)_2CFOK \xrightarrow{n CF_2{=}CF_2,\ I_2} (CF_3)_2CFO(CF_2CF_2)_nI$$

Nucleophiles, such as OH^- and NH_3, do not react with perfluoroalkyl iodides and therefore intermediates, that would be suitable for further fluorosurfactant synthesis, cannot be obtained at once. Hence, at first the reaction with ethylene in presence of a free radical catalyst is carried out:

$$C_2H_5(C_2F_4)_nI + CH_2{=}CH_2 \xrightarrow{\Delta} C_2H_5(C_2F_4)_nCH_2CH_2I$$

The resultants, 1,1,2,2-tetrahydroperfluoroalkyl iodides, can be easily converted, e.g., into alcohols, thiols, carboxylic acids and ethoxylated products. Thus, direct hydrolysis of 2-perfluoroalkyl iodides leads to perfluoroalkyl-2-ethanols which show surface activity in non-aqueous solvents. Such approaches to fluorosurfactant synthesis have been put on stream by *Du Pont*, *Ciba-Geigy*, *Hoechst*, *Asahi Glass* and *Daikin Kogyo*.

(3) The oligomerisation process consists in anionic polymerisation of tetrafluoroethylene in suitable aprotic solvents, e.g., diglyme or dimethylformamide, using KF, CsF or tetraalkylammonium fluoride as catalyst. The oligomerisation products are branched perfluoroolefins able to by further modified. Trimers, tetramers and pentamers of tetrafluoroethylene as well as dimers and trimers of hexafluoropropylene are useful essentially as a lyophobic backbone of fluorinated surfactants. This approach was initiated by *ICI* and *Neos* (Jap.), respectively.

The anionic oligomerisation of hexafluoropropylene oxide or tetrafluoroethylene oxide is an alternative source of the hydrophobic/oleophobic fluorocarbon fragment synthesis [126, 128]:

$$n CF_3CF_2\text{-}CF_2\text{(O)} \xrightarrow{F^-} CF_3CF_2\text{-}CF_2O(CF(CF_3)\text{-}CF_2O)_{n-2}CF(CF_3)COF \xrightarrow{\text{Alkali}} CF_3CF_2\text{-}CF_2O(CF(CF_3)\text{-}CF_2O)_{n-2}CF(CF_3)COONa\ (NH_4)$$

The process was brought to a commercial level with the Italian *Montedison* ("Fomblin" perfluoroether fluids). Further perfluorinated carbon chain modifications to manufacture any required kind of fluorocarbon surfactants encounter no much difficulties.

1.6.2. Structure and synthesis of fluorinated surfactants

Straight-chain perfluoroalkanoic or perfluoroalkanesulphonic acids fluorides derived by electrofluorination can be subjected to hydrolysis, esterification, amidation and other modifying, as illustrated with the following reactions [124, 126]:

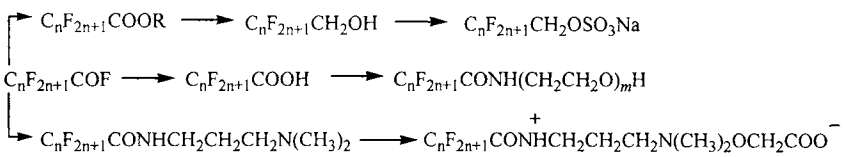

Ethoxylated fluorosurfactants can be further modified with proper reactants, such as P_2O_5, benzyl chloride, allyl chloride, glycidyl (meth)acrylate, epichlorohydrin, etc., to obtain either required dispersing effects, or inert behaviour in aprotic and aggressive media, or cross-linking with finishing substrates.

The addition of solubilising groups has often much specificity for fluorinated surfactants. Thus, perfluoroalkylethyl iodides obtained by a telomerisation process (see above) can be converted into intermediates and surfactants described in a great number of patents and scientific literature. Some examples are shown schematically in Fig. 1.5.

Fluorinated nonionics are synthsised by the base-catalysed nucleophilic replacement in tetrafluoroethylene or hexafluoropropylene oligomers with PEG and end-capped PEG. Similar reactions between branched-chain perfluoroolefins and phenol gives rise to perfluoroalkenyl phenyl ethers, which show surface activity in organic liquids. The extent of the surface tension lowering depends on the balance between the oleophobic fluorinated chain and the oleophilic phenol group. The latter can be hydrophilised by sulphonation with oleum or other sulphonation agent followed by a neutralisation with a base [126]. This and some other useful reactions for perfluoroolefin oligomers modifications are shown below in Fig. 6. The branched-chain fluorosurfactants cannot pack so tightly at the surface as their straight-chain counterparts and hence give some higher surface tension (20-23 mN/m). Thus, the 0.001 M aqueous solution of the nonionic fluorosurfactant "Monflor 51" (*ICI*) of the formula $C_{10}F_{19}O(CH_2CH_2O)_mC_{10}F_{19}$, $m \approx 23$ reaches a surface tension of 22 mN/m at 20 °C [129]. At the same time the branched-chain fluorochemicals work at very low concentrations (< 0.1 %) and are more attractive from the economical point of view [123, 126, 130].

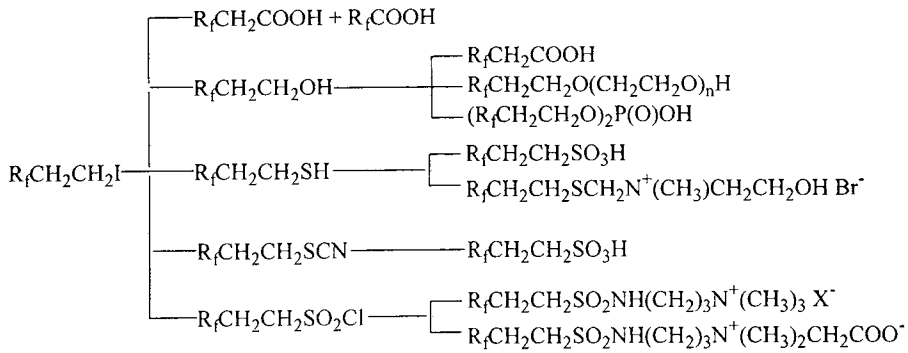

Figure 1.5 Some opportunities of fluorosurfactant synthesis from perfluoroalkylethyl iodides

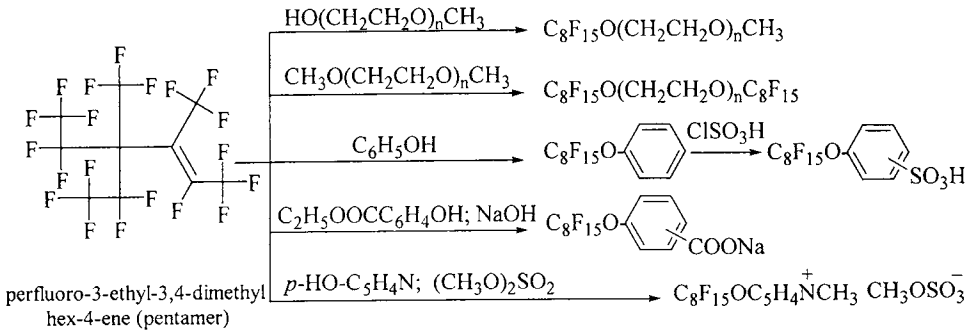

Figure 1.6. Some reactions of the TFE pemtamer for making fluorinated surfactats

The acid fluorides resulting from the hexafluoropropylene oxide oligomerisation are capable to condense with benzene or toluene by means of a Friedel-Crafts catalyst such as $AlCl_3$ [128c]:

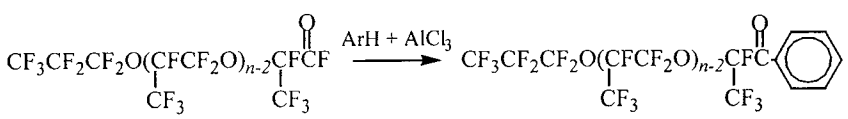

Ar = benzene or toluene

The flexible perfluoroether chain provides the surfactant a low melting point, low Krafft point and excellent surface activity. Thus, the toluene-modified HFPE hexamer lower the surface tension of toluene and m-xylene up to 12 mN/m (!) at conc. 0.46 wt. %, whereas the sodium

salt of the corresponding toluenesulphonic derivative lower the surface tension of water to 15.9 mN/m at 0.20 wt. % only [128c].

In some cases the modification of silicones with fluorocarbon groups provides the unique opportunity to achieve ultralow surface tensions [126]. On the other hand, a semifluorinated surfactant behaves in some respects as a conventional hydrocarbon surfactant. Just one hydrogen atom in the fluorocarbon tail, as in the case of ω-hydrofluorinated amphiphiles, is sufficient to deteriorate the surface tension reduction. The comparison of single-headed and ω,ω'-double-headed fluorosurfactants demonstrates that the latter, such as hydrocarbon bolaphiles [107a], show higher CMCs and surface tension values [128d, 131]. The base-catalysed reaction between fluorinated alcohols and glycidol results in polyglycerol ethers showing excellent surface activity without thermal clouding in water [132].

Head groups of fluorinated surfactants providing the required hydrophilicity, as a rule, have not much specificity as compared with the head groups of the hydrocarbon counterparts. These can be: carboxylic, sulphonic, sulphate and phosphate groups in anionics; quaternary ammonium, amino-, pyridinium, morpholinium or piperazinium groups in cationics; polyalkylene oxide, polyglycerine chain, dimethylamine oxide, or carbohydrate residues in nonionics; amino acid and betaine groups in amphoterics and zwitter-ionic surfactants. Presumably, perfluoroketones with an asymmetrical position of the ketogroup is the only exception to the general picture because in watery solvents it forms *gemi*diol showing high surface activity [133]. Such behaviour is not characteristic to aliphatic ketones. The leading suppliers as well as their selling ranges are given in Table 1.9.

The principal features of fluorinated surfactants may be summarized as the chemical and thermal stability, the ability to reduce surface tensions to extremely low values, strong hydrophobic and oleophobic character, and effectiveness at low concentrations. When they are adsorbed or anchored at solids, the surfaces often acquire antistatic, oil- and soil-repellent properties that found use in paper and polymer processing. The field of reactive F-alkylated soil-release agents for fabrics finishing deserves a separate consideration [134]. Excellent spreading and levelling properties of fluorosurfactants are widely used in modern film-forming fire-extinguishing foams (in combination with hydrocarbon surfactants), printing inks,

polishing aids, adhesives, in antifoaming, electroplating, etching, and other formulations. They are excellent emulsifiers for polymerisation of fluoromonomers. A wider application of fluorinated surfactants lies in the cost reduction, their reclamation and solving of environmental problems.

Table 1.9 Fluorinated surfactants and finishing aids: Main suppliers, registered trade names and methods of the R_f synthesis

Company	Trade name	Method of synthesis
3 M	Fluorad, Scotchgard, Scotchban	Electrochemical fluorination
Bayer	Bayowet FT	Electrochemical fluorination
Dainippon Ink & Chemicals	Megafac	Electrochemical fluorination
Tohoku Hiryo	Eftol	Electrochemical fluorination
Du Pont	Zonyl, Zepel	Telomerisation of TFE
Atofina	Forafac, Foraperle	Telomerisation of TFE
Asahi Glass	Surflon, Asahiguard	Telomerisation of TFE
Ciba Spec. Chemicals	Lodyne, Rodaine	Telomerisation of TFE
Daikin Kogyo/ Sumitomo	Sumifluol	Telomerisation of TFE
ICI	Monflor	Oligomerisation of TFE
Neos	Ftergent	Oligomerisation of HFP
Ausimont/ Montedison	Fomblin	Oligomerisation of PFPE

Fluorinated nonionics offer the advantage of being stable in saline conditions and variable pH that, along with their mildness, high dispersing to fluorocarbons and solubilisation of gases, can be advantageous for temporary blood substitutes and other biological applications [126, 135-137]. Such as ordinary double-chained surfactants, the amphiphiles with two fluorinated tails can form stable vesicular aggregates under ultrasonification having peculiar physicochemical properties [138].

1.7. Structure/Performance Relations in Surfactants

Two kinds of behaviour are significant for a surfactant, the adsorption at interfaces and the aggregation in the solution bulk. Adsorbing at interfaces and forming micelles, surfactants play an important role in wetting, dispersing, foaming, solubilising and a great number of other phenomena. In order to understand and predict their action in practically important phenomena

and technological processes, it is important to know general relationships between structure and performance, mechanisms of interactions among amphiphiles and other species as well as their behaviour in complex systems, such as detergents.

1.7.1. Performance in adsorption

There is large body of data on the surface and interfacial tensions of aqueous surfactant solutions. This data show that the structure of the surfactant molecule has a pronounced effect on its ability to reduce these tensions. As the length of the alkyl or fluorinated alkyl chain increases, the CMC decreases and the surface excess concentration increases, causing a drop in the interfacial tension at a fixed surfactant concentration. At low surfactant concentrations the reduction in surface tension (or increase in surface pressure $\Pi = \gamma_0 - \gamma$) is linear with the molar bulk solute concentration c (in the case of the dilute solution)

$$g = (d\Pi / dc)_{c \to 0}, \qquad (1.1)$$

where g is the surface activity. The Traube rule is related to the standard free energy of adsorption $\Delta G^0_{CH_2}$ (or the work of adsorption $-\Delta G^0_{CH_2}$) per CH_2 group via

$$\Delta G^0_{CH_2} = -RT \ln(g_{n+1} / g_n) \qquad (1.2)$$

where n is the number of CH_2 groups, and for nonionic $g_{n+1}/g_n = 3 \div 3.5$. Thus, $\Delta G^0_{CH_2} \cong 3$ kJ/mol.

According to the Langmuir principle [139], the surface free energy of adsorption of any straight-chain amphiphilic molecule $CH_3(CH_2)_{n-1}X$ can be considered as a linear combination of increments of hydrophobic and hydrophilic groups, namely the free energy changes associated with the transfer of the terminal methyl group, of the (n -1) CH_2 groups and of the hydrophilic "head" of the molecule, i.e.:

$$\Delta G^0 = \Delta G^0_{CH_3} + (n-1)\Delta G^0_{CH_2} + \Delta G^0_p \qquad (1.3)$$

The third term is a function of chemical nature of the head (polar) group and its environment.

The free energy of adsorption is considered in more detail in the chapters 2 (paragraph 2.10) and 3 (paragraph 3.5).

The derivative of the surface tension or surface pressure with respect to concentration is characterised by the relationship

$$-d\gamma / dc = d\Pi / dc \qquad (1.4)$$

and has a maximum ($d\Pi / dc = RT\Gamma / c$) at $c \rightarrow 0$ and a minimum at the c = CMC. Unfortunately, precise surface tension data in the initial part of the isotherm at high dilutions are difficult to obtain. Hence, $(d\Pi/dc)_{CMC}$ can be proposed as a measure of the "effectiveness" of the amphiphile in respect to surface tension reduction. The finite differences, $-\Delta\gamma/\Delta c$, was assumed to be more acceptable as a practical measure of the surfactant effectiveness [140]

$$-\Delta\gamma / \Delta c = -(\gamma_0 - \gamma_{CMC}) / CMC\,, \qquad (1.5)$$

where $\gamma_0 - \gamma_{CMC} = \Pi_{CMC}$ refers to the surface pressure at the critical micelle concentration CMC beyond which Π remains nearly constant. For true nonionic and ionic surfactants, Π_{CMC} is moderately affected by the change in the length of alkyl chain whereas the chain isomerism and head group nature can cause marked changes of the effectiveness in surface or interfacial tension reduction [141].

For most of the conventional amphiphiles it was demonstrated by Rosen [141] that at a surface pressure Π = 20 mN/m the surface excess concentration reaches 84-100 % of its saturation value. Then, the $(1/c)_{\Pi=20}$ value can be related to the change in free energy of adsorption at infinite dilution ΔG^0, the saturation adsorption Γ_∞ and temperature T using the Langmuir and von Szyszkowski equations. The negative logarithm of the amphiphile concentration in the bulk phase required for a 20 mN/m reduction in the surface or interfacial tension can be used as a measure of the efficiency of the adsorbed surfactant:

$$pc_{20} = -\log c_{(\Pi=20)}. \qquad (1.6)$$

Similar to the surface activity g, the parameter pc_{20} rises linearly with the increase of the carbon number in straight-chain surfactants, reflecting the negative free energy of adsorption of a methylene group at the interface. When the hydrophobic group is lengthened by one CH_2-group, pc_{20} increases by about 0.28÷0.31 for most of the hydrocarbon surfactants and by up to 1.0 for fluorocarbon surfactants. The effectiveness in surface or interfacial tension reduction by a surfactant in a liquid–fluid system can be characterised by the surfactant concentration in the

entire system required to produce a given interfacial tension. Both pc_{20} and Π_{CMC} increase with rising ionic strength, especially for ionic surfactants, with lengthening of the hydrophobic group, under addition of synergistic co-surfactants, and to a lesser degree with elevation of temperature [141-143].

Ethoxylated nonionics show the lowest interfacial tension as well as high solubilisation and detergency around their cloud points [36, 54]. Sterically, their polyoxyethylene chains can assume two different conformations in aqueous solution: at the low ethoxylation is has a fully extended *trans* or "zig-zag" form and at higher ethoxylation it has a more compact *gauche* or "meander" form. In the second case the saturation adsorption is not so high but the steric stabilisation of dispersions may be quite effective [7, 8].

The surface or interfacial tension of a solution of long-chain surfactants, non-ionics or ionics in the presence of surface-inactive electrolyte with the same counterion, is given by the bulk concentration c via the fundamental Gibbs adsorption equation

$$\Gamma = -\frac{d\gamma}{RT\, d\ln c}, \qquad (1.7)$$

where Γ is the surface excess concentration, R is the gas constant. The surfactant solution should be diluted enough to use the concentration instead of the activity.

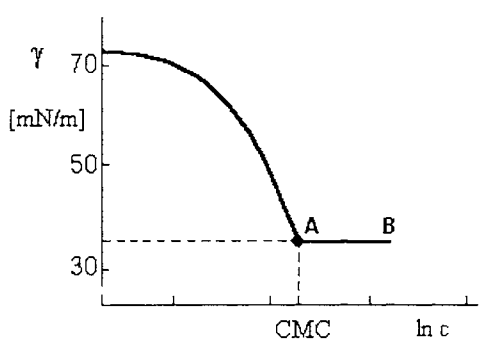

Figure 1.7 Typical plot of surface tension vs logarithm of surfactant concentration

According to the Gibbs adsorption equation, the linear plot of surface or interfacial tension vs logarithm of the bulk concentration must indicate that the surface saturation has reached the

maximal value Γ_∞ (largest slope of the curve γ(ln c) before point A as shown in Fig. 1.7. Above the CMC (A-B) the surface tension of the surfactant solution remains nearly constant since the formed micelles are not surface-active and the monomeric surfactant concentration is essentially constant. For more details, Chapter 5 gives a comprehensive overview of micelle formation thermodynamics and kinetics and its impact on the properties of interfacial layers.

For 1:1 ionic surfactants and in absence of indifferent electrolyte, the equation (1.7) should be modified in the following way

$$\Gamma = -\frac{d\gamma}{2\,RT\,d\ln c}. \qquad (1.8)$$

The coefficient "2" takes into account the dissociation of the surfactant, such as sodium dodecyl sulphate, SDS, into two species. At moderate salt concentrations a coefficient $1< f < 2$ should be used. Correspondingly, a coefficient "3" has to be inserted into Eq. (1.8) for a 2:1 or 1:2 ionic surfactant. The increase in salt concentration leads to rising Γ up to the limiting value Γ_∞ which is mainly dependent on the nature and structure of the hydrophobic part [141, 143-146]. In 50^{th} to 70^{th} of the last century a large number of experiments have been performed using the foam bubble separation technique and radiotracer method to measure directly the surface excess concentrations of pure surfactants at the gas-liquid interface, and the measured surface composition was in a good agreement with those calculated from the surface tension data. Recently developed techniques, such as ellipsometry and neutron reflection at liquid interfaces, provide even more accurate results. Details will be given in Chapters 3 and 4.

The position of point A in the curve shown in Fig. 1.7 is characteristic for a sufficient purity of the surfactant and solvent. The point is located at a definite surface tension and concentration (CMC). As a rule, a minimum in the γ(c) or γ(log c) plot is evidence of traces of highly surface-active impurities which affect the results [147]. In chapters 2 to 4 the effect of lateral molecular interaction with increasing alkyl chain length, the effects of changes in orientation and conformation, essentially shown by polymeric surfactants such as proteins, may also lead to significant changes in the adsorption behaviour.

The incremental changes in the excess free energies of adsorption per added CH_2 group in homologous series of different straight-chain amphiphiles are essentially of the same order at

the air/water (A/W) and oil/water (O/W) interfaces: $\Delta G^0_{CH_2}$ ranges from –2.6 kJ/mol to –3.2 kJ/mol for nonionics and ionics with or without electrolyte (in more details for the A/W interface see paragraph 3.5). For perfluorinated amphiphiles $\Delta G^0_{CF_2}$ can attain even –4.0 kJ/mol. For many surfactants the temperature coefficient of surface tension $d\gamma/dT$ changes the sign of surface entropy from minus to plus when passing the CMC [148].

Major practical needs related with colloidal systems, such as the formation of stable emulsions and microemulsions [2, 149-170], detergency and powder dispersion [2, 45, 99, 145, 171-173], oil recovery [153, 161, 174-177], formation of aqueous films onto hydrocarbons and stability of biliquid foams [22a, 125, 126, 178], etc., require extremely low interfacial tensions. The strong reduction in surface and/or interfacial tension can be obtained by a proper selection of surfactant, its concentration, adjustment in ionic strength, addition of one or more surface active compounds. Particularly, high-molecular petroleum sulphonates and di(alkyl)benzene sulphonates with equal and preferably branched alkyl chains are more effective than others in reducing the oil-water interfacial tension. On the other hand, structural requirements can be in contradiction with environmental standards bearing in mind the worse biodegradation of higher branched-chain surfactants [40, 41]. Attaining ultra-low O/W tension with a given surfactant depends also on the kind of oil [174, 176]. Microemulsion surfactant systems proposed for tertiary oil recovery contain lower aliphatic alcohols, typically propanol, butanol and pentanol. The alcohols increase both surfactant's solubility and oil solubilisation, they sharpen the oil-brine interfacial tension minimum (down to < 0.01 mN/m) as result of the growth in the chemical potential in the adjacent phases.

In order to cause spontaneous spreading of an aqueous surfactant solution (W) over a second immiscible liquid (O) as substrate, the definite relationship between surface and interfacial tension, known as the spreading (Harkins) coefficient S_{WO} should be fulfilled. If S_{WO}, as defined by the equation

$$S_{OW} = \gamma_O - (\gamma_W + \gamma_{OW}), \tag{1.9}$$

is positive, spreading occurs spontaneously; while for negative S_{WO}, the solution will not spread spontaneously over the surface. The more the initial difference between γ_O and $(\gamma_W + \gamma_{OW})$ the larger is the driving force of film spreading.

In spite of very low surface tension, the aqueous solution of a single fluorinated surfactant cannot spread on a burning fuel due to its poor affinity (oleophobicity) to O/W interface as manifested by the high value of γ_{OW}. On the contrary, the affinity of a hydrocarbon surfactant for the O/W interface is generally higher than for the A/W interface. Taking into account the known non-ideality of mixing of conventional and fluorinated surfactants at interfaces and in micelles [126, 179-182], we can expect that such surfactant combinations can spread well over oil surfaces the surface tension of which is approximately 20 mN/m. The resulting asymmetrical liquid film covering a hydrocarbon substrate is schematically presented in Fig. 1.8.

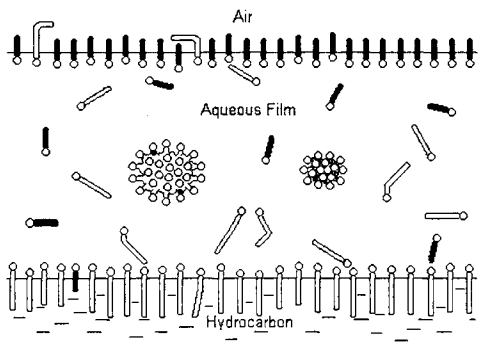

Fig.1.8 Aqueous film formation at hydrocarbon as a result of immiscibility of conventional and fluorinated surfactants in adsorbed layers and micelles

Progress in the understanding of such films initiated the use in modern film formation processes and the preparation of fluoroprotein and universal foams for fire fighting [22a, 22d, 178b]. In practice, to attain better effects and economy, both fluorinated and hydrocarbon surfactants are used as binary, ternary or more complex synergistic mixtures.

Spreading of a surfactant solution over solid surface, among other things, depends on its texture and quality. A number of surfactants, particularly low-ethoxylated ones, are known as excellent wetting agents.

It is generally accepted that silicone surfactants are more effective than ordinary aliphatic surfactants in lowering the surface tension of water and non-aqueous liquids [21]. However, they are weaker surfactants in comparison to perfluorinated ones.

The adsorption kinetics of a surfactant to a freshly formed surface as well as the viscoelastic behaviour of surface layers have strong impact on foam formation, emulsification, detergency, painting, and other practical applications. The key factor that controls the adsorption kinetics is the diffusion transport of surfactant molecules from the bulk to the surface [184] whereas relaxation or repulsive interactions contribute particularly in the case of adsorption of proteins, ionic surfactants and surfactant mixtures [185-188]. At liquid/liquid interface the adsorption kinetics is affected by surfactant transfer across the interface if the surfactant, such as dodecyl dimethyl phosphine oxide [189], is comparably soluble in both liquids. In addition, two-dimensional aggregation in an adsorption layer can happen when the molecular interaction between the adsorbed molecules is sufficiently large. This particular behaviour is intrinsic for synergistic mixtures, such as SDS and dodecanol (cf. the theoretical treatment of this system in Chapters 2 and 3). The huge variety of models developed to describe the adsorption kinetics of surfactants and their mixtures, of relaxation processes induced by various types of perturbations, and a number of representative experimental examples is the subject of Chapter 4.

Concerning to the adsorption of surfactants at liquid-fluid interfaces, it is worse to mention the theory of hydrophile-lipophile balance (HLB) most recently extensively described by Kruglyakov in a volume of this series [190]. The HLB method has been firstly introduced by Griffin [191] as a numerical scale of the relative hydrophilicity and emulsifying efficiency of surfactants. According to the method, the HLB number is assigned to the role each surfactant plays as emulsifier. Another number we can refer to is the "required HLB" of an oil subjected to emulsification. Low HLB values correspond to lipophilic (oil-soluble) surfactants and high HLB values correspond to hydrophilic surfactants as it was illustrated for nonionics in Table 1.1 in section 1.2.3. A number of studies was performed to find reproducible and rapid methods of determination of the HLB by calculation or experimental evaluation. There have been numerous studies to correlate HLB numbers and other physicochemical properties of surfactans, e.g. partition coefficient, solubility parameter, spreading coefficient, CMC, cloud point of nonionics, their phenol index, emulsion inversion point, analysis of NMR spectrum, retention value in GLC, interfacial tension minimum, solubilisation of water in the emulsifier soluble in the oil phase, etc [54, 144-146, 149-153, 190, 192].

A simple rule to choose a surfactant required for emulsification of an oil is provided by the Bancroft rule stating that oil-in-water emulsions (having water as continuous phase) will be more stable when the emulsifying agent is better soluble in the aqueous phase than in the oil phase. And vice versa, water-in-oil emulsions are generally stable when the emulsifying agents are better soluble in the oil phase as compared to the aqueous. In general, instead of water, any other second phase may be used which is immiscible in the oil phase, such as PEG or glycerine.

In determining the emulsification temperature for emulsions stabilised with EO containing nonionics, the consideration of the phase inversion temperature (PIT or HLB-temperature) suggested by Shinoda and co-workers [193] can be also important in order to select the surfactant of optimum HLB. The PIT of an emulsion depends not only on the structure of surfactant(s), but also on many other parameters, such as the surfactant concentration, nature of the oil, phase ratio, or the presence of salts. The lowest interfacial tension at the PIT is the important factor for obtaining emulsions with small average droplet size and hence good stability.

Adsorption layers of the same kind as at fluid interfaces are also formed at low-energy solid – water surfaces, as it was established on PE, polystyrene, paraffin, carbon black, and other related materials. The classical Langmuir or Frumkin adsorption isotherm is often applicable to describe this behaviour. Studies on surfactant adsorption at various solid surfaces have been summarised in a great number of reviews [2, 7, 8, 54, 98, 101, 111, 121, 126, 141, 144, 145, 177, 186, 190, 194-198]. The adsorption at the solid/liquid interfaces is governed by a number of factors:

- nature of the solid surface - chemical composition, morphology, existing charged groups;
- molecular structure, ionic and hydrophobic nature of the surfactant;
- properties of the liquid from which the adsorption of the surfactant proceeds (composition, pH, temperature, etc.).

In general, following mechanisms participate in the adsorption of surface-active solutes at a solid/liquid interface [141]:

- ion exchange and pairing (onto charged surfaces having ionic sites);

- hydrogen bonding (through hydrogen bond formation between adsorbate and adsorbent);
- ion-dipole, dipole-dipole and induced dipole-dipole interactions;
- hydrophobic bonding peculiar to aqueous surfactant solutions to minimize the contact between hydrocarbon chains and the surrounding water [199, 200];
- universal dispersion forces acting as a supplementary mechanism in all other interactions.

The surface filling and the molecular orientation are determined also by the nature of interaction forces between solvent species and surface-active species as well as with the solid substrate.

On polar adsorbents, such as zeolite or metal oxide, and essentially apolar adsorbents, such as acetylene black, the formation of tri-dimensional micelle-like aggregates or two-dimensional "hemi-micelles" was observed [194-198]. This kind of surfactant aggregation at a solid substrate occurs at low bulk concentrations and medium surface monolayer filling or just above the CMC (the latter is generally observed for nonionics) and it is due mainly to lateral and hydrophobic interactions. Adsorption isotherms of technical grade surfactants, especially on heterogeneous substrates, often pass through a maximum due to surfactant redistribution and solubilisation effects. The ionic surfactant binding to biological substrates, such as hair keratin [44, 45, 122] is rather complicated adsorption process accompanied by swelling and conformational changes.

Adsorption of surfactants on solids is an important problem in a number of phenomena and industrial processes. In processes of waste treatment, pigment dispersion and froth flotation, the surfactant adsorption on a material is essential for their successful realisation. Surfactant loss due to the adsorption on rock minerals is unfavourable for tertiary oil recovery by surfactant flooding [176, 177]. In addition, the surfactant adsorption controls other interfacial processes such as cleaning, etching, dyeing, sizing, hydrophobisation, antistatic effects, lubrication, disinfection, chromatography, etc. Each of the particular adsorption processes in various systems has been discussed in a great number of special publications and some of them are presented in more detail in Chapter 6.

1.7.2. Structural relations in aggregation

Surfactants in aqueous media form colloidal aggregates known as micelles and vesicles. The gain in total free energy due to minimising the hydrocarbon/water contact is the main driving force for surfactant aggregation. For the first time spherical micelles were recognised by Hartley in the 30th [201]. They are formed from the molecular or ionic, generally single long-chain, amphiphiles within a narrow concentration range called critical micelle concentration, CMC. As a result, the hydrophobic part of the amphiphile "hides" itself inside the micelle, the hydrophilic part is oriented towards the aqueous environment. As soon as the CMC is reached, many properties of a surfactant solution in function of the bulk concentration show a remarkable change as presented schematically in Fig. 1.9. Above the CMC the monomeric surfactant concentration remains nearly constant and all additional surfactants form micelles of a quite narrow size distribution and approximately spherical shape. The mean micellar aggregation number n can be of order of few tens or hundreds. Micelles are characterised by a certain lifetime, the rate of monomer exchange, counterion binding and other properties.

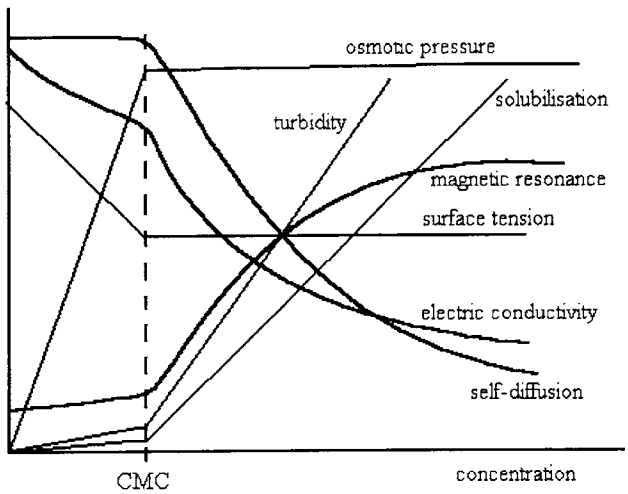

Fig. 1.9. Schematic representation of changes in some physical properties for solutions of a micelle-forming surfactant, according to [203]

There are a number of synthetic and natural surfactants where the CMC cannot be identified by an abrupt change in the solution properties. Short-chained surfactants, like as sodium octanoate, and amphiphiles with weakly pronounced hydrophobic groups, like as bile salts [202], often show a non-cooperative stepwise aggregation over a broad concentration range, so that the CMC concept is not applicable.

After the CMC is reached, ionic as well as non-ionic micellar solutions display further changes in their properties such as the osmotic pressure, solubilising capacity, refractive index, viscosity, water binding, etc, which can evidence for the change in the mean aggregation number and micellar shape from slightly oblate spheroid to disks, lamellae or rods. For ionic micelles, the transition to the non-spherical shape can be stimulated by lowering the temperature, addition of electrolyte or solubilisate [98, 203-212] as well as by specific binding of some kind of counter-ions, as in the case of the worm-like cationic micelle formation induced by the salicylate ions or other organic anions [98, 207, 209-212]. Sometimes emulsion-droplet-like giant micelles having a mean aggregation number $n \cong 1000$ are formed presumably due to the incorporation of ionic pairs into the micellar interior [213].

With increasing temperature in close proximity to the cloud point polyoxyethylene-type nonionics show a micellar growth slightly dependent on the concentration as result of a secondary aggregation in the solution [54, 214-216]. The cloud point is registered as the temperature at which the solution displays turbidity under heating in consequence of dehydration of the polyoxyethylene chains. The upper concentration limit of existing micelles is given by some kind of a liquid crystalline phase [217].

In the same way as hydrocarbons lose sharply the solubility in water with longer chains length, the hydrophobic tails of a surfactant "avoid" more and more the surrounding by water that tends to segregation and self-aggregation. As a rule, the ability to form micelles is shown by molecules with seven or more carbon atoms and a proper hydrophilic group (or several groups) rendering certain water affinity. The distribution of hydrophilic groups along a surfactant molecule diminishes the aggregation potential. For ionic surfactants the cooperativity for micellisation rises (CMC drops) under the following structural modifications:

- with the size of the hydrophobic part,
- with the distance between the geometric centre of charge and the α-carbon atom in the alkyl chain,
- with increase of charge of the head group (compare, for example, CMC of SDS and disodium salt of monododecyl phosphate).

Table 1.10 CMC, Krafft points and aggregation numbers of some surfactants

Surfactant	CMC (10^{-3} mole/l) at different temperatures						Krafft point, °C	n at 25°C
	10 °C	20 °C	25 °C	30 °C	40 °C	50 °C		
Nonionic straight-chain surfactants								
$C_{12}H_{25}(EO)_6$		0.074						400
$C_{10}H_{21}(EO)_8$		1.2	1.0	0.93	0.76			
$C_{12}H_{25}(EO)_8$		0.083	0.071	0.069	0.058			
$C_{12}H_{25}(EO)_7$ [1]			0.05			0.02		123
$C_{14}H_{29}(EO)_8$		0.0098	0.009	0.008	0.0072			
Sodium *n*-alkyl sulphates								
$C_8H_{17}SO_4Na$	141.6	133.3	130.2	131.8	135.9	142.1		
$C_{10}H_{21}SO_4Na$	35.0	33.3	33.0	32.9	33.7	35.5	8	50
$C_{12}H_{25}SO_4Na$	8.66	8.25	8.16	8.24	8.56	9.18	8-20 [2]	55-62
$C_{14}H_{29}SO_4Na$			2.05	2.08	2.22	2.43	20.5-36 [2]	
$C_{12}H_{25}SO_4$ ½Mg			1.76				24, 29 [2]	
Anionic surfactants having dodecyl as hydrophobe								
$C_{12}H_{25}SO_3Na$					9.7		32, 38.3 [2]	54 (40 °C)
$C_{12}H_{25}COONa$					11.7		39.8	
$C_{12}H_{25}OPO_3Na_2$			57			50	ca 20	
$C_{12}H_{25}(EO)SO_4Na$			4.2				5	
$C_{12}H_{25}(EO)_5CH_2$– –$COONa$ [1]			3.5 ± 0.4		3.5 ± 0.4 (45 °C)		< 0	
Other surfactants having dodecyl as hydrophobe								
$C_{12}H_{25}N(CH_3)_3Br$			16, 15.4 [2]					50
$C_{12}H_{25}N(CH_3)_2HCl$ 0.05 M NaCl 0.20 M NaCl			14.9 6.8 3.5				-4	56-65 70-74 86-91
$Br(C_4H_9)_3NC_{12}H_{24}$– –$N(C_4H_9)_3Br$	No micelle formation up to 0.05 mole/l							
$C_{12}H_{25}\overset{\oplus}{N}(CH_3)_2$– –$CH_2COO^-$		2.0, 2.4 [2]		2.5				63

[1] Technical-grade surfactants with statistical distribution of polyoxyethylene chains.

[2] CMC and Krafft points according the experimental data of different authors [91, 141, 211, 218-229].

As expected, the CMCs of individual surfactants, such as sodium alkyl sulphates (compiled in Table 1.10), are highly dependent on the alkyl chain length according to the following equation [91, 141-146, 203, 212]:

$$\log \mathrm{CMC} = p - qn_C \tag{1.10}$$

where p and q are constants. The slope of the straight line q is about –0.5 for most nonionic, amphoteric and zwitter-ionic surfactants, while it is ca –0.3 for 1:1 ionic surfactants, such as alkyl sulphates and alkylpyridinium halides, and it is ca –0.25 for 1:2 ionic surfactants, such as disodium alkyl phosphates or sulphosuccinates. If the surfactant activities are used instead of the concentrations, the slope q is almost constant, between –0.50 and –0.58 irrespective the nature of the head group [230].

CMCs of nonionics are related to the free energy change accompanied the micellisation, ΔG_m, by the expression

$$\Delta G_m = RT \ln x_{CMC}. \tag{1.11}$$

Here $x_{CMC} = \mathrm{CMC}/55.6$ is the surfactant mole fraction in the aqueous solution. Hence

$$\ln \mathrm{CMC} = \Delta G_m/RT + \ln 55.6. \tag{1.12}$$

No wonder that the slope of the straight line from Eq. (1.10) is directly proportional to the methylene group increment in ΔG_m, taking into account the additivity of the hydrophobic groups' contributions, CH_3- and (n_C-1) CH_2-, and the hydrophilic group contribution to ΔG_m

$$q = -\Delta G_{m(CH2)} / RT, \tag{1.13}$$

and the constant p reflects the free energy change mainly due to transfer of the hydrophilic group from an aqueous media to the micellar surface. The ratio of counterions to long-chain ions in the ionic micelle β should be taken into account in Eq. (1.13) as a correction factor (1 + β) in the denominator. Recently Zana [231] proposed for ionic micelles another correction factor for the charge fraction not neutralised by bound counterions. The constants p and q compiled elsewhere [141, 219] and obtained other sources for some homologous series of straight-chain surfactants are given in Table 1.11. The variation of the CMC for most nonionics and ionics is very similar to each other: q = 0.45-0.53 and q = 0.27-0.31, respectively. Unlike single charged ionics, for disodium and dipotassium salts of monoalkyl malonates and sulphosuccinates q drops to ca 0.21-0.23. The slope q rises for double-chained surfactants, as

illustrated by sodium dialkyl sulphosuccinates and dialkyldimethylammonium chlorides, as well as for dimeric [107a, 143] and perfluorinated surfactants [126].

The straight line slopes for different homologous surfactant series allow to derive the free energy change for the methylene unit: $\Delta G_{m(CH2)}$ is from -2.84 to -3.25 kJ/mol, while for the perfluromethylene unit of fluorinated surfactants $\Delta G_{m(CF2)}$ is of the order of 4-5 kJ/mol. The logarithm of the CMC for the homologous surfactant series is a linear function of the length of the surfactant molecule or ion n_C and its HLB number. More fine structural effects on the CMC are offered by the isomery of the hydrophobic part, the nature of head group substituents at nitrogen atom of cationics and substituents in the aromatic ring of alkylbenzene sulphonates, alkylnaphthalene sulphonates or alkylpyridinium halides, the nature of spacer groups in alcohol ether sulphates and ether carboxylates, in carboxy- and sulphobetaines, the ester group or amide group isomery, chirality, counterion geometry, and other structural changes [54, 98, 101, 142, 143, 211, 212].

As it was recognised by Corrin and Harkins [232], the CMC values of ionic surfactants are highly influenced by the electrolyte concentration according to the following equation

$$\log CMC = -a' \log c_{el} + b', \qquad (1.14)$$

where the coefficient a' means the counterion/monomer ratio (β), the coefficient b' is dependent on the nature of the head group and c_{el} is the total concentration of counterion [232, 233].

For the most ionic surfactants the constant b' varies from –0.4 to –0.95. If the c_{el} is replaced by the counterion activity a_{el}, the slope of $\log a_{CMC}$ *vs* $\log a_{el}$ becomes surprisingly identical both for the single-charged surfactants (–0.9) and double-charged surfactants (ca –1.8) [230].

The equation like as Eq. (1.14) remains true also for nonionics and ampholytes but the electrolyte has not so strong influence as before [7, 8, 54, 111, 141]

$$\log CMC = -k\, c_{el} + \text{constant}. \qquad (1.15)$$

Here k is the constant depended on the kind of surfactant, electrolyte and temperature. Practically all anions and cations diminish the CMC of ethoxylated nonionics in accordance with their lyotropic numbers of constituting ions following the sequence

$$F^- \cong 1/2SO_4^{-2} > Cl^- > Br^- > NO_3^- > I^- > CNS^- \text{ and } NH_4^+ > K^+ > Na^+ > Li^+ > 1/2Ca^{+2} > 1/2Mg^{+2}$$

Table 1.11 Coefficients in the equation log CMC = p – q n_C for some homologous surfactant series

Surfactant series	p	q	Temperature, °C
Nonionic surfactants			
$RO(CH_2CH_2O)_6H$	1.82	0.49	25
$RO(CH_2CH_2O)_8H$	1.89	0.50	25
$RO(CH_2CH_2O)_8H$	1.66	0.48	40
$ROC_6H_{11}O_5$ (alkyl glucosides)	1.64	0.53	25
$RN(CH_3)_2\rightarrow O$ (aminoxides)	3.626	0.446	27
Anionic surfactants			
RCOONa	1.85	0.30	20
RCOOK	1.92	0.29	25
$RCH(COOK)_2$ (alkyl malonates)	1.30	0.219	20-25
R_fCOONa	1.53	0.44	20-30
R_fCOONH_4	1.40	0.40	20-25
$ROSO_3Na$	1.43	0.29	25
$ROSO_3Na$	1.42	0.30	45
$ROSO_3Na$	1.35	0.28	60
$ROSO_3Na$ (secondary alkylsulphates)	1.28	0.27	55
RSO_3Na	1.59	0.29	40
RSO_3Na	1.42	0.28	60
RSO_3H	0.928	0.274	25-50
p-$RC_6H_4SO_3Na$	1.68	0.29	55
p-$RC_6H_4SO_3Na$	1.33	0.27	70
$R\text{-}CH{=}CH_2SO_3Na$	1.82	0.31	40
$R\text{-}CH(OH)CH_2CH_2SO_3Na$	2.065	0.305	40
$ROOCCH_2SO_3Na$	1.263	0.303	40
$ROOCCH_2CH_2SO_3Na$	1.108	0.301	40
$RCOOCH_2CH_2CH_2SO_3Na$	0.99	0.296	50
$ROOCCH_2CH(SO_3Na)COOR$	2.08	0.681	50
Cationic surfactants			
$RNH_2{\cdot}HCl$	1.25	0.27	25
$RN(CH_3)_3Br$	1.72	0.30	25
$RN(CH_3)_3Cl$ in 0.1 M NaCl	1.23	0.33	25
$R_2N(CH_3)_2Cl$	2.77	0.548	30
RNC_5H_5Br (alkylpyridinium bromides)	1.72	0.31	30
Zwitter-ionic surfactants			
$RN^+(CH_3)_2CH_2COO^-$	3.109	0.485	20
$RN^+(CH_3)_2CH_2CH_2CH_2SO_3^-$	3.757	0.517	30
$RS^+(CH_3)CH_2COO^-$	3.27	0.50	30

Some hydrophobic cations, such as tetrabutyl ammonium, appear to have the opposite action on the CMC. OH^- acts as normal anion whereas H^+ practically has no effect up to ca 0.5 M and it rise the CMC at higher concentrations in view of the ether oxygen protonation of the ethylene oxide chain. As a result of electrolyte addition, strong specific binding of ions may make surfactants sometimes more soluble and, in contrast, it may cause coacervation. Surfactant precipitation or strong aggregation occurs in many cases.

As it is well known, the solubility of any ionic surfactants in water rise abruptly at a definite temperature, which is known as the Krafft point, T_K, characteristic for each surfactant [146, 212, 234]. The Krafft point is characterised by a narrow concentration range, attributed to the CMC at T_K, and the temperature at which the solubility becomes equal to the CMC of the surfactant. Below T_K surfactant species are dissolved only in a single-dispersed state and above T_K all additional surfactant forms micelles so the solubility rises sharply. For homologous series of soaps, alkyl sulphates, sulphonates and other surfactants, the T_K values increase with the alkyl chain, and drop with its branching and unsaturation. A remarkable feature is that the Krafft points show a pronounced alternation between straight-chained homologues with even and odd numbers of carbon atoms in the alkyl chain [212, 223]. The even-numbered homologues have systematically lower T_K, i.e. higher colloidal solubilities than the odd-numbered ones. By the way, similar alternation is observed for the CMC vs n_C. Dealing with commercial surfactant fractions, one should bear in mind that the solubility is always more governed by the short-chained homologues.

The minimum in the interfacial free energy predetermines three kinds of geometry in nature: spheres, cylinders and planes. Correspondingly, the most stable amphiphile aggregation structures are: i) spherical (Hartley) micelles, ii) rod-shaped micelles and anisotropic middle phases, iii) disk-shaped micelles and lamellar mesophases. They exist as aggregates in a water continuum with a hydrocarbon core surrounded by hydrated polar groups (the normal type) and as aggregates in a hydrocarbon continuum (the reverse or inverted type) where water and

hydrated polar groups are surrounded with hydrocarbon chains. Quite general approaches to design the surfactant molecule for producing stable aggregate structure were developed by Tanford [235], Israelashvili, et al. [236] and more recently by Rusanov [146]. The self-assembly of amphiphiles, as molecules or ions, is closely related to the molecular parameters and aggregation conditions. Parameters of importance are the volume of the hydrocarbon tail(s) v, its effective length l and the head group area ω. For $v/l\omega < 1/3$ one has normal micelles, for $1/3 < v/l\omega < 1/2$ – rod-shaped micelles, and for $1/2 < v/l\omega < 1$ – vesicles or bilayers [236]. Increase in salt concentration, polar solubilisate or co-surfactant will screen head-group repulsion and decreases ω that often stimulates, for example, the transition of spherical micelles into oblate, cylindrical or disk-like micelles. The specific counterion binding and interaction of head groups of different nature can have dramatic effects on the aggregate shape and size [204-212, 237-239].

In view of the geometrical restrictions, surfactants having two or three hydrophobic tails form essentially lamellar structures or reverse micelles with a hydrocarbon continuum. On sonication or other mechanical action the lamellar systems are turned into metastable unilamellar vesicles. These liposome-like colloidal aggregates are formed by a number of long-chain natural and synthetic surfactants, such as phospholipids, saccharose diesters, polyoxyethylene hydrogenated castor oil, some anionics neutralised with bivalent cations, dialkyl dimethyl ammonium salts, and some dimeric surfactants having a long spacer group [31, 98, 107a, 143, 235, 236, 238-243]. Vesicles show unique encapsulation and storage properties along with conventional solubilisation by the membrane.

There is a large scope of literature concerning the surfactant self-assembly in non-aqueous media, particularly in hydrocarbons, which presents much interest in relation to the micro-heterogeneous reactions and catalytic action [199, 244-248], greases, dry cleaners, pharmaceuticals, and some other applications [101, 121, 141, 164, 165, 249-252].

It is not the aim of this paragraph to cover in a brief all aspects of this problem in view of the great variety and behaviour features of modern surfactants. The unbounded opportunities of organic synthesis, as well as domestic, science and high-tech needs have resulted in the creation of a large number of compounds and their combinations having specific structures and unique

properties. The limited scope of the chapter does not allow us to refer to all necessary quotations from the majority of works, patents including. So, this is a kind of a basic review that can lead everybody interested in similar problems to original publications. The links given to subsequent Chapters intend to make it easier for the reader to recognise how the different parameters and behaviour of surfactants and their ensembles are interrelated and what the impact on each other is.

Acknowledgements

Theauthor thanks Dr. Reinhard Miller, Max Planck Institute of Colloids and Interfaces, for valuable comments concerning structure–performance relations in surfactants as well as polishing the English. Fruitful assistance in preparation of the manuscript by my colleague, Dr. Nadezhda Glukhareva is highly acknowledged.

1.8 References

1. a) A.M. Raymond, Proceedings of the 4th World Surfactants Congress, Vol. 1, Barcelona, 3-7 VI 1996, AEPSAT, Barcelona, 1996, p. 21-32; b) J. Granados, ibid., p. 100-121.
2. J. Falbe (Ed.), Surfactants in Consumer Products: Theory, Technology and Application, Springer-Verlag, Berlin, 1987.
3. R.G. Laughlin, Y.-C. Fu, F.C. Wireko, J.J. Scheibel and R.L. Munyon, in "Novel Surfactants: Preparation, Application, and Biodegradability", Surfactant Sci. Ser., Vol. 74, Marcel Dekker, New York, 1998, p. 1-30.
4. a) W. von Rybininski and K. Hill, in "Novel Surfactants: Preparation, Application, and Biodegradability", Surfactant Sci. Ser., Vol. *74*, Marcel Dekker, New York, 1998, p. 31-85; b) Idem, Angew. Chem. Intern. Edn., 37 (1998) 1328-1345.
5. H. Luders and D. Balzer, in "Compte-rend. 2e Congr. mondial des agents de surface", Vol. 2, CESIO-ASPA, Paris, 1988, p. 81-93.
6. E. Lomax, Spec. Chem., 14 (1994) 21, 26; Y. Paik and G. Swift, Chem. & Ind. (1995) 55.
7. M.J. Schick (Ed.), Nonionic Surfactants, Surfactant Sci. Ser., Vol. 1, Marcel Dekker, New York, 1966.
8. N. Schönfeldt, Grenzflächenaktive Äthylenoxid-Addukte, Ihre Herstellung, Eigenschaften, Anwendung und Analyse (Surface Active Ethylene Oxide Derivatives, Their Production, Application and Analysis), Wissenschaft Verlag, Stuttgart, 1976.
9. N.M. van Os (Ed.), Nonionic Surfactants: Organic Chemistry, Surfactant Sci. Ser., Vol. 72), Marcel Dekker, New York, 1997.

10. W.M. Linfield (Ed.), Anionic Surfactants, Surfactant Sci. Ser., Vol. 7, New York: Marcel Dekker, 1976 (in two parts).
11. H.W. Stache (Ed.), Anionic Surfactants: Organic Chemistry, Surfactant Sci. Ser., Vol. 56, Marcel Dekker, New York, 1995.
12. S.M. Loktev (Ed.), Vysshiye Zhirnye Spirty (Higher Fatty Alcohols), Khimiya, Moscow, 1970.
13. E. Woollatt, The Manufacture of Soaps, Other Detergents and Glycerine, Ellis Horwood, Chichester, 1985.
14. G. Colombo, E. Faccetti, L. Valtorta, A. Zarbo and A. Zatta, Proceedings of the 4th World Surfactants Congress, Vol. 1, Barcelona, 3-7 VI 1996, AEPSAT, Barcelona, 1996, p. 213-226.
15. V.I. Bavika, G.V. Bakulina, in "Novye Processy Organicheskogo Sinteza" (New Processes in Organic Synthesis), S.P. Chernykh (Ed.), Khimiya, Moscow, 1989, pp. 199
16. a) I.R. Schmolka, J. Amer. Oil Chem. Soc., 54 (1977) 110-116; b) I.R. Schmolka, Cosmet. Toilet., 91 (1976) 64 ff.; c) I.R. Schmolka, Cosmet. Toilet., 97 (1982) 61 ff.; d) V.M. Nace, J. Am. Oil Chem. Soc., 73 (1996) 1-8.
17. S. Kucharski, Surface Active Alkylene Oxide Adducts: Structure and Properties, Monogr. Ser. ,Vol. 5, Wyd. Polytech. Wroclawskej, Wroclaw, 1978.
18. F.E. Bailey jr. and J.V. Koleske, Alkylene Oxide and Their Polymers, Surfactant Sci. Ser., Vol. 35, Marcel Dekker, New York, 1991.
19. P. Bahadur and G. Ries, Tenside Surfactants Detergents, 28 (1991) 173-179.
20. V.M. Nace (Ed.), Nonionic Surfactants: Polyoxyalkylene Block Copolymers, Surfactant Sci. Ser., Vol. 60, Marcel Dekker, New York, 1996.
21. I. Schlachter and G. Feldmann-Krane, in "Novel Surfactants: Preparation, Applications, and Biodegradability", Surfactant Sci. Ser., Vol. 74, K. Holmberg (Ed.), Marcel Dekker, New York, 1998, pp. 201-239.
22. a) D.R. Karsa (Ed.), Industrial Applications of Surfactants, Spec. Publ. Royal Soc. Chem., Vol. 59, Royal Soc. Chem., London 1987; b) D.R. Karsa (Ed.), Industrial Applications of Surfactants II, Spec. Publ. Royal Soc. Chem., Vol. 77, Royal Soc. Chem., London, 1990; c) D.R. Karsa (Ed.), Industrial Applications of Surfactants III, Spec. Publ. Royal Soc. Chem., Vol. 107, Royal Soc. Chem., London, 1993; d) D.R. Karsa, J.M. Goode and P.J. Donnely (Eds.), Surfactants Applications Directory, Blackie & Son, Glasgow, 1991.
23. M. Sagitani, Y. Hayashi and M. Ochiai, J. Am. Oil Chem. Soc. 66 (1989) 146-152.
24. *a*) J. Knaut and G. Kreienfeld, Chim. Oggi, 11 (1993) 41-46; *b*) P. Busch, H. Hensen and H. Hensen, Tenside Surf. Deterg., 30 (1993) 116-121.
25. Water-Soluble Polymers/ Ed. by N.M. Bikales, Plenum Press, New York-London, 1973.

26. V.Y. Bytenski and E.P. Kuznetsova, Proizvodstvo efirov tsellulozy (The Production of Cellulose Ethers), Khimiya, Leningrad, 1974.
27. Water-Soluble Synthetic Polymers: Properties and Behavior, CRC Press, Boca Raton, (USA), 1984.
28. a) W. Steiner, D. Haltrich and R.M. Lafferty, in „Biosurfactants: Production, Properties, Applications, Surfactant Sci. Ser., Vol. 48)"/. ,Marcel Dekker, New York, 1994, pp. 175-203; b) S. Lang and F. Wagner, Ibid., pp. 205-229.
29. *a*) L.M. Landoll, J. Polym. Sci. Polym. Chem. Ed. 20 (1982) 443-455; b) P. Hodul, Tenside Deterg. 22 (1985) 114-116.
30. I. Piirma, Polymeric Surfactants, Surfactant Sci. Ser., Vol. 42, Marcel Dekker, New York, 1993.
31. a) Biosurfactants and Biotechnology, Surfactant Sci. Ser., Vol. 25, N. Kosaric, W.L. Cairns and N.C. Gray (Eds.), Marcel Dekker, New York, 1987; b) Biosurfactants: Production, Properties, Applications, Surfactant Sci. Ser., Vol. 48, N. Kosaric (Ed.), Marcel Dekker, New York, 1994.
32. a) E. Rosenberg, CRC Crit. Rev. Biochem. 3 (1988) 109-132; b) J.D. Desai and I.M. Banat, Microbiol. & Molec. Biol. Rev. 61 (1997) 47-64.
33. E. Vulfson, in „Novel Surfactants: Preparation, Application, and Biodegradability, Surfactant Sci. Ser., Vol. 74, Marcel Dekker, New York, 1998, p. 279-299.
34. M. Svensson, In „Novel Surfactants: Preparation, Application, and Biodegradability", Surfactant Sci. Ser., Vol. 74, Marcel Dekker, New York, 1998, p. 179-200.
35. K.W. Dillan, G.C. Johnson and P.A. Siracusa, HAPPI 23 (1986) 52-54, 123.
36. a) K.L. Matheson, T.P. Matson and K. Yang, J. Am. Oil Chem. Soc. 63 (1986), 365-370; b) M.F. Cox – *Ibid.* 66 (1989) 367-374.
37. W. Hreczuch and J. Szymanowski, J. Am. Oil Chem. Soc. 73 (1996) 73-78.
38. Y.C. Chiu, L.J. Chen and W.I. Pien, Colloids Surfaces, 34 (1988/89) 23-42.
39. McCutcheon's Emulsifiers and Detergents, Intern. Edn. - Glen Rock, N.J.: MC Publ. Co., 1982.
40. R.D. Swisher, Surfactant Biodegradation, 2nd Edn., Surfactant Sci. Ser., Vol. 18, Marcel Dekker, New York, 1987.
41. Detergents in the Environment, Surfactant Sci. Ser., Vol. 65, M.J. Schwuger (Ed.), Marcel Dekker, New York, 1996.
42. a) S. Friberg (Ed.), Food Emulsions, Food Sci. Ser., Vol. 5, Marcel Dekker, New York, 1976; b) G. Schuster, Emulgatoren für Lebensmittel, Emulsifiers in Food, Springer-Verlag, Heidelberg-Berlin, 1985.
43. G. Charalambous and G. Doxostakis (Eds.), Food Emulsifiers: Chemistry, Technology, Functional Properties and Applications, Develop. Food Sci., Vol. 19, - Amsterdam: Elsevier Sci. Publ., 1989.

44. Surfactants in Cosmetics, Surfactant Sci. Ser., Vol. 16, M.M. Rieger (Ed.), Marcel Dekker, New York, 1985.
45. M.Y. Pletnev, Kosmetiko-gigienitcheskije moyushchije sredstva, Cosmetic and Personal Care Detergents, Khimiya, Moscow, 1990.
46. D.F. Williams and W.M. Schmitt, Chemistry and Technology of the Cosmetics and Toiletries, Chapman & Hall, New York, 1992.
47. a) G. De Grandis and L. Maggesi, Riv. Ital. Essenze Parfumi Piante Offic. Aromi Saponi Cosmet. Aerosol 56 (1974), 371-379; b) A.L.L. Hunting, Cosmet. Toilet., 96(1981)29-34.
48. a) H. Meijer, Seifen-Öle-Fette-Wachse 113 (1987) 135-139; b) H. Meijer, Ibid. 116 (1990) 251-257.
49. D.L. Chang and H.L. Rosano, in „Structure/Performance Relations in Surfactants, ACS Symp. Ser., Vol. 253, Am. Chem. Soc., Washington, 1984, pp. 129-140.
50. J.G. Weers, J.F. Rathman and D.R. Scheuing, Colloid Polym. Sci. 268 (1990), 832-846.
51. Z.H. Zhu, D. Yang and M.J. Rosen, J. Am. Oil Chem. Soc. 66 (1989) 998-1001.
52. P.S. Belov, V.I. Frolov and B.E. Tshistyakov, Novye poverkhnostno-aktivnye veschestva na osnove zamschennykh imidazolinov (New Surfactants Based on Substituted Imidazolines), NIITEKhim, Moscow, 1975.
53. Y. Koide, in „Structure – Performance Relations in Surfactants, Surfactant Sci. Ser., Vol. 70, K. Esumi and M. Ueno (Eds.), Marcel Dekker, New York, 1997, p. 227-254.
54. Nonionic Surfactants: Physical Chemistry, Surfactant Sci. Ser., Vol. 23, M.J. Schick (Ed.), Marcel Dekker, New York, 1987.
55. B. Fell, in „Anionic Surfactants: Organic Chemistry, Surfactant Sci. Ser., Vol. 56, Marcel Dekker, New York, 1995, pp. 1-37.
56. H. Stüpel, Synthetische Wasch- und Reinigungsmittel: Chemie, Klassifikation, Technologie, Komposition, Anwendung, Untersuchungsmethoden und Wirtschaftliche Bedeutung, 2. Auflage (Synthetic Washing and Cleaning Agents, 2nd Edn.), Konradin-Verlag, Stuttgart, 1957, Ch. 2.
57. A.M. Schwartz, J.W. Perry and J. Berch, Surface Active Agents and Detergents, Interscience, New York, 1958, Ch. 2.
58. G.L. Bitman, V.R. Gurevich, Ya.I. Isakov, V.V. Lobkina, A.S. Loktev, G.P. Pavlov, S.L. Plaskunova, et al., in „Novye Processy Organicheskogo Sinteza (New Processes in Organic Synthesis)", S.P. Chernykh (Ed.), Khimiya, Moscow, 1989, pp. 128-163.
59. G. Hons, in „Anionic Surfactants: Organic Chemistry", Surfactant Sci. Ser., Vol. 56, Marcel Dekker, New York, 1995, pp. 39-108.
60. B.V. Vora, P.R. Pujado, T. Imai and T.R. Fritsch, Tenside Surfactants Detergents, 28 (1991) 287-293.
61. E.E. Gilbert, Sulfonation and Related Reactions, Wiley-Interscience, New York, 1965.

62. W.H. De Groot, Sulfonation Technology in the Detergent Industry, Kluwer Academic, Dordrecht, 1991.
63. V.G. Pravdin, M.A. Podustov and D.I. Zemenkov, Sulphonation and Sulphation of Petrochemical Products with Gaseous SO_3 in the Production of Surfactants, Subject Review (in Russian), TsNIITE-Neftekhim, Moscow, 1981.
64. G.F. Moretti, I. Adami and W.H. de Groot, in „Anionic Surfactants: Organic Chemistry", Surfactant Sci. Ser., Vol. 56, Marcel Dekker, New York, 1995, pp. 647-696.
65. D.W. Roberts, Org. Process Res. & Develop. 2 (1998) 194-202.
66. H. Berthold, S. Brandel, K. Dietzsch, et al., Alkan Sulfonate (Alkanesulphonates), H.G. Hauthal (Ed.), Deutsch. Verlag für Grundstoffind., Leipzig, 1985.
67. J.M. Quack and M. Trautmann, Tenside Deterg. 22 (1985) 281-289.
68. Alpha Olefins Applications Handbook, G.R. Lappin and J.D. Sauer (Eds.), Marcel Dekker, New York, 1989, p. 139 ff.
69. N.M. van Os, R. van Ginkel, A. van Zon, et al., in „Anionic Surfactants: Organic Chemistry", Surfactant Sci. Ser., Vol. 56, Marcel Dekker, New York, 1995, pp. 363-459.
70. M.J. Schwuger and H. Lewandowski, in „Anionic Surfactants: Organic Chemistry", Surfactant Sci. Ser., Vol. 56, Marcel Dekker, New York, 1995, pp. 461-499.
71. K. Schmid, H. Baumann, W. Stein and H. Dolhaine, in „Welt-Tensid-Kongress: Tenside in unserer Welt heute und morgen (Proc. World Surfactants Congr., 2, Munich)", Kürle Verlag, Gelnhausen, 1984, p. 105 ff.
72. A.E. Sherry, B.E. Chapman, M.T. Creedon, J.M. Jordan and R.L. Moese, J. Am. Oil Chem. Soc. 72 (1995) 835-841.
73. R.B. Login, HAPPI 21 (1984) 56, 58, 60, 88.
74. S.I. Faingold, A.E. Kuusk and H.E. Kijk, Khimiya anionnykh i amfolitnykh azotsoderzhashchikh poverkh-nostno-aktivnyh veshchestv (Chemistry of Nitrogen-Containing Anionic and Amphoteric Surfactants), Valgus, Tallinn, 1984.
75. E.K. Anufriev and I.G. Reznikov, Poverkhnostno-aktivnye proizvodnye sulfoyantarnoj kisloty (Surfase-Active Derivatives of Sulphosuccinic Acid), TsNIITENeftekhim, Moscow, 1966.
76. A. Domsch and B. Irrgang, in „Anionic Surfactants: Organic Chemistry", Surfactant Sci. Ser., Vol. 56, Marcel Dekker, New York, 1995, pp. 501-549.
77. a) S. Yanagida, Y. Shimada, I. Ikeda, et al., Yukagaku 26 (1977) 283-286; b) T. Takeda, Kagaku to Kogyo 60 (1986) 48-56; c) A.S. Gordeev, N.M. Shevereva, R.V. Rodionova and V.A. Volkov, Kolloidn. Zh. 52 (1990) 574-578.
78. a) G. Barker, Soap Cosmet. Chem. Spec. 61 (1985) 30-32, 44, 45; b) Z.P. Perel, R.S. Vasko and N.F. Kolpina, in „Novye razrabotki i dostizheniya v tekhnologii proizvodstva PAV (New Developments and Advances in the Technology of Surfactants)", TsNIITENeftekhim, Moscow, 1987, pp. 14-18.

79. I.G. Reznikov and E.K. Anufriev, Poverkhnostno-aktivnye proizvodnye monoamidov sulfoyantarnoj kisloty (Surface Active Derivatives of Sulphosuccinic Acid Monoamides), TsNIITENeftekhim, Moscow, 1971.
80. a) I.S. Akhmetzhanov, L.V. Androsova, A.I. Menyajlo, S.N. Sementsov, and V.I. Yakovleva, Anionnye PAV na osnove oxietilirovannykh spirtov i alkylfenolov (Anionic Surfactants Derived from Ethoxylated Alcohols and Alkylphenols, Review), TsNIITENeftekhim, Moscow, 1988; b) R.A. Jacobs, Soap Cosmet. Chem. Spec. 63 (1987) 41-42, 57.
81. R. Tsushima, Proceedings of the 4th World Surfactants Congress, Vol. 1, Barcelona, 3-7 VI 1996, AEPSAT, Barcelona, 1996, pp. 43-56.
82. X. Domingo, In „Anionic Surfactants: Organic Chemistry", Surfactant Sci. Ser., Vol. 56, Marcel Dekker, New York, 1995, pp. 223-312.
83. K. Rasheed, J. Gray and J. Fulton, Proceedings of the 4th World Surfactants Congress, Vol. 1, Barcelona, 3-7 VI 1996, AEPSAT, Barcelona, 1996, pp. 578-584.
84. a) M. Hato, M. Tahara and Y. Suda, J. Colloid Interface Sci. 72 (1979) 458-464; b) K. Shinoda and K. Fontell, Adv. Colloid Interface Sci. 54 (1995) 55-72.
85. a) W.M. Linfield, Rev. Franc. Corps Gras 32 (1985) 371-375; b) W.M. Linfield, in „Detergency: Theory and Technology" Surfactant Sci. Ser., Vol. 20, Marcel Dekker, New York, 1987, pp. 441-457; c) W.M. Linfield, Tenside Surfactants Detergents 27 (1990) 159-161.
86. P. Hövelmann, In „World Conference and Exhibition on Environmental Challenges in Oilseeds Processing, Surfactants, Detergents, and Oleochemicals. Abstr.", AOCS, Champaign, 1997.
87. Anonym, HAPPI 27 (1990) 18.
88. K.D. Haase, A.J. Heynen and N.L.M. Laane, Fat Sci. Technol. 91 (1989) 350-353.
89. N.A. Glukhareva and M.Y. Pletnev, in „Intern. Conference on Colloid Chemistry and Physical-Chemical Mechanics Dedicated to the Centennial of the Birthday of P.A. Rehbinder, 4-8 Oct. 1998", Russ. Acad. Sci., Moscow, 1998, Sec. B.
90. a) M. Frenkel, C. Krauz and N. Garti, Colloids Surfaces 5 (1982) 353-362; b) N. Garti and A. Aserin, J. Dispers. Sci. & Technol. 6 (1985) 175-191.
91. H. Meijer and J.K. Smid, in „Anionic Surfactants: Organic Chemistry" Surfactant Sci. Ser., Vol. 56, Marcel Dekker, New York, 1995, pp. 313-361.
92. W.W. Schmidt, D.R. Durante, R. Gingell and J.W. Harbell, J. Amer. Oil Chem. Soc. 74 (1997) 25-31.
93. a) K. Sakamoto, Yukagaku 44 (1995) 256-265; b) M. Takehara, Hyomen 22 (1984) 459-473, 512-527; c) V.N. Iyer and V.V.R. Subrahmanyam, J. Indian Chem. Soc. 562 (1985) 507-512.

94. B.E. Tchistyakov, I.T. Polkovnichenko and P.E. Tchaplanov, Fosforsoderzhashchie poverkhnostno-aktivnye veshchestva (Phosphorus-Containing Surfactants. Subject Rev.), TsNIITENeftekhim, Moscow, 1979.
95. a) T. Kurosaki, G. Imokawa and A. Ishida, Yukagaku 36 (1987) 629-640; b) T. Kurosaki, H. Furugaki, A. Matsunaga, M. Yuzawa and A. Nanba, ibid. 39 (1990) 250-258.
96. G. Wasow, in „Anionic Surfactants: Organic Chemistry" Surfactant Sci. Ser., Vol. 56, Marcel Dekker, New York, 1995, pp. 551-629.
97. D.N. Rubingh and T. Jones, Ind. Eng. Chem. Prod. Res. Dev. 21 (1982) 176-182.
98. Cationic Surfactants. Physical Chemistry, Surfactant Sci. Ser., Vol. 37. D.N. Rubingh and P.M. Holland (Eds.), Marcel Dekker, New York, 1991.
99. Liquid Detergents, Surfactant Sci. Ser., Vol. 67, K.-L. Lai (Ed.), Marcel Dekker, New York, 1996.
100. Powdered Detergents, Surfactant Sci. Ser., Vol. 71, M.S. Showell (Ed.), Marcel Dekker, New York, 1997.
101. Cationic Surfactants, Surfactant Sci. Ser., Vol. 4, E. Jungermann (Ed.), Marcel Dekker, New York, 1970.
102. a) Cationic Surfactants: Organic Chemistry, Surfactant Sci. Ser., Vol. 34, J.M. Richmond (Ed.), Marcel Dekker, New York, 1990; b) S. Billenstein and G. Blaschke, J. Am. Oil Chem. Soc. 61 (1984) 353-357.
103. Oleochemicals, Proc. World Conference, Montreux, Switz., Sept. 18-23, 1983 in J. Am. Oil Chem. Soc. 61 (1984).
104. A.D. Russell, W.B. Hugo and G.A.J. Ayliffe (Eds.), Principles and Practice of Desinfection, Preservation and Sterilisation, Blackwell Sci. Publ., Oxford, 1982.
105. M.L. Schlossman, Seifen-Öle-Fette-Wachse 103 (1977) 187-190.
106. a) Cospha Protein Hydrolysates and Protein Derivatives, Henkel KGaA, Düsseldorf, 1992; b) Cospha Products from A to Z, Henkel KGaA, Düsseldorf (Ger.), 1997.
107. a) R. Zana, in „Novel Surfactants: Preparation, Application, and Biodegradability", Surfactant Sci. Ser., Vol. 74, Marcel Dekker, New York, 1998, pp. 241-275; b) R.M. Infante, L. Pérez and A. Pinazo, Ibid., pp. 87-114; c) L. Pérez, I. Ribosa, T. Garcia, A. Manresa, and M.R. Infante, in "Proceedings of the 4th World Surfactants Congress", Vol. 1, Barcelona, 3-7 VI 1996", AEPSAT, Barcelona, 1996, pp. 558-565.
108. G. Krüger, D. Boltersdorf and K. Overkempe, in „Novel Surfactants: Preparation, Application, and Biodegradability" Surfactant Sci. Ser., Vol. 74, Marcel Dekker, New York, 1998, pp. 115-137.
109. H. Yokota, SÖFW-J. 121 (1995) 115-117.
110. D. Schaefer, Tenside Surfactants Detergents 27 (1990) 154-158.
111. Amphoteric Surfactants, Surfactant Sci. Ser., Vol. 12, B.R. Bluestein and C.L. Hilton (Eds.), Marcel Dekker, New York, 1982.

112. T. Takeda, Kagaku to Kogyo 58 (1984) 86-95.
113. Y. Chevalier, S. Brunel and P. Leperchec, J. Chim. Phys. Phys.-Chim. Biol. 92 (1995) 1025-1042.
114. a) T. Takeshita, I. Wakebe and S. Maeda, J. Am. Oil Chem. Soc. 57 (1980) 430-434; b) T. Takeshita, T.A. Shimohara and S. Maeda, Ibid. 59 (1982) 104-107; c) S. Maeda, K. Nagayama, M. Imayoshi and T. Tekeshita, Yukagaku 31 (1982) 47-51; d) S. Maeda, M. Fukushima, M. Imayoshi and T. Takeshita, Yukagaku 31 (1982) 1027-1029; e) B.A. Parker and J.J. Crudden, Proceedings of the 4th World Surfactants Congress, Vol. 1, Barcelona, 3-7 VI 1996, AEPSAT, Barcelona, 1996, pp. 446-460.
115. Protein Structure, Function and Industrial Applications, E. Hofmann and E. Pfeil (Eds.), Pergamon Press, Elmsford (UK), 1979.
116. J.J. Bikerman, Foams, Appl. Phys. Eng., Vol. 10, Springer-Verlag, New York, 1973, pp. 128-132.
117. H. Yokota, K. Sagawa, Ch. Eguchi and M. Takehara, J. Am. Oil Chem. Soc. 62 (1985) 1716-1719.
118. V.A. Garrand, Cosmet. Toilet. 100 (1985) 77-80.
119. R. Ohme, D. Ballschuh and H. Seibt, Tenside Surfact. Deterg. 28 (1991) 180-184, 235-240.
120. a) M. Okazaki and I. Hara, Yukagaku 30 (1981) 553-557; b) F. Kanetani, K. Negoro and E. Okada, Nippon Kagaku Kaishi (1984), 1452-1458.
121. D. Attwood and A.T. Florence, Surfactant Systems: Their Chemistry, Pharmacy and Biology, Chapman & Hall, London, 1983.
122. J. Knowlton and S. Pearce, Handbook of Cosmetic Science and Technology, Elsevier, London, 1993.
123. H.C. Fielding, in „Organofluorine Chemicals and Their Industrial Applications"/ Ed. by R.E. Banks, SCI-Publishing, London-Chichester, 1979, pp. 214-233.
124. J.N. Meussdörffer and H. Niederprüm, Chem.-Ztg. 104 (1980) 45-52.
125. M. Matzuo, in "Novoye v tekhnologii soedinenij ftora" (Rus./Jap. Transl.: "Fluorine Compounds. Modern Technology and Application"), N. Ishikawa (Ed.), Mir Publ., Moscow, 1984, pp. 385-422.
126. E. Kissa, Fluorinated Surfactants – Synthesis, Properties, Applications, Surfactant Sci. Ser., Vol. 50, Marcel Dekker, New York, 1993.
127. a) A.T. Kuhn (Ed.), Industrial Electrochemical Processes, Elsevier, Amsterdam, 1971; b) T. Abe and S. Nagase, in „Preparation, Properties and Industrial Applications of Organofluorine Compounds" R.E. Banks (Ed.), Ellis Horwood, Cichester; Halsted Press, New York, 1982, pp. 19-43.
128. a) L.A. Shits, L.V. Dikhtievskaya, S.P. Krukovskii, L.V. Cherednitchenko and V.A. Ponomarenko, Kolloidn. Zh. 38 (1976) 1130-1135; b) K. Ogino, H. Murakami,

N. Ishikawa and M. Sasabe, Yukagaku 32 (1983) 96-101; c) N. Ishikawa and M. Sasabe, J. Fluorine Chem. 25 (1984) 241-253; d) G. Caporiccio, F. Burzio, G. Carniselli and V. Biancardi, J. Colloid Interface Sci. 98 (1984) 202-209.

129. Th.F. Tadros, J. Colloid Interface Sci. 74 (1980) 196-200.
130. I. Ikeda, M. Tsuji and M. Okahara, Tenside Surfactants Detergents 24 (1987) 272-274.
131. V. Krier, C. Bassilana, B. Martin and A. Cambon, Tenside Surfactants Detergents 35 (1998) 160-164.
132. a) L.L. Gervitz, K.N. Makarov and L.F. Komarova, Izvest. AN SSSR Ser. Khim. (1974), 2256-2259; b) L.L. Gervitz, K.N. Makarov and M.Y. Pletnev, Zhurn. VkhO im. Mendeleeva 30 (1985) 578-580.
133. M.Y. Pletnev, A.F. Eleev and A.F. Ermolov, Kolloidn. Zh. 52 (1990) 804-805.
134. E. Kissa, in „Chemical Processing of Fibers and Fabrics. Functional Finishes. Pt. B, Handbook Fiber Sci. & Technol., Vol. 2, M. Lewin and S.B. Sello (Eds.), Marcel Dekker, New York, 1984, pp. 211-289.
135. M. LeBlanc and J.G. Riess, in „Preparation, Properties and Industrial Applications of Organofluorine Compounds", R.E. Banks (Ed.), Ellis Horwood, Cichester, Halsted Press, New York, 1982, pp. 83-138.
136. a) K. Yokoyama, T. Suyama and R. Naito, in „Biomedical Aspects of Fluorine Chemistry", R. Filler and Y. Kobayashi (Eds.), Kodansha, Tokyo; Elsevier, Amsterdam, 1982, 191-212; b) Y. Kobayashi, I. Kumagane and T. Taguchi, in „Novoye v tekhnologii soedinenij ftora (Rus./Jap. Transl.: Fluorine Compounds. Modern Technology and Application)", N. Ishikawa (Ed.), Mir Publ., Moscow, 1984, pp. 447-499.
137. G. Mathis, P. Leempoel, J.-C. Ravey, C. Selve and J.-J. Delpuech, J. Am. Chem. Soc. 106 (1984) 6162-6171; b) C. Selve, E.M. Moumi and J.-J. Delpuech, J. Chem. Soc. Chem. Commun. (1987), 1437-1438; c) S. Achilefu, C. Selve, M.-J. Stebe, *et al.*, Langmuir 10 (1994) 2131-2138; d) J.C. Ravey and M.-J. Stebe, Colloids Surfaces A, 84 (1994) 11-31.
138. a) S. Szönyi, H.J. Watzke and A. Cambon, Progr. Colloid & Polym. Sci. 89 (1992) 149-155; b) T. Kunitake, in „Templating, Self-Assembly, and Self-Organisation", Comprehens. Supramol. Chem., Vol. 9, J.-P. Sauvage and M.W. Hosseini (Ed.), Plenum/ Elsevier, Oxford, 1996, pp. 351-406.
139. I. Langmuir, in „Colloid Symposium Monograph" Book Dep. Chem. Catalog Comp., New York, 1925, p. 48.
140. a) P. Rehbinder, Zhurn. VKhO im. Mendeleeva 11 (1966) 362-369; b) P. Rehbinder, Izbrannye trudy: Poverkhnostnye yavleniya v dispersnykh sistemakh. Kolloidnaya khimiya (Selected Works: Surface Phenomena in Disperse Systems. Colloid Chemistry), Nauka, Moscow, 1978, pp. 157-181.

141. M.J. Rosen, Surfactants and Interfacial Phenomena, 2nd Edn., John Wiley, New York, 1989.
142. M.J. Rosen (Ed.), Structure/Performance Relations in Surfactants, ACS Symp. Ser., Vol. 253, Am. Chem. Soc., Washington, 1984.
143. K. Esumi and M. Ueno (Eds.), Structure-Performance Relationships in Surfactants, Surfactant Sci. Ser., Vol. 70, Marcel Dekker, New York, 1997.
144. J.T. Davies and E.K. Rideal, Interfacial Phenomena, Academic Press, New York, 1961.
145. L.I. Osipow, Surface Chemistry: Theory and Industrial Applications, Reinhold, New York, 1963.
146. A.I. Rusanov, Micelloobrazovanie v rastvorakh poverkhnostno-aktivnyh veshchestv (Micelle Formation in Surfactant Solutions), Khimiya, St.-Petersburg, 1992.
147. K.J. Mysels, Langmuir, 2 (1986) 423-428.
148. a) K. Motomura, Adv. Colloid Interface Sci., 12 (1980) 1-42; b) K. Motomura, S.-I. Iwanaga, M. Yamanaka, M. Aratono and R. Matura, J. Colloid Interface Sci., 86 (1982) 151-157; c) M. Yamanaka, M. Aratono, H. Iyota, K. Motomura and R. Matura, Bull. Chem. Soc. Jap., 55 (1982) 2744-2748.
149. P. Sherman (Ed.), Emulsion Science, Academic Press, London - New York, 1968.
150. K.J. Lissant (Ed.), Emulsions and Emulsion Technology, Surfactant Sci. Ser., Vol. 6, Marcel Dekker, New York, 1974/84.
150. B.J. Carrol, in "Surface and Colloid Science", Vol. 9, E. Matievič (Ed.), Wiley-Interscience, New York, 1976, pp. 1-67.
151. S. Friberg (Ed.), Food Emulsions, Food Sci. Ser., Vol. 5, Marcel Dekker, New York – Basel, 1976.
152. P. Becher (Ed.), Encyclopedia of Emulsion Technology, Vol. 1: Basic Theory, Marcel Dekker, New York, 1983.
153. L.L. Schramm (Ed.), Emulsions: Fundamentals and Applications in the Petroleum Industry, Adv. Chem. Ser., Vol. 231, Am. Chem. Soc., Washington, DC, 1992.
154. a) K. Shinoda and S. Friberg, Adv. Colloid Interface Sci. 4 (1975) 281-300; b) S.E. Friberg, Progr. Colloid Polym. Sci. 68 (1983) 41-47; c) S.E. Friberg, J. Dispers. Sci. Technol. 6 (1985) 317-337; d) S.E. Friberg and P. Rothorel (Eds.), Microemulsions: Structure and Dynamics, CRC Press, Boca Raton, FL, 1987.
155. L.M. Prince (Ed.), Microemulsions: Theory and Practice, Academic Press, New York - San Francisco –London, 1977.
156. M. Rosoff, Progr. Surface & Membrane Sci. 12 (1978) 405-477.
157. S.L. Holt, J. Dispers. Sci. & Technol. 1 (1980) 423-464.
158. I.D. Robb, Microemulsions: Proc. Conf. Phys. Chem.: Microemulsions, 1980, Plenum Press, New York – London, 1982.
159. E.D. Shchukin and L.A. Kochanova, Kolloidn. Zh. 45 (1983) 726-736.

160. A.M. Bellocq, J. Biais, P. Bothorel, et al., Adv. Colloid Interface Sci. 20 (1984) 167-272.
161. D.O. Shah (Ed.), Macro- and Microemulsions: Theory and Applications. Symp. 186th Meet. Amer. Chem. Soc., Wash., Aug. 28-Sept.2, 1983, Am. Chem. Soc., Washington, D.C., 1985.
162. J.Th.G. Overbeek, Proc. Konink. Ned. B, 89 (1986) 61-78.
163. H.L. Rosano and M. Clausse (Eds.), Microemulsion Systems, Surfactant Sci. Ser., Vol. 24, Marcel Dekker, New York, 1987.
164. M. Bourrel and R.S. Schechter, Microemulsions and Related Systems: Formulation, Solvency, and Physical Properties, Surfactant Sci. Ser., Vol. 30, Marcel Dekker, New York, 1988.
165. S.-H. Chen and R. Rajagopalan, Micellar Solutions and Microemulsions, Springer, Berlin, 1990.
166. J. Pore, Emulsions, Microemulsions, and Multiple Emulsions (in French), Ed. Techn. Ind. Corps Gras, Neuilly/Seine, 1992.
167. K. Stickdorn, M.J. Schwuger and R. Schomacker, Tenside Surfact. Deterg. 31 (1994) 218-228.
168. C. Solans and H. Kunieda, Industrial Applications of Microemulsions, Surfactant Sci. Ser., Vol. 66, Marcel Dekker, New York, 1996.
169. S.P. Moulik and B.K. Paul, Adv. Colloid Interface Sci. 78 (1998) 99-195.
170. D.J. McClements, Food Emulsions: Principles, Practice, and Techniques, CRC Press, Boca Raton, FL, 1998.
171. G. Jakobi and A. Lohr, Detergents and Textile Washing: Principles and Practice, VCH Publ., New York, 1987.
172. W.G. Cutler and E. Kissa (Eds.), Detergency: Theory and Technology, Surfactant Sci. Ser., Vol. 20, Marcel Dekker, New York, 1987.
173. W. Black in „Dispersion of Powders in Liquids", 3rd Edn/ Ed. by G.D. Parfitt, Appl. Sci. Publ., London, 1981, pp. 149-201.
174. V.K. Bansal and D.O. Shah in „Micellization, Solubilization and Microemulsions", Vol. 1, K.L. Mittal (Ed.), Plenum Press, New York, 1977, pp. 87-103.
175. J.C. Morgan, R.S. Schechter and W.H. Wade in „Solution Chemistry of Surfactants", Vol. 2, K.L. Mittal (Ed.), Plenum Press, New York – London, 1979, pp. 749-775.
176. D.H. Smith (Ed.), Surfactant-Based Mobility Control: Progress in Miscible-Flood Enhanced Oil Recovery, ACS Symp. Ser., Vol. 373, Am. Chem. Soc., Washington, D.C., 1988.
177. N.R. Morrow (Ed.), Interfacial Phenomena in Petroleum Recovery, Surfactant Sci. Ser., Vol. 36, Marcel Dekker, New York, 1991.

178. a) F. Sebba, Foams and Biliquid Foams – Aphrons, John Wiley, New York, 1987; b) R.K. Prud'homme and S.A. Khan (Eds.), Foams: Theory, Measurements, and Applications, Surfactant Sci. Ser., Vol. 57, Marcel Dekker, New York, 1996.
179. J.F. Scamehorn (Ed.), Phenomena in Mixed Surfactant Systems, ACS Symp. Ser., Vol. 311, Am. Chem. Soc., Washington, D.C., 1986.
180. M.Y. Pletnev in „Uspekhi kolloidnoi Khimii (Progress in Colloid Chemistry)", A.I. Rusanov (Ed.), Khimiya, St.-Petersburg, 1991, pp. 60-82.
181. P.M. Holland and D.N. Rubingh (Eds.), Mixed Surfactant Systems, ACS Symp. Ser., Vol. 501, Am. Chem. Soc., Washington, D.C., 1992.
182. K. Ogino and M. Abe (Eds.), Mixed Surfactant Systems, Surfactant Sci. Ser., Vol. 46, Marcel Dekker, New York, 1993.
183. V.B. Fainerman, Usp. Khimii 54 (1985) 1613-1631.
184. C.A. Miller and P. Neogi (Eds.), Interfacial Phenomena: Equilibrium and Dynamic Effects, Surfactant Sci. Ser., Vol. 17, Marcel Dekker, New York, 1985.
185. S.G. Dukhin, G. Kretzschmar, and R. Miller (Eds.), Dynamics of Adsorption at Liquid Interfaces: Theory, Experiment, Application, Studies in Interface Science, Vol. 1, Elsevier, Amsterdam, 1995.
186. a) R. Miller, K. Lunkenheimer, Colloid Polym. Sci. 260 (1982) 1148-1150; b) R. Miller, K.-H. Schano, Ibid. 264 (1986) 277-281; c) K. Lunkenheimer, K. Haage, and R. Miller, Colloids Surfaces 22 (1987) 215-228.
187. F. Ravera, M. Ferrari, L. Liggieri, and R. Miller, Progr. Colloid Polym. Sci. 105 (1997) 346-350.
188. E.H. Lucassen-Reynders (Ed.), Anionic Surfactants. Physical Chemistry of Surfactant Action, Surfactant Sci. Ser., Vol. 11, Marcel Dekker, New York, 1981.
189. a) B.A. Noskov, D.O. Grigoriev, R. Miller, J. Colloid Interface Sci. 188 (1997) 9-15; a) B.A. Noskov, D.O. Grigoriev, R. Miller, Langmuir 13 (1997) 295-298.
190. P.M. Kruglyakov, Hydrophyle-Lypophile Balance of Surfactants and Solid Particles. Physicochemical Aspects and Applications, Studies in Interface Science, Vol. 9, Elsevier, Amsterdam - New York, 2000.
191. a) W.C. Griffin, J. Soc. Cosmet. Chem. 1 (1949) 311-326; b) W.C. Griffin, J. Soc. Cosmet. Chem. 5 (1954) 249-262.
192. R. Sowada, J.C. McGowan, Tenside Surfact. Deterg. 29 (1992) 109-113.
193. a) K. Shinoda, H. Arai, J. Phys. Chem. 68 (1964) 3485-3490; b) K. Shinoda, J. Colloid Interface Sci. 24 (1967) 4-9; c) K. Shinoda, T. Yoneyama, and H. Tsutsumi, J. Dispersion Sci. & Technol. 1 (1980) 1-12.
194. A.M. Koganovski and N.A. Klimenko, Physico-Chemical Backgrounds of Recovery of Surfactants from Aqueous Solutions and Sewage (in Russ.), Naukova Dumka, Kiev, 1978.

195. a) J.S. Clunie and B.T. Ingram in „Adsorption from Solution at the Solid/Liquid Interface", Academic Press, London - New York, 1983, pp. 105-152; b) D.B. Hough and H.M. Rendall, ibid, pp. 247-319.
196. B. Dobias, Structure & Bonding 56 (1984) 91-147.
197. Th.F. Tadros (Ed.), Surfactants, Academic Press, London, 1984.
198. P. Somasundaran and B.M. Moudgil (Eds.), Reagents in Mineral Technology, Surfactant Sci. Ser., Vol. 22, Marcel Dekker, New York, 1987.
199. A.K. Chattopadhyay and K.L. Mittal (Eds.), Surfactants in Solution, Surfactant Sci. Ser., Vol. 64, Marcel Dekker, New York, 1996.
200. F. Franks in „Water: a Comprehensive Treatise, Vol. 4: Aqueous Solutions of Amphiphiles and Macromolecules", Plenum Press, New York – London, 1979, Chap. 1.
201. G.S. Hartley, Aqueous Solutions of Paraffin-Chain Salts: a Study in Micelle Formation, Hermann & Co., London, 1936.
202. C.J. O'Connor and R.G. Wallace, Adv. Colloid Interface Sci. 22 (1985) 1-111.
203. B. Lindman and H. Wennerström, in „Micelles (Top. Current Chem., Vol. 87)", Springer-Verlag, Berlin, 1980, pp. 1-83.
204. S. Ozeki, Hyomen 20 (1982) 632-648.
205. a) P.J. Missel, N.A. Mazer, M.C. Carey, and G.B. Benedek, in „Solution Behavior of Surfactants", Vol. 1, K.L. Mittal and E.J. Fendler (Eds.), Plenum Press, New York, 1982, pp. 373-388; b) Idem, J. Phys. Chem. 87 (1983) 1264-1277.
206. a) P.T.T. Wong, H.H. Mantsch, J. Phys. Chem. 87 (1983) 2436-2443; b) W.E. McMullen, A. Ben-Shaul, W.H. Gelbart, J. Colloid Interface Sci. 98 (1984) 523-536.
207. a) H. Rehage and H. Hoffmann, Faraday Discuss. Chem. Soc. (1983) 363-373; b) H. Hoffmann, H. Rehage, W. Schorr, and H. Thurn, in „Surfactants in Solution", Vol. 1, K.L. Mittal and B. Lindman (Eds.), Plenum Press, New York, 1984, pp. 425-454; c) O. Bayer, H. Hoffmann, W. Ulbricht, and H. Thurn, Adv. Colloid Interface Sci. 26 (1986) 177-203; d) H. Hoffmann, Ber. Bunsen-Ges. Phys. Chem. 98 (1994) 1433-1455.
208. A.I. Serdyuk and R.V. Kucher, Micellar Transitions in Surfactant Solutions (in Russ.), Naukova Dumka, Kiev, 1987.
209. a) T. Shikata, Y. Sakaiguchi, H. Uragami, H. Hirata, J. Colloid Interface Sci. 119 (1987) 291-293; b) Idem, Colloid Polym. Sci. 265 (1987) 750-753; c) T. Shikata, H. Hirata, Langmuir 3 (1987) 1081-108; d) Y. Sakaiguchi, T. Shikata, H. Urakami, A. Tamura, H. Hirata, J. Electron Microsc. 36 (1987) 168-176; e) H. Hirata, M. Sato, Y. Sakaiguchi, Y. Katsube, Colloid Polym. Sci. 266 (1988) 862-864.
210. S.J. Bachofer, R.M. Turbitt, J. Colloid Interface Sci. 135 (1990) 325-334.

211. a) F.M. Menger, D.Y. Williams, A.L. Underwood, E.W. Anacker, J. Colloid Interface Sci. 90 (1982) 546-548; b) A.L. Underwood, E.W. Anacker, Ibid. 117 (1987) 242-250.
212. Y. Moroi, Micelles: Theoretical and Applied Aspects, Plenum Press, New York, 1992.
213. a) H. Hoffmann, W. Ulbricht, B. Tagesson, Z. Phys. Chem. 113 (1978) 17-36; b) H. Hoffmann, G. Platz, H. Rehage, K. Reizlein, W. Ulbricht, Makromol. Chem. 182 (1981) 451-481.
214. E.J. Staples, G.J.T. Tiddy, J. Chem. Soc. Faraday Trans. Pt. 1 74 (1978) 2530-2541.
215. A. Malliaris, J. Le Moigne, J. Sturm, R. Zana, J. Phys. Chem. 89 (1985) 2709-2713.
216. N. Nishikido, Langmuir 6 (1990) 1225-1228.
217. R.G. Laughlin, The Aqueous Phase Behaviour of Surfactants, Academic Press, London, 1996.
218. P. Mukerjee, K.J. Mysels, Critical Micelle Concentration of Aqueous Surfactant Systems (NSRDS-NBS No. 36), US Nat. Bur. Stand., Washington, D.C., 1971.
219. H. Gerrens, G. Hirsch in „Polymer Handbook", 2nd Edn., J. Brandrup and E.H. Immergut (Eds.), John Wiley, New York – London, 1975, pp. II-483–II-497.
220. Y. Moroi, N. Nishikido, H. Uehara, and R. Matuura, J. Colloid Interface Sci. 50 (1975) 254-263.
221. M. Hato, M. Tahara, and Y. Suda, J. Colloid Interface Sci. 72 (1979) 458-464.
222. a) H. Hirai, Y. Ishikawa, K. Suga, and S. Watanabe, Yukagaku 16 (1967) 75-80; b) T. Hikota and K. Meguro, J. Am. Oil Chem. Soc. 52 (1975) 419-422.
223. a) H. Lange and M.J. Schwuger, Kolloid Z. Z. Polym. 223 (1968) 145-149; b) K. Ogino and Y. Ichikawa, Bull. Chem. Soc. Jap. 49 (1976) 2683-2686.
224. J.P. Kratohvil, J. Colloid Interface Sci. 75 (1980) 271-275.
225. J. Arakawa, B.A. Pethica, J. Colloid Interface Sci. 75 (1980) 441-450.
226. D.F. Evans, M. Allen, B.W. Ninham, A. Fouda, J. Solut. Chem. 13 (1984) 87-101.
227. K. Meguro, Y. Takasawa, N. Kawahashi N., Tabata Y. and Ueno M.. J. Colloid Interface Sci. 83 (1981) 50-56.
228. M. Saito, Y. Moroi and R. Matuura, J. Colloid Interface Sci. 88 (1982) 578-583.
229. a) Y. Gama and H. Narasaki, Yukagaku 29 (1980) 414-418; b) B. Sesta and C. La Mesa, Colloid Polym. Sci. 267 (1989) 748-752.
230. M. Nakagaki and T. Handa, in „Structure/Performance Relations in Surfactants", ACS Symp. Ser., Vol. 253, Am. Chem. Soc., Washington, 1984, pp. 73-86.
231. R. Zana, Langmuir 12 (1996) 1208-1211.
232. M.L. Corrin and W.D. Harkins, J. Am. Chem. Soc. 69 (1947) 683-688.
233. K. Shinoda, T. Nakagawa, B. Tamamushi and T. Isemura, Colloidal Surfactants, Academic Press, New York – London, 1963.
234. R. Sowada, Tenside Surfactants Detergents 31 (1994) 195-199.

235. Ch. Tanford, The Hydrophobic Effect: Formation of Micelles and Biological Membranes, 2nd Edn., John Wiley, New York, 1979.
236. a) J.N. Israelachvili, D.J. Mitchell and B.W. Ninham, J. Chem. Soc. Faraday Trans. Pt. II 72 (1976) 1525-1568; b) J.N. Israelachvili, S. Marcelja and R.G. Horn, Quart. Rev. Biophys. 13 (1980) 121-200.
237. K. Yamada, H. Shosenji, H. Ihara and O. Hotta, Chem. Lett. (1983) 43-46.
238. a) J.E. Brady, D.F. Evans, D.F. Warr, F. Grieser and B.W. Ninham, J. Phys. Chem. 90 (1986) 1853-1859; b) D.O. Miller, J.R. Bellare, T. Kaneko and D.F. Evans, Langmuir 4 (1988) 1363-1367.
239. M. Ambuel, F. Bangerter, P. Luisi, P. Strabal and H. Watzke, Progr. Colloid Polym. Sci. 93 (1993) 183-184.
240. a) J.H. Fendler, Science 223 (1984) 888-894; b) J.H. Fendler, CHEMTECH 15 (1985) 686-691.
241. M. Tanaka, H. Fukuda, T. Horiuchi, J. Am. Oil Chem. Soc. 67(1990) 55-60.
242. D.A. Vanhal, J.A. Bouwstra, A. Vanrensen, E. Jeremiasse, T. Devringer and H.E. Junginger, J. Colloid Interface Sci. 178 (1996) 263-273.
243. Y.A. Schipunov, Usp. Khimii 66 (1997) 328-352.
244. J.H. Fendler and E.J. Fendler, Catalysis in Micellar and Macromolecular Systems, Academic Press, New York, 1975.
245. P.P. Infelta, in "Energy Resources through Photochemistry and Catalysis", M. Grätzel (Ed.), Academic Press, New York – London, 1983, Ch. 2.
246. I.V. Berezin, Dejstvie fermentov v obraschennykh micellakh (Action of Enzymes in Reverse Micelles), Nauka, Moscow, 1985.
247. M.P. Pileni, Structure and Reactivity in Reverse Micelles, Elsevier, Amsterdam, 1989.
248. M. Grätzel and K. Kalynasundaram (Eds), Kinetics and Catalysis in Microheterogeneous Systems, Surfactant Sci. Ser., Vol. 38, Marcel Dekker, New York, 1991.
249. N. Pilpel, Chem. Rev., 63 (1963) 221-234.
250. A.S. Kertes and H. Gutman, in „Surface and Colloid Chemistry", Vol. 8, E. Matijevic (Ed.), John Wiley, New York – London, 1976, pp. 193-295.
251. a) H.-F. Eicke, Top. Current Chem., 87 (1980) 85-145;
b) H.-F. Eicke, Pure & Appl. Chem., 53 (1981) 1417-1424.
252. V.A. Volkov, Surface Active Agents in Detergents and Dry Cleaning Boosters (in Russ.), Legpromizdat, Moscow, 1985.

This Page Intentionally Left Blank

2. THERMODYNAMICS OF ADSORPTION OF SURFACTANTS AT THE FLUID INTERFACES

V.B. Fainerman[1] and R. Miller[2]

[1] International Medical Physicochemical Centre, Donetsk Medical University, 16 Ilych Avenue, Donetsk 83003, Ukraine

[2] Max-Planck-Institut für Kolloid- und Grenzflächenforschung, Forschungscampus Golm, 14424 Potsdam/Golm, Germany

2.1. Introduction

The thermodynamics and dynamics of interfacial layers have gained large interest in interfacial research. An accurate description of the thermodynamics of adsorption layers at liquid interfaces is the vital prerequisite for a quantitative understandings of the equilibrium or any non-equilibrium processes going on at the surface of liquids or at the interface between two liquids. The thermodynamic analysis of adsorption layers at liquid/fluid interfaces can provide the equation of state which expresses the surface pressure as the function of surface layer composition, and the adsorption isotherm, which determines the dependence of the adsorption of each dissolved component on their bulk concentrations. From these equations, the surface tension (pressure) isotherm can also be calculated and compared with experimental data. The description of experimental data by the Langmuir adsorption isotherm or the corresponding von Szyszkowski surface tension equation often shows significant deviations. These equations can be derived for a surface layer model where the molecules of the surfactant and the solvent from which the molecules adsorb obey two conditions:

(i) not interaction between adsorbed molecules

(ii) equal molecular areas at the interface.

In a number of cases, deviations from the Langmuir behaviour can be explained by a break of the former condition, for example by the presence of interactions between adsorbed molecules [1-14] or differences in the molecular areas [15-19].

The adsorption isotherm and the equation of state for adsorption layers proposed by Frumkin [1] describe the adsorption of low molecular weight surfactants rather well, provided the systems to be described deviate only slightly from an ideal (Langmuir) behaviour. Reasonable agreement between theory and experiment was found when interactions between all components in the system were taken into consideration [13, 14, 20]. However, the intermolecular interaction parameters which can be estimated from a comparison of experimental data with the isotherms do not always correlate with the properties of the surfactants or solvents. Often they have to be regarded simply as matching parameters. A better understanding of the physical reasons for deviations between experimental data and theoretical models should result from new models for the adsorption isotherm and the corresponding equation of state. In our opinion, such new models should account for the effects of, e.g., the size of the surfactant or protein molecules, molecular reorientation within the surface, dimerisation, cluster formation, etc.

Differences in the molecular area are of obvious relevance in mixed monolayers, where larger molecules have a larger partial molar area than smaller ones. Such differences lead to a situation where the smaller molecules are increasingly preferentially adsorbed with increasing surface pressure, even in the absence of any surface interactions [16]. In adsorption layers consisting of a single surface-active compound similar effects can occur if, due to the asymmetry in different adsorption states the molecules can occupy different areas [3, 4, 15, 19, 21, 22]. The fraction of molecules which are in the state characterised by a particular partial molar area depends on the surface pressure. In a thermodynamic study by Joos and Serrien [21] it was shown that if the molecule possesses, say, the two modifications 1 and 2, with different partial molar surface areas ω_1 and ω_2 (in absence of intermolecular interactions) their ratio in the surface layer obeys the equation

$$\frac{x_2^s}{x_1^s} = K_{12} \exp\left[\frac{\Pi(\omega_1 - \omega_2)}{RT}\right], \qquad (2.1)$$

where K_{12} is a constant, R is the gas law constant, T is the temperature, $\Pi = \gamma_0 - \gamma$ is the surface pressure, γ_0 and γ are the surface tension of solvent and solution, respectively, $x_i = m_i / \Sigma m_i$ are the molar fractions, and m_i are the numbers of moles of the i^{th} state. If $\omega_1 > \omega_2$, then with increasing Π the concentration of modification 2 in the surface layer increases. Equation (2.1) is the analytical expression for the general physico-chemical principle of Braun-Le Châtelier, applied by P. Joos [19] to adsorption layers of surfactants or proteins. It shows that the surface pressure acts as a self-regulation mechanism of the adsorption layer. This model cannot only be used in many cases as an alternative to the known equations based on the intermolecular interaction concept, but it can also predict new effects [21-26]. Recently it was shown [22, 23] that a "superdiffusion" kinetics of octylphenyl polyethylene glycol ethers may be described by a model assuming two different orientations of the polyethylene glycol chain, i.e. flat and normal oriented molecules, depending on the interfacial pressure. Corresponding equations for the adsorption and surface layer state were derived recently for surfactants and proteins displaying a change in the partial molar area with increasing surface pressure due to orientation changes [24-31].

Thus, deviations from the ideal Langmuir isotherm can be caused both by intermolecular interactions, which result in an enthalpy of mixing, and by area differences between molecules, which produce a non-ideal entropy of mixing [18]. For a simple case where the interactions are of the Frumkin type and the partial molar areas of solvent and surfactant are constant the entropic effect of area differences results in typical features of macromolecular adsorption, e.g., a steep initial increase of adsorption ("high affinity" adsorption) and a very slow rise once the surface is approximately half filled [18].

These estimates oversimplify both the enthalpic effects of interaction and the entropic effects of size differences. First, interactions between adsorbed molecules as described by Frumkin type models do not allow for the formation of dimers or larger aggregates in the surface layer which can occur in practice. Equations of state for monolayers showing such two-dimensional aggregation have been proposed for various models [32-42]. Second, proteins differ from surfactants in more than just the size. For proteins, surface denaturation can take place, leading to their unfolding at the surface, at least at low surface pressures. The partial molar surface area for proteins, in contrast to surfactants, is large and variable. The interrelation between the

protein denaturation process at the surface and the activity of the solvent molecules (typically water) was demonstrated by Ter-Minassian-Saraga [43], while Joos [17] showed that the degree of surface denaturation decreases with increasing surface pressure. Joos and Serrien [21], in deriving Eq. (2.1), demonstrated that the surface pressure controls both the composition and the thickness of a protein surface layer. This concept was further developed for an arbitrary number of different modifications of protein molecules at a surface [26].

Various models discussed so far have all been formulated in the framework of a two-dimensional solution theory among which the equation proposed by Butler [44] is the earliest example. One of the aims of this chapter is to demonstrate the general principle of deriving equations of state and adsorption isotherms on this basis. By this method most of the existing relationships can be obtained, for ideal and non-ideal surface layers of single or mixed surfactants. Equations will also be derived from this general principle resulting from models which consider interfacial reorientations [24-26] or aggregations [35, 41]. Moreover, introducing relatively simple corrections (taking into account the mean activity of ions [2, 5] and introducing the electrochemical potential [45-47]) one can apply this approach also to ionic surfactants and polyelectrolytes. The adsorption behaviour of the solutions of proteins and their mixtures with surfactants can also be satisfactorily described in the framework of this general approach [26]. In this chapter we analyse the dependence of the shape of isotherms on the parameters of the theoretical model. Also selected examples will be described to demonstrate the principle application of these new models to experimental surface tension isotherms for particular surfactants. However, a systematic analysis of the adsorption characteristics of various surfactants and complete homologous series will be presented in Chapter 3.

2.2. Chemical potentials of surface layers

The chemical potentials of components within surface layer μ_i^s depend on the composition of the layer and its surface tension γ. The dependence of μ_i^s on the composition of a surface layer is given by the known relation [48]

$$\mu_i^s = \mu_i^{0s}(T,P,\gamma) + RT\ln f_i^s x_i^s \qquad (2.2)$$

where $\mu_i^{0s}(T,P,\gamma)$ is the standard chemical potential of component i and depends on temperature T, pressure P and surface tension γ, and the f_i are the activity coefficients. Here the

superscript 's' refers to the surface (interface). The standard chemical potential can be presented as a function of pressure and temperature only, if one introduces an explicit dependence of $\mu_i^{0s}(T,P,\gamma)$ on the surface tension into Eq. (2.2). To do this, the well-known expression for the variation of the free enthalpy of the Gibbs dividing surface at constant pressure and temperature [48] can be used

$$dG = -Ad\gamma + \sum \mu_i^s dm_i^s , \tag{2.3}$$

where A is the surface area. As dG is a total differential, each component at the surface obeys the following Maxwell relationship

$$\left(\frac{\partial \mu_j^s}{\partial \gamma}\right)_{m_j^s} = -\left(\frac{\partial A}{\partial m_j^s}\right)_{\gamma} \tag{2.4}$$

at constant p, T and numbers of molecules except j. The derivative on the right hand side of Eq. (2.4) is by definition the partial molar area of the j^{th} component

$$\left(\frac{\partial A}{\partial m_j^s}\right)_{\gamma} = \omega_j \tag{2.5}$$

at constant p, T and numbers of molecules other than j. Using Eqs. (2.4) and (2.5) one can transform Eq. (2.2) into the form

$$\mu_i^s = \mu_i^{0s}(T,P) - \int_0^{\gamma} \omega_i d\gamma + RT\ln f_i^s x_i^s . \tag{2.6}$$

In this equation, in contrast to Eq. (2.2), the standard chemical potential $\mu_i^{0s}(T,P) = \mu_i^{0s}$ is already independent of surface tension. Assuming that ω_i is also independent of γ, and integrating Eq. (2.6), one obtains the expression

$$\mu_i^s = \mu_i^{0s} + RT\ln f_i^s x_i^s - \gamma\omega_i , \tag{2.7}$$

which is called the Butler equation [44]. Butler's equation is often used to derive surface equations of state and adsorption isotherms. The equation is to be applied to a Gibbs dividing surface chosen by a convention which results in positive values for all adsorptions, including

that of the solvent. Such a convention can be formulated by choosing numerical values for the partial molar surface areas of all components, as first recognised by Joos [15].

2.3. Interfacial layer model

Equations of state for surface layers, adsorption isotherms (below referred to as simply 'isotherms') and surface tension isotherms can be derived by equating the expressions for the chemical potentials at the surface, Eq. (2.7), to those in the solution bulk

$$\mu_i^{\alpha} = \mu_i^{0\alpha} + RT \ln f_i^{\alpha} x_i^{\alpha}, \tag{2.8}$$

where the superscript 'α' refers to the bulk solution. The standard chemical potentials $\mu_i^{0\alpha}$ depend on pressure and temperature. At equilibrium, for non-ionic surfactants and electroneutral combinations of ions, this yields

$$\mu_i^{0s} + RT \ln f_i^{s} x_i^{s} - \gamma \omega_i = \mu_i^{0\alpha} + RT \ln f_i^{\alpha} x_i^{\alpha}. \tag{2.9}$$

Now the standard state has to be formulated. For the solvent (i = 0) usually a pure component is assumed. This means $x_o^s = 1$, $f_o^s = 1$, $x_o^{\alpha} = 1$, $f_o^{\alpha} = 1$ and $\gamma = \gamma_o$. From Eq. (2.9) one obtains

$$\mu_0^{0s} - \gamma_o \omega_0 = \mu_0^{0\alpha}. \tag{2.10}$$

For the i surface active components, infinite dilution ($x_i^{\alpha} \to 0$) is experimentally better accessible than the pure state. It should be mentioned that setting the activity coefficients to 1 at infinite dilution is not necessarily consistent with setting the activity coefficient for pure components to unity. Therefore, for the case of infinite dilution of a multicomponent system, an additional normalisation of the potentials of the components should be performed [49]. This yields unity for the activity coefficient of pure components, while the activity coefficients at infinite dilution, in general should not be equal to 1. Indicating parameters at infinite dilution by the subscript (0), and those in the pure state by the superscript 0, the two standard potentials are interrelated by

$$\mu_{(0)i} = \mu_i^0 + RT \ln f_{(0)i} \tag{2.11}$$

for the bulk phase α and for the interface s. In combination with Eq (2.9) this leads to

$$\mu_{0i}^{s} + RT \ln x_i^{s}\Big|_{x_i^{\alpha}\to 0} - \gamma_o \omega_i = \mu_{0i}^{\alpha} + RT \ln x_i^{\alpha}\Big|_{x_i^{\alpha}\to 0} \tag{2.12}$$

and

$$\mu_{0i}^{\alpha} - \mu_{0i}^{s} = -\gamma_o \omega_i + RT \ln K_i . \tag{2.13}$$

$K_i = (x_i^s / x_i^\alpha)_{x_i^\alpha \to 0}$ are the distribution coefficients at infinite dilution. From Eqs. (2.9) and (2.10) the following relationship results

$$\ln \frac{f_0^s x_0^s}{f_0^\alpha x_0^\alpha} = -\frac{(\gamma_o - \gamma)\omega_0}{RT} . \tag{2.14}$$

and from (2.9) and (2.13) one obtains

$$\ln \frac{f_i^s x_i^s / f_{(0)i}^s}{K_i f_i^\alpha x_i^\alpha / f_{(0)i}^\alpha} = -\frac{(\gamma_o - \gamma)\omega_i}{RT} . \tag{2.15}$$

It is seen that the additional (normalised) activity coefficients introduced in Eq. (2.10) to establish the consistency between the standard potentials of the pure components and those at infinite dilution, can be incorporated into the constant K_i in Eq. (2.15). Therefore, if a diluted solution with activity coefficients of unity is taken as the standard state, the form of Eqs. (2.13) and (2.14) remains unchanged. The equations (2.14) and (2.15) are the most general relationships from which many well-known isotherms for non-ionic surfactants can be obtained. For further derivation it is necessary to express the surface molar fractions, x_j^s, in terms of their Gibbs adsorption values Γ_j. For this we introduce the degree of surface coverage, i.e. $\theta_j = \Gamma_j \omega_j$ or $\theta_j = \Gamma_j \omega$. Here ω is the partial molar area averaged over all components or all possible states. It is necessary to choose a proper ω_0 and the average partial molar surface area ω for all components or states. The Analysis of the Eqs. (2.14) and (2.15) shows that the system is invariant in relation to different values of θ_j ($\Gamma_j \omega_j$ or $\Gamma_j \omega$) and, therefore, also in relation to ω_0 (for instance $\omega_0 = \omega$). However the use of a realistic surface demand for ω_0 (approximately 0.1 nm² for one H_2O molecule) will contradict with experimental data. Let us consider first that there is only one dissolved species, existing in one state, and assume that

both the surface layer and bulk are ideal. For $\omega_0 = \omega_1$ the Eqs. (2.14) and (2.15) transform into the well-known equations of von Szyszkowski [50] and Langmuir [51]

$$\Pi = \gamma_0 - \gamma = \frac{RT}{\omega_1}\ln\left(1 + K_1 x_1^{\alpha}\right) = \frac{RT}{\omega_1}\ln\left(1 + b_1 c_1\right), \tag{2.16}$$

$$\Gamma_1 = \frac{1}{\omega_1}\frac{b_1 c_1}{1 + b_1 c_1}, \tag{2.17}$$

respectively, were the constant b_1 is the surface-bulk distribution coefficient related to the concentration c rather than to the mole fraction x. In order to derive Eq. (2.16) we have to employ a surface layer model where the molar surface area of the solvent in Eqs. (2.14) and (2.15) is chosen equal to the molar surface area of the surfactant. This requirement can be satisfied [2, 16, 52] if one chooses the position of the dividing surface in such a way that the total adsorption of the solvent and surfactant are equal to $1/\omega_1$, i.e.

$$\Gamma_0 + \Gamma_1 = 1/\omega_1 = \Gamma_1^{\infty}, \tag{2.18}$$

For a saturated monolayer ($\Gamma_1 = 1/\omega_1$), the dividing surface defined by Eq. (2.18) coincides with the dividing surface of the Gibbs convention, for which $\Gamma_0 = 0$. For $\Gamma_1 = 0$, however, the convention of Eq. (2.18) shifts the dividing surface towards the bulk solution by the distance $\Delta = (\omega_1 x_0^{\alpha})^{-1}$ as compared to the Gibbs convention [53]. Using a realistic surface demand for small molecules, e.g., $\omega_0 = \omega_1 = 0.2\ \mathrm{nm}^2$, implies a distance of 0.15 nm between the two dividing surfaces. Note that for large molecules, such as proteins ($\omega_1 \gg \omega_0$) the value of Δ becomes negligibly small, and therefore for any adsorptions the Lucassen-Reynders dividing surface practically coincides with the Gibbs dividing surface.

For surfactant mixtures or single molecules having several adsorption states within the surface the corresponding values of ω_i differ from each other and the definition of the dividing surface transforms into a more general relationship

$$\sum_{i=0}^{n}\Gamma_i = 1/\omega\,. \tag{2.19}$$

Equations defining an average molecular area demand for all surfactant components of a mixture taking into account different ω_i, have been proposed by Rusanov [48], Lucassen-

Reynders [16, 52] and Joos [15, 54]. An example in which the contribution of each component to ω is determined by its adsorption relative to the other adsorptions [16, 19] reads

$$\omega = \left(\sum_{i\geq 1}\Gamma_i\omega_i\right)\Big/\left(\sum_{i\geq 1}\Gamma_i\right). \tag{2.20}$$

Reasons for this particular choice of the dividing surface have been discussed in [24-26]. We can only add here that for this particular choice of the dividing surface ($\omega_0 = \omega$), the part of the surface occupied by the i^{th} surfactant molecule or a surfactant in the i^{th} state ($\theta_i = \Gamma_i\omega$) is equal to its mole fraction in the surfactant mixture at the surface ($x_i^s = \Gamma_i/\sum_{j\geq 0}\Gamma_j \equiv \Gamma_i\omega$). Another important consequence following from the location of the dividing surface according to Eq. (2.19) and ω according to Eq. (2.20) is that there is no contribution of non-ideality of the entropy of mixing (see below). And finally, using this definition of the dividing surface the adsorption layer thickness can be excluded from any further considerations. In this approach the actual number of water molecules displaced from the adsorption layer during the adsorption of protein or surfactant molecules does not need to be accounted for. On the other hand, the disadvantages of this convention are that (i) the partial molar surface area of the solvent does not have any connection with the molecular properties of the solvent, even not in the limit of infinite dilution of the solutes, and (ii) the mathematical treatment becomes rather awkward as all partial molar areas vary with the composition of the surface mixture. A treatment in terms of a convention based on constant different values for all partial molar areas, is therefore often simpler and more easily related to molecular dimensions of solvent and solutes [15, 18].

If dissolved components are ionised, and the charges are separated resulting in the formation of an electric double layer (DEL), then the electrochemical potential [45,46] has to be used instead of the chemical potential [cf. Eq. (2.7)]

$$\mu_i^S = \mu_i^{0S}(T,P,\gamma) + RT\ln f_i^S x_i^S + z_i F\psi, \tag{2.21}$$

where F is the Faraday constant, z_i is the charge of the ion, ψ is the electric potential. Unfortunately, in this case the dependence of the standard potential on surface tension cannot be excluded, in contrast to the development presented above for non-ionised components, because it can be easily seen that the right hand side of Eq. (2.4) now involves partial derivatives of ψ with respect to m_i^s and γ. However, in [55] a generalisation of Butler's

equation (2.7) was proposed for ionised compounds, simply by adding the term $z_i F\psi$ to the right hand side of Eq. (2.7). This unproved modification is clearly incorrect. In the solution bulk outside the DEL no charge separation takes place, therefore the chemical potential μ_i^{α} for both ionised and non-ionised components obeys the same equation (2.8).

2.4. Mixtures of non-ionic surfactants

The most widely used approach for the description of multicomponent monolayers consisting of molecules of different size is the integration of the Gibbs equation

$$d\Pi = \sum_{i=0}^{n} \Gamma_i d\mu_i \,, \tag{2.22}$$

using model equations for the adsorption isotherms [3, 4, 56]. This approach, however, has the problem that the adsorption isotherms for the different components of the mixture have to be mutually consistent. From the requirement for the differential of the surface tension for the ideal solution of two surfactants (here denoted by the subscripts 1 and 2) to be exact (total), Eq. (2.22) yields [57]

$$\frac{\partial}{\partial c_2}\left[\frac{\Gamma_1(c_1,c_2)}{c_1}\right] = \frac{\partial}{\partial c_1}\left[\frac{\Gamma_2(c_1,c_2)}{c_2}\right]. \tag{2.23}$$

If the condition (2.23) does not hold, then the adsorption isotherms are thermodynamically inconsistent. It should be noted that Eq. (2.23) was derived for the Gibbs dividing surface, located such that the adsorption of the solvent is zero (i=0) in Eq. (2.22). For other positions of the dividing surface Eq. (2.23) is meaningless.

For the description of mixed monolayers, the choice of the dividing surface proposed by Lucassen-Reynders (see Eqs. 2.18, 2.19) is superior [58, 59]. The results obtained using the Butler equation (2.7) and Lucassen-Reynders' dividing surface model for the description of mixed monolayers of non-ionic or ionic surfactants, and proteins assuming reorientation or aggregation of adsorbed molecules were presented and discussed in overviews [58, 59]. In this chapter, these concepts are discussed and further developed.

Assuming ideality of the solution bulk, the equation of state for a non-ideal surface layer can be obtained from Eq. (2.14)

$$\Pi = -\frac{RT}{\omega_0}\left(\ln x_0^s + \ln f_0^s\right), \tag{2.24}$$

and the adsorption isotherm from Eqs. (2.14) and (2.15)

$$\ln \frac{f_i^s x_i^s}{K_i x_i^\alpha} = \frac{\omega_i}{\omega_0}\left(\ln x_0^s + \ln f_0^s\right). \tag{2.25}$$

If all partial molar areas are identical, the surface coverage θ_i can be used instead of the mole fractions in the form $x_i^s = \theta_i = \Gamma_i\omega_i$ or $\theta_i = \Gamma_i\omega$, and Eqs. (2.24) and (2.25) transform into

$$\Pi = -\frac{RT}{\omega_0}\left[\ln\left(1 - \sum_{i\geq 1}\theta_i\right) + \ln f_0^s\right], \tag{2.26}$$

$$K_i x_i = \frac{\theta_i f_i^s}{\left(1 - \sum_{i\geq 1}\theta_i\right)^{n_i}\left(f_0^s\right)^{n_i}}, \tag{2.27}$$

where $n_i = \omega_i/\omega_0$. The activity coefficients determined by intermolecular interactions (enthalpic non-ideality, f_i^{sH}) can be calculated using the regular solution theory [60-62]

$$RT\ln f_k^{sH} = \sum_i\sum_j\left(A_{ik}^s - \frac{1}{2}A_{ij}^s\right)\theta_i\theta_j, \tag{2.28}$$

where $A_{ij}^s = U_{ii}^s + U_{jj}^s - 2U_{ij}^s$, U_{ii}^s and U_{ij}^s are the energies of interaction between the species in the surface layer. Lucassen-Reynders [18] has derived the following expressions for the activity coefficient of any surface layer component for non-ideal entropy of mixing

$$\ln f_k^{sE} = 1 - n_k\sum_i\left(\theta_i\ n_i\right). \tag{2.29}$$

The additivity of enthalpy and entropy in the Gibbs free energy results in

$$f_i^s = f_i^{sH}\cdot f_i^{sE} \quad \text{or} \quad \ln f_i^s = \ln f_i^{sH} + \ln f_i^{sE}. \tag{2.30}$$

For solutions of two surfactants or for two states of the same surfactant in the surface layer, the substitution of Eqs. (2.28) - (2.30) into Eqs. (2.26) and (2.27) leads to

$$\Pi = -\frac{RT}{\omega_0}\left[\ln(1-\theta_1-\theta_2)+\theta_1\left(1-\frac{1}{n_1}\right)+\theta_2\left(1-\frac{1}{n_2}\right)+a_1\theta_1^2+a_2\theta_2^2+2a_{12}\theta_1\theta_2\right], \quad (2.31)$$

$$b_i c_i = \frac{\theta_i}{(1-\theta_1-\theta_2)^{n_i}}\exp(-2a_i\theta_i-2a_{12}\theta_j)\cdot\exp\left[(1-n_i)(a_1\theta_1^2+a_2\theta_2^2+2a_{12}\theta_1\theta_2)\right], \quad (2.32)$$

where $a_1 = A_{01}$; $a_2 = A_{02}$; $a_{12} = (A_{01} + A_{02} - A_{12})/2$; c_i are the bulk concentrations, $b_i = (K_i/\rho)\exp(n_i - a_i - 1)$; ρ is the ratio of the solvent (water) density to its molecular weight, $\rho \approx 1000/18 = 55.6$ [mol H_2O/l]; $i = 1, 2$; $j = 1, 2$ ($j \neq i$). If the Eqs. (2.32) have to describe two interfacial states of the same surfactant, then $c_1 = c_2 = c$. The equation of state for the surface layer (2.31) is similar to that proposed in [4]. One can easily verify that all known equations describing the interfacial state of solutions of one or two surfactants involving both intermolecular interaction and non-ideality of entropy (cf. [1-11, 15, 63-73]) are limiting cases of Eqs. (2.31) and (2.32). Some examples can be considered here. If the enthalpy of mixing is ideal, i.e. $a_1 = a_2 = a_{12} = 0$, then the following relationships result [7, 8, 18]

$$\Pi = -\frac{RT}{\omega_0}\left[\ln(1-\theta_1-\theta_2)+\theta_1\left(1-\frac{1}{n_1}\right)+\theta_2\left(1-\frac{1}{n_2}\right)\right], \quad (2.33)$$

$$b_i c_i = \frac{\theta_i}{(1-\theta_1-\theta_2)^{n_i}}. \quad (2.34)$$

If the entropy of mixing for the surface layer components is ideal, $n_1 = n_2 = 1$, then the generalised Frumkin equation of state and isotherm [2-5] are obtained

$$\Pi = -\frac{RT}{\omega_0}\left[\ln(1-\theta_1-\theta_2)+a_1\theta_1^2+a_2\theta_2^2+2a_{12}\theta_1\theta_2\right], \quad (2.35)$$

$$b_i c_i = \frac{\theta_i}{(1-\theta_1-\theta_2)}\exp(-2a_i\theta_i-2a_{12}\theta_j). \quad (2.36)$$

For the solution of a single surfactant, i.e. for $\theta_2 = 0$ and $c_2 = 0$, the last expressions transform into the usual Frumkin equations [1]

$$\Pi = -\frac{RT}{\omega_0}\left[\ln(1-\theta)+a\theta^2\right], \quad (2.37)$$

$$bc = \frac{\theta}{(1-\theta)} \exp(-2a\theta). \tag{2.38}$$

Finally, for an ideal surface layer of a n-component ideal bulk solution, Eqs. (2.26) and (2.27) transform into a generalised von Szyszkowski-Langmuir equation of state

$$\Pi = -\frac{RT}{\omega_0} \ln\left(1 - \sum_{i\geq 1} \theta_i\right) = \frac{RT}{\omega_0} \ln\left(1 + \sum_{i\geq 1} b_i c_i\right), \tag{2.39}$$

and a generalised Langmuir adsorption isotherm given by

$$b_i c_i = \frac{\theta_i}{\left(1 - \sum_{i\geq 1} \theta_i\right)}. \tag{2.40}$$

For the solution of a single surfactant the last expressions (2.39) and (2.40) transform into the usual von Szyszkowski equation [50]

$$\Pi = \frac{RT}{\omega_0} \ln(bc + 1). \tag{2.41}$$

A direct consequence of the equality of all ω_i is that the adsorption ratio of two surfactants remains constant when their concentrations are varied in the same proportion, i.e., at constant c_1/c_2. However, for surfactant molecules with different ω_i, Butler's equation (2.7) predicts that with increasing surface pressure the adsorption of the smaller molecules is preferentially increased. This has been shown experimentally [16] and is conveniently theoretically illustrated for an ideal surface behaviour [19] by the equation

$$\frac{\Gamma_1}{\Gamma_2} = \frac{b_1 c_1}{b_2 c_2} \exp\left(\frac{\Pi(\omega_2 - \omega_1)}{RT}\right). \tag{2.42}$$

This implies that a smaller molecule will expel a larger one from the surface when their total concentration is increased at constant c_1/c_2. Thus, a two-dimensional solution treatment which expresses the chemical potentials of the surface layer components by means of Eq. (2.7) enables us to derive equations of state and adsorption isotherms at fluid interfaces depending on the system considered (ideal or non-ideal surface layer, single surfactant or mixture of

surfactants). Similar options are provided by the approach proposed by Diamant and Andelman [74] which is based on the analysis of the free energy of the surface layer.

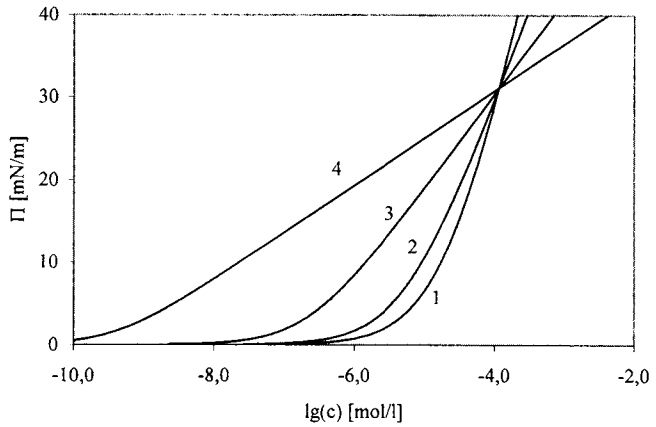

Fig. 2.1 The dependence of surface pressure on the bulk concentration for the Szyszkowski equation (2.41) with $\omega = 1.5 \cdot 10^5$ m²/mol (1), $2.5 \cdot 10^5$ m²/mol (2), $5.0 \cdot 10^5$ m²/mol (3) and 10^6 m²/mol (4).

It is seen from the von Szyszkowski-Langmuir surface tension isotherm, Eq. (2.41), that at a given temperature the shape of the surface tension isotherm is determined by only one parameter $\omega_0 = \omega_1 = \omega$. The other parameter b enters this equation as a dimensionless variable bc, in combination with the concentration. Therefore, the value of b does not affect the shape of surface tension isotherm, and only scales this curve with respect to the concentration axis. It should be noted that this dependence on b is characteristic to all the equations presented above. The dependence of the surface pressure isotherm on the molar area ω is illustrated by Fig. 2.1. It is seen, that the lower ω is, hence the higher the limiting adsorption $\Gamma_\infty = 1/\omega$, the steeper is the slope of the $\Pi(c)$-curve.

The Frumkin equation of state and adsorption isotherm (2.37) - (2.38) involve one extra parameter a. Thus, the Frumkin model can better fit experimental data. The effect of the parameter a for fixed ω values is illustrated by Fig. 2.2.

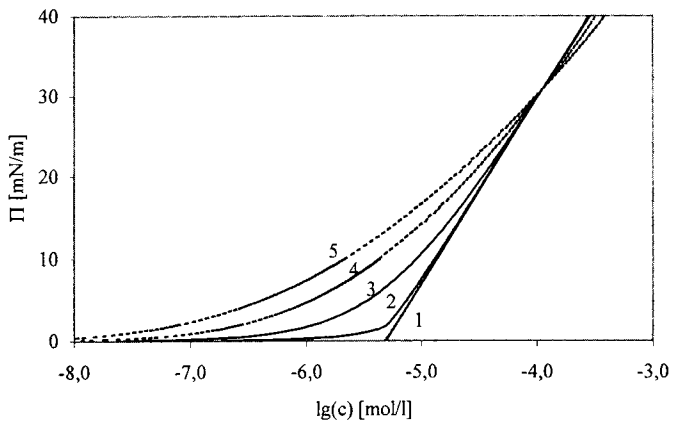

Fig. 2.2 The same as in Fig. 2.1 for a Frumkin isotherm, Eqs. (37) and (38), with $\omega = 2.5 \cdot 10^5$ m²/mol and: a = 4 (1), a = 2 (2), a = 0 (3), a = -2 (4), a = -4 (5).

For negative values of a (which can result from intermolecular repulsion in the surface layer, which is the case for ionic surfactants) the shape of the curve is steeper as compared with the Langmuir isotherm, while for positive a-values (intermolecular attraction in the monolayer) the curve becomes steeper at low concentrations, and is almost a straight line at higher concentrations. All the curves shown in Figs. 2.1 and 2.2 are normalised with respect to the constant b in such a way that the concentration 10^{-4} mol/l corresponds to a surface pressure of 30 mN/m.

2.5. Mixtures of ionic surfactants

2.5.1 Model of electroneutral surface layers of ionised molecules

The von Szyszkowski equation (2.41) and Frumkin equations (2.37)-(2.38) have been used for the description of experimental surface tension isotherms of ionic surfactants [40, 58]. Thus the constant a in the Eqs. (2.37)-(2.38) reflects simultaneously intermolecular attractive (van der Waals) and interionic repulsive interactions. As a result, for the ionic surfactants the constant a can have either a positive or negative sign.

Lucassen-Reynders' approach regards the surface as a two-dimensional solution described by Eq. (2.7) applied to an electroneutral dividing surface which contains only electroneutral

combinations of ions [2, 5]. Any additional effects of ionisation in this approach should be accounted for in the activity coefficients f_i. This model therefore assumes that the dividing surface is located at the external border of the DEL. More rigorously, as the model [2, 5] involves excess surface values, the assumption about the electroneutrality of the surface layer is better applicable to ionic surfactant solutions with addition of inorganic electrolytes, where the thickness of the double layer becomes smaller. However, it will be shown below that for ionic compositions, the DEL does not contribute to both surface tension and adsorption. Therefore the excess values are not affected by the actual thickness of the DEL. The surface equation of state is still given by Eq. (2.14), but the distribution of surfactant between surface and solution is now obtained for electroneutral combinations of ions, say R^- and X^+ for an anionic surfactant RX (where R^- is the surface-active ion and X^+ is the counterion). This means that for both surface and solution the average ionic product $(c_R c_X)^{-1/2}$ replaces the molar concentration c_i [2, 5, 15, 67]. This does not make any difference to the adsorption isotherm if there is only one salt RX, but it does when the solution contains in addition an inorganic electrolyte with the same counterion X^+ as the surfactant, for example a salt XY. In such a case it is necessary to take into account the average activity of surface active ions and all counterions in the solution. Also, the ionic sum enters into the convention for specifying the position of the dividing surface: the simplest convention now is to choose $\omega_{jk} = 2\omega_0$, where the factor of 2 represents the dissociation into 2 ions. This corresponds to a constant total amount of surface excess, as in the nonionic case, but now we have $\Gamma_0 + \Gamma_j + \Gamma_k = 1/\omega_0 = 2/\omega_{jk}$ .Using the conditions which require the ionic equilibrium in the bulk ($\mu^{\alpha}_{RX} = \mu^{\alpha}_{R} + \mu^{\alpha}_{X}$) and in the surface layer ($\mu^{s}_{RX} = \mu^{s}_{R} + \mu^{s}_{X}$), the Eqs. (2.7) and (2.8) yield

$$\ln \frac{f^s_R f^s_X x^s_R x^s_X}{K_{RX} f^{\alpha}_R f^{\alpha}_X x^{\alpha}_R x^{\alpha}_X} = -\frac{(\gamma_o - \gamma)\omega_{RX}}{RT}, \qquad (2.43)$$

instead of Eq. (2.15). As the surface layer is electroneutral, and therefore $x^s_R = x^s_X$, from Eqs. (2.14) and (2.43) for non-ideal (Frumkin) surface layers and non-ideal bulk solutions of one ionic surfactant, with or without additional non-surface active electrolyte, the following equation of state and adsorption isotherm is obtained

$$\frac{\Pi\omega_0}{RT} = \frac{\Pi\omega_{RX}}{2RT} = -\ln(1-\theta) - a\theta^2 \tag{2.44}$$

$$b\left(c_{R^-}c_{X^+}\right)^{1/2} f_{\pm} = \frac{\theta}{1-\theta}\exp(-2a\theta) \tag{2.45}$$

where $\theta(=2x_R^s = \Gamma_{RX}/\Gamma_{RX}^{\infty})$ is the surface mole fraction of the salt RX, Γ_R=Γ_X=Γ_{RX} because of electroneutrality, b is defined as $2K_{RX}^{1/2}$ converted into units l/mol by using ρ, $f_{\pm}$ is the average activity coefficient in the bulk solution, $c_{X^+} = c_{RX} + c_{XY}$, and $c_{R^+} = c_{RX}$.

For ideal surface layers (a=0), Eq. (2.45) is reduced to [2, 5]

$$\theta = \frac{bf_{\pm}\left(c_R c_X\right)^{1/2}}{1 + bf_{\pm}\left(c_R c_X\right)^{1/2}} \tag{2.46}$$

corresponding to the following $\Pi(c)$-relationship

$$\Pi = 2RT\Gamma_{RX}^{\infty}\ln\left[bf_{\pm}\left(c_{RX}c_{X^-}\right)^{1/2} + 1\right] \tag{2.47}$$

where $\Gamma_{RX}^{\infty} = 1/2\omega_0 = 1/\omega_{RX}$. The forms of Eqs. (2.46) and (2.47) are similar to the equations of Langmuir and von Szyszkowski, respectively, but with the molar concentration replaced by the average ionic product of RX.

It was shown in [2, 5, 67] that Eq. (2.47) describes quite well the surface tension isotherms of anionic and cationic surfactant solutions in a wide range of added inorganic electrolyte (from 0 to 0.5 mol/l). Irrespectively of the added inorganic electrolyte, all surface tension isotherms plotted in the co-ordinates of Eq. (2.47) fall on one curve, characterised by one and the same value of b independent of the electrolyte concentration. In such systems the main effect of the inorganic salt is simply to increase the thermodynamic potential of the ionic surfactant in the solution, resulting in increased adsorption and surface pressure at a given c_{RX}. This effect is completely analogous to the well-known salting-out effect where an electrolyte can be precipitated from its solution by adding a better soluble salt with a common ion.

Figure 2.3 illustrates the results of studies on dodecyl trimethyl ammonium bromide (DTAB) at different additions of NaBr [75]. It is seen that with increasing salt concentration the shape of the curve varies and becomes displaced towards lower surfactant concentrations. The

variation of the shape of the curve (the decrease of the limiting slope with increasing electrolyte concentration) is due to changes in the counterion adsorption. According to the Gibbs equation, for 1:1-charged surfactants in the presence of a 1:1-charged inorganic electrolyte (see, e.g., [19]), we have

$$d\sigma = -RT\Gamma_{DTA^+}\left[1 + \frac{c_{DTAB}}{c_{DTAB} + c_{NaBr}}\right] d\ln c_{DTAB},$$

and for low electrolyte concentration ($c_{DTAB} \gg c_{NaBr}$) the coefficient in the square brackets is equal to 2, while at excess of inorganic electrolyte ($c_{DTAB} \ll c_{NaBr}$) this coefficient is equal to 1. Thus, if changes in the adsorption of surface active ions with the electrolyte concentration is low, then the slope of the surface tension isotherm in absence of electrolyte should be two times steeper as compared with the case where the electrolyte is in excess. This agrees with the data presented in Fig. 2.3 for the cationic surfactant dodecyl trimethyl ammonium bromide (DTAB).

In Figure 2.4 the results discussed above for NaBr concentrations lower than 0.5 M are presented in the coordinates of Eq. (2.47), i.e., the abscissa variable is taken to be $c^* = f_{\pm} \cdot (c_{DTAB+NaBr} \cdot c_{DTAB})^{1/2}$, where $f_{\pm}$ is the average activity coefficient of ions in the solution bulk.

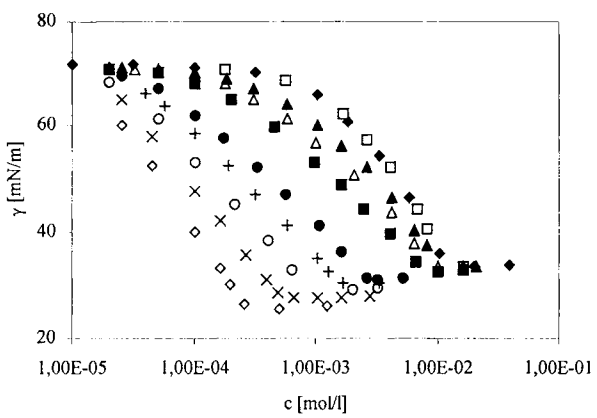

Fig. 2.3. Experimental surface tension isotherms (DTAB) without salt (Φ) and with various additions of NaBr, according to [75]: (□) 0,0001, (▲) 0.005, (△) 0.01, (■) 0.02, (●) 0.1, (+) 0.2, (O) 0.5, (×) 1.0 and (◇) 2.0 M NaBr.

For NaBr concentrations lower than 0.01 M the activity coefficient was taken to be 1, while for higher concentrations this coefficient was calculated from the Debye-Hückel theory. For NaBr concentrations exceeding 0.5 M the Debye-Hückel theory becomes incorrect, so that data for these concentrations are not presented in Fig. 2.4.

It is seen that the experimental isotherms plotted *vs* c* correspond quite satisfactorily with this master curve in a wide range of added inorganic electrolyte, and well describes by Eqs. (2.44) and (2.45) with $\omega = 2.8 \cdot 10^5$ m^2/mol, b=125 mol/l and a = 1.7. Figure 2.4 also shows that many precise details of the adsorption process in the framework of the model described by Eq. (2.44)-(2.45) remain unaccounted for.

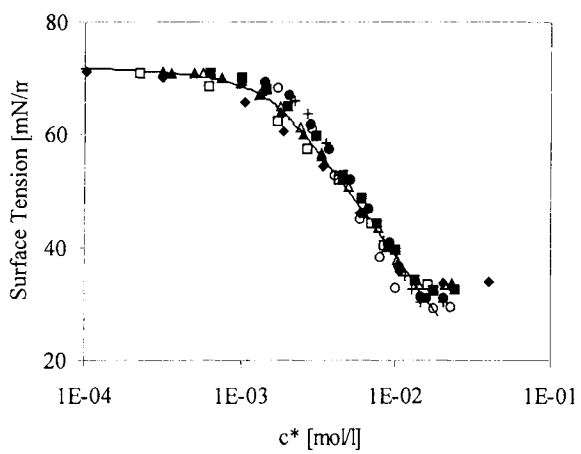

Fig. 2.4. Same data as in Fig. 2.3 plotted in the coordinates of Eq. (2.47).

Let us consider now the case when a solution contains a mixture of two anionic (or cationic) surfactants (for example, homologues R_1X and R_2X with a common counterion X^+) with addition of inorganic electrolyte XY. In such systems the counterion concentration X^+ is given by the sum of concentrations of R_1X, R_2X and XY. For simplicity, the saturation adsorptions of the two homologues will be taken as equal, i.e., $\omega_{1X} = \omega_{2X} = 2\omega_0$. After consideration of the surface-to-bulk distribution of both electroneutral combinations of ions, the surface layer equation of state for the Frumkin-type non-ideality of a mixture of two ionic surfactants can be written in a form similar to Eq. (2.35), where it is assumed that $1/\omega_0 = \Gamma_{RX}^{\infty}$. Corresponding

equations for mixtures of n ionic homologues are given in [67]. For ideal surface layers ($a_1 = a_2 = a_{12} = 0$) one obtains the following surface pressure isotherm

$$\Pi = 2RT\Gamma_{RX}^{\infty} \ln\left[\left((b_1 f_{1\pm})^2 c_{R_1X} c_{X^-} + (b_2 f_{2\pm})^2 c_{R_2X} c_{X^-}\right)^{1/2} + 1\right]. \qquad (2.48)$$

One can easily see that Eq. (2.48) is the straightforward consequence of Eqs. (2.7)- (2.8) for the compositions of ions within the surface layer $x_i^s = (x_{R_i}^s x_X^s)^{1/2}$ and within the solution bulk $x_i^{\alpha} = (x_{R_i}^{\alpha} x_X^{\alpha})^{1/2}$, provided that the following conditions are satisfied: $x_{R_1}^s + x_{R_2}^s = x_X^s$ (surface layer electroneutrality), $x_0^s + x_{R_1}^s + x_{R_2}^s + x_X^s = 1$ (balance between the molar portions of all components in the surface layer), and $\Gamma_0 + \Gamma_{R_1} + \Gamma_{R_2} + \Gamma_X = \Gamma_{RX}^{\infty}$ (dividing surface chosen after Lucassen-Reynders). For non-ideal surface layers the following equation of state is obtained

$$\Pi = -\frac{2RT}{\omega_{RX}}\left[\ln(1-\theta_1-\theta_2) + a_1\theta_1^2 + a_2\theta_2^2 + 2a_{12}\theta_1\theta_2\right], \qquad (2.49)$$

where for the ionic solutes $\theta_1 = 2x_1^s$ and $\theta_2 = 2x_2^s$. After consideration of the surface-to-bulk distribution of both electroneutral combinations of ions, we arrive at the equation for the adsorption isotherm for the surfactant R_1X

$$b_1 f_{\pm}\left(c_{R_1} c_X\right)^{1/2} = \frac{\left((\theta_1(\theta_1+\theta_2)\right)^{1/2}}{1-(\theta_1+\theta_2)} \exp\left(-2a_1\theta_1 - 2a_{12}\theta_2\right), \qquad (2.50)$$

and a similar equation for the surfactant R_2X. As one can see from Eq. (2.50) the simple summation of adsorbed ions is used for the calculation of the coefficients' activity of solvent and ions. The ionic products are used only for the activity of ions in a monolayer. Equations (2.48)-(2.50), first derived by Lucassen-Reynders [2, 5], shows that the presence of inorganic electrolyte in solutions of surface active homologues increases the adsorption activity of the ionic surfactant more than additively, in contrast to what is observed for non-ionic surfactant mixtures. This additivity is expressed by the generalised von Szyszkowski-Langmuir equation (2.39). If the same additivity would apply to the case of two mixed ionic surfactants, one should expect the experimental results obey the following equation rather than Eq. (2.48):

$$\Pi = 2RT\Gamma_{RX}^{\infty} \ln\left[b_1 c_{R_1X} f_{1\pm} + b_2 c_{R_2X} f_{2\pm} + 1\right] \qquad (2.51)$$

In fact, experimental surface tensions of mixtures of sodium decyl sulphate SDeS (component 1) and sodium dodecyl sulphate SDS (component 2) are described satisfactorily by Eq. (2.48) whereas the application of Eq. (2.51) leads to large differences between theory and experiment [67]. The best agreement between experimental and theoretical values of Π was received by using the Frumkin analogue of Eqs. (2.48)-(2.50) with a_1=0.7, a_2=0.85 and $a_{12}=(a_1+a_2)/2$=0.77. Similarly, mixtures of decyl ammonium chloride and dodecyl ammonium chloride were very well described by these equations with a_1=1.2, a_2=1.56 and $a_{12}=(a_1+a_2)/2$=1.38 [16]. The latter system also reveals a reverse salting-out effect: as an excess of inorganic counterions in the solution increases the adsorption activity of an ionic surfactant, by the same token such an excess in the surface decreases the adsorption activity. As a result, the effect of a second ionic surfactant with a common counterion on the surface pressure is smaller than it would have been according to the additivity rule for non-ionic surfactants expressed in Eq. (2.51).

Finally, very large effects on adsorption and surface pressure have been described for mixtures of anionic RX (R^-X^+) and cationic RY (R^+Y^-) surfactants in the solution. In such systems, the adsorption is represented almost completely by the equimolar composition R^-R^+ which has a very high surface activity without any noticeable contribution of R^-X^+ and R^+Y^- over a large rage of mixing ratios [76]. Thus one can describe the surface tension of this mixture for ideal surface layers without any consideration of the DEL influence by

$$\Pi = RT\Gamma_{R^-R^+\infty} \ln\left[b_{R^-R^+} f_{\pm}\left(c_{RX}c_{RY}\right)^{1/2} + 1\right] \qquad (2.52)$$

The adsorption equilibrium constant for the composition R^-R^+ can be approximated by the constants of adsorption equilibrium of R^-X^+ and R^+Y^- in the individual solutions [67]. The experimental data for mixed systems of SDS and DTAB [76] are described satisfactory by Eq. (2.52).

2.5.2. Model of charged monolayers of ionic surfactants

The advantages of the electroneutral surface layer model presented above can be regarded also as a deficiency, because this model cannot describe the structure of the surface layer, electric potential of the surface, etc. In addition, no satisfactory analysis of the adsorption of proteins

and other polyelectrolytes can be given, if the contribution of the DEL to the surface pressure of the adsorption layer is ignored.

As there is no analogue of Butler's equation for ionised surface layers, the procedure used to derive the equation of state has to be based on the Gibbs adsorption equation and a model adsorption isotherm. The isotherm equation can also be derived from the theoretical analysis of the expressions for electrochemical potentials of ions. For the solution of a single ionic surfactant RX, with the addition of inorganic electrolyte XY, starting from Eqs. (2.2) and (2.21) for the electrochemical potentials, one obtains the adsorption isotherm

$$Kf_R c_R = \frac{\theta}{(1-\theta)} \exp(-2a\theta) \exp\left(\frac{z_R F\psi}{RT}\right), \tag{2.53}$$

where f_R is the activity coefficient of the ion R in the solution bulk, and $\theta = \Gamma_R / \Gamma_R^{\infty}$. It was taken into account by Kalinin & Radke [77] that part of the counterions is bonded to surface active ions within the Stern-Helmholtz (S-H) layer, while another (not bonded) part is located in the diffuse region of the DEL. Therefore, this model employs two adsorption isotherms: one for free ions, Eq. (2.53), and another for bonded surface active ions. Equation (2.53) is similar to that derived by Davies [45], and was used subsequently by many other authors [46, 47, 74, 78, 79].

For our system, the Gibbs adsorption equation has the form

$$-d\gamma = \Gamma_R d\mu_R^{\alpha} + \Gamma_X d\mu_X^{\alpha} + \Gamma_Y d\mu_Y^{\alpha}. \tag{2.54}$$

Clearly, Gibbs' dividing surface is used in Eq. (2.54), where $\Gamma_0 = 0$. The adsorption isotherm Eq. (2.53) involves another definition of the dividing surface (Lucassen-Reynders' surface with $\Gamma_0 \neq 0$), which inevitably introduces some deficiency when the two Eqs. (2.53) and (2.54) are used simultaneously. The difference between the positions of these surfaces is of the order of the dimensions of an inorganic ion.

For a fixed concentration of inorganic electrolyte, in ideal bulk solution Eq. (2.54) becomes (see [46]):

$$\frac{\partial\gamma}{\partial c_R} = \Gamma_R \frac{\partial\mu_R^{\alpha}}{\partial c_R} + \Gamma_X \frac{\partial\mu_X^{\alpha}}{\partial c_R} \tag{2.55}$$

The adsorption of ions R^- and X^+ can be calculated from the integration over the total solution volume, i.e.,

$$\Gamma_i = \int_0^\infty [c_i(y) - c_{i0}]dy \tag{2.56}$$

where c_{i0} is the concentration of the ions outside the DEL, and y the spatial co-ordinate. The concentration of ions within the DEL in Eq. (2.56) can be calculated from the Gouy-Chapman theory. Finally, the relationship

$$\frac{\partial\gamma}{\partial c_R} = RT\frac{\Gamma_R}{c_R} + \frac{2RT}{F}\left(\frac{2\varepsilon RT}{c_R + c_Y}\right)^{1/2}\left[\cosh\left(\frac{z_R F\psi^0}{2RT}\right) - 1\right] \tag{2.57}$$

follows from Eqs. (2.55) and (2.56) (see [46, 77, 78]), where ψ^0 is the electric potential of the surface. Introducing now Γ_R (cf. adsorption isotherm (2.53)) into Eq. (2.57) and integrating, one obtains the equation of state for the surface layer of an ionic surfactant solution [45, 46, 77]

$$\Pi = -2RT\Gamma_{RX}^{\infty}\left[\ln(1-\theta) + a\theta^2\right] + \frac{4RT}{F}(2\varepsilon RTc_\Sigma)^{1/2}\left[\mathrm{ch}\left(\frac{z_R F\psi^0}{2RT}\right) - 1\right]. \tag{2.58}$$

Thus, the inter-ion interaction results in an additional surface pressure contribution

$$\Delta\Pi = \frac{4RT}{F}(2\varepsilon RTc_\Sigma)^{1/2}[\mathrm{ch}\varphi - 1], \tag{2.59}$$

where c_Σ is the total concentration of ions in the solution, and $\varphi = z_i F\psi^0/2RT$. The electric potential is determined by the surface charge density

$$\mathrm{sh}\varphi = \frac{z_R\Gamma_R F}{(8\varepsilon RTc_\Sigma)^{1/2}}. \tag{2.60}$$

More complicated expressions for $\Delta\Pi$ were derived when the contribution by the S-H layer was taken into account, that is, when part of the counterions is bound by surface active ions [77]. The theory developed by Poberezhnyi *et al.* [79] also assumes that part of the counterions penetrates into the adsorption layer. The equations analogous to Eqs. (2.57)-(2.60) can be

developed in the framework of this theory [79]. The counterparts of Eqs. (2.57)-(2.59) involve additional terms on the right hand sides, while the counterpart of Eq. (2.60), which determines the surface charge density, contains the difference $\Gamma_R - \Gamma_X^s$ instead of Γ_R, where Γ_X^s is the adsorption of counterions localised in the surface layer. Similar concepts concerning the structure of the adsorption layer for ionic surfactants were used elsewhere [80, 81]. It follows from the model described by Eqs. (2.57)-(2.60) that if all counterions are localised within the surface layer (in the S-H layer), then $\Delta\Pi = 0$. However, this is not exactly true. If no bulk charge separation takes place, and oppositely charged ions are located at the interface (two-dimensional electrolyte solution model), the Coulomb interaction leads to a certain arrangement of the ions. In this case an additional contribution to the surface pressure $\Delta\Pi$ also exists as was shown by Muller and Derjaguin [82]. This contribution, however, is negative, and its value is significantly lower than that given by Eq. (2.59) for the case of a DEL formation. The analysis of Eq. (2.59) has shown that for 1:1 ionics, at low bulk concentration the approximation $\varphi \gg 1$ holds [83]. This approximation leads to a linear dependence of $\Delta\Pi$ on Γ in Eq. (2.59) [74, 84]

$$\Delta\Pi = 2RT\Gamma . \qquad (2.61)$$

For the opposite case of large ion bulk concentrations and low φ values, $\Delta\Pi$ is proportional to the squared adsorption amount [74, 84]. Moreover for 1:1 ionic surfactant the value of $\Delta\Pi$ is small enough so that the effect of the DEL can be neglected.

Examples of a successful application of Eqs.(2.53) and (2.58) to experimental Π *vs* c_{RX} curves are given in [46, 77]. It should be noted that Eqs. (2.53) and (2.58) describe quite satisfactorily dependencies measured for both anionic and cationic surfactants, irrespective of the presence of inorganic electrolyte, and a single value of the constant K in Eq. (2.53) is obtained for various concentrations of the added electrolyte.

It was shown in [77] that, irrespective of the electrolyte concentration, for a surface coverage exceeding 20%, the portion of adsorbed surface active 1:1-charged ions bonded to counterions in the S-H layer is approximately 90%, that is, the surface layer is almost electroneutral. The calculations performed in [80] for sodium tetradecyl sulphate solutions, with or without added NaCl, revealed that the extent of bonded counterions, while being somewhat lower than that reported in [77], is quite high, and amounts up to 80% for concentrated solutions. These results

explain why Lucassen-Reynders' theory, which assumes the existence of an electroneutral layer of ionic surfactants, can be successfully applied to these systems. However, even without regard to these results, rigorous theoretical considerations can be presented to support Lucassen-Reynders' model. It can be shown that for compositions of ions the effect produced by the DEL is weak which follows directly from the main relations describing charged layers. According to Eq. (2.56) the compositions of ions can be presented as

$$(\Gamma_R \Gamma_X)^{1/2} = \int_0^{\infty} \left[(c_R(y) c_X(y))^{1/2} - (c_{R0} c_{X0})^{1/2} \right] dy . \tag{2.62}$$

The integration domain on the right hand side of Eq. (2.62) can be split into two intervals: 0 to H and H to ∞, respectively, where H is the thickness of the S-H layer.

For the diffuse part of the DEL (y > H), Eq. (2.21) becomes

$$\mu_i^d = \mu_i^{0d}(T,P) + RT \ln f_i^d x_i^d + z_i F \psi . \tag{2.63}$$

As for this region of the solution the surface tension makes no contribution to the chemical potential, $\mu_i^{0d}(T,P) = \mu_i^{0\alpha}(T,P)$, the compositions of ions are obtained from Eqs. (2.8) and (2.63),

$$f_{\pm}^d \left(x_R^d x_X^d \right)^{1/2} = f_{\pm}^{\alpha} \left(x_R^{\alpha} x_X^{\alpha} \right)^{1/2} \exp\left(- \frac{(z_R + z_X) F \psi}{2RT} \right). \tag{2.64}$$

For symmetric 1:1 electrolytes $z_X = -z_R$, therefore the contribution to adsorption caused by the diffuse part of the DEL, calculated for the compositions of ions according to Eq. (2.62) vanishes

$$\left(\Gamma_R^d \Gamma_X^d \right)^{1/2} = B \int_H^{\infty} \left[\left(x_R^d x_X^d \right)^{1/2} - \left(x_R^{\alpha} x_X^{\alpha} \right)^{1/2} \right] dy = 0 , \tag{2.65}$$

where the constant B arises from the recalculated molar portions to the bulk concentrations, $B = (c_{R0} c_{X0})^{1/2} / \left(x_R^{\alpha} x_X^{\alpha} \right)^{1/2}$. According to Eq. (2.62), only the contribution of the S-H layer should be considered

$$(\Gamma_R \Gamma_X)^{1/2} = \int_0^{H} \left[(c_R(y) c_X(y))^{1/2} - (c_{R0} c_{X0})^{1/2} \right] dy . \tag{2.66}$$

The thickness of the S-H layer is of the order of the dimension of ions, therefore the choice of the location of the dividing surface according to Lucassen-Reynders' condition $\Gamma_0 + \Gamma_{R_1} + \Gamma_{R_2} + \Gamma_X = \Gamma_{RX}^{\infty}$, almost does not vary the location of the surface upon increasing surface coverage. It is seen that the considerations in terms of the compositions of ions, in contrast to the summation over particular ions, as in Eq. (2.57), enables one to exclude the contribution of the DEL to the adsorption of ions and the surface pressure of the solution of symmetric electrolytes. As applied to Lucassen-Reynders' theory, the inclusion of the DEL into the surface layer model is a merely formal development. This explains why this theory leads to quite good results irrespective of the concentration of added inorganic electrolyte. Surely, for non-symmetric electrolytes, for example proteins, one cannot exclude the contribution by the DEL in the framework of the composition approach, and the model of a charged surface layer should be preferred. Such models, in which the ability of the protein molecule to vary its configuration and partial molar area with changes of the surface pressure was taken into account, were recently proposed in [85 , 86].

The above procedure for the derivation of the adsorption isotherm and equation of state including the effect of the DEL can be performed for two or more ionic surfactants in the solution. Following the lines of the previous derivation the solution of a mixture of two anionic homologues of R_1X (1) and R_2X (2) with the same counterion X^+ in the presence of inorganic salt XY can easily be described. In this system the concentration of counterions X^+ is equal to the sum of the concentrations of R_1X, R_2X and XY. Then the adsorption isotherms have the form

$$K_1 f_{R1} c_{R1} = \frac{\theta_1}{(1-\theta_1-\theta_2)} \exp(-2a_1\theta_1 - 2a_{12}\theta_2) \exp\left(\frac{z_{R1}F\psi}{RT}\right), \tag{2.67}$$

$$K_2 f_{R2} c_{R2} = \frac{\theta_2}{(1-\theta_1-\theta_2)} \exp(-2a_2\theta_2 - 2a_{12}\theta_1) \exp\left(\frac{z_{R2}F\psi}{RT}\right). \tag{2.68}$$

Gibbs' adsorption equation (2.54) for this system at fixed concentration of inorganic electrolyte can be presented as

$$\partial\gamma = \left(\Gamma_{R1}\frac{\partial\mu_{R1}^{\alpha}}{\partial c_{R1}} + \Gamma_X\frac{\partial\mu_X^{\alpha}}{\partial c_{R1}}\right)\partial c_{R1} + \left(\Gamma_{R2}\frac{\partial\mu_{R2}^{\alpha}}{\partial c_{R2}} + \Gamma_X\frac{\partial\mu_X^{\alpha}}{\partial c_{R2}}\right)\partial c_{R2} \ . \tag{2.69}$$

The simultaneous solution of Eqs. (2.67)-(2.69) results in the following equation of state

$$\Pi = -2RT\Gamma_{RX}^{\infty}\left[\ln(1-\theta_1-\theta_2)+a_1\theta_1^2+a_2\theta_2^2+2a_{12}\theta_1\theta_2\right]+\Delta\Pi \qquad (2.70)$$

where $\Delta\Pi$ is again determined from Eq. (2.59) with $c_\Sigma = c_{R_1X} + c_{R_2X} + c_{XY}$, and the electric potential of the surface is defined by

$$sh\varphi = \frac{(z_{R1}\Gamma_{R2} + z_{R1}\Gamma_{R2})F}{(8\varepsilon RTc_\Sigma)^{1/2}} . \qquad (2.71)$$

Again one obtains zero contribution to the adsorption for compositions formed by the ions of symmetric electrolyte $x_i^{\alpha d} = \left(x_{R_i}^d x_X^d\right)^{1/2}$ when the summation is performed over the DEL. This fact substantiates the application of Lucassen-Reynders' relations (2.44) with $1/\omega_0 = \Gamma_{RX}^{\infty}$ and (2.48) for the uncharged surface layer model.

Therefore, the two known adsorption models for ionic surfactants (the one which accounts for the DEL, and the one disregarding it) are applicable. The choice of the particular model should be determined by the aim of the study: Lucassen-Reynders' model is more suitable for a formal description of the system, while the model assuming a separation of charges provides information on the structure of the adsorption layer.

2.6. Surface layers of surfactants able to change orientation

2.6.1 Non-ideal surface layers

The equations which describe the reorientation of surfactant molecules in the surface layer can be derived from Eqs. (2.26) and (2.27). It is assumed that the reorientation results in a variation of the partial molar area ω_i. Note that for the derivation of Eq. (2.7) it was assumed that the ω_i are independent of γ. This requirement, however, does not contradict with the assumption of variable molar areas, because only the ratio of the surfactant adsorptions in different states, i.e., the states with different ω_i-values, depends on γ.

If there are two possible adsorption states, then Eqs. (2.31) and (2.32) can be applied. These equations comprise seven parameters (n_1, n_2, b_1, b_2, a_1, a_2 and a_{12}) for two components or for two states of one surfactant. It is clear that in this form the equations are not readily applicable.

One can derive simpler equations for describing the adsorption of one surfactant possessing i different states (ω_i) of the molecule in the surface layer.

If we assume that the solvent-surfactant and surfactant-surfactant intermolecular interactions do not depend on the adsorption state of the surfactant molecules (ω_i), the regular solution theory (cf. [60-62], and Eq. (2.28)) for the convention of Eq. (2.19) yields

$$\ln f_0^{sH} = a\Gamma_\Sigma^2\omega^2, \ \ln f_i^{sH} = a(1-\Gamma_\Sigma\omega)^2, \tag{2.72}$$

where a is the intermolecular interaction constant, and $\Gamma_\Sigma = \Sigma_{i\geq 1}\Gamma_i$ is the total adsorption of surfactants in all states. For our choice of the dividing surface, Eqs. (2.29) can be transformed into

$$\ln f_i^{sE} = 1-\omega_i\sum_{j\geq 0}\Gamma_j = 1-n_i, \quad i\geq 1, \tag{2.73}$$

$$\ln f_0^{sE} = 1-\omega_0\sum_{j\geq 0}\Gamma_j = 0. \tag{2.74}$$

The convention $\omega_0 = \omega$ means that the enthalpic contribution to the activity coefficient of the solvent in the surface layer depends on the intermolecular interaction, and that the entropic contribution vanishes.

Using Eqs. (2.30), (2.72)-(2.74), from (2.26) and (2.27) and with $K_i = K = \text{const}$, one obtains

$$\Pi = -\frac{RT}{\omega}\left[\ln(1-\Gamma_\Sigma\omega)+a(\Gamma_\Sigma\omega)^2\right], \tag{2.75}$$

$$bc = \frac{\Gamma_i\omega}{(1-\Gamma_\Sigma\omega)^{n_i}}\exp(-n_i)\exp\left[-2a\Gamma_\Sigma\omega+a(1-n_i)(\Gamma_\Sigma\omega)^2\right], \tag{2.76}$$

where $b = K\exp(-a-1)$. In contrast to Eqs. (2.31) and (2.32), for solutions of a single surfactant in two adsorption states (1 and 2) the resulting expressions (2.75) and (2.76) depend on four parameters only: ω_1, ω_2, b and a. An important relationship proposed by Joos [21] follows from Eq. (2.76) for any two states i and j

$$\frac{\Gamma_i}{\Gamma_j} = \exp\left(\frac{\omega_i-\omega_j}{\omega}\right)\cdot\exp\left(\frac{(\omega_j-\omega_i)\Pi}{RT}\right), \tag{2.77}$$

which is equivalent to Eq (2.1). Using Eq. (2.77), the total adsorption can be expressed via the adsorption in any particular state. In terms of state 1 the equation reads

$$\Gamma_\Sigma = \Gamma_1 \sum_{i\geq 1} \exp\left(-\frac{\omega_1 - \omega_i}{\omega}\right)\exp\left[\frac{(\omega_1 - \omega_i)\Pi}{RT}\right]. \tag{2.78}$$

Using (2.20), (2.77) and (2.78) one can express the mean partial molar area of all states by

$$\omega = \frac{\sum_{i\geq 1} \omega_i \exp\left(-\frac{\omega_1 - \omega_i}{\omega}\right)\exp\left[\frac{(\omega_1 - \omega_i)\Pi}{RT}\right]}{\sum_{i\geq 1} \exp\left(-\frac{\omega_1 - \omega_i}{\omega}\right)\exp\left[\frac{(\omega_1 - \omega_i)\Pi}{RT}\right]}. \tag{2.79}$$

If there are only two possible orientations of the surfactant molecules at the surface (states 1 and 2, with $\omega_1 > \omega_2$), Eq. (2.76) can be again simplified. Expressing the adsorption in the i^{th} state via the total adsorption, one can transform Eq. (2.76) into

$$bc = \frac{\Gamma_\Sigma \omega \exp\left(-\frac{\omega_2}{\omega_1}\right)\exp\left[-2a\Gamma_\Sigma\omega + a\left(1-\frac{\omega_2}{\omega}\right)(\Gamma_\Sigma\omega)^2\right]}{(1-\Gamma_\Sigma\omega)^{\omega_2/\omega}\left\{1+\exp\left(\frac{\omega_1-\omega_2}{\omega}\right)\exp\left[-\frac{(\omega_1-\omega_2)\Pi}{RT}\right]\right\}}. \tag{2.80}$$

On the other hand, the number of possible states for adsorbed molecules, corresponding to different partial molar areas ω_i, can be quite large. Theoretically one can assume a continuous change of ω between ω_{min} and ω_{max}, and successive values varying from each other by an infinitesimal increment of the molar area $\Delta\omega$. The transition from a discrete to a continuous reorientation model can be performed formally, replacing the summation in Eqs. (2.78) and (2.89) by an integration.

The values of the adsorption equilibrium constants for different states of adsorbed molecules can be different. The oxyethylated surfactants can be referred to as a typical example. These surfactants differ from other surface active substances in that the oxyethylene chain exhibits the adsorption activity at low surface coverages [22, 23], affecting the total activity of the molecule in the unfolded state. In [24], a power dependence of b_i on ω_j was assumed

$$b_1 = b_2(\omega_1/\omega_2)^\alpha, \tag{2.81}$$

with $\alpha \geq 0$. $\alpha = 0$ means that the adsorption activity id independent of the molecular surface area, while for $\alpha > 0$ the orientation with the larger molecular surface area is stronger surface active. There is an analogue to the well-known experimentally confirmed fact of the dependence of the constant b on the number of carbon atoms in the alkyl chain of a homologous series of a surfactant

$$b_n = b_0 \exp(\beta n), \tag{2.82}$$

were b_0 and β are constants. It is worth noticing that Eq. (2.82) contains the balance between hydrophobic and hydrophilic groups in the molecule, whereas Eq. (2.81) points only to a dependence on orientation.

Using Eq. (2.81), one can transform Eq. (2.77) into a more general form

$$\frac{\Gamma_i}{\Gamma_j} = \exp\left(\frac{\omega_i - \omega_j}{\omega}\right) \cdot \left(\frac{\omega_i}{\omega_j}\right)^{\alpha} \cdot \exp\left(\frac{(\omega_j - \omega_i)\Pi}{RT}\right). \tag{2.83}$$

Equations (2.78) - (2.80) should be also modified correspondingly. It is seen from Eq. (2.83) that positive α lead to an increase of the fraction of the states with larger molar area in the surface layer.

1.6.2 Ideal surface layers and model isotherms

For ideal (with respect to the enthalpy) surface layers of a surfactant capable of adsorbing in two states (1 and 2) with different partial molar areas ω_i ($\omega_1 > \omega_2$) and different adsorption equilibrium constants, Eqs. (2.26) and (2.27) can be transformed into a generalised von Szyszkowski-Langmuir equation of state [25]

$$\Pi = -\frac{RT}{\omega}\ln(1 - \Gamma\omega), \tag{2.84}$$

while the adsorption isotherm is

$$bc = \frac{\Gamma_2\omega}{(1 - \Gamma\omega)^{\omega_2/\omega}}. \tag{2.85}$$

The corresponding values of equilibrium adsorption in these two states are Γ_1 and Γ_2, respectively, with the total adsorption expressed as $\Gamma = \Gamma_1 + \Gamma_2$. The ratio of the adsorption values and the average molar area are given by the expressions

$$\frac{\Gamma_1}{\Gamma_2} = \beta \exp\left[\frac{\Pi(\omega_2 - \omega_1)}{RT}\right] \tag{2.86}$$

$$\omega = \frac{\Gamma_1\omega_1 + \Gamma_2\omega_2}{\Gamma_1 + \Gamma_2} = \frac{\omega_2 + \omega_1 \cdot \beta \cdot \exp[\Pi(\omega_2 - \omega_1)/RT]}{1 + \beta \cdot \exp[\Pi(\omega_2 - \omega_1)/RT]} \tag{2.87}$$

where

$$\beta = \exp\left(\frac{\omega_1 - \omega_2}{\omega}\right)(\omega_1 / \omega_2)^{\alpha}, \tag{2.88}$$

The pre-exponential factor β expresses the relative activity of the states of the surfactant molecule with different areas, and involves two co-factors: the first results from the theory which takes into account the non-ideality of the surface layer entropy caused by differences in the molar areas, while the second co-factor (involving the constant α) reflects the effect of the additional surface activity of state 1 as compared with state 2.

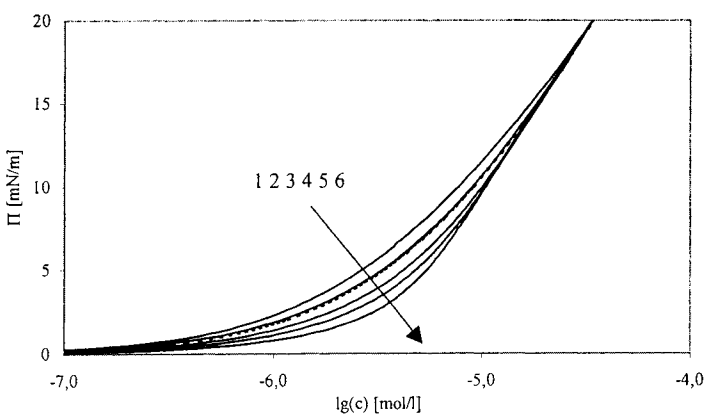

Fig. 2.5. Dependence of surface pressure on the bulk concentration for the following parameter values: $\alpha = 0$, $\omega_2 = 2.5 \cdot 10^5$ m²/mol and: $\omega_1 = 5 \cdot 10^5$ m²/mol (1), 10^6 m²/mol (2), $2.5 \cdot 10^5$ m²/mol (3) (corresponds to the Langmuir model), $1.5 \cdot 10^6$ m²/mol (4), $2.0 \cdot 10^6$ m²/mol (5) and $4.0 \cdot 10^6$ m²/mol (6).

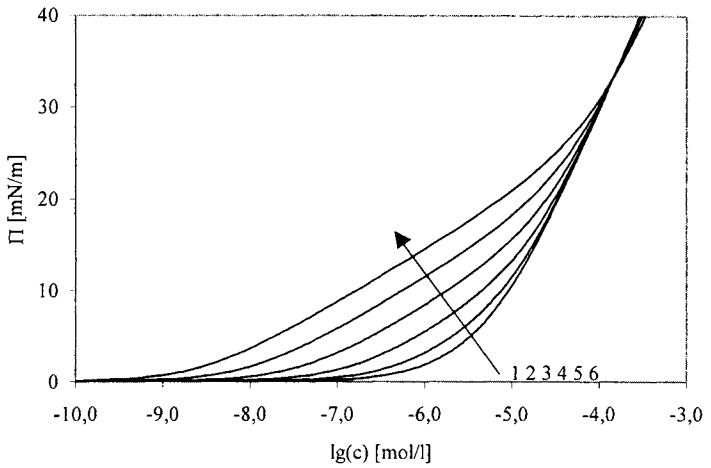

Fig. 2.6 The same as in Fig. 2.5 with the parameter values $\omega_2 = 2.5 \cdot 10^5$ m²/mol, $\omega_1 = 10^6$ m²/mol and: $\alpha = 0$ (1), 1 (2), 2 (3), 3 (4), 4 (5) and 5 (6).

Let us consider now the dependence of the shape of surface pressure isotherms on the parameters of the reorientation model. The dependence of surface pressure on the maximum area ω_1 is illustrated in Fig. 2.5. Here Eqs. (2.84)-(2.88) are employed with $\omega_2 = \text{const}$ and $\alpha = 0$. All calculated curves are normalised in such a way that for the concentration 10^{-4} mol/l, the surface pressure is 30 mN/m. One can see in Fig. 2.5 that with the increase of ω_1 the inflection of the isotherm becomes more pronounced, however, for the ratio $\omega_1/\omega_2 = 4$ the calculated curve almost coincides with the one calculated from the von Szyszkowski-Langmuir equation (2.41) which assumes only one adsorption state with $\omega_0 = \omega = \text{const}$.

For lower ratios ω_1/ω_2 the shape of the isotherms is less convex than for the Langmuir isotherm. For non-zero α, which are especially characteristic for oxyethylated alcohols [87], this difference becomes even more significant. For example, the isotherms calculated for various α values (0 to 5) and $\omega_1/\omega_2 = 4$ are presented in Fig. 2.6, while the calculations performed for the same α range and $\omega_1/\omega_2 = 8$ are illustrated by Fig. 2.7.

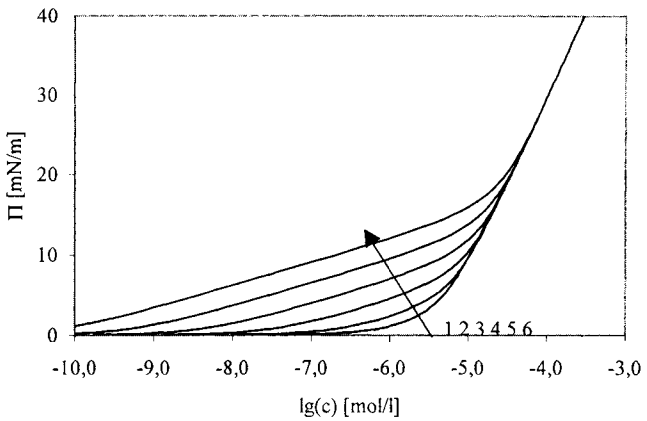

Fig. 2.7 The same as in Fig. 2.5 with the parameter values $\omega_2 = 2.5 \cdot 10^5$ m²/mol, $\omega_1 = 2.0 \cdot 10^6$ m²/mol and: $\alpha = 0$ (1), 1 (2), 2 (3), 3 (4), 4 (5) and 5 (6).

An increase of α corresponds to a sharp increase in the surface activity of the surfactant at very low concentrations. Here the surface pressure isotherm appears to consist of two curves with quite different shape. This behaviour can be attributed to the fact that in the low and medium Π-range the adsorption of the surfactant molecules existing in the state with the molar surface area ω_1 is preferred, while for high Π-values the molecules are mainly adsorbed in the state with the lower area value ω_2.

This is illustrated in Fig. 2.8, where the surface layer coverage is plotted *vs* the bulk concentration. Here the 'partial coverage' $\Gamma_i\omega_i$ was calculated for the two states of the adsorbed molecules (i = 1, 2) with isotherm parameters $\omega_1 = 10^6 m^2 mol$, $\omega_2 = 2.5 \cdot 10^5 m^2 mol$ and $\alpha = 3$, which are typical for oxyethylated alcohols (see below). It is seen that the maximum coverage by the molecules in state 1 is reached for a concentration of about $2 \cdot 10^{-6}$ mol/l, while for $c = 5 \cdot 10^{-5}$ mol/l, i.e., when the curve corresponding to this parameter set at Fig. 2.6 exhibits a sharp increase, the coverages for the two states of the adsorbed molecules become approximately equal to each other (see Fig. 2.8). It should be noted that at concentrations above $2 \cdot 10^{-6}$ mol/l the total adsorption increases only due to a decrease of the fraction of molecules adsorbed in the state with maximum partial molar area.

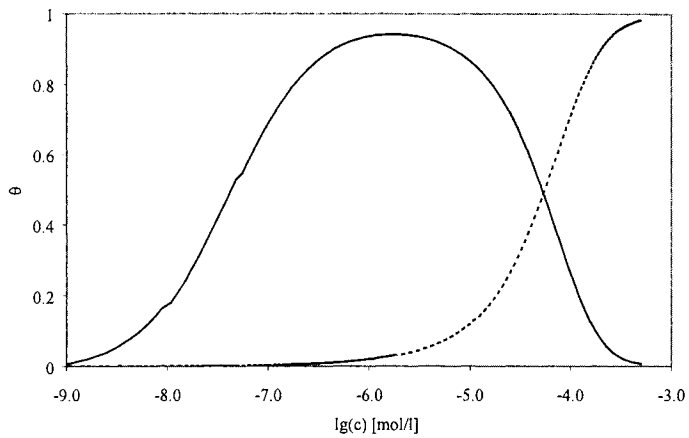

Fig. 2.8 The dependence of the adsorption layer coverage ($\Gamma_1\,\omega_1$) in state 1 (solid line) and 2 (dotted line) on the bulk concentration for $\omega_2 = 2.5 \cdot 10^5$ m²/mol, $\omega_1 = 10^6$ m²/mol and $\alpha = 3$.

2.6.3. Example of experimental results

Let us consider an example where the reorientation isotherm can be successfully applied to experimental data. In Fig. 2.9 the surface pressure isotherm of (N-16-alkyl-N,N-dimethylammonio)-acetic acid bromide [13, 25] is presented.

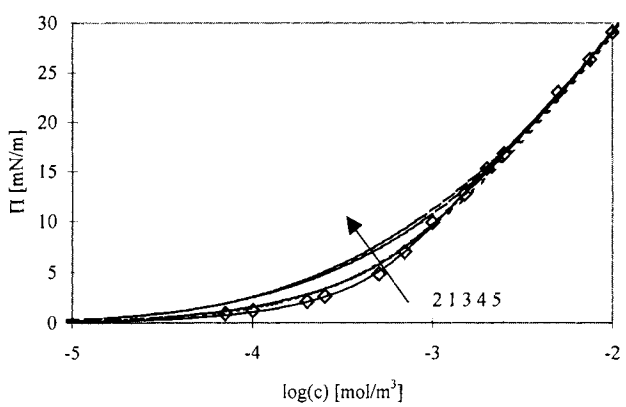

Fig. 2.9 Equilibrium surface pressure for $BHBC_{16}$ solutions; symbols - experimental data from [13, 25] , curves - theoretical calculations: curve 1 - Langmuir-Szyszkowski equation; curves 2 - 5 - reorientation model for 2, 3, 7 and over 50 adsorption states of the $BHBC_{16}$ molecule, respectively; $\omega_{min}=2.52\cdot10^5$m²/mol, $\omega_{max}=19.8\cdot10^5$ m²/mol, b=$1.7\cdot10^6$ l/mol and $\alpha=0$.

At pH 7 (N-16-alkyl-N,N-dimethylammonio)-acetic acid bromide is transformed into a betaine ($BHBC_{16}$). To determine optimum parameters of Eqs. (2.84)-(2.88), a best fit procedure was used, the details of which are discussed in Chapter 3. In brief, for each set of ω_1, ω_2 and α, the values of b_i in each of the m experimental points $\Pi_i = \Pi_i(c_i)$, i = 1, 2, ... , m are calculated and then the mean value of b averaged weighted with the relative surface pressure interval

$$b = \sum_{i=1}^{m} b_i \frac{\Delta\Pi_i}{\Pi_n - \Pi_1}. \tag{2.89}$$

$\Delta\Pi_i = (\Pi_{i+1} - \Pi_{i-1})/2$ is the Π range corresponding to the i^{th} point. The values of the parameters ω_1, ω_2 and α were varied stepwise within respective intervals and that set of parameters ω_1, ω_2 and α was considered optimum where the value of the 'target function' ε was minimum

$$\varepsilon = \sum_{i=1}^{m} \frac{\Delta c_i}{c_{ex,i}} \frac{\Delta\Pi_i}{\Pi_m - \Pi_1} = \min. \tag{2.90}$$

Here $\Delta c_i = |c_{ex,i} - c_{cal,i}|$; the subscripts 'ex' and 'cal' refer to the experimental and calculated surfactant concentrations, respectively; ε is the target function weighted over the relative deviations between the experimental and calculated c_i values. For the Langmuir model, only the parameter ω is varied.

The theoretical isotherms are shown in Fig. 2.9. The difference between the Langmuir and the reorientation isotherms is rather significant, especially in the low surface pressure region where, according to Eq. (2.83), the surfactant molecules are more likely to be adsorbed in the state with the maximum partial molar area ω_1. This effect cannot be reproduced by the Langmuir-von Szyszkowski isotherm. It is essential that the value of α calculated by the fitting program is zero, that is, the activity of the $BHBC_{16}$ molecule remains the same for all adsorption states. The results in Fig. 2.9 also demonstrate that the increasing number of possible adsorption states (for states more than 2 the general formulae Eqs. (2.75)-(2.80) were employed for $\alpha = 0$) yields an increasing discrepancy between theory and experimental data. This discrepancy is especially significant for the continuous reorientation model with an infinite number of states. One can thus conclude that the $BHBC_{16}$ molecule adsorbs in two

states only, corresponding to the maximum and minimum molar surface area, respectively. However, for betaine homologues of shorter alkyl chain lengths, only one adsorption state exists. A detailed discussion of this homologous series of betaine surfactants will be given in Chapter 3.

2.6.4. The elasticity modulus

The reorientation of molecules in the adsorption layer should have a strong effect on the surface elasticity modules (cf. paragraph 4.5 of Chapter 4). The Gibbs' elasticity modulus $\varepsilon_0 = -(d\gamma/d\ln\Gamma)_A = (d\gamma/d\ln A)_\Gamma$ can be calculated from the equation of state (2.84) together with the relationships (2.85)-(2.88). Therefore, this value should reflect the processes involved in the equilibrium transition between the adsorption states .

The viscoelasticity is a complex number determined by the dilatational elasticity and viscosity [19, 94, 95]. The viscoelasticity modulus (or surface dilatational modulus) incorporates a real and imaginary constituent, elasticity and viscosity, respectively,

$$|\varepsilon| = \left(\varepsilon_r^2 + \varepsilon_i^2\right)^{1/2} = \frac{\varepsilon_0}{\left(1 + 2\varsigma + 2\varsigma^2\right)^{1/2}} \tag{2.91}$$

where ε_0 is the Gibbs elasticity modulus. The value ς characterises the ratio of the so-called diffusion relaxation frequency ϖ_0 to the angular frequency of surface oscillations ϖ:

$$\varsigma = \left(\varpi_0 / 2\varpi\right)^{1/2}. \tag{2.92}$$

The diffusion relaxation frequency, in turn, is determined by the diffusion coefficient, adsorption and bulk concentration of the surfactant

$$\varpi_0 = D\left(dc/d\Gamma\right)^2. \tag{2.93}$$

Using Eq. (2.91) both the elasticity and viscosity can be expressed via the surface dilatational modulus as $\varepsilon_r = |\varepsilon|(1+\varsigma)/\left(1 + 2\varsigma + 2\varsigma^2\right)^{1/2}$ and $\varepsilon_i = |\varepsilon|\varsigma/\left(1 + 2\varsigma + 2\varsigma^2\right)^{1/2}$ [94, 95].

As example we will calculate the elasticity module for $C_{10}EO_8$, using the following parameters (compare with Chapter 3, Table 3.13): water/air interface - $\omega_2 = 4.0\cdot10^5$ m²/mol, $\omega_1 = 1.2\cdot10^6$ m²/mol, $\alpha = 3.0$, water/hexane interface - $\omega_2 = 4.1\cdot10^5$ m²/mol,

$\omega_1 = 1.06 \cdot 10^6$ m²/mol, $\alpha = 7.3$. Figure 2.10 illustrates the dependence of the Gibbs' elasticity modulus on the equilibrium surface pressure simulated for a $C_{10}EO_8$ adsorption layer. In contrast to the Langmuir model (with $\omega = 5.6 \cdot 10^5$ m²/mol), which predicts a monotonous increase of the elasticity modulus, the reorientation of adsorbed $C_{10}EO_8$ molecules results in a extremal dependency of $\varepsilon_0(\Pi)$. It should be noted that at high Π values, that is, when the monolayer is almost saturated, both models predict a sharp increase in the elasticity modulus. A maximum of the elasticity modulus was observed at $\Pi = 7$ mN/m for water/air interface, and at $\Pi = 11$ mN/m for water/hexane interface. At these surface pressure values (see Fig. 2.11), the surface layer is saturated with $C_{10}EO_8$ molecules in state 1, possessing the maximum molar area.

It seems instructive to discuss the nature of the minima in the plots of Fig. 2.10. For $C_{10}EO_8$ at the water/hexane interface the elasticity modulus attains a minimum at $\Pi = 25$ mN/m. This can be explained by the influence of the surface pressure on the composition of the surface layer comprised of surfactant molecules capable to adsorb in two states, see Fig. 2.11. Moreover, at $\Pi > 11$ mN/m for the water/hexane interface, and $\Pi > 7$ mN/m for the water/air interface, the adsorption in state 1 starts to decrease significantly. At the same time, adsorption in state 2 increases continuously as usual - with increasing pressure the adsorption becomes higher. As the changes of adsorption in states 1 and 2 are opposite to each other, the resulting changes in the total adsorption and surface tension are small.

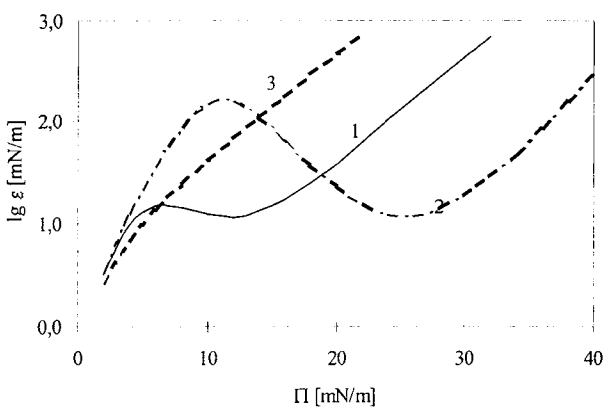

Fig.2.10. Dependence of the Gibbs elasticity modulus $C_{10}EO_8$ solutions on surface pressure; reorientation model water/air interface (1); reorientation model water/hexane interface (2); von Szyszkowski-Langmuir equation for both interfaces (3).

The minimum of the elasticity modulus corresponds to the situation when, for such opposite variations, the adsorptions in the states 1 and 2 are close to each other, see Fig. 2.11.

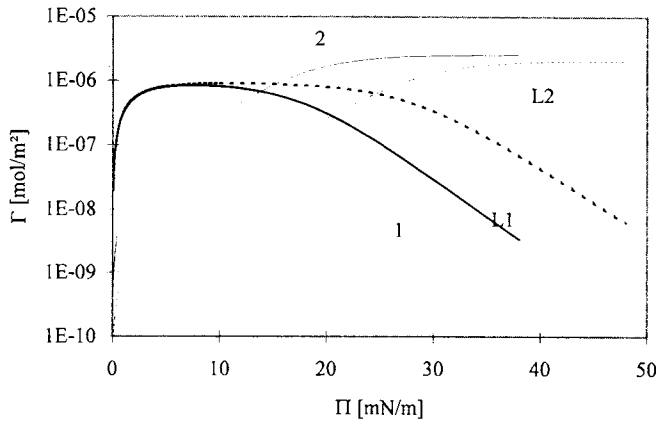

Fig.2.11. Dependencies of the adsorption in state 1 (1 and L1) and 2 (2 and L2) on the interfacial pressure for the two-state model at the water/air (solid lines), and water/hexane (dotted lines) interfaces; according to [87]

The above analysis of the viscoelastic behaviour for adsorption layers of a reorientable surfactant leads to important conclusions. It is seen that the most important prerequisite for a realistic prediction of the elastic properties is the adequacy of the theoretical model used to describe the equilibrium adsorption of the surfactant. For example, when we use the von Szyszkowski-Langmuir equation instead of the reorientation model to describe the interfacial tension isotherm, this rather minor difference drastically affects the elasticity modulus of the surface layer. The elasticity modulus, therefore, can be regarded to as a much more sensitive parameter to find the correct equation of state and adsorption isotherm, rather than the surface or interfacial tension. Therefore the study of viscoelastic properties can give much more insight into the nature of subtle phenomena, like reorientation, aggregation etc.

Let us consider another example in order to emphasise the extraordinary importance of the dilational elasticity for the understanding of the adsorption state of surfactant molecules. The experimental values of the viscoelasticity for two homologues of alkyl dimethyl phosphine oxides (C_{14} and C_{10}) measured using the oscillating bubble method [96] are presented in Fig. 2.12. The existence of the maxima in the experimental curves are due to the finite magnitude of the oscillations of the bubble surface (~10%) resulting in an over-saturation of the surface layer at higher surfactant concentrations in the bulk phase and at the interface.

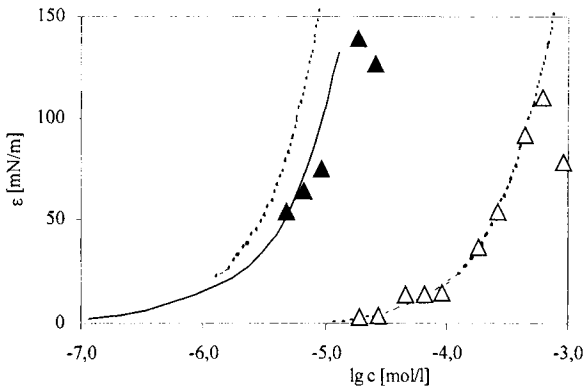

Fig.2.12. Dependence of the elasticity modulus for C_{10}DMPO (△) and C_{14}DMPO (▲) from the data reported in [96]; dotted lines - calculated from the Szyszkowski-Langmuir equation, solid line - calculated using the reorientation model.

It follows from Eqs. (2.91) - (2.93) that when the frequency of surface oscillations is high enough, and the concentration of the surfactant is low, say, for $\varsigma < 0.1$, the viscous modulus is negligibly small and, therefore, the surface behaves completely elastic. In this particular case the dilatational modulus is equal to the Gibbs elasticity modulus. For higher frequencies, the diffusional exchange between the solution bulk and the surface layer can be neglected as compared with the processes taking place in the surface layer. The experiments reported in [96] were performed at higher oscillation frequencies, therefore the results obtained can be compared with the Gibbs elasticity modulus. The theoretical curves presented in Fig. 2.12 were calculated using the parameters of the equilibrium surface tension isotherm. It is seen that the experimental data obtained for C_{10}DMPO agree well with the values calculated from the Langmuir model, while for C_{14}DMPO the two-state reorientation model provides better agreement with the experiment. Therefore, the results obtained from the analysis of the viscoelasticity modulus are in perfect agreement with the surface tension measurements summarised in Chapter 3: while the C_{14}DMPO molecules undergo reorientation in the surface layer the C_{10}DMPO molecules adsorbed in a single state only.

2.7. Aggregation of adsorbing molecules

2.7.1. Equations of state and adsorption isotherms

The aggregation of surfactant molecules in the solution bulk (e.g., micelle formation) affects significantly the shape of surface tension isotherms. For a non-ionic surfactant solution with c > CMC, the Gibbs adsorption equation has the form $d\gamma / d\ln c \cong -RT\Gamma / n$, where n is the micellar aggregation number, usually between 50 and 100 [97]. It follows that for non-ionic surfactants in the region where micelles exist, the dependence of γ on ln c is very weak. For 1:1 charged ionic surfactants the corresponding dependence has the form $d\gamma / d\ln c \cong -RT\Gamma_1(1-\beta)$ [97], where β is the degree of bonding of counterions by micelles, usually ca. 0.8 to 0.9, and Γ_1 is the adsorption of surface active ions. The slope of the dependence of γ on ln c for this case is rather significant, and can be used to determine the value of β. However, the mechanism through which the aggregation of surfactants in the bulk affects the dependence $\gamma(c)$ is rather different from that responsible for surfactant aggregation in the surface layer $\gamma(\Gamma)$: while the aggregation of molecules in the solution bulk leads to the formation of adsorption inactive micelles and hence to a decrease of the concentration of surface active monomers in the bulk, the surface aggregation of surfactants leads to a decrease of the number of kinetic units, because both the aggregates and the monomers introduce quite similar contribution to the surface pressure of the interface [35, 41].

For the formation of aggregates at the surface, the equilibrium between monomers and n-mers can be described by

$$\mu_n^s = n\mu_1^s. \qquad (2.94)$$

Combining Eqs. (2.7) written for monomers and aggregates with Eq. (2.94), and assuming ideal mixing, one obtains

$$x_n^s = K_n \left(x_1^s\right)^n \exp(\Pi\Delta\omega/RT), \qquad (2.95)$$

where K_n is the aggregation constant, $K_n = \exp\left\{\left[\left(n\mu_1^\circ - \mu_n^\circ\right) - \gamma_0\Delta\omega\right]/RT\right\}$ and $\Delta\omega = n\omega_1 - \omega_n$. For very small aggregates (dimers, trimers, etc.) the value of $\Delta\omega$ is negligibly small, for large aggregation numbers $\Delta\omega$ can have significant values, because the net area of free monomers

can differ from that of the molecules in the aggregates [34, 35, 98]. If $\Delta\omega > 0$, then, according to Eq. (2.95), the monomer/aggregate equilibrium is shifted towards the formation of aggregates. The adsorption of aggregates (n-mers) is described by the relationship

$$\Gamma_n = K_n \Gamma_1^n \omega^{n-1} \exp(\Pi \Delta\omega / RT). \tag{2.96}$$

Regarding the formation of small aggregate only ($\Delta\omega = 0$), and introducing a critical aggregation adsorption Γ_c, one can represent the aggregation constant K_n by

$$K_n = \Gamma_c^{-(n-1)} \omega^{-(n-1)}. \tag{2.97}$$

Then the equation for aggregate adsorption (2.96) simplifies to

$$\Gamma_n = \Gamma_1 \left(\frac{\Gamma_1}{\Gamma_c} \right)^{n-1}. \tag{2.98}$$

Introducing Eq. (2.98) into Eqs. (2.26), and assuming $\omega_0=\omega_1$ and an ideal enthalpy of mixing (Eq. (2.33) instead of Eq. (2.26) in this case can be used), one can represent the equation of state for surface layer of aggregating surfactants as

$$\Pi = -\frac{RT}{\omega_1} \left[\ln \left[1 - \omega_1 \Gamma_1 \left(1 + n \left(\frac{\Gamma_1}{\Gamma_c} \right)^{n-1} \right) \right] + \omega_1 n \Gamma_1 \left(\frac{\Gamma_1}{\Gamma_c} \right)^{n-1} \left(1 - \frac{1}{n} \right) \right] \tag{2.99}$$

where (see Eq. (2.33)) $n=n_2=\omega_n/\omega_1$, and $n_1=\omega_1/\omega_0=1$. Adsorption isotherm Eq. (2.27) or Eq. (2.34) of monomers for the same conditions given by

$$bc = \frac{\Gamma_1 \omega_1}{\left[1 - \Gamma_1 \omega_1 \left(1 + n (\Gamma_1 / \Gamma_c)^{n-1} \right) \right]}. \tag{2.100}$$

More realistic equations can be obtained if we assume $\omega_0 = \omega$ (the convention $\omega_0 = \omega$ means that the entropic contribution to the activity coefficient of the solvent in the surface layer vanishes). Moreover, the convention $\omega_0 = \omega$ shows that n-mer similar to the monomer are represented by one kinetically independent entity only. Introducing Eq. (2.98) into Eqs. (2.20), (2.26) and (2.27) we get the equation of state for surface layers of aggregating surfactants in the form

$$\Pi = -\frac{RT}{\omega}\ln\left[1-\Gamma_1\omega\left(1+\left(\frac{\Gamma_1}{\Gamma_c}\right)^{n-1}\right)\right], \tag{2.101}$$

and the adsorption isotherm of monomers

$$bc = \frac{\Gamma_1\omega}{\left[1-\Gamma_1\omega\left(1+(\Gamma_1/\Gamma_c)^{n-1}\right)\right]^{\omega_1/\omega}}. \tag{2.102}$$

Here the mean molar area of monomers and aggregates is defined by

$$\omega = \frac{\Gamma_1\omega_1+\Gamma_n\omega_n}{\Gamma_1+\Gamma_n} = \omega_1\frac{1+n(\Gamma_1/\Gamma_c)^{n-1}}{1+(\Gamma_1/\Gamma_c)^{n-1}}. \tag{2.103}$$

If we now assume the formation of dimers, then the equation of state (2.101) transforms into

$$\Pi = -\frac{RT}{\omega}\ln\left[1-\Gamma_1\omega-K_2\Gamma_1^2\omega^2\right] \tag{2.104}$$

For values $K_2\Gamma_1^2\omega^2$ much smaller than $\Gamma_1\omega$ and 1, the logarithmic function in Eq. (2.104) can be developed into a series, which results in

$$\Pi = -\frac{RT}{\omega}\left[\ln(1-\Gamma_1\omega)-K_2\Gamma_1^2\omega^2\right]. \tag{2.105}$$

This equation coincides with Frumkin's equation of state (2.37) in which the intermolecular interaction a is given now by the constant of dimerisation in the adsorption layer ($K_2 = -a$).

For the formation of large aggregates, so-called clusters ($n \gg 1$), the approximations $\Gamma_1 \cong \Gamma_c$ and $1+(\Gamma_1/\Gamma_c)^{n-1} \cong 1$ are valid in the transition region of adsorption $\Gamma_\Sigma = \Gamma_1+\Gamma_n > \Gamma_1$ [35]. With these approximations and Eq. (2.103), we get the mean molar area of adsorbed monomers and aggregates in the form

$$\omega = \omega_1\frac{\Gamma}{\Gamma_c}. \tag{2.106}$$

Therefore, in the limiting case of large aggregates, the equation of state for the surface layer (2.101) and the respective adsorption isotherm (2.102), expressed via the molar area of monomers and the critical adsorption of aggregation, can be written in the following form

$$\Pi = -\frac{RT\Gamma_c}{\omega_1\Gamma}\ln[1-\omega_1\Gamma], \tag{2.107}$$

$$bc = \frac{\Gamma\omega_1}{[1-\omega_1\Gamma]^{\Gamma_c/\Gamma}}. \tag{2.108}$$

In equations (2.106)-(2.108) adsorption of kinetic entities Γ_Σ is expressed via the observable total adsorption recalculated into monomers

$$\Gamma = \Gamma_1 + n\Gamma_n. \tag{2.109}$$

Using the condition $\Gamma_1 \cong \Gamma_c$ one obtains the following approximate relation

$$\Gamma_\Sigma = \frac{\Gamma_c(n-1)+\Gamma}{n} \cong \Gamma_c + \Gamma/n. \tag{2.110}$$

For low surface coverage we get

$$\Pi = RT\Gamma_\Sigma = RT(\Gamma_c + \Gamma/n). \tag{2.111}$$

Eq. (2.111) predicts that above the critical adsorption Γ_c, or above the corresponding critical bulk concentration c_c, determined from Eq. (2.102) as

$$bc_c = \frac{\Gamma_c\omega_1}{[1-\Gamma_c\omega_1]}, \tag{2.112}$$

the increase in equilibrium surface pressure is much slower as compared to the case where molecules do not form aggregates (at the same conditions $\Pi = RT\Gamma$).

For very large aggregates, a quite simple relationship can be proposed which provides a correction of Γ_c with respect to the ratio of the molar areas of molecules existing in aggregates and as monomers, and to the surface pressure change [98]

$$\Gamma_c = \Gamma_c^0 \exp\left(-\frac{(\Pi-\Pi_c)(\omega_1-\omega_n/n)}{RT}\right) \tag{2.113}$$

where Γ_c^0 is the value of Γ_c which corresponds to the inset of phase transition, i.e. at $\Pi = \Pi_c$. For $\Pi > \Pi_c$ and $1-\omega_n/n\omega_1 > 0$ (the packing of monomers in aggregates is closer) the value of Γ_c decreases, which according to Eqs. (2.107)-(2.111), results in a decrease of surface pressure. Therefore, the dependence of surface pressure on concentration at $c > c_c$ becomes flatter.

2.7.2. Example of experimental results

Let us first demonstrate the effect of the model parameters on the shape of the surface pressure isotherms. The results in Fig. 2.13 illustrate the process of dimer formation in the adsorption layer at various Γ_c. The smaller Γ_c is, the more pronounced is the difference between the dimerisation isotherm and the Langmuir isotherm (n = 1). At the same time, for $\Gamma_c < 10^{-10}$ mol/m^2 the shape of the surface pressure isotherm does no longer depend on Γ_c, because for sufficiently small Γ_c the adsorption layer consists of aggregates only.

Figure 2.14 illustrates the effect of the aggregation number for the case where the surface layer is free of monomers ($\Gamma_c < 10^{-10}$ mol/m^2). In this case, when the aggregation number exceeds a certain value (n > 20), the curves also become independent of n. Here, if the critical adsorption Γ_c is not too small, the curves exhibit a characteristic fracture which indicates the formation of clusters in the adsorption layer (cf. Fig. 2.15). However, for n > 50 (that is, for very large clusters) the shape of the curves becomes independent of n.

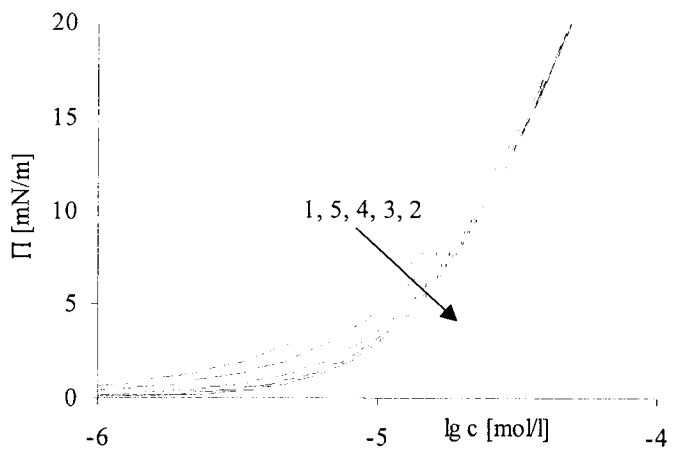

Fig. 2.13. Surface pressure isotherm for a surfactant solution, calculated from the Langmuir equation for monomers (1), and for the formation of surface dimers: $\Gamma_c = 10^{-10}$ mol/m² (2); $\Gamma_c = 10^{-8}$ mol/m² (3); $\Gamma_c = 10^{-7}$ mol/m² (4) and $\Gamma_c = 10^{-6}$ mol/m² (5). The ω_1 value was varied in the range $(1\text{-}1.5)\cdot 10^5$ m²/mol to obtain the same slope of all curves at Π > 20 mN/m; the constant b was chosen such that Π = 30 mN/m was reached at a concentration of 10^{-4} mol/l.

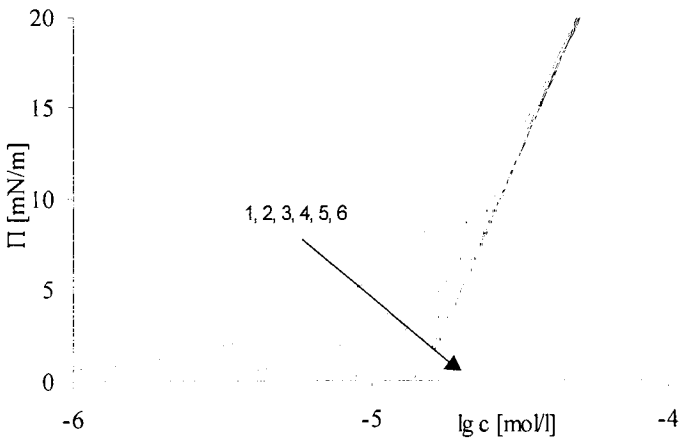

Fig. 2.14. The same as in Fig. 2.13 for $\Gamma_c = 10^{-10}$ mol/m² and different aggregation numbers n = 1 (1), n = 2 (2), n = 3 (3), n = 5 (4), n = 10 (5) and n = 20 (6).

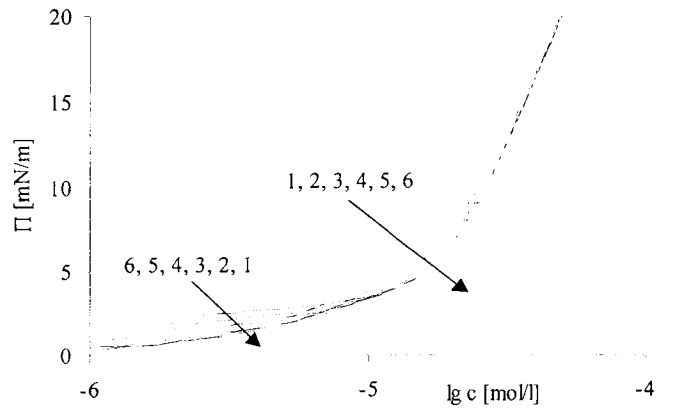

Fig. 2.15. The same as in Fig. 2.13 for $\Gamma_c = 10^{-6}$ mol/m² and different aggregation numbers, n = 2 (1), n = 3 (2), n = 5 (3), n = 10 (4), n = 20 (5) and n = 100 (6).

The position of the inflection point in the surface pressure isotherm for large clusters depends on Γ_c: the higher Γ_c is, the higher is the surfactant concentration at which the cluster formation sets in, the less pronounced is the inflection, and the less steep is the isotherm beyond the

inflection point (cf. Fig. 2.16). Similar features are characteristic to the dependence of surface pressure on area per surfactant molecule [35, 98].

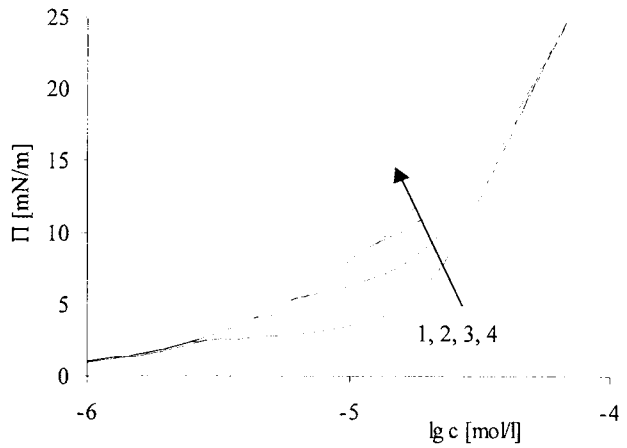

Fig. 2.16. The same as in Fig. 2.15 for the aggregation number n = 100 and different critical adsorptions $\Gamma_c = 10^{-6}$ mol/m² (1), $\Gamma_c = 2 \cdot 10^{-6}$ mol/m² (2), $\Gamma_c = 3 \cdot 10^{-6}$ mol/m² (3), and $\Gamma_c = 4 \cdot 10^{-6}$ mol/m² (4).

It was shown recently [36, 37, 40] that neither the von Szyszkowski-Langmuir (2.41), nor the Frumkin isotherm (2.37), (2.38) can provide a correct description of experimental surface tension isotherms for sodium dodecyl sulphate (SDS) and decanol at the water/air interface. To achieve satisfactory agreement with experimental data, for decanol solutions an additional parameter was introduced in the Frumkin equation [36, 37]. On the other hand, the experimental and theoretical dependencies $\Pi = \Pi(c)$ for decanol solutions showed excellent agreement with the aggregation model within experimental accuracy (cf. Fig. 2.17). The Langmuir (target function ε=0.18) and Frumkin equations (ε=0.041) are rather inconsistent with the experimental data which is maybe caused by the almost complete aggregation ($\Gamma_c < 10^{-10}$ mol/m^2) of decanol molecules at the surface with a formation of dimers and trimers (the best agreement with $\varepsilon = 0.011$ was obtained for $n = 2.6$).

The surface pressure isotherms of SDS in presence of large NaCl concentration reported in [99] look unusual on a first glance. Part of the data are reproduced in Fig. 2.18 for 0.1 M NaCl. The surface pressure isotherm for SDS exhibits a characteristic inflection at a pressure of ca. 8 mN/m which was ascribed to the aggregation of SDS in the surface layer [99]. Similar

dependencies with inflection points at 8-10 mN/m were also obtained for SDS at higher NaCl concentrations [99]. It should be noted that besides the results reported in [99] similar dependencies were obtained also for other surfactants [93, 100-102].

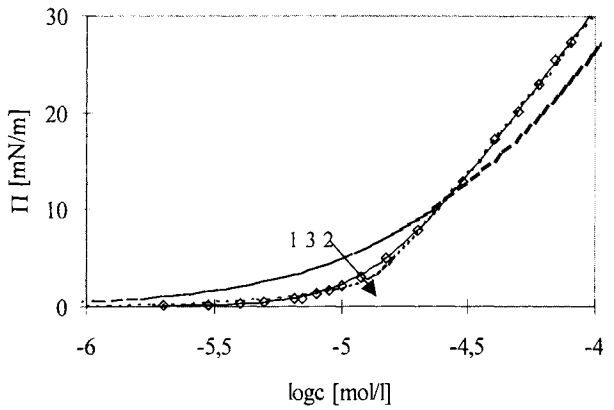

Fig. 2.17. Surface pressure isotherm for 1-decanol solutions: ◇ -experimental data [36, 37]; calculations from the von Szyszkowski equation (1), Frumkin equation (2), and aggregation model (3).

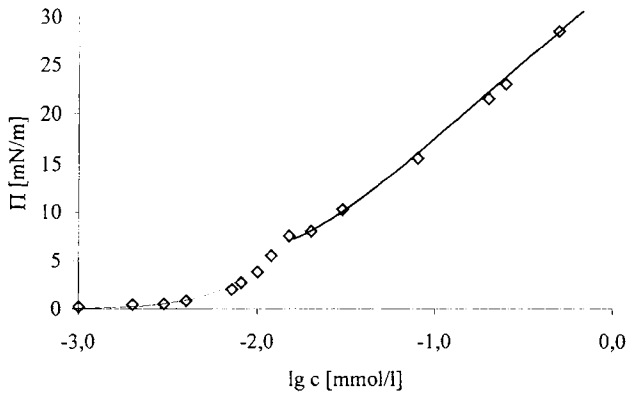

Fig. 2.18. Surface pressure isotherm for the SDS in the presence of 0.1 M NaCl, ◇ - experimental data from [99]; lines - calculated in the pre-critical region with $\omega_1 = 2.0 \cdot 10^{-5}$ m²/mol, $\Gamma_c = 10^{-10}$ mol/m² and n = 2, and in the transition region with $\omega_1 = 3.6 \cdot 10^{5}$ m²/mol, $\Gamma_c = 1.8 \cdot 10^{-6}$ mol/m² and n = 100.

To achieve agreement between theoretical calculations and experimental results it can be supposed that at pre-critical concentrations (region 1) small aggregates are formed, while in the transition region (2) the surfactant forms large aggregates. In Fig. 2.18 it is shown that the results calculated from the aggregation model for two parts of the experimental curve are quite consistent with the experimental data. The values of the parameters suggest that in region 1 only dimers exist at the surface. It should be noted that the critical adsorption Γ_c is so small that this parameter does not affect the shape of the curve and is therefore irrelevant. The value $\omega_1 = 2 \cdot 10^5$ mol/m^2 in region 1 agrees well with that estimated from the radiotracer method, giving $\omega_1 = 2.3 \cdot 10^5$ mol/m^2 [103]. In region 2 only large clusters ($n > 50$) exist, and therefore the aggregation number is irrelevant. There seems to be an inconsistency between the parameters obtained from the fitting procedure in regions 1 and 2: in the first region a monomer-dimer equilibrium exists without almost any monomers ($\Gamma_c < 10^{-10}$ mol/m^2), while in the second region a significant number of monomers are present ($\Gamma_c = 1.8 \cdot 10^{-6}$ mol/m^2), and a monomer-cluster equilibrium exists in the surface layer. Moreover, the total adsorption of monomers and dimers (recalculated to monomers) at the end of region 1 is almost twice as much as Γ_c ($3.5 \cdot 10^{-6}$ mol/m^2 against $1.8 \cdot 10^{-6}$ mol/m^2). However, it should be kept in mind, that the value of ω_1 for the second region is almost twice as large as the value estimated for the first region. Therefore the monomers in the second region are nothing else but the SDS dimers, so that a dimer-cluster equilibrium exists in this region.

2.7.3. Phase transitions in adsorption layers

There are critical phenomena taking place in a three-dimensional non-ideal gas, or in a two-dimensional insoluble monolayers at the interface between two liquid bulk phases, which have been explained qualitatively using an equation of the van der Waals type. Similar considerations can be applied to the condensation in an adsorption layer, which can be described by the Frumkin equation of state for a surfactant solution [1, 104, 105]. If the interaction parameter a is large enough, then at constant temperature Eq. (2.37) has three real roots: three different values the surface coverage θ (or area per mole $A=1/\Gamma$) correspond to the same surface pressure Π. As the monolayer should be mechanically stable, $d\Pi/dA \leq 0$, so that the system undergoes a jump through the instability region, from a value of θ determined by

the smallest root of Eq. (2.37) to that corresponding to the largest root. This jump is known as two-dimensional condensation of the monolayer.

The dependence of the dimensionless pressure $\Pi^* = \Pi\omega_1/RT$ (as $\omega_0 = \omega_1$) on the surface coverage θ, calculated for various values of the intermolecular interaction constant a is shown in Fig. 2.19.

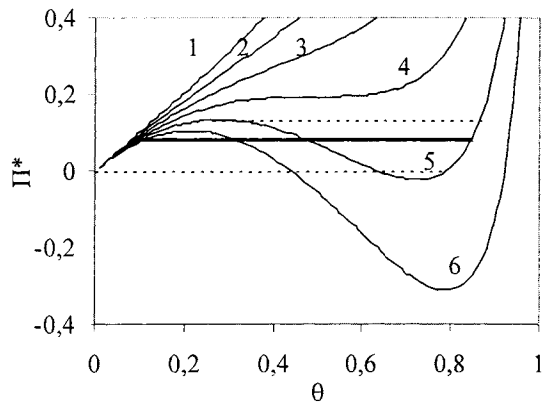

Fig. 2.19. Dependence of dimensionless surface pressure $\Pi^* = \Pi\omega_1/RT$ calculated for the Frumkin model (2.37) with a = 0.5 (1); a = 1 (2); a = 1.5 (3); a = 2.0 (4); a = 2.5 (5); and a = 3.0 (6); for details see text.

Three different roots of Eq. (2.37) exist for $a > 2$. The region enclosed by the dashed lines (shown in Fig. 2.19 for $a = 2.5$) corresponds to unstable states of the system. The surface pressure that corresponds to the coexistence of a condensed and gaseous state can be determined by using the so-called Maxwell construction [1, 104, 105]. That is, the areas enclosed by the dashed lines corresponding to this coexistence pressure and the two portions of the loop should be equal to each other on the Π^* vs A dependence. For $a = 2.5$ this pressure is marked in Fig. 2.19 by the solid line.

In spite of the obvious capability of the models described by Eq. (2.37) to provide explanation of the phenomenon of surface condensation due to strong intermolecular interaction, there is evidence that this model is incompatible with the actual physical process governing the two-dimensional condensation of surfactants in either spread or adsorbed interfacial layers. In both regions, precritical and transcritical, Eq. (2.37) involves the same surface layer entities, namely the monomers and no distinction is made between free monomers and molecules involved into

aggregates. It is known from experiments that in the transcritical region of spread monolayers or adsorption layers, aggregates start to form, and the relative fraction of the surface occupied by monomers decreases with increasing surfactant surface concentration [106-115]. Clearly, the intermolecular interaction between the molecules in the aggregates (condensed phase) cannot affect the surface pressure in the same manner as the interaction between non-aggregated monomers does. Moreover, the degree of freedom characteristic to condensed monomers is insufficient to produce an appreciable effect on the surface pressure even in an ideal monolayer. More rigorous theoretical models, developed recently [32, 33, 35, 98, 116-118], take into account different effects of monomers and aggregates on the surface pressure.

The curve shown in Fig. 2.19 for $a = 2.5$ exhibits a step-like variation of the monolayer coverage, from 0.1 to 0.85, that is, the adsorptions of monomers and aggregates become several times larger. Note that for this case the Frumkin adsorption isotherm (2.38) predicts a relatively small jump of the surfactant bulk concentration, namely by 20 to 30%. Therefore, in the framework of the van der Waals approach, the two-dimensional condensation in the adsorption layer should be accompanied by a sharp increase in the adsorption at constant pressure, and at the same time involving no significant increase in the surfactant bulk concentration. This concept was widely used in the analysis of surface tension *vs* concentration isotherms $\gamma(c)$ for solutions of various surfactants adsorbed at liquid/gas and liquid/liquid interfaces [101, 119-128]. Sharp inflections in $\gamma(c)$-isotherms accompanied by an increase in the slope was ascribed to a surfactant condensation at the interface. For the interpretation of these results, the authors in [101, 119-128] have used the Gibbs equation in the following form

$$\Gamma = -\frac{1}{RT}\frac{d\gamma}{d\ln c} \tag{2.114}$$

Applying Eq. (2.114) to experimental data the authors obtained surface pressure Π *vs* molar area A isotherms which exhibit horizontal sections. (As $\Gamma = 1/A$, the form of these curves corresponds to a mirror reflection of the curves shown in Fig. 2.19 with respect to the ordinate.)

This interpretation of the experimental data is erroneous. Indeed, a two-dimensional aggregation (or condensation) in an adsorption layer or a spread insoluble monolayer should be regarded to as the formation of another type of adsorbed particles, namely two-dimensional aggregates (n-mers) or domains. It is important to note that the surface concentration of the

monomers for $A < A_c$, i.e. the molar area of states below the critical value A_c remains virtually unchanged with decreasing average area per molecule A. At the same time, however, the number and size of aggregates in the surface layer increases [106-115]. Therefore, Eq. (2.114) is valid only in the region, which corresponds to concentrations lower than the critical concentration, while for concentrations higher than the critical one, the Gibbs equation correctly reads

$$\Gamma_{\Sigma} = \Gamma_1 + \Gamma_n = -\frac{1}{RT}\frac{d\gamma}{d\ln c}. \qquad (2.115)$$

For monolayers in a condensed state the value of n is very high (10^3 or more), so that in Eq. (2.115) the adsorption of aggregates Γ_n can be neglected as compared with the adsorption of monomers Γ_1 ($\Gamma_n \ll \Gamma_1$). Therefore, the adsorption corresponding to states below the critical concentration should be approximately the same as the adsorption of monomers immediately above the critical concentration. Hence, from Eq. (2.115) we can conclude that the values of $d\gamma/d \ln c$ corresponding to states below the presumed phase transition point should be roughly the same as those values corresponding to states immediately above this point. It follows then that the phase transition could not be identified from an inflection point in the $\gamma(c)$ isotherm. A more rigorous theory describing the aggregation in adsorption layers (see Section 2.7.1) indeed predicts the existence of an inflection point in the $\gamma(c)$ isotherm. However, according to this theory, the slope of the curve $d\gamma/d \ln c$ for the states above this point becomes lower than for the states below this point.

More rigorous thermodynamic relations valid for adsorption layers which undergo a phase transition could be derived based on the requirement that the chemical potentials in either phase should be equal to each other. The phases are represented by the surfactant bulk solution, the non-condensed (surface solution) and the condensed part of the surface layer. The dependence of μ_i^s on the composition of a surface layer is given by the Butler equation (2.7). The chemical potential of the i^{th} component in the condensed phase comprised of the given component only ($f_i^s x_i^s = 1$) can be derived from Eq. (2.7) as

$$\mu_{i(n)}^s = \mu_{i(n)}^{0s} - \gamma\omega_{i(n)}. \qquad (2.116)$$

From Eqs. (2.7) and (2.116), using the condition $\mu_i^s = \mu_{i(n)}^s$ and assuming that the molecular area of monomers within the condensed phase is equal to that outside the aggregates, $\omega_1=\omega_{1(n)}$, one obtains

$$x_{ic}^s = \exp\left(-\frac{\mu_1^{0s} - \mu_{1(n)}^{0s}}{RT}\right) = \text{const}. \qquad (2.117)$$

Therefore the surface molar fraction of the free monomers is constant throughout the whole range of phase coexistence.

When two phases coexist with each other, the monolayer is comprised of non-aggregated molecules with a surface coverage θ_c, and of a condensed fraction of the monolayer with the coverage θ_n. Assuming that the total coverage of the monolayer is θ, one can express these 'partial coverages' via corresponding values of adsorptions and molar areas as $\Gamma_i\omega_i$. Applying the obvious relationship $x_0^s = 1-\theta$ and Eqs. (2.106) and (2.14) an equation of state for the monolayer in the coexistence region is obtained

$$\Pi = -\frac{RT\theta_c}{\omega_1\theta}\ln(1-\theta). \qquad (2.118)$$

The dependence of the dimensionless surface pressure $\Pi^* = \Pi\omega_1 / RT$ on the total surface coverage θ for various values of θ_c, calculated from Eq. (2.118), are presented in Fig. 2.20.

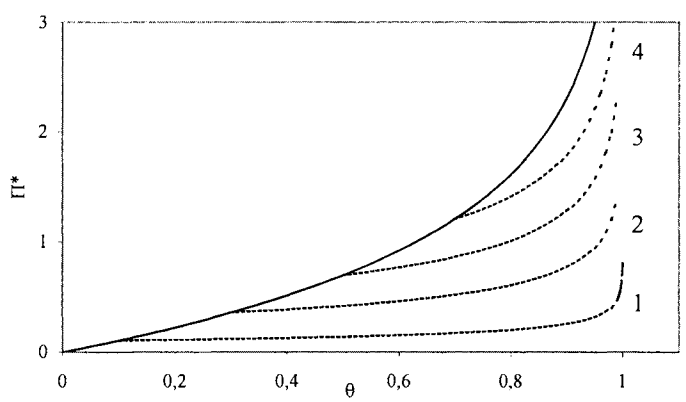

Fig. 2.20. Theoretical dependencies of the dimensionless surface pressure Π^* as a function of the total surface coverage θ for θ_c = 0.1, 0.3, 0.5 and 0.7 (dotted lines) calculated from Eqs. (2.118); solid line - calculated from Eq. (2.39) for $\omega_0 = \omega_1$ and i=1.

It is seen that the phase transition (condensation) in the monolayer is accompanied by a significant decrease of the slope of the surface pressure isotherm. In contrast to the model based on Frumkin's equation and Maxwell's construction (see Fig. 2.19), the dependence of Π^* on θ in the phase coexistence region does not generally have a horizontal line, except for very small θ_c values.

To derive the adsorption isotherm valid for the coexistence region, one has to assume $x_{ic}^s = \text{const}$ (or $\Gamma_c = \text{const}$) in Eq. (2.15), cf. Eq. (2.117). The value $x_c^s = \Gamma_c \omega_1$ is correct only if the concentrations of all other soluble components in the surface layer are zero. If a phase transition takes place, then a significant portion of the monolayer is covered by the condensed phase. In the previous sections we took into account the existence of other components in the monolayer by introducing the degree of surface coverage, as $\theta_i = \Gamma_i \omega$ (in Eq. (2.101)-(2.103), as $\theta_c = \Gamma_c \omega$). Then the portion of the surface occupied by the i^{th} molecules θ_i is equal to its mole fraction x_i^s at the surface (see Section 2.3). If we use the condition (2.117) as $\Gamma_c = \text{const}$, the surface coverage for monomers should depend on the fraction of the surface occupied by the condensed phase. As the condensation leads to an increase of the molar area per adsorbed monomer, the value of $\theta_c = \Gamma_c \omega_1$ should be corrected by the factor $\omega/\omega_1 = \theta/\theta_c$. Other explanations fort he need of the given correction for the phase coexistence region can be: i) the increase of the surface occupied by monomers and hence free of the condensed phase ; and ii) dependence of the value $K_i = (x_i^s / x_i^\alpha)_{x_i^\alpha \to 0}$ (the distribution coefficient at infinite dilution in Eq. (2.15)) on the surface fraction occupied by the condensed phase. Introducing the correction of θ_c the Eqs. (2.15) and (2.117) yield an adsorption isotherm similar to Eq. (2.108) and valid in the phase coexistence region,

$$bc = \frac{\theta}{(1-\theta)^{\theta_c/\theta}}. \qquad (2.119)$$

The dependencies of Π^* on B for various θ_c values, calculated from Eqs. (2.118) and (2.119), are shown in Fig. 2.21. It is seen that the phase transition in the monolayer is characterised by a decreased slope of the Π^*(B)-curves, in contrast to the two-dimensional condensation model based on the Gibbs equation (2.114) [119-128] or that derived in [1, 104, 105] employing the Frumkin equation and Maxwell construction. With increasing B, all isotherms exhibiting a

phase transition move closer to that calculated from Eq. (2.42). This phenomenon can be easy explained: the behaviour of a monolayer extremely saturated by monomers should be the same as that of a condensed monolayer.

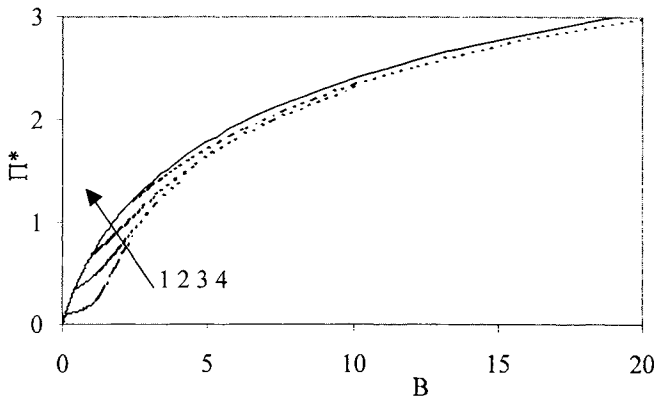

Fig. 2.21. Theoretical dependencies of the dimensionless surface pressure Π* on the dimensionless concentration B = bc for $\theta_c = 0.1$ (1), 0.3 (2), 0.5 (3) and 0.7 (4), dotted lines - calculated from Eqs. (2.118) and (2.119); solid line - calculated from Eq. (2.42) for $\omega_0 = \omega_1$.

If one does not introduce any corrections to the θ_c in the phase coexistence region, results similar to those reported in [1, 104, 105, 119-128] are obtained. In the phase coexistence region ($\theta > \theta_c$) we then have $\Gamma_c \neq \text{const}$ and the critical monomer adsorption is less than Γ_c for $\theta = \theta_c$ by a factor of $\omega_1/\omega = \theta_c/\theta$. Introducing $x_1^s = \theta_c$, one obtains from Eq. (2.15) and (2.117) the following adsorption isotherm

$$bc = \frac{\theta_c}{(1-\theta)^{\theta_c/\theta}}. \qquad (2.120)$$

The dependencies of Π* on B for various θ_c values, calculated with Eqs. (2.118) and (2.120), are shown in Fig. 2.22. In agreement with the models given in [1, 104, 105, 119-128], the curve exhibits a sharp inflection accompanied by an increase in the slope at the condensation onset point. In contrast to curves presented in Fig. 2.21, the saturation of the monolayer does not move these curves towards that calculated for the case when no phase transition takes place. We find, that the lower the θ_c-value, the steeper is the dependence of Π* on B, which seems incorrect. For example, for $\theta_c = 0.01$ (not shown in Fig. 2.22) the Π*(B)-curve coincides

almost with the ordinate axis. Moreover, the condition $\Gamma_c \neq \text{const}$ leads to incorrect Eqs. (2.106) and (2.118).

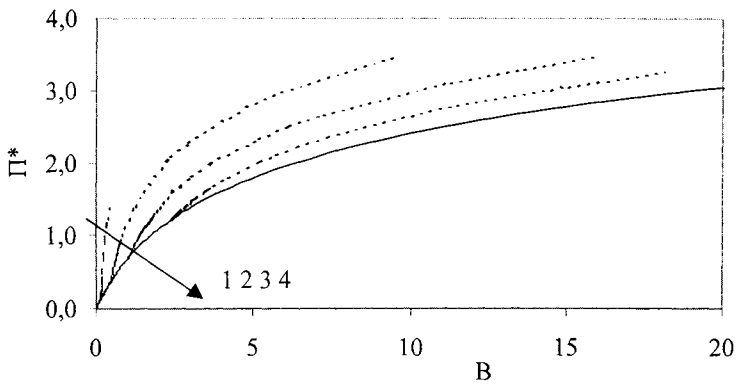

Fig. 2.22. The same as in Fig. 2.21, calculated from Eqs. (2.118) and (2.120).

Experimental surface tension data have been reported in [128] for the $C_{20}OH$ solution in hexane at the water/hexane interface. In addition we know that $C_{18}OH$ forms domains at this interface [129]. This domain formation process should be far more probable for $C_{20}OH$. In Fig. 2.23 the experimental results from [128] are compared with calculations for the Frumkin, aggregation and phase transition models. It was argued in [128] that the inflexion point observed at a concentration of 11 mmol/kg is caused by a condensation process, while according to the aggregation model the 'retarded' shape of the curve at a concentration of about 5 mmol/kg should be ascribed to the onset of the formation of large clusters ($n>100$) or of a phase transition. We suppose therefore that for concentrations below 5 mmol/kg small aggregates are formed, while for higher concentrations larger clusters (phase transition) appear in the monolayer. The theoretical curves calculated for this case are in perfect agreement with the experimental data. The calculations predict that saturation of the $C_{20}OH$ adsorption layer is reached at a concentration of about 12 mmol/kg. It is essential that the inflexion points in the $\gamma(c)$ isotherms with a sharp increase of the slope can be explained by the saturation of the surface layer by monomers and aggregates. Here the important prerequisite is that the condensation onset should corresponds to the state of the monolayer far from saturation. This can be easily seen from the analysis of the curves shown in Figs. 2.20 and 2.21, calculated with $\theta_c = 0.1$ for the phase transition model given by Eqs. (2.118) and (2.119). This explanation is in contrast to the explanation given in the literature claiming that it were caused by the onset of a

two-dimensional aggregation process in the surface layer, as treated in the framework of the van der Waals – Frumkin model.

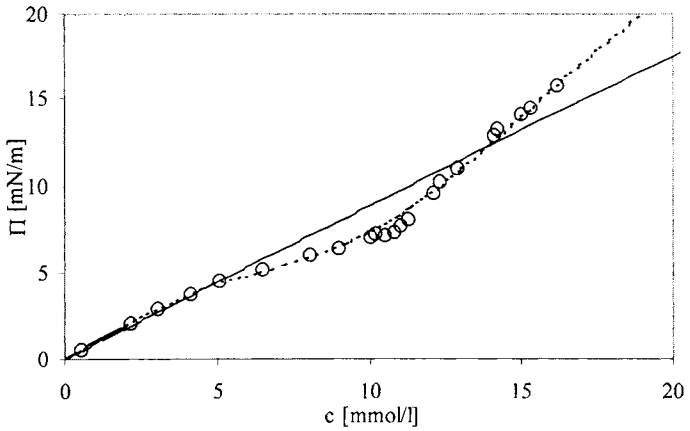

Fig. 2.23. Dependence of surface pressure on concentration for $C_{20}OH$ in hexane at the water/hexane interface at 25°C; experimental points from [127]; solid curve - calculated for the Frumkin model with $\omega = 1.0 \cdot 10^5$ m²/mol and a = 2.0 (ε = 10.8%); dashed curve - calculated for the aggregation model: in the region c < 5 mmol/kg for $\omega_1 = 1.0 \cdot 10^5$ m²/mol, n = 3.5 and $\Gamma_c = 1.4 \cdot 10^{-6}$ mol/m² (ε = 0.9%), in the region c > 5 mmol/kg for the phase transition model, Eqs. (2.118) and (2.119), for $\omega_1 = 1.0 \cdot 10^5$ m²/mol and $\Gamma_c = 1.4 \cdot 10^{-6}$ mol/m² (ε = 2.0%).

Recently, the formation of clusters was reported for adsorption layers and spread monolayers of 1-dodecanol at the water/air interface [130]. In analogy to the systems discussed above, good agreement between the experimental results and theoretical calculations for 1-dodecanol was achieved when small aggregates (dimers-trimers) in the pre-critical region, and larger clusters in the trans-critical region were assumed. Hence, certain general properties in the behaviour of normal alcohols at the two interfaces compared are evident.

2.8. Adsorption of proteins and protein/surfactant mixtures

2.8.1. Protein solutions

A review of various theoretical (molecular-statistical, scaling and thermodynamic) models which describe the adsorption of proteins at liquid/fluid interface was presented in [86]. Here the thermodynamic models derived to describe the protein adsorption are discussed briefly. The adsorption isotherm (2.27), and also the equation of state (2.26) accounting for the

Coulomb contribution can be used as a basis to describe adsorption layers of proteins. It should be kept in mind that the subscript 'i' refers to various states of the protein molecule at the surface. Problems arising from a non-ideality of the surface layer, the inter-ion interactions in the adsorption layer and the dependence of K_i on the adsorption state of large molecules at the surface have been addressed in [26, 85, 86, 131].

In analogy to surfactant molecules able to reorient, we assume here that protein molecules can exist in a number of states with different molar areas and that the non-ideality of enthalpy for protein adsorption layers does not depend on the state of molecules at the surface, that is, the activity coefficients are given by Eqs. (2.72). Assuming an entropy non-ideality (the convention $\omega_0 = \omega_1$) and enthalpic non-ideality contribution of the Frumkin type, and taking into account the contribution of the DEL, Eq. (2.59), one can transform the equation of state for the surface layer (2.26) into

$$\Pi = -\frac{RT}{\omega_1}\left[\ln\left(1-\sum\Gamma_i\omega_i\right)+\sum\Gamma_i\omega_i\left(1-\frac{1}{n_i}\right)+a\left(\sum\Gamma_i\omega_i\right)^2\right]+\frac{4RT}{F}\left(2\varepsilon RTc_\Sigma\right)^{1/2}\left[ch\varphi-1\right], \quad (2.121)$$

where ω_1 is the minimum molar area (the area of the kinetically independent parts – fragments - of protein molecule, or the area of one or more monomers for the polymer molecule) and $n_i=\omega_i/\omega_1 \geq 1$. This equation is the most general and very complicate to analyse, but can be simplified by introducing an ideal entropy of mixing (convention $\omega_0 = \omega$). The convention $\omega_0 = \omega$ also shows that the protein molecules are existing in states with different molar areas and represents only one kinetically independent entity. This convention is more or less true for globular protein molecules. In line with this assumption, the non-ideality of the surface layer entropy will be described by Eqs. (2.73) and (2.74). This corresponds to the choice of the dividing surface embodied in Eqs. (2.19) and (2.20), which for the case of proteins results in a significantly lower deviation from the Gibbs dividing surface as for surfactant solutions. For protein solutions at high ion concentrations the Debye length $\lambda = (\varepsilon RT/F^2c_\Sigma)^{1/2}$ is small; e.g., for $c_\Sigma = 0.1$ mol/l we have $\lambda = 1.3$ nm. This means that for protein solutions the DEL thickness can be smaller than the adsorption layer thickness. Therefore, the concentration of ions in Eqs. (2.60) and (2.121) is just their concentration in the adsorption layer, which can exceed 1 mol/l due to the degree of ionisation of hydroxyl and amino groups, and the contribution of counterions. It follows from Eqs. (2.60) and (2.121) that for large c_Σ the approximation $\varphi \ll 1$

can be used. Thus, introducing the first members of the series expansions $sh\varphi = \varphi + \varphi^3/6$ and $ch\ \varphi = 1 + \varphi^2/2$ into Eq. (2.60) and (2.121), one obtains an equation of state for non-ideally charged surface layers of adsorbed proteins

$$\Pi = -\frac{RT}{\omega}\left[\ln(1-\Gamma_\Sigma\omega) + (a - a_{el})(\Gamma_\Sigma\omega)^2\right], \tag{2.122}$$

where $\Gamma_\Sigma = \Sigma_{i \geq 1}\Gamma_i$ is the total adsorption of the protein in all states, $a_{el} = z^2F/\omega\ (8\varepsilon RTc_\Sigma)^{1/2}$, z is the number of non-bound unit charges in the protein molecule. Using expressions (2.72)-(2.74) and the relation $\exp(2\varphi) = (ch\varphi + sh\varphi)^2$, one obtains from Eq. (2.27) the protein adsorption isotherm for any i^{th} state of the adsorbed molecule [85, 86]

$$b_i c = \frac{\Gamma_i\omega \exp\left[-a\Gamma_\Sigma^2\omega^2\left(i\frac{\omega_1}{\omega} - 1\right) - i\frac{\omega_1}{\omega} - 2a\Gamma_\Sigma\omega + 2\frac{a_{el}}{z}\Gamma_\Sigma\omega + \left(\frac{a_{el}}{z}\Gamma_\Sigma\omega\right)^2\right]}{i^\alpha(1-\Gamma_\Sigma\omega)^{i\omega_1/\omega}}. \tag{2.123}$$

Here α is a constant which determines the variation in surface activity of the protein molecule in the i^{th} state with respect to the state 1 characterised by a minimum partial molar area $\omega_i = \omega_{min}$, $b_i = b_1 i^\alpha$. The value i can be either integer or fractional and the increment is defined by $\Delta i = \Delta\omega/\omega_1$. For $\alpha = 0$ one obtains $b_i = b_1 = const$, while for $\alpha > 0$ the b_i increase with increasing ω_i.

The simplifications discussed in [85, 86] allow us to transform the equation of state for protein surface layers (2.122) and the adsorption isotherm (2.123) into the simpler form

$$\Pi = -\frac{RT}{\omega}\left[\ln(1-\Gamma_\Sigma\omega) - a_{el}\Gamma_\Sigma^2\omega^2\right], \tag{2.124}$$

$$b_i c = \frac{\Gamma_i\omega}{(1-\Gamma_\Sigma\omega)^{\omega_1/\omega}}. \tag{2.125}$$

The total adsorbed amount in these equations can be expressed from Eq. (2.123) via the adsorption in state 1

$$\Gamma_\Sigma = \Gamma_1\sum_{i=1}^{n} i^\alpha \exp\frac{\omega_1(i-1)}{\omega}\exp\left[-\frac{(i-1)\Pi\omega_1}{RT}\right], \tag{2.126}$$

where the first exponential factor arises due to the non-ideality of entropy of mixing. This factor, and also i^{α} correspond to a relative increase in adsorption of the states with $\omega_i > \omega_1$. To simplify Eq. (2.126) and subsequent expressions, this factor can be omitted when a value of $\alpha = 0.5$ is used which can compensate the effect. A more general approach results when the ratio $b_i = b_1 i^{\alpha}$ as pre-exponential factor is used. The mean partial molar area for all states, and the adsorption in any i^{th} state can be expressed by

$$\omega = \omega_1 \frac{\sum_{i=1}^{n} i^{(\alpha+1)} \exp\left(-\frac{i\Pi\omega_i}{RT}\right)}{\sum_{i=1}^{n} i^{\alpha} \exp\left(-\frac{i\Pi\omega_1}{RT}\right)}, \tag{2.127}$$

$$\Gamma_i = \Gamma_{\Sigma} \frac{i^{\alpha} \exp\left[-\frac{(i-1)\Pi\omega_1}{RT}\right]}{\sum_{i=1}^{n} i^{\alpha} \exp\left[-\frac{(i-1)\Pi\omega_1}{RT}\right]}, \tag{2.128}$$

respectively.

The adsorption model described above assumes the existence of different discrete states of protein molecules in the surface layer, with neighbouring states differing from one another by the molar area increment $\Delta\omega$. From the viewpoint of scaling analysis, $(\Delta\omega)^{1/2}$ has to be close to the size of an electrostatic blob [132]. In adsorption layers of proteins the flexibility of chains increases due to the high concentration of both protein and inorganic electrolyte [133]. This allows to consider, instead of discrete states, an infinitesimal change $d\omega$ in the molar area. To perform the transition from the discrete to the continuous model one has to replace formally the summations in Eqs. (2.126)-(2.128) by an integration [86].

The main feature of the theoretical model given by Eqs. (2.124)-(2.128) is the self-regulation of both the state of the adsorbed molecules and the adsorption layer thickness via the surface pressure. The theory is based on the concept first formulated by Joos [19, 21]. The mechanism of self-regulation is inherent in the Butler equation (2.7), from which all main equations are derived. Of course, surface pressure cannot be regarded as the only self-regulating parameter, but for the solution/fluid interface this is possibly the main factor. From Eq. (2.128) one can calculate the portion of adsorbed molecules which exist in the state ω_i. The dependence of the

distribution function Γ_i/Γ_{max} on ω_i for Π = 1.2 mN/m, and also the Π dependence of ω_i which corresponds to the maximum adsorbed amount Γ_{max} are shown in Fig. 2.24.

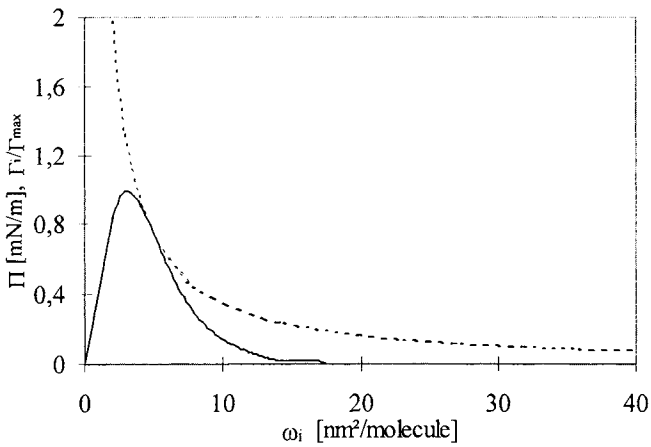

Fig. 2.24. Distribution of protein adsorption in various states Γ_i with respect to the surface area ω_i covered by the protein molecule in the adsorption layer at Π = 1.2 mN/m (1), and surface pressure as a function of area per protein molecule in the maximum of the distribution function (2); parameters used: M = 24000 g/mol, ω_{max} = 40 nm²/molecule, ω_{min} = 2 nm²/molecule, $\Delta\omega$ = 1 nm²/molecule, a_{el} = 100, α = 1.

It is seen that for low values of Π the adsorption achieves its maximum at $\omega_i = \omega_{max}$ = 40 nm²/molecule. With the increase of Π the value of $\omega_i(\Gamma_{max})$ decreases monotonously, while finally at $\Pi \approx 2.0$ mN/m the maximum adsorption corresponds to the state which possesses minimum partial molar area of ω_{min} = 2 nm²/molecule. Therefore, the protein adsorption layer is characterised by almost a complete denaturation at low surface pressure while at large surface pressures the adsorption layer is comprised of molecules in a state with minimum surface area demand.

The theoretical model described by Eqs. (2.124)-(2.128) predicts for $\Pi \geq 20 - 25$ mN/m a subsequent unrealistically sharp increase of surface pressure with a weak increase of protein concentration, and simultaneously a slight increase in adsorption. This contradicts with experimental data which show, starting from some protein concentration, that Π remains almost constant, while the adsorption continues to increase. This results in an increased

coverage leading to an almost complete saturation of the adsorption layer at higher protein concentration [75, 133, 134]. Graham & Phillips [134] had attributed their results to the formation of a second adsorption layer at the side of the interface adjacent to the solution. Subsequently some attempts were made to apply this hypothesis to explain the fact that surface pressure does not depend on the adsorption value in concentrated surface layers. Theoretical adsorption isotherm which matches experimental data [134] was derived by Guzman *et al.* [135]. Douillard & Lefebvre [136] also employed the two-layer model of protein adsorption, which assumes that the composition of the first layer only affects the surface pressure. This theory exhibits good agreement with the data reported by Graham & Phillips [134]. However, the fact that the surface pressure of concentrated protein solutions is independent of the bulk concentration can also be satisfactorily explained in the framework of the monolayer model: here either the weakening of the inter-ion interactions in the concentrated surface layer [75, 76], or the possibility of 2D aggregation of protein molecules in the monolayer [131] should be taken into account.

2.8.2. Surfactant/protein mixtures

Let us now discuss mixtures of proteins with low-molecular weight surfactants. These mixtures are of great practical importance for the stabilisation of emulsions and foams, and play an important role in biological systems. Let us consider equilibrium ideal (with respect to the enthalpy) solutions of proteins and surfactants. If such a solution contains i different surfactants (or proteins) which exist in j different states at the interface, the following system of equations from (2.26) and (2.27) may be formulated [24, 25]:

equation of state for the interface

$$\Pi = -\frac{RT}{\omega}\ln\left[1-\omega\sum_{i,j}\Gamma_{ij}\right], \tag{2.129}$$

adsorption isotherm

$$b_{il}c_i = \frac{\Gamma_{il}\omega}{\left[1-\omega\sum_{i,j}\Gamma_{ij}\right]^{\omega_{il}/\omega}}, \tag{2.130}$$

where the mean molar area of all states and monolayer components is

$$\omega = \frac{\sum_{i,j} \Gamma_{ij} \omega_{ij}}{\sum_{i,j} \Gamma_{ij}}. \tag{2.131}$$

The ratio of the adsorption in any arbitrary state j to the adsorption in certain state k (e.g., the state with minimum surface area) is expressed by the generalised formula (2.83)

$$\frac{\Gamma_{ij}}{\Gamma_{ik}} = \exp\left(\frac{\omega_{ik} - \omega_{ij}}{\omega}\right)\left(\frac{\omega_{ij}}{\omega_{ik}}\right)^{\alpha_i} \exp\left[\frac{\Pi(\omega_{ik} - \omega_{ij})}{RT}\right]. \tag{2.132}$$

For the non-ideal behaviour of a system which contains a single component able to exist in different states, the rigorous thermodynamic expressions are far more complicated than those given above. The relevant mathematical formalism becomes yet more involved if the contributions of ionisation to the surface pressure of the adsorption layer and the chemical potentials of surface active ions located in the diffuse region of the double electric layer are taken into account. Therefore, to describe the adsorption behaviour of a protein/surfactant mixture, some assumptions have to be introduced which simplify the problem significantly.

The mixture of a protein (component 1) existing in the state with minimal molar area (i.e., when the surface pressure is not too high) and the surfactant existing in a single adsorption state (component 2) characterised by an ideal behaviour, was considered in [137]. The equation of state for this mixed layer reads

$$\Pi = -\frac{RT}{\omega}\left[\ln(1 - \Gamma_\Sigma \omega) - a_{el}\Gamma_1^2 \omega_1^2\right], \tag{2.133}$$

while the expressions for the adsorption isotherm of protein and surfactant are

$$b_1 c_1 = \frac{\Gamma_1 \omega_1}{(1 - \Gamma_\Sigma \omega)^{\omega_1/\omega}}, \tag{2.134}$$

$$b_2 c_2 = \frac{\Gamma_2 \omega_2}{(1 - \Gamma_\Sigma \omega)^{\omega_2/\omega}}, \tag{2.135}$$

respectively, with $\Gamma_\Sigma = \Gamma_1 + \Gamma_2$. The average molar area of adsorbed components 1 and 2 can be expressed by [3]

$$\omega = \frac{\Gamma_1\omega_1 + \Gamma_2\omega_2}{\Gamma_1 + \Gamma_2}. \tag{2.136}$$

The relation between the adsorptions of protein and surfactant can be derived from the adsorption isotherms given by Eqs. (2.134) and (2.135)

$$\frac{\Gamma_1\omega_1}{\Gamma_2\omega_2} = \frac{b_1c_1}{b_2c_2}\left(1 - \Gamma_\Sigma\omega\right)^{\frac{\omega_1-\omega_2}{\omega}}. \tag{2.137}$$

For $\omega_1 \gg \omega_2$ at a given ratio of the concentrations in the solution bulk, the portion of protein in the surface layer decreases sharply with the increase of the total adsorption Γ_Σ. For $a_{el} = 0$ Eq. (2.137) is reduced to the known relationship (2.1) for a mixture of two surfactants in an ideal surface layer

$$\frac{\Gamma_1\omega_1}{\Gamma_2\omega_2} = \frac{b_1c_1}{b_2c_2}\exp\left[-\frac{\Pi\left(\omega_1 - \omega_2\right)}{RT}\right]. \tag{2.138}$$

At low surfactant concentrations (and adsorptions), as $\omega_1/\omega \cong 1$ and $\omega_2/\omega \ll 1$, an approximation follows from Eqs. (2.134) and (2.135)

$$\Gamma_1\omega_1 = b_1c_1\left(1 - b_2c_2\right)/\left(1 + b_1c_1\right) \text{ and } \Gamma_2\omega_2 = b_2c_2. \tag{2.139}$$

Using Eq. (2.133) and the corresponding equation of state for the protein solution, one obtains the expression for the surface pressure jump for the protein/surfactant mixture

$$\Delta\Pi_{12} = \frac{RT}{\omega_1}\ln\left(\frac{1}{1 - b_2c_2}\right) - \frac{RTa_{el}}{\omega_1}\left(\frac{b_1c_1}{1 + b_1c_1}\right)^2\left[2b_2c_2 - \left(b_2c_2\right)^2\right]. \tag{2.140}$$

$\Delta\Pi_{12}$ is the extra decrease of surface tension for the solution of component 1, caused by the addition of component 2. It can be seen that, for certain relationships between the parameters in Eq. (2.140), the first term in this equation can be neglected as compared with the second term. This results in a negative value of the surface pressure change of the mixture, that is, the surface tension of the protein/surfactant mixture can exceed that characteristic to the system where no surfactant is added. Moreover, calculating the extreme value of the second term of Eq. (2.140) one sees that the surface tension maximum of the mixture is located at $b_2c_2 = 1$. In the region where the surfactant concentration is high, Eq. (2.137) yields that almost all protein

molecules are expelled from the surface layer. This constitutes a crucial difference between surfactant/protein mixtures and mixtures of different surfactants or proteins. For such mixtures, the exponential factor can be excluded from Eq. (2.138) and a simple expression follows for $\Delta\Pi_{21}$ (that is, for the variation of the surfactant surface tension caused by the addition of protein). If the inequalities $\Gamma_2 \gg \Gamma_1$ and $\omega_2\Gamma_2 \gg \omega_1\Gamma_1$ hold Eqs. (2.132) and (2.133) transform into

$$\Delta\Pi_{21} = \frac{RTa_{el}}{\omega_2}(\Gamma_1\omega_1)^2 \cong \frac{RTa_{el}}{\omega_2}(b_1c_1)^2\left(\frac{1}{1+b_2c_2}\right)^{2\omega_1/\omega} \tag{2.141}$$

As the power index in Eq. (2.141) is extremely high, the value of $\Delta\Pi_{21}$ does not exceed 1 mN/m.

This approximate theoretical model which attempts to explain the anomalous behaviour of protein/surfactant mixtures was recently confirmed for the HSA/C_{10}DMPO mixture as an example [137]. The equilibrium surface tension isotherms for mixed and pure C_{10}DMPO solutions at 22°C are shown in Fig. 2.25. It is seen that for $c > 10^{-4}$ mol/l, the two isotherms are almost identical. For these C_{10}DMPO concentrations the adsorption of HSA is negligible. The conclusion concerning the sharp change in the composition of the surface layer within a narrow C_{10}DMPO concentration range is supported by the analysis of the surface shear viscosity η_s of mixed monolayers [137].

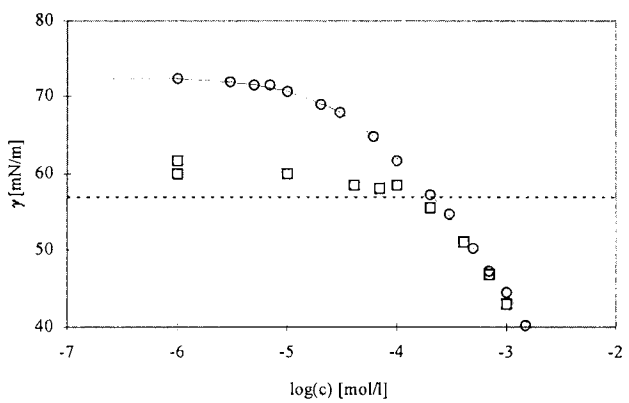

Fig. 2.25. Equilibrium surface tension isotherms for individual C_{10}DMPO solutions (○ and solid line) and mixed C_{10}DMPO/HSA solutions for a HSA concentration of 10^{-7} mol/l (□); the dotted line shows the equilibrium surface tension of the pure HSA solution averaged over 6 measurements (γ = 57±1 mN/m).

For C_{10}DMPO concentrations below $2 \cdot 10^{-5}$ mol/l, the monolayer possesses a rather high viscosity, characteristic for the individual HSA solution. However, already at a concentration of $7 \cdot 10^{-5}$ mol/l, the shear viscosity decreases sharply almost to zero, which is characteristic for surfactant solutions. Therefore, both tensiometric and rheological studies indicate that the compatibility of HSA and C_{10}DMPO in the mixed monolayer is very poor, in contrast to mixtures of surface active homologues [9, 11, 138]. For such mixtures no range of 'components antagonism' exists, i.e., the addition of a second component always results in an extra surface tension decrease for the mixture. This fact can be easily explained from a theoretical point of view. The generalised von Szyszkowski-Langmuir equation for two-component mixtures yields

$$\Delta\Pi_{12} = \frac{RT}{\omega} \ln\left(1 + \frac{b_2 c_2}{1 + b_1 c_1}\right), \tag{2.142}$$

i.e., the surface tension of the solution decreases significantly due to the addition of the second component, except when $b_1 c_1 \gg b_2 c_2$.

From Fig. 2.25 we also see that in the C_{10}DMPO concentration range $c = (10^{-6} - 10^{-4})$ mol/l, the surface tensions of the mixtures exceed the values for the pure HSA solution. For C_{10}DMPO concentrations $< 5 \cdot 10^{-7}$ mol/l, the surface tension of the mixtures is equal to that of the pure HSA solution. For $c = (4\text{-}10) \cdot 10^{-5}$ mol/l the surface tension excess amounts only to about 1 mN/m. However, for $c < 4 \cdot 10^{-5}$ mol/l, the surface tension of the mixed solutions exceeds that of the HSA solution by 3 to 4 mN/m. The theoretical model of Eq. (2.142) cannot explain such increase in surface tension. Negative values of $\Delta\Pi_{12}$ cannot be obtained from Eq. (2.142) for the addition of a second component, however, this phenomena can be explained quite well by Eq. (2.140). The location of the maximum at the curve at $b_2 c_2 \approx 1$ corresponds approximately to the value estimated from Eq. (2.140). For low values of a_{el}, the mixing of components 1 and 2 cannot lead, as it follows from Eq. (2.140), to any increase in surface tension. Therefore, the anomalous behaviour of surface tension for HSA/C_{10}DMPO mixtures results from the large

free charge of protein molecules [85, 86]. This phenomenon can be explained rather simply from a physical point of view. The addition of C_{10}DMPO results in an increase of the total surface layer coverage, which lowers the first term of Eq. (2.140). However, as it follows from the isotherm equation (2.139), the addition of C_{10}DMPO results in the decrease of the HSA adsorption. This decreases the second term of Eq. (2.133), which depends quadratically on the HSA adsorption leading to a surface pressure decrease for the mixture. One has also to note, that all the discussion based on the thermodynamic models does not consider a change in the surface activity of the protein molecules. Due to hydrophobic interaction with the surfactant it seems obvious that protein/surfactant complexes are formed which are less surface active, which can lead to the observed increase in surface tension.

To summarise, it can be seen from the above discussion of some simple limiting cases of the adsorption behaviour of protein/surfactant mixtures that these systems can exhibit rather unusual features. In general, for arbitrary concentrations of the components, surfactant ionisation in the monolayer and the intermolecular interaction of the components in the bulk and at the surface, one can expect that equilibrium and dynamic mixed protein/surfactant monolayers could display various and often unpredictable features.

2.9. Penetration thermodynamics

The equilibrium and dynamic behaviour of mixed monolayers of soluble and insoluble amphiphiles at fluid/liquid interfaces plays an important role in various technological and biological processes, which was studied in numerous publications [139-157]. However, even for very simple systems, say, gaseous mixed monolayers, the thermodynamic analysis is not trivial. For more complicated systems (the formation of two-dimensional domains) such an analysis is very cumbersome due to mathematical difficulties.

The main problem in the thermodynamic theory of penetration is to determine the dependence of the adsorption of a soluble surfactant on its bulk concentration for any given (constant) adsorption of the insoluble surfactant (surface concentration), and the onset of the surface pressure jump in mixed monolayers, caused by the adsorption of a soluble surfactant in the presence of the insoluble component. There exist several main theoretical approaches to the description of the penetration thermodynamics. One is based on the Gibbs adsorption equation for multicomponent monolayers [143-146]. Another approach, initially proposed by Pethica

[139, 140], employs either his original equation [155-156], or more general expressions of the same type [142]. Another method of the analysis was proposed in [155], i.e., the application of Butler's equation (2.7) to express the chemical potentials of the surface layer components.

2.9.1 Theoretical approaches

In the Gibbs adsorption equation for multicomponent surface layers (2.22) the value of μ for soluble components can refer both to the bulk and to the surface layer (as equilibrium exists), and for the insoluble components to the surface layer only. For systems with one insoluble and one soluble component, denoted by subscripts 1 and 2, respectively, and the assumption that the area per mole of the insoluble component 1 is $A_1 = 1/\Gamma_1$, Eq. (2.22) can be rewritten as

$$d\mu_1 = A_1 d\Pi - A_1\Gamma_2 d\mu_2 , \tag{2.143}$$

which leads to the Maxwell equation

$$\left(\frac{\partial \Pi}{\partial \mu_2}\right)_{A_1} = \left(\frac{\partial A_1 \Gamma_2}{\partial A_1}\right)_{\mu_2} . \tag{2.144}$$

The integration for constant μ_2 between the limits corresponding to two states of the monolayer (I and II, respectively) with different Γ values for the soluble or insoluble component, yields the difference of the product $(A_1\Gamma_2)$ in these states [143, 146]

$$(A_1\Gamma_2)_{II} - (A_1\Gamma_2)_I = \int_I^{II} \left(\frac{\partial \Pi}{\partial \mu_2}\right)_{A_1} dA_1 , \tag{2.143}$$

where Γ_1 is the surface concentration of the insoluble component, and Γ_2 the adsorption of the dissolved surfactant. Thus, for any given μ_2, the change in the adsorption of the soluble surfactant can be calculated from the experimentally measured dependence of the surface pressure on A_1 and μ_2.

The Gibbs equation which expresses the total differential of the difference between the surface pressure of the mixed layer and that in absence of the insoluble surfactant (denoted by subscript 0) can be derived from Eq. (2.22)

$$d(\Pi - \Pi_0) = d\mu_1 / A_1 + (\Gamma_2 - \Gamma_2^0) d\mu_2 , \tag{2.144}$$

which leads to a relation similar to Eq. (2.143)

$$\left(A_1(\Gamma_2 - \Gamma_2^0)\right)_{II} - \left(A_1(\Gamma_2 - \Gamma_2^0)\right)_I = \int_I^{II} \left(\frac{\partial(\Pi - \Pi_0)}{\partial \mu_2} \right)_{A_1} dA_1 . \tag{2.145}$$

Hall argued this equation is more correct than Eq. (2.143) because, for infinitesimal adsorption of the two components, the products on the left hand side converge to a certain limiting value.

Equation (2.144) leads also to a relation which expresses the difference in adsorption [146] assuming that the chemical potential of component 1 is constant

$$\left(\frac{\partial(\Pi - \Pi_0)}{\partial \mu_2} \right)_{\mu_1} = \Gamma_2 - \Gamma_2^0 . \tag{2.146}$$

Hall proposed an experimental procedure, in which changes in the area of the monolayer in equilibrium with the soluble surfactants should be performed to keep constant or control the chemical potential of the first component when the activity of the second component is varied.
To summarise, the rigorous thermodynamic analysis of the penetration equilibrium, based on the Gibbs equation, can neither provide an equation of state of the monolayer, nor an adsorption isotherm for the soluble component. This analysis only enables one to formulate the conditions for a penetration experiment, which are, however, very difficult to implement. Therefore, to describe the thermodynamic behaviour of real mixed monolayers, at present one should use some approximate theoretical models.

Assuming fixed coverage or adsorbed amounts of all the components except the j^{th} one, the expression for the partial derivative $\partial\Pi/\partial\mu_j$ can be calculated from Eq. (2.22) as

$$\left(\frac{\partial \Pi}{\partial \mu_i} \right)_{\Gamma_{i \neq j}} = \Gamma_j + \sum_{i \neq j}^{n} \Gamma_i \left(\frac{\partial \mu_i}{\partial \mu_j} \right)_{\Gamma_{i \neq j}} . \tag{2.147}$$

The sum on the right hand side of Eq. (2.147) can be expressed as

$$\sum_{i\neq j}^{n}\Gamma_i\left(\frac{\partial\mu_i}{\partial\mu_j}\right)_{\Gamma_{i\neq j}}=\left(\frac{\partial\Pi}{\partial\mu_j}\right)_{\Gamma_{i\neq j}}\sum_{i\neq j}^{n}\Gamma_i\left(\frac{\partial\mu_i}{\partial\Pi}\right)_{\Gamma_{i\neq j}}. \tag{2.148}$$

Then, introducing (2.148) into Eq. (2.147), one obtains

$$\left(\frac{\partial\Pi}{\partial\mu_j}\right)_{\Gamma_{i\neq j}}=\Gamma_j\left[1-\sum_{i\neq j}^{n}\Gamma_i\left(\frac{\partial\mu_i}{\partial\Pi}\right)_{\Gamma_{i\neq j}}\right]^{-1}. \tag{2.149}$$

Note that in Eqs. (2.149), Γ (adsorption or surface concentration) of all components except the Γ_j are kept constant, while in Eqs. (2.4) the number of moles of all components are fixed. Ignoring this difference, taking into account that $d\gamma = -d\Pi$, and using Eqs. (2.4) and (2.5) instead of Eq. (2.149) we obtain

$$\left(\frac{\partial\Pi}{\partial\mu_j}\right)_{\Gamma_{i\neq j}}=\Gamma_j\left[1-\sum_{i\neq j}^{n}\theta_i\right]^{-1}, \tag{2.150}$$

where $\theta_i=\Gamma_i/\Gamma_{\infty i}$ are the surface coverages of component i. For the soluble components, the value of the chemical potential in the bulk is equal to that within the surface layer, provided equilibrium conditions exist, and Eq. (2.150) for these components can be expressed by the generalised Pethica equation [11, 64, 65]

$$\left(\frac{\partial\Pi}{\partial\ln a_j}\right)_{\Gamma_{i\neq j}}=RT\Gamma_j\left[1-\sum_{i\neq j}^{n}\theta_i\right]^{-1}. \tag{2.151}$$

Here a_i is the activity of the i^{th} component in the solution bulk. For one insoluble and one soluble component, and an ideal bulk solution, the ordinary Pethica equation [139] follows from Eq. (2.151)

$$\left(\frac{\partial\Pi}{\partial\ln c_2}\right)_{\theta_1}=\frac{RT\Gamma_2}{(1-\theta_1)}, \tag{2.152}$$

where c_2 is the bulk concentration of the soluble component. Eq. (2.151) is the most general form of Pethica's equation.

A possible error introduced into Eqs. (2.151) and (2.152) by keeping fixed the Γ values (adsorption or surface concentration) of all the components except the j^{th} component in Eqs. (2.149) and fixing the number of moles of all the components in Eqs. (2.4) was considered in [142], where a more general expression was obtained for the derivative on the left hand side of Eq. (2.152). It follows from this analysis that Eqs. (2.151) and (2.152) can be used, when

$$\left(\frac{\partial \mu_1}{\partial \Gamma_2}\right)_{\Pi,\Gamma_1}\left(\frac{\partial \Gamma_2}{\partial \Pi}\right)_{\Gamma_1} = 0. \tag{2.153}$$

As the second term in Eq. (2.153) is non-zero, the chemical potential of the insoluble component does not depend on the adsorption of the soluble component provided that both surface pressure and adsorption of the insoluble component are fixed. In turn, as the surface concentration of the insoluble component is fixed, the requirement for constant activity of this component implies the independence of this activity coefficient of adsorption of the soluble component. Clearly, this requirement is satisfied not only for the trivial case of an ideal monolayer, but also for non-ideal monolayers, provided that the activity cross-coefficients of the components (or intermolecular interaction parameters) vanish. For example, if the equation of state Eq. (2.35) is used for a non-ideal (with respect to the enthalpy) mixed two-component monolayer, it follows from Eq. (2.153) that Eqs. (2.151) and (2.152) are applicable when $a_{12} = 0$. Clearly, the condition of Eq. (2.153) imposes certain restrictions to the applicability of Pethica's model. The generalised Pethica equation (2.151) was thermodynamically analysed in [64, 65]. Moreover, an attempt to verify Eq. (2.151) experimentally was undertaken in [65], which also confirms its validity for mixed monolayers comprised of two non-ionic surfactants, or for mixtures of non-ionic and ionic surfactant, or two ionic surfactants.

The efficiency of Pethica's equation can be shown by a simple example. Suppose that the behaviour of both surfactants in a mixed surface layer can be described by the generalised Szyszkowski-Langmuir equation (2.39)

$$\Pi = -\frac{RT}{\omega}\ln(1-\theta_1-\theta_2), \tag{2.154}$$

where ω is the mean molar area defined by (2.20). Differentiation of Eq. (2.154) with respect to θ_2 at θ_1 = const (with the additional approximate assumption ω = const) yields

$$\left(\frac{\partial \Pi}{\partial \theta_2}\right)_{\theta_1} = \frac{RT}{\omega}\frac{1}{1-\theta_1-\theta_2}. \qquad (2.155)$$

It follows from Eqs. (2.152) and (2.155) that

$$d\ln c_2 = \frac{1-\theta_1}{\theta_2(1-\theta_1-\theta_2)}d\theta_2. \qquad (2.156)$$

Integrating Eq. (2.156) one obtains the adsorption isotherm for a soluble surfactant in presence of an insoluble monolayer

$$b_2c_2 = \frac{\theta_2}{1-\theta_1-\theta_2}. \qquad (2.157)$$

It can be seen that Eq. (2.157) is just the ordinary Langmuir equation in its generalised form (2.40) which follow rigorously from the analysis of chemical potentials of the components of a mixed monolayer. It was demonstrated that Pethica's equation provides the description of quite complicated systems, including the penetration of a soluble protein into the monolayer of insoluble phospholipids able to form 2D aggregates [155]. In another paper, the case of mixed layers composed of a soluble and a 2D aggregating insoluble surfactant is considered [156].

The main guidelines for the application of the Butler equation (2.7) and numerous examples for mixtures of soluble surfactants were presented above in Sections 2.4-2.8. It should be noted that, as the solubility or insolubility of the i^{th} component does not affect Eq. (2.7), it can be used for the analysis of penetration processes in a way quite similar to how it was employed for mixed soluble components only, however, the expression for the chemical potentials of the components in the bulk solution (2.8) is applicable to soluble components only. Therefore, adsorption isotherms can be derived only for the soluble components of the monolayer.

The application of Butler's equation has been illustrated in form of the equation of state and adsorption isotherm for non-ideal monolayers (with respect to both enthalpy and entropy) comprised of an insoluble 1 and a soluble 2 component. In this case the equation of state is Eq. (2.31), but the adsorption isotherm (2.32) is true for the soluble component 2 only

$$b_2c_2 = \frac{\theta_2}{(1-\theta_1-\theta_2)^{n_2}}\exp\left(-2a_2\theta_2-2a_{12}\theta_1\right)\cdot\exp\left[(1-n_2)\left(a_1\theta_1^2+a_2\theta_2^2+2a_{12}\theta_1\theta_2\right)\right]. \qquad (2.158)$$

For an ideal monolayer and $n_2 = 1$, this expression is reduced to the adsorption isotherm (2.157) derived using Pethica's equation. It can be concluded therefore, that the two approaches lead to similar results. At the same time, Butler's equation (2.7) always leads to a logarithmic form of the equation of state for mixed monolayers, which often disagrees with the experimental results. For these systems, Volmer's or van der Waals' equations of state are more appropriate [58, 98]. Therefore the method based on Pethica's equation is advantageous, enabling one to apply semi-empirical model equations of state for mixed monolayers.

2.9.2 Penetration theory for homologues

The theoretical description of the equilibrium penetration of a soluble surfactant into insoluble monolayers becomes less complicated if the partial molar areas of the two components are approximately equal to each other. This case includes the penetration of a soluble homologue into the monolayer of an insoluble homologue. Obviously, the range of the systems which can be thus described covers other mixtures composed of molecules with similar geometry. For low surface coverage by the insoluble component, the generalised Szyszkowski-Langmuir equation (2.154) works well. For low adsorption of the soluble component, the generalised Volmer equation can be used to describe the two components of the monolayer [58, 98]

$$\Pi = RT\frac{\sum_i \Gamma_i}{1-\sum_i \Gamma_i \omega_i} - B \tag{2.159}$$

where Γ_i is the adsorption (surface concentration) of the i^{th} component or state, and B is Volmer's integration constant.

The equation of state (2.154) and adsorption isotherm (2.157) correspond to insoluble/soluble mixtures of two homologues, in absence of any 2D aggregation. These equations can be transformed then into

$$\Pi = \frac{RT}{\omega}\ln\frac{(1+bc)}{(1-\theta_1)}, \tag{2.160}$$

$$\Gamma_2 = \frac{1-\theta_1}{\omega}\frac{bc}{1+bc}, \tag{2.161}$$

which leads to interesting conclusions. First, it follows from Eq. (2.160) that changes in the surface pressure (difference between the surface pressures of the mixed monolayer and the pure insoluble monolayer $\Delta\Pi$) due to the adsorption of the soluble surfactant, does not depend on θ_1, but depends on bc only, $\Delta\Pi = (RT/\omega)\ln(1+bc)$. Second, according to the isotherm (2.161), the monolayer coverage by the soluble component $\theta_2 = \omega\Gamma_2$ in presence of the insoluble component decreases proportionally to $(1 - \theta_1)$. Therefore, the θ_2 value, which corresponds to some $\Delta\Pi$ values for the mixed monolayer, is lower than the θ_2 value that corresponds to the same $\Delta\Pi$ for adsorption layers in absence of the insoluble amphiphile. This behaviour can result in a faster achievement of the adsorption equilibrium of the mixed surface layer.

When the formation of large aggregates of an insoluble surfactant is stimulated by the adsorption of a soluble surfactant, the von Szyszkowski-Langmuir equation of state and adsorption isotherm for the soluble surfactant read [157]

$$\Pi = -\frac{RT(A/A_c)}{\omega(1+\Gamma A)}\ln[1-\omega(\Gamma+1/A)], \tag{2.162}$$

$$bc = \frac{\Gamma\omega A_c(1+\Gamma A)}{A-\omega(1+\Gamma A)}, \tag{2.163}$$

where Γ is the adsorption of the soluble surfactant in the mixed monolayer at bulk concentration c, A is the area per mole of the insoluble surfactant for $A > A_c$, A_c is the critical area per mole of the insoluble component for the individual monolayer at the inset point of aggregation.

As aggregation of the insoluble component occurs only when its surface concentration is sufficiently high, the description of the two components based on Volmer's equation seems to be more appropriate than that based on the Szyszkowski-Langmuir equation. If a first-order phase transition does not occur in the monolayer, i.e. no aggregates are formed, then the simultaneous solution of Volmer's equation (2.159) for the components 1 and 2, and Pethica's equation (2.152) yields the adsorption isotherm for the soluble component 2 (see [156])

$$bc = \left(\frac{\theta_2}{1-\theta_1-\theta_2}\right)^{\frac{1}{1-\theta_1}} \cdot \exp\left[\frac{\theta_2}{(1-\theta_1)(1-\theta_1-\theta_2)}\right]. \tag{2.164}$$

Assuming that, according to the quasi-chemical aggregation model [97], mixed aggregates are formed, one can transform the generalised Volmer equation (2.159) into

$$\Pi = RT\frac{\Gamma_{1l} + \Gamma_{2l} + \Gamma_n}{1-\omega(\Gamma_{1l} + \Gamma_{2l} + n\Gamma_n)} - B, \tag{2.165}$$

where the second subscript 1 refers to monomers, Γ_n is the adsorption of aggregates, and $n = n_1 + n_2$ is the total aggregation number for both components. It is seen from Eq. (2.165) that the surface pressure behaviour of the mixed monolayer depends on the type of the formed aggregates [156, 157]. The denominator of Eq. (2.165) represents the part of the surface not covered by the monolayer. Therefore, with our assumptions concerning the molar areas of the components, it does not depend on the aggregation conditions. However, the numerator of Eq. (2.165) depends on these conditions. For example, if the soluble component 2 is not involved in the mixed aggregates, that is, assuming $n_2 = 0$ and $n_1 \gg 1$, Eq. (2.165) can be transformed into the expression

$$\Pi = RT\frac{\Gamma_2 + \Gamma_{1c}}{1-\omega(\Gamma_1 + \Gamma_2)} - B. \tag{2.166}$$

When mixed aggregates are formed, and the conditions $n_1 \gg 1$ and $n_2 \gg 1$ hold, Eq. (2.165) yields

$$\Pi = RT\frac{\Gamma_{1c} + \Gamma_{2c}}{1-\omega(\Gamma_1 + \Gamma_2)} - B, \tag{2.167}$$

where Γ_{2c} is the adsorption of component 2 corresponding to the inset of its 2D transition.

The case that the critical surface concentration Γ_{1c} of the insoluble component depends on the adsorption of the soluble component, but, at the same time, the soluble surfactant does not form mixed aggregates and leads to an increase of the total adsorption of the monomers only, was discussed in [155, 157]. This situation exists when newly adsorbed (penetrated) molecules compensate the incorporation of free insoluble molecules into the condensed phase domains.

Differentiating the equations of state (2.166)-(2.167) with respect to Γ_2, and solving the resulting differential equations simultaneously with the Pethica equation, one obtains the following adsorptions isotherm for the soluble component:

a) from Eq. (2.166)

$$bc = \left(\frac{\theta_2}{1-\theta_1-\theta_2}\right)^{1+\theta_{1c}/(1-\theta_1)} \exp\left[\frac{\theta_2\theta_{1c}+(1-\theta_1)}{(1-\theta_1)(1-\theta_1-\theta_2)}\right], \tag{2.168}$$

b) from Eq. (2.167)

$$bc = \left(\frac{\theta_2}{1-\theta_1-\theta_2}\right)^{(\theta_{1c}+\theta_{2c})/(1-\theta_1)} \exp\left[\frac{\theta_2(\theta_{1c}+\theta_{2c})}{(1-\theta_1)(1-\theta_1-\theta_2)}\right]. \tag{2.169}$$

The theory which describes the penetration of a soluble surfactant into a monolayer formed by molecules possessing equal partial molar area (mixtures of homologues), was extended recently to include the actual process of protein penetration into 2D aggregating phospholipid monolayer [155, 157]. This extension was based on the concept of independent segments of the protein molecules, occupying an area equal to that of the phospholipid molecule. In the theoretical models, various mechanisms for the effect of the soluble surfactant on the aggregation of the insoluble component can be considered:

(i) no effect on the aggregate formation process;

(ii) formation of mixed aggregates;

(iii) influence on the aggregating process by changing the aggregation constant without any formation of mixed aggregates.

These models predict different forms of the equations of state and the adsorption isotherms of the soluble surfactant depend on the mechanism. Based on the shape of experimental Π-A isotherms respective conclusions can be drawn on the actual penetration mechanism.

2.10. Effect of temperature on the surface tension of surfactant solutions

There exists a large pool of experimental data regarding the effect caused by temperature on the dynamics and equilibrium surface and interfacial tension of solutions of various surfactants. In particular, solutions of ionic surfactants with and without the additions of inorganic

electrolytes were studied in [83, 121, 158-163], while mixtures of ionic surfactants were considered in [164-166].

The results of these studies can be summarised as follows. For low concentrated solutions of ionic surfactants, the increase of the temperature leads to a decrease in the equilibrium surface tension. This can be explained by the decrease of the surface tension of the solvent. In the range of medium ionic surfactant concentrations, almost no temperature dependence of surface tension is observed, while at concentrations close to CMC the most common trend is an increase of surface tension with temperature. The rate of surface tension changes usually slightly increase with increasing temperature.

For solutions of non-ionic surfactants and their mixtures, the temperature effect is more significant, see [22, 23, 167-175]. In the range of low surfactant concentration, a temperature increase is usually accompanied not only by a decrease of surface tension, but also by an increase of surface pressure. Therefore, the surface activity of the surfactant is increased. A significant decrease of surface tension was also observed for non-ionic surfactants in the medium concentration range. When the concentration is close to the CMC, the temperature effect depends on the EO chain length: for molecules with long EO chains (and therefore rather high surface tension in the CMC region) the increase in temperature results in a decrease of surface tension however less significant than at low concentrations. At the same time, for very short EO chains, the surface tension can either remain constant or even exhibit a slight increase with temperature. Similarly to ionic surfactants, the rate of surface tension decrease for the oxyethylated surfactants becomes higher with increasing temperature. In some cases, however, an anomalous sharp increase of this rate was observed, as described in [174]. It can be supposed that in such systems the surfactant molecules form aggregates at low temperature, which is known to result in a slower surface tension decrease [176, 177].

The data on the temperature dependence of surface tension of surfactant solutions are often used to estimate the thermodynamic characteristics of adsorption and micelle formation. One of such characteristics is the standard free energy of adsorption ΔG^0 [83, 160, 178-191]. To derive the expression for ΔG^0, one can use the relations for the chemical potential in the surface layer and in the solution bulk. The chemical potentials μ_i^s depend on the composition of the surface layer and its surface tension γ and are given by the relation (2.2), the potentials

in the solution bulk are given by Eq. (2.8). Assuming constant chemical potentials in the bulk and at the surface, Eqs (2.2) and (2.8) yield

$$\mu_i^{0s}(T,P,\gamma) + RT \ln f_i^s x_i^s = \mu_i^{0\alpha}(T,P) + RT \ln f_i^\alpha x_i^\alpha . \qquad (2.170)$$

In contrast to Eq. (2.9) discussed above, Eq. (2.170) does not involve explicitly the surface tension of the solution. Now the standard state has to be formulated. This state is similar to that used in Section 2.3, that is, for the solvent (i = 0) usually a pure component is assumed. This means $x_o^s = 1$, $f_o^s = 1$, $x_o^\alpha = 1$, $f_o^\alpha = 1$ and $\gamma = \gamma_0$. From Eq. (2.170) one obtains

$$\mu_0^{0s}(T,P,\gamma) = \mu_0^{0\alpha}(T,P) . \qquad (2.171)$$

The standard state for the i surface-active components is an infinitely diluted solution. Therefore, $x_i^\alpha \to 0$, $f_i^\alpha = 1$, $f_i^S = 1$, $\gamma = \gamma_0$, and Eq. (2.170) leads to

$$\mu_i^{0s}(T,P,\gamma) + RT \ln x_i^s\Big|_{x_i^\alpha \to 0} = \mu_i^{0\alpha}(T,P) + RT \ln x_i^\alpha\Big|_{x_i^\alpha \to 0} \qquad (2.172)$$

and

$$\mu_i^{0\alpha}(T,P) - \mu_i^{0s}(T,P,\gamma) = RT \ln K_i . \qquad (2.173)$$

$K_i = (x_i^s / x_i^\alpha)_{x_i^\alpha \to 0}$ is the distribution coefficient for infinite dilution. The difference $\mu_i^{0s}(T,P,\gamma) - \mu_i^{0\alpha}(T,P)$ is by definition the standard free energy of adsorption ΔG^0. Therefore,

$$\Delta G^0 = -RT \ln K_i . \qquad (2.174)$$

From Eqs. (2.170) and (2.173) and ideal surface layer and ideal solution bulk the Henry adsorption isotherm is obtained . Thus, K_i can be calculated from experimental data

$$K_i x_i^\alpha = x_i^s . \qquad (2.175)$$

The bulk concentration is usually denoted by c_i and expressed in mol/l. The molar portion of surfactant at the surface is equal to the monolayer coverage θ_i, if the dividing surface is chosen according to Lucassen-Reynders (see Eq. 2.18). Therefore, instead of expression (2.175) one obtains

$$\theta_i = b_i c_i = K_i c_i / \rho , \tag{2.176}$$

where ρ is the ratio of the solvent (water) density to its molecular weight, $\rho \approx 1000/18 = 55.6$ [mol H_2O/l]. Thus, one can replace K_i by $b_i\rho$ in Eq. (2.174). The Henry constant b_i is exactly equal to the constant of the Langmuir adsorption isotherm (2.17), because for low monolayer coverage or low bulk concentrations the expressions (2.17) can be simplified to Eq. (2.176).

Equation (2.174) is widely used to calculate the standard free energy of surfactant adsorption at water/air or water/oil interfaces [83, 160, 178, 179, 181-188]. For various surfactants, the values of ΔG^0 are in the range -20 to -60 kJ/mol, and usually decrease with temperature.

To consider the expression for the standard free energy of adsorption in more detail, one can take into account the contribution of surface tension to the standard chemical potential of the surface layer. This can be done by using Butler's equation (2.7) instead of Eq. (2.2). In this expression both standard chemical potentials of the surface and the bulk depend on temperature and pressure only. From Eqs. (2.11) and (2.2) one obtains Eqs. (2.9), (2.11)-(2.13) instead of Eqs. (2.170)-(2.173). Therefore, the standard free energy of adsorption is given by

$$\Delta G^0 = \mu_i^{0s}(T,P) - \mu_i^{0\alpha}(T,P) - \gamma_0 \omega_i . \tag{2.177}$$

This equation was first derived by Ross & Morrison [179]. It is seen that the standard free energy of adsorption of the i^{th} component comprises also the free surface energy per mole of this component.

To calculate the standard free energy of micelle formation for non-ionic surfactants, the expression

$$\Delta G_m^0 = RT \ln x_{cmc} = RT \ln(c_{cmc}\rho) \tag{2.178}$$

can be used (see [180-182, 184, 185, 190, 191]). In this case the standard free energy of adsorption is expressed via the standard energy of micelle formation as

$$\Delta G^0 = \Delta G_m^0 - (\gamma_0 - \gamma_{cmc})\omega_i . \tag{2.179}$$

One can easily see that Eq. (2.179) follows from Eqs. (2.9) and (2.177), in consideration that at the CMC the relations $x_i^s = 1$ and $\gamma_i = \gamma_{cmc}$ are valid. Therefore, the standard free energy of adsorption can also be calculated from the standard free energy of micelle formation [185,

101]. This calculation method is often simpler, because it does not require the measurements of the adsorption isotherm parameters in the region of low surfactant concentrations, while the measurements of surface and interfacial tension in the concentration range close to the CMC are experimentally much easier performed.

The results obtained for ΔG^0 at various temperatures are used to estimate the standard enthalpy (ΔH^0) and standard entropy of adsorption (ΔS^0)

$$\Delta G^0 = \Delta H^0 - T\Delta S^0, \tag{2.180}$$

$$-\frac{\Delta H^0}{T^2} = \frac{\partial}{\partial T}\left(\frac{\Delta G^0}{T}\right). \tag{2.181}$$

Introducing the relation (2.174) into the Gibbs-Helmholtz equation (2.181), one obtains the van't Hoff equation

$$\Delta H^0 = RT^2\left(\frac{\partial \ln K_i}{\partial T}\right). \tag{2.182}$$

Equation (2.182) is commonly used to calculate the standard enthalpy of adsorption [83, 160, 171, 186, 187]. The constant K_i usually exhibits a weak dependence on temperature. The value of ΔH^0 calculated from Eq. (2.182) was found to be in the range of +10 to -20 kJ/mol for various surfactants. As mentioned above ΔG^0 lies in the range -20 to -60 kJ/mol, hence the standard free energy of adsorption is mainly controlled by the adsorption entropy, see Eq. (2.180), and the value of $T\Delta S^0$ can amount to 10 to 50 kJ/mol. The most significant contribution of entropy was found for the water/oil interface [160]. The increase of ΔS^0 due to adsorption can be ascribed mainly to the disorder of water structure in the solution bulk [83, 160]. In solution the hydrocarbon chains of the surfactant molecules are surrounded by a structured water shell, while during the adsorption these shells are destructed. This leads to an increase in entropy of the system. The entropy also increases due to the transfer of hydrocarbon chains from the water phase to the gas phase and, especially, to the oil phase where they become more flexible.

We consider now the changes which should be introduced into the equations for the standard free energy of adsorption of ionic surfactants. For non-ionic surfactants, the relation between

the values of b and K are given by Eq. (2.176) which follows from Eqs. (2.15)-(2.16) according to the choice of the dividing surface after Lucassen-Reynders. However, for ionic surfactants, no proportionality between b and K exists. The generalised Butler equation for 1:1 ionic surfactants can be written as [192]

$$\mu_{jk}^{s} = \mu_{jk}^{0s} + RT \ln f_j^s f_k^s x_j^s x_k^s - \gamma\omega_{jk}. \tag{2.183}$$

Therefore, Eq. (2.15) which is valid for non-ionic surfactants, has to be replaced for ionic surfactants by Eq. (2.43). The constant b in the adsorption isotherm (2.45) is related to the constant K_{RX} of ionic surfactant distribution between surface and bulk as

$$b\rho = 2K_{RX}^{1/2}. \tag{2.184}$$

Inserting the adsorption equilibrium constant b into the distribution constant in Eq. (2.174), which is valid for non-ionic and ionic surfactants), we obtain for non-ionic surfactants

$$\Delta G^0 = -RT \ln(b\rho) \tag{2.185}$$

and for 1:1 ionic surfactants:

$$\Delta G^0 = -2RT \ln(b\rho/4). \tag{2.186}$$

Thus, the standard free energy of adsorption ΔG^0 for ionic surfactants calculated from the isotherm parameter b via Eq. (2.45), is roughly two times higher than the corresponding value for non-ionic surfactants. This increase is due to the simultaneous adsorption of surface-active ion and counterion (note that the surface layer is electroneutral). For the calculation of the standard free energy per surface-active ion one can, of course, use corresponding equations for non-ionic surfactants. The standard free energy of micelle formation for ionic surfactants is also approximately two times higher than for non-ionics, cf. Eq. (2.178), because the counterions are involved in the aggregation [193]

$$\Delta G_m^0 = (1+\beta)RT \ln x_{cmc} = (1+\beta)RT \ln(c_{cmc}/\rho). \tag{2.187}$$

Here β is the degree of bonding of counterions to the micelles, usually ca. 0.7 to 0.9 [97, 202]. Therefore, for ionic surfactants, instead of Eq. (2.179) one obtains

$$\Delta G^0 = \Delta G_m^0 - (\gamma_0 - \gamma_{cmc})\omega_{RX}, \tag{2.188}$$

where $\omega_{RX} = 2\omega_0$, in agreement with the choice of the dividing surface (the ionic sum convention for specifying the position of the dividing surface). The validity of Eqs. (2.179), (2.185) for non-ionic surfactants and (2.186), (2.188) for ionic surfactants will be verified in the following chapter. It will be shown that the proposed model leads to the same values of the standard free energy of adsorption as calculated either from b or CMC and ω_{RX}. Moreover, it will be shown that the Eqs. (2.185) and (2.186) lead to similar increments of the free energy adsorption per carbon atom in the hydrocarbon chain for both non-ionic and ionic surfactants.

2.11. Conclusions

Since the first decades of this century, when von Szyszkowski, Langmuir and Frumkin published their famous equations, great progress has been achieved in the theoretical description of adsorption at liquid/fluid interfaces. Thousands of relevant studies have been published since that time, and it appears almost impossible to compile a comprehensive review of the results obtained so far. Therefore, we have restricted ourselves to the presentation of some general principles used to derive equations of state and adsorption isotherms for surface active molecules at liquid/fluid interfaces. It is shown that the majority of all known equations can be derived via a two-dimensional solution theory applying Butler's equations for the chemical potentials in a Gibbs dividing surface. A number of additional assumptions or theoretical considerations are necessary, e.g., a convention for locating the dividing surface, the assumption of multiple states of adsorbed molecule within the surface layer, theories of enthalpic and entropic non-ideality of surface layers and, finally, the mass action law for molecular aggregation within a surface layer.

Some new equations of state and adsorption isotherms are presented in this chapter which describe mixed surface layers of surfactants possessing different molar areas, or which comprise surfactants and proteins able to change orientation or conformation. The influence of the main parameters of the respective adsorption models on the shape of surface pressure isotherms for surfactants which undergo reorientation or aggregation in the monolayer is analysed and illustrated graphically. These isotherms as compared with traditional ones, described by the Langmuir and Frumkin equations, provide a better agreement with experimental data for a number of systems (most recent results are presented in some papers just published [194 -203]). For systems allowing reorientation and aggregation the effect of

self-regulation of the surface layer composition governed by the surface pressure is considered. This physical approach goes back to the studies by Joos and co-workers. The effect is especially pronounced in protein adsorption layers, where not only the composition, but also the thickness of the adsorption layer depends on surface pressure. The general theoretic concept is also used for the analysis of the adsorption process based on the temperature dependence of surface and interfacial tension.

Some consequences which result from the proposed models of equilibrium surface layers are of special practical importance for rheological and dynamic surface phenomena. For example, the rate of surface tension decrease for the diffusion-controlled adsorption mechanism depends on whether the molecules undergo reorientation or aggregation processes in the surface layer. This will be explained in detail in Chapter 4. It is shown that the elasticity modulus of surfactant layers is very sensitive to the reorientation of adsorbed molecules. For protein surface layers there are restructuring processes at the surface that determine adsorption/desorption rates and a number of other dynamic and mechanical properties of interfacial layers.

While this chapter was dedicated to the description of the theoretical basis of surfactant adsorption layers, the subsequent Chapter 3 will now give a large number of examples taken from literature. The main aim will be to find the optimum isotherm for a given surfactant or homologous series. It will also be shown how isotherm parameters depend on the surfactant chain length, temperature, and added electrolyte.

2.12. References

1. A.N. Frumkin, Z. Phys. Chem. (Leipzig), 116(1925)466.
2. E.H. Lucassen-Reynders, J. Colloid Sci. 19(1964)584, J. Phys. Chem., 70(1966)1777.
3. B.B. Damaskin, A.N. Frumkin, S.L. Djatkina, Izv. AN SSSR, Ser. Chim., (1967)2171.
4. B.B. Damaskin, Izv. AN SSSR, Ser. Chim., (1969)346.
5. E.H. Lucassen-Reynders, In: Anionic Surfactants (Physical Chemistry of Surfactant Action), (Ed. E.H. Lucassen-Reynders), Marcel Dekker Inc., New York-Basel, 1981, pp.1.
6. J.A. Tedoradze, R.A. Arakeljan, E.D. Belokolos, Elektrokhimija, 2(1966)563.
7. B.B. Damaskin, Elektrochimija, 5(1969)249.
8. B.B. Damaskin, A.N. Frumkin, N.A. Borovaja, Elektrokhimija, 8(1972)807.

9. M.J. Rosen, X.Y. Hua, J. Colloid Interface Sci., 86(1982)164.
10. X.Y. Hua, M.J. Rosen, J. Colloid Interface Sci., 87(1982)469.
11. V.B. Fainerman, S.V. Lylyk, Koll. Zh., 45(1983)500.
12. V.B. Fainerman, Zh. Fiz. Khim., 60(1986)681.
13. R. Wüstneck, R. Miller, J. Kriwanek, H.-R. Holzbauer, Langmuir, 10(1994)3738.
14. R. Wüstneck, R. Miller, J. Kriwanek, J. Colloid Interface Sci., 81(1993)1.
15. P. Joos, Bull. Soc. Chim. Belg., 76(1967)591.
16. E.H. Lucassen-Reynders, J. Colloid Interface Sci., 41(1972)156.
17. P. Joos, Biochim. Biophys. Acta, 375(1975)1.
18. E.H. Lucassen-Reynders, Colloids and Surfaces A, 91(1994)79.
19. P. Joos, *Dynamic Surface Phenomena,* VSP, Utrecht, The Netherland, 1999
20. E.H. Lucassen-Reynders, J. Colloid Interface Sci., 42 (1973) 563
21. P. Joos, G. Serrien, J. Colloid Interface Sci., 145(1991)291.
22. V.B. Fainerman, A.V. Makievski, P. Joos, Colloids Surfaces A, 90(1994)213.
23. V.B. Fainerman, R. Miller, A.V. Makievski, Langmuir, 11(1995)3054.
24. V.B. Fainerman, R. Miller, R. Wüstneck, A.V. Makievski, J. Phys. Chem., 100(1996)7669.
25. V.B. Fainerman, R. Miller, R. Wüstneck, J. Phys. Chem., 101(1997)6479
26. V.B. Fainerman, R. Miller, R. Wüstneck, J. Colloid Interface Sci., 183(1996)26.
27. L. Liggieri, F. Ravera, A. Passerone, J. Colloid Interface Sci., 169(1995)226.
28. G. Geeraerts, P. Joos, F. Ville, Colloids Surfaces A, 75(1993)243.
29. G. Kretzschmar, D. Vollhardt, Monatsber. Dtsch. Akad. Wiss. Berlin, 10(1968)206.
30. Ch. Böhm, F. Leveiller, D. Jacquemain, H. Möhwald, K. Kjaer, J. Als-Nielsen, W. Weissbuch, L. Lieserowitz, Langmuir, 10(1994)880.
31. G. Brezesinski, Ch. Böhm, A. Dietrich, H. Möhwald, Physika B, 198(1994)146.
32. E. Ruckenstein, A. Bhakta, Langmuir, 10(1994)2694.
33. J. Israelachvili, Langmuir, 10(1994)3774.
34. E. Ruckenstein, B. Li, Langmuir, 11(1995)3510.
35. V.B. Fainerman, D. Vollhardt, V. Melzer, J. Phys. Chem., 100(1996)15478.
36. S.-Y. Lin, K. McKeigue, C. Maldarelli, Langmuir, 7(1991)1055.
37. S.-Y. Lin, T.-L. Lu, W.-B. Hwang, Langmuir, 10(1994)3442.

38. S.-Y. Lin, W.-B. Hwang, T.-L. Lu, Colloids & Surfaces A, 114(1996)143.
39. K. Lunkenheimer, R. Hirte, J. Phys. Chem., 96(1992)8683.
40. K. Lunkenheimer, G. Czichocki, R. Hirte, W. Barczyk, Colloids Surfaces A, 101(1995)187.
41. V.B. Fainerman, R. Miller, Langmuir, 12(1996)6011.
42. E.H. Lucassen-Reynders, Colloids Surfaces, 25 (1987) 231.
43. L. Ter-Minassian-Saraga, J. Colloid Interface Sci., 80(1981)393.
44. J.A. Butler, V. Proc. Roy. Soc. Ser. A, 138(1932)348.
45. J.T. Davies, Proc. Roy. Soc., Ser. A, 208(1951)224; 245(1958)417, 419.
46. R.P. Borwankar, D.T. Wasan, Chem. Eng. Sci., 43(1988)1323.
47. C.A. MacLeod, C.J. Radke, Langmuir, 10(1994)3555.
48. A.I. Rusanov, *Fazovye Ravnovesija i Poverchnostnye Javlenija*, Khimija, Leningrad, 1967.
49. J.M. Prausnitz, *Molecular Thermodynamics of Fluid Phase Equilibria*, Prentice-Hall Englewood Cliffs, New York, 1969.
50. B. von Szyszkowski, Z. Phys. Chem. (Leipzig), 64(1908)385.
51. I. Langmuir, J. Amer. Chem. Soc., 39 (1917) 1848.
52. E.H. Lucassen-Reynders, J. Colloid Interface Sci., 85(1982)178.
53. E.H. Lucassen-Reynders, Progress in Surface and Membrane Science, 10(1976)253.
54. R. Van den Bogaert, P. Joos, J. Phys. Chem., 84(1980)190.
55. L.K. Filippov, J. Colloid Interface Sci., 182(1996)330.
56. R. Parsons, J. Electroanal. Chem., 7(1964)136.
57. E.I. Franses, F.A. Siddiqui, D.J. Ahn, C.-H. Chang, N.-H.L. Wang, Langmuir, 11(1995)3177
58. V.B. Fainerman, E.H. Lucassen-Reynders, R. Miller, Colloids & Surfaces A, 143(1998)141
59. V.B. Fainerman, A.V. Makievski, R. Miller, Rev. in Chem. Eng., 14(1998)373.
60. I. Prigogine, *The Molecular Theory of Solutions*, North-Holland, Amsterdam, 1968.
61. E.A Guggenheim, *Mixtures*, Clarendon Press, Oxford, 1952.
62. R.C. Read, J.M. Prausnitz, T.K. Sherwood, *The Properties of Gases and Liquids*, 3rd Ed., McGraw-Hill Inc. , New York, London, Paris, Tokyo, 1977.

63. K. Lunkenheimer, R. Hirte, J.Phis.Chem, 96(1992)8683.
64. V.V. Krotov, Kolloidn. Zh., 47(1985)1075.
65. V.B. Fainerman, Zh. Fiz. Khim., 62(1988)1003.
66. V.B. Fainerman, Zh. Fiz. Khim., 60(1986)681.
67. V.B. Fainerman, Kolloidn. Zh., 48(1986)512.
68. J. Rodakiewicz-Nowak, J. Colloid Interface Sci. , 85(1982)586.
69. M. Karolczak, D.M. Mohilner, J. Phys. Chem., 86(1982)2840.
70. D.M. Mohilner, H. Nakadomari, P.R. Mohilner, J. Phys. Chem., 81(1977)244.
71. E. Helfand, H.L. Frisch, J.L. Lebowitz, J. Chem. Phys., 34(1961)1037.
72. R. Parsons, J. Electroanal. Chem., 7(1964)136.
73. E. Tronel-Peyroz, J. Phys. Chem., 88(1984)1491.
74. H. Diamant, D. Andelman, J. Phys. Chem., 100(1996)13732.
75. H. Okuda, S. Ozeki, S. Ikeda, Bull. Chem. Soc. Japan, 57(1984)1321.
76. E.H. Lucassen-Reynders, J. Lucassen, D. Giles, J. Colloid Interface Sci., 81(1981)150.
77. V.V. Kalinin, C.J. Radke, Colloids Surfaces A, 114(1996)337.
78. V. Ya. Poberezhnyi, L.A. Kul'skiy, Kolloidn. Zh., 46(1984)735.
79. V. Ya. Poberezhnyi, T.Z. Sotskova, L.A. Kul'skiy, Khim. i Tekhnol. Vody., 18(1996)570.
80. P.M. Vlahovska, K.D. Danov, A. Mehreteab, G. Broze, J. Colloid Interface Sci., 192(1997)194.
81. P.A. Kralchevsky, K.D. Danov, G. Broze, A. Mehreteab, Langmuir, 15(1999)2351.
82. V.M. Muller, B.V. Derjaguin, J. Colloid Interface Sci., 61(1977)361.
83. V.B. Fainerman, Colloids Surfaces, 57(1991)249.
84. V.B. Fainerman, Zh. Fiz. Khim., 56(1982)2506.
85. A.V. Makievski, V.B. Fainerman, M. Bree, R. Wüstneck, J. Krägel, R. Miller, J. Phys. Chem., 102(1998)417.
86. V.B. Fainerman and R. Miller, Adsorption Isotherms of Proteins at Liquid Interfaces, monograph in "Proteins at Liquid Interfaces", in "Studies of Interface Science", D. Möbius and R. Miller (Eds.), Vol. 7, Amsterdam, Elsevier, 1998, p. 51-102
87. R. Miller, E.V. Aksenenko, L. Liggieri, F. Ravera, M. Ferrari, V.B. Fainerman, Langmuir, 15(1999)1328.

88. A.V. Makievski, D. Grigoriev, Colloid Surfaces A, 143(1998)233.
89. E.V. Aksenenko, A.V. Makievski, R. Miller, V.B. Fainerman, Colloids & Surfaces A, 143(1998)311.
90. M. Ueno, Y. Takasawa, H. Miyashige, Y. Tabata, K. Meguro, Colloid Polym. Sci., 259(1981)761.
91. J.R. Lu, Z.X. Li, T.J. Su, R.T. Thomas, J. Penfold, Langmuir, 9(1993)2408
92. J.R. Lu, Z.X. Li, R.T. Thomas, E.J. Staples, I. Tucker, J. Penfold, J. Phys. Chem., 97(1993)8012
93. S. Ozeki, T. Ikegava, S. Inokuma, T. Kuwamura, Langmuir, 5(1989)222.
94. J. Lucassen, M. Van den Tempel, Chem. Eng. Sci., 17(1972)1283.
95. J. Lucassen, M. Van den Tempel, J. Colloid Interface Sce., 41(1972)41.
96. K.-D. Wantke, K. Lunkenheimer, C. Hempt, J. Colloid Interface Sci., 159 (1993)28.
97. A.I. Rusanov, V.B. Fainerman, Dokl. Akad. Nauk SSSR, 308(1989)651.
98. V.B. Fainerman and D. Vollhardt, J. Phys. Chem. B, 103(1999)145.
99. A. Nikolov, G. Martynov, D. Exerowa, J. Colloid Interface Sci., 81(1981)116.
100. J.C. Eriksson, S. Ljungrenn, Prog. Colloid Polym. Sci., 76(1988)188.
101. M. Aratono, S. Uryu, Y. Hayami, K. Motomura, R. Matuura, J. Colloid Interface Sci., 98(1984)33.
102. B.P. Binks, P.D.I. Fletcher, W.F.C. Sagere, R.L. Thompson, Langmuir, 11(1995)977.
103. K. Tajima, Bull. Chem. Soc. Japan, 43(1970)3063.
104. J.K. Ferry, K.J. Stebe, Colloids & Surfaces A, 156(1999)567
105. J.K. Ferry, K.J. Stebe, J. Colloid Interface Sci.,208(1999)1.
106. H. Möhwald, Annu. Rev. Phys. Chem., 41(1990)441.
107. D. Vollhardt, Adv. Colloid Interface Sci., 64(1996)143.
108. A.-F. Mingotaud, C. Mingotaud, L.K. Patterson, *Handbook on Monolayers*, Academic Press, New York, 1993.
109. M.B. Sankaram, D. Marsh, T.E. Thompson, Biophys. J., 63(1992)340.
110. J. Zhu, A. Eisenberg, R.B. Lennox, Macromolecules, 25(1992)6547.
111. D. Vollhardt, U. Gehlert, S. Siegel, Colloids Surf. A, 76(1993)187.
112. U. Gehlert, G. Weidemann, D. Vollhardt, J. Coll. Interf. Sci., 174(1995)392.
113. V. Melzer, D. Vollhardt, Physical Review Letters, 76(1996)3770

114. D. Vollhardt, V. Melzer, J. Phys. Chem B., 101(1997)3370.
115. V. Melzer, D. Vollhardt, G. Brezesinski, H. Möhwald, J. Phys. Chem B, 102(1998)591.
116. E. Ruckenstein, B. Li, J. Phys. Chem., 100(1996) 3108.
117. E. Ruckenstein, B. Li, Langmuir, 12(1996)2309.
118. E. Ruckenstein, B. Li, J. Phys. Chem. B, 102(1998)981
119. M. Lin, J.-L. Firpo, P. Mansoura, J.F. Baret, J. Chem. Phys., 71(1979)2202.
120. K. Motomura, S.-I. Iwanaga, Y.Hayami, S. Uryu, R. Matuura, J. Colloid Interface Sci., 80(1981)32.
121. K. Motomura, M. Aratono, N. Matubayasi, R. Matuura, J. Colloid Interface Sci., 67(1978)347.
122. N. Matubayasi, K. Motomura, M. Aratono, R. Matuura, Bull. Chem. Soc. Japan, 51(1978)2800.
123. Y. Hayami, A. Uemura, N. Ikeda, M. Aratono, K. Motomura, J. Colloid Interface Sci., 172(1995)142.
124. T. Takiue, A. Yanata, N. Ikeda, K. Motomura, M. Aratono, J. Phys. Chem., 100(1996)13743.
125. T. Takiue, A. Yanata, N. Ikeda, Y. Hayami, K. Motomura, M. Aratono, J. Phys. Chem., 100(1996)20122.
126. T. Takiue, A. Uemura, N. Ikeda, K. Motomura, M. Aratono, J. Phys. Chem. B, 102(1998)3724.
127. T. Takiue, A. Uemura, N. Ikeda, K. Motomura, M. Aratono, J. Phys. Chem. B, 102(1998)4906.
128. T. Takiue, T. Toyomasu, N. Ikeda, M. Aratono, J. Phys. Chem. B, 103(1999)6547.
129. S. Uredat, G. H. Findenegg, Langmuir, 15(1999)1108.
130. D. Vollhardt, V.B. Fainerman, G. Emrich, submitted to J. Phys. Chem B.
131. V.B. Fainerman, R. Miller, Langmuir, 15(1999)1812.
132. A.V. Dobrynin, R.H. Colby and M. Rubinstein, Macromolecules, 28(1995)1859.
133. R. Douillard, M. Daoud, J. Lefebvre, C. Minier, G. Lecannu and J. Coutret, J. Colloid Interface Sci., 163(1994)277.
134. D.E. Graham, M.C. Phillips, J. Colloid Interface Sci., 70(1979)415
135. R.Z. Guzman, R.G. Carbonel, P.K. Kilpatrick, J. Colloid Interface Sci., 114(1986)536.

136. R. Doullard, J. Lefebvre, J. Colloid Interface Sci., 139(1990)488.
137. R. Miller, V.B. Fainerman, A.V. Makievski, J. Krägel and R. Wüstneck, Colloids Surfaces A, 161(2000)151.
138. E. Hutchinson, J. Colloid Sci., 3(1948)413.
139. B.A. Pethica, Trans. Faraday Soc., 51(1955)1402.
140. P.J. Anderson, B.A. Pethica, Trans. Faraday Soc., 52(1956)1080.
141. M.A. McGregor, G.T. Barnes, J. Colloid Interface Sci., 69(1977)408.
142. D.M. Alexander, G.T. Barnes, J. Chem. Soc. Faraday Trans. 1, 76(1980)118.
143. K. Motomura, I. Hayami, M. Aratono, R. Matuura, J. Colloid Interface Sci., 87(1982)333.
144. I. Panaiotov, L. Ter-Minassian-Saraga, G. Albrecht, G. Langmuir, 1(1985)395.
145. L. Ter-Minassian-Saraga, Langmuir, 1(1985)391
146. D.G. Hall, Langmuir, 2(1986)809
147. K. Tajima, M. Koshinuma, A. Nakamura, Langmuir, 7(1991)2764.
148. Q. Jiang, C.J. O'Lenick, J.E. Valentini, Y.C. Chiew, Langmuir, 11(1995)1138.
149. K. Asano, K. Miyano, H. Ui, M. Shimomura, I. Ohta, Langmuir, 9(1993)3587.
150. D. Vollhardt, M. Wittig, Colloids Surfaces, 47(1990)233.
151. S. Siegel, D. Vollhardt, Colloids Surfaces A, 76(1993)197.
152. S. Sundaran, K.J. Stebe, Langmuir, 13(1997)1729.
153. N.S. Santos Magalhaes, H.M. de Oliveira, A. Baszkin, Colloid and Surfaces A, 118(1996)63
154. S. Sundaram, J.K. Ferri, D. Vollhardt, K.J. Stebe, Langmuir, 14(1998)1208.
155. V.B. Fainerman, D. Vollhardt, Langmuir, 15(1999)1784.
156. V.B. Fainerman, A.V. Makievski, D. Vollhardt, S. Siegel, R. Miller, J. Phys. Chem. B, 103(1999)330.
157. V.B. Fainerman, J. Zhao, D. Vollhardt, A.V. Makievski, J.B. Li, J. Phys. Chem. 103(1999)8998.
158. K. Motomura, N. Matubayasi, M. Aratono, R. Matuura, J. Colloid Interface Sci., 64(1978)356.
159. D.K. Owens, J. Colloid Interface Sci., 29(1969)496.
160. Z.N. Markina, N.M. Zadymova, O.P. Bovkun, Colloids Surfaces, 22(1987)9.

161. V.B. Fainerman, A.V. Makievski, R. Miller, Colloids Surfaces A, 87(1994)61.
162. V.B. Fainerman, Kolloid. Zh., 40(1978)924.
163. V.B. Fainerman, A.V. Makievski, Kolloid. Zh., 54, (1992)75.
164. L.-H. Zhang, G.-X. Zhao, J. Colloid Interface Sci., 127(1989)353.
165. D. Goralczyk, J. Colloid Interface Sci., 88(1982)590.
166. L.-W. Chen, J.-H. Chen, N.F. Zhou, J. Chem. Soc. Faraday Trans., 91(1995)3873.
167. M.J. Schick, J. Colloid. Sci., 17(1962)801.
168. J.M. Corkill, J.F. Goodman, R.N. Ottewill, Trans. Faraday Soc., 57(1961)1627.
169. J.M. Corkill, J.F. Goodman, S.P. Harrold, Trans. Faraday. Soc., 60(1964)202.
170. J.E. Carless, B.A. Challis, B.A. Mulley., J. Colloid. Sci., 19(1964)201.
171. G. Bleys, P. Joos, J. Phys. Chem., 89(1985)1027.
172. A.V. Makievski, V.B. Fainerman, P. Joos, J. Colloid Interface Sci., 166(1994)6.
173. V.B. Fainerman, Kolloid. Zh., 54, N4(1992)200.
174. J. Eastoe, J.S. Dalton, P.G.A. Rogueda, P.C. Griffiths, Langmuir,14(1998)979.
175. J. Eastoe, J.S. Dalton, P.G.A. Rogueda, E.R. Crooks, A.R. Pitt, E.A. Simister, J. Colloid Interface Sci., 188(1997)423.
176. V.B. Fainerman, D. Vollhardt, V. Melzer, J. Chem. Phys., 107(1)(1997)243.
177. E.V. Aksenenko, V.B. Fainerman, R. Miller, J. Phys. Chem. B, 102(1998)6025.
178. J.T. Davies, E.K. Rideal, Interfacial Phenomena, Acad. Press, New York, 1963.
179. S. Ross, L.D. Morrison, Colloids Surfaces, 7(1983)121.
180. J.L. Katz, J. Colloid Interface Sci., 56(1976)179.
181. N. Kishimoto, K. Sumida, Chem. Pharm. Bull., 24(1976)1226.
182. M.J. Rosen, Surfactants and Interfacial Phenomena, John Wiley & Sons, New York, 1978.
183. H. Lange, In: Nonionic Surfactants, Ed. M. Schick, Marcel Dekker, New York, 1967, p. 443.
184. M.J. Rosen, In: Solution Chemistry of Surfactants, Vol.1, Ed. K.L. Mittal, Plenum Publ. Corp., New York, 1979, p.45.
185. M.J. Rosen, A.W. Cohen, M. Dahanayake, X.-Y. Hua, J. Phys. Chem., 86(1982)541.
186. M. Nakagaki, M. Yamamoto, Bull. Chem. Soc. Japan, 50(1977)873.
187. N.M. Zadymova, Z.N. Markina, Kolloid. Zh., 48(1986)15; 355.

188. V.B. Fainerman, Zh. Fiz. Khim., 64(1990)1611.
189. V.Ya. Poberezhny, T.Z. Sotskova, Khim. i Tekhnol. Vody, 14(1992)883.
190. A.A. Abramzon, Russian J. Appl. Chem., 69(1996)1159.
191. M.E. Haque, A.R. Das, S.P. Moulik, J. Phys. Chem., 99(1995)14032.
192. V.B. Fainerman, E.H. Lucassen-Reynders, Adv. Colloid Interface Sci., (2001).
193. A.I. Rusanov, Micellization in Surfactant Solutions, In: Chemical Reviews, 27(1997)1-326.
194. V.B. Fainerman, R. Miller, E.V. Aksenenko, J. Phys. Chem. B, 104(2000)5744.
195. V.B. Fainerman, R. Miller, J. Phys. Chem. B, 104(2000)8471.
196. V.B. Fainerman, R. Miller, E.V. Aksenenko, Langmuir, 16(2000)4196.
197. V.B. Fainerman, R. Miller, J. Colloid Interface Sci., 232(2000)254.
198. R. Miller, V.B. Fainerman, A.V. Makievski, J. Krägel, R, Wüstneck, Colloids Surfaces A, 161(2000)151.
199. D. Vollhardt, V.B. Fainerman, G. Emrich, J. Phys. Chem. B, 104(2000)8536.
200. R. Miller, V.B. Fainerman, A.V. Makievski, J. Krägel, D.O. Grigoriev, V.N. Kazakov, O.V. Sinyachenko, Adv. Colloid Interface Sci., 86(2000)39.
201. V.B. Fainerman, R. Miller, E.V. Aksenenko, A.V. Makievski, J. Krägel, G. Loglio, L. Liggieri, Adv. Colloid Interface Sci., 86(2000)83.
202. D. Vollhardt, V.B. Fainerman, Adv. Colloid Interface Sci., 86(2000)103.
203. R. Miller, E.V. Aksenenko, V.B. Fainerman, J. Colloid Interface Sci., 236(2001)35.

3. EQUILIBRIUM ADSORPTION PROPERTIES OF SINGLE AND MIXED SURFACTANT SOLUTIONS

V.B. Fainerman[1], R. Miller[2], E.V Aksenenko[3] and A.V. Makievski[2,4]

[1] International Medical Physicochemical Centre, Donetsk Medical University, 16 Ilych Avenue, Donetsk 83003, Ukraine

[2] Max-Planck-Institut für Kolloid- und Grenzflächenforschung, Forschungscampus Golm, 14424 Potsdam/Golm, Germany

[3] Institute of Colloid Chemistry and Chemistry of Water, Ukrainian National Academy of Sciences, 42 Vernadsky avenue, Kiev 03680, Ukraine

[4] SINTECH Surface and Interface Technology, Volmerstrasse 5-7, D-12489 Berlin, Germany

3.1 Introduction

The problem of interrelation between the chemical structure of a surfactant and its ability to be adsorbed at a liquid interface is one of the main questions in physical chemistry of surfactant solutions. Studies of the theoretical and experimental aspects of this interrelation were reviewed in a number of publications [1-16]. These studies revealed some general principles which enable one to deduce the adsorption activity of a surfactant, the character of the dependence of surface tension on bulk concentration of the surfactant and some details of the adsorption layer composition from the structure of the surfactant molecule. However, in spite of significant progress achieved mainly during the last two or three decades, there is no generalisation of the results even not for the most popular homologous series of surfactants. Also, data concerning the main parameters of adsorption isotherms of these surfactants are scattered and should be systematised. Usually the experimental isotherms are compared with the Langmuir or Frumkin models, which cannot be regarded to as universal theoretical description of adsorption layers. Even less attention is paid in the literature to the more complicated and more practically important problem, the adsorption behaviour of mixed surfactant solutions. The most interesting aspect of this problem, the prediction of the adsorption behaviour of a mixture from data obtained for individual solutions, is still in the initial stage.

In this chapter, we present systematised experimental results for equilibrium surface (in some cases interfacial) tensions for several homologous series of non-ionic and ionic surfactants. In contrast to what is generally believed to be trivial, we paid large attention to the selection of reliable experimental equilibrium data. Two main principles were employed here:

(i) high purity of the surfactants and solutions used,

(ii) control of experimental conditions under which the equilibrium was established.

The related questions were extensively discussed in the monograph [17]. We believe that all data obtained in our laboratories are in full compliance with these requirements. Also, the conditions of equilibrium establishment were controlled in studies performed in the groups of Joos, Lucassen-Reynders, Lin and other authors. For surfactants with high adsorption activity, e.g., oxyethylated alcohols or ethers, the concentration in the solution is low, and the time necessary to attain the equilibrium is usually tens of hours. Therefore the data published for such systems are not necessarily equilibrium ones. To illustrate this, we present below some results published in the literature, which do not satisfy the requirement (ii). Hence, it is no surprise that these data do not agree with the general trends observed.

In the preceding chapter, theoretical models were presented which provide the description of the adsorption behaviour for individual and mixed surfactant solutions involving not only the nonideality of a surfactant in the adsorption layer, but also possible reorientation or aggregation of molecules at the interface. These new theoretical models are used below to analyse the experimental dependencies of equilibrium surface tension on concentration (or activity for ionic surfactants) for several homologous series of surface active substances. To process the experimental data, a problem-oriented software was developed in form of fitting programs. These were used to establish the relations between the adsorption equilibrium constants, intermolecular interaction parameters, molar areas of molecules corresponding to their different orientations in the monolayer etc., and the number of methylene groups and the type of the polar group specific to the surfactant molecule. From the comparison of the deviations obtained from fitting of experimental data to various theoretical models, one can deduce which of the models seems to be the most appropriate, conjecturing therefore about the adsorption process mechanism for the particular surfactant. However, it is also shown in this chapter that the most reliable conclusions about the correspondence between the theoretical model and the experimental data can be provided by a comparison between the equilibrium tensiometry data

and results obtained in dynamic surface (interfacial) tension studies, and also with data from other experimental techniques (ellipsometry, neutron and X-ray reflection, Brewster angle microscopy and other optical methods).

The structure of this chapter is as follows. First, the results obtained for individual surfactant solutions are presented, which are preceded, for the sake of convenience, by a summary of the main equations corresponding to the various theoretical models discussed in Chapter 2. The software used for fitting the models to experimental data will be described in Chapter 7. Then, surfactant mixtures are considered with a number of experimental and theoretical examples. A summary of the main theoretical equations for mixtures of ionic and non-ionic surfactants (the corresponding fitting software again is described in Chapter 7). Also some approximate theoretical models for the mixture of two or more surfactants is presented and compared with experimental results.

3.2. Theoretical models for individual surfactant solutions

The equation of state and adsorption isotherm for the Frumkin model (which becomes the Langmuir model for a = 0, cf. Chapter 2) are

$$-\frac{\Pi\omega}{RT} = \ln(1-\theta) + a\theta^2, \tag{3.1}$$

$$bc = \frac{\theta}{1-\theta}\exp(-2a\theta). \tag{3.2}$$

The reorientation model for molecules which can exist in two states (conformational changes) in the adsorption layer, 1 and 2, respectively (for definiteness we assume $\omega_1 > \omega_2$) involves the equation of state of the surface layer

$$-\frac{\Pi\omega}{RT} = \ln(1-\Gamma\omega) \tag{3.3}$$

and the adsorption isotherm

$$bc = \frac{\Gamma_2\omega}{(1-\Gamma\omega)^{\omega_2/\omega}}\ . \tag{3.4}$$

Here the total adsorption Γ and mean molar area ω are defined by the relationships

$$\Gamma = \Gamma_1 + \Gamma_2 \tag{3.5}$$

$$\omega\Gamma = \omega_1\Gamma_1 + \omega_2\Gamma_2, \tag{3.6}$$

The model also involves the ratio of adsorptions in the two possible adsorption states of the molecule (the so-called generalised Joos adsorption equation)

$$\frac{\Gamma_1}{\Gamma_2} = \exp\left(\frac{\omega_1 - \omega_2}{\omega}\right)\left(\frac{\omega_1}{\omega_2}\right)^{\alpha} \exp\left[-\frac{\Pi(\omega_1 - \omega_2)}{RT}\right]. \tag{3.7}$$

The model for aggregation in the adsorption layer with the arbitrary aggregation number n is described by the following equation of state and adsorption isotherm

$$-\frac{\Pi\omega}{RT} = \ln\left\{1 - \Gamma_1\omega\left[1 + (\Gamma_1/\Gamma_c)^{n-1}\right]\right\} \tag{3.8}$$

$$bc = \frac{\Gamma_1\omega}{\left\{1 - \Gamma_1\omega\left[1 + (\Gamma_1/\Gamma_c)^{n-1}\right]\right\}^{\omega_1/\omega}}. \tag{3.9}$$

Here Γ_1 and Γ_c are the partial and critical adsorption of monomers, respectively, and the average molar area ω should be expressed via the equation

$$\frac{\omega}{\omega_1} = \frac{1 + n(\Gamma_1/\Gamma_c)^{n-1}}{1 + (\Gamma_1/\Gamma_c)^{n-1}}. \tag{3.10}$$

The results discussed below for a number of homologous series were all obtained using the program IsoFit which was developed for fitting experimental dependencies of $\Pi(c)$ or $\gamma(c)$ against the equations for the particular model (cf. Chapter 7).

3.3. Non-ionic and amphoteric surfactants

3.3.1. Normal alcohols

The series of normal alcohols (C_nOH) is the most frequently studied homologous series of surfactants. Figure 3.1 illustrates the experimental surface tension isotherms for the aqueous solutions of alcohols in the range from C_3 to C_{10}, as summarised from the data reported elsewhere by different authors [18-24].

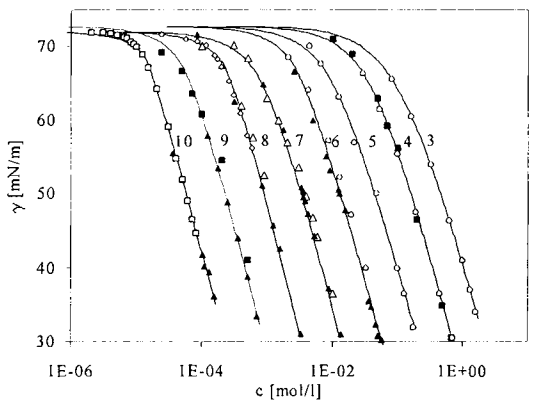

Fig. 3.1. The dependence of equilibrium surface tension on concentration for the solutions of normal alcohols in the range of 1-propanol to 1-decanol (the number of carbon atoms is shown by figures at the curves); (O), data from [18], 20°C; (▲), data from [19], 20°C; (△), data from [20], 25°C; (◇), data from [21], 25°C; (■), data from [22], 20°C; (□), data from [23,24], 25°C, theoretical curves were calculated from Frumkin's model, model parameters are listed in Table 3.1.

Table 3.1. Adsorption parameters for normal alcohols using Frumkin's model of Eqs. (3.1)-(3.2),.

C_nOH	ω_1, 10^5 m^2/mol	a	b, l/mol	ε, %	Ref.
C_3OH	1.75	0.16	7.77	1.4	18
C_4OH	1.71	0.6	$1.48 \cdot 10^1$	4.6	18, 22
C_5OH	1.75	0.52	$5.87 \cdot 10^1$	5.4	18
C_6OH	1.72	1.04	$1.23 \cdot 10^2$	9.1	18, 19
C_7OH	1.67	0.8	$5.33 \cdot 10^2$	2.2	19, 20
C_8OH	1.65	1.37	$1.17 \cdot 10^3$	3.1	19, 20, 21
C_9OH	1.65	1.2	$5.82 \cdot 10^3$	6.0	19, 22
$C_{10}OH$	1.67	1.8	$1.21 \cdot 10^4$	4.6	19, 23, 24

The temperature of the solutions in all the experiments presented was almost the same, 20 - 25°C. The correspondence between the data reported by different authors is remarkably well. For the processing of experimental data the Frumkin model was employed and the resulting model parameters are presented in Table 3.1. Here the value ε characterises the deviation between the theoretical isotherm and the experimental values. Figures 3.2-3.4

illustrate the dependence of the parameters ω, a and b on the number of carbon atoms (methylene groups) n_C in the alcohol molecule.

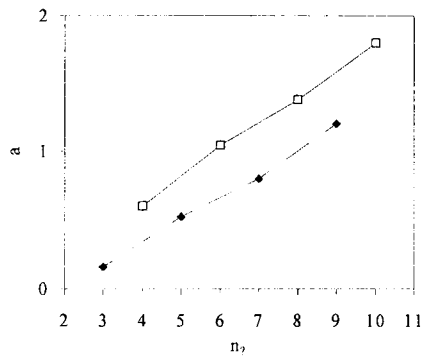

Fig. 3.2. Dependence of the attraction constant (Frumkin's constant) a on n_C for normal alcohols.

It is seen that with increasing n_C the molar area ω only slightly decreases, while the attraction constant a increases almost linearly, with difference between the even and odd homologues. It is seen from Fig. 3.4 that the addition of one methylene group in the range of C_3 to C_{10}, the average value b becomes 3 times higher. According to Eq. (2.185) the standard free energy of adsorption depends only on temperature and the constant K (or b)

$$\Delta G^0 = -RT\ln(b\rho). \tag{3.11}$$

where $\rho \cong 55.6$. Hence the increment in b per methylene group (b_i/b_{i-1}) corresponds to the increment in free energy of adsorption of $\Delta G^0_{CH_2} = -2.73$ kJ/mol per methylene group in the homologous series of normal alcohol.

For 1-decyl alcohol the model which assumes the aggregation of molecules in the adsorption layer leads to much better agreement with the experiment, cf. Fig. 2.17. The processing of the data reported in [23, 24] assuming aggregation with n = 2.6 leads to ε = 1.1%, while for the Frumkin model we obtain ε = 4.1%. Also for 1-decanol the aggregation model yields better agreement with the data. It is seen from Fig. 3.2 that for 1-decanol the value of a is close to the critical value of a = 2 which corresponds to the onset of phase transition in the monolayer, cf. Section 2.7.3 and Fig. 2.19. As for 1-dodecanol the predicted value of a = 2.2 exceeds the critical value, it can be supposed that, in addition to the formation of small aggregates, a

condensed phase is also formed in the monolayer. This conjecture was recently supported experimentally [25].

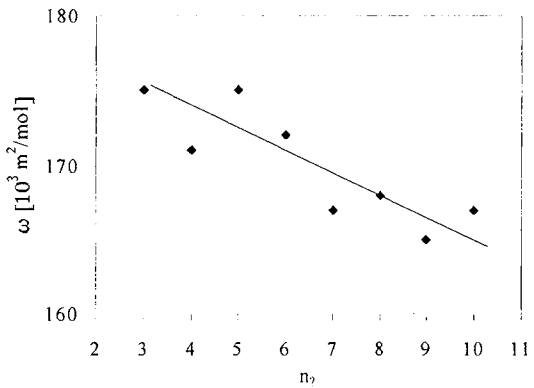

Fig. 3.3. Dependence of molar area ω on n_C for Frumkin's model obtained for the homologous series of normal alcohols.

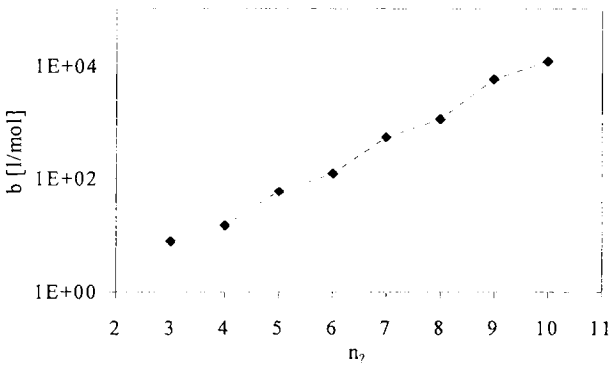

Fig. 3.4. Dependence of adsorption equilibrium constant b on n_C obtained for the homologous series of normal alcohols.

It was shown that the formation of 1-dodecanol adsorption layers is accompanied by inflection points in the surface pressure *vs* time plots, a feature characteristic to two-dimensional condensation. Also the compression of a spread 1-dodecanol monolayer leads to characteristic inflections in the surface pressure (Π) *vs* area per mole (or molecule) curves. The surface

pressure in the critical points at a given temperature does not depend on the process of monolayer formation (adsorption or spread monolayer). The presence of clusters in the monolayer at pressures exceeding the critical value is also demonstrated by Brewster angle spectroscopy [25]. The compression isotherms for spread monolayers of 1-dodecanol at 10°C and 15°C are shown in Fig. 3.5.

Comparing the experimental Π-A isotherms with the theoretic models one can conclude that small aggregates are formed in 1-dodecanol monolayer, and this aggregation process precedes the formation of larger clusters. The same conclusion follows from the analysis of the dynamic surface pressure of the adsorbed monolayers [25].

The generalised Volmer equation (2.159) is the basis for the theoretic analysis of the behaviour of insoluble monolayers. The equation of state for insoluble monolayers with a bimodal distribution (large clusters and monomers or small aggregates) was derived in [25-27]

$$\Pi = \frac{(RT/n)(A/A_{c\Pi})\beta}{A - \omega_1[1 + \varepsilon((A/A_{c\Pi})\beta - 1)]} - B. \tag{3.12}$$

Here

$$\beta = 1 + \frac{\omega_1(1-\varepsilon)}{A_{c\Pi}} - \frac{\omega_1(1-\varepsilon)}{A}, \text{ or } \beta \cong \frac{A}{A_{c\Pi}}, \tag{3.13}$$

$$A_{c\Pi} = A_c \exp\left(\frac{(\Pi - \Pi_c)\varepsilon\omega_1}{RT}\right), \tag{3.14}$$

where $A = 1/\Gamma$, n is the aggregation number for small aggregates, B is the Volmer constant, $\varepsilon = 1 - \omega_a/n_a\omega_1$, ε is a value (positive or negative) which is much less than unity, $\omega_a/n_a = \omega_{(a)}$ is the area per mole of monomers in a cluster (large aggregates with an aggregation number $n_a >> 1$), $A_c = 1/\Gamma_c$ is the molar area which corresponds to the commencement of phase transition, i.e., at $\Pi = \Pi_c$.

Equation (3.11) is valid for the region $A \leq A_c$. For $A = A_c$, Eq. (3.11) becomes the Volmer equation for small aggregates or monomers (n=1) [25],

$$\Pi = \frac{RT/n}{A - \omega_1} - B \tag{3.15}$$

which is valid within the range $A \geq A_c$.

Theoretical Π *vs* A isotherms are also presented in Fig. 3.5, while the parameters used are listed in Table 3.2.

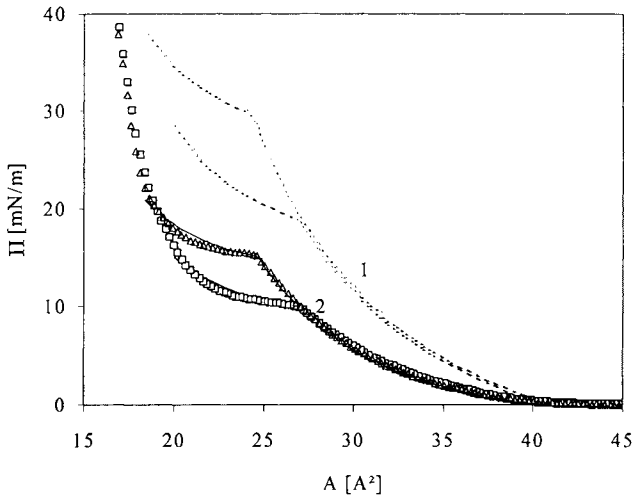

Fig. 3.5. Experimental and theoretical Π-A isotherms for 1-dodecanol at 10°C (□) and 15°C (△), the parameters in Eqs. (3.12)-(3.14) are shown in Table 3.2., curves 1 are for n = 1 and curves 2 for n = 2.

Table 3.2. Parameters of Volmer's model, Eqs. (3.12)-(3.14) for a spread monolayer of 1-dodecanol.

T, °C	10	10	15	15
B, mN/m	9.0	17.0	9.0	17.0
n	2	1	2	1
ω, nm^2/molecule	0.165*	0.165*	0.165*	0.165*
ε	0.1	0.1	0.2	0.2
A_c, nm^2/molecule	0.27*	0.27*	0.25*	0.25*

* The values are underestimated due to the desorption of 1-dodecanol

The curves in Fig. 3.5 show that the model assuming dimerisation (n = 2) for $A \geq A_c$ and a cluster/dimer equilibrium for $A \leq A_c$ leads to a perfect agreement with the experiment. At the same time, the model of gaseous monolayers formed by monomers (n = 1) disagrees with the experimental results in the $A \geq A_c$ region. Moreover, it was shown in [25] that the values of dynamic surface tension for 1-dodecanol adsorption from solution in the range $\Pi < \Pi_c$ agree satisfactorily with the diffusion model, assuming the formation of surface dimers.

Therefore, as the intermolecular Van der Waals interaction in the monolayer of normal alcohols becomes larger with increasing number of methylene groups, different theoretical models should be applied to describe the adsorption: the Langmuir model for $n_C \leq 3$, the Frumkin model for the intermediate n_C values, and aggregation and cluster models for $n_C \geq 10$.

3.3.2. Diols

Diols differ from normal alcohols due to the presence of a second OH group ($C_n(OH)_2$). Data obtained for the 1,4-butanediol in [28] and for 1,8-octanediol, 1,9-nonanediol and 1,10-decanediol in [29] are shown in Fig. 3.6.

The data in Table 3.3 obtained from the Frumkin model parameters for diols show, that the molar area of diols is roughly two times larger than that of the normal alcohols. This means that the two polar OH groups are localised in the surface layer.

The presence of the second polar group leads to a Frumkin constant a which is much lower than that for alcohols. However, the most significant decrease is obtained for the adsorption equilibrium constant b, as demonstrated in Fig. 3.7.

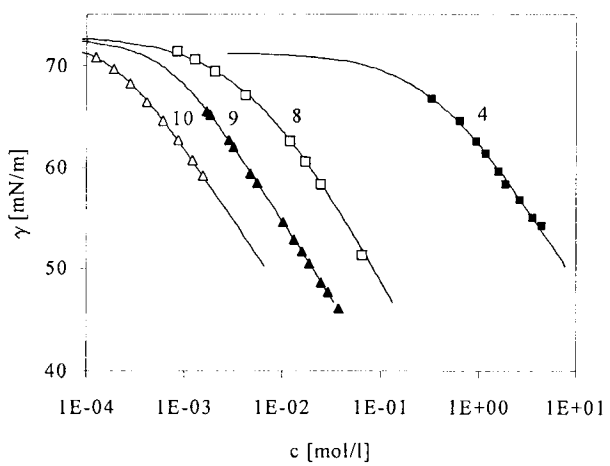

Fig. 3.6. The dependence of equilibrium surface tension on concentration for 1,4-butanediol (data [28], 30°C), and 1,8-octanediol, 1,9-nonanediol and 1,10-decanediol (data [29], 20°C), numbers denote the carbon atoms number, theoretical curves are calculated from Frumkin's model using the parameters listed in Table 3.3.

Table 3.3. Frumkin's model parameters, Eqs. (3.1), (3.2), for diols.

$C_n(OH)_2$	ω_1, 10^5 m^2/mol	a	b, l/mol	ε, %	Ref.
$C_4(OH)_2$	3.76	0.0	2.80	2.9	28
$C_8(OH)_2$	3.67	0.0	$3.06 \cdot 10^2$	3.2	29
$C_9(OH)_2$	3.63	0.8	$6.41 \cdot 10^2$	0.8	29
$C_{10}(OH)_2$	3.80	0.8	$2.29 \cdot 10^3$	1.7	29

The corresponding dependence $b(n_C)$ for normal alcohols is also shown. Both curves have the same slopes, which shows that the increments of b and hence the free energy of adsorption per methylene group $\Delta G^0_{CH_2} = -2.75$ kJ/mol are equal for the two series, while the absolute values of b for the diol molecule is approximately 6 times lower than that for the corresponding normal alcohol molecule with the same alkyl chain length n_C. Therefore, the existence of the second polar OH group leads to a decrease in the absolute value of standard free energy of adsorption for diols as compared with normal alcohols.

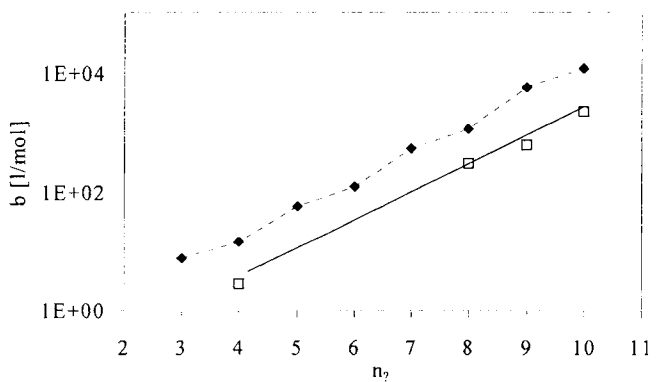

Fig. 3.7. Dependence of the adsorption equilibrium constant b on n_C for the homologous series of diols (□), data for alcohols (◆) are those from Fig. 3.4.

3.3.3. Normal fatty acids

To prevent dissociation in water the studies of fatty acids (C_nO_2H) are performed in a medium of strong acidity (pH = 1), arranged by addition of HCl. The results for some fatty acids in acidic solution obtained in different studies [30-33] are illustrated in Fig. 3.8.

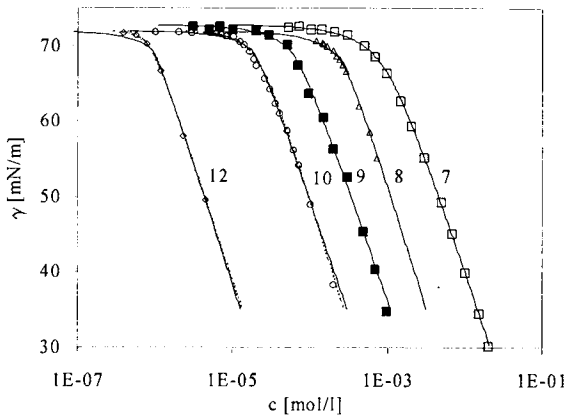

Fig. 3.8. Dependence of equilibrium surface tension on concentration for heptanoic and nonanoic acids ([30], 20°C), octanoic acid ([31], 25°C), decanoic acid ([32], 25°C), and dodecanoic acid ([33], 20°C), numbers denote the number of carbon atoms, the theoretical curves are calculated from the Frumkin (solid line, Table 3.4) and aggregation models (dashed line, Table 3.5), respectively.

Table 3.4. Frumkin's model parameters, Eqs. (3.1), (3.2), obtained for fatty acids.

C_nO_2H	ω_1, 10^5 m^2/mol	a	b, l/mol	ε, %	Ref.
C_7O_2H	1.81	1.06	$3.79 \cdot 10^2$	2.6	30
C_8O_2H	1.71	1.60	$7.89 \cdot 10^2$	2.8	31
C_9O_2H	1.87	1.50	$3.62 \cdot 10^3$	6.2	30
$C_{10}O_2H$	1.86	1.86	$8.16 \cdot 10^3$	4.9	32
$C_{12}O_2H$	1.75	2.0	$1.44 \cdot 10^5$	5.2	33

Table 3.5. Aggregation model parameters, Eqs. (3.8)-(3.10), obtained for fatty acids.

C_nO_2H	ω_1, 10^5 m^2/mol	n	b, l/mol	ε, %	Ref.
C_7O_2H	1.82	1.6	$2.2 \cdot 10^1$	2.0	30
C_8O_2H	1.54	2.2	$1.3 \cdot 10^2$	3.2	31
C_9O_2H	1.58	1.5	$6.93 \cdot 10^1$	6.9	30
$C_{10}O_2H$	1.72	2.3	$1.56 \cdot 10^2$	2.6	32
$C_{12}O_2H$	1.86	4.0	$9.83 \cdot 10^2$	1.9	33

* For all systems $\Gamma_c = 10^{-10}$ mol/m^2

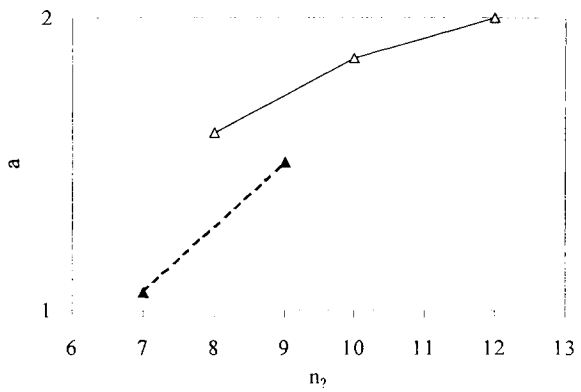

Fig. 3.9. Dependence of the Frumkin constant a on n_C for fatty acids

It is seen from Fig. 3.9 that for lower acids (C_7–C_9) the corresponding theoretical curves are indistinguishable, i.e. both theoretical models provide good description of the adsorption behaviour. However, for decanoic and lauric acids the aggregation model leads to essentially smaller deviation from the experimental data (by a factor of 2 for lauric acid) then the Frumkin model. Similarly to the normal alcohol series, the increase of the Frumkin constant a with n_C takes place, and for even homologues the value of a is essentially higher, cf. Fig. 3.9.

The slope of the dependence $b(n_C)$ for fatty acids is the same as for normal alcohols, i.e. the increments of free energy per CH_2 group for these substances are approximately equal ($\Delta G^0_{CH_2} = -2.88$ kJ/mol). However the values of b for the fatty acids are 1.5 times lower than those for normal alcohols, cf. Fig. 3.10. It follows than that the higher hydrophilicity of the polar group results in a standard free energy of adsorption for fatty acids 1.0 kJ/mol lower as compared with the normal alcohols.

For the dodecanoic acid, in contrast to 1-dodecanol, the aggregation model yields a quite high aggregation number of n = 4, while no indications exist for the formation of larger clusters. Also, no data for spread dodecanoic acid monolayers could be found in literature which exhibit characteristic inflection points in the Π-A isotherm. The dependencies at 15-20 °C usually correspond to the type of gaseous monolayers [34]. Therefore, a certain similarity exists in the behaviour of fatty acids and alcohols, i.e. for a smaller number of methylene groups the system

is better described by the Frumkin model, with increasing number of methylene groups the behaviour of the system becomes more 'aggregation-like'. However, as the solubility of the acids is higher (and therefore the b values are lower) condensation sets in for the acids only at C_{13} [35], but not at C_{12}, which is characteristic to the normal alcohols.

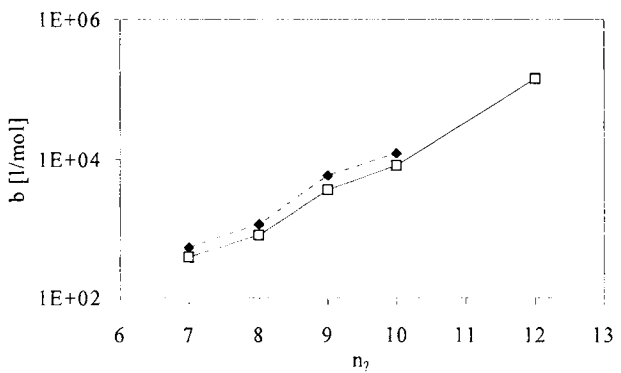

Fig. 3.10. Dependence of adsorption equilibrium constant b on n_C for the fatty acids series (□), data for alcohols (◆) as given in Fig. 3.4.

3.3.4. Alkyl dimethyl phosphine oxides

The surface tension isotherms for alkyl dimethyl phosphine oxides (C_nDMPO) in the interval from C_8 to C_{16} at 25 °C are shown in Fig. 3.11. It should be noted that the experimental data reported in [36] for C_8, C_{10}, C_{12} and C_{14} are in a good agreement with the data presented in [37, 38], and therefore the results for these experimental data are also shown in Fig. 3.11. The parameters of the Frumkin and reorientation models are summarised in Tables 3.6 and 3.7. Both isotherms agree well with the experimental data. Small differences between the calculated isotherms exist only for $n_C \geq 13$, while for lower n_C the curves for the two models perfectly coincide. It follows then that neither of the two models can be preferred if one takes into account only the agreement between the experimental and theoretical data. However, the negative values of the Frumkin constant a for lower homologues, and the unusual shape of this dependence on n_C (cf. Fig. 3.12) indicate that for the Frumkin model the coincidence with the experiment is only formal.

Table 3.6. Frumkin's model parameters, Eqs. (3.1), (3.2), for C_nDMPO.

C_nDMPO	ω_1, 10^5 m^2/mol	a	b, l/mol	ε, %	Ref.
C_8DMPO	2.94	0.0	$2.45 \cdot 10^3$	4.4	36, 37
C_9DMPO	2.80	-0.6	$1.12 \cdot 10^4$	4.3	36
C_{10}DMPO	2.52	-0.22	$2.19 \cdot 10^4$	4.4	36, 37
C_{11}DMPO	2.52	-0.5	$9.72 \cdot 10^4$	11.2	36
C_{12}DMPO	2.44	0.35	$1.5 \cdot 10^5$	5.7	36, 37
C_{13}DMPO	2.32	0.05	$2.32 \cdot 10^5$	11.7	36
C_{14}DMPO	2.52	0.8	$7.63 \cdot 10^5$	7.6	36
C_{15}DMPO	2.71	1.0	$2.91 \cdot 10^6$	5.0	36
C_{16}DMPO	2.42	1.6	$5.45 \cdot 10^6$	5.7	36

Table 3.7. Reorientation model parameters, Eqs. (3.3)-(3.7), for C_nDMPO.

C_nDMPO	ω_1, 10^5 m^2/mol	ω_2, 10^5 m^2/mol	b, l/mol	ε, %	Ref.
C_8DMPO	2.94	2.94	$2.45 \cdot 10^3$	4.4	36, 37
C_9DMPO	4.8	2.67	$4.71 \cdot 10^3$	5.4	36
C_{10}DMPO	5.0	2.28	$1.18 \cdot 10^4$	3.9	36, 37
C_{11}DMPO	7.6	2.68	$7.18 \cdot 10^4$	10.8	36
C_{12}DMPO	12.7	2.38	$1.95 \cdot 10^5$	6.5	36, 37
C_{13}DMPO	13.0	2.37	$7.06 \cdot 10^5$	11.9	36
C_{14}DMPO	14.6	2.39	$2.15 \cdot 10^6$	6.5	36
C_{15}DMPO	16.0	2.52	$1.05 \cdot 10^7$	6.1	36
C_{16}DMPO	17.0	2.16	$1.84 \cdot 10^7$	5.9	36

* For all systems α=0 has been assumed

Negative values of Frumkin's constant, which could be expected for ionic surfactants, cannot be explained for the case of non-ionic surfactants. Usually one obtains negative values when trying to match the Frumkin model to results obtained for surfactants with reorientation in the adsorption layer. This is especially evident for oxyethylated alcohols, where the values obtained are $a = -(5 \div 10)$, as shown below. Another argument in favour of the applicability of the reorientation isotherm is the dynamic surface tension for C_nDMPO solutions, studied in [39]. It is known (see Chapter 4) that, if adsorbed molecules change their orientation in the adsorption layer a higher surface coverage results, and the rate of surface tension decrease for

the diffusion adsorption mechanism becomes essentially higher (provided that the transition between the adsorption states at the surface is not slow). Therefore, reorientation mimics a diffusion controlled adsorption with a strongly increased diffusion coefficient. The data obtained agree the diffusion model and real values of the diffusion coefficient when the reorientation model used with the parameters listed in Table 3.7 [39]. Hence, we can conclude that for higher C_nDMPO homologues the reorientation model is physically consistent.

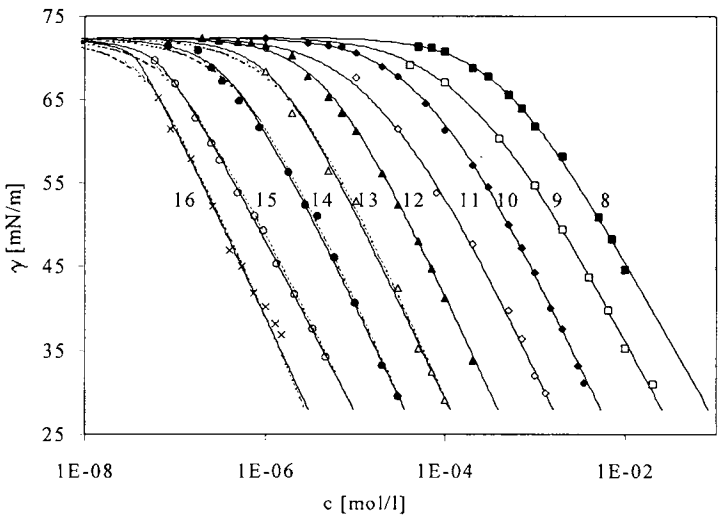

Fig. 3.11. Dependence of equilibrium surface tension on concentration for C_nDMPO solutions, according to [36, 37], numbers denote the carbon atoms number, the theoretical curves are calculated from the Frumkin (solid line, Table 3.6) and reorientation models (dashed line, Table 3.7).

The dependence of molar area for the two states of C_nDMPO molecules on the number of carbon atoms in the hydrocarbon chain is shown in Fig. 3.13. While the minimum area per C_nDMPO mole (or per molecule) ω_2 is almost independent of n_C, the area per mole (or molecule) in the unfolded state ω_1, calculated from the best fit to the experimental data, is increased with the chain length for C_{12} and larger n_C. It is interesting to note that the area per mole C_nDMPO calculated in [36] from the atomic radii and bond lengths for the state with maximum area (see dashed line in Fig. 3.13) agrees well with the data obtained from tensiometry for $n_C > 11$. For lower C_nDMPO homologues the molecule in the unfolded state

cannot exist in the monolayer, which was already discussed in [40]. For lower homologues, exact coincidence is observed between the experimental data obtained from the dynamic surface tension experiments and calculations made for the diffusion theory in absence of any reorientation [39].

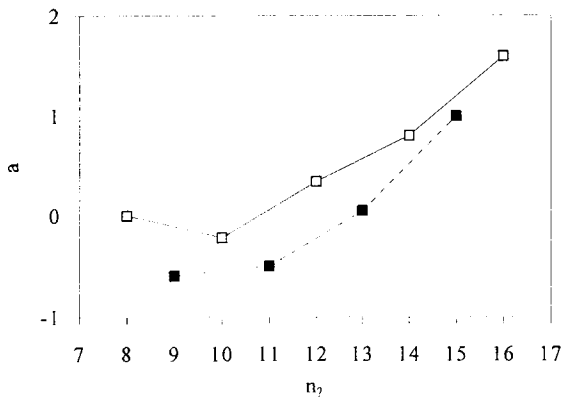

Fig. 3.12. Dependence of Frumkin's constant a on n_C for the homologous series of C_nDMPO.

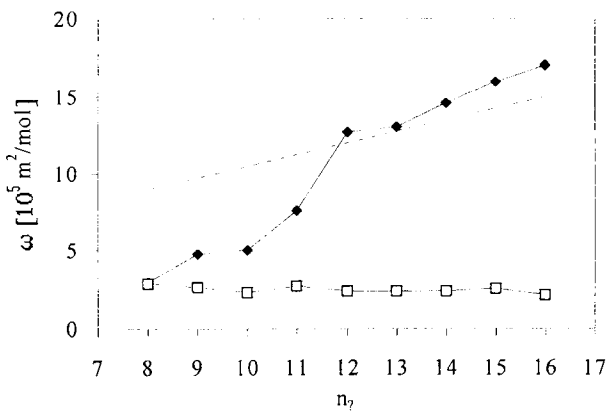

Fig. 3.13. Dependence of molar area in the states 1 (◆) and 2 (□) on the number of carbon atoms n_C for the C_nDMPO, dashed line - values estimated from the molecular geometry.

The dependence b(n_C) calculated from the two models is shown in Fig. 3.14. Here also the data for fatty acids are shown for comparison.

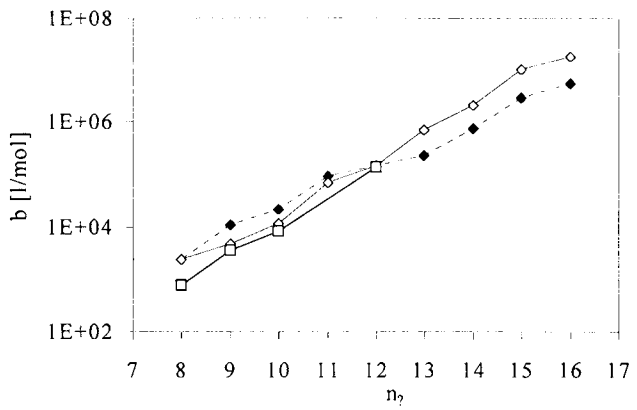

Fig. 3.14. Dependence of the adsorption equilibrium constant b on n_C for C_nDMPO as calculated from the Frumkin (◆) and reorientation (◇) models, (□) - the data for fatty acids reproduced from Fig. 3.10.

The slope of the dependence for the data calculated for the Frumkin isotherm is lower than that for the reorientation model. The increment of the free energy of adsorption calculated from the reorientation model, $\Delta G^0_{CH_2} = -3.0$ kJ/mol, is almost equal to the value obtained for normal alcohols and acids, $\Delta G^0_{CH_2} \cong -2.8$ kJ/mol. The absolute values of the constant b for C_nDMPO at $n_C \leq 10$ are identical to those obtained for the normal alcohols.

3.3.5. Betains

(N-n-R-N,N-dimethylammonio)-acetic acid bromide (C_nBHB) is a typical amphoteric surfactant with the ionic form dependent on the pH of the solution. For pH = 7 the $BHBC_n$ molecules are transformed into betains with the structure [41]:

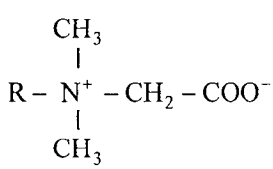

where R is the alkyl radical. Therefore, at this pH the C_nBHB molecule as a whole is electroneutral, and possesses the highest adsorption activity. The surface tension isotherms for C_nBHB solutions at 20°C and pH = 7 as reported in [42] are shown in Fig. 3.15.

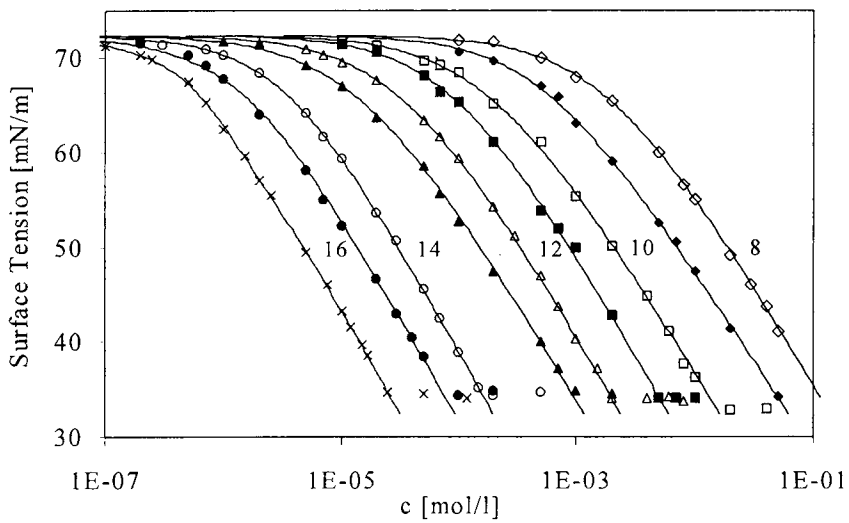

Fig. 3.15. Dependence of equilibrium surface tension on the concentration for C_nBHB solutions (data [42]), numbers denote the carbon atoms number, theoretical curves are calculated from the Frumkin and reorientation model, Table 3.8 and 3.9.

Table 3.8. Frumkin's model parameters, Eqs. (3.1), (3.2), calculated for C_nBHB.

C_nBHB	ω_1, 10^5 m^2/mol	a	b, l/mol	ε, %	c_{cmc}, mol/l	ΔG^0_a, kJ/mol	ΔG^0_m, kJ/mol	$\Delta G^0_{a(m)}$, kJ/mol
C_8BHB	2.69	-0.1	$6.0 \cdot 10^2$	3.1				
C_9BHB	2.98	0.04	$1.89 \cdot 10^3$	3.3				
$C_{10}BHB$	2.78	-0.20	$6.56 \cdot 10^3$	5.2	$1.5 \cdot 10^{-2}$	-31.4	-20.0	-30.6
$C_{11}BHB$	2.62	0.0	$1.12 \cdot 10^4$	4.1	$5.0 \cdot 10^{-3}$	-32.7	-22.8	-32.8
$C_{12}BHB$	2.63	-0.20	$3.49 \cdot 10^4$	2.8	$2.0 \cdot 10^{-3}$	-35.5	-25.0	-35.0
$C_{13}BHB$	2.32	0.15	$7.72 \cdot 10^4$	3.7	$9.3 \cdot 10^{-4}$	-37.4	-26.9	-35.7
$C_{14}BHB$	2.54	0.28	$2.27 \cdot 10^5$	2.5	$1.7 \cdot 10^{-4}$	-40.1	-31.1	-40.8
$C_{15}BHB$	2.90	0.6	$5.49 \cdot 10^5$	4.3	$7.5 \cdot 10^{-5}$	-42.2	-33.1	-44.1
$C_{16}BHB$	2.65	0.75	$1.05 \cdot 10^6$	2.6	$2.6 \cdot 10^{-5}$	-43.8	-35.7	-45.8

Table 3.9. Reorientation model parameters, Eqs. (3.3)-(3.7), calculated for C_nBHB.

C_nBHB	ω_1, 10^5 m^2/mol	ω_2, 10^5 m^2/mol	b, l/mol	ε, %	ΔG^0_a, kJ/mol	$\Delta G^0_{a(m)}$, kJ/mol
C_8BHB	2.70	2.68	$2.79 \cdot 10^2$	3.1		
C_9BHB	2.96	2.95	$9.51 \cdot 10^2$	3.5		
$C_{10}BHB$	3.6	2.60	$3.00 \cdot 10^3$	5.3	-29.5	-30.1
$C_{11}BHB$	3.6	2.27	$5.38 \cdot 10^3$	3.8	-30.9	-31.4
$C_{12}BHB$	8.1	2.58	$2.67 \cdot 10^4$	2.2	-34.8	-34.8
$C_{13}BHB$	9.4	2.74	$7.07 \cdot 10^4$	3.2	-37.2	-37.3
$C_{14}BHB$	13.8	2.52	$2.89 \cdot 10^5$	2.3	-40.6	-40.7
$C_{15}BHB$	14.7	2.64	$7.3 \cdot 10^5$	4.1	-42.9	-43.1
$C_{16}BHB$	17.2	2.51	$1.86 \cdot 10^6$	2.1	-45.2	-45.2

The used Frumkin and reorientation models agree perfectly well with the experimental isotherms. Also the deviations for lower homologues ($n_C < 11$, cf. Tables 3.8 and 3.9) are quite similar. However, for higher homologues the deviation obtained for the reorientation isotherm is smaller, and therefore the reorientation model can be considered to be more adequate for the description of the adsorption behaviour of this group of surfactants. Table 3.8 also lists the critical micellisation concentration (CMC). The two tables show also the free energies of adsorption and micellisation, which however will be discussed further below. The behaviour of C_nBHB in the adsorption layer for $n_C < 12$ is almost ideal (cf. Table 3.8 and Fig. 3.16). For higher homologues the Frumkin constant deviates from zero.

Similar to the alkyl dimethyl phosphine oxides discussed in the previous section, the minimum area ω_2 per mole (molecule) of C_nBHB is almost independent of n_C, while the area ω_1 per mole (molecule) of C_nBHB in the unfolded state, estimated from the best fit to the experimental isotherm, becomes higher with the increasing alkyl chain length for $C_{12}BHB$ and larger molecules in the series (cf. see Fig. 3.17). Therefore, for lower C_nBHB homologues the unfolding of the molecule in the monolayer does not take place. A possible explanation for this result is that the hydrophilic/hydrophobic balance for these lower C_nBHB homologues is shifted towards hydrophilicity. As result, some methylene groups of C_nBHB adjacent to the

polar group are drawn into the water phase due to strong interaction with water, while the limited flexibility of C-C bonds prevents the remaining part of the alkyl chain from laying flat at the solution/air interface. For longer alkyl chains, however, the situation is rather different. The area per mol C_nBHB calculated for $n_C > 13$ in [43] by molecular dynamics for the state characterised by the maximum area (Fig. 3.17, dashed line) agrees well with the surface tension data.

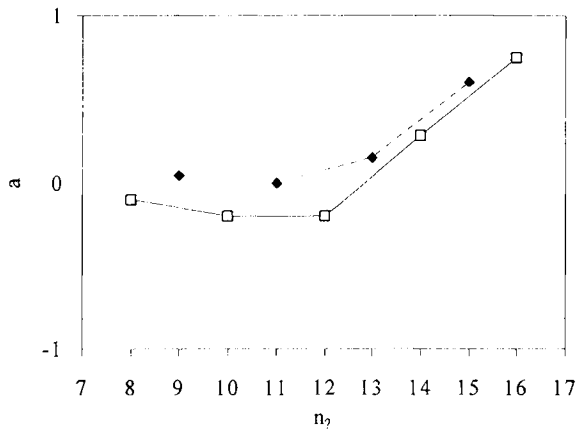

Fig. 3.16. Dependence of Frumkin's constant a as a function of n_C for C_nBHB.

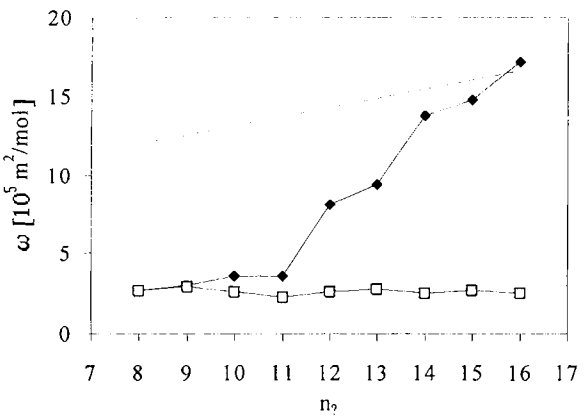

Fig. 3.17. Dependence of molar area in the states 1 (◆) and 2 (□) on n_C for C_nBHB, dashed curve - estimation of the molar area from molecular dynamics.

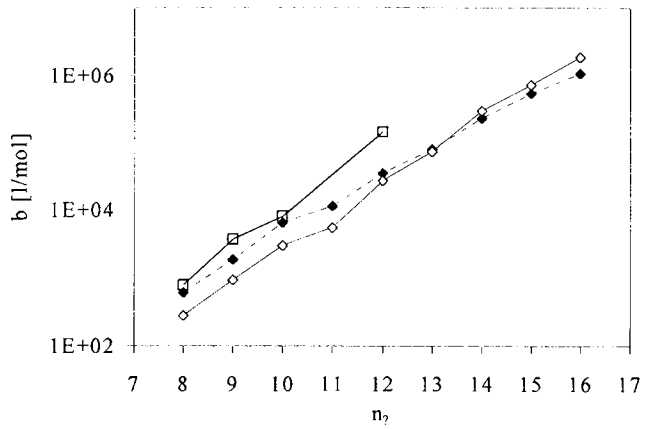

Fig. 3.18. Dependence of adsorption equilibrium constant b on nC for C_nBHB calculated from the Frumkin (◆) and reorientation (◇) models, (□) - data for fatty acids as in Fig. 3.10.

The slope of the dependence b on n_C calculated for the Frumkin isotherm is also lower than that calculated for the reorientation isotherm. The increment of adsorption free energy, calculated from the b values for the reorientation model, $\Delta G^0_{CH_2} = -2.78$ kJ/mol, is almost equal to the value obtained for normal alcohols and fatty acids ($\Delta G^0_{CH_2} \cong -2.8$ kJ/mol), however, the absolute values of b for C_nBHB are 3.7 times lower than the corresponding values for fatty acids, and 5.5 times lower than those for normal alcohols.

It was shown in Chapter 2 that the standard free energy of adsorption ΔG^0 can be calculated from the standard free energy of micellisation ΔG^0_m via the relationship (2.179),

$$\Delta G^0 = \Delta G^0_m - \Pi_{cmc}\omega, \tag{3.16}$$

where $\Pi_{cmc} = \gamma_0 - \gamma_{cmc}$ is the surface pressure of the solution at CMC. In turn, the standard free energy of micellisation can be determined from the CMC as

$$\Delta G^0_m = RT \ln x_{cmc} = RT \ln(c_{cmc}/\rho), \tag{3.17}$$

where $\rho \cong 55.6$. The ΔG^0_m values calculated from the CMC are listed in Table 3.8. Here also the standard free energy of adsorption is shown as calculated in two ways: from the values of b via Eq. (3.11) (denoted by subscript 'a'), and from the CMC and ω values via Eq. (3.16)

(denoted by subscript 'a(m)'). In a similar way, these values were calculated for the reorientation model and summarised in Table 3.9. In Figs. 3.19 and 3.20 we present the dependencies of ΔG^0 and ΔG^0_m on n_C for C_nBHB molecule for the Frumkin and reorientation models, respectively.

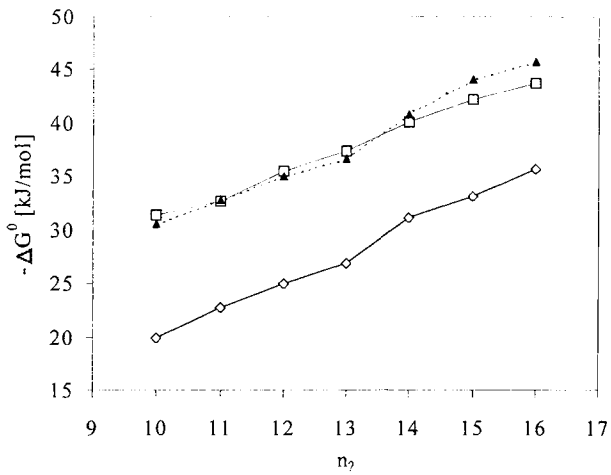

Fig. 3.19. Dependence of ΔG^0_m (◇) and standard free energy of adsorption ΔG^0_a (□) and $\Delta G^0_{a(m)}$ (▲) on n_C for C_nBHB, calculated from the Frumkin model.

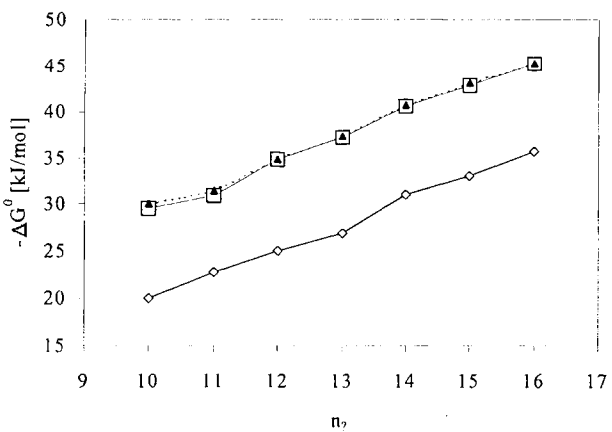

Fig. 3.20. The dependence of ΔG^0_m (◇) and standard free energy of adsorption ΔG^0_a (□) and $\Delta G^0_{a(m)}$ (▲) on n_C for C_nBHB, from the reorientation model.

It is seen that for the Frumkin model, the two methods give somewhat different values of the standard free energy of adsorption, while for the reorientation model the values obtained by these two methods are equal. This fact can be easily explained: equating the ΔG^0 values given by Eqs. (3.11) and (3.16) to each other, one obtains:

$$-RT\ln(b\rho) = RT\ln(c_{cmc}/\rho) - \Pi_{cmc}\omega \,. \tag{3.18}$$

From Eq. (3.18), the usual von Szyszkowski equation follows for the case of very high surfactant concentration, $bc_{cmc} >> 1$,

$$\frac{\Pi_{cmc}\omega}{RT} = \ln(bc_{cmc}) \,. \tag{3.19}$$

Therefore, for the reorientation model the two methods lead to similar values of ΔG^0, because, on the one hand, this model transforms into the ideal (Langmuir – von Szyszkowski) model at high surface pressure, when only one of two possible adsorption states exists, namely that possessing the minimum area, cf. Eq. (3.7). On the other hand, this coincidence also indicates that the CMC and the adsorption characteristics (b and ω_2) calculated from the fitting program, are reliable.

3.3.6. Maleic acid mono[2-(4-alkylpiperazinyl)ethyl esters]

Maleic acid mono[2-(4-alkylpiperazinyl)ethyl esters] (C_nPIP) also are amphoteric surfactants and the ionic form depends on the pH, [44, 45]. Four ionic forms are known, of which the most surface active one is similar to the betain, with two oppositely charged atoms N^+ and O^-. At pH = 6.2 approximately 99.6% of all C_nPIP molecules in solution exist in the betain form, while each of the other two forms, containing one ionised atom (either N^+ or O^-) is represented by 0.2% [45]. The experimental and theoretical surface tension isotherms of C_nPIP solutions at pH = 6.2 and 24°C are presented in Fig. 3.21. The theoretical curves calculated from the Frumkin and reorientation models are essentially the same with similar deviations, and therefore neither model could be preferred. The dependencies of the main parameters on n_C for the two models are shown in Figs. 3.22 – 3.24.

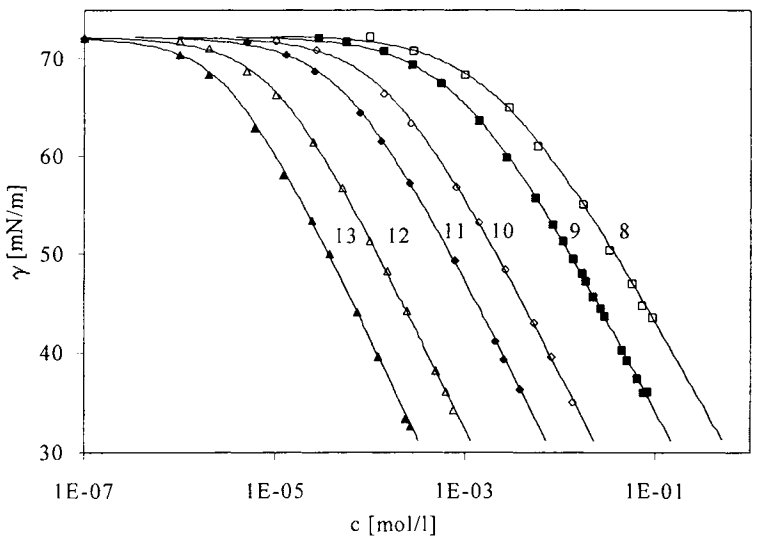

Fig. 3.21. Dependence of equilibrium surface tension on the concentration for C_nPIP solutions, according to [44], numbers denote the alkyl chain length, the theoretical curves are calculated from the Frumkin and reorientation models, Tables 3.10 and 3.11, respectively.

The increments of the adsorption free energy calculated from b for the reorientation model ($\Delta G^0_{CH_2} = -3.2$ kJ/mol) and the Frumkin model ($\Delta G^0_{CH_2} = -2.86$ kJ/mol) are similar to those for normal alcohols and acids ($\Delta G^0_{CH_2} = -2.8$ kJ/mol). The absolute values of b for C_nPIP in both models are 1.7 times lower than those for fatty acids, and 2.5 times lower than the values for normal alcohols.

Table 3.10. Frumkin's model parameters, Eqs. (3.1), (3.2), calculated for C_nPIP.

C_nPIP	ω_1, 10^5 m^2/mol	a	b, l/mol	ε, %
C_8PIP	3.32	-0.5	$7.92 \cdot 10^2$	8.1
C_9PIP	3.12	-0.36	$1.68 \cdot 10^3$	3.8
$C_{10}PIP$	3.09	0.04	$6.82 \cdot 10^3$	4.1
$C_{11}PIP_1$	3.02	0.08	$1.86 \cdot 10^4$	3.2
$C_{12}PIP$	2.95	0.35	$7.99 \cdot 10^4$	4.8
$C_{13}PIP$	2.85	0.52	$2.06 \cdot 10^5$	8.1

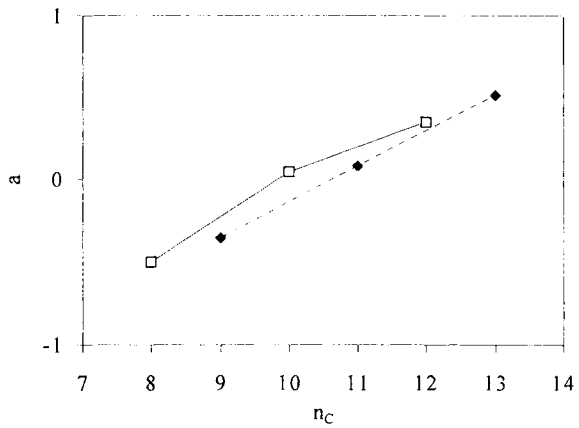

Fig. 3.22. Dependence of the Frumkin constant a on n_C for C_nPIP.

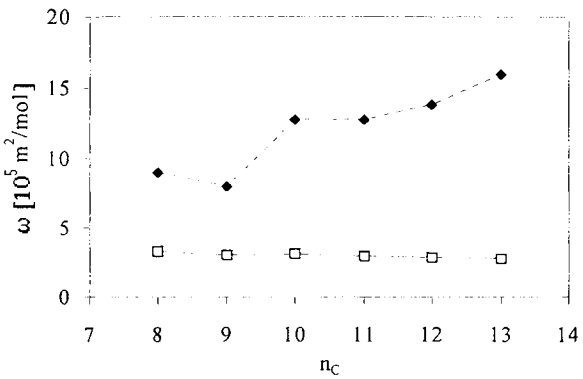

Fig. 3.23. Dependence of molar area in the states 1 (◆) and 2 (□) on n_C for C_nPIP.

Table 3.11. Reorientation model parameters, Eqs. (3.3)-(3.7), calculated for $C_nП$ assuming α=0.

C_nPIP	ω_1, 10^5 m^2/mol	ω_2, 10^5 m^2/mol	b, l/mol	ε, %
C_8PIP	9.0	3.3	$4.81 \cdot 10^2$	8.3
C_9PIP	8.0	3.02	$1.04 \cdot 10^3$	3.4
$C_{10}PIP$	12.7	3.1	$7.06 \cdot 10^3$	4.0
$C_{11}PIP_1$	12.7	3.0	$1.95 \cdot 10^4$	3.1
$C_{12}PIP$	13.8	2.86	$9.96 \cdot 10^4$	4.9
$C_{13}PIP$	16.0	2.75	$2.97 \cdot 10^5$	8.0

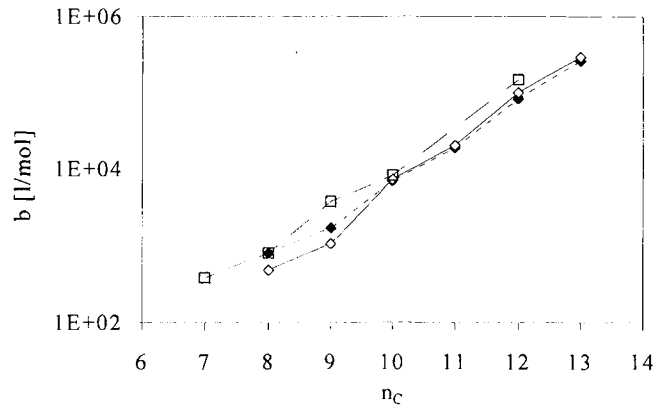

Fig. 3.24. Dependence of adsorption equilibrium constant b on n_C for C_nPIP calculated from the Frumkin (◆) and reorientation (◇) models, data for fatty acids (□) as shown in Fig. 3.10.

3.3.7. Oxyethylated alcohols

Equilibrium surface and interface tension of oxyethylated alcohols (C_nEO_m) was studied by many authors. The values for C_nEO_m with various length of the hydrocarbon (n) and oxyethylene (m) chain were reported in a number of publications [46-55].

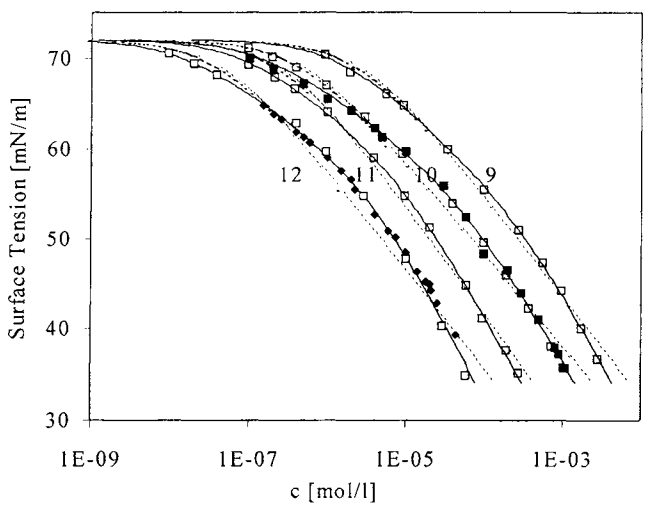

Fig. 3.25. Dependence of equilibrium surface tension on concentration for C_nEO_8 solutions at 25°C with n = 9 – 12, numbers denote the alkyl chain length, (□) - [46]; (△) - [48]; (■) - [49]; (◆) - [50], theoretical curves are calculated from the Langmuir (dashed line) and reorientation models (solid line) using the parameters listed in Tables 3.12 and 3.13, respectively.

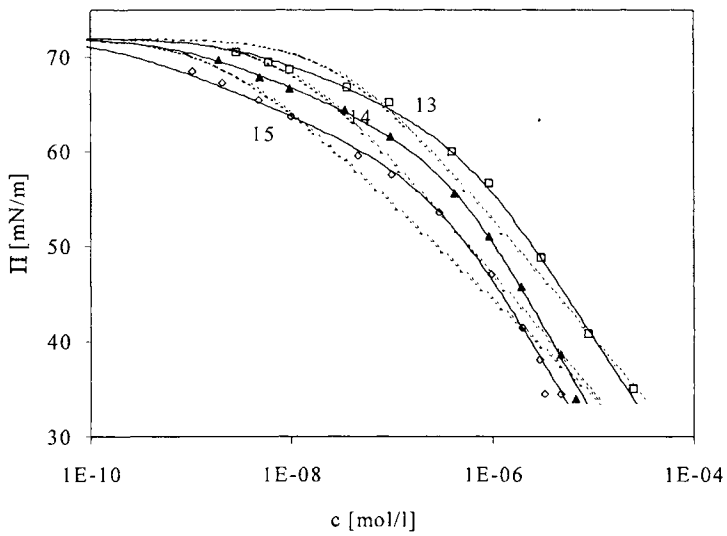

Fig. 3.26. The same as in Fig. 3.25 for n = 13 – 15, according to [46].

Table 3.12. Langmuir model parameters, Eqs. (3.1), (3.2) with a = 0, calculated for C_nEO_m.

C_nEO_m	ω, 10^5 m^2/mol	b, l/mol	ε, %	Ref.
C_9EO_8	5.15	$3.76 \cdot 10^5$	20.5	46
$C_{10}EO_5$	3.78	$4.16 \cdot 10^5$	12.4	51, 52
$C_{10}EO_6$	4.65	$1.27 \cdot 10^6$	21.0	54
$C_{10}EO_8$	5.6	$2.1 \cdot 10^6$	27.3	46, 49
$C_{11}EO_8$	4.8	$3.68 \cdot 10^6$	20.9	46
$C_{12}EO_3$	2.3	$1.94 \cdot 10^6$	2.0	53
$C_{12}EO_4$	2.6	$2.31 \cdot 10^6$	8.6	55
$C_{12}EO_5$	3.44	$4.3 \cdot 10^6$	2.0	51
$C_{12}EO_6$	3.65	$5.3 \cdot 10^6$	13.4	47, 53, 54
$C_{12}EO_8$	4.82	$2.28 \cdot 10^7$	36.2	46, 50, 48
$C_{13}EO_8$	4.56	$3.39 \cdot 10^7$	38.8	46
$C_{14}EO_8$	4.62	$1.05 \cdot 10^8$	49.0	46
$C_{15}EO_8$	5.64	$5.3 \cdot 10^8$	49.0	46

The surface tension isotherms of C_nEO_8 solutions at 25°C in a high range of n from the data presented in [46,48-50] are summarised in Figs. 3.25 and 3.26. For some compounds, the data obtained by various authors are presented; these data are in a quite good mutual agreement. Note that the data given in [48] for $C_{12}EO_8$ are in a satisfactory agreement with those presented in [46, 50] only in the concentration range above $3 \cdot 10^{-6}$ mol/l. For lower concentrations the values measured in [48] (not shown in Fig. 3.25) up to 3 mN/m higher. Possibly the adsorption equilibrium in the experiments [48] was not reached. For example, it was shown in [50], where the bubble shape method was employed, that the time necessary to achieve equilibrium in the solutions for such concentration is $5 \cdot 10^3$ s or more. In Figs. 3.25 and 3.26 also the results for the reorientation and Langmuir models are shown. For some oxyethylated alcohols these calculations were performed earlier in [56]. The model parameters for various oxyethylated alcohols are listed in Tables 3.12 and 3.13.

Considering the data shown in Tables 3.12 and 3.13, one notes the significant difference between the values of ε calculated for the two models: for the Langmuir model these values are 2 to 10 times higher than for the reorientation model. This difference becomes more pronounced with increasing n and m in the C_nEO_m molecule.

A satisfactory agreement with the experiment can also be formally achieved in the framework of the Frumkin model. This, however, results in physically unrealistic values of intermolecular interaction constant for C_nEO_8: $a = -(4 \div 6)$ for the water/air interface, and $a = -10.8$ for the water/hexane interface as shown in [57]. A negative value of the constant a corresponds to a repulsion between adsorbed molecules, which is characteristic to solutions of ionic surfactants, where the parameter a compensates the Coulomb interaction. In these cases, however, the value of this parameter is usually much lower than that estimated for C_nEO_8. We therefore conclude that for the non-ionic surfactant, the Frumkin constant a should be regarded to as a pure fitting parameter, which has no physical meaning.

Comparing the experimental data with the calculated surface tension isotherms one can see that perfect agreement exists between the predictions given by the reorientation model and the experimental results, while the correspondence with the Langmuir model is rather poor.

It is seen from the curves shown in Figs. 3.25 and 3.26 that, with increasing n in the C_nEO_8 molecule the isotherm becomes more and more different from the Langmuir isotherm: a decrease in surface tension becomes apparent already for very low surfactant concentrations.

This tendency is observed also with increasing number oxyethylene groups in the C_nEO_m molecule. The surface pressure isotherms of C_nEO_m solutions for various m at fixed n (n=10 and n=12, respectively) obtained in [46, 47, 49-54] are shown in Figs. 3.27 and 3.28. Here the surface pressure data are used to compare the results of various authors at different temperatures (20 and 25°C).

Table 3.13. Reorientation model parameters, Eqs. (3.3)-(3.7), calculated for C_nEO_m.

C_nEO_m	ω_1, 10^5 m^2/mol	ω_2, 10^5 m^2/mol	α	b, l/mol	ε, %	Ref.
C_9EO_8	7.0	2.8	3.5	$1.53 \cdot 10^4$	3.7	46
$C_{10}EO_5$	6.5	3.2	0.9	$1.92 \cdot 10^5$	9.0	51, 52
$C_{10}EO_6$	8.0	3.52	2.1	$2.92 \cdot 10^5$	6.0	54
$C_{10}EO_8$	10.2	3.94	3.0	$2.77 \cdot 10^5$	12.5	46, 49
$C_{11}EO_8$	9.8	3.7	2.2	$9.33 \cdot 10^5$	3.8	46
$C_{12}EO_3$	4.0	2.0	0.0	$1.09 \cdot 10^6$	1.6	53
$C_{12}EO_4$	6.5	2.15	0.95	$1.18 \cdot 10^6$	3.6	55
$C_{12}EO_5$	4.6	2.96	0.73	$1.79 \cdot 10^6$	2.1	51
$C_{12}EO_6$	5.7	2.97	1.5	$1.81 \cdot 10^6$	10.4	47, 53, 54
$C_{12}EO_8$	10.0	3.42	2.75	$2.34 \cdot 10^6$	8.6	46, 50, 48
$C_{13}EO_8$	13.4	3.46	2.3	$6.78 \cdot 10^6$	6.8	46
$C_{14}EO_8$	13.4	3.0	2.76	$1.18 \cdot 10^7$	4.2	46
$C_{15}EO_8$	13.0	3.2	3.45	$2.50 \cdot 10^7$	7.8	46

It is seen from these dependencies that, with the increase of m, the onset of surface tension decrease (or the surface pressure increase) corresponds to lower surfactant concentrations; at the same time, the decrease of the isotherm slope at high concentrations takes place. The increase of surface activity with the increase of m for low pressure in the framework of reorientation model can be qualitatively explained by strong increase of the molar area of C_nEO_m molecule in the state 1 (ω_1), while the decrease of the isotherm slope (and also the decrease of surface activity) at high concentrations can be ascribed to slight increase of the ω_2 value. Therefore, the intersection of the isotherms which is observed for the oxyethylated alcohols with different m values is the consequence of the fact that these two molar areas are increased with the increase of m, but the rate of this increase is different for ω_2 and ω_2 values. In Figs. 3.29 and 3.30 which are plotted using the data listed in Tables 3.12 and 3.13, the

dependence of the reorientation isotherm parameters on n and m is illustrated. A certain dependence exists of the reorientation isotherm parameters on the length of the ether molecule hydrocarbon chain, which cannot be attributed to the experimental or calculation errors. It is essential to note that the parameter α, which characterises the extra adsorption activity of the molecule existing in the unfolded state, that is, solely the effect of the oxyethylene chain EO_8, is almost independent of the hydrocarbon chain length.

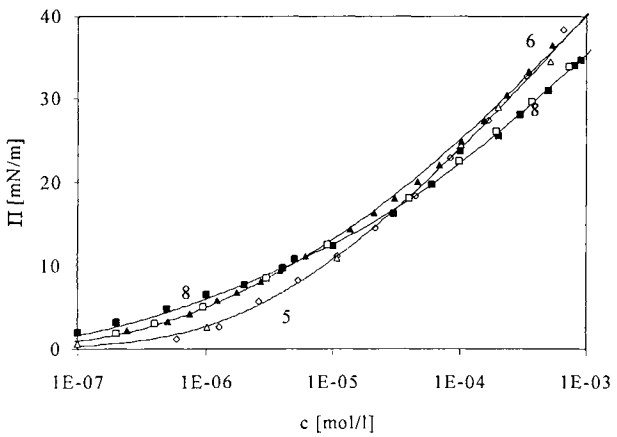

Fig. 3.27. Dependence of equilibrium surface pressure on the concentration of $C_{10}EO_m$ for different m: m = 8, (□), data [46], 25°C; (■), data [49], 25°C; m = 6, (▲), data [54], 25°C; m=5, (◇), data [52], 20°C; (△), data [51], 20°C. Theoretical curves were calculated from the reorientation model, see Table 13.

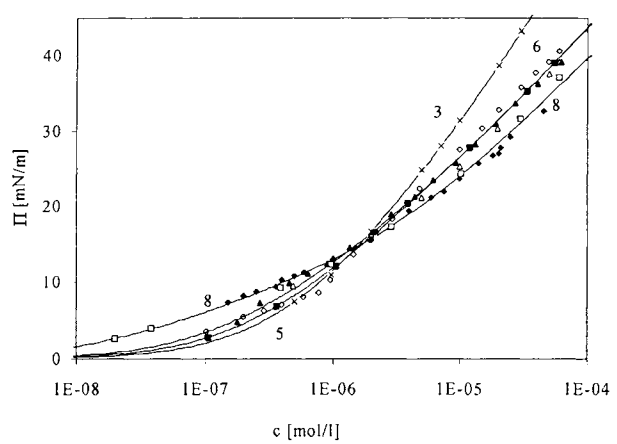

Fig. 3.28. The same as in Fig. 3.27 for $C_{12}EO_m$ with different m: m = 8: (□) - [46], 25°C; (◆) - [50], 25°C; m = 6: (△) - [53], 20°C; (◇) - [47], 25°C; (▲) - [54], 25°C; m = 5: (■) - [51], 20°C; m = 3: (×) - [53], 20°C.

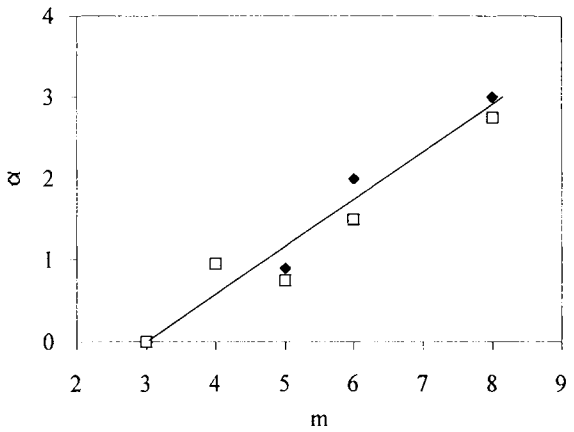

Fig. 3.29. Dependence of the parameter α on the oxyethylene groups number m in the C_nEO_m molecule: (□) - n=12; (◆) - n=10.

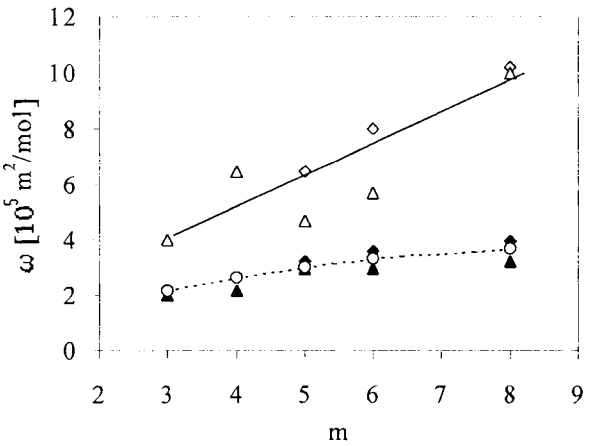

Fig. 3.30. Dependence of molar area in states 1 (△,◇) and 2 (▲,◆) on the number of oxyethylene groups m in the C_nEO_m molecule for n = 10 (◇, ◆) and n=12 (△, ▲). The values of ω obtained in [14] by neutron reflection method for $C_{10}EO_m$ at CMC are denoted as (○) and shown by dashed line.

For the solution/water interface the value of this parameter is ca. 3.0, while the adsorption behaviour in the homologous series of betains and dimethyl alkyl phosphine oxides (as was already mentioned above) is well described by the two-states model with $\alpha = 0$. The

dependence of α on m plotted in Fig. 3.29 clearly shows that this is the presence of the oxyethylene groups which leads to the increase of the surface activity in state 1. It is seen that, with the increase of m from 3 to 8, the parameter α increases from 0 to 3. At the same time, the variation of the methylene groups in the C_nEO_m molecule affects this tendency only slightly. Figure 3.30 shows the dependence of molar areas ω_1 and ω_2 on m.

The increase of m leads to an increase in both ω_1 and ω_2. However, the increase of ω_2 is relatively low, by approximately 70% for the increase of m from 3 to 8, at the same time, the value of ω_1 becomes 2.5 times higher. Perfect agreement is noted between the ω_2 values obtained from the isotherms with the values ω_{cmc} for $C_{10}EO_m$ obtained by neutron reflection [14]. At large surface pressure, the state 1 (that with the maximum molar area) disappears according to Eq. (3.7), as

$$\exp\left[-\frac{\Pi_{cmc}(\omega_1-\omega_2)}{RT}\right]\cong 0. \qquad (3.20)$$

The dependence of adsorptions in states 1 and 2 for $C_{10}EO_8$ is shown in Fig. 3.31 as an example.

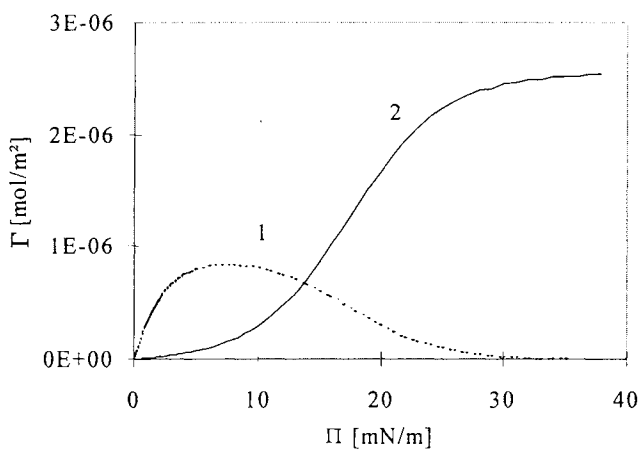

Fig. 3.31. Dependencies of the adsorption in the state 1 (curve 1) and 2 (curve 2) on the surface pressure.

For surface pressures > 30 mN/m the adsorption layer consists of molecules only in the state with minimum molar area ω_2. Therefore, physically the ω_{cmc} is identical to the quantity ω_2. Perfect agreement between the molar areas calculated from the reorientation model and measured by neutron reflection strongly supports the proposed theory. Note that for the Langmuir model the ω values are approximately 1.5 times higher than the ω_2 values obtained for the reorientation model, cf. Tables 3.12 and 3.13. Also, the attempt to describe the surface tension isotherms of C_nEO_m solutions in the framework of the Frumkin model leads not only to unexplainably high negative values of a, but to the ω values which are 1.5 times lower than the ω_2 value obtained in the reorientation model. Therefore, the Langmuir and Frumkin models disagree with the neutron reflection data.

The significant increase in ω_1 with increasing m is caused by the localisation of the oxyethylene chain in the surface layer. This result which is implied by the reorientation model also agrees with the neutron reflection data. It was shown in [14] that, with the increase of the area per C_nEO_m molecule in the adsorption layer, i.e., with surface pressure decrease, the thickness of the layer occupied by the oxyethylene groups of C_nEO_m becomes lower. At the same time, a decrease in the tilt angle of the oxyethylene groups to the interface is observed. These results were discussed in [14] in the context of the adsorption of oxyethylene groups in the non-saturated adsorption layer of oxyethylated alcohols. The dependence of molar areas in the two states on n is shown in Fig. 3.32.

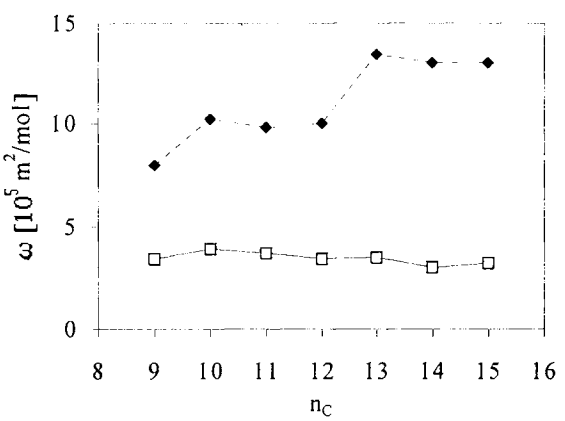

Fig. 3.32. Dependence of molar area in states 1 (◆) and 2 (□) on n_C for C_nEO_8.

It is seen that the ω_2 value remains almost unchanged with increasing n. This feature is characteristic also for other homologous series of non-ionic surfactants. The quite small (as compared with the alkyl dimethyl phosphine oxides or betains) increase of ω_1 with n is due to the fact that the main contribution to ω_1 comes from the oxyethylene groups.

We compare now the adsorption behaviour of oxyethylated alcohols (with $C_{10}EO_8$ as an example) at the water/air and water/hexane interfaces, with reference to the data reported in [57]. The experimental and theoretic isotherms at the water/hexane interface are shown in Fig. 3.33. It was mentioned above that the experimental data agree satisfactorily with the Frumkin model for a physically unrealistic value of $a = -10.8$. Comparing the reorientation model parameters for $C_{10}EO_8$ at the two interfaces (cf. Fig. 3.33 and Table 3.13), one can see that the molar areas are almost the same, while the value of α for the water/hexane interface is 2.5 times higher than that for the water/air interface. Thus the adsorption activity of the oxyethylene groups at the water/hexane interface is significantly higher than that at the water/air interface.

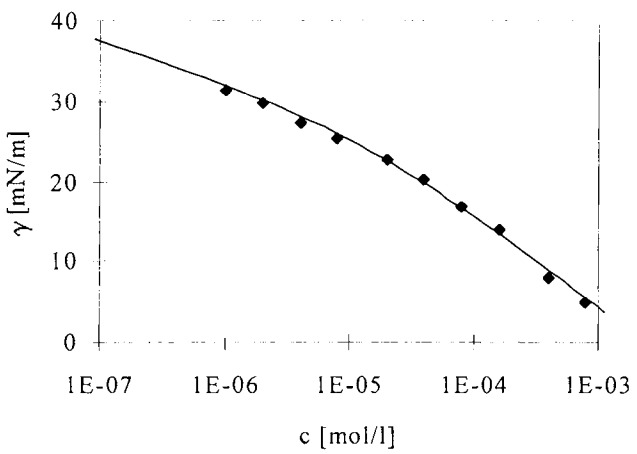

Fig. 3.33. Surface tension isotherm for $C_{10}EO_8$ at water/hexane interface, solid line – reorientation model for two states ($\omega_2 = 4.0 \cdot 10^5$ m^2/mol, $\omega_1 = 1.1 \cdot 10^6$ m^2/mol, $\alpha = 7.5$, b=$2.25 \cdot 10^6$ l/mol).

This result also agrees with the fact that the adsorption equilibrium constant b for $C_{10}EO_8$ at the water/hexane interface is higher than that at the water/air interface. For the water/air interface,

$b = 2.77 \cdot 10^5$ l/mol, while for the water/hexane interface the value is $b = 2.25 \cdot 10^6$ l/mol, i.e. almost 10 times higher. The increase of the constant α results in an earlier (i.e., at lower Π) saturation of surface layer and later desorption of molecules in the state with a maximum molar area as compared with the adsorption process at the solution/air interface [57].

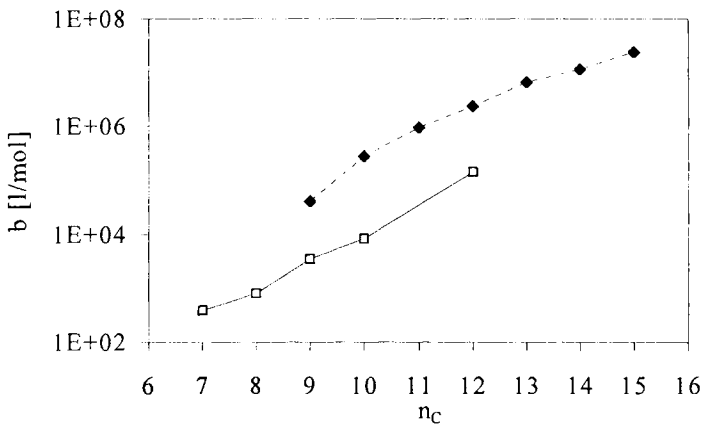

Fig. 3.34. Dependence of adsorption equilibrium constant b on n_C for C_nEO_8, calculated from the reorientation model (◆); (□) – data for fatty acids from Fig. 3.10.

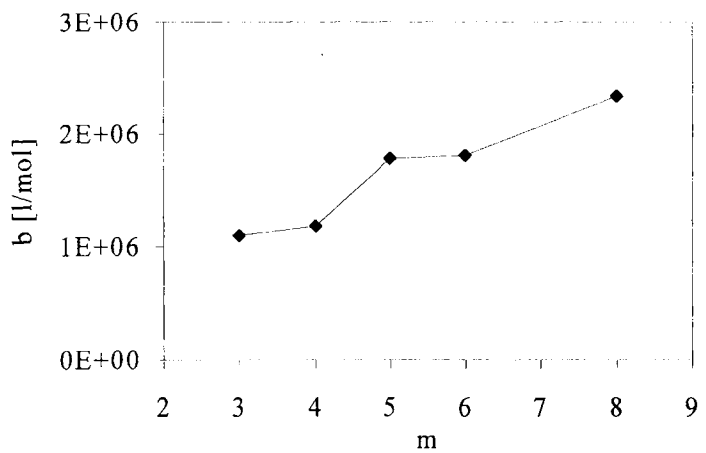

Fig. 3.35. Dependence of adsorption equilibrium constant b on m for $C_{12}EO_m$, calculated from the reorientation model (◆).

To summarise, the experimental interfacial tension isotherms of $C_{10}EO_8$ at the solution/air and solution/hexane interfaces exhibit perfect agreement with the reorientation models. The presence of the hexane phase results not only in an increase of the adsorption activity of the $C_{10}EO_8$ molecule as a whole, but also in a significant increase in the adsorption activity of the oxyethylene chain. This effect is explained by an additional (as compared with the water/air interface) decrease of the free energy of the system due to the interaction of the EO-groups with the hexane molecules. The dependencies of the adsorption equilibrium constant b on n_C for C_nEO_8 and on m for $C_{12}EO_m$ at water/air interface are shown in Figs. 3.34 and 3.35, respectively.

The surface activity of oxyethylated alcohols is much higher than that of fatty acids. This is caused by the additional contribution of the oxyethylene groups. This contribution, however, becomes lower with the increase of n_C, as one can see in Fig. 3.34. For example, for $n_C = 9 \div 11$ the presence of the EO_8 group is roughly equivalent to the elongation of the hydrocarbon chain by 2-3 methylene groups, while for $n_C = 15 \div 16$ this effect becomes almost non-perceivable. The increment of standard free energy of C_nEO_8 adsorption ($\Delta G^0_{CH_2} = -2.86$ kJ/mol) is almost identical to the value obtained for normal alcohols and fatty acids ($\Delta G^0_{CH_2} \cong -2.8$ kJ/mol). The increase in the number of EO groups leads to an increase in b (cf. Fig. 3.35). This fact is in agreement with the concept of partial hydrophobicity of the oxyethylene groups.

Similarly to the situation with other surfactants, additional support for the reorientation model for C_nEO_m yield the dynamic surface tensions. The two-state model agrees well with the experimental data for $C_{10}EO_8$ at the water/air and water/hexane interfaces [57], predicting a faster (as compared to the Langmuir model) kinetics of the surface tension decrease in the short time range for the diffusion adsorption mechanism.

3.3.8. Tritons

The adsorption behaviour of polyethylene glycol octylphenyl ethers (Tritons X-45, X-100, X-165 and X-305) is similar to that of the oxyethylated alcohols. The experimental data [58-62] and the results of the calculations according to the Frumkin and reorientation models are presented in Figs. 3.36, 3.37 and Tables 3.14 and 3.15.

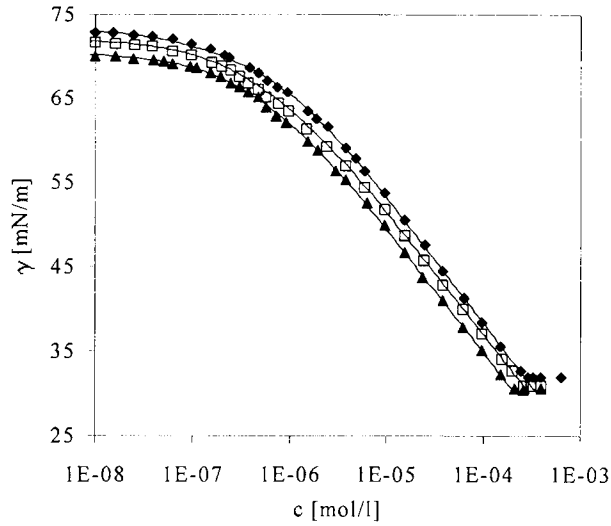

Fig. 3.36. The dependence of equilibrium surface tension on the concentration of Triton X-100 solution at: 15°C (◆); 25°C (□) and 35°C (▲), according to [59], theoretical curves calculated from the reorientation model using the parameters listed in Table 3.15.

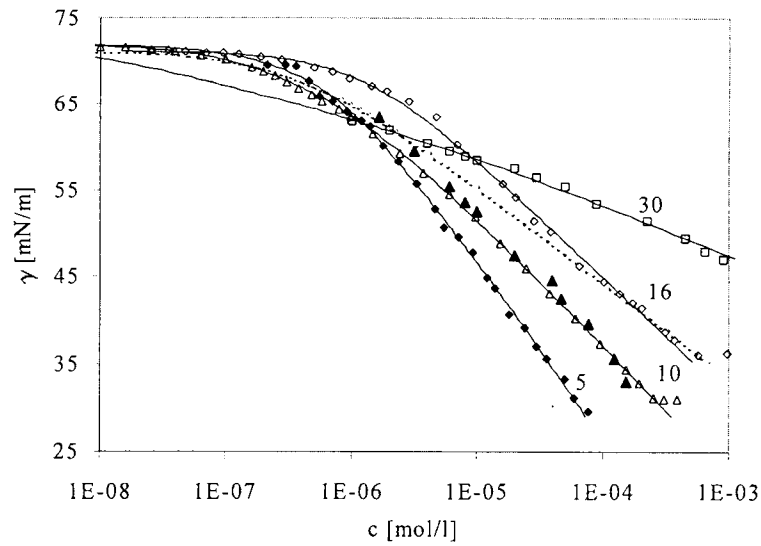

Fig. 3.37. Dependence of equilibrium surface tension on the Tritons solutions concentration: (◆), X-45, data [60,61], 25°C; (△), X-100, data [59], 25°C; (▲), data [58, 60, 61], 25°C; (◇), X-165, data [62], 30°C; (□), X-305, data [60, 61], 25°C, theoretical curves calculated from the reorientation model using the parameters listed in Table 3.15, dashed line shows the calculations according to data [62] at high concentrations.

Table 3.14. Frumkin's model parameters, Eqs. (3.1), (3.2), for Tritons.

Tritons	°C	ω_1, 10^5 m^2/mol	a	b, l/mol	ε, %	Ref.
X-45	25	2.8	0.4	$1.14 \cdot 10^6$	5.0	60, 61
X-100	15	3.47	-0.98	$4.16 \cdot 10^6$	6.2	59
	25	3.87	-0.48	$3.74 \cdot 10^6$	1.0	58 - 61
	35	3.98	-0.3	$3.27 \cdot 10^6$	3.3	59
X-165*	30	5.27	0.0	$2.71 \cdot 10^6$	4.4	62
X-165	30	4.23	0.4	$5.4 \cdot 10^5$	9.7	62
X-305	25	10.9	0.0	$3.85 \cdot 10^7$	15.2	60, 61

* Without results for concentrations < 10^{-5} mol/l

Table 3.15. Reorientation model parameters, Eqs. (3.3)-(3.7), for Tritons.

Tritons	°C	ω_1, 10^5 m^2/mol	ω_2, 10^5 m^2/mol	α	b, l/mol	ε,%	Ref.
X-45	25	15.0	2.75	0.0	$1.57 \cdot 10^6$	5.4	60, 61
X-100	15	15.6	3.67	0.98	$2.08 \cdot 10^6$	5.5	59
	25	11.8	3.96	0.2	$2.39 \cdot 10^6$	1.0	58 - 61
	35	12.6	3.99	0.0	$2.46 \cdot 10^6$	3.3	59
X-165*	30	20.0	5.25	0.0	$2.63 \cdot 10^6$	4.5	62
X-165	30	23.0	4.08	0.0	$7.0 \cdot 10^5$	10.3	62
X-305	25	20.0	9.8	4.0	$1.64 \cdot 10^7$	10.5	60, 61

* Without results for concentrations < 10^{-5} mol/l

Similarly to the oxyethylated alcohols, the adsorption behaviour of Tritons agrees better with the two-state model. It is seen from the analysis of the experimental results reported in [62] that only in the high concentration range (dashed line in Fig. 3.37) the results are consistent with those obtained for the Tritons with other degrees of oxethylation, cf. Tables 3.14 and 3.15. Higher surface tension values exhibited by Triton X-165 for the concentration below $5 \cdot 10^{-5}$ mol/l can be possibly ascribed to the lack of adsorption equilibrium in the experiments [62]. Similar results were obtained in [62] also for Triton X-100 (not shown in Fig. 3.37). We do not believe that the data listed in Table 3.15 are sufficient to make unambiguous

conclusions about the trends in the variations of adsorption isotherm parameters with the variation of m value in the Triton series. Here only certain increase in molar areas (especially significant in the state 2) with the m increase could be definitely noted.

The dynamic surface tension studies of Tritons indicate that the surface tension decrease in the short time range is faster (as compared with the usual diffusion models) [60,61]. This fact supports the conclusion about the existence of a reorientation process for Tritons at the surface. Similarly to the C_nEO_m, in the homologous series of Tritons the b value also increases with the m (cf. Fig. 3.38). This again supports the hydrophilic-hydrophobic character of the EO groups.

From the temperature dependence of the adsorption equilibrium constant b (cf. Table 3.15), one can estimate the thermodynamic characteristics of Triton X-100 adsorption at the water/air interface. In particular, the ΔG^0 values can be calculated at various temperatures using Eq. (3.11), and then estimate the standard enthalpy (ΔH^0) and standard entropy of adsorption (ΔS^0) via Eqs. (2.180) and (2.181).

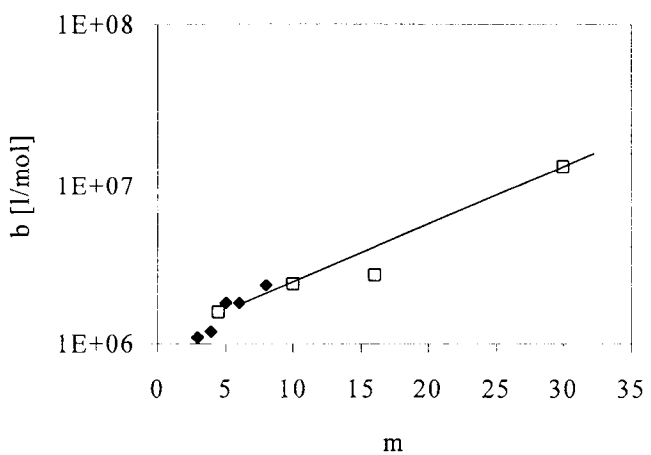

Fig. 3.38. Dependence of the adsorption equilibrium constant b on the oxyethylene groups number m in the molecules: (□), Tritons; and (◆), $C_{12}EO_m$.

The calculations with Eq. (3.11) show that, with the temperature increase from 15 to 35°C, ΔG^0 for Triton X-100 varies from −44.4 kJ/mol to −48.0 kJ/mol. According to Eq. (2.181), this leads to a negative standard enthalpy of adsorption, $\Delta H^0 = -7.2$ kJ/mol, and Eq. (1.180) yields therefore a positive variation of the system entropy during the adsorption, $\Delta S^0 = 130$ J/(mol·K),

or $T\Delta S^0 = 39$ kJ/mol. These results are consistent with the data obtained for other surfactants (cf. Section 2.10), and indicate that the adsorption of surfactants at the water/air interface is a mainly entropy-driven process.

3.3.9. Crown ethers

In contrast to the C_nEO_6 molecule which contains a linear oxyethylene chain, the crown ether molecule possesses a closed crown ring as shown schematically here:

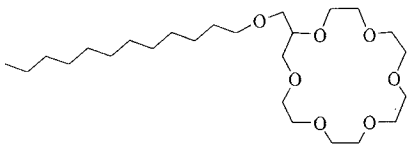

In Fig. 3.39 the surface tension isotherms [47] for the aqueous solutions of the linear ether $C_{12}EO_6$, and the crown ether $C_{12}H_{25}OCH_2$-18-crown-6 (C_{12}-OM-crown) in water and in 0.01 M KCl are shown. One can see that the difference in the structure of the ether group results in a significant difference in the adsorption behaviour of the C_{12}-OM-crown as compared with $C_{12}EO_6$. Note that the adsorption activity of the C_{12}-OM-crown ether at low concentration is significantly lower than that of $C_{12}EO_6$. It was mentioned above that the increased activity of $C_{12}EO_6$ at low concentrations can be explained by the reorientation and adsorption of the oxyethylene group at the solution/fluid interface.

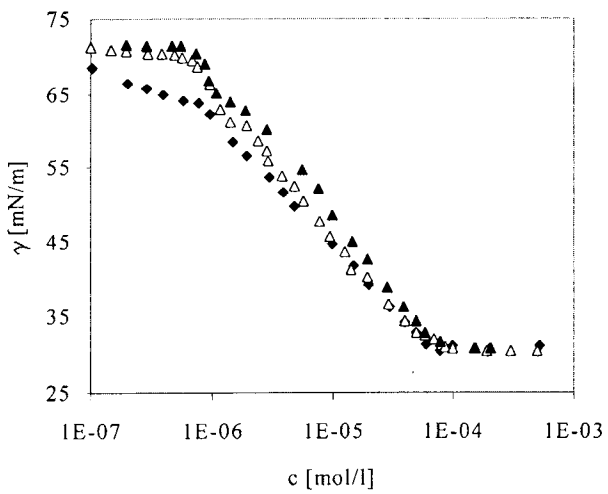

Fig. 3.39 Surface tension isotherms for aqueous solutions of linear ether $C_{12}EO_6$ (◆) and crown ether C_{12}-OM-crown in water (△) and 0.01 M KCl (▲), according to [47]

For the crown ether, the reorientation of the oxyethylene group in the monolayer is quite impossible. As the oxyethylene ring plane of the adsorbed crown ether molecule is located approximately perpendicular to the interface (which follows from the estimation of the area occupied by the crown ether molecule in a monolayer [47, 63]), strong interaction between the ether rings can arise due to the formation of hydrogen bonds. This can result in an aggregation of the C_{12}-OM-crown molecules both in the solution bulk and at the surface. The fact that a slight decrease of the surface tension at concentrations $< 10^{-6}$ mol/l was observed, could be indicative of the formation of small aggregates at the interface. However, the most interesting phenomenon in this regard is the existence of the inflection point in the surface tension isotherms of the crown ether at a concentration just above 10^{-6} mol/l. Similar inflection points were observed for C_{12}-OM-crown at KCl concentrations of 0.1, 0.2, 0.4 and 1.0 M [47]. The experimental dependencies for C_{12}-OM-crown at 0.0 and 0.01 M KCl are presented in Fig. 3.40, along with the results of the calculations using Eqs. (3.8) – (3.10) [57].

It is seen that the theoretical results are in excellent agreement with the experimental data. Table 3.16 summarises the values of parameters calculated in the two concentration regions - below (region 1) and above (region 2) the critical point.

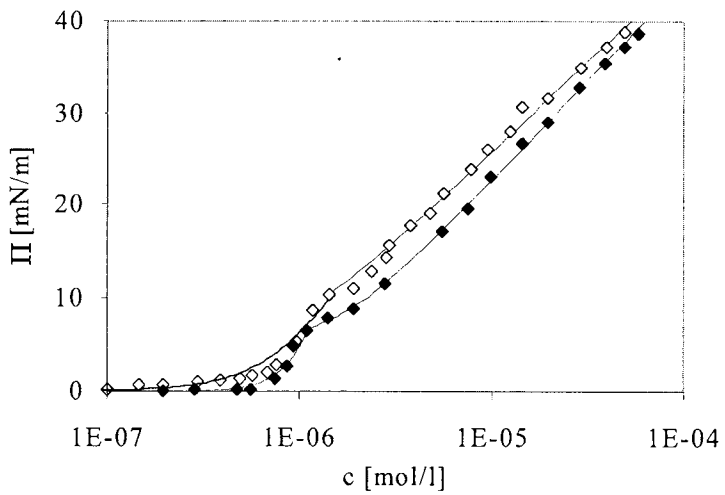

Fig. 3.40 Experimental [47] and theoretical surface pressure isotherms for the C_{12}-OM-crown solution without (◇) and with 0.1 M KCl (◆), model parameters are listed in Table 3.16.

Table 3.16. Parameters obtained from fitting the aggregation model to the surface tension data for C_{12}-OM-crown (Eqs. (3.8) – (3.10)).

c_{KCl}, mol/l	Region	ω_1, m²/mol	Γ_c, mol/m²	n
0.0	1	$1.5 \cdot 10^5$	$1 \cdot 10^{-10}$	2
0.0	2	$2.9 \cdot 10^5$	$2 \cdot 10^{-6}$	>50
0.01	1	$1 \cdot 10^5$	$1 \cdot 10^{-10}$	3-4
0.01	2	$2.7 \cdot 10^5$	$1.9 \cdot 10^{-6}$	>50

Analysing these results, one can see that in region 1 the monolayer is comprised mainly either of dimers (if no salt was added to the solution), or of tri- and quadrumers, at a salt concentration of 0.01 M. In both cases the behaviour is the consequence of the very small critical adsorption ($\Gamma_c = 10^{-10}$ mol/m²). For the same solutions in region 2 there is equilibrium between dimers (which possess an area per aggregate of ca. 0.5 nm² or $2.9 \cdot 10^5$ m²/mol), and large clusters. In fact, the critical adsorption of aggregates in region 2 ($\Gamma_c = 2.0 \cdot 10^{-6}$ mol/m²) is equal to the adsorption of small aggregates before the critical point, that is, the two portions of the theoretical curve presented in Fig. 3.40 are mutually consistent.

3.4. Ionic surfactants

It was shown in Chapter 2 that the theoretical models defined by Eqs. (3.1)-(3.10) can be used also to describe the behaviour of the solutions of ionic surfactant RX in absence and presence of inorganic electrolyte XY. In this case, the Frumkin constant, in addition to the Van der Waals interaction, involves also the inter-ion interaction in the surface layer. Now instead of the concentration c the corresponding adsorption isotherms should be a function of the mean ionic products $c^* = f_\pm \cdot (c_{RX+XY} \cdot c_{RX})^{1/2}$, where $f_\pm$ is the average activity coefficient of ions in the solution bulk. An equation accurately representing measured values of $f_\pm$ is the Debye-Hückel euqation corrected for short-range interactions

$$\log f_\pm = -\frac{0.5115\sqrt{I}}{1+1.316\sqrt{I}} + 0.055I . \qquad (3.21)$$

Here I is the ionic strength in mol/l and the numerical constants correspond to 25°C [64]. The dissociation of the surfactant results in a variation in the number of adsorbed particles, thus

affecting the localisation of the dividing surface. It was shown in the previous chapter that the simplest convention is to choose $\omega = 2\omega_0$, where the factor of 2 represents the dissociation into 2 ions. This corresponds to a constant total amount of surface excess, as in the nonionic case, but now we have $\Gamma_0 + \Gamma_j + \Gamma_k = 1/\omega_0 = 2/\omega_{jk}$. Therefore, for ionic surfactants Eq. (3.1) reads:

$$-\frac{\Pi\omega}{2RT} = \ln(1-\theta) + a\theta^2. \qquad (3.22)$$

In the equations for non-ionic surfactants the choice of the dividing surface was made according to the condition $\omega = \omega_0$. Therefore, omitting the factor of 2 in the right hand side of Eqs. (3.3) and (3.8) we imply that ω is in fact $\omega/2$, and the molar area of a surface active ion. In the tables below, for ionic surfactants the values of molar area of a surface active ion are listed which follow from the IsoFit program with implementation of Eqs. (3.1)-(3.10). To distinguish between the molar area of an ion and the molar area of the surfactant, the former will be denoted by ω_I. To obtain the molar area of an ionic surfactant, the value should be doubled.

3.4.1. Sodium salts of fatty acids (Soaps)

Surface tension isotherms for some sodium salts of fatty acids (C_nO_2Na) are shown in Fig. 3.41: sodium decanoate (n=10), laurate (n=12) and myristate (n=14). Here the experimental data of [33, 65] are presented, where NaOH [65] or NaOH + $NaHCO_3$ [33] were added to the solutions of C_nO_2Na to prevent the solutions from hydrolysis. In both cases the concentration of added sodium ions was 0.1 M. This counterion concentration was introduced in the calculations of the average ionic product as $c^* = f_\pm \cdot (c_{RX+XY} \cdot c_{RX})^{1/2}$.

The experimental isotherms are in perfect agreement with the Frumkin model. Note that a increases with n_c as expected However, as compared with fatty acids (cf. Table 3.4) the values of a for soaps are by a factor of 0.5-0.6 lower than the values for the corresponding acids. This is possibly due to the Coulomb interaction of likely charged ions. The molar areas of surface active ions in soaps ω_I remain almost unchanged in the n_C range between 10 and 14, being approximately 1.5 times lower than the corresponding ω values for fatty acids (cf. Table 3.4). To recalculate the ω_I value given in Table 3.17 to an electroneutral molecule it has to be doubled, which yields $\omega = 2.6 \cdot 10^5$ m^2/mol for C_nO_2Na.

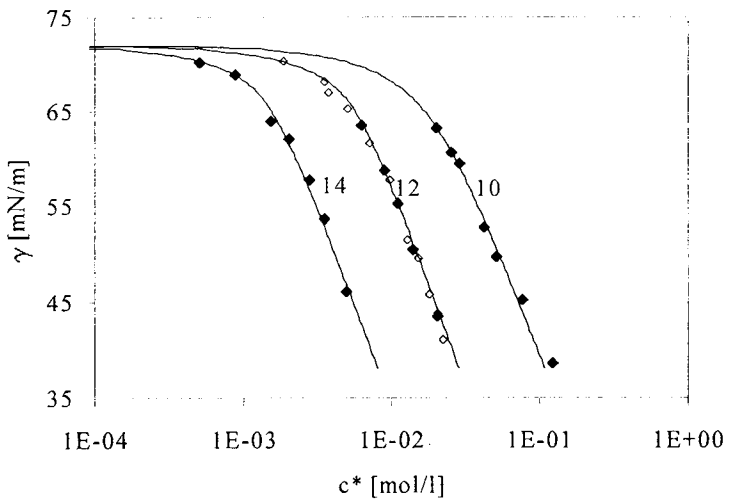

Fig. 3.41. Dependence of the equilibrium surface tension on c* in the solutions of sodium salts of fatty acids, data reported in: (◆), [65]; and (◇), [33]; at 25°C and sodium ions concentration 0.1 M, theoretical curves calculated from the Frumkin model using the model parameters listed in Table 3.17.

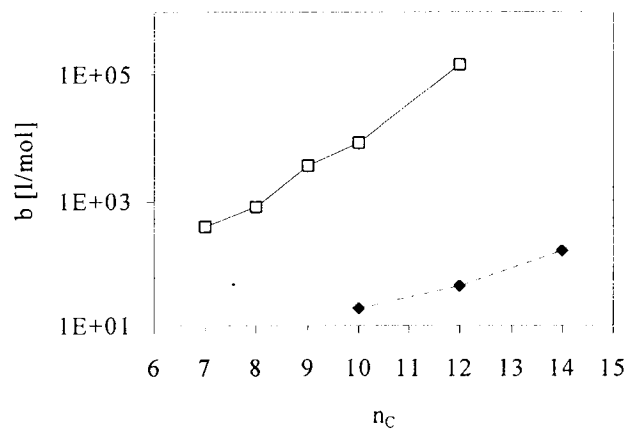

Fig. 3.42. Dependence of b on n_C for C_nO_2Na (◆), (□) - data for fatty acids as shown in Fig. 3.10.

The dependence $b(n_C)$ for soaps is characterised not only by a much lower slope as compared to fatty acids, but also the values of b are by 3 to 4 orders of magnitude lower, as shown in Fig. 3.42. The increment of standard free energy of adsorption, calculated from the values of b

via Eq. (2.186) for soaps ($\Delta G^0_{CH_2} = -2.68$ kJ/mol) is close to that obtained for normal alcohols and fatty acids ($\Delta G^0_{CH_2} \cong -2.8$ kJ/mol).

Table 3.17. Frumkin's model parameters, Eqs. (3.1), (3.2) calculated for C_nO_2Na.

C_nO_2Na	ω_I, 10^5 m^2/mol	a	b, l/mol	ε, %	Ref.
$C_{10}O_2Na$	1.35	1.1	$1.83 \cdot 10^1$	2.2	65
$C_{12}O_2Na$	1.25	1.45	$4.31 \cdot 10^1$	8.9	33, 65
$C_{14}O_2Na$	1.3	1.5	$1.58 \cdot 10^2$	5.3	65

3.4.2. Sodium alkyl sulphates

Among ionic surfactants, the adsorption behaviour of sodium alkyl sulphates (more precisely, sodium dodecyl sulphate, $C_{12}SO_4Na$, and, to the lesser extent, sodium decyl sulphate, $C_{10}SO_4Na$) are the most extensively studied compounds. Here we refer to the classic study by Elworthy and Mysels [66], where the data obtained for $C_{12}SO_4Na$ until 1965 were summarised and reviewed critically. For the analysis of the adsorption behaviour of C_nSO_4Na, we use here the data reported in [67-76]. It should be noted that the data given in [71] for $C_{12}SO_4Na$ include not only the values measured by Fang and Joos obtained from various methods, but also the data reported by Elworthy and Mysels [66] and some other authors. It will be shown below that the surface tension isotherms for $C_{12}SO_4Na$ given in [67-74] are in very good agreement.

The results for $C_{10}SO_4Na$ and $C_{12}SO_4Na$ obtained in water and with addition of NaCl are illustrated in Figs. 3.43 and 3.44. The presence of the inorganic salt alters the shape of the curve and shifts it to lower surfactant concentrations. The alteration of the shape – in particular, the decrease of the limiting slope with increasing electrolyte concentration – is in agreement with Gibbs' adsorption equation [77],

$$d\gamma = -RT\Gamma_R \left[1 + \frac{c_{RNa}}{c_{RNa} + c_{NaCl}} \right] d \ln c_{RNa}, \qquad (3.23)$$

where the index R stands for the residual C_nSO_4. For low electrolyte concentrations, $c_{NaCl} << c_{RX}$, and the limiting slope is equal to $2\Gamma_R$, while in the presence of a large constant

excess of inorganic electrolyte ($c_{NaCl} >> c_{RX}$) the slope is equal to Γ_R. Thus, at adsorptions close to saturation, the slope of the surface tension isotherm in absence of electrolyte should be twice as high as in the presence of excess electrolyte, as is the case for the data presented in Figs. 3.43 and 3.44.

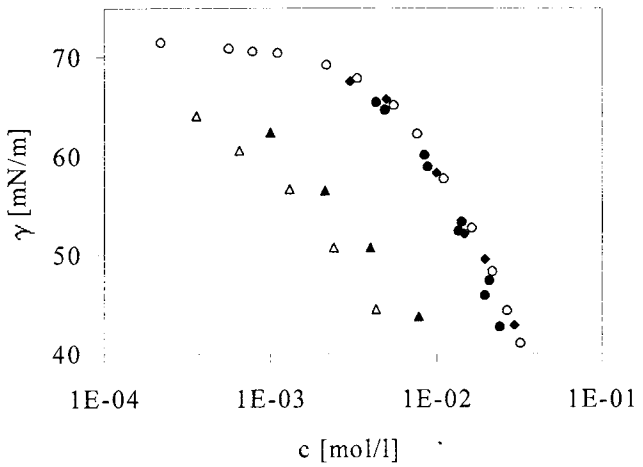

Fig. 3.43. Experimental surface tension *vs* concentration of $C_{10}SO_4Na$ at 25°C without salt: (●) - [68]; (○) - [67]; (◆) - [76]; and with additions of inorganic salt: (▲), 0.1 M NaCl and (△), 0.5 M NaCl [68].

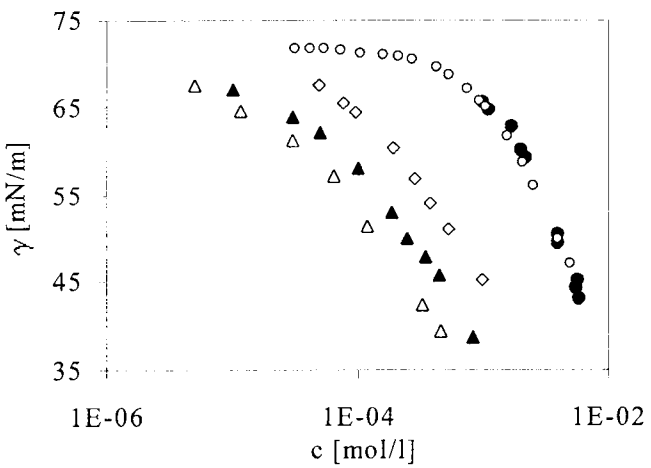

Fig. 3.44. Experimental surface tension *vs* concentration of $C_{12}SO_4Na$ at 25°C without salt: (●) - [68]; (○) - [67]; and with additions of inorganic salt: (◇) - 0.03 M NaCl [70]; (▲) - 0.1 M NaCl and (△) - 0.5 M NaCl [68]

Similar results were also obtained for dodecyl trimethyl ammonium bromide ($C_{12}TAB$) with different additions of NaBr (cf. Fig. 2.3). However, the shape of the surface tension isotherm becomes essentially different when the mean value of the ionic product c* is used instead of the surfactant concentration c. The experimental isotherms of $C_{12}TAB$ plotted *vs* the mean ionic product $c^* = f_{\pm} \cdot (c_{DTAB+NaBr} \cdot c_{DTAB})^{1/2}$ in a wide range of inorganic electrolyte concentrations merge into a single curve (cf. Figure 2.4).

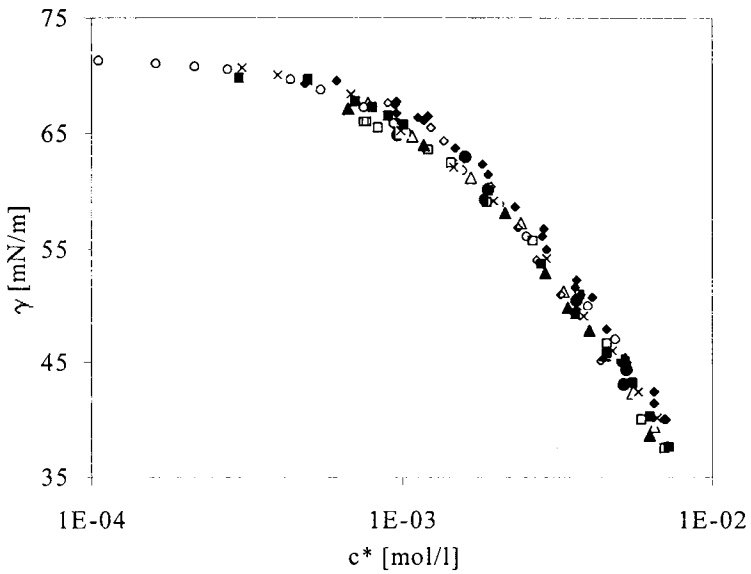

Fig. 3.45. The dependence of surface tension for $C_{12}SO_4Na$ solutions at 25°C on the mean ionic activity c*. Without salt: (●) [68]; (○) [67]; (×) [69]; (◆) [71]; (■) [72-74]; and with additions of inorganic salt: (◇) 0.03 M NaCl [70]; (□) 0.115 M NaCl [72-74]; (▲) 0.1 M NaCl and (△) 0.5 M NaCl [68].

Figure 3.45 summarises the experimental results for $C_{12}SO_4Na$ both with and without NaCl as the dependence of the mean ionic product $c^* = f_{\pm} \cdot (c_{RNa+NaCl} \cdot c_{RNa})^{1/2}$. Once again, we see the data merge into a single curve when re-plotted as a function of c*, indicating that the adsorption and the surface tension depend only on the mean ionic activity in the solution. The experimental results reported by several authors are in a good agreement: the absolute error in all experiments does not exceed ±1.5 mN/m. The experimental and theoretic surface tension isotherms for sodium alkyl sulphates at 25°C are shown in Fig. 3.46.

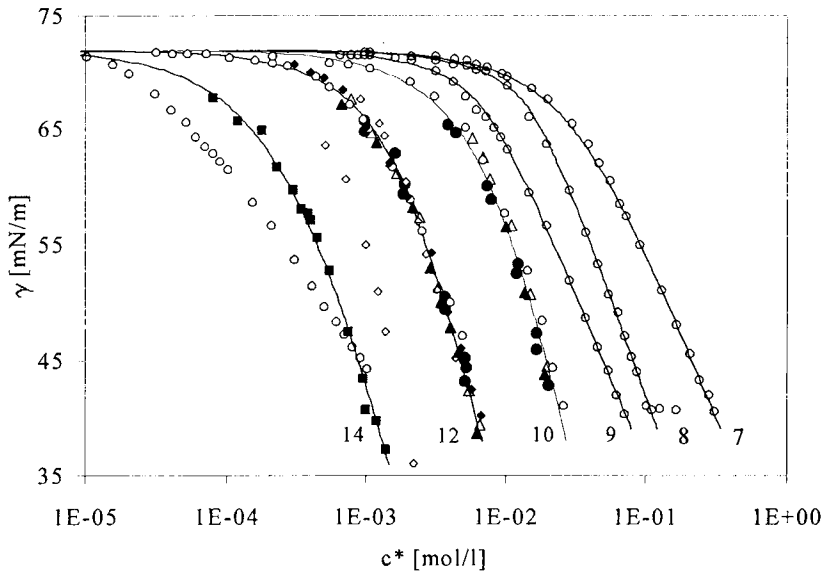

Fig. 3.46. Dependence of surface tension for C_nSO_4Na solutions on the mean ionic activity c*, numbers correspond to the carbon atoms number, without salt: (●) - [68]; (○) - [67]; (◆) - [69]; (■) - [75]; and with additions of inorganic salt: (◇) - 0.03 M NaCl [70]; (▲) - 0.1 M NaCl and (△) - 0.5 M NaCl [68], theoretical curves are calculated from the Frumkin model with the parameters listed in Table 3.18.

The lower homologues of sodium alkyl sulphates were studied in [67] only. Essential differences exist between the data presented in [67, 70, 75] for $C_{14}SO_4Na$. Therefore, to estimate the adsorption isotherm parameters for this substance we used the data [75], which are seen from Fig. 3.46 to be in a better agreement with the surface tension isotherms measured for other homologues. The data obtained in [67] for $C_{11}SO_4Na$ and $C_{13}SO_4Na$ are not shown in Fig. 3.46; however, the calculated isotherm parameters are listed in Table 3.18. Of all the parameters for the Frumkin isotherm summarised in Table 3.18, only those for $C_{10}SO_4Na$ and $C_{12}SO_4Na$ can be considered to be reliable. The analysis of the data shows that no definite trend could be seen in the variations of the molar area of the surface active ion or the constant a as function of n_C. To make the situation clear, new experiments are obviously needed.

Table 3.18. The parameters of Frumkin's model, Eqs. (3.1), (3.2) calculated for C_nSO_4Na.

C_nSO_4Na	ω_l, 10^5 m^2/mol	a	b, l/mol	ε, %	Ref.
C_7SO_4Na	1.85	0.68	$1.66 \cdot 10^1$	4.0	67
C_8SO_4Na	1.59	1.4	$1.67 \cdot 10^1$	3.8	67
C_9SO_4Na	1.90	1.27	$4.30 \cdot 10^1$	3.0	67
$C_{10}SO_4Na$	1.10	0.8	$6.30 \cdot 10^1$	9.7	67, 68, 76
$C_{11}SO_4Na$	1.88	1.68	$2.07 \cdot 10^2$	3.1	67
$C_{12}SO_4Na$	1.15	0.9	$2.55 \cdot 10^2$	5.3	67–74
$C_{13}SO_4Na$	2.3	1.14	$4.06 \cdot 10^3$	5.0	67
$C_{14}SO_4Na$	1.1	0.2	$2.28 \cdot 10^3$	4.7	75

The constant b for C_nSO_4Na (similarly to that for soaps), as compared with fatty acids, not only exhibits significantly lower increments, but also the absolute values are essentially lower (cf. Fig. 3.47. Note that the values of b calculated for odd homologues C_7, C_9 and C_{11} from the data in [67] are approximately the same as those for the next even homologues, and the value for C_{13} is even higher than that for C_{14}. This fact disagrees with the trends shown to exist in other surfactant homologous series. For normal alcohols and fatty acids the molar area is usually low ($\omega \cong 1.7 \cdot 10^5$ m^2/mol) and, as the size of the polar group is small, the hydrocarbon tails are rather closely packed. The conformation of dimers and other van der Waals entities for even and odd homologues can be different. This is one possible explanation of the fact that the lg(b) values for odd homologues lie somewhat above the straight line lg(b) *vs* n_C for even homologues (cf. Figs. 3.4 and 3.10), while, on the contrary, the parameters a for odd homologues are lower than those expected from the values for even homologues (cf. Figs. 3.2 and 3.9). For surfactants with larger molar area ω, for example $2.4 \div 3.2 \cdot 10^5$ m^2/mol (that is, for less packed hydrocarbon tails) the adsorption characteristics of even and odd homologues becomes less, as it was observed for the homologous series C_nDMPO, C_nBHB and C_nPIP (cf. Figs. 3.12, 3.14, 3.16, 3.18, 3.22 and 3.24). For C_nSO_4Na the molar areas $\omega = 2\omega_l$ estimated from Table 3.18 are between $2.2 \cdot 10^5$ m^2/mol and $3.6 \cdot 10^5$ m^2/mol, which is roughly the same as for C_nDMPO, C_nBHB and C_nPIP. Thus, both the anomalous values of the parameter b for odd

C_nSO_4Na homologues and the ambiguous trends in the dependence of the molar area and the parameter a on n_C could be thought of as problems which are still to be studied experimentally.

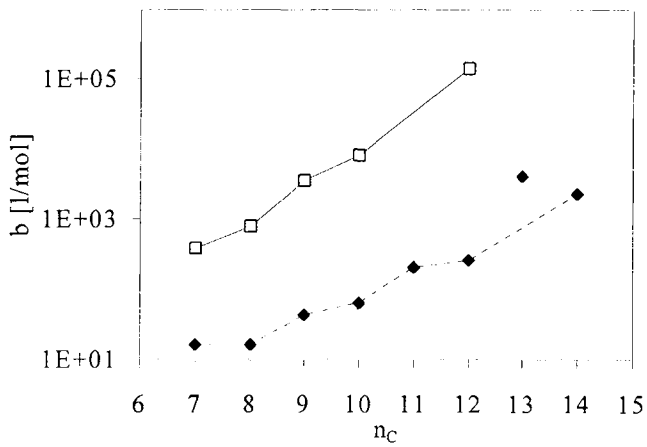

Fig. 3.47. Dependence of adsorption equilibrium constant b on n_C for $C_{12}SO_4Na$ (◆), (□) - data for fatty acids as given in Fig. 3.10.

The value of the increment of the standard free energy of adsorption for C_nSO_4Na calculated via Eq. (2.186) from the parameter b (except the data for $C_{13}SO_4Na$ and $C_{14}SO_4Na$), $\Delta G^0_{CH_2} = -3.17$ kJ/mol, is somewhat higher than that obtained for normal alcohols and acids ($\Delta G^0_{CH_2} = -2.8$ kJ/mol)..

The data reported in [78] for $C_{12}SO_4Na$ with additions of 0.1 M NaCl was presented in Chapter 2, see Fig. 2.18. The surface pressure isotherms exhibits a characteristic inflection at a pressure of ca. 8 mN/m. These results were well described by the theoretical model which assumes the formation of small aggregates in the precritical surface pressure range, and cluster formation in the transcritical region. These data do not contradict with the results shown in Fig. 3.45. To support this statement, we presented the most reliable experimental results obtained for $C_{12}SO_4Na$ together with the data from [78] shown in Fig. 2.18, however re-plotted as a function of the mean ionic product c* (cf. Fig. 3.48).

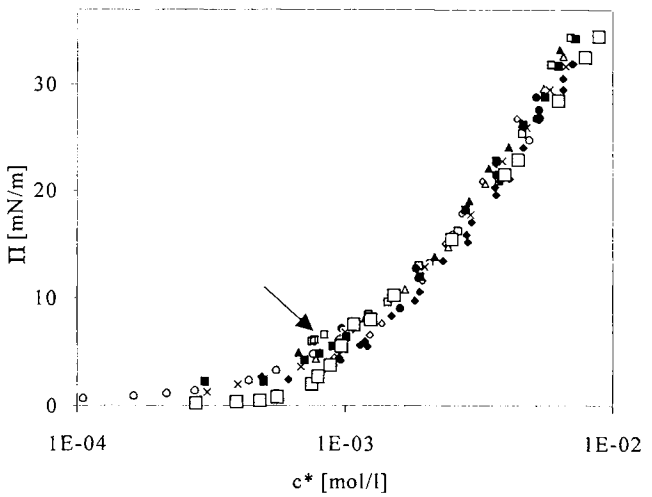

Fig. 3.48. Dependence of surface pressure of $C_{12}SO_4Na$ solutions on the mean ionic activity c*, small symbols correspond to the data shown in Fig. 3.45; □ - data from [78] for $C_{12}SO_4Na$ in 0.1 M NaCl.

The data from [78] are consistent with the group of best experimental results characterised by an experimental error of ±1.5 mN/m. Moreover, the location of the critical point in the $C_{12}SO_4Na$ isotherm at 0.1 M NaCl for the data from [78] (approximately at $c^* = 10^{-3}$ mol/l), and the inflection-like agglomeration of the experimental data from other publications (indicated by an arrow at $c^* = 8 \cdot 10^{-4}$ mol/l in Fig. 3.48) occur both at similar surface pressures (ca. 8 mN/m). Note that the results indicated by the arrow in Fig. 3.48 correspond to an electrolyte concentration of 0.1 to 0.5 M NaCl. To summarise, the supposition that $C_{12}SO_4Na$ undergoes a condensation in the adsorption monolayers at sufficiently high NaCl concentration can be regarded to as a reliable hypothesis, which however, still requires further experimental verification.

3.4.3. Oxyethylated sodium alkyl sulphates

The presence of EO groups in the oxyethylated sodium alkyl sulphate molecule ($C_nEO_mSO_4Na$), similarly to other ionic surfactants, affects significantly the adsorption behaviour at the water/air interface [76]. The experimental data for $n_C = 8$, 10 and 12, and m = 1, 2, 3 obtained in [69, 76] are presented in Fig. 3.49. For comparison the isotherms for sodium alkyl sulphates with the same hydrocarbon chain length are shown. One can see that the

addition of 1 to 3 EO groups into the C_nSO_4Na molecule results in a significant increase in the surface activity, as the respective isotherms are shifted drastically towards lower concentrations. Also, the shape of the adsorption isotherms becomes similar to those obtained for C_nEO_m, cf. Figs. 3.27 and 3.28. Therefore, the experimental isotherms for $C_nEO_mSO_4Na$ exhibit a better correspondence with the reorientation model, as we can learn from the data given in Table 3.20.

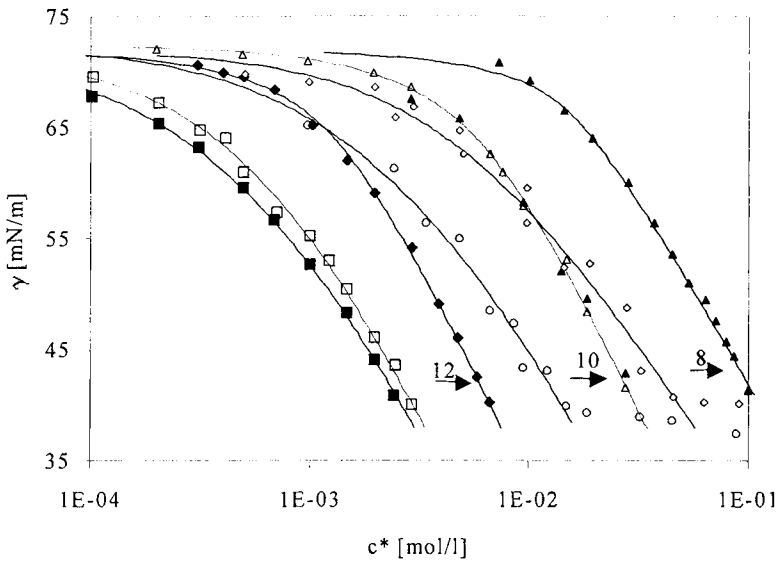

Fig. 3.49. Dependence of surface tension for $C_nEO_mSO_4Na$ solutions as a function of the mean ionic activity c* for various n and m; n=8: m = 0 (▲) [67], m = 3 (◇) [76]; n=10: m = 0 (▲,△), [76, 67], m=1 (O) [76]; n=12: m = 0, (◆), m = 1 (□), m = 2 (■), [69], theoretical curves calculated from Frumkin's model with the model parameters listed in Table 3.19.

The addition of one, two and three EO groups results in an approximately six, nine and eleven times increase of the constant b for the corresponding sodium alkyl sulphate, respectively. In Figure 3.50 the dependencies lg(b) *vs* n_C are compared for $C_nEO_2SO_4Na$ with the data for non-oxyethylated C_nSO_4Na homologues.

When the number of oxyethylene groups in the $C_nEO_mSO_4Na$ molecule is small, their effect on the adsorption characteristics is quite the same as the effect of the hydrophobic methylene groups. This result is consistent with that obtained for oxyethylated alcohols, which exhibits the diphility character of the EO groups. In this case, the absolute standard free energy of adsorption is significantly increased (by 10.3 kJ/mol, as compared with C_nSO_4Na), but the

increment of the standard free energy of adsorption for one methylene group for $C_nEO_2SO_4Na$, $\Delta G^0_{CH_2} = -3.3$ kJ/mol is the same as that obtained for C_nSO_4Na, $\Delta G^0_{CH_2} = -3.17$ kJ/mol.

Table 3.19. Frumkin's model parameters, Eqs. (3.1), (3,2), calculated for $C_nEO_mSO_4Na$.

$C_nEO_mSO_4Na$	ω_I, 10^5 m^2/mol	a	b, l/mol	ε, %	Ref.
$C_{12}SO_4Na$	1.36	1.1	$2.68 \cdot 10^2$	3.8	69
$C_{12}EOSO_4Na$	1.32	0.1	$1.41 \cdot 10^3$	5.0	69
$C_{12}EO_2SO_4Na$	1.25	-0.5	$2.23 \cdot 10^3$	3.0	69
$C_{10}SO_4Na$	1.3	0.92	$6.65 \cdot 10^1$	5.2	76, 67
$C_{10}EOSO_4Na$	1.3	-0.55	$4.93 \cdot 10^2$	11.1	76
$C_{10}EO_2SO_4Na$	1.5	0.0	$5.14 \cdot 10^2$	7.5	76
C_8SO_4Na	1.59	1.4	$1.66 \cdot 10^2$	3.9	67
$C_8EO_3SO_4Na$	1.77	0.0	$1.82 \cdot 10^2$	16.9	76

Table 3.20. Reorientation model parameters, Eqs. (3.3)-(3.7), calculated for some $C_nEO_mSO_4Na$ homologues.

$C_nEO_mSO_4Na$	ω_{I1}, 10^5 m^2/mol	ω_{I2}, 10^5 m^2/mol	α	b, l/mol	ε, %	Ref.
$C_{12}EO_2SO_4Na$	11.8	1.7	0.8	$2.98 \cdot 10^3$	2.4	69
$C_{10}EOSO_4Na$	8.0	1.4	0.8	$4.05 \cdot 10^2$	10.5	76

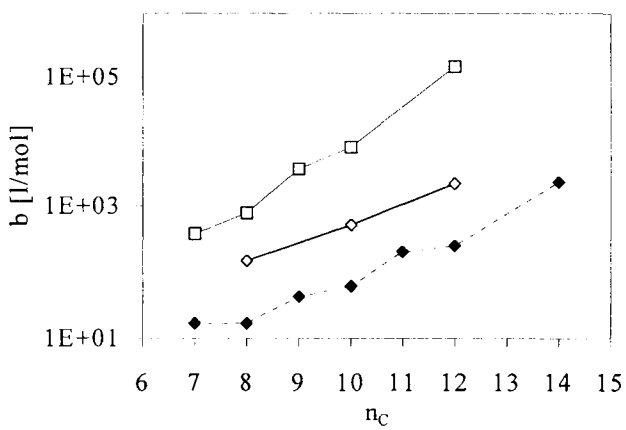

Fig. 3.50 Dependence of the adsorption equilibrium constant b on n_C for: (◆), C_nSO_4Na and (◇), $C_nEO_2SO_4Na$, (□) - data for fatty acids as shown in Fig. 3.10.

3.4.4. Alkyl trimethyl ammonium bromides

The Fig. 2.4 of Chapter 2 illustrates the surface tension of dodecyl trimethyl ammonium bromide ($C_{12}TAB$) at different NaBr concentrations [79] as a function of the mean ionic product $c^* = f_{\pm} \cdot (c_{DTAB+NaBr} \cdot c_{DTAB})^{1/2}$. These results, and also the experimental data reported in [80, 81] are shown in Fig. 3.51.

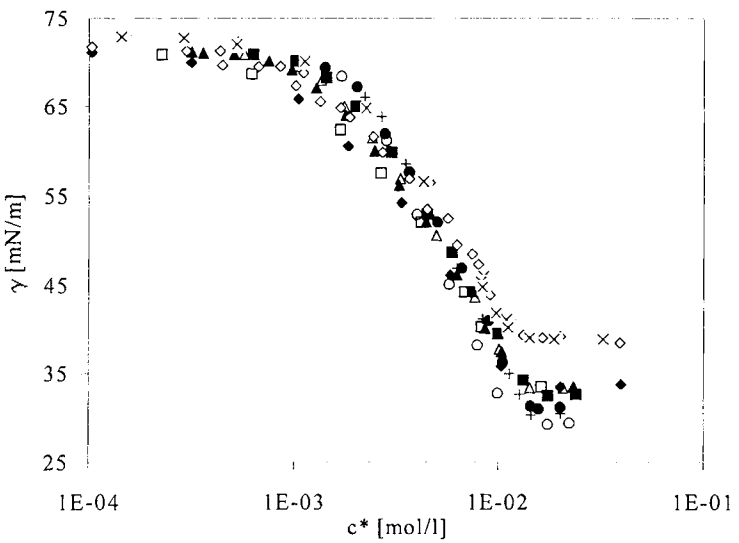

Fig. 3.51 Experimental surface tension of $C_{12}TAB$ solutions at 25°C *vs* mean ionic activity $c^* = f_{\pm} \cdot (c_{DTAB+NaBr} \cdot c_{DTAB})^{1/2}$; without salt: (◆) - 25°C [79], (◇) - 20°C [80], (×) - 20°C [81]; with the addition of NaBr at 25°C: 0.0001 (□),0.005 (▲),0.01 (△), 0.02 (■),0.1 (●), 0.2 (+), 0.5 (O) M NaBr [79].

The data obtained by various authors for the $C_{12}TAB$ solutions, both with and without the electrolyte, are quite consistent, however, the maximum experimental error in all experiments amounts to ±3.0 mN/m, which is twice as large as that for $C_{12}SO_4Na$ (cf. Fig. 3.45). The experimental and theoretical surface tension isotherms for various alkyl trimethyl ammonium bromides are summarised in Fig. 3.52 (data from [80-83]).

To calculate the isotherm parameters, the data from [80] were employed, while the data from [81-83] were used only in the surface tension region $\gamma < 60$ mN/m. These results obtained by various authors are quite consistent. The parameters for the two adsorption models are summarised in Tables 3.21 and 3.22. Table 3.21 also lists the CMC and the standard free

energy of micellisation calculated from Eq. (2.187). In both Tables the value of standard free energy of adsorption are shown calculated by two methods: (i) from the constant b via Eq. (2.186) (denoted by the subscript 'a'), and (ii) from Eq. (2.188) via the parameters for the CMC (with $\beta = 0.8$) and ω (denoted by the subscript 'a(m)').

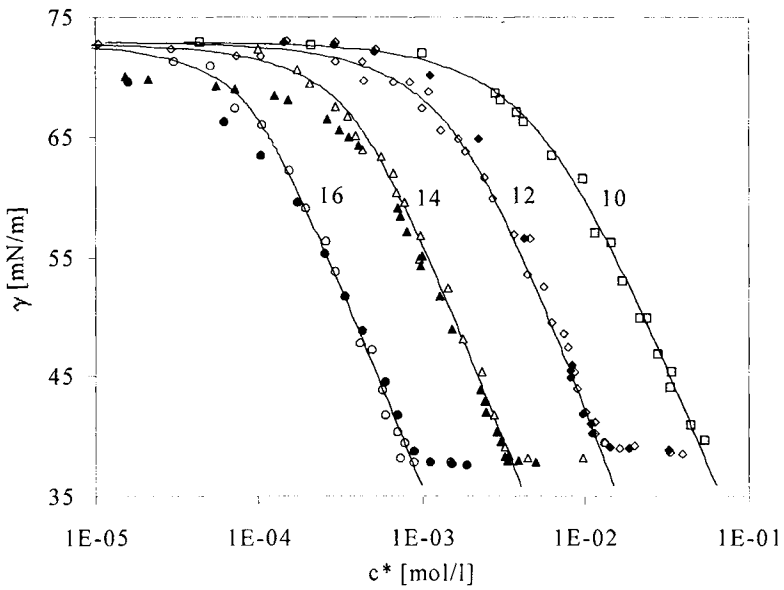

Fig. 3.52. Dependence of surface tension for C_nTAB solutions as a function of the mean ionic activity c*: (□,◇,△, O) at 20°C [80]; (◆) at 20°C [81]; (▲) at 25°C [82]; (●) at 30°C [82], numbers denote the number of carbon atoms, the theoretical curves were calculated from the Frumkin model using the parameters listed in Table 3.21.

Table 3.21. The parameters of the Frumkin model, Eqs. (3.1), (3.2), for C_nTAB.

C_nTAB	ω_l, 10^5 m^2/mol	a	b, l/mol	ε, %	c_{cmc}, mol/l	ΔG^0_a, kJ/mol	ΔG^0_m, kJ/mol	$\Delta G^0_{a(m)}$, kJ/mol	Ref.
$C_{10}TAB$	1.60	0.58	$9.42 \cdot 10^1$	8.6	$5.0 \cdot 10^{-2}$	-38.4	-30,8	-42.4	80
$C_{12}TAB$	1.48	0.8	$2.63 \cdot 10^2$	15.2	$1.2 \cdot 10^{-2}$	-43.4	-36.9	-46.9	80, 81
$C_{14}TAB$	1.56	1.1	$8.46 \cdot 10^2$	11.3	$3.6 \cdot 10^{-3}$	-49.2	-42.3	-52.1	80, 82
$C_{14}TAB$	1.32	0.0	$1.52 \cdot 10^3$	12.2					82
$C_{16}TAB$	1.61	1.3	$3.05 \cdot 10^3$	6.7	$9.0 \cdot 10^{-4}$	-55.4	-48.4	-59.6	80, 83
$C_{16}TAB$	1.36	0.0	$5.60 \cdot 10^3$	4.4					83

In the low concentration region the surface tensions for C_{14}TAB from [82] and C_{16}TAB from [83] are essentially smaller than those given in [80]. This difference cannot be ascribed to the fact that the measurement temperatures in [82, 83] were 5-10°C higher. As a control of the equilibration conditions was implemented in [82, 83], it can be supposed that the observed disagreement with data from [80] is due to lack of equilibrium in the experiments with higher C_nTAB homologues. That is why the data from [82,83] were analysed here separately. The results of calculations for the two models are summarised in Tables 3.22, 3.23 and in Fig. 3.53.

Table 3.22. The parameters of the reorientation model, Eqs. (3.3)-(3.7), calculated for some C_nTAB.

C_nTAB	ω_{l1}, 10^5 m^2/mol	ω_{l2}, 10^5 m^2/mol	α	b, l/mol	ε, %	ΔG^0_a, kJ/mol	$\Delta G^0_{a(m)}$, kJ/mol	Ref.
C_{10}TAB	9.6	1.53	0.0	$1.42 \cdot 10^2$	9.2	-40.4	-40.8	80
C_{12}TAB	12.4	1.46	0.0	$5.02 \cdot 10^2$	14.9	-46.6	-47.7	80, 81
C_{14}TAB	16.0	1.47	0.0	$2.0 \cdot 10^3$	12.1	-53.4	-52.5	80, 82
C_{14}TAB	15.0	1.61	0.8	$3.31 \cdot 10^3$	6.5			82
C_{16}TAB	15.9	1.50	0.0	$8.38 \cdot 10^3$	7.3	-60.4	-58.8	80, 83
C_{16}TAB	15.0	1.74	0.6	$9.38 \cdot 10^3$	2.3			83

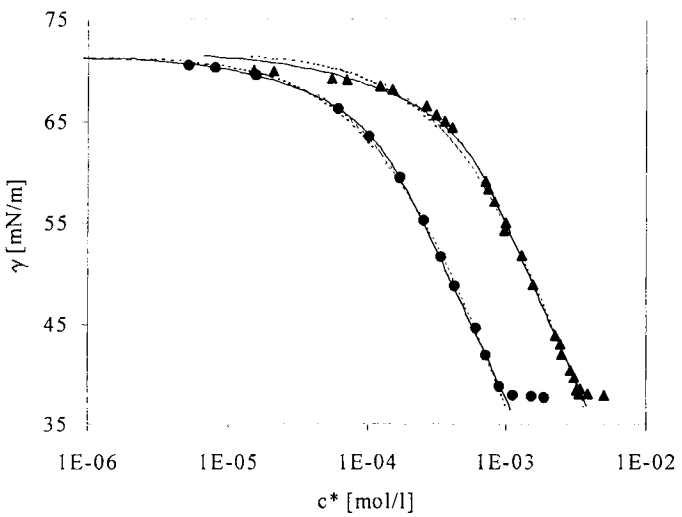

Fig. 3.53. Dependence of surface tension for C_{14}TAB solutions as a function of the mean ionic activity c*: (▲) - at 25°C [82] and for C_{16}TAB solutions (●) at 30°C [82], the theoretical curves were calculated from Frumkin's model (solid line) and the reorientation model (dashed line) with parameters listed in Tables 3.21 and 3.22.

It is seen that the calculated deviation for the reorientation model is two times lower than for the Frumkin model. The dependencies of the isotherm parameters of C_nTAB on n_C are similar to those obtained for other surfactants: the Frumkin constant a increases with n_C (cf. Table 3.21), the minimum area of the surface active ion ω_{I2} is almost independent of n_C, and the molar area in the unfolded state ω_{I1} becomes higher with increasing n_C (cf. Table 3.22 and Fig. 3.54).

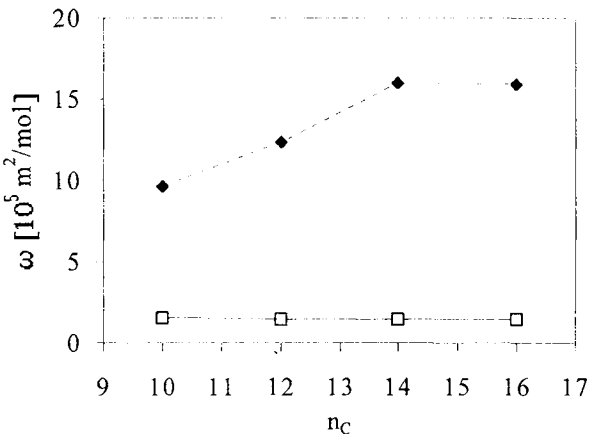

Fig. 3.54. Dependence of the molar area per surface active ion ω_I in states 1 (◆) and 2 (□) on the number of carbon atoms n_C calculated for C_nTAB.

Similarly to other ionic surfactants, the values of the constant b for C_nTAB are by several orders of magnitude lower than for corresponding non-ionic surfactants. However, the increment of the standard free energy of adsorption for C_nTAB, $\Delta G^0_{CH_2} = -2.88$ kJ/mol, calculated from the constant b via Eq. (2.186), is quite similar to the values obtained for normal alcohols and fatty acids, $\Delta G^0_{CH_2} \cong -2.8$ kJ/mol. The dependencies of ΔG^0 and ΔG^0_m on the alkyl chain length of C_nTAB for the Frumkin and reorientation models are shown in Figs. 3.55 and 3.56, respectively. Similarly to C_nBHB (cf. Figs. 3.19 and 3.20), for the Frumkin model the two methods of the calculation of the standard free energy of adsorption lead to certain differences, while for the reorientation model the two models yield perfectly the same results. The reasons of this agreement were discussed above for non-ionic surfactants. It indicates that

the CMC and the adsorption characteristics (parameter b and molar area ω) are reliable thermodynamic results. We can conclude that our theoretical model (see Eqs. (2.186)-(2.188)) is also correct for ionic surfactants, with the choice of the dividing surface such that $\omega = 2\omega_0$.

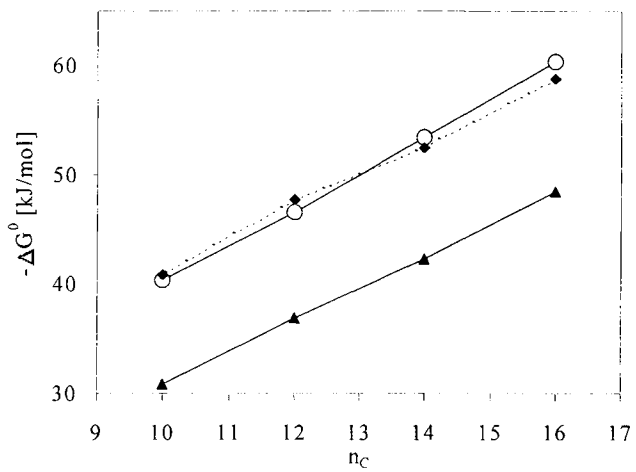

Fig. 3.55. Dependence of ΔG_m^{υ} (◇) and standard free energy of adsorption ΔG_a^0 (□) and $\Delta G_{a(m)}^0$ (▲) on n_C for C_nTAB, calculations according to the Frumkin model.

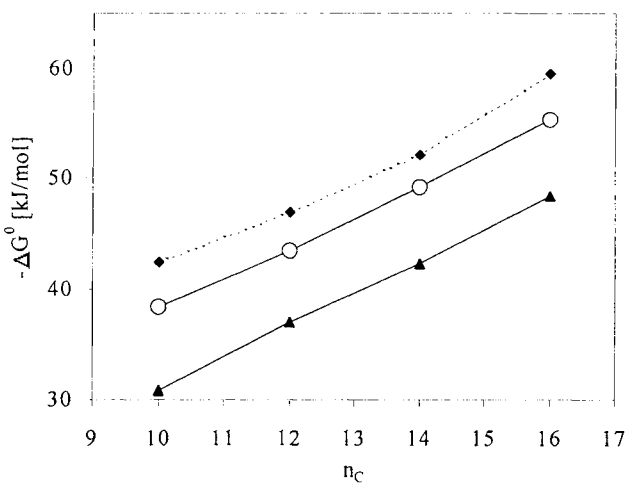

Fig. 3.56. The dependence of ΔG_m^0 (◇) and standard free energy of adsorption ΔG_a^0 (□) and $\Delta G_{a(m)}^0$ (▲) on n_C for C_nTAB, calculated according to the reorientation model.

3.4.5. Alkyl ammonium chlorides

Figure 3.57 presents experimental data for decyl ammonium chloride ($C_{10}ACl$) and dodecyl ammonium chloride ($C_{12}ACl$) in presence of 0.005 M HCl [33]. The molar area ω_1 is somewhat lower than that for C_nTAB. At the same time, the Frumkin constant a is somewhat higher which underlines the interrelation of these parameters. The dependencies of b on n_C for C_nACl and C_nTAB are compared with the data for fatty acids in Fig. 3.58.

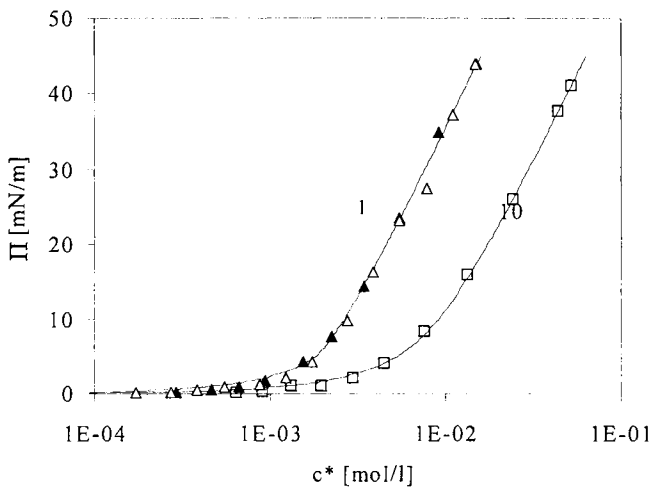

Fig. 3.57. Experimental surface pressure vs mean ionic activity, $c^* = \gamma_{\pm}(c_R.c_{Cl})^{1/2}$, for $C_{10}ACl$ (□) and $C_{12}ACl$ (▲ without and △ with NaCl to give total c_{Cl}=20 mmol/l); c_{HCl}=5 mmol/l, at 20 °C [33], the theoretical curves were calculated from the Frumkin model using the parameters listed in Table 3.23.

The values of b for C_nACl and C_nTAB are by several orders of magnitude lower than those for respective non-ionic surfactants, while the increments of the standard free energy of adsorption are close to those for non-ionics.

Table 3.23. The parameters of the Frumkin model, Eqs. (3.1), (3.2), calculated for $C_{10}ACl$.

C_nAcl	ω_l, 10^5 m^2/mol	A	b, l/mol	ε,%	Ref.
$C_{10}ACl$	1.18	1.25	$3.72 \cdot 10^1$	3.4	33
$C_{12}ACl$	1.16	1.7	$9.31 \cdot 10^1$	3.9	33

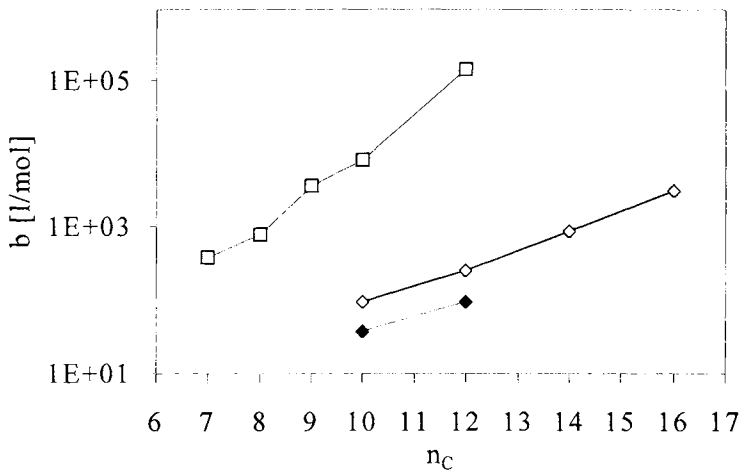

Fig. 3.58. Dependence of the adsorption equilibrium constant b on n_C for: (◆), C_nACl; and (◇), C_nTAB, (□) - data for fatty acids as given in Fig. 3.10.

3.5. General features of the adsorption of individual surfactants.

To predict the adsorption behaviour of surfactants at liquid interfaces, purely theoretical and semi-empirical approaches were proposed. In [16, 84] the attempt was made to calculate theoretically all parameters of the equation of state and adsorption isotherm for ionic or non-ionic surfactants. The area per molecule was calculated from bond lengths and angles for surfactants having compact hydrophilic head groups, or via Monte Carlo simulations for surfactants having flexible, polymer-like hydrophilic heads. The intermolecular interaction parameters were also be calculated theoretically, assuming electrostatic interaction to form an additive contribution to the surface pressure. However, it is impossible to reliably estimate the difference between the chemical potentials of the component in the bulk and at the surface which determines the adsorption activity of a surfactant. Therefore, to implement the model proposed in [16] one has to know experimental surface tension values of individual solutions at least at one concentration. More common is another approach to predict the adsorption behaviour of surfactants, the so called additive-group method. This method was first proposed by Davies [4, 85] to explain Griffin's concept of hydrophilic-lipophilic balance (HLB) [86]. As applied to the adsorption behaviour of surfactants, this method was extensively developed by

Rosen [1, 4] and Abramzon [87]. It was assumed that the physicochemical properties of a surfactant, e.g., the free energy of adsorption, adsorption equilibrium constant b, the bulk concentration corresponding to a certain (usually by 20 mN/m [1, 4]) surface tension decrease, CMC etc. can be estimated by the additive summation of the contributions from the hydrophilic and hydrophobic groups of the surfactant molecule or their fragments. To calculate the standard free energy of adsorption the additive-group approach allows to calculate the adsorption equilibrium constant b together with the theoretical estimation of other parameters. Hence this is possibly the most efficient method to predict the adsorption behaviour of a surfactant. The results presented in the previous sections enable one to derive or specify more precisely some general features characteristic for the adsorption isotherm parameters of various surfactants.

It should be noted first that the Frumkin model is the most general one with respect to its application to surfactants of different nature. In spite of the fact that, e.g., for oxyethylated non-ionic or ionic surfactants this model is essentially biased, in the majority of practical cases it can be recommended irrespectively of the nature of the surfactant. In the Frumkin model, three parameters are necessary to describe the adsorption and surface tension isotherm. Leaving aside the molar area ω which can be estimated from the molecular geometry [16, 84], we concentrate on the results which follow from our development for the parameters a and b for surfactant molecules with linear hydrocarbon chain. Figure 3.59 illustrates the dependence of the Frumkin constant a on the molar area ω of various surfactants at $n_C = 10$. Note that for ionic surfactants the ω values are equal to the doubled values of ω_i from corresponding tables.

It is seen that the lower is the molar area, the higher is the a value. This can be ascribed to the fact that the nonideality results from the Van der Waals interaction of the methylene groups, which is the stronger, the less is the area of the polar group. This polar group area always exceeds the cross-section area of the hydrocarbon tails, and therefore, it is the polar group area which determines the molar area of the surfactant in a densely packed adsorption layer. For $\omega > 3 \cdot 10^5$ m^2/mol the behaviour of the adsorption layer can be thought of as almost ideal (cf. Fig. 3.59). It is interesting to note that the development above does not differentiate between non-ionic and ionic surfactants. This possibly results from the concept of an electroneutral surface layer and the mean ionic products involved in the derivation of the adsorption isotherm equation for ionic surfactants. If the number of carbon atoms in the

molecule differs from 10, the dependence shown in Fig. 3.59 can be corrected using the value of the increment of the parameter a per methylene group. It follows from our data that $\Delta a_C = 0.2 \pm 0.05$; therefore, for $n_C = 14$ the curve shown in Fig. 59 should be shifted towards high areas by approximately $\Delta\omega = 0.5 \cdot 10^5$ m^2/mol, while for $n_C = 6$ the shift would take place by the same value towards lower molar areas (dashed lines in Fig. 3.59).

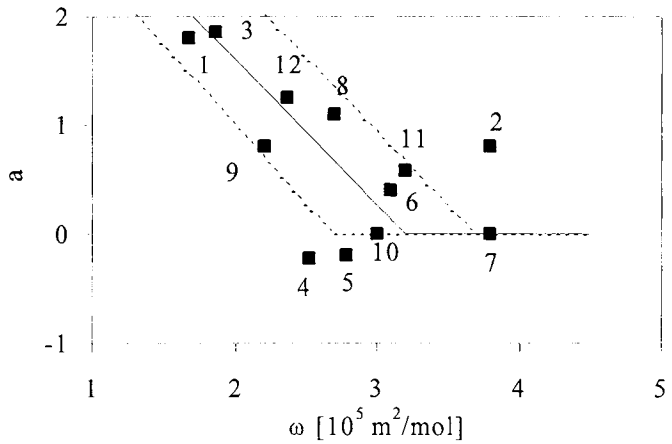

Fig. 3.59. Dependence of Frumkin's constant a on the molar area ω at $n_C = 10$ for various surfactants: 1 - C_nOH; 2 - $C_n(OH)_2$; 3 - C_nO_2H; 4 - C_nDMPO; 5 - C_nBHB; 6 - C_nPIP; 7 - C_nEO_8; 8 - C_nO_2Na; 9 - C_nSO_4Na; 10 - $C_nEO_2SO_4Na$; 11 - C_nTAB; 12 - C_nACl.

For all homologous series with linear hydrocarbon chains, discussed in this chapter, the linear dependence of lg(b) on n_C was shown to be approximately valid. Therefore, according to Eq. (3.11) and keeping in mind the linear dependence mentioned above, one can express the standard free energy of adsorption as

$$\Delta G^0 = \Delta G^0_{CH_2} \cdot n_C + \Delta G^0_P, \qquad (3.24)$$

where ΔG^0_P is the standard free energy of adsorption of the polar group plus the difference of $\Delta G^0_{CH_3} - \Delta G^0_{CH_2}$. Instead of Eq. (3.11), the expression for the so called transfer energy into the surface layer was used in [1, 4]

$$\Delta G^0_{tr} = -RT \ln(1/c_{20}), \qquad (3.25)$$

where c_{20} is the surfactant concentration at which the surface tension is reduced by 20 mN/m. It is easily seen that, for the Langmuir isotherm, Eqs. (3.11) and (3.25) lead to the same value of the free energy increment $\Delta G^0_{CH_2}$. However, unlike the absolute term of Eq. (3.24), the absolute term in the corresponding equation for ΔG^0_{ir} [1 ,4] involves not only the free energy of adsorption of the polar groups at the surface, but also an unknown numerical factor.

Combining Eqs. (2.186), (3.11) and (3.24) one obtains an expression for the surfactant adsorption equilibrium constant involving the corresponding increments

$$b = \frac{1}{\rho\alpha^2}\exp\left(-\frac{(\Delta G^0_{CH_2}\cdot n_C + \Delta G^0_P)\alpha}{RT}\right), \qquad (3.26)$$

where $\alpha = 1$ for non-ionic surfactants, and $\alpha = 1/2$ for ionic surfactants. For most surfactants (except oxyethylated ones) the polar group remains in the aqueous environment rather than at the interface [14]. Therefore, in the initial approximation one can assume $\Delta G^0_P = 0$ in Eq. (3.24). This form of the equation (zero ΔG^0_P term) was first proposed by Abramzon [87], however, instead of the expression $\ln(b\rho\alpha^2)$ in Eq. (3.11) (note that the $b\rho\alpha^2$ value gives the ratio of the surfactant molar fraction at the surface to that in the bulk), he used the expression $\ln(b/\omega\delta)$ to account for the surface layer of finite thickness δ, and $\delta = 1$ nm was assumed. As $\rho \cong 55.6$, and $1/\omega\delta \cong (2\div4)\cdot10^4$, then for the same increments $\Delta G^0_{CH_2}$ and ΔG^0_P our model and the model of Abramzon lead to different values of b in the limit $n_C = 0$. It follows from Eq. (3.26) for $n_C = 0$ and $\Delta G^0_P = 0$ that $b_0\rho\alpha^2 = 1$, or $b_0 \cong 0.018$ l/mol for non-ionic surfactants, and $b_0 \cong 0.072$ l/mol for ionic surfactants. The condition $b_0\rho\alpha^2 = 1$ means that no adsorption takes place, i.e., the molar fraction of the polar groups in the bulk is approximately equal to the fraction at the surface. At the same time for the model given in [87] in the limit $n_C = 0$, and therefore $b/\omega\delta = 1$ (for $\Delta G^0_P = 0$) yields a value of $b_0 \cong 3\cdot10^{-5}$ mol/l. In the following we will compare the theoretical values of b_0 with experimental results.

Figure 3.60 summarises all the experimental dependencies of b on n_C for different surfactants considered in this chapter. For the oxyethylated surfactants, C_nDMPO, C_nBHB and C_nPIP the values of b calculated from the reorientation model are shown, while for all other surfactants the Frumkin model was used.

The theoretical dependencies were constructed with $b_0 \cong 0.018$ l/mol for non-ionic surfactants and $b_0 \cong 0.072$ l/mol for ionic surfactants at $n_C = 0$ and $\Delta G_P^0 = 0$. It is seen that the theoretical lines are in a satisfactory agreement with most experimental data. On the contrary, if the value $b_0 \cong 3 \cdot 10^{-5}$ l/mol at $n_C = 0$ is assumed which follows from [87], then the theory disagrees with the experiment, as one can see from the dashed lines in Fig. 3.60.

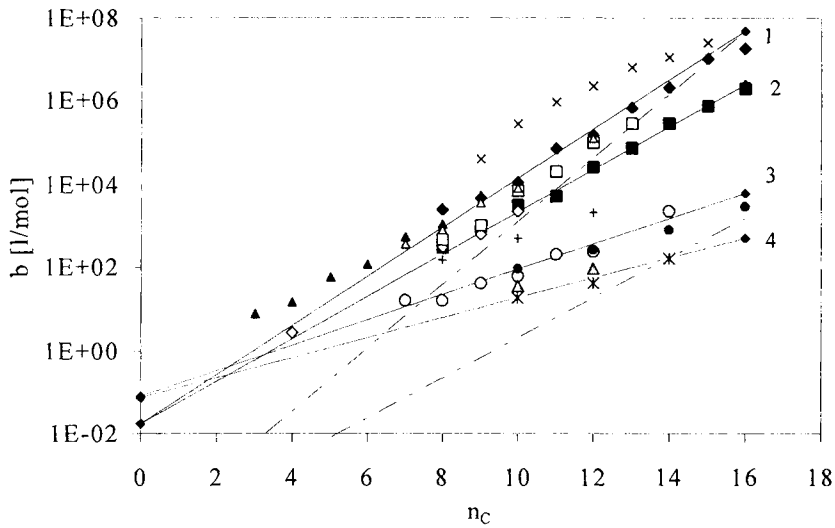

Fig. 3.60. Dependence of adsorption equilibrium constant b on n_C for various surfactants: (▲) - C_nOH; (◇) - $C_n(OH)_2$; (△) - C_nO_2H; (◆) - C_nDMPO; (■) - C_nBHB; (□) - C_nPIP; (×) - C_nEO_8, (∗) - C_nO_2Na; (O) - C_nSO_4Na; (+) - $C_nEO_2SO_4Na$; (●) - C_nTAB; (▲) - C_nACl, straight lines are calculated from Eq. (3.26) for $\Delta G_P^0 = 0$ and $b_0 = 0.018$ l/mol for non-ionic surfactants, $b_0 \cong 0.072$ l/mol for ionic surfactants (solid line), and $b_0 \cong 3 \cdot 10^{-5}$ l/mol (dashed line).

Lines 1 and 2 in Fig. 3.60 extend over the region characteristic for non-ionic or amphoteric surfactants (except for the oxyethylated ones), and correspond to $\Delta G_{CH_2}^0 = -(2.9 \div 3.3)$ kJ/mol. Lines 3 and 4 confine the region of ionic surfactants, yielding the values $\Delta G_{CH_2}^0 = -(2.7 \div 3.8)$ kJ/mol. These values of the increments are approximately 10% larger than those calculated for these surfactants in the previous sections. This inconsistency is possibly due to the fact that the ΔG_P^0 value is not exactly equal to zero (as also the difference $\Delta G_{CH_3}^0$ -

$\Delta G^0_{CH_2}$ is included into ΔG^0_P), and therefore the value b_0 at $n_C = 0$ is different from that determined by the condition $b_0\rho\alpha^2 = 1$.

The best agreement with the entire scope of the experimental data was obtained for $\Delta G^0_P = -4.25$ kJ/mol; the theoretical lines calculated from Eq. (3.26) with this ΔG^0_P value are shown in Fig. 3.61. For the non-ionic and amphoteric surfactants the lines 1 and 2 correspond to $\Delta G^0_{CH_2} = -(2.6 \div 3.0)$ kJ/mol, and for ionic surfactants the lines 3 and 4 correspond to $\Delta G^0_{CH_2} = -(2.6 \div 3.3)$ kJ/mol, i.e. exactly the values presented in the previous sections and agree with the generally accepted increments for non-ionic surfactants [1, 87]. For the oxyethylated non-ionic surfactants (C_nEO_8, line 5) $\Delta G^0_{CH_2} = -2.86$ kJ/mol, and for the oxyethylated ionic surfactants ($C_nEO_2SO_4Na$, line 6) we have $\Delta G^0_{CH_2} = -3.3$ kJ/mol. These values coincide with the results presented for ordinary surfactants, but ΔG^0_P for oxyethylated surfactants is higher than for ordinary surfactants (−10.9 kJ/mol and −7.8 kJ/mol for C_nEO_8 and $C_nEO_2SO_4Na$ respectively). Therefore, with increasing number of EO groups, the absolute value of the increment of free energy of adsorption of the polar group becomes higher.

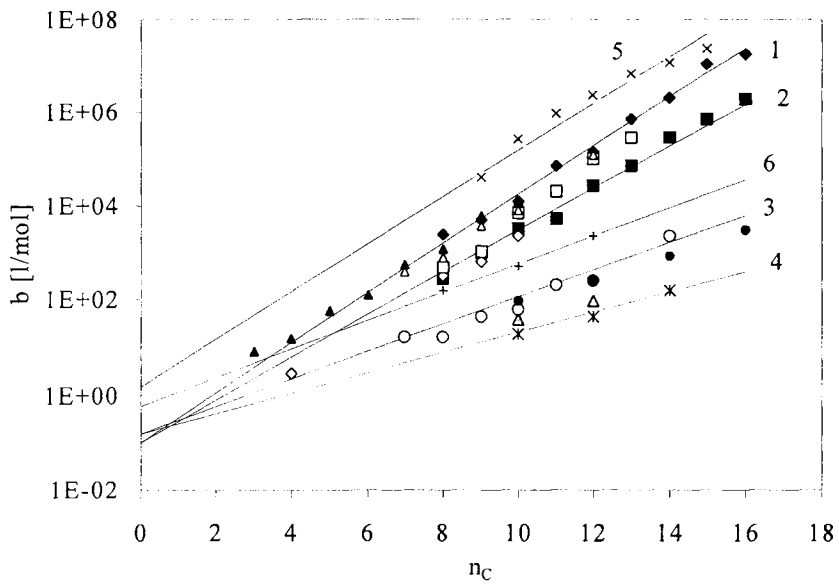

Fig. 3.61. The same as in Fig. 3.60, theoretical lines were calculated from Eq. (3.26) with $\Delta G^0_P = -4.25$ kJ/mol.

From these results, considered together with the lg(b) dependencies on m for C_8EO_8 and Tritons, presented in Figs. 3.35 and 3.38, and the data for $C_nEO_mSO_4Na$ shown in Fig. 3.49, it is possible to estimate the contribution of the EO groups into the increment of free energy of adsorption of the polar group ΔG_P^0. It is seen from these data that the dependence of this contribution on the oxyethylene groups number m is non-linear, cf. Fig. 3.38. The best fit of all experimental results available for C_nEO_m, Tritons and $C_nEO_mSO_4Na$ in the m range from 1 to 30 is given by the lg(b) *vs* m^x dependence with $x \cong 0.5$. Therefore, in addition to the increment −4.25 kJ/mol associated with the polar groups, common for all surfactants (for oxyethylated surfactants this value is constituted by the difference $\Delta G_{CH_3}^0 - \Delta G_{CH_2}^0$, the contribution due to the adsorption of a hydroxyl (for C_nEO_m) or sulphate (for $C_nEO_mSO_4Na$) group, and other unknown items), the additional contribution by m oxyethylene groups should be accounted for as $\Delta G_{EO_m}^0 = -2.35m^{1/2}$ [kJ/mol]. The values calculated via the relationship $\Delta G_P^0 = -(4.25 + 2.35m^{1/2})$ kJ/mol are $\Delta G_P^0 = -10.9$ kJ/mol for C_nEO_8, and $\Delta G_P^0 = -7.6$ kJ/mol for $C_nEO_2SO_4Na$, which are in a perfect agreement with the results obtained from the experimental dependencies lg(b) vs n_C in Fig. 3.61 and Eq. (3.26).

Thus, from Eq. (3.26) and the increment values summarised above it is possible to predict the constant b, if the nature of the surfactant molecule and the hydrocarbon chain length are given. It should be noted that the experimental values of the increments $\Delta G_{CH_2}^0$ for various ionic and non-ionic surfactants are scattered in a quite narrow range (±10%), and the ΔG_P^0 value (=−4.25 kJ/mol) is independent of the type of the polar group and the nature of the non-oxyethylated surfactant. The additional contribution by m EO groups can be accounted for by $\Delta G_{EO_m}^0 = -2.35m^{1/2}$ [kJ/mol]..

At the same time, for this deviation from the mean increment, the uncertainty in the standard free energy of adsorption at $n_C = 10$ becomes approximately equal to the increment $\Delta G_{CH_2}^0$. Thus, the constant b calculated from Eq. (3.26) and the mean increments can differ from its correct value by a factor of 3 for non-ionic surfactants, and by a factor of 1.8 for ionic surfactants. For higher n_C numbers this uncertainty can be even larger. The exact values of the increments $\Delta G_{CH_2}^0$ and ΔG_P^0 calculated using the least squares method from experimental

dependencies b *vs* n_C, shown in Fig. 3.60, and Eq. (3.26) are listed for all the surfactants studied in Table 3.24.

As one can see the Frumkin model does not reflect all the details of the adsorption process. In some cases, the reorientation and aggregation models lead to better results. The scope of the data available is still insufficient to formulate a criterion for the best choice of the adsorption model. However, it follows from the results summarised in this chapter, that the reorientation model can be successfully applied to oxyethylated surfactants, and also for surfactants with relatively large molar area ($\omega > 2.5 \cdot 10^5$ m^2/mol). At the same time, the surfactant molecules with relatively high values of the Frumkin constant and low molar area ($\omega < 2.5 \cdot 10^5$ m^2/mol) are more capable for aggregation in the surface layer.

Table 3.24. The values of increments $\Delta G^0_{CH_2}$ and ΔG^0_P for various surfactants.

Surfactants	n	$\Delta G^0_{CH_2}$, kJ/mol	ΔG^0_P, kJ/mol
C_nOH	4-10	–2.82	–5.2
$C_n(OH)_2$	4-10	–2.75	–1.56
C_nO_2H	7-12	–2.88	–3.78
C_nDMPO	8-16	–3.0	–3.97
C_nBHB	8-16	–2.78	–1.56
C_nPIP	8-13	–3.2	1.47
C_nEO_8	9-15	–2.86	–10.9
C_nO_2Na	10-14	–2.68	–0.17
C_nSO_4Na	7-12	–3.17	–1.8
$C_nEO_2SO_4Na$	8-12	–3.3	–7.8
C_nTAB	10-16	–2.88	–3.2
C_nACl	10-12	–2.6	–4.0

3.6. Mixtures of non-ionic surfactants

It was shown in the previous section that Frumkin's model is the most general capable for the description of the adsorption behaviour of surfactants of different nature. Therefore this model is expected to be applicable to mixtures. The equation of state for a non-ideal (in the

framework of the regular two-dimensional solution theory) surface layer and the adsorption isotherm equations for two non-ionic surfactants were derived in Chapter 2. As the DEL contribution in the electroneutral surface layer model is included in the Frumkin constant, Eqs. (2.31) and (2.32) can be used to describe the mixture of one non-ionic surfactant with one ionic surfactant as well. In the next section we will also consider the mixture of two ionic surfactants. For the present case, the appropriate set of equations reads

$$\Pi = -\frac{RT}{\omega_0}\left[\ln(1-\theta_1-\theta_2)+\theta_1\left(1-\frac{1}{n_1}\right)+\theta_2\left(1-\frac{1}{n_2}\right)+a_1\theta_1^2+a_2\theta_2^2+2a_{12}\theta_1\theta_2\right], \quad (3.27)$$

$$b_1c_1 = \frac{\theta_1}{(1-\theta_1-\theta_2)^{n_1}}\exp(-2a_1\theta_1-2a_{12}\theta_2)\cdot\exp\left[(1-n_1)(a_1\theta_1^2+a_2\theta_2^2+2a_{12}\theta_1\theta_2)\right], \quad (3.28)$$

$$b_2c_2 = \frac{\theta_2}{(1-\theta_1-\theta_2)^{n_2}}\exp(-2a_2\theta_2-2a_{12}\theta_1)\cdot\exp\left[(1-n_2)(a_1\theta_1^2+a_2\theta_2^2+2a_{12}\theta_1\theta_2)\right]. \quad (3.29)$$

Here $\theta_i = \Gamma_i\omega_i$ is the monolayer coverage, Γ_i is the adsorption, $\Pi = \gamma_0 - \gamma$ is the surface pressure, γ_0 is the surface tension of solvent, $n_i = \omega_i/\omega_0$, ω_i and ω_0 are the partial molar surface areas of the surfactant and solvent, respectively, b_i is the adsorption constant, c_i is the surfactants concentration in the solution bulk. The Frumkin parameters a_1 and a_2 represent the interactions of components 1 and 2 with the solvent, while the parameter a_{12} accounts for interactions between the two surfactants 1 and 2 in the ternary regular mixture (see Eq. 2.32): $a_1 = H_{01}^s/RT; a_2 = H_{02}^s/RT; a_{12} = (H_{01}^s + H_{02}^s - H_{12}^s)/2RT$, where H_{ij}=A_{ij}RT. Choosing the dividing surface after Lucassen-Reynders (cf. Chapter 2), one can eliminate the contributions from the entropic non-ideality of the solvent, thus reducing Eq. (3.27) to a much simpler form

$$\Pi = -\frac{RT}{\omega}\left[\ln(1-\theta_i-\theta_2)+a_1\theta_1^2+a_2\theta_2^2+2a_{12}\theta_1\theta_2\right], \quad (3.30)$$

where

$$\omega = \frac{\omega_1\Gamma_1+\omega_2\Gamma_i}{\Gamma_1+\Gamma_2}. \quad (3.31)$$

Note that, while the choice of the dividing surface after Lucassen-Reynders does not affect the form of the adsorption isotherm, Eqs. (3.28) and (3.29), the values of n_i are now given by $n_i = \omega_i/\omega$. To apply Eqs. (3.28)-(3.31), one needs to have information about the adsorption characteristics of the individual surfactants (b_i, a_i, ω_i).

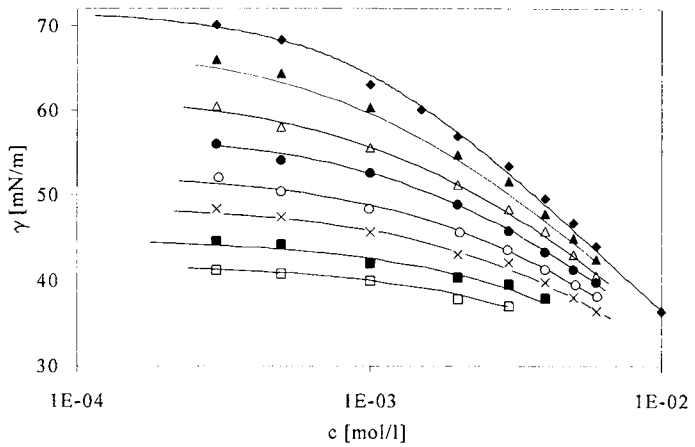

Fig. 3.62. Dependencies of surface tension for 1-heptanol solution at various concentrations of 1-octanol: (◆) 0, (▲) 0.2, (△) 0.4, (●) 0.6, (O) 0.9, (×) 1.2, (■) 1.6, (□) 2.0 mmol/l; theoretical isotherms for individual solutions were calculated from the Frumkin equation (3.1)-(3.2): for 1-heptanol $\omega_i = 1.72 \cdot 10^5$ m^2/mol, $a_i = 0.86$ and $b_i = 4.75 \cdot 10^2$ l/mol; for 1-octanol $\omega_i = 1.75 \cdot 10^5$ m^2/mol, $a_i = 1.15$ and $b_i = 1.27 \cdot 10^3$ l/mol; theoretical curves for mixtures calculated from Eqs. (3.28)-(3.31) with $a_{12} = 1.0$; data reported in [20].

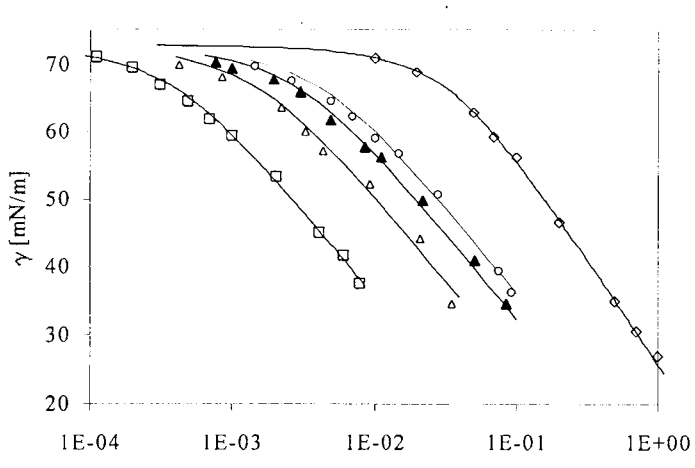

Fig. 3.63. Surface tension isotherms for $C_{12}SO_4Na$ (◇), 1-butanol (□) and their mixtures with ratios 1:2.89 (△), 1:6.81 (▲) and 1:10.63 (O); theoretical isotherms for individual solutions calculated from the Frumkin equation (3.1)-(3.2): for $C_{12}SO_4Na$ $\omega_i = 2.2 \cdot 10^5$ m^2/mol, $a_i = 0.6$ and $b_i = 1.485 \cdot 10^3$ l/mol; for 1-butanol $\omega_i = 1.7 \cdot 10^5$ m^2/mol, $a_i = 0.74$ and $b_i = 12.93$ l/mol; theoretical curves for mixtures calculated from Eqs. (3.28)-(3.31) with $a_{12} = 0.67$; data reported in [22].

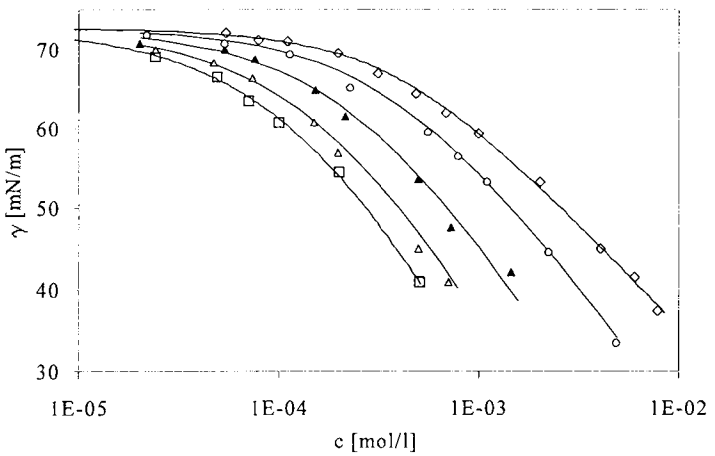

Fig. 3.64. Surface tension isotherms for 1-nonanol (◇), $C_{12}SO_4Na$ (□) and their mixtures with ratios 2:1 (△), 1:2 (▲) and 1:9 (○); theoretical isotherms for individual solutions calculated from the Frumkin equation (3.1)-(3.2): for $C_{12}SO_4Na$ - see Fig. 3.63; for 1-nonanol $\omega_i = 1.7 \cdot 10^5$ m^2/mol, $a_i = 0.8$ and $b_i = 7.74 \cdot 10^3$ l/mol; theoretical curves for mixtures calculated from Eqs. (3.28)-(3.31) with $a_{12} = 0.7$; data reported in [221.

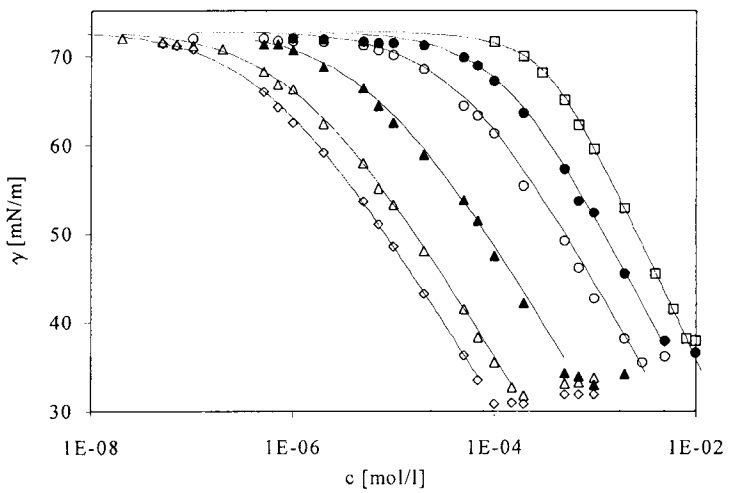

Fig. 3.65. Surface tension isotherms for $C_{10}EO_5$ (◇), $C_{12}SO_4Na$ in 0.01M NaCl (□) and their mixtures in 0.01M NaCl with ratios 1:1 (△), 1:10 (▲), 1:100 (○) and 1:500 (■); theoretical isotherms for individual solutions calculated from the Frumkin equation (3.1)-(3.2): for $C_{10}EO_5$ $\omega_i = 3.32 \cdot 10^5$ m^2/mol, $a_i = 0.0$ and $b_i = 2.823 \cdot 10^6$ l/mol; for $C_{12}SO_4Na$ in 0.01M NaCl $\omega_i = 2.24 \cdot 10^5$ m^2/mol, $a_i = 0.95$ and $b_i = 1.135 \cdot 10^3$ l/mol; theoretical curves for mixtures calculated from Eqs. (3.28)-(3.31) with $a_{12} = 1.1$; data reported in [41].

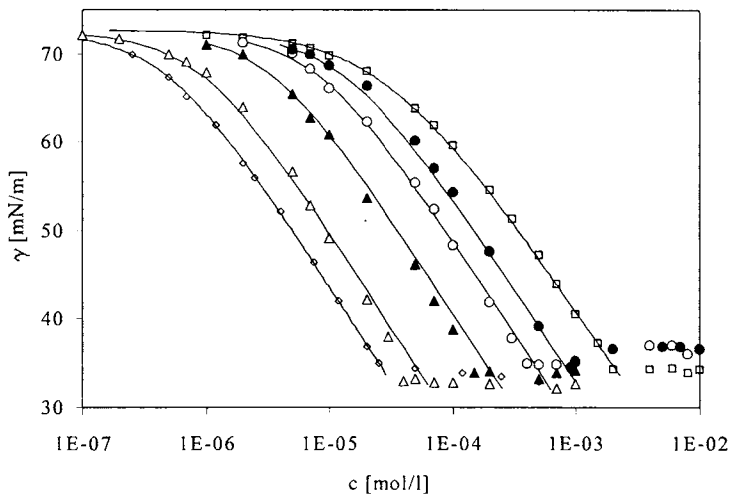

Fig. 3.66. Surface tension isotherms for C_{16}BHB (◇), C_{12}BHB (□) and their mixtures with ratio 1:1 (△), 1:9 (▲), 1:30 (O) and 1:80 (■); theoretical isotherms for individual solutions calculated from the Frumkin equation (3.1)-(3.2): for C_{12}BHB $\omega_i = 2.63 \cdot 10^5$ m^2/mol, $a_i = -0.2$ and $b_i = 3.49 \cdot 10^4$ l/mol; for C_{16}BHB $\omega_i = 2.65 \cdot 10^5$ m^2/mol, $a_i = 0.75$ and $b_i = 1.05 \cdot 10^6$ l/mol; theoretical curves for mixtures calculated from Eqs. (3.28)-(3.31) with $a_{12} = 0.7$; data reported in [41].

If no specific interaction exists between the molecules of different species, we can approximately assume $a_{12} = (a_1 + a_2)/2$. To calculate the surface pressure and adsorption of a mixture from the individual solution parameters, and to estimate the value of a_{12} by fitting to experimental data, the NonIonMix utility was developed which is briefly explained in Chapter 7. In the following some results are presented which were obtained using this fitting tool. Figures 3.62 to 3.66 illustrate experimental results for some surfactant mixtures, as reported in [20, 22, 41].

All systems shown in these figures can be perfectly described by the model defined by Eqs. (3.28)-(3.31) which supports this theoretical model based on Butler's equation for the chemical potentials of the surface layer, and the regular solution theory. In addition, this agreement is due to the certain choice of the dividing surface after Lucassen-Reynders, and to the fact that Eq. (3.31) was used to calculate the mean molar area of the surfactants mixture. It is important to note that in some cases (for mixtures of normal alcohols, Fig. 3.62, and mixtures of sodium dodecyl sulphate ($C_{12}SO_4Na$) with 1-butanol and 1-nonanol, Figs. 3.63 and

3.64) the value a_{12} was quite close to the arithmetic average $a_{12} = (a_1 + a_2)/2$. However, for other systems (mixture of $C_{10}EO_5$ with $C_{12}SO_4Na$ in 0.01 M NaCl, Fig. 3.65, and mixture of betain homologues $C_{12}BHB + C_{16}BHB$, Fig. 3.66) it was found that $a_{12} > (a_1 + a_2)/2$. However, the differences in the a_{12} values calculated from the best fit between the experimental results, and from additivity are quite small. Hence, it can be suggested that in practice the model given by Eqs. (3.28)-(3.31) can be used with $a_{12} = (a_1 + a_2)/2$.

It will be demonstrated below that much simpler theoretical models, which additionally account for processes actually taking place in the adsorption layer, can be used instead of the complicated set of Eqs. (3.28)-(3.31) with $a_{12} = (a_1 + a_2)/2$. Moreover, the use of these models does not require any preliminary consideration of isotherms of individual solutions, but rather involves information about the surface tension at certain surfactant concentrations.

3.7. Mixtures of ionic surfactants

The adsorption behaviour of mixtures of ionic surfactants is essentially different from that of non-ionic ones, because

(i) the counterions of one surfactant increase the adsorption activity of the second surfactant due to increase of the mean ionic product,

(ii) according to Eq. (3.21) the introduction of additional ions to the solution affects the mean activity coefficient of all ions.

The adsorption behaviour of mixtures of surfactants possessing surface active ions with equal or opposite charges was discussed in Chapter 2 and in the recent review [88]. Here we present the principal equations for such systems and some examples of experimental data.

3.7.1. Mixtures of surfactants of same charge

In the mixture of two anionic (or cationic) surfactants (for example ionic homologues R_1X and R_2X with the common counterion X^+) with addition of inorganic electrolyte XY the counterion concentration X^+ is given by the sum of concentrations of R_1X, R_2X and XY. For simplicity, the molar areas of the two homologues are assumed to be roughly the same: $\omega_{R1X} \cong \omega_{R2X} \cong \omega = 2\omega_0$, therefore the second exponential terms in the corresponding adsorption isotherms, see Eqs. (3.28) and (3.29) for non-ionic surfactants, can be omitted, and the small difference in the molar areas of the homologues can be included into the surface pressure

calculation via Eq. (3.31). The surface equation of state for a Frumkin-type non-ideality of such a mixed system is found by considering the distribution of the solvent and evaluating f_0^s from the ternary regular mixture model [88]

$$\Pi = -\frac{2RT}{\omega}\left[\ln(1-\theta_1-\theta_2)+a_1\theta_1^2+a_2\theta_2^2+2a_{12}\theta_1\theta_2\right]. \tag{3.32}$$

As in the binary system, $\theta_0 = x_0^s$, but for the ionic solutes $\theta_1 = 2x_1^s$ and $\theta_2 = 2x_2^s$. In Eq. (3.32) the factor 2 can be omitted when the molar area of the ions ω_I is introduced instead of ω. After consideration of the surface-to-bulk distribution of both electroneutral combinations of ions, we arrive at the equation for the adsorption isotherm of the two surfactants R_1X and R_2X, respectively

$$b_1 f_\pm (c_{R_1} c_X)^{1/2} = \frac{((\theta_1(\theta_1+\theta_2))^{1/2}}{1-(\theta_1+\theta_2)} \exp(-2a_1\theta_1 - 2a_{12}\theta_2), \tag{3.33}$$

$$b_2 f_\pm (c_{R_2} c_X)^{1/2} = \frac{((\theta_2(\theta_1+\theta_2))^{1/2}}{1-(\theta_1+\theta_2)} \exp(-2a_2\theta_2 - 2a_{12}\theta_1). \tag{3.34}$$

When we restrict ourselves to the case of ideal surface layers ($a_1 = a_2 = a_{12} = 0$) we obtain the surface pressure isotherm (2.48). Eqs. (3.33), (3.34) and (2.48) show that the presence of inorganic counterions in solutions of ionic surface active homologues increases the adsorption activity of the ionic surfactants more than additively, in contrast to what is observed for non-ionic surfactant mixtures (see Eqs. (3.28)-(3.29)). To calculate the surface tension and the adsorption of the mixture of ionic homologues from the parameters found for individual solutions, and to determine the value of a_{12} from experimental data for the mixture of two homologues, the program IonMix was developed as described in Chapter 7.

Figure 3.67 shows the comparison between the experimental [68] and theoretical values of Π for mixtures of $C_{10}SO_4Na$ and $C_{12}SO_4Na$ assuming the specific interaction parameter H_{12} =0. Similarly, Figure 3.68 illustrates that the experimental data [33] for mixtures of decyl ammonium chloride ($C_{10}ACl$) and dodecyl ammonium chloride ($C_{12}ACl$) are very well described by Eqs. (3.31)-(3.34), again with H_{12}=0, over a broad range of surface compositions.

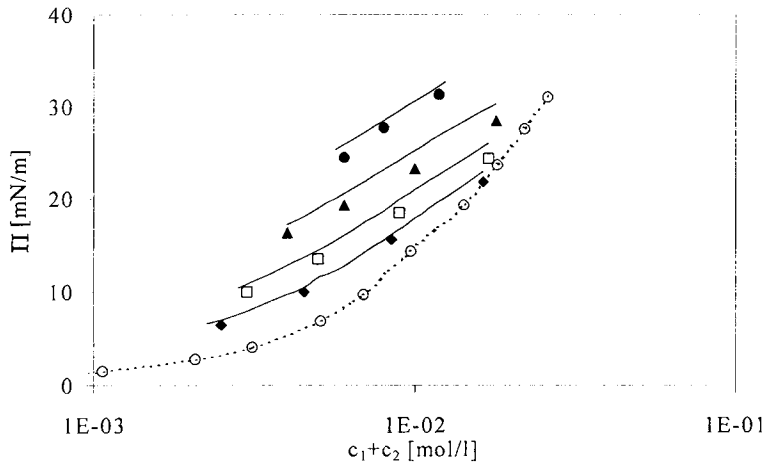

Fig. 3.67. Surface pressure *vs* total concentration $c = c_1 + c_2$ for mixtures of $C_{10}SO_4Na$ (1) and $C_{12}SO_4Na$ (2) at concentrtions of $C_{12}SO_4Na$: (○) 0.0; (◆) 0.5; (□) 1.0; (▲) 2.0 and (●) 4.0 mmol/l, experiments points from [68] and [67], solid lines – calculated from Eqs. (3.31)-(3.34) for parameters of Table 3.17 and $H_{12} = 0$ ($a_{12}=(a_1+a_2)/2$).

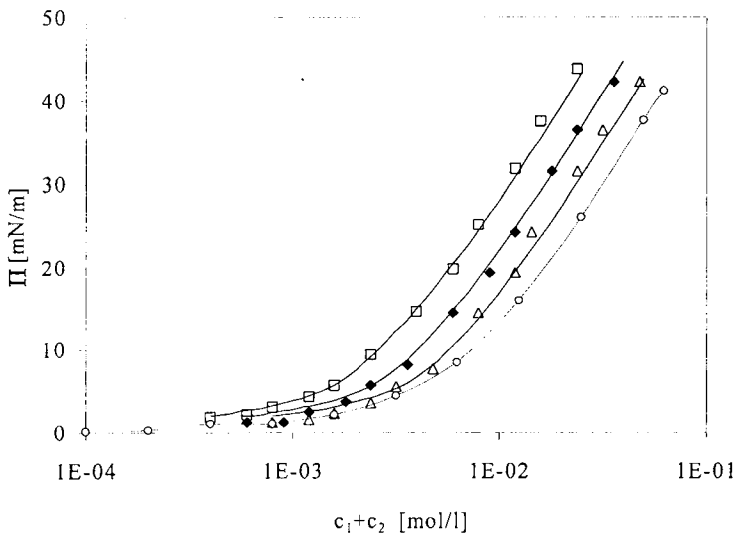

Fig. 3.68. Surface pressure *vs* concentration $c = c_1 + c_2$ for mixtures of $C_{10}ACl$ (1) and $C_{12}ACl$ (2) in 5 mmol/l HCl at 20 °C, experiments according to [33], $c_2=0$ (○); $c_1/c_2=15$ (△); 5 (◆) and 1.67 (□), solid lines calculated from Eqs. (3.31)-(3.34) for parameters of Table 3.22 and $H_{12}=0$ ($a_{12}=(a_1+a_2)/2$).

It may be concluded that the theory presented for single ionic surfactants can be extended to predict the surface properties of mixed ionic surfactant solutions from the characteristic parameters of the single surfactants.

3.7.2. Mixtures of anionic and cationic surfactants

Very large effects on adsorption and surface pressure have been described for mixtures of anionic RX (R^-X^+) and cationic RY (R^+Y^-) surfactants [88]. For example, in mixtures of $C_{12}SO_4Na$ and $C_{12}TAB$ the surface pressure increased from less than 1 mN/m to about 40 mN/m after mixing the two single-surfactant solutions at a constant total concentration of 0.03 mmol/l [89]. The surface pressure is determined not just by the adsorption of the long-chain ions, but by the total adsorption of all ions: $\Gamma_t = \Gamma_{R^+} + \Gamma_{Br^-} + \Gamma_{Na^+} + \Gamma_{R^-}$, where the electroneutrality condition prescribes $\Gamma_{R^+} + \Gamma_{Na^+} = \Gamma_{Br^-} + \Gamma_{R^-}$. In the single-surfactant monolayers, both inorganic ions are adsorbed as counterions to satisfy the electroneutrality condition, but in the mixed monolayer neither is required any more since the long-chain ions on their own can ensure electroneutrality. Consequently, sodium and bromide ions can and will be desorbed from the surface mixture. However, transfer of NaBr from the surface to the solution is not the only effect of mixing. We can also expect considerable transfer of the new electroneutral combination, R^+R^-, from the solution to the surface. In the above example of the C_{12} mixture, the effect of R^+R^- adsorption is very much larger than that of NaBr desorption. The adsorption isotherms of all electroneutral combinations are governed by the surface-to-solution distribution coefficients b_{jk}. In cationic/anionic mixtures, these are interrelated by

$$b_{R^+Y^-} b_{R^-X^+} = b_{R^+R^-} b_{X^+Y^-} \tag{3.35}$$

since bringing the four ions from their standard solution state to that in the surface involves the same amounts of energy regardless of whether they are considered to go as R^+Y^- and X^+R^- or as R^+R^- and X^+Y^- [88, 90]. It has been suggested [68] that the value of b for the double-chain salt can be approximated by

$$b_{R^-R^+} = \left(b_{RX} b_{RY}\right) / V, \tag{3.36}$$

where V is the average molar volume of the surfactants in the surface layer, and the assumption was made that the volume concentration of the inorganic salt XY in the surface layer is roughly

the same as in the bulk solution. If one ionic combination has a very low surface activity, e.g, $b_{XY} << (b_{RY} \cdot b_{RX})^{1/2}$, then the surface activity of the salt R^+R^- must be very high, i.e., $b_{RR} >> (b_{RY} \cdot b_{RX})^{1/2}$. In $C_{12}SO_4Na/C_{12}TAB$ surface layers there will not only be desorption of NaBr but also strong additional adsorption of the new combination R^+R^- because of the high value of $b_{R^+R^-}$. This is confirmed by the experimental surface mixing ratios of anionic and cationic, which generally has been found to be 1:1 over a wide range of mixing ratios in the solution bulk [89, 91, 92]. Figure 3.69 presents measurements on sodium dodecyl sulphate (Na^+R^-) and dodecyl trimethyl ammonium bromide (R^+Br^-) and their mixtures, with bulk mixing ratios c_{RBr}/c_{NaR} ranging from 1/64 to 8/1.

All mixture data in Figure 3.69 merge to a single curve for R^+R^- when plotted as a function of the ionic product of the three electroneutral combinations. In such mixtures, the adsorption is represented almost completely by the equimolar composition R^-R^+, which has a very high surface activity, without any noticeable contribution of Na^+R^- and R^+Br^- over the entire range of mixing ratios [89]. Thus one can describe the surface tensions of the mixtures by Eq. (3.1) combined with an isotherm equation for R^+R^-:

$$b_{R^+R^-}\left(c_{R^+}c_{R^-}\right)^{1/2} = \frac{\theta_{R^+R^-}}{1-\theta_{R^+R^-}} \exp\left(-2a_{R^+R^-}\theta_{R^+R^-}\right) \tag{3.37}$$

without any consideration of electric double layer effects.

The surface-to-solution distribution coefficient b for the composition R^-R^+ is $6.25 \cdot 10^4$ l/mol, i.e., approximately 300 times higher than the constants $b_{Na^+R^-}$ and $b_{R^+Br^-}$ in the individual solutions. It is worth noting that the relationship (3.36) yields an estimate of $8.8 \cdot 10^4$ l/mol for $b_{R^-R^+}$ if we use the reasonable value V = 0.5 l/mol for the average molar volume of Na^+R^-, R^+Br^- and the double-chain salt R^-R^+, in fair agreement with the experiments in Figure 3.69 interpreted by Eq. (3.37). The solvent-surfactant interaction parameter, $a_{R^+R^-}$, is also considerably larger than in the individual solutions. We suggest that this is mainly due to higher inter-chain cohesion in the double-chain compound. Together, the differences in the parameters b and a shift the curve for R^+R^- by 3 orders of magnitude to lower concentrations, as shown in Figure 3.69. The mixtures of the anionic surfactant with several cationic surfactants were studied in [93]. The surface tension isotherms obtained in [93] also indicate

the formation of double-chain salts R^-R^+ in the surface layer, however, these data were not discussed by the authors in the framework of the model defined by Eq. (3.37). The increased adsorption of R^+R^- implies a gigantic increase of surface pressure upon mixing cationic and anionic solutions at constant total concentration. This is illustrated by Figure 3.70.

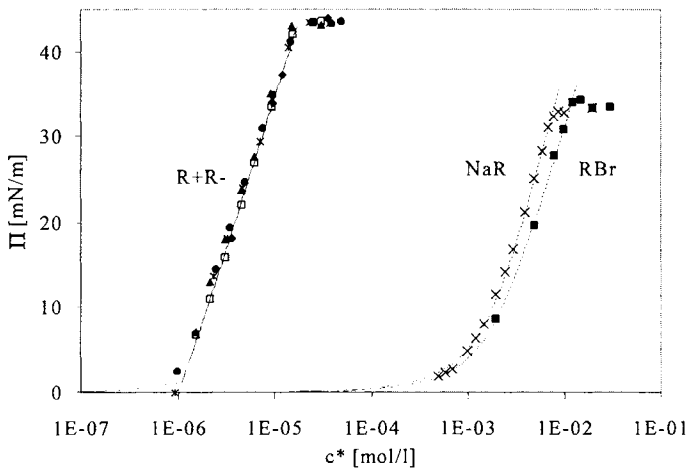

Fig. 3.69. Surface pressure *vs* mean ionic product c* at 25 °C,: experiments according to [89], mixing ratios c_{R^+}/c_{R^-} = 0/1; 1/64; 1/8; 1/2; 1/1; 8/1; 1/0, solid lines: theory for regular surface behaviour, Eqs (3.1) and (3.37), parameter for Na^+R^-: RT/ω_I= 20 mN/m; b=2.2·10^2 l/mol; a=1, for R^+Br^-: RT/ω_I= 17 mN/m; b=2.1·10^2 l/mol; a=1, For R^+R^-: RT/ω_I= 17 mN/m; b=6.25·10^4 l/mol; a=2.5.

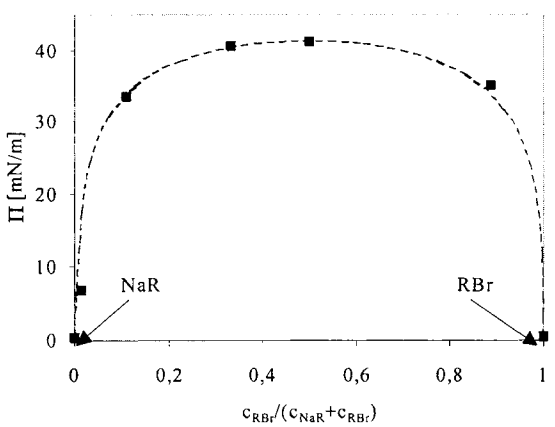

Fig. 3.70. Mixtures of sodium dodecyl sulphate (Na^+R^-) and dodecyl trimethyl ammonium bromide (R^+Br^-), at constant total concentration of 0.03 mmol/l, experiments according to [89], solid line - theory for adsorption of R^+R^- and desorption of NaBr.

The theoretical line in Figure 3.70 reflects the variations in the ionic product of R^+ and R^- in the solution, it says however nothing about any surface interactions of R^+R^- with either Na^+R^- or R^+Br^-, because inorganic ion adsorption is negligible at the chosen low total concentration. At higher total concentrations, the increase in ω is smaller than in Figure 3.70, since ω can no longer increase once micellisation of the R^+R^- salt sets in (cf. the constant value of ω in Fig. 3.69).

3.8. Simple model for mixed surfactant solutions

First, an exact expression should be derived which gives a relationship between the surface pressure of a surfactant mixture and the surface pressure of the individual solutions. For an ideal ($a_1 = a_2 = a_{12} = 0$) mixture of homologues ($\omega = \omega_1 = \omega_2$), Eq. (3.27) can be rewritten in the form of a generalised von Szyszkowski equation

$$\Pi = \frac{RT}{\omega}\ln\left(\frac{\theta_1}{1-\theta_1-\theta_2} + \frac{\theta_2}{1-\theta_1-\theta_2} + 1\right) = \frac{RT}{\omega}\ln\left(b_1c_1 + b_2c_2 + 1\right). \tag{3.38}$$

Using the corresponding equations for the individual surfactants 1 and 2 (in the following the subscript 0 refers to the individual solution),

$$\Pi_i = -\frac{RT}{\omega}\ln\left(1-\theta_{0i}\right) = \frac{RT}{\omega}\ln\left(1+b_ic_i\right), \tag{3.39}$$

$$b_ic_i = \frac{\theta_{0i}}{\left(1-\theta_{0i}\right)}, \tag{3.40}$$

and substituting the terms b_ic_i in Eq. (3.38) by the corresponding products from Eqs. (3.39), one can express the equation of state (3.38) as [94]

$$\exp\overline{\Pi} = \exp\overline{\Pi}_1 + \exp\overline{\Pi}_2 - 1, \tag{3.41}$$

where $\overline{\Pi} = \Pi\omega/RT$, $\overline{\Pi}_1 = \Pi_1\omega/RT$ and $\overline{\Pi}_2 = \Pi_2\omega/RT$ are dimensionless surface pressures of the mixture and individual solutions of components 1 and 2, respectively, at identical surfactant concentrations as in the mixture.

The use of Eq. (3.41) would require only the knowledge of one pair of experimental surface pressure (tension) of individual solutions. The only parameter of the isotherm in Eq. (3.41), the molar area ω, can be either calculated from the molecular geometry of the surfactant, or

determined experimentally from the limiting slope of the γ *vs* lnc curve for the individual surfactant (slope of the surface tension isotherm near the CMC or solubility limit). Moreover, it was shown in [94] that calculations according to Eq. (3.41) are quite insensitive with respect to the choice of ω. Therefore for estimation one can assume that this parameter is equal to the value typical for the surfactant type considered, e.g., $(1.2 \div 2.5) \cdot 10^5$ m^2/mol for fatty alcohols, acids and most anionic and cationic surfactants.

In the subsequent sections more complicated mixtures of surfactants, characterised by intermolecular interactions, different molar areas of the components, mixtures of ionic surfactants and other systems are considered.

3.8.1. Non-ideal mixture of homologues

The equation of state and adsorption isotherm for a non-ideal surface layer of two surfactants with the same molar areas are Eq. (3.30) and

$$b_i c_i = \frac{\theta_i}{\left(1-\theta_1-\theta_2\right)} \exp\left(-2a_i\theta_i - 2a_{12}\theta_j\right). \tag{3.42}$$

It can be shown that Eq. (3.41) can be used also for the approximate description of non-ideal mixtures of surfactants. Π in Eq. (3.30) can be expressed via the terms $b_i c_i$ using the isotherms (3.42). These products can in turn be expressed via the Π_i values for individual solutions using Eqs. (3.1) and (3.2). This leads to a (dimensionless) equation of state for a mixed surface layer

$$\exp\overline{\Pi} = k_1 \exp\overline{\Pi}_1 + k_2 \exp\overline{\Pi}_2 - k_3. \tag{3.43}$$

Here $k_1 = \exp\left[a_1(\theta_{01}^2 - \theta_1^2 + 2\theta_1 - 2\theta_{01}) - a_2\theta_2^2\right]$, $k_2 = \exp\left[a_2(\theta_{02}^2 - \theta_2^2 + 2\theta_2 - 2\theta_{02}) - a_1\theta_1^2\right]$ and $k_3 = \exp(2a_1\theta_1 - a_1\theta_1^2 - a_2\theta_2^2) + \exp(2a_2\theta_2 - a_1\theta_1^2 - a_2\theta_2^2) - \exp(-a_1\theta_1^2 - a_2\theta_2^2)$, the subscript 0 refers to the coverage for the individual solution. Equation (3.43) and the expressions for k_i given above were obtained from Eqs. (3.30) and (3.42) and $a_{12} = 0$. If the more correct expression $a_{12} = (a_1 + a_2)/2$ is introduced, then the resulting equation has also the form of Eq. (3.43), but the expressions for k_i become more cumbersome. Analysing the values of k_i it becomes evident that the signs of the terms in the expression are opposite, and, assuming only small deviations from ideality, one obtains the approximation $k_1 \cong k_2 \cong k_3 \cong 1$. It should be noted that if the requirement $a_{12} = (a_1 + a_2)/2$ is imposed, all coefficients k_i are also

approximately equal to 1. Therefore, Eq. (3.43) which describes a non-ideal surface layer can be approximately transformed into Eq. (3.41) derived for an ideal mixture of homologues. Note that for ideal surface layers, as $a_1 = a_2 = 0$ and thus $k_1 = k_2 = k_3 = 1$, Eq. (3.43) coincides exactly with Eq. (3.41). In Figs. 3.71 and 3.72 the experimental surface tension isotherms for mixtures of homologues of normal alcohols and betains, respectively, are compared with values calculated from Eq. (3.41).

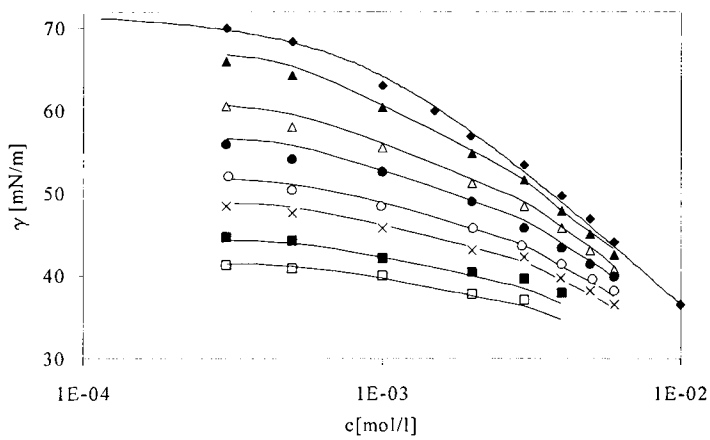

Fig. 3.71. The same as in Fig. 3.62, theoretical curves for mixtures are calculated from Eq. (3.41).

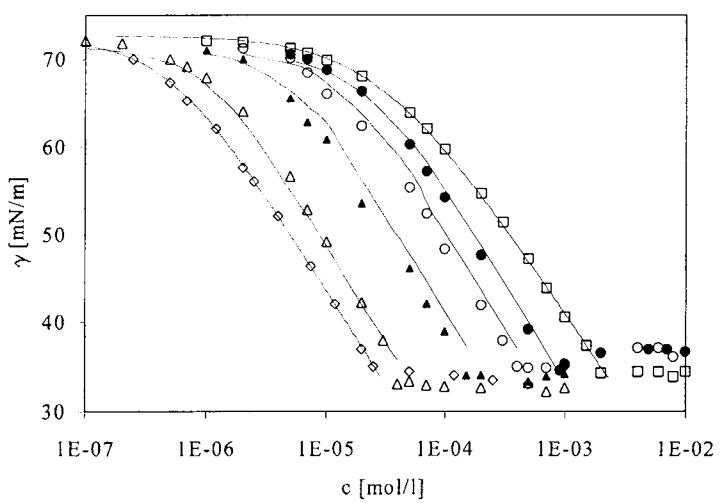

Fig. 3.72. The same as in Fig. 3.66, theoretical curves for mixtures are calculated from Eq. (3.41).

Both systems exhibit good agreement. For the mixtures of 1-heptanol with 1-octanol (Figs. 3.62 and 3.71) and mixtures of C_{12}BHB with C_{16}BHB (Figs. 3.66 and 3.72) theoretical calculations were performed using both the exact and approximate models. The comparison of the corresponding results shows that the difference between the two models is rather insignificant.

3.8.2. Mixture of ionic homologues

Mixtures of an ionic and a non-ionic surfactant are quite similar to those considered above, because the contribution of the DEL to the surface pressure for an ionic surfactant can be treated approximately as a non-ideality factor. If the solution of individual ionic surfactants and their mixtures are studied at a fixed ionic strength (which is usually accomplished by addition of an indifferent electrolyte), then the surface pressure of a mixed solution, similarly to non-ionic surfactants, is calculated from the data obtained for individual solutions according to Eq. (3.41).

Mixtures of ionic surfactants at any arbitrary ionic strength can be satisfactorily described by the Frumkin equation of state and isotherm if the electroneutral combination of the corresponding ions is considered. In a mixture of two anionic (or cationic) surfactants the counterion concentration X^+ is given by the sum of the concentrations of R_1X, R_2X and XY. For an ideal surface layer ($a_1 = a_2 = a_{12} = 0$) it follows from Eqs. (3.32)-(3.34) that:

$$\Pi = \frac{2RT}{\omega} \ln\left[\left((b_1 f_{1\pm})^2 c_{R_1X} c_{X^-} + (b_2 f_{2\pm})^2 c_{R_2X} c_{X^-}\right)^{1/2} + 1\right]. \tag{3.44}$$

where ω is the molar area of the ionic surfactant. The surface pressure of the solution of an individual ionic surfactant R_iX (with or without addition of an indifferent electrolyte XY) obeys the equation

$$\Pi_i = \frac{2RT}{\omega} \ln\left[\left((b_i f_{i\pm})^2 c_{R_iX} c_{X^-}\right)^{1/2} + 1\right]. \tag{3.45}$$

Combining Eqs. (3.44) and (3.45), one obtains the expression which describes the surface tension of a mixed solution

$$\exp\overline{\Pi} = \left((\exp\overline{\Pi}_1 - 1)^2 + (\exp\overline{\Pi}_2 - 1)^2\right)^{1/2} + 1. \tag{3.46}$$

Unlike the cases of non-ionic surfactants or ionic surfactants in the presence of electrolyte excess, when calculations are made according to Eq. (3.41), one should choose the concentrations (activities) of the individual solutions such that the products of the concentrations of the corresponding surface-active ions and counterions in the individual solutions and in the mixture of surfactants are equal. For example, assuming that the R_1X concentration in the mixture is c_1, and the concentration of R_2X is c_2, then the surface pressure in the individual solutions should be determined for the concentrations $c_{01}=[c_1(c_1+c_2)]^{1/2}$ and $c_{02}=[c_2(c_1+c_2)]^{1/2}$, respectively. This means, the increase of the counterion concentrations in the surfactant mixture due to the addition of the second surfactant's counterion has to be taken into account. In a similar way the influence of small additions of indifferent electrolyte with a common counterion has also to be considered.

The account for the non-ideality of the components in the surface layer of an ionics mixture does not affect the form of Eq. (3.46). Thus, Eq. (3.41) in the case of counterion excess, and Eq. (3.46) in absence of indifferent electrolyte (and the correction of the concentrations in the individual solutions as described above) allow an approximate description of non-ideal mixtures of ionic surfactants with identical values of the molar areas of the components.

Figure 3.73 illustrates the surface pressure isotherms for $C_{12}SO_4Na$ and $C_{14}SO_4Na$ solutions and their 3:1 molar fraction mixture in presence of 0.03 M NaCl.

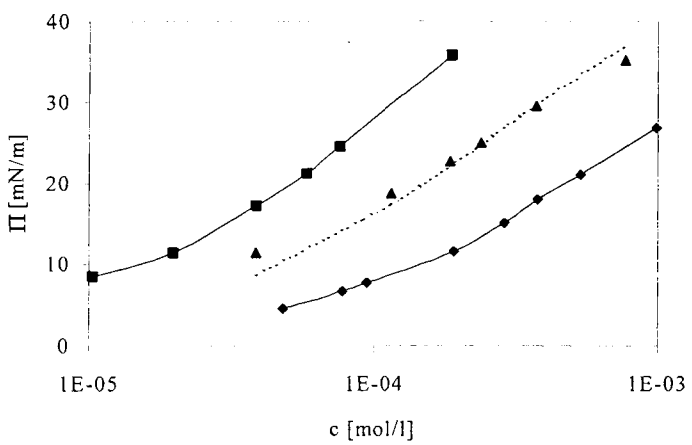

Fig. 3.73. Concentration dependences of surface pressure for $C_{12}SO_4Na$ (◆) and $C_{14}SO_4Na$ (■) solutions and their 3:1 (molar fractions) mixture (▲) in the presence of 0.03 M NaCl; theoretical values for the mixture calculated from Eq. (3.41); data reported in [70].

The theoretical calculations for the mixture performed with Eq. (3.41) are in perfect agreement with the experimental data. The dependence of surface pressure of aqueous sodium decyl sulphate ($C_{10}SO_4Na$) solutions for various additions of $C_{12}SO_4Na$ (without any addition of electrolyte) is shown in Fig. 3.74.

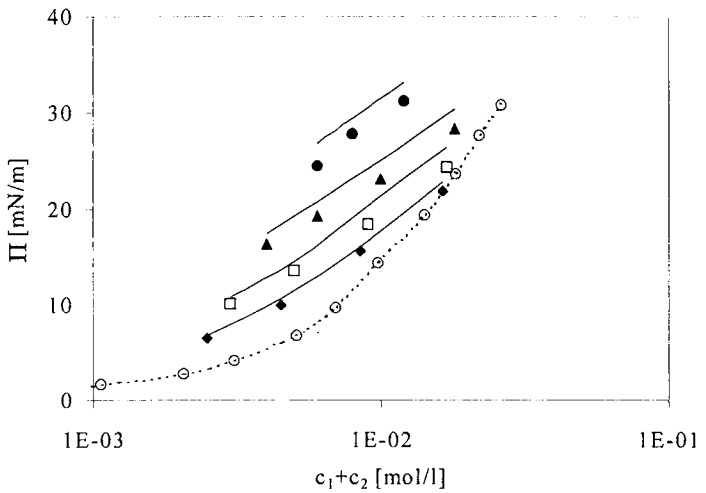

Fig. 3.74. The same as in Fig. 3.67, theoretical curves for mixtures are calculated from Eq. (3.46).

The theoretical curves for this system are calculated from Eq. (3.46), where the surface pressure isotherms for individual $C_{10}SO_4Na$ and $C_{12}SO_4Na$ solutions (see Fig. 3.46) are used, and the above expressions for the concentrations in the individual solutions, $c_{01}=[c_1(c_1+c_2)]^{1/2}$ and $c_{02}=[c_2(c_1+c_2)]^{1/2}$, respectively. The error of this approximate equation (3.46) as compared to the rigorous model is relatively small, cf. Fig. 3.67. A significant difference (up to 2 mN/m) was found only for large additions of $C_{12}SO_4Na$ to $C_{10}SO_4Na$ solutions.

The changes in the state of adsorbed molecules in the surface layer (reorientation, aggregation or cluster formation) have also a minor effect on the form of the equation which relates the surface pressure of mixed solutions with the corresponding values for the individual solutions. This will be demonstrated below for mixtures, where one component is able to form surface clusters.

3.8.3. Mixture of surfactants capable of surface aggregation

For a surfactant forming aggregates in the adsorption layer the equations of state and adsorption isotherms were derived in Chapter 2. In the limiting case of large aggregates these equations expressed via the molar area of monomers ω and the critical adsorption of aggregation Γ_{1c}, can be written in the form of Eqs. (2.107)-(2.108).

For the ideal mixture (both in the bulk and at the surface) of two surfactants with similar molar areas, where only component 1 is able to form large two-dimensional aggregates in the adsorption layer, the following equations were derived in [95]

$$\Pi = -\frac{RT(\theta_c + \theta_2)}{\omega(\theta_1 + \theta_2)} \ln(1 - \theta_1 - \theta_2), \tag{3.47}$$

$$b_1 c_1 = \frac{\theta_1}{(1 - \theta_1 - \theta_2)^{(\theta_c + \theta_2)/(\theta_1 + \theta_2)}}, \tag{3.48}$$

$$b_2 c_2 = \frac{\theta_2}{(1 - \theta_1 - \theta_2)^{(\theta_c + \theta_2)/(\theta_1 + \theta_2)}}, \tag{3.49}$$

where $\theta_1 = \omega\Gamma_1 = \omega(\Gamma_{11} + n\Gamma_{1n})$, $\theta_2 = \omega\Gamma_2$ and $\theta_c = \omega\Gamma_{1c}$ are the degrees of surface coverage by component 1 (aggregates and monomers), by component 2, and the critical monolayer coverage of component 1, respectively. Eq. (3.47) can be transformed to

$$\exp(\overline{\Pi}/\alpha) = b_1 c_1 (1 - \theta_1 - \theta_2)^{\alpha - 1} + b_2 c_2 (1 - \theta_1 - \theta_2)^{\alpha - 1} + 1, \tag{3.50}$$

where $\overline{\Pi} = \Pi\omega/RT$ is the dimensionless pressure, and $\alpha = (\theta_c + \theta_2)/(\theta_1 + \theta_2)$ is the fraction of monomers of the net surfactant adsorption. Similarly to the previous development, in this equation the $b_i c_i$ can be expressed via the corresponding surface pressures of the individual solutions using Eqs. (2.107) and (2.108) for the aggregating surfactant 1, and the Szyszkowski-Langmuir equation (3.39) for the individual solution of surfactant 2. This results in an expression similar to Eq. (3.43), with $k_1 = \exp(1/\beta - 1/\alpha)\dfrac{(1 - \theta_1 - \theta_2)^{\alpha - 1}}{(1 - \theta_{01})^{\beta - 1}}$, $k_2 = \exp(-1/\alpha)(1 - \theta_1 - \theta_2)^{\alpha - 1}$ and $k_3 = \exp(-1/\alpha)$. Here $\theta_{01} = \omega\Gamma_{01}$ is the degree of surface coverage by component 1 for the individual solution, and $\beta \doteq \Gamma_{01c}/\Gamma_{01}$. As $\alpha > \beta$, and also

$\alpha < 1$ and $\beta < 1$, it follows that $k_1 > 1$, $k_2 < 1$, and $k_3 < 1$. As the coefficients k_i are quite close to 1, one can approximately write $k_1 = k_2 = k_3 = 1$. Therefore, Eq. (3.41) can be used for an approximate estimation of the surface pressure of the mixed solution of two surfactants both in the pre-critical and trans-critical adsorption range of the aggregating component.

A successful application of Eq. (3.41) is the calculation of surface tensions of mixed $C_{12}SO_4Na$ /1-dodecanol solution [95]. It was shown in [25] that 1-dodecanol forms surface aggregates (see Fig. 3.5). As the $C_{12}SO_4Na$ adsorption is completed before any appreciable adsorption of 1-dodecanol starts, and 1-dodecanol adsorbs due to the diffusion mechanism the Eq. (3.41) remains valid also for the dynamic surface pressure. The approximate model correctly predicts the existence of a significant shift towards shorter times corresponding to the critical point of phase transition in the mixed surface layer. The time of the aggregation onset of 1-dodecanol in the mixed solution is 4 times lower as compared to the individual 1-dodecanol solution [95].

3.8.4. Mixture of components with different molar areas

This case is of practical importance, because surfactants with essentially different molar areas are often present in a mixture. The equation of state for the ideal mixture of two surfactants with different ω_i is also given by Eq. (3.38) expressed here in the form

$$\Pi = -\frac{RT}{\omega}\ln(1-\theta_1-\theta_2). \tag{3.51}$$

However, the ω value is no longer a constant but depends on the corresponding partial molar areas ω_i and adsorptions of components 1 and 2, and is given by Eq. (3.31). For this mixture, the adsorption isotherms read

$$b_i c_i = \frac{\theta_i}{(1-\theta_1-\theta_2)^{n_i}}, \tag{3.52}$$

where $n_i = \omega_i/\omega$. Following the lines of the preceding sections, one can use Eq. (3.52) to substitute the terms $b_i c_i$ in Eq. (3.51) by the corresponding terms for the individual solutions from Eqs. (3.39). This results in Eq. (3.43) where the coefficients are now defined by $k_1 = (1-\theta_1-\theta_2)^{1-n_1}$, $k_2 = (1-\theta_1-\theta_2)^{1-n_2}$ and $k_3 = 1-(1-\theta_1-\theta_2)^{1-n_1}-(1-\theta_1-\theta_2)^{1-n_2}$. If the

values n_i are close to 1, then all coefficients k_i are also close to 1, i.e., Eq. (3.41) is valid also for this case. Note that, in contrast to the examples given above, the dimensionless pressures in Eq. (3.41) are: $\overline{\Pi} = \Pi\omega/RT$, $\overline{\Pi}_1 = \Pi_1\omega_1/RT$ and $\overline{\Pi}_2 = \Pi_2\omega_2/RT$. To determine the average of ω for the mixture, the same substitution procedure for b_ic_i should be used and Eq. (3.31) becomes

$$\omega = \frac{\omega_1(\exp\overline{\Pi}_1 - 1) + \omega_2(\exp\overline{\Pi}_2 - 1)(1-\theta_1-\theta_2)^{n_2-n_1}}{\exp\overline{\Pi}_1 - 1 + (\exp\overline{\Pi}_2 - 1)(1-\theta_1-\theta_2)^{n_2-n_1}}. \tag{3.53}$$

Estimations using this equation show that even if the difference between the ω_i values is relatively small, but the surface coverage is medium or large, the term $(1-\theta_1-\theta_2)^{n_2-n_1}$ cannot be omitted. However, one can use other expressions for the mean area, which do not involve unknown quantities. As the adsorption is roughly proportional to the surface pressure (for extremely diluted surface layers $\Pi = RT\Gamma$), then the mean molar area, Eq. (3.31), is given by

$$\omega = \frac{\omega_1\Pi_1 + \omega_2\Pi_2}{\Pi_1 + \Pi_2} = \omega_1 \frac{\overline{\Pi}_1 + \overline{\Pi}_2}{\overline{\Pi}_1 + \overline{\Pi}_2(\omega_1/\omega_2)}. \tag{3.54}$$

Assuming that the adsorptions of surfactants characterised by different molar areas in a densely packed layer (at sufficiently large Π) are roughly inverse proportional to ω_i, instead of Eq. (3.54) we obtain

$$\omega = \frac{\omega_1\Pi_1/\omega_1 + \omega_2\Pi_2/\omega_2}{\Pi_1/\omega_1 + \Pi_2/\omega_2} = \omega_1 \frac{\Pi_1 + \Pi_2}{\Pi_1 + \Pi_2(\omega_1/\omega_2)}. \tag{3.55}$$

Both models provide quite a satisfactory description of surfactant mixtures with essentially (more than twice) different values of the molar areas of the components.

Figure 3.75 illustrates the dependencies obtained for solutions of pure C_{12}BHB and 1-butanol, and for their mixture with a molar ratio 1:9.

As the ω_i for the two components are remarkably different, Eqs. (3.54) and (3.55) were used to calculate the mean value of ω in the mixture. It is seen from the calculations in Fig. 3.75 that the two models yield very similar results. In general, the results of the calculations made from Eq. (3.41) are in perfect agreement with the experimental dependence obtained for C_{12}BHB/1-butanol mixtures.

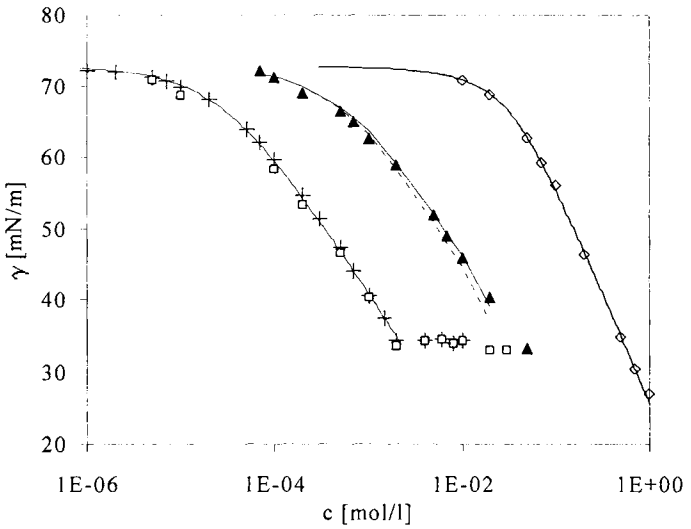

Fig. 3.75. Surface tension isotherms for C_{12}BHB (+, data reported in [41], □, data reported in [96]), 1-butanol (◇) and their mixture with ratio 1:19 (▲), theoretical isotherms for individual solutions were calculated from Frumkin equation: for C_{12}BHB see Table 3.8; for 1-butanol see Table 3.1, theoretical calculations for the mixture were performed according to Eqs. (3.41) and (3.54) (solid line), and from Eqs. (3.41) and (3.55) (dotted line), respectively.

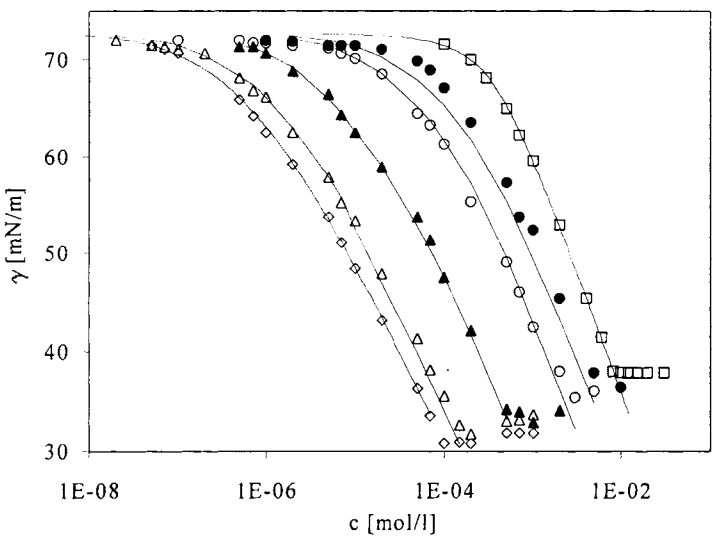

Fig. 3.76. The same as in Fig. 3.65, theoretical curves for mixtures calculated from Eq. (4.41) and (3.55).

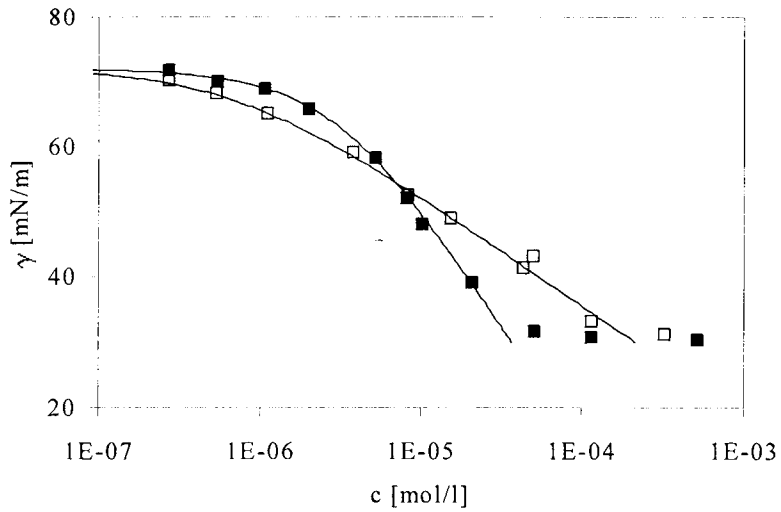

Fig. 3.77. Surface tension isotherms for non-ionic surfactants Triton X-100 (□) and $C_{12}EO_5$ (■); theoretical isotherms calculated from the Frumkin equation (3.1)-(3.2): Triton X-100 ($\omega_1 = 3.4 \cdot 10^5$ m^2/mol, $b_1 = 1.455 \cdot 10^6$ l/mol, $a_1 = 0$); $C_{12}EO_5$ ($\omega_2 = 1.5 \cdot 10^5$ m^2/mol, $b_2 = 1.795 \cdot 10^5$ l/mol, $a_2 = 0.6$); data reported in [97].

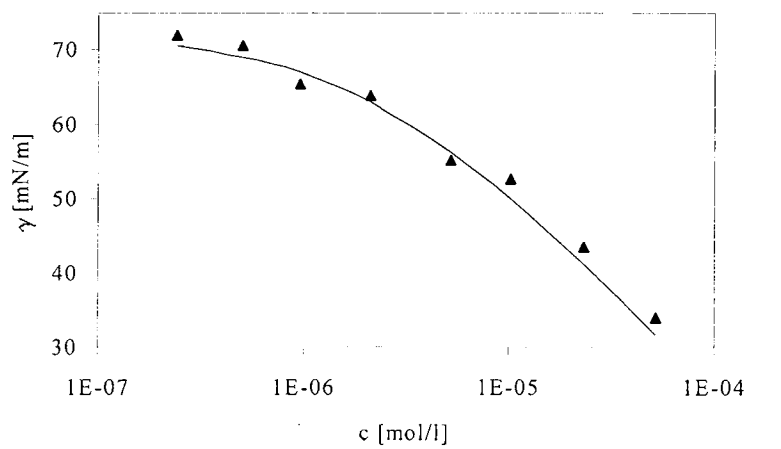

Fig. 3.78. Surface tension isotherm for the mixture of Triton X-100 and $C_{12}EO_5$ for a ratio of 1:1; theoretical curve calculated from Eqs. (3.41) and (3.55); data reported in [97].

Fig. 3.76 illustrates surface tension isotherms for mixtures of $C_{10}EO_5$ with $C_{12}SO_4Na$ in 0.01 M NaCl. The agreement between values calculated from the simple Eq. (3.41) and the experimental data is very satisfactory. Comparison of the results calculated from the approximate equations (3.41) and (3.55) with the exact results from Eqs. (3.28) - (3.31) (see Figure 3.65) shows that both models give quite similar results.

Another example of a system comprised of molecules with essentially different molar areas is illustrated in Figs. 3.77 and 3.78, which show the surface tension isotherms for individual solutions of Triton X-100 and $C_{12}EO_5$, and their mixture at a molar fractions ratio of 1:1.

The calculations from Eqs. (3.41) and (3.55) describe the experimental data very well.

3.8.5. Mixture of n components

The Eq. (3.41) can be easily generalised to mixtures of any number of different components (ideal or non-ideal), including ionic surfactants in presence of electrolytes and surfactants with different molar area. Starting from the generalised von Szyszkowski equation (2.39) one an equation for the mixture of n surfactants results

$$\exp\overline{\Pi} = \sum_{i=1}^{n} \exp\overline{\Pi}_i + 1 - n . \tag{3.56}$$

When the molar areas of the components are different, the average area for the mixture can be estimated by

$$\omega = \frac{\sum \omega_i \Pi_i}{\sum \Pi_i} . \tag{3.57}$$

For m ionic surfactants with a common counterion, in absence of any additional inorganic electrolytes, instead of Eq. (3.46) we can use:

$$\exp\overline{\Pi} = \sum_{i=1}^{n} \exp\overline{\Pi}_i + \left[\sum_{i=1}^{m} (\exp\overline{\Pi}_i - 1)^2 \right]^{1/2} + 1 - n . \tag{3.58}$$

Eqs. (3.56)-(3.58) allow to estimate the surface pressure for a mixture of any number of surfactants from the pressures of the individual solutions.

3.9. Conclusions

This chapter presents experimental surface pressure data for some homologous series of non-ionic and ionic surfactants: C_nOH, $C_n(OH)_2$, C_nO_2H, C_nDMPO, C_nBHB, C_nPIP, C_nEO_m, Tritons, C_nO_2Na, C_nSO_4Na, $C_nEO_mSO_4Na$, C_nTAB and C_nACl reported by a number of authors. The experimental surface tension isotherms were processed in the framework of the Frumkin model, for some systems, the reorientation and aggregation models also were employed. The Frumkin model provides a rather good description of the adsorption behaviour of surfactants of different nature, and therefore this model can be recommended for the practical use in the majority of cases. The analysis of results obtained in this way reveals some general features of the Frumkin model parameters for the surfactant molecules with linear hydrocarbon chains. It was found that the lower the molar area of the surfactant is, the higher is the intermolecular interaction constant a. Equ. (3.26) enables one to make quite satisfactory predictions of the parameter b from the surfactant molecule structure. The experimental values of the increment of standard free energy per methylene group $\Delta G^0_{CH_2}$ for various ionic and non-ionic (non-oxyethylated or oxyethylated) surfactants vary in a rather narrow range, –2.6 kJ/mol to -3.3 kJ/mol, while the free energy increment for the non-oxyethylated polar group ΔG^0_P=–4.25 kJ/mol does neither depend on the type of the polar group nor on the surfactant nature. For oxyethylated non-ionic surfactants (C_nEO_m) and for oxyethylated ionic surfactants ($C_nEO_mSO_4Na$) the increments for the polar group ΔG^0_P are higher than for ordinary surfactants, which can be ascribed to the partial adsorption of the oxyethylene chain. The additional contribution to the increment of the polar group ΔG^0_P from m EO groups can be accounted as $\Delta G^0_{EO_m} = -2.35m^{1/2}$ [kJ/mol]..

In some cases, a better agreement with the experimental surface tension isotherms and other data (dynamic surface tension, optical methods) is provided by the reorientation or aggregation model, respectively. It follows from the presented results that the reorientation model is more appropriate for oxyethylated surfactants and for surfactants which possess relatively high molar area, $\omega > 2.5 \cdot 10^5$ m^2/mol. At the same time, the aggregation and cluster models describe better the behaviour of surfactants with a relatively large Frumkin constant and low molar area, $\omega < 2.5 \cdot 10^5$ m^2/mol.

A theoretical model is presented which describes the equilibrium behaviour of a surfactant mixture at liquid/fluid interfaces. The theory accounts for the nonideality of the surface layer (with respect to both enthalpy and entropy of mixing), thus comprising mixtures of surfactants with different molar areas. The theoretical results are in a good agreement with experimental data. The parameter describing the interaction between molecules of different species is quite close to the value calculated from additivity.

For the ionic surfactants solutions, the model of electroneutral two-dimension solutions provides good agreement with experiments. In this approach, the adsorption of any ion is the sum of its excesses in the monolayer and in the electrical double layer; while no assumptions are made about the spatial distribution of charges. In many cases, measurements of Π *vs* mean ionic activity at different salt concentrations merge into a single curve. Such generalised dependencies were obtained for the solutions of C_nSO_4Na, C_nTAB и C_nACl.. In addition, the electroneutral 2-D solution approach has resulted in a simple explanation of several typical features of mixed ionic surfactant solutions. For the mixtures of ionic homologues, a model is presented which accounts for the mutual influence of the mixed ions. Here the calculations made using the corresponding software agree well with the experiment, assuming additivity of the Frumkin constants.

The rigorous equation of state for mixed surface layers can be transforms into a simple relationship (3.41) for surfactants possessing different adsorption parameters. To calculate the surface tension of the surfactant mixtures one can use various types of surface tension information of the individual components, either experimental values for a given concentration in the pure solutions, or the parameters of the corresponding adsorption isotherms.

The derived expressions are valid for several surfactant systems, where the molar areas of the components and other parameters of the adsorption isotherm are quite different. This validity can be ascribed primarily to the fact that many particular features of the adsorption of the components (the non-ideality of the surface layer, capability for reorientation or cluster formation in the surface layer) are accounted for 'automatically', because the surface tensions of the individual solutions entering the Eq. (3.41) carry this information. The proposed approach is an approximation, however, it is important and useful for the estimation of systems for which information is unavailable. This can be especially important with respect to the practical application of surfactant mixtures.

3.10. References

1. M.J. Rosen, Surfactants and Interfacial Phenomena, John Wiley & Sons, New York (1978).
2. H. Lange, In: Nonionic Surfactants, Ed. M. Schick, Marcel Dekker, New York (1967)443.
3. M.J. Schick, Nonionic Surfactants: Physical Chemistry, Surfactant Science Series 23, Marcel Dekker, New York (1986).
4. M.J. Rosen, In: Solution Chemistry of Surfactants, Vol.1, Ed. K.L. Mittal, Plenum Publ. Corp., New York (1979)45.
5. J.T. Davies and E.K. Rideal, Interfacial Phenomena, Acad. Press, New York (1963).
6. E.H. Lucassen-Reynders, Anionic Surfactants: Physical Chemistry of Surfactant Action, Surfactant Science Series, Vol. 11, Marcel Dekker Inc., New York-Basel (1981).
7. C.-H. Chang and E.I. Franses, Colloids Surfaces A, 100(1995)1.
8. P.M. Holland, In: Relation between Structure and Performance of Surfactants, M.J. Rosen (ed.), ACS Symposium Series, 253(1984)141.
9. I.W. Osborne-Lee and R.S. Schechter, In: Phenomena in Mixed Surfactant Systems, J.F. Scamehorn (ed.), ACS Symposium Series, 311(1986)30.
10. D.N. Rubingh and P.M. Holland, Cationic Surfactants: Physical Chemistry, Surfactant Science Series, Vol. 37, Marcel Dekker, New York (1991).
11. N.M. van Os, J.P. Haak and L.A.M. Rupert, Physico-Chemical Properties of Selected Anionic, Cationic and Nonionic Surfactants, Elsevier (1993).
12. K. Ogino and M. Abe, In: Mixed Surfactant System, K. Ogino and M. Abe (eds.), Surfactant Science Series, Vol. 46, Marcel Dekker Inc., New York-Basel (1993).
13. K. Motomura and M. Aratono, In: Mixed Surfactant System, K. Ogino and M. Abe (eds.), Surfactant Science Series. Vol. 46, Marcel Dekker Inc., New York (1993)100 .
14. J.R. Lu, R.K. Thomas and J. Penfold, Adv. Colloid Interface Sci., 84(2000)143.
15. M. Aratono and N. Ikeda, In: Structure-Performance Relationships in Surfactants, Surfactant Science Series, Vol. 70, Marcel Dekker Inc., New York, Basel, Hong Kong (1997)83.

16. M. Mulqueen and D. Blankschtein, Langmuir, 15(1999)8832.

17. S.S. Dukhin, G. Kretzschmar and R. Miller, Dynamics of Adsorption at Liquid Interfaces: Theory, Experiment, Application, in Studies of Interface Science, Vol. 1, D. Möbius and R. Miller (eds.), Elsevier, Amsterdam, 1995

18. C.C.Addison, J. Chem. Soc., (1945)98.

19. J. R. Hommelen, J. Colloid Science, 14(1959)385.

20. V.B. Fainerman and S.V. Lylyk, Koll. Zh., 45(1983)500.

21. M. Aratono, S. Uryu, Y. Hayami, K. Motomura and R. Matuura, J. Colloid Interface Sci., 98(1984)33.

22. R. Wüstneck and R. Miller, Colloids Surfaces, 47(1990)15.

23. S.-Y. Lin, K. McKeigue and C. Maldarelli, Langmuir, 7(1991)1055.

24. S.-Y. Lin, T.-L. Lu and W.-B. Hwang, Langmuir, 10(1994)3442.

25. D. Vollhardt, V.B. Fainerman and G. Emrich, J. Phys. Chem B, 104(2000)8536.

26. D. Vollhardt and V.B. Fainerman, Colloids Surfaces A, 176(2000)117.

27. R. Wüstneck, V.B. Fainerman and V. Zauls, J. Phys. Chem. B, 103(1999)3587.

28. K. Nakanishi, T. Matsumoto and M. Hayatsy, J. Chem. Eng. Data, 16(1971)44.

29. G. Petre and P. Debelle, V. Tagung Grenzflächenakt. Stoffe 1968, II(1969), 559.

30. K. Malysa, R. Miller and K. Lunkenheimer, Colloids and Surfaces, 53(1991)47.

31. M. Aratono, S. Uryu, Y. Hayami, K. Motomura and R. Matuura, J. Colloid Interface Sci., 98(1984)33.

32. K. Lunkenheimer and R. Hirte, J. Phys. Chem., 96(1992)8683.

33. E.H. Lucassen-Reynders, J. Colloid Interface Sci., 41(1972)156.

34. L. Ter Minassian-Saraga, J. Colloid Sci., 11(1956)398.

35. E. Boyd, J. Phys. Chem., 62(1958)536.

36. A.V. Makievski and D. Grigoriev, Colloid Surfaces A, 143(1998)233.

37. K. Lunkenheimer, K. Haage and R. Miller, Colloids Surfaces, 22(1987)215.

38. J.-P. Fang, K.-D. Wantke and K. Lunkenheimer, J. Phys. Chem., 99(1995)4632.

39. E.V. Aksenenko, A.V. Makievski, R. Miller and V.B. Fainerman, Colloids & Surfaces A, 143(1998)311.

40. V.B. Fainerman, E.H. Lucassen-Reynders and R. Miller, Colloids & Surfaces A, 143(1998)141.

41. R. Wüstneck, J. Kriwanek, M. Herbst, G. Wasow and K. Haage, Colloids Surfaces, 66(1992)1.

42. R. Wüstneck, R. Miller, J. Kriwanek and H.-R. Holzbauer, Langmuir, 10(1994)3738.

43. V.B. Fainerman, R. Miller and R. Wüstneck, J. Phys. Chem., 101(1997)6479

44. H. Fiedler, R. Wüstneck, B. Weiland, R. Miller and K. Haage, Langmuir, 10(1994)3959.

45. R.Wüstneck, H.Fiedler, R. Miller and K. Haage, Langmuir, 10(1994)3966.

46. M. Ueno, Y. Takasawa, H. Miyashige, Y. Tabata and K. Meguro, Colloid Polym. Sci., 259(1981)761.

47. S. Ozeki, T. Ikegava, S. Inokuma and T. Kuwamura, Langmuir, 5(1989)222.

48. M.J. Rosen and X.Y. Hua, J. Colloid Interface Sci., 86(1982)164.

49. H.C. Chang, C.-T. Hsu and S.-Y. Lin, Langmuir, 14(1998)2476.

50. S.-Y. Lin, R.-Y. Tsay, L.-W. Lin and S.-I. Chen, Langmuir, 12(1996)6530.

51. R.J. Pugh and E.D. Manev, J. Colloid Interface Sci., 152(1992)582.

52. A. Asnacios, D. Langevin and J.-F. Argillier, Macromolecules, 29(1996)7412.

53. J. Lucassen and D. Giles, J.C.S Faraday Trans., 71(1975)217.

54. B.V. Zhmud, F. Tiberg, and J. Kizling, Langmuir, 16(2000)2557.

55. C.-T. Hsu, M.-J. Shao and S.-Y. Lin, Langmuir, 16(2000)3187.

56. V.B. Fainerman, R. Miller and E.V. Aksenenko, Langmuir, 16(2000)4196.

57. R. Miller, E.V. Aksenenko, L. Liggieri, F. Ravera, M. Ferrari and V.B. Fainerman, Langmuir, 15(1999)1328.

58. J. Van Hunsel, P. Joos, Colloids and Surfaces, 24(1987)139

59. B. Janczuk, J.M. Bruque, M.L. Gonzalez-Martin and C. Dorado-Calasanz, Langmuir, 11(1995) 4515.

60. V.B. Fainerman and R. Miller, Colloids Surfaces A, 97(1995)65.

61. V.B. Fainerman, R. Miller and A.V. Makievski, Langmuir, 11(1995)3054.

62. A. El Ghzaoui, E. Fabreque, G. Cassanas, J.M. Fulconis and J. Delagrange, Colloid Polymer Sci., 278(2000)321.

63. S. Ozeki, T. Ikegava, S. Inokuma and T. Kuwamura, Langmuir, 4(1988)1070.

64. R.A. Robinson and R.H. Stokes, Electrolyte Solutions, Butterworths, London, 1965.

65. R. van den Bogaert and P. Joos, J. Phys. Chem., 84(1980)190.

66. P.H. Elworthy and K.J. Mysels, J. Colloid Interface Sci., 21(1966)331.

67. K. Lunkenheimer, G, Czichocki, R. Hirte and W. Barzyk, Colloids Surfaces A, 101(1995)187.

68. V.B. Fainerman, Kolloidn. Zh., 48(1986)512.

69. D. Vollhardt, G. Czichocki and R. Rudert, Colloids Surfaces A, 76(1993)217.

70. L.-W. Chen and J.-H. Chen, J. Chem. Soc. Faraday Trans., 91(21)(1995)3873.

71. J.P. Fang and P. Joos, Colloids Surfaces, 65(1992)113.

72. K. Tajima, M. Muramatsu and T. Sasaki, Bull. Chem. Soc. Japan, 43(1970)1991.

73. K. Tajima, Bull. Chem. Soc. Japan, 43(1970)3063.

74. M. Muramatsu, K. Tajima, M. Iwahashi and K. Nukina, J. Colloid Interface Sci., 43(1973)499.

75. K. Tajima, J. Chem. Soc. Japan, 5(1973)883.

76. G. Czichocki, A.V. Makievski, V.B. Fainerman and R. Miller, Colloids Surfaces A, 122(1997)189.

77. P. Joos, *Dynamic Surface Phenomena,* VSP, Utrecht, The Netherland, 1999.

78. A. Nikolov, G. Martynov and D. Exerowa, J. Colloid Interface Sci., 81(1981)116.

79. H. Okuda, S. Ozeki and S. Ikeda, Bull. Chem. Soc. Japan, 57(1984)1321.

80. V. Bergeron, Langmuir, 13(1997)3474

81. D. Langevin, and J.-F. Argillier, Macromolecules, 29(1996)7412.

82. J.R. Lu, R.K. Thomas, R. Aveyard, B.P. Binks, P. Cooper, P.D.I. Fletcher, A. Sokolowski, and J. Penfold, J. Phys. Chem., 96(1992)10971.

83. E.D. Shchukin, Z.N. Markina, and N.M. Zadymova, Progr. Colloid Polymer Sci., 68(1983)90.

84. Y.J. Nikas, S. Puvvada and D. Blankschtein, Langmuir, 8(1992)2680.

85. J.T. Davies, Proc. 2nd Int. Congr. Surface Activity, Vol. 1, London, Butterworths, 1957, p.440.

86. W.C. Griffin, J. Soc. Cosmetic. Chem., 1(1949)311; 5(1954)249.

87. A.A. Abramzon, Russian J. Appl. Chem., 69(1996)1159.

88. V.B. Fainerman and E.H. Lucassen-Reynders, Adv. Colloid Interface Sci., (2001).

89. E.H. Lucassen-Reynders, J. Lucassen and D. Giles, J. Colloid Interface Sci., 81(1981)150.

90. E.H. Lucassen-Reynders, Progress in Surface and Membrane Science, 10(1976)253.

91. J.M. Corkill, J.F. Goodman, C.P. Ogden and J.R. Tate, Proc. Roy. Soc. London Ser. A 273(1963) 24.

92. M.J. Schwuger, Kolloid-Z. u. Z. Polymere, 243(1971) 129.

93. Z.-G. Cui and J.P. Canselier, Colloid Polym. Sci., 279(2001)254.

94. V.B. Fainerman and R. Miller, J. Phys. Chem. B, submitted.

95. V.B. Fainerman, D. Vollhardt and G. Emrich, J. Phys. Chem. B, submitted.

96. V.B. Fainerman and R. Miller, Tenside Surfactants Detergents, in press.

97. F.A. Siddiqui and E.I. Franses, Langmuir, 12(1996)354.

This Page Intentionally Left Blank

4. DYNAMICS OF ADSORPTION FROM SOLUTIONS

R. Miller[1], A.V. Makievski[1,2] and V.B. Fainerman[3]

[1] Max-Planck-Institut für Kolloid- und Grenzflächenforschung, Am Mühlenberg 1, D-14424 Potsdam/Golm, Germany

[2] SINTECH Surface and Interface Technology, Volmerstrasse 5-7, D-12489 Berlin, Germany

[3] International Medical Physicochemical Centre, Donetsk Medical University, 16 Ilych Av., Donetsk 83003, Ukraine

In the preceding Chapters 1 to 3 it was demonstrated how surfactants of different nature and structure modify the properties of interfaces due to their adsorption. It was also shown that there is not only one parameter, which allows classifying the action of a surfactant. While some surfactants are called highly surface active when they adsorb and decrease the interfacial tension at extremely low bulk concentrations, others deserve this attribute due to their capability to decrease the interfacial tension to extremely low values. It was also shown that the surfactants' properties correlate with each other in a particular way, and the Traube rule is only one of the simple correlations valid for each homologous series.

Later in Chapter 6 a large variety of technologies based on adsorption effects will be described. It will also be shown that in general, these technologies work under dynamic conditions and an improvement of the surfactant's efficiency, made in the by past trial and error or thanks personal experience, is now more and more based on a systematic analysis of the entire technology and the particular impact of the surfactants used. The optimisation of surfactants and their mixtures requires specific knowledge of their dynamic adsorption behaviour [1]. The most frequently used parameter to characterise the dynamic properties of liquid adsorption layers is the dynamic interfacial tension. Many techniques exist to measure dynamic tensions of liquid interfaces having different time windows from milliseconds to hours and days. As direct measurements of the time process of adsorption of surfactants at liquid interfaces are rare

and applicable only at long adsorption times, respective theories are required then to deduce the adsorption dynamics from the measured dynamic interfacial tensions [2].

The aim of this chapter is to present the fundamentals of adsorption kinetics of surfactants at liquid interfaces. Theoretical models will be summarised to describe the process of adsorption of surfactants and surfactant mixtures. As analytical solutions are either scarcely available or very complex and difficult to apply, also approximate and asymptotic solutions are given and their ranges of application demonstrated. For particular experimental methods specific initial and boundary conditions have to be considered in these theories. In particular for relaxation theories the experimental conditions have to be met in order to quantitatively understand the obtained results. In respect to micellar solutions and the impact of micelles on the adsorption layer dynamics a detailed description on the theoretical basis as well as a selection of representative experiments will follow in Chapter 5.

This chapter will also present a selected number of experiments representative for the various models discussed. This refers especially to surfactant systems where recently new phenomena have been observed and explained, i.e. the possibility of changes in the orientation of adsorbed molecules are alternatively the formation of aggregates at the interface. Adsorption kinetics as well as interfacial relaxation experiments will be reported and the results discussed in terms of the specific parameters of these new theories. This will include also some data on proteins as particular type of surface active molecules able to change their conformation at an interface and hence changing the molar area at the interface.

The studies of adsorption layers at the water/alkane interface give excess to the distribution coefficient of a surfactant, which is a parameter of particular relevance for many applications. Theoretical models and experimental measurements of surfactant adsorption kinetics at and transfer across the water/oil interface will be presented. The chapter will be concluded by investigations on mixed surfactant systems comprising experiments on competitive adsorption of two surfactants as well as penetration processes of a soluble surfactant into the monolayer of a second insoluble compound. In particular these penetration kinetics experiment can be used to visualise separation processes of the components in an interfacial layer.

4.1 General models for adsorption kinetics and relaxations of surfactants

The present state of research allows to describe the adsorption kinetics of surfactants at liquid interfaces in most cases quantitatively. The first model for interfaces with constant area was derived by Ward & Tordai [3]. It is based on the assumption that the time dependence of interfacial tension, which is directly related to the interfacial concentration Γ of adsorbed molecules via an equation of state, is mainly caused by the surfactant transport to the interface. In the absence of any external influences this transport is controlled by diffusion and the result, the so-called diffusion controlled adsorption kinetics model, has the following form

$$\Gamma(t) = 2\sqrt{\frac{D}{\pi}}\left(c_0\sqrt{t} - \int_0^{\sqrt{t}} c(0, t-\tau)\mathrm{d}\sqrt{\tau} \right), \tag{4.1}$$

where D is the diffusion coefficient and c_0 is the surfactant bulk concentration. The integral equation describes the change of $\Gamma(t)$ with time t. The application of the Ward and Tordai equation (4.1) to dynamic surface tension data $\gamma(t)$ is not simple and often avoided due to numerical difficulties. In the following paragraphs we first show the general physical idea of all adsorption kinetics models, and then the main equations are discussed necessary to describe the various adsorption kinetics models.

4.1.1 Physical picture

There are two general ideas to describe the dynamics of adsorption at liquid interfaces. The diffusion controlled model assumes the diffusional transport of interfacial active molecules from the bulk to the interface to be the rate-controlling process, while the so-called kinetic controlled model is based on transfer mechanisms of molecules from the solution to the adsorbed state and vice versa. A schematic picture of the interfacial region is shown in Fig. 4.1 showing the different contributions, transport in the bulk and the transfer process.

Transport in the solution bulk is controlled by diffusion of adsorbing molecules if any liquid flow is absent. The transfer of molecules from the liquid layer adjacent to the interface, the so-called subsurface, to the interface itself is assumed to happen without transport. This process is determined by molecular movements, such as rotations or flip-flops. The adsorption of surface active molecules at an interface is a dynamic process. In equilibrium the two fluxes, the adsorption and desorption fluxes, are in balance. If the actual surface concentration is smaller

than the equilibrium one, $\Gamma < \Gamma_o$, the adsorption flux to the interface predominates, if $\Gamma > \Gamma_o$, the actual amount adsorbed at the interface is higher than the equilibrium value Γ_o, and the desorption flux prevails.

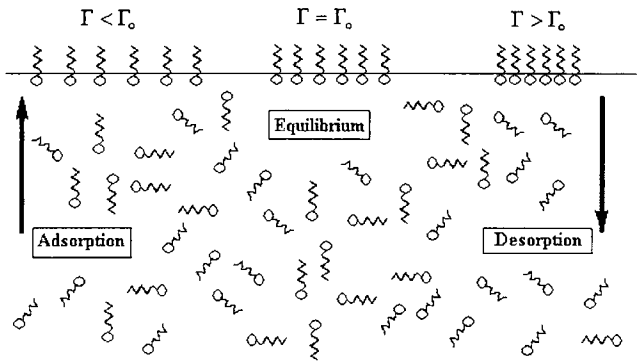

Fig. 4.1. Schematic diagram of the fluxes of adsorbing molecules near and at a liquid interface in absence of any forced liquid flow

If processes happen in the adsorption layer, such as changes in the orientation or conformation or the formation of aggregates due to strong intermolecular interaction, additional fluxes in the adsorption layer have to be considered. These fluxes are also shown schematically in Fig. 4.1.

Milner [4] was the first to discuss diffusion as a process responsible for the time dependence of surface tension of soap solutions. Later, several models took into account transfer mechanisms in form of rate equations [5, 6, 7, 8]. More complicated models take into account diffusion and transfer mechanisms simultaneously [9, 10, 11, 12, 13, 14].

Some very simple diffusion models have been given by Dukhin et al. [2], however these models are only useful for estimating the order of magnitude of adsorption or desorption processes. Based on comprehensive quantitative models approximations have been derived the application of which is often very useful [15, 16].

Temperature or density gradients in the bulk phase can initiate flows in a direction, which is controlled by the direction of these gradients. Surface tension gradients along the interface can generate Marangoni-Gibbs effects. Theoretical models for describing the adsorption kinetics usually neglect these particular effects as they can be avoided by a proper choice of the experimental conditions. However, there are specially designed experiments on the adsorption

dynamics which make use of freshly formed surfaces and have to consider particular types of controlled bulk flows, mainly laminar radial flows as it is the case in growing drop or bubble experiments [17].

Models considering diffusion in the bulk as the only rate controlling process are called pure diffusion controlled. When the diffusion is assumed to be fast in comparison to the transfer of molecules between the subsurface and the interface the model is called kinetic-controlled or barrier-controlled. Both steps are taken into account in so-called mixed diffusion kinetic controlled models. Van den Tempel proposed processes within the adsorption layer to be considered instead of hypothetical adsorption barriers [18, 19, 20]. We believe that such models, which account for actual physical processes within adsorption layers, such as reorientation of molecules, their dimerisation and formation of clusters, although explanations for all known cases of anomalous adsorption kinetics do not exist yet, have to be preferred over any formal model. However, reliable experimental evidence for a slower surface tension decrease caused by aggregation within the adsorption layer does not allow the conclusion that this is an exclusive mechanism.

Models regarding for molecular processes in the adsorption layer itself can also be considered as mixed models. In this case, three different characteristic times can exist and the one with the largest value controls the rate of the whole adsorption process. One can even imagine that the control is changing during the adsorption process from one to the other mechanism as it was discussed by Joos [16]. As an example, at a freshly formed surface the adsorption is first controlled only by diffusion while after a certain surface coverage is reached the process of interfacial reorientation becomes time controlling.

For mixed surfactant systems, various types of experiments exist. The adsorption layer of a two-component system can be formed from one mixed solution or from two sides of a liquid/liquid system. A special case is the penetration layer, where one component forms an insoluble monolayer and the second one penetrates from the bulk phase. For such systems, theoretical models and experimental data will be presented here as well.

4.1.2 Diffusion model

A quantitative description of adsorption kinetics processes is so far usually based on the model derived in 1946 by Ward and Tordai [3]. The various models developed on this basis use mainly different boundary and initial conditions [2], as it becomes clear from the schematic in Fig. 4.1. The diffusion-controlled adsorption model of Ward and Tordai assumes that the step of transfer from the subsurface to the interface is fast compared to the transport from the bulk to the subsurface. It is based on the following general equation,

$$\frac{\partial c}{\partial t} + (v \cdot \mathrm{grad})\, c = D\, \mathrm{div}\, \mathrm{grad}\, c. \tag{4.2}$$

If any flow in the bulk phase is neglected the diffusion equation (4.2) can be simplified to

$$\frac{\partial c}{\partial t} = D \frac{\partial^2 c}{\partial x^2} \quad \text{at } x > 0,\ t > 0. \tag{4.3}$$

To solve the transport problem respective initial and boundary conditions have to be defined. A very suitable boundary condition is Fick's first law defined at the surface located at x=0, which reads in its general form

$$\frac{\partial \Gamma}{\partial t} + (v_s \cdot \mathrm{grad}_s)\, \Gamma = D_s\, \mathrm{div}_s \mathrm{grad}_s \Gamma - \Gamma \mathrm{div}_s v_s + D \frac{\partial c}{\partial x}. \tag{4.4}$$

This law describes the surfactant flux from the bulk to the interface and along the interface during the adsorption or desorption process. As long as the surface concentration Γ is lower than the respective equilibrium value Γ_0 the adsorption flux dominates while in the opposite case a desorption flux results. If any flow and fluxes other than bulk diffusion is neglected the boundary condition has the following very simple form

$$\frac{\partial \Gamma}{\partial t} = j = D \frac{\partial c}{\partial x} \quad \text{at } x = 0;\ t > 0. \tag{4.5}$$

For a mixture of different surfactants the diffusion problem can be described in an analogous way and the generalised diffusion equations read

$$\frac{\partial c_i}{\partial t} + (v \cdot \mathrm{grad})\, c_i = \sum_{j=1}^{r} D_{ij}\, \mathrm{div}\, \mathrm{grad}\, c_i. \tag{4.6}$$

where r is the number of adsorbing species. At low surfactant concentrations the mixed diffusion coefficients can be replaced by the individual ones $D_{ij} = D_i$ (cf. [21]) and equations of the form of Eq. (4.3) for each component results. In the same way as above also the boundary conditions for each component is obtained having the form of Eq. (4.5).

To complete the transport problem one additional boundary condition and an initial condition are necessary. Typical boundary conditions are an infinite bulk phase

$$\lim_{x\to\infty} c(x,t) = c_0 \text{ at } t > 0 \tag{4.7}$$

or a bulk phases of limited depth h where a diminishing concentration gradient is assumed

$$\frac{\partial c}{\partial x} = 0 \text{ at } x = h;\ t > 0. \tag{4.8}$$

The usual initial condition is a homogenous concentration distribution and a freshly formed interface with no surfactant adsorption

$$c(x,t) = c_0 \text{ at } t = 0 \tag{4.9}$$

$$\Gamma(0) = 0. \tag{4.10}$$

Any other initial condition, according to the actual experimental conditions can be chosen, however a simple analytical solution is not possible then. In many cases, an initial load of the interface is more realistic than Eq. (4.10):

$$\Gamma(0) = \Gamma_d \neq 0. \tag{4.11}$$

For surfactant mixtures, the initial conditions are chosen equivalent to those for a single surfactant system. The solution of the given initial and boundary condition problem for Γ_d=0 is Eq. (4.1) which can be most easy found by applying the Laplace operator method [22]. Via this deviation an equivalent relation to Eq. (4.1) can be found

$$c(0,t) = c_0 - \frac{2}{\sqrt{D\pi}} \int_0^{\sqrt{t}} \frac{d\Gamma(t-\tau)}{dt} d\sqrt{\tau} \tag{4.12}$$

This equation is sometimes more useful than Eq. (4.1). Up to here, both resulting equations (4.1) and (4.12) are of very general nature as no particular assumption about the surfactants involved had been made. The effect of various adsorption isotherms is shown in Section 4.3.1.

4.1.3 Mixed kinetics model

As mentioned above many adsorption kinetics models were discussed in the literature. These models consider specific mechanisms of the molecular transfer from the subsurface to the interface, or vice versa in the case of desorption [5, 6, 7, 8, 9, 10, 11, 12, 14, 23]. The models, which assume only the transfer mechanism as rate determining step are called kinetic-controlled. More advanced models, the so-called mixed models, consider both the transport by diffusion in the bulk and the transfer mechanism (cf. Fig. 4.1). Such mixed models were first derived by Baret in 1969 [9] who combined Eq. (4.1) with a certain transfer mechanism.

The most frequently used transfer mechanism is the type Langmuir rate equation, which reads in its general form,

$$\frac{d\Gamma}{dt} = k_{ad}\, c_o \left(1-\frac{\Gamma}{\Gamma_\infty}\right) - k_{des}\frac{\Gamma}{\Gamma_\infty}. \tag{4.13}$$

At very small surface coverage we can assume $\frac{\Gamma_o}{\Gamma_\infty} \ll 1$ and obtain the so-called Henry rate equation

$$\frac{d\Gamma}{dt} = k_{ad} c_o - k_{des}\Gamma. \tag{4.14}$$

The rate constants of adsorption and desorption k_{ad} and k_{des} results from the equilibrium condition $\frac{d\Gamma}{dt} = 0$. For the Frumkin isotherm the following mechanism was proposed by Fainerman [24] and later used by MacLeod and Radke [25]

$$\frac{d\Gamma}{dt} = k_{ad}\, c_o \left(1-\frac{\Gamma}{\Gamma_\infty}\right) - k_{des}\frac{\Gamma}{\Gamma_\infty}\exp\left(a\frac{\Gamma}{\Gamma_\infty}\right) \tag{4.15}$$

The solution of these adsorption models is easy and results in exponential expressions.

Following Baret [9] the coupling of transfer mechanisms with the diffusion equation (4.12) can be arranged by replacing the bulk concentration c_o by the subsurface concentration $c(0, t)$ which for the Langmuir mechanism (4.13) leads to

$$\frac{d\Gamma}{dt} = k_{ad}\, c(0,t)\left(1-\frac{\Gamma}{\Gamma_\infty}\right) - k_{des}\frac{\Gamma}{\Gamma_\infty}. \tag{4.16}$$

The two Eqs (4.12) and (4.13) are coupled and yield an integro-differential equation system which can be solved numerically [10, 26].

Other theoretical models of surfactant adsorption kinetics take into account specific experimental conditions or surfactant properties: surfactant charge [27, 28, 29, 30, 31, 32, 33], micelle formation [34, 35, 36, 37, 38] or other specific effects [39, 40, 41, 12, 13, 42, 43]. These other effects however will not further discussed here, as most of the surfactants studied in literature turned out to follow a diffusion mechanism. Thus, below we will give more details mainly on models based on a diffusion mechanism.

4.1.4 Interfacial molecular processes

Since the first work by Nikolov et al. [44] in 1981 on the possibility of coexisting states in a soluble surfactant monolayer, mainly qualitative discussions on this subject have been published [39, 45]. The systematic thermodynamic work by Fainerman then gives a new understanding of the surface state of soluble surfactants at liquid interfaces [46, 47, 48, 49] as reviewed recently [50, 51]. The impact of these new ideas on adsorption dynamics is immense and up to now has been started only. It appears to be possible to answer to many open questions still existing in the interpretation of surfactant adsorption layer dynamics, and even of protein layers.

As it was shown in detail in Chapters 2 and 3 some surfactants can change their interfacial orientation or conformation and this process happening at the interface can influence the adsorption kinetics. The respective equations of state describing this type of adsorption layers are given by Eqs. (2.84) to (2.88). In Fig. 4.2 three possibilities are shown of molecular arrangements with changing the molar area in the adsorption layer. In order to take these molecular processes of reorientation or re-conformation into consideration, an additional relationship has to be added to the system of equations derived for the diffusion-controlled adsorption, as it will be discussed in detail in Section 4.3.2.

Another possibility discussed in Chapter 2 is the formation of small clusters or aggregates within the adsorption layer. It was shown that all those surfactants, which had been discussed as strongly interacting in the adsorption layer adsorb according to the surface aggregation model of Eqs. (2.110) – (2.112). The process of aggregation formation/dissolution as

schematically shown in Fig. 4.3 is equivalent to the micelle kinetics discussed in detail in Chapter 5.

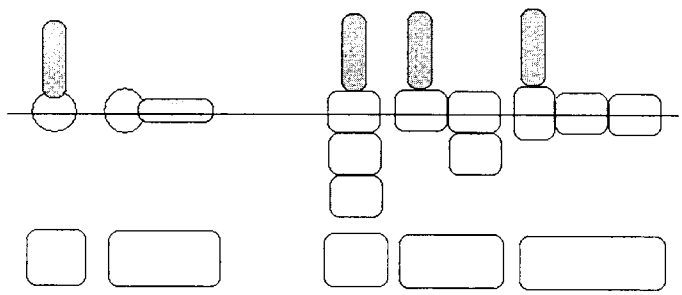

Fig. 4.2 Change of the molar area of an adsorbed molecule:
due to molecular reorientation (a), due to molecular reconformation (b)

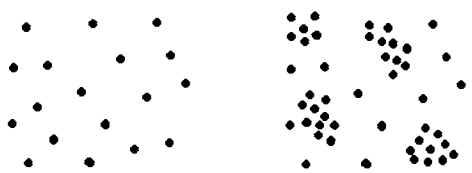

Fig. 4.3 Aggregation of adsorbed molecules at the interface due to strong intermolecular interactions

Again, in order to take the process of molecular aggregation into consideration, an additional relationship has to be added to the initial and boundary problem. Model calculations for the dynamics of this type of adsorption layers are shown below in Section 4.3.3 while experimental examples showing the different molecular interfacial processes on the adsorption dynamics are given in Section 4.7.

4.1.5 Models for mixed surfactant systems

There are different possibilities to form mixed surfactant layers and respective quantitative theories have to consider the particular initial and boundary conditions. The general description of the adsorption kinetics of a surfactant mixture however can be made in an analogous way as for a single surfactant solution. Instead of Eq. (4.5) a set of transport equations has to be used, one for each of the r different surfactants. The initial and boundary conditions are defined for

each component, in analogy to Eqs (4.5) through (4.11) and finally a system of r integral equations results, either in the form

$$\Gamma_i(t) = 2\sqrt{\frac{D_i}{\pi}}\left(c_{oi}\sqrt{t} - \int_0^t c_i(0,t-\tau)d\sqrt{\tau}\right), \quad i = 1,\ldots, r \tag{4.17}$$

or

$$c_i(0,t) = c_{oi} - \frac{2}{\sqrt{D_i\pi}}\int_0^{\sqrt{t}} \frac{d\Gamma_i(t-\tau)}{dt} d\sqrt{\tau}\,, \quad i = 1\ ,\ldots, r. \tag{4.18}$$

The set of r integral equations is linked together via a multi-component adsorption isotherm. In the simplest case a set of r independent relations of the type of Eq. (4.17) results when linear adsorption isotherms Eq. (2.144) are assumed for each of the surfactants [52]

$$\Gamma_i(t) = \Gamma_{oi}\left(1 - \exp(D_i t/K_i^2)\operatorname{erfc}(\sqrt{D_i t}/K_i)\right), \quad i = 1,\ldots,r. \tag{4.19}$$

The r equations are independent of each other and give reasonable results only for very dilute solutions of surfactant mixtures. Except in this very simple case, no other analytical solution exists.

As it was shown in Chapter 2 there are thermodynamic models that allow a quantitative description of the adsorption behaviour of surfactant mixtures in the equilibrium state. Using such isotherms a correct description of the adsorption kinetics is also possible, however, sophisticated numerical procedures are required as analytical solutions will not be available.

Mixed interfacial layers can be formed in various ways, as shown schematically in Fig. 4.4.

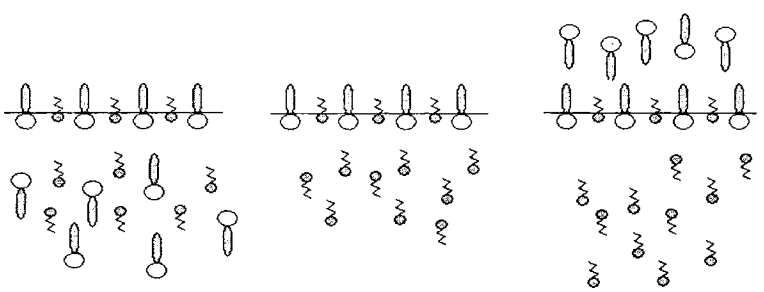

Fig. 4.4 Formation of mixed interfacial layers; a) from a mixed bulk solution, b) as penetration of one component into an insoluble layer, c) from two bulk solutions at the joint interface

The situations a) and c) can be described by one and the same model, as for diluted solutions there is no difference in the diffusitivities of the components in dependence of the presence of others. For case b) a particular model is required, as the behaviour of an insoluble monolayer, already existing at the interface, cannot be described by a classical adsorption isotherm. The thermodynamics of such systems was discussed in Section 2.8.2 and a more detailed description on penetration kinetics models will be given in Section 4.3.6.

4.2 Diffusion controlled adsorption kinetics

The diffusion controlled adsorption model is the most useful one as it is at present the main basis for all particular adsorption kinetics theories. It has also been demonstrated that for most of the systems for which an adsorption barrier controlled mechanism was discussed surface active impurities had been detected. These impurities can simulate a kinetic controlled adsorption mechanism [53, 54, 55].

4.2.1 Comparison of different isotherms

Based on a linear isotherm Eq. (2.144), a simple equation was derived by Sutherland in 1952 [56] . It leads to the following analytical relation, which can be used as a first approximation

$$\Gamma(t) = \Gamma_0 \left(1 - \exp(Dt/K^2)\,\mathrm{erfc}(\sqrt{Dt}/K)\right). \tag{4.20}$$

its range of application however is very limited [57]. The determination of the function $\exp(\xi^2)\,\mathrm{erfc}(\xi)$ is difficult and discussed in detail elsewhere [2, 58]. Via the Gibbs equation (2.22) in the form

$$\Gamma(t) = -\frac{1}{RT}\frac{d\sigma(t)}{d\ln c(0,t)}, \tag{4.21}$$

which is valid under the condition of local equilibrium between the interface and the adjacent bulk phase (the subsurface), a relation for the dynamic interfacial tension results,

$$\gamma(t) = \gamma_0 - RT\Gamma_0\left(1 - \exp(Dt/K^2)\,\mathrm{erfc}(\sqrt{Dt}/K)\right). \tag{4.22}$$

As soon as the equilibrium surface tensions deviate from a linear dependence on c this relation becomes invalid and a full use of Eq. (4.1) is required or a direct solutions of the transport problem with respective boundary conditions.

The diffusion controlled adsorption model has be solved by the so-called orthogonal collocation method using the Langmuir isotherm (2.17) [59]. If we define a dimensionless time by $\Theta = Dt / (\Gamma_o / c_o)^2$, the solution can be given in form of a polynomial

$$\frac{\Gamma(\Theta)}{\Gamma_o} = \sum_{i=1}^{N} \xi_i \tau^i , \tag{4.23}$$

where the coefficients ξ_i are functions of the reduced concentration c_o/a_L and τ is defined by:

$$\tau = 1 - \frac{1}{1 + \sqrt{\Theta + \Theta^2 c_o / a_L}} . \tag{4.24}$$

For the region of practical interest, $0 \le c_o / a_L \le 100$, the coefficients ξ_i are tabulated by Miller and Kretzschmar [60] (cf. also [2]). Another rather complicated polynomial solution was derived by Yousef and McCoy [61]. The use of Eq. (4.23) is quite simple: from the measured $\gamma(t)$ - value the corresponding $\Gamma(t)$ -values are calculated via Eq. (4.25), which is the equivalent relationship to the Langmuir isotherm

$$\Gamma(t) = \Gamma_\infty \left(1 - \exp\left[\frac{\gamma(t) - \gamma_o}{RT\Gamma_\infty} \right] \right) . \tag{4.25}$$

By variation of D, the values of $\Gamma(\Theta)$ via Eqs (4.23) are calculated and compared to the corresponding experimental $\Gamma(t)$ - values, i.e., the model equation is fitted to the experimental $\gamma(t)$ - values. For these calculations the specific parameters Γ_∞ and a_L for the studied surfactant are needed, which can be determined from the corresponding equilibrium interfacial tension isotherm. If the fitting yields a reasonable value for D the studied surfactant adsorbs diffusion-controlled. Pure surfactant systems follow a diffusion-controlled mechanism. Experimental results with different surfactant systems proof this statement (cf. Section 4.3).

To demonstrate the influence of the adsorption isotherm on the adsorption kinetics of a surfactant, the change in surface tension with time $\gamma(t)$ for a Frumkin isotherm is shown in Fig. 4.5 for three values of the interaction parameter a in Eq. (2.37). The case a = 0 is identical with the Langmuir isotherm. The parameter b was chosen such that the equilibrium surface tension is 25 mN/m. As one can see, the shape of the adsorption isotherm has a significant influence on the course of the adsorption kinetics, here given in terms of dynamic surface pressure as a function of time.

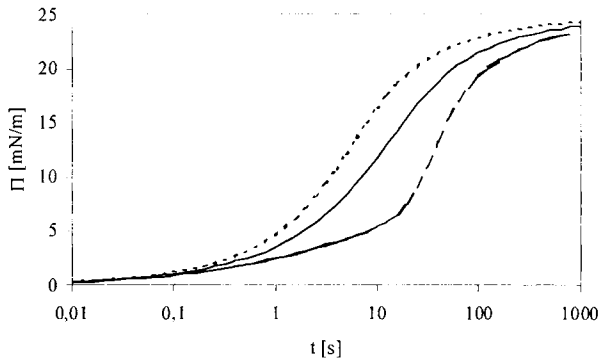

Fig. 4.5 Dynamic surface pressure calculated for the Frumkin isotherm; $c_0 = 5 \cdot 10^{-8}$ mol/cm^3, $D = 6 \cdot 10^{-10}$ m^2/s, $\omega = 1.5 \cdot 10^5$ m^2/mol; a = 0 (solid line - Langmuir isotherm); a = 1.5 – dotted line; a = -1.5 – dashed line

Recently, Ferri and Stebe [62] proposed a scaling low in order to directly compare the adsorption dynamics of different surfactants. By plotting dynamic surface tensions in a dimensional format $\Pi(t/\tau_D)/\Pi_0$, where $\Pi_0=\gamma(t)-\gamma_0$ is the equilibrium surface pressure and the diffusion relaxation time τ_D is defined by the following relationship

$$\tau_D = \frac{1}{D}\left(\frac{\Gamma_0}{c_0}\right)^2 . \tag{4.26}$$

The authors show that depending on the chosen adsorption isotherm, all experimental curves fall into one or deviate from each other. The degree of scattering of the received normalized curves is discussed as a measure for the correctness of the chosen isotherm.

Analytical solutions as presented above are based on the very simple Henry isotherm, while for the frequently applied Langmuir isotherm an approximate solution as a power series can be obtained. For any other, more sophisticated isotherm, an analytical solution does not exist. Thus, a direct integration of the initial and boundary value problem of the diffusion-controlled model is required. Using a difference scheme [63] numerical results can be obtained for any type of an adsorption isotherm. The following models rely on such numerical methods.

4.2.2 Consideration of interfacial reorientation

In the thermodynamic model derived by Fainerman et al. [49, 64], which has been described in detail in the preceding Chapter 2, it was supposed that, depending on the surface coverage, surfactant molecules can adsorb in two different states. These states are characterised respectively by two different molar surface areas ω_1 and ω_2 and by the parameters b_1 and b_2, which are related to the respective surface activities. Then it was demonstrated in Chapter 3 that n-alkyl dimethyl phosphine oxides [65] and poly-oxyethylated surfactants at the water/air and water/alkane interfaces could be described by this model perfectly [66, 67, 68].

In order to describe the evolution of the surface pressure during the adsorption process, the three involved dynamic processes have to be considered, i.e. the diffusion process in the bulk, the adsorption-desorption exchange between the surface and the subsurface, and the change in the orientation of the adsorbed molecules. In the present model, adsorption is considered to proceed in the following way. The molecules, which are randomly oriented in the bulk, adsorb either in the state 1 or 2, with the respective probabilities χ and $1-\chi$. The diffusion sets in when there is a concentration gradient established in the bulk. As the distribution of the freshly adsorbed molecules between the two states is out of equilibrium, a re-orientation process is induced. The time evolution of the partial adsorptions Γ_1 and Γ_2 is described then by

$$\frac{d\Gamma_1}{dt} = j_{a1} - j_{d1} + j_{or} \tag{4.27}$$

$$\frac{d\Gamma_2}{dt} = j_{a2} - j_{d2} - j_{or} \tag{4.28}$$

where j_a and j_d are the adsorption and desorption fluxes. j_{or} is the contribution of the orientation which is assumed to be a kinetic process involving only the adsorbed molecules and can be expressed in the following way

$$j_{or} = k_{21}\Gamma_2 - k_{12}\Gamma_1 \tag{4.29}$$

The change of the total adsorption with time then reads

$$\frac{d\Gamma}{dt} = j_{a1} + j_{a2} - j_{d1} - j_{d2} \tag{4.30}$$

i.e., the variation of the total adsorption $\Gamma=\Gamma_1+\Gamma_2$ does not depend on the orientation process and the adsorption dynamics is completely described when the time dependence of two of the quantities Γ, Γ_1 and Γ_2 is known.

For the orientation process two rate coefficients k_{12} and k_{21} exist which describe the transfer from one state into the other. Using the equilibrium state, a relationship between Γ_1 and Γ_2 and the rate constants is found [64]

$$k_{21} = \left(\frac{\Gamma_1}{\Gamma_2}\right)_0 k_{12} \tag{4.31}$$

where the index "0" refers to the orientation equilibrium. Thus, by using Eq. (2.42), Eq (4.31) becomes

$$k_{21} = \left(\frac{\omega_1}{\omega_2}\right)^{\alpha} (1-\omega\Gamma)^{\frac{\omega_1-\omega_2}{\omega}} k_{12} \tag{4.32}$$

and the orientation term has the form

$$\Phi_{or} = k_{12}\left(\left(\frac{\omega_1}{\omega_2}\right)^{\alpha} (1-\omega\Gamma)^{\frac{\omega_1-\omega_2}{\omega}} \Gamma_2 - \Gamma_1\right) \tag{4.33}$$

The contribution of the subsurface-surface transfer has also been considered by Ravera et al. [69], however this will not be discussed here further in detail. The complete adsorption kinetics problem consists now of the transport by diffusion and the boundary condition (4.30). In order to estimate the influence of the three main processes going on simultaneously, a comparison of the characteristic times is helpful. The characteristic time of the diffusion process is given by the diffusion relaxation time as defined above in Eq. (4.26), which depends on the diffusion coefficient D and the surface properties of the surfactant expressed by the ratio Γ_0/c_0. The characteristic time of the orientation process is found by assuming the other processes to be at equilibrium [69]

$$\tau_{or} = \frac{1}{k_{12}\left[1+\frac{\Gamma_{1,0}}{\Gamma_{2,0}}\right]} \tag{4.34}$$

which depends both on the orientation rate constant k_{12} and the partitioning between the two adsorption states at equilibrium. Finally, the characteristic time of the transfer kinetics reads

$$\tau_k = \frac{1}{k_a \omega c_0} \tag{4.35}$$

The estimation of these characteristic times can be used to verify the possibility that different processes can govern the adsorption dynamics. If both the kinetic exchange and the molecular orientation processes are at equilibrium with respect to the diffusional transport, i.e. $\tau_D \gg \tau_k$ and $\tau_D \gg \tau_{or}$, the adsorption increases only due to the diffusive flux to the surface. Assuming that the process of exchange of molecules between the interface and the sublayer (kinetic transfer) is at equilibrium in comparison to diffusion and orientation, i.e. $\tau_k \ll \tau_{or} \approx \tau_D$, the time evolution of the total adsorption $\Gamma(t)$ is controlled by these two latter processes. Model calculations have been performed in [69] as well showing the effect of the reorientation kinetics mechanism. Under certain conditions, this effect can be significant. As an example, results of calculations are given in Fig. 4.6 showing the influence of the ratio between the molar surface areas corresponding to the two adsorption states. The behaviour of the surface pressure strongly changes only when the ratio of ω_2/ω_1 exceeds a value of 3. This ratio is typical for surfactants of the type C_nEO_m. Note that $\omega_2/\omega_1 = 1$ corresponds to the Langmuir model. As one can see, in the beginning the reorientation process enhances the change in surface tension while at larger adsorption time the trend can change.

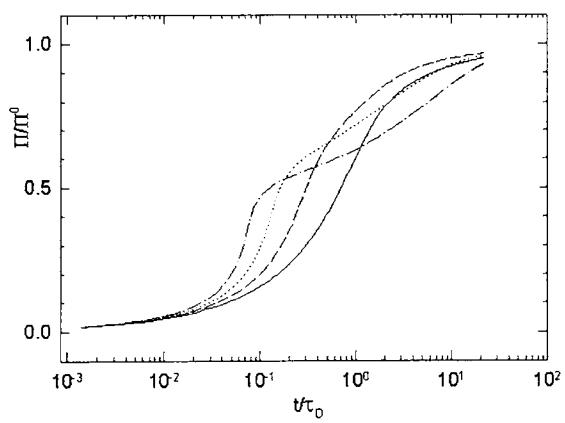

Fig. 4.6 Influence of the ratio ω_2/ω_1 on the dimensionless surface pressure Π/Π_0 versus dimensionless time t/τ_D, K_{12}=0.2 (corresponding to $\tau_D/\tau_{or} \approx 1$); c_0=6 10^{-8} mol/cm³, b_2=1.4 10^8 cm³/mol, α=2.2, ω_1=6.7 10^9 cm²/mol; ω_2/ω_1= 1 (—), 2 (---), 3 (····), 4 (-·-), according to [69]

The adsorption kinetics of proteins follows the same principles, however, these molecules can undergo conformational changes in the adsorption layer. Thus, more then two interfacial states are imaginable, while the number of adsorption states depend on the protein structure and the surface coverage or surface pressure (cf. Chapter 2, paragraph 2.8). Due to increasing adsorption, the degree of unfolding becomes smaller with advancing time. At low bulk concentrations, however, the area at the interface covered by adsorbed molecules is small and the molecules can occupy a maximum interfacial area. A kinetics model should take all this into consideration, so that at present a comprehensive kinetic adsorption theory for proteins can certainly not be worked out. For the moment, only some general conclusions can be made which result from the evolution of protein molecules in different states in an adsorption layer.

Adsorbed protein molecules rearrange at the interface to establish the equilibrium value Γ_i^0, which is determined by Γ_Σ^0, ω, and the number of different adsorption states. For an ideal equilibrium adsorption layer, the amount of molecules adsorbed in the i^{th} state has the form

$$\Gamma_i^0 = \frac{c_0 b_1 i^\alpha}{\omega}\left(1-\Gamma_\Sigma\omega\right)^{i\omega_1/\omega}. \tag{4.36}$$

This equation results from the model characterised by Eqs. (2.84) - (2.88). Under dynamic conditions $\Gamma_i < \Gamma_i^0$, and protein molecules increase their number of adsorbed segments each occupying an area ω_1, while when $\Gamma_i > \Gamma_i^0$ earlier adsorbed segments rearrange to leave the interface. The transfer between the different states may be described by a first order reaction

$$\Gamma_{i-1} \underset{k_i^-}{\overset{k_i^+}{\leftrightarrow}} \Gamma_i \underset{k_{i+1}^-}{\overset{k_{i+1}^+}{\leftrightarrow}} \Gamma_{i+1}, \tag{4.37}$$

A rate constant with "+" indicates an increase, a constant marked by "-" leads to a decrease of the partial molar surface of the protein by a value $\Delta\omega = \omega_1$. From Eq. (4.37) follows the equation of adsorption kinetics for a protein in i states

$$\frac{d\Gamma_i}{dt} = -\Gamma_i\left(k_i^- + k_{i+1}^+\right) + \Gamma_{i-1}k_i^+ + \Gamma_{i+1}k_{i+1}^-,\ i = 2, 3, ..., n \tag{4.38}$$

For i = 1 instead of Eq. (4.38) we have to add the diffusion flux from the bulk

$$\frac{d\Gamma_1}{dt} = \Gamma_2 k_2^- - \Gamma_1 k_2^+ + D\left(\frac{\delta c}{\delta x}\right)_{x=0}, \tag{4.39}$$

A good approximation for the diffusion flux is [70]

$$D\left(\frac{\delta c}{\delta x}\right)_{x=0} = \left[c_o - c(\Gamma_1)\right]\left(\frac{D}{\pi t}\right)^{1/2}, \tag{4.40}$$

The protein concentration in the sublayer $c(\Gamma_1)$ can be determined via the adsorption isotherm Eqs. (2.117) to (2.119). The Eq. (4.38) is quite complicated for a further analysis and simplifications are necessary. From experimental data, it is known that the adsorption of proteins at the air/water interfaces follows a diffusion-controlled mechanism, at least for small surface pressures $\Pi \leq 2$ mN/m [71, 72, 73, 74, 75]. Moreover, the so-called induction time t^*, the time at which the surface pressure Π starts to increase, can be used for an estimation of the adsorption mechanism. For this time interval the relation $c^2 t^* \cong$ const should hold [71, 74, 76]. A diffusion model for the range of small Γ as approximation was given in [77]

$$\Gamma_{\Sigma / \Pi \to 0} = 2c_o\sqrt{\frac{Dt}{\pi}}. \tag{4.41}$$

Usually, at surface pressures $\Pi > 2$ mN/m the rate of adsorption is slower than predicted by Eq. (4.41), and we can conclude that for low concentrations the conformational changes and desorption of adsorbed segments of the protein molecules are comparatively fast and do not control the overall adsorption process. At higher surface concentration or surface pressure these processes become more important.

A more advanced model was suggested very recently by [78] based on the adsorption isotherm for proteins given by Eq. (2.124). In addition to diffusion of the molecules in the bulk, a kinetic process was assumed equivalent to the mechanism used in the mixed kinetic model. The configuration changes, i.e. orientation of a globular protein molecule to the surface, were characterised by one rate constant k. The following Fig. 4.7 shows model calculations where the following parameters were used: $\omega_1 = 2.5 \cdot 10^7$ m²/mol, $\omega_2 = 5.0 \cdot 10^7$ m²/mol (i.e. $\omega_2/\omega_1 = 2$), $a_{el} = 200$. These parameters correspond to those for HSA adsorbed at the water/air interface [79]. The diffusion coefficient was taken to be $D = 10^{-6}$ cm²/s and the protein concentration as 10^{-8} mol/l. The equilibrium surface pressure of the protein solutions was taken to be 20 mN/m, typical for HSA at this concentration. It should be noted first that the time required for an experimentally observable decrease of the surface tension, say by 0.5 mN/m, is about 3100 s

(see Fig. 4.7), while for a lower concentration of 10^{-6} mol/l this time becomes less than one second.

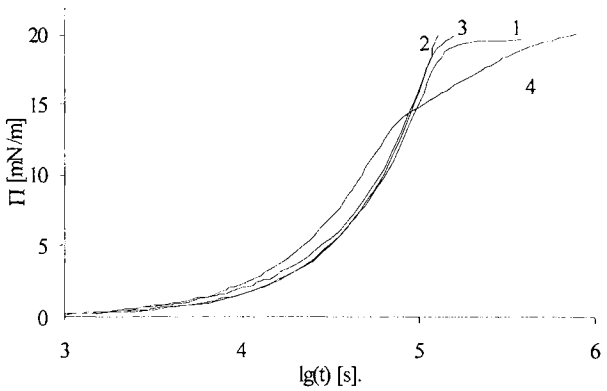

Fig. 4.7. Dynamic surface tension of model protein solution ($\omega_1 = 2.5 \cdot 10^7$ m^2/mol, $\omega_2 = 5.0 \cdot 10^7$ m^2/mol, $a_{el} = 200$) at concentration 10^{-8} mol/l; calculations were made for the quasi-equilibrium model (1) and the kinetic model with k = 10^{-3} (2), 10^{-4} (3), 10^{-5} s^{-1} (4).

This time is usually called induction time, a phenomenon which is explained by the fact that for protein molecules the molar area ω_1 is very high (by one or two orders of magnitude higher than for usual surfactants), and therefore at low adsorption layer coverage the contribution by the first (logarithmic) term in the right hand side of Eq. (2.124) is negligibly small. The contribution by the second (quadratic) term is also very small. Therefore, the surface tension deviates from zero only when the coverage exceeds 10 - 20 % [80]. Comparison with experimental data will be shown below in paragraph 4.7.5.

4.2.3 Consideration of interfacial aggregation

In Chapter 3 the adsorption isotherms where discussed for some surfactant systems showing the formation of small aggregates (dimers or trimers) within the adsorption layer. There are quite a number of surfactants, which can be described by this model perfectly, for example the homologous series of fatty acids or alcohols or the alkyl sulphates [81].

The modelling of adsorption kinetics of surfactants, which show interfacial aggregation has not been extensively studied yet. A first attempt to analyse this effect on the adsorption kinetics

was done recently by Aksenenko and co-workers [65]. As another example, the dynamic surface tension for aqueous solutions of the slightly soluble n-dodecyl-γ-hydroxy-butyric acidamide (DHBA) was studied. The kinetics exhibit a sharp decrease of the slope when the surface pressure attains a critical value which corresponds to the beginning of 2D aggregation of DHBA molecules within the adsorption layer [82]. Theoretical calculations based on an approximate diffusion model, which assumes the formation of large two-dimensional aggregates (with aggregation numbers exceeding 1000 as supported by Brewster angle microscopy) show good agreement with the experiments. The studies reported by Lin et al. [83, 84] also provide a satisfactory description for the deviation of the adsorption kinetics of 1-decanol from the Langmuir-type behaviour by assuming a 2D-aggregation within the surface layer (cf. Chapter 2). The data agree perfectly with the aggregation model when assuming a mean surface aggregation number of 2.5.

To derive an adsorption kinetics model the Ward and Tordai equation (4.1) is again the main relationship between the dynamic adsorption $\Gamma(t)$ and the subsurface concentration $c(0,t)$. As it was described in detail in paragraph 4.1.2, an adsorption isotherm as additional function $\Gamma(c)$ is needed for a kinetic model. The isotherm equations (2.110) - (2.112) given in Chapter 2 represent such type of function, which accounts for a 2D-aggregation in the adsorption layer [48]. The set of equation is too complex to find an analytical solution. Only for the short time range and for low adsorption layer coverage, the following approximation is valid [65]

$$\Pi = \frac{2c_0 RT}{n}\left(\frac{Dt}{\pi}\right)^{1/2}, \tag{4.42}$$

which is equivalent to Eq. (4.77) for not aggregating molecules. The aggregation number n is an additional parameter in the denominator, leading to a slower adsorption caused by the formation of aggregates within the adsorption layer.

For arbitrary times, surface layer coverage and critical adsorption Γ_c, the set of equations (2.110) - (2.112) together with the transport equation has to be solved numerically. This model assumes that the aggregation process itself does not require additional time, i.e. there is always equilibrium between monomers and aggregates in the adsorption layer. To solve this set of equations numerically, first-order finite difference schemes can be applied as described in

detail elsewhere [85]. The entire numerical procedure allows to calculate step-wise the time dependencies of $\Gamma(t)$ or $\Pi(t)$ to be used for comparison with experimental data.

As illustration the dependencies of dynamic surface pressure for a surfactant solution of $c_0 = 5 \cdot 10^{-8}$ mol/cm^3 and $D = 6 \cdot 10^{-6}$ cm^2/s assuming formation of small aggregates in the surface layer are shown in Fig. 4.8. The effect of the aggregation number on the dynamic surface pressure of a surfactant solution is very strong and leads to a sharp deceleration of the surface tension decrease for larger aggregation number.

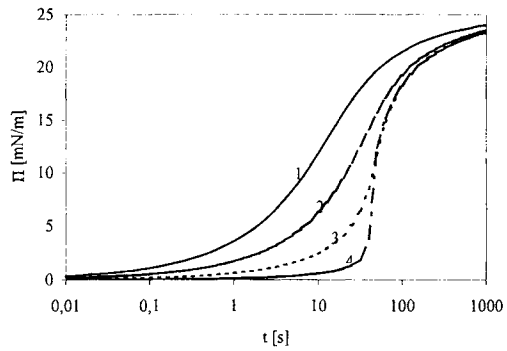

Fig. 4.8 Dynamic surface pressure for aggregation isotherm and $c_0 = 5 \cdot 10^{-8}$ mol/cm^3, $D = 6 \cdot 10^{-6}$ cm^2/s, $\omega_1 = 1.5 \cdot 10^5$ m^2/mol; curve (1) corresponds to the Langmuir isotherm; aggregation model: $\Gamma_c = 10^{-13}$ mol/cm^2, n=2 (2); n=5 (3); n=20 (4), according to [85]

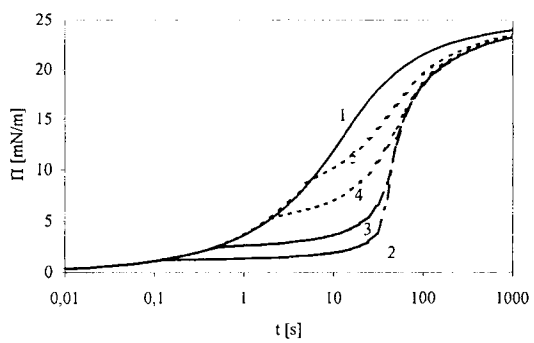

Fig. 4.9 Dynamic surface pressure for aggregation isotherm and $c_0 = 5 \cdot 10^{-8}$ mol/cm^3, $D = 6 \cdot 10^{-10}$ m^2/s, $\omega_1 = 1.5 \cdot 10^5$ m^2/mol; curve (1) corresponds to the Langmuir isotherm; aggregation model n=100: $\Gamma_c = 5 \cdot 10^{-11}$ mol/cm^2 (2); $\Gamma_c = 10^{-10}$ mol/cm^2 (3); $\Gamma_c = 2 \cdot 10^{-10}$ mol/cm^2 (4); $\Gamma_c = 3 \cdot 10^{-10}$ mol/cm^2 (5).

Further calculations were performed for various values of the critical adsorption of aggregation Γ_c and an aggregation umber of n = 100, which is realistic for slightly soluble surfactants able to form larger aggregates. For easy comparison, the equilibrium surface pressure Π_0 was set to 25 mN/m (cf. Fig. 4.9). For comparison the calculations for a Langmuir isotherm are also included. With decreasing Γ_c the values of Π for a given surface lifetime also decrease. At sufficiently low values of Γ_c one can see a significant kink point in the dynamic surface pressure curves, which has been really observed for special slightly soluble surfactants, such as by Melzer and Vollhardt [86, 87].

4.2.4 Adsorption processes at interfaces at time variable area

Depending on the technical equipment of the trough various types of area deformations can be produced by the moving barrier. In a very detailed analysis Joos [16] has demonstrated that the adsorption to or desorption from a liquid interface with changing interfacial area can be described in a very general way. The derivation of a respective diffusion controlled model leads to the following equation

$$\Gamma f(t) = \Gamma_e + 2\left(\frac{D\tau}{\pi}\right)^{1/2} c_0 - 2\left(\frac{D}{\pi}\right)^{1/2} \int_0^{\sqrt{\tau}} c_s(c-\lambda)\,d\sqrt{\lambda} \tag{4.43}$$

This equation has the same structure as the famous equation (4.1) of Ward and Tordai [3] discussed above. Joos introduced here the function f(t)

$$f(t) = \frac{A(t)}{A_0} \tag{4.44}$$

which is the relative change of the interfacial area A(t) with time and A_0 is the initial area. Based on this model the effective interfacial age can be determined from

$$t_{eff} = \frac{\tau}{f^2(t)} \tag{4.45}$$

with

$$\tau = \int_0^t f^2(t)\,dt = \int_0^t \left(\frac{A}{A_0}\right)^2 dt \tag{4.46}$$

In the book by Joos [16] as well as in original papers, some special cases of this general approach have been discussed. It was shown that such stress relaxation experiments are well suited for studying the dilational rheology of interfacial layers, which yield the dilational elasticity as a function of the effective surface age t_{eff}

$$\varepsilon = \varepsilon_0 \exp\left(\frac{t_{eff}}{\tau_D}\right)\operatorname{erfc}\sqrt{\frac{t_{eff}}{\tau_D}} \tag{4.47}$$

with the dilational elasticity modulus ε_0 and the diffusion relaxation time τ_D as defined by Eq. (4.26). For sufficiently long adsorption times, i.e.

$$\tau_D \ll t_{eff} \tag{4.48}$$

the following equation was derived by Joos and Petrov [88]

$$\Delta\gamma = \varepsilon_0 \frac{f(t)-1}{f(t)} \frac{1}{\left(\dfrac{4\tau}{\pi\tau_D f^2(t)}\right)^{1/2}} = \varepsilon_0 (f(t)-1)\sqrt{\tau_D}\left(\frac{\pi}{4\tau}\right)^{1/2} \tag{4.49}$$

Among various cases, the so-called peak tensiometry is worth mentioning [89, 90]. This relaxation process is observed when the interfacial area is changed in a linear way, i.e. $A(t)=A_0(1+\alpha*t)$ and Eq.(4.49) simplifies to the following relationship

$$\Delta\gamma = \varepsilon_0 \sqrt{\alpha\tau_D}\left(\frac{3\pi}{4}\right)^{1/2}\left(\frac{\alpha t}{\alpha^2 t^2 + 3\alpha t + 3}\right)^{1/2} \tag{4.50}$$

This function has a maximum at $t_p = \sqrt{3}/\alpha$ which makes this type of experiments very useful to confirm or reject the diffusion mechanism for a surfactant system under study.

4.2.5 Consideration of micelles in the bulk

When an adsorption layer is pre-equilibrated with a micellar solution and expanded, then monomers will adsorb at the surface. As this decreases the monomer concentration locally, the monomers and micelles are out of equilibrium and micelles will disintegrate. Hence, locally the concentration of micelles decreases and micelles will diffuse too. As the result the presence of micelles in the solution bulk can be seen as extra source of matter, i.e. the micellar kinetics represents an additional relaxation mechanism to interfacial perturbations.

The coupling of the diffusion of monomers and micelles is given by the micellar kinetics, which consists of different physical processes: a fast process in the range of microseconds (exchange of monomers between the micellar and the aqueous solution phase), and a second in the range of milliseconds (total disintegration of micelles into monomers). The entire variety of micellar kinetics was discussed by Aniansson et al. [91, 92, 93].

A quantitative model must consider the diffusion of monomers and micelles, and the micellar kinetics mechanisms as it was reviewed in the paper by Dushkin [94] or in the book by Joos [16]. As example the transport equations for a continuously expanding surface can be given in the following form

$$\frac{\partial c_1}{\partial t} - \theta z \frac{\partial c_1}{\partial z} = D_1 \frac{\partial^2 c_1}{\partial z^2} - k_1 c_1 + k_m n c_m \tag{4.51}$$

$$\frac{\partial c_m}{\partial t} - \theta z \frac{\partial c_m}{\delta z} = D_m \frac{\partial^2 c_m}{\partial z^2} + \frac{k_1 c_1}{n} - k_m c_m \tag{4.52}$$

where the subscripts 1 and m refer to monomers and micelles, respectively, k_1 and k_m are the rate constants for micellisation and demicellisation, and n is the aggregation number of micelles. For small area jumps the following relationship can be derived [95]

$$\Delta\gamma = \frac{\Delta\gamma_0 e^{-k_m t}}{\sqrt{\omega_0 + 4k_m}} \left[\sqrt{s_2} \exp(s_2 t) \operatorname{erfc} \sqrt{s_2 t} - \sqrt{s_1} \exp(s_1 t) \operatorname{erfc} \sqrt{s_1 t} \right] \tag{4.53}$$

$$\sqrt{s_1} = \frac{-\sqrt{\omega_0} - \sqrt{\omega_0 + 4k_m}}{2}, \quad \sqrt{s_2} = \frac{-\sqrt{\omega_0} + \sqrt{\omega_0 + 4k_m}}{2} \tag{4.54}$$

where $\omega_0 = D\left(\frac{dc}{d\Gamma}\right)^2$ is the relaxation frequency. This equation represents a generalization of the Sutherland equation. In general, when the jump is not small so that a linearisation is not allowed, we get the equation

$$\Gamma = \sqrt{D} \left\{ \frac{c_0}{\sqrt{k_m}} \left[\left(\frac{1}{2} + k_m t \right) \operatorname{erf} \sqrt{k_m t} + \sqrt{\frac{k_m t}{\pi}} e^{-k_m t} \right] - \int_0^t c_s(t-\lambda) \left[\frac{e^{-k_m t}}{\sqrt{\pi t}} + \sqrt{k_m} \operatorname{erf} \sqrt{k_m t} \right] d\lambda \right\} \tag{4.55}$$

which is the generalised equation of Ward and Tordai accounting additionally for the micellisation process. The short time approximation of eq. (4.55) for $c_s \approx 0$ is

$$\Gamma = \sqrt{\frac{D}{k_m}} c_0 \left[\left(\frac{1}{2} + k_m t \right) \operatorname{erf} \sqrt{k_m t} + \sqrt{\frac{k_m t}{\pi}} e^{-k_m t} \right] \tag{4.56}$$

while for long times we can approximate

$$\Gamma = \sqrt{\frac{D}{k_m}} (c_0 - c_s) \left[\left(\frac{1}{2} + k_m t \right) \operatorname{erf} \sqrt{k_m t} + \left(\frac{k_m t}{\pi} \right)^{1/2} e^{-k_m t} \right] \tag{4.57}$$

These equations can serve to estimate the influence of micellar kinetics on the adsorption process. Much more details will be given in Chapter 5 where the various micelle kinetics models and their practical relevance for interfacial studies are discussed.

4.2.6 Effect of surfactants charge

The existence of an electric double layer can remarkably influence the dynamic interfacial properties of ionic surfactant solutions [96, 97, 98, 99, 100]. The equilibrium state of such interfacial layers has been described in much detail in Paragraph 2.5. The dynamic problems, however, are rather complex and difficulties arise in solving the respective set of non-linear equations.

First models have been derived by Dukhin et al. [27, 28, 30, 101], and Borwankar and Wasan [102]. They used a quasi-equilibrium model by assuming that the characteristic diffusion time is much greater than the relaxation time of the electrical double layer, and thus, the complicated electro-diffusion problem is reduced to a simply transport problem. Datwani and Stebe [103] analysed this model and performed extensive numerical calculations, however, they did not include the electro-migration term into the diffusion equation so that the results are not relevant for further discussions.

For small periodic surface perturbations as it is the case in longitudinal wave experiments Bonfillon and Langevin [104] derived a respective solution. Joos et al. [105] demonstrated that the kinetic problem becomes extremely simple for solutions of mixed anionic and cationic surfactants, and the adsorption of the resulting electroneutral combination of the two molecules is governed by the simple diffusion model [106, 107].

MacLeod and Radke [108] obtained numerical solutions of the electro-diffusion problem without making simplifying assumptions. Although the advantage of their rigorous approach is

indisputable, the numerical solution is much time-consuming when applied to process experimental data, and it does not entirely elucidate the course of the underlying physical processes. Besides, the model of MacLeod and Radke [108] does not take into account the effect of counterion binding, i.e. the formation of a Stern layer.

During the process of adsorption of surfactant ions at a liquid-fluid interface the surface electric potential and charge density increase with time. This leads to the formation of an electric double layer inside the solution. The charged surface repels the new-coming surfactant molecules (Fig. 4.10), which results in an apparent deceleration of the adsorption process. On the other hand, the existence of the electric double layer (DEL in agreement with the nomination given in [2]) changes the amount of adsorbed surfactant ions needed to reach equilibrium. This decreases the rate of adsorption so that the total rate is a counterbalance of various influences and it cannot be estimated a priori if a deceleration or an acceleration of the equilibration of an adsorption layer results. The most recent analysis of the different relaxation processes inherent in the adsorption process of ionic surfactants has been performed by Danov et al. [33]. In this work the inclusion of counterions into the Stern layer was performed for the first time.

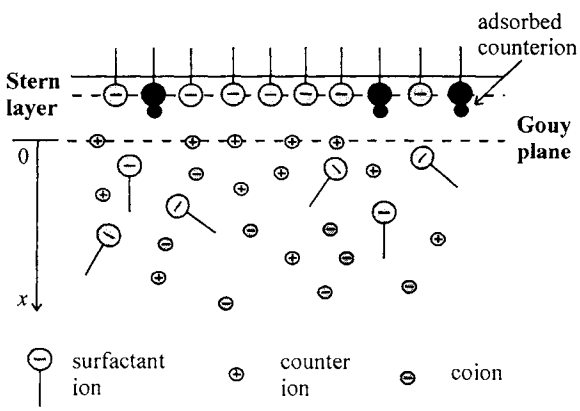

Fig. 4.10 Interfacial zone of a solution of an anionic surfactant in presence of an indifferent electrolyte, according to Danov et al. [33]

In this section, we will not discuss all the peculiarities of the electric charge effect on the adsorption kinetics as the state of experiments is still discouraging and deserves much more attention in future.

To get the main idea of the charge effect on adsorption kinetics, it is sufficient to consider an aqueous solution of a symmetric (z:z) ionic surfactant in the presence of an additional indifferent symmetric (z:z) electrolyte. When a new interface is created or the equilibrium state of an interfacial layer disturbed a diffusion transport of surface active ions, counterions and coions sets in. This transport is affected by the electric field in the DEL. According to Borwankar and Wasan [102], the Gouy plane as the dividing surface marks the boundary between the diffuse and Stern layers (see Fig. 4.10). When we denote the surfactant ion, the counterion and the coion, respectively, with the indices i = 1, 2 and 3, the transport of the ionic species with valency z_i and diffusion coefficient D_i , under the influence of electrical potential ψ, is described by the equation [2, 33]:

$$\frac{\partial c_i}{\partial t} = D_i \frac{\partial}{\partial x}\left(\frac{\partial c_i}{\partial x} + \frac{z_i e}{kT} c_i \frac{\partial \psi}{\partial x}\right) \text{ for } i = 1,2,3\ , \tag{4.58}$$

where c_i are the bulk concentrations of the respective ions which depends on time t and the distance x to the interface. k and T are the Boltzmann constant and the absolute temperature. The second term on the right hand side of Eq. (4.58) is the so-called "electro-migration" term, which accounts for the effect of the electric field on diffusion. The electric potential ψ is given by the well-known Poisson equation

$$\frac{\partial^2 \psi}{\partial x^2} = -\frac{4\pi e}{\varepsilon}\left[z_1 c_1 + z_2 c_2 + z_3 c_3\right] \tag{4.59}$$

where ε is the dielectric permittivity. The initial condition for the electric potential at time t=0 reads

$$\psi(x,0) = \begin{cases} \psi_0 \text{ at } x = 0 \\ \psi_{eq} \text{ at } x \neq 0 \end{cases}, \tag{4.60}$$

where ψ_0 is the initial value of the surface potential corresponding to the initial adsorption; $\psi_{eq} = \psi_{eq}(x)$ is the equilibrium potential distribution throughout the DEL. All other initial conditions are the same as for non-ionic surfactants.

The interfacial mass balance, interrelating the change of the surfactant or counterion adsorptions Γ_i with time and the respective electro-diffusion influx from the bulk, reads

$$\frac{d\Gamma_i}{dt} = D_i\left(\frac{\partial c_i}{\partial x} + \frac{z_i e}{kT} c_i \frac{\partial \psi}{\partial x}\right) \quad \text{at x=0 for i =1, 2.} \tag{4.61}$$

In addition the electroneutrality condition for the solution as a whole is needed

$$\int_0^\infty [c_{10} - c_{20} + c_{30}]dx + \Gamma_{10} - \Gamma_{20} = 0, \tag{4.62}$$

Here we use the fact that both the surfactant and the salt are symmetric z:z-electrolytes, so that $z_1 = -z_2 = z_3$ (the counterions of the surfactant and the electrolyte are assumed to be the same).

The distributions of the various ionic species at equilibrium are non-uniform and obey the Boltzmann equation

$$c_{i0} = c_{i\infty} \exp\left[(-1)^i \phi^{(e)}\right], \quad i = 1, 2, 3; \; \phi_{eq} \equiv \frac{ze}{kT}\psi_{eq}, \tag{4.63}$$

which results as solution of Eq. (4.58). From here it is again interesting to argue about the total adsorption or relaxation rate of ionic surfactants. As the ion distribution in equilibrium is similar to the temporary ion concentration gradient in the diffusion layer, one can again expect that it is faster to approach the equilibrium state although all the ions have to migrate against the electric field.

The Eqs. (4.59) and (4.63) yield the Poisson-Boltzmann equation for the dimensionless potential ϕ_{eq} within the equilibrium DEL

$$\frac{d^2\phi_{eq}}{dx^2} = \kappa^2 \sinh(\phi_{eq}), \; \kappa^2 \equiv \frac{8\pi z^2 e^2}{\varepsilon kT} c_{2\infty}, \tag{4.64}$$

(κ denotes the Debye screening length) which has the following solution [109]

$$\tanh\left(\frac{\phi_{eq}}{4}\right) = \tanh\left(\frac{\phi^*_{eq}}{4}\right)\exp(-\kappa x), \tag{4.65}$$

with ϕ^*_{eq} being the equilibrium surface potential. Eqs. (4.62) to (4.65) give the formula of Gouy

$$\Gamma_{1,eq} - \Gamma_{2,eq} = \frac{4c_{2\infty}}{\kappa}\sinh\left(\frac{\phi^*_{eq}}{2}\right). \tag{4.66}$$

This equation relates the surface charge density with the surface potential at equilibrium and is equivalent with Eq. (2.60) derived in Chapter 2.

Based on these basic equations Danov et al. [33] derived several expressions especially for the relaxation of adsorption layers after a transient perturbation. For a small perturbation of the interfacial layer from equilibrium the change in the adsorption of the surfactant ion and the counterions is obtained in the following

$$\frac{\Gamma_i(t)-\Gamma_{i,eq}}{\Gamma_i(0)-\Gamma_{i,eq}}=\sqrt{\frac{\tau_i}{\pi t}}, \tag{4.67}$$

where the adsorption relaxation times τ_i are defined by

$$\tau_i=\frac{1}{\kappa^2}\left(g_{i1}G_1+\frac{2}{p}\frac{q}{\sqrt{D}}g_{i2}+gG_2\right)^2 \ (i=1,2). \tag{4.68}$$

To obtain the values of the two relaxation times τ_1 and τ_2 the values of the coefficients g_{ij} and G_i have to be calculated. All these coefficients depend on the adsorption isotherms of the surfactant and the counterions, and the equilibrium state of the DEL [33].

Vlahovska et al. [32] discussed a particular case of a solution containing an ionic surfactant but no additional salt. Under these conditions, the parameters g_{ij} are zero and the following relationship for the change in surface tension was obtained

$$\gamma(t)-\gamma_{eq}=\left(\frac{\partial\gamma}{\partial\Gamma_1}\right)_{eq}\left[\Gamma_1(0)-\Gamma_{1,eq}\right]\sqrt{\frac{\tau_1}{\pi t}}. \tag{4.69}$$

The relaxation time τ_1 is then defined in the same way as the diffusion relaxation time given in paragraph 4.2 by Eq. (4.26).

4.2.7 Penetration kinetics models

Penetration systems at the air-water interface in which a dissolved amphiphile (surfactant, protein) penetrates into a Langmuir monolayer are interesting models for a better understanding of various complex processes. Most of all, penetration systems can simulate properties of biological membranes typically comprised of lipids mixed with proteins. First penetration experiments have been described by Schulman and Hughes in 1935 [110]. In the

meantime a huge number of experiments have been performed and theoretical models derived in order to understand such systems quantitatively. The theoretical and experimental progress achieved in recent years was summarised in a review by Vollhardt and Fainerman [111].

The theoretical analysis of penetration systems has not only to account for processes going on in the monolayer itself, but also for the effect induced by adsorbing surfactant molecules on two-dimensional aggregation processes in the insoluble monolayer. The quantitative analysis of penetration systems became possible due to the following achievements: a) use of Butler's equation to construct equations of state and adsorption isotherms for multicomponent solutions and monolayers, including protein solutions; b) application of the generalised Pethica adsorption equation to derive the adsorption isotherm for a soluble surfactant in the presence of a Langmuir monolayer; and c) use of the generalised Volmer equation to derive equations of state for insoluble and mixed monolayers assuming a 2D-aggregation.

Studies on the penetration dynamics, i.e., the time dependence of the surface pressure of a penetration system during the adsorption of the soluble surfactant, are rather scarce [112, 113, 114, 115, 116].

The penetration kinetics of a component 2 into an insoluble monolayer, can be monitored by measurements of the rate of the surface pressure change $\Delta\Pi(t)$. The above discussed integro-differential equation (4.1) derived by Ward and Tordai [3] is again the basis for a theoretical description of penetration processes. As shown in paragraph 2.9, a simple model for the diffusion mechanism of the penetration process can be obtained by using an equation of the following type interrelating the subsurface concentration and the adsorption

$$\Gamma_2(t) = \frac{1-\Theta_1}{\omega_2}\frac{b_2 c_2(0,t)}{1+b_2 c_2(0,t)} \tag{4.70}$$

Here component 2 is the soluble species with the bulk concentration $c_2(0, t)$, while component 1 is the monolayer covering a certain part of the interface Θ_1. b_2 and ω_2 are the adsorption constant and the area per molecule of the penetrating species. A simultaneous numerical solution of Eqs. (4.1) and (4.70) was performed by Fainerman et al. [115] using the collocation method proposed in [59]. The variation of the dynamic surface pressure for mixed monolayers caused by the penetration of the soluble component can be calculated from the equation

$$\Delta\Pi(t) = \frac{RT}{\omega}\ln(1 + bc(0,t)) \tag{4.71}$$

which follows from the respective relation equivalent to Eq. (4.70)

$$\Pi = \frac{RT}{\omega_2}\ln\frac{(1 + b_2c_2(0,t))}{(1-\Theta_1)} \tag{4.72}$$

As example of the calculations performed for various monolayer coverages of the insoluble component by Fainerman et al. [115] Fig. 4.11 shows the variation of surface pressure with time $\Delta\Pi(t)$ for different initial surface coverage.

With increasing Θ_1 a decrease of the time necessary to achieve the equilibrium state is observed, and the final value of $\Delta\Pi$ increases also significantly. This phenomenon is caused by the decrease of the equilibrium adsorption value for the soluble surfactant in presence of an insoluble monolayer. There are more recent attempts to describe the penetration kinetics, for example the diffusion model for dissolved homologues and ideal monolayers as developed by Sundaram et al. [113].

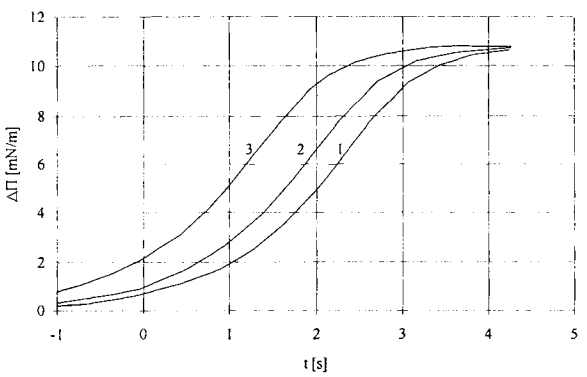

Fig. 4.11 Model calculations for the penetration kinetics of a soluble surfactant into a monolayer at different surface coverage $\Theta 1$=0 (1), 0.35 (2) and 0.7 (3), D = 5.10-6cm²/s, ω = 2.28.109 cm²/mol, b = 1.69.108 cm³/mol; according to [115]

4.2.8 Approximate solutions

The Ward & Tordai equation (4.1) is comparatively complex and large numerical efforts are necessary for its application. Therefore, simple asymptotic and approximate solutions are very

valuable and the approximation derived in 1952 by Sutherland [56] in the form of Eq. (4.20) has been very often used. In the literature a number of further approximation for small surface coverage and small and large adsorption times were discussed. Hansen [117] for example expressed the change in surface concentration as a function of the dimensionless time $\Theta = Dt / (\Gamma_o / c_o)^2$

$$\frac{\Gamma(t)}{\Gamma_o} \approx 2\sqrt{\frac{\Theta}{\pi}}\left(1 - \frac{\sqrt{\pi\Theta}}{2} \pm \ldots\right) \text{ for } \sqrt{\Theta} \le 0.2 \tag{4.73}$$

$$\frac{\Gamma(t)}{\Gamma_o} \approx 1 - \frac{1}{\sqrt{\pi\Theta}}\left(1 - \frac{1}{2\Theta} \pm \ldots\right) \text{ for } \sqrt{\Theta} \ge 5.0 \tag{4.74}$$

Rillaerts and Joos [118] derived an approximate solution at long time t by assuming that c(0,t) is almost constant and can be placed outside the integral of Eq. (4.1), which leads to

$$\Gamma(t) = 2\sqrt{\frac{D}{\pi}}(c_o\sqrt{t} - c(0,t)\sqrt{t}). \tag{4.75}$$

The most simple and often used short time approximation is

$$\Gamma = 2c_o\sqrt{\frac{Dt}{\pi}}, \tag{4.76}$$

obtained from Eq. (4.1) by neglecting the integral. Using the linear relation between γ and Γ, the interfacial tension of a surfactant solution at $t \to 0$ is given then by

$$\gamma_{t\to 0} = \gamma_o - 2nRTc_o\sqrt{\frac{Dt}{\pi}} \tag{4.77}$$

where γ_o is the surface tension of the solvent and n is 1 for non-ionic and 2 for ionic surfactants, respectively. The derivative of Eq. (4.77) with respect to $\sqrt{t}$ yields

$$\left(\frac{d\gamma}{d\sqrt{t}}\right)_{t\to 0} = -2nRTc_o\sqrt{\frac{D}{\pi}}. \tag{4.78}$$

For a diffusion-controlled adsorption at a non-deforming surface, the experimental values in the form of $\gamma(\sqrt{t})$ must give a straight line. The slope of this plot is equal to the expression on the right hand side of Eq. (4.78) and thus yields the diffusion coefficient.

There is one point important to note here, the experimental data plotted as $\gamma(\sqrt{t})$ must cross the ordinate at a value identical to the surface tension of the surfactant-free system, i.e. the surface tension of water for a water/air interface. This is often not the case, in particular for drop volume or maximum bubble pressure experiments where due to the peculiarities of the measurement an initial surfactant load of the interface exists. It has been demonstrated in the book by Joos [16] that even in these cases, assumed it is the initial period of the adsorption time, the slope of the plot $\gamma(\sqrt{t})$ yields the diffusion relaxation time defined by Eq. (4.26) and hence information about the diffusion coefficient. For small deviation from equilibrium we have the relationship

$$\Delta\gamma(t) = \Delta\gamma_0 \exp\left(\frac{t}{\tau_D}\right) \operatorname{erfc}\sqrt{\frac{t}{\tau_D}} \tag{4.79}$$

with $\Delta\gamma(t) = \gamma(t) - \gamma_e$ and $\Delta\gamma_0 = \gamma_0 - \gamma_e$. When setting $\Delta\Gamma \approx RT\Delta\gamma$ we get from Eq. (4.73) the approximation

$$\Delta\gamma(t) = 2\Delta\gamma_0\sqrt{\frac{t}{\tau_D}} \tag{4.80}$$

and hence

$$\frac{d(\Delta\gamma)}{d\sqrt{t}} = 2\Delta\gamma_0/\sqrt{\tau_D}\,. \tag{4.81}$$

In Chapter 2 it was shown that molecules can undergo aggregation in the adsorption layer. This is common to all surfactants having strong intermolecular interactions, such as fatty acids or alcohols. Provided a complete aggregation of all adsorbed molecules takes place, for the short time range and for low adsorption layer coverage, one can derive an approximate solution from Eqs. (4.1) and (2.104) by retaining the leading term of the expansion of the logarithm in Eq. (2.104), which finally yields Eq. (4.42). In contrast to the relation (4.77) valid for non-aggregating molecules, the denominator of Eq. (4.42) is proportional to the aggregation number n. This means that if the formation of aggregates within the monolayer takes place, then the rate of surface tension decrease becomes lower, and the value of dynamic surface pressure becomes inversely proportional to the aggregation number.

Additional short and long time approximations have been summarised by Fainerman et al. [99] based on diffusion-controlled, barrier-controlled and mixed kinetic models. An analysis of the known long time approximations was given by Makievski et al. [15]. They compared the long time approximations given by Hansen and by Joos. While Hansen's approximation [22, 117] yields

$$\Delta\gamma\big|_{t\to\infty} = \gamma(t) - \gamma_{eq} = \frac{RT\Gamma^2}{c_0\sqrt{\pi Dt}} \tag{4.82}$$

Joos derived the relationship [119]

$$\Delta\gamma\big|_{t\to\infty} = \gamma(t) - \gamma_{eq} = \frac{RT\Gamma^2}{2c_0}\left(\frac{\pi}{Dt}\right)^{1/2} \tag{4.83}$$

which both differ by a factor of $2/\pi$. Makievski et al. [15] demonstrate that the approximation by Joos reflects the real long time data much more accurate. However, it was shown that it is difficult to estimate the range of application of this equation for experimental data. Thus, the use of this long time approximation can lead to significant errors when applied in a wrong time interval.

For a multi-component solution and the same diffusion-controlled mechanism as $t \to 0$ we obtain the total adsorption,

$$\Gamma_T = \sum_{i=1}^{r}\Gamma_i = \sum_{i=1}^{r} 2c_{oi}\sqrt{\frac{D_i t}{\pi}} \tag{4.84}$$

and finally

$$\left(\frac{d\gamma}{dt^{1/2}}\right)_{t\to 0} = -2RT\sum_{i=1}^{r} n_i c_{oi}\sqrt{\frac{D_i}{\pi}}\,. \tag{4.85}$$

From Eq. (4.85) we can learn that surface-active contaminants eventually present in the solution of a surfactant under study, do not influence the dependence of $\gamma(t)$ at short adsorption times $t \to 0$. This of course is true only for the beginning of the adsorption process while for the remaining period impurities can take over the determining role in the adsorption layer.

4.3 Non-diffusional kinetics and mixed models

4.3.1 Adsorption barriers

As mentioned above, the adsorption kinetics for a kinetic-controlled mechanism is given by the balance of surfactant adsorption and desorption fluxes to and from the interface and for the Langmuir kinetics this balance has the form of Eq. (4.15). The rate constants k_{ad} and k_{des} are functions of the activation energies adsorption and desorption and can be specified on the basis of the molecular kinetic [9, 120] or transition state theory [121]. Eq. (4.15) was applied to adsorption kinetics data of surfactants at the water/air interface by many authors, for example in [24, 39, 83, 97, 122, 123, 124, 125, 126, 127]. In these works, it was shown that the values of k_{ad} and k_{des} are not constant but depend on the surfactant bulk, the degree of adsorption layer saturation, or its lifetime. To obtain better correspondence with the experimental data, some authors had assumed that the adsorption and desorption activation energies depend on the degree of adsorption layer saturation. These rather complicated kinetic equation are more or less empirical, although they transforms into a valid adsorption isotherm at equilibrium ($d\Gamma/dt = 0$).

For the practical use a criterion is needed to decide whether it is justified that such a kinetic equation is applied. This criterion must ensure that the kinetic constants are independent of the parameters of the adsorption process, mainly the surfactant concentration and the monolayer coverage. Experimental data for various surfactants show that for surface lifetimes shorter than 20 ms the reduced desorption rate constant $k'_{des} = k_{des}/\Gamma_\infty$ is nearly constant and of the order of $100\ s^{-1}$ [16]. This important result allows to define a simple criterion for a non-diffusional adsorption mechanism by comparing the characteristic times of diffusion and adsorption kinetics according to the model of Eq. (4.15). The condition for mixed or kinetic controlled adsorption mechanisms [122] then reads $\frac{\Gamma_\infty^2 k'_{des}}{a_L^2 D} < 1$. For $k'_{des} = 100\ s^{-1}$ it follows, that for usual surfactants a non-diffusional adsorption kinetics can be expected for $a_L > 10^{-6}\ mol/cm^3$. Thus, for $c_0 > a_L$ the adsorption reaches values for which a non-diffusional (barrier) adsorption mechanism could be observed.

Other theoretical approaches allow a description of non-diffusional adsorption kinetics in the framework of a purely diffusional approach. In these models, a diffusion coefficient D^s is

assumed within a certain layer of thickness δ adjacent to the surface, which is lower than the bulk diffusion coefficient [12, 34, 61, 128, 129]. Setting $k_{ad} = D^s/\delta$ one can see that this approach is only an alternative formulation of the Langmuir adsorption kinetics.

4.3.2 Effect of a non-equilibrium adsorption layers

It is known that the surface energy depends not only on the composition of the surface layer, but also on that of the bulk phases [130]. To formulate the Gibbs law for the non-equilibrium chemical potential, additional so-called cross-chemical potentials (the partial derivatives of the surface free energy with respect to the component concentrations in the bulk phases) have been introduced. Rusanov and Prokhorov [131] derived the Gibbs equation and the expression for the free energy of the surface layer in terms of the ordinary chemical potentials by dividing the transition layer adjacent to the surface into *n* thin layers. For each layer an equilibrium state was assumed. The expression for surface energy was derived by the summation of the equilibrium equations over all these layers. Further, the expression for the additional contribution to the surface tension due to the non-equilibrium diffusion layer was derived in [48, 132]

$$\Delta\gamma = RT\int_0^s c(x,t)\ln\left[c_0/c(x,t)\right]dx \tag{4.86}$$

Here Δγ is the non-equilibrium surface tension jump, x is the co-ordinate normal to the surface, s is the thickness of the layer assumed to be in a non-equilibrium adsorption state.

An estimation of Δγ obtained from Eq. (4.86) shows that it is essential to this non-equilibrium effect into account when $c_0 > 5\cdot10^{-6}$ mol/cm^3, which coincides very good with the criterion for the non-diffusional adsorption kinetics in the Langmuir model discussed above. If we consider the von Szyszkowski-Langmuir equation, then the adsorption layer in equilibrium obeys

$$\gamma(t) = \gamma_0 + RT\Gamma_\infty \ln\left(1-\Gamma(t)/\Gamma_\infty\right) \tag{4.87}$$

while under the conditions of a dynamic surface layer we obtain (Fainerman et al. 1998a)

$$\gamma(t) = \gamma_0 + RT\Gamma_\infty \ln\left(1-\Gamma(t)/\Gamma_\infty\right) + RT\int_0^s c(x,t)\ln\left[c_0/c(x,t)\right]dx \tag{4.88}$$

Calculations show that the model of a non-equilibrium surface layer is an alternative to kinetic-controlled adsorption models. On the basis of the purely diffusion-controlled adsorption mechanism the proper consideration of a non-equilibrium diffusion layer leads to a satisfactory agreement between theory and experimental data for various studied systems, systematically demonstrated for the short-chain alcohols [132]. The non-equilibrium model is applicable in the concentration range from 10^{-6} to 10^{-5} mol/cm^3 at different values of the Langmuir constant a_L. For $a_L < 10^{-6}$ mol/cm^3 a consideration of non-equilibrium layer effects is not necessary. For $a_L > 10^{-5}$ mol/cm^3 and large surfactant concentration the $\Delta\gamma$ values calculated from the proposed theory do not compensate the discrepancy to the experimental data so that other mechanisms have to be taken into account. An empirical formula also proposed in [132] for the estimation of the non-equilibrium surface layer thickness leads to a better agreement with experimental data, however this expression restricts the validity of the non-equilibrium surface layer model as alternative to non-diffusional adsorption kinetics.

4.4 Adsorption and transfer across the interface

The description of adsorption processes at liquid-liquid interfaces requires some specific consideration. The main reason that almost each surfactant is soluble in both the aqueous and the oil phases which can practically never be neglected. This implies that a theoretical modelling of the adsorption kinetics has to consider the transfer of surfactant across the interface during the adsorption process. Moreover, experiments have to carefully define the initial partition state, so that the relative volumes of the bulk phases become important parameters for the adsorption dynamics [133, 134]. For these reasons the knowledge of the distribution coefficient K for the adsorbing surfactant is a key parameter, which is defined as the ratio between the equilibrium surfactant concentrations in the two phases. For dilute and ideal solutions in the two liquids α and β, the ratio between the equilibrium concentrations c_α and c_β can be written as [135]

$$K = \frac{c_\alpha}{c_\beta} = \frac{v_\alpha}{v_\beta} \exp\left(-\frac{\mu^{0\alpha} - \mu^{0\beta}}{RT} \right) \qquad (4.8$$

where v_α and v_β are the molar volumes. Although K describes properties of the liquid bulk phases, this parameter influences the adsorption dynamics of a surfactant at the liquid-liquid

interface significantly [133, 134,136, 137]. The transfer of surfactant across an interface can cause interfacial instabilities which has to be considered in experiments as well [138, 139].

4.4.1 General model

As mentioned above the adsorption dynamic at liquid-liquid is considered, the partitioning of the surfactants between the two phases has an important role. In spite of the good knowledge of the adsorption dynamics at solution surfaces, only a few investigations have been devoted to the study of dynamic and equilibrium adsorption properties of surfactants at liquid-liquid interfaces.

In the general diffusion model it is possible to assume for most of the surfactants that there is a local equilibrium between the interface and the sub-layer as discussed above in paragraph 4.1.2. For the present case we have to generalise the model as diffusion happens in both liquid phases. By considering a plane interface between two semi-infinite liquid phases 1 and 2 characterised by a the diffusion coefficients D_1 and D_2, respectively, the boundary condition Eq. (4.5) becomes

$$\frac{d\Gamma}{dt} = -D_1 \left.\frac{\partial c}{\partial x}\right|_{x=0^+} + D_2 \left.\frac{\partial c}{\partial x}\right|_{x=0^-} \tag{4.90}$$

Due to the assumption of a local equilibrium condition at the interface, for t>0, the sub-layer concentrations $c_{10}(t)=c(0^+,t)$ and $c_{20}(t)=c(0^-,t)$ are always at partition equilibrium

$$c_{20}(t) = Kc_{10}(t) \tag{4.91}$$

The classical problem of adsorption dynamics is the prediction of the evolution of the interfacial adsorption $\Gamma(t)$ for a "freshly" formed interface, i.e. with the initial condition of Eq. (4.10), and a homogeneous surfactant distribution in the two bulk phases

$$c(x,0)=c_1^{\infty} \text{ for } x>0 \tag{4.92}$$

$$c(x,0)=c_2^{\infty} \text{ for } x<0 \tag{4.93}$$

By solving the diffusion equation in both bulk phases with the boundary condition (4.90) and the given initial conditions we obtain

$$\Gamma(t) = 2c_1^{\infty}\left[\sqrt{\frac{D_1 t}{\pi}} + K\sqrt{\frac{D_2 t}{\pi}}\right] - \frac{1}{\sqrt{\pi}}\int_0^t \left[\sqrt{D_1} + K\sqrt{D_2}\right]\frac{c_{01}(\chi)}{\sqrt{t-\chi}}\,d\chi \tag{4.94}$$

which is a generalisation of the Eq. (4.1) derived by Ward-Tordai (1946).

Assuming a local equilibrium at the interface, the adsorption isotherm can be used at any t to describe the relationship between Γ and c_{01}, which is needed to solve Eq. (4.94). This assumption also allows to used Eq. (4.91). So far, no theories describe the adsorption dynamics at liquid-liquid interfaces when a local equilibrium cannot be assumed. For liquid-vapour systems, some models are available to describe this situation, often called mixed adsorption dynamics.

The models of adsorption from semi-infinite bulk phases predict in general a monotonic decrease of the interfacial tension even when a transfer of matter across the interface exists. In particular, if the initial bulk concentrations are in partition equilibrium the adsorption reaches asymptotically the equilibrium state, while otherwise the system achieves a stationary state.

For some application, however, the assumption of semi-infinite bulk phases is not realistic, for example for drops of surfactant solution in a liquid. The effect of the transfer across the interface on adsorption dynamics is particularly remarkable when such system of limited volume are considered which are initially far from the partitioning equilibrium. A first theoretical approach to this problem has been given by Rubin and Radke [136], where stirred bulks are considered.

A diffusion controlled model can be applied to describe these experiments, in which a spherical drop of radius R_1 is considered embedded in a spherical shell of radius R_2 representing the external phase. The volume ratio Q can be adjusted by varying the R_1/R_2 ratio. The model is characterised by the following set of equations

$$\frac{d\Gamma}{dt} = -D_1 \left.\frac{\partial c}{\partial r}\right|_{r=R_1^-} + D_2 \left.\frac{\partial c}{\partial r}\right|_{r=R_1^+} \tag{4.95}$$

where c=c(r,t) is the surfactant concentration at time t and at distance r from the origin of the coordinates. This equation is equivalent to Eq. (4.90) and has to be used as a boundary condition at the interface $r=R_1$ for the diffusion problem in the bulk phases described by the Fick equations

$$\frac{\partial c}{\partial t} = D_1 \left(\frac{\partial^2 c}{\partial r^2} + \frac{2}{r}\frac{\partial c}{\partial r} \right) \quad \text{for} \quad 0 < r < R_1 \tag{4.96}$$

$$\frac{\partial c}{\partial t} = D_2\left(\frac{\partial^2 c}{\partial r^2} + \frac{2}{r}\frac{\partial c}{\partial r}\right) \quad \text{for} \quad R_1 < r < R_2 \tag{4.97}$$

The initial conditions are

$$c(r,0) = c_0 \quad \text{for} \quad 0 < r < R_1 \tag{4.98}$$

$$c(r,0) = 0 \quad \text{for} \quad R_1 < r < R_2 \tag{4.99}$$

When the surfactant is initially contained in the external phase, the conditions change respectively. Another boundary condition is needed expressing the closure of the system

$$\left.\frac{\partial c}{\partial r}\right|_{r=R_2^-} = 0 \tag{4.100}$$

Finally, since the interface is considered at local equilibrium with both the adjacent phases, the concentrations at both sides of the interface are assumed at partition equilibrium

$$c(R_1^-, t) = K\, c(R_1^+, t) \tag{4.101}$$

and the equilibrium relation holds between the boundary concentration $c(R_1^-,t)$ and the adsorption Γ

$$\Gamma = \Gamma(c(R_1^-, t)) \tag{4.102}$$

The described set of equations can be solved by using a finite difference scheme. The model gives the general features observed for practical systems (cf. 4.7.6).

4.4.2 Surfactant distribution

As shown above, the distribution coefficient K is the key parameter for the adsorption of surfactants at any liquid/liquid interface. There are only few attempts known from literature where K is determined. A straightforward procedure is the measurement of the bulk concentrations after equilibration of the two immiscible phases. This, however, only works for particular surfactants, and common analytic techniques usually fail at low surfactant concentration. An indirect method consists in the measurement of the surface tension of the aqueous phase. Via the γ-c isotherm as a master curve, the concentration can be evaluated then and hence the distribution coefficient [140].

More recently, the adsorption dynamics of C_{13}DMPO, C_{12}DMPO and C_{10}DMPO at freshly formed water-hexane interfaces has been investigated as a function of the initial partition conditions and as a function of the relative volumes between the two liquids [141]. The Table 4.1 summarises some K-values for the system water-hexane.

Table 4.1 Distribution coefficient K of some surfactants in the water-hexane system at 20 °C; according to Miller et al. [142]

Surfactant	K	Surfactant	K
C_8DMPO	0.14 ± 0.02	Triton X-405	0.098 ± 0.004
C_{10}DMPO	1.30 ± 0.05	Triton X-100	0.82 ± 0.03
C_{12}DMPO	7.7 ± 0.3	$C_{10}EO_5$	1.65 ± 0.04
C_{13}DMPO	34.7 ± 0.6	$C_{10}EO_8$	0.85 ± 0.08
		$C_{16}EO_{20}$	0.14 ± 0.02

As one can see these surfactants have large values of the partition coefficient, which enhances the influence of the transfer on the adsorption rate.

Direct methods such as HPLC can be used to determine the amount of surfactant in both phases having been in contact before to reach the distribution equilibrium. For the non-ionics of the Triton type experiments have been described by Czichocki et al. [143]. It is shown that such analytical methods are very time consuming, however once available they provide very accurate results. For ionic surfactants there are several other methods which can determine the amount of the surfactant at least in the aqueous phase, such as selective electrodes.

4.5 Interfacial relaxations

Interfacial relaxation methods are typically based on a perturbation of the equilibrium state of an interfacial layer (equilibrium within the interfacial layer and with the adjacent bulk phases) by small changes of the interfacial area. The small relative change in area is defined by

$$d\ln A = \frac{\Delta A}{A_0} \ll 1 \tag{4.103}$$

where A_0 is the initial area and ΔA the amplitude of the surface deformations. As a result the surface tension γ changes by the amount $\Delta\gamma$. The ratio of the two amplitudes gives the modulus of elasticity ε, defined as

$$\varepsilon = -\frac{d\gamma}{d\ln\Gamma} = \frac{d\gamma}{d\ln A} = -\frac{d\gamma}{d\ln\Gamma}\frac{d\ln\Gamma}{d\ln A} \approx \frac{\Delta\gamma}{\Delta A}A_0 \qquad (4.104)$$

There are transient and harmonic perturbations of the interfacial area. As it was shown by Loglio et al. [144] the theoretical basis is the same and therefore transient relaxations correspond also to a certain characteristic frequency. For harmonic relaxation processes there is a phase difference between the generation of the oscillation and the response function which is a measure of the exchange of matter.

The most popular methods, the capillary wave and the oscillating bubble methods, use harmonic disturbances of the equilibrium adsorption layer to generate relaxation processes. Their frequency intervals are very different. Methods applicable with arbitrary area changes (transient methods) to induce relaxation processes are the Langmuir trough technique [145], the elastic ring [146, 147], different surface dilational methods [16], or the modified pendent drop experiment [148, 149]. By moving a barrier at the trough, changing the shape of the elastic ring, lifting the funnel or the strip, or increasing/decreasing the volume of a pendent drop, a variety of area changes can be performed, such as jumps, square waves, ramp type, trapezoidal, and again harmonic area changes. In the so-called stress-relaxation methods (for example the oscillating jet, inclined plate) the surface is expanded in such a way that initially a bare surface with no adsorbed surfactant is obtained, and the decay of the surface tension with time is measured.

The most recently developed methods to investigate the surface relaxation of soluble adsorption layers due to harmonic disturbances is the oscillating bubble or drop method. The technique involves the generation of radial oscillations of a gas bubble or a liquid drop at the top of a capillary immersed into the solution under study. The first set-up was described by Lunkenheimer & Kretzschmar [150] and Wantke et al. [151] followed by a number of new designs of apparatus using novel pressure transducers to monitor the pressure changes inside a bubble or a drop [67, 152, 153, 154].

If area changes are performed in an anisotropic way, for example in trough experiments, the theoretical model has also to take into account the lateral transport of adsorbed molecules [145, 155, 156].

4.5.1 Harmonic relaxations

Assuming isotropic area deformations, the diffusional flux at the interface is given by

$$\frac{1}{A}\frac{d(\Gamma A)}{dt} = D\frac{\partial c}{\partial x} \text{ at } x = 0, \tag{4.105}$$

where A(t) is the time function of the interfacial area. If the relaxation is assumed to be based on the transport of molecules in the bulk by diffusion the solution to the problem has the general form [157]

$$c(x,t) = c_0 + \alpha \exp(\beta x)\exp(i\omega t). \tag{4.106}$$

The boundary condition (4.105) can be rearranged to

$$\frac{d\ln\Gamma}{d\ln A} = -\left(1 + D\frac{\partial c/\partial x}{(d\Gamma/dc)(\partial c/\partial t)}\right)^{-1}. \tag{4.107}$$

Using the definition of the dilational elasticity (4.104), the following relation is obtained

$$\varepsilon = -\frac{d\gamma}{d\ln\Gamma}\left(1 + D\frac{dc}{d\Gamma}\frac{\partial c/\partial x}{(\partial c/\partial t)}\right)^{-1}. \tag{4.108}$$

The introduction of Eq. (4.106) leads to the expression for $\varepsilon(i\omega)$ as the final result,

$$\varepsilon(i\omega) = \varepsilon_0 \frac{\sqrt{i\omega}}{\sqrt{i\omega} + \sqrt{2\omega_0}} \tag{4.109}$$

with

$$\varepsilon_0 = -\left(\frac{d\gamma}{d\ln\Gamma}\right)_A \text{ and } \omega_0 = \left(\frac{dc}{d\Gamma}\right)^2 \frac{D}{2}. \tag{4.110}$$

To model the exchange of matter at the interface of a mixed surfactant solution the same principle can be used as for the system containing only one surfactant. However, one term for each of the r surface active compounds in the system is needed [158]

$$\varepsilon_0 = \frac{d\gamma}{d\ln\Gamma_T}\sum_{i=1}^{r}\frac{\Gamma_i}{\Gamma_T}\frac{d\ln\Gamma_i}{d\ln A} \tag{4.111}$$

with the total interfacial concentration $\Gamma_T = \sum_{i=1}^{r}\Gamma_i$. The solution to Eq. (4.111) is found in the same way as described for a single surfactant system and was given in its general form also by [158],

$$\varepsilon(i\omega) = \varepsilon_0\sum_{i=1}^{r}\frac{\Gamma_i}{\Gamma_T}\frac{\sqrt{i\omega}}{\sqrt{i\omega}+\sqrt{2\omega_{i0}}} \tag{4.112}$$

with

$$\omega_{i0} = \left(\frac{dc_i}{d\Gamma_i}\right)^2\frac{D_i}{2}. \tag{4.113}$$

Only for a generalised linear adsorption isotherm the adsorption of the components i are independent and consequently the functions ω_{i0}.

As mentioned above in Section 4.4, on adsorption kinetics at liquid/liquid interfaces, one must consider that the surfactant is usually soluble in both adjacent phases. Therefore, the exchange of matter takes place in both bulk phases and the diffusion law must also be considered in both bulk phases. The result is obtained in an analogous way, but the exchange function contains both the diffusion coefficients of the surfactant in the respective phase and the distribution coefficient K of the surfactant between the two liquids. The characteristic frequency ω_0 is now defined by

$$\omega_o = \left(\frac{dc}{d\Gamma}\right)^2\frac{(\sqrt{D_1}+\sqrt{D_2}/K)^2}{2}. \tag{4.114}$$

Calculations for adsorption layers described by a reorientation isotherm have been also performed, however, analytical solutions cannot be given [159]. Based on the reorientation model given by Eqs. (2.84) to (2.88) the exchange of matter function was calculated and compared with experimental data. It was shown that the particularities of the adsorption model has a significant influence on the resulting dilational elasticities. Hence one can conclude that dilational elasticity experiments are much more sensitive to processes of adsorbed molecules,

such as changes in the orientation. Therefore, the so far rarely performed experiments have to be significantly extended in order to produce a sufficient amount of experimental data for proving this statement.

4.5.2 Transient relaxations

The whole theoretical treatment of the derivation of interfacial response functions was discussed recently by Miller et al. [160]. It was shown by Loglio et al. [144, 161, 162] that exchange of matter functions derived for harmonic disturbances can be applied to transient ones. As the result for a diffusion-controlled exchange of matter, using the theory of Lucassen and van den Tempel [157], the following functions result for a trapezoidal area change [162]

$$\Delta\gamma_1(t) = \frac{\Theta\varepsilon_0}{2\omega_0}\exp(2\omega_0 t)\mathrm{erfc}(\sqrt{2\omega_0 t}) + \frac{2\Theta\varepsilon_0\sqrt{t}}{\sqrt{2\pi\omega_0}} - \frac{\Theta\varepsilon_0}{2\omega_0}, \qquad 0 < t < t_1, \qquad (4.115)$$

$$\Delta\gamma_2(t) = \Delta\gamma_1(t) - \Delta\gamma_1(t - t_1), \qquad t_1 < t < t_1 + t_2, \qquad (4.116)$$

$$\Delta\gamma_3(t) = \Delta\gamma_2(t) - \Delta\gamma_1(t - t_1 - t_2), \qquad t_1 + t_2 < t < 2t_1 + t_2, \qquad (4.117)$$

$$\Delta\gamma_4(t) = \Delta\gamma_3(t) - \Delta\gamma_1(t - 2t_1 - t_2), \qquad t > 2t_1 + t_2, \qquad (4.118)$$

Here, the relative area change is denoted by $\Theta = \frac{d\ln A}{dt} = \frac{1}{t_1}\ln(1 - \frac{\Delta A}{A_0})$. t_1 and t_2 are the characteristic times of the trapezoidal perturbation. For a diffusion controlled exchange of matter the characteristic frequency ω_0 is defined by Eq. (4.110), as it was defined for a harmonic area change. The trapezoidal area change is a general perturbation which contains area changes such as the jump or ramp type and the square pulse as particular cases. The derivation of $\Delta\gamma(t)$ for surfactant mixtures and the consideration of specific peculiarities of the l/l interface was described by Miller et al. [160].

The surface tension response function $\Delta\gamma(t)$ of relaxations at the liquid/liquid interface has exactly the same form as the one at the liquid/air interface, except the characteristic frequency is defined in a different way, taking into account the peculiarity of solubility of the surfactant in both adjacent phases.

As it is the case in adsorption kinetics models, besides the diffusion theory, other models exist to describe the exchange of matter. We refer here only to the review by Miller et al. [1] and the book by Dukhin et al. [2].

4.6 Experimental techniques

As mentioned above, the study of the dynamics of adsorption layers at liquid interfaces is mainly restricted to surface and interfacial tension measurements. Only for slow adsorption processes, methods such as radiotracer technique [163, 164], the significantly improved surface ellipsometry [165, 166], or the very recently developed technique of neutron reflectivity [167, 168, 169, 170] can be used to directly follow the change of surface concentration with time. Neutron reflectivity allows even distinguishing between different species adsorbed at a fluid interface [171, 172, 173]. These techniques are reviewed in more detail in the preceding chapter 3 as they yield data most of all for the equilibrium state of adsorption layers.

The surface activity of surfactants varies over a broad concentration range and hence a broad time interval has to be studied. Therefore, complementary experiments are necessary to cover the extensive time range from less than a millisecond up to minutes, hours and sometime days. The following Table 4.2 summarises the most frequently used surface tension methods, their available time and temperature intervals and suitability for studying the liquid/air and liquid/liquid interface. The given values represent the interval available by standard instruments, while particular modifications certainly allow to go beyond these limits.

In the following a brief overview will be given of the most frequently used surface and interfacial tension methods, mostly available as commercial set-ups.

4.6.1 Dynamic surface tension measurements

There are a number of techniques available to measure the surface or interfacial tension of liquid systems, which together cover a wide range of time. In many cases, several methods are required in order to receive the complete surface tension time dependence of a surfactant system. One of the important points in this respect is that the data obtained from different experimental techniques have to be recalculated such that a common time scale results, i.e. one has to calculate the effective surface age from the experimental time, which is typically determined by the condition of the methods. For example, the maximum bubble pressure

method yields the surface tension in function of the bubble frequency, the drop volume a function of the drop formation time. A general procedure for the recalculation of experimental time scales to the effective age of the respective fluid surface was discussed in detail by Joos in his recently published book [16].

Table 4.2 Overview of dynamic surface tension and surface relaxation methods

Method	Suitability for liquid/liquid interface	Suitability for liquid/gas interface	Typical available time range	Typical temperature range
Capillary rise	possible	good	10 s - 24 h	20 - 25 °C
Drop volume*	good	good	1 s - 1000 s	10 - 90 °C
Growing drop/bubble	good	good	0.01s - 600 s	10 - 90 °C
Inclined plate	problematic	good	0.1 s – 10 s	20 – 25 °C
Maximum bubble pressure*	possible	good	0.1 ms - 100 s	10 - 90 °C
Oscillating jet	problematic	good	0.001s - 0.02s	20 - 25 °C
Drop/bubble shape*	good	good	10 s - 24 h	20 - 90 °C
Plate tensiometer*	possible	good	10 s - 24 h	20 - 45 °C
Ring tensiometer*	problematic	good	30 s - 24 h	20 - 45 °C
Sessile drop*	possible	possible	10 s - 24 h	10 - 90 °C
Spinning drop*	good	possible	-	10 - 90 °C
Static drop volume*	good	good	10 s – 1000 s	10 - 90 °C
Transient drop/bubble relaxation	good	good	1 s - 300 s	10 - 90 °C
Capillary waves	possible	possible	0.001 – 0.1 s	20 - 25 °C
Longitudinal waves	problematic	good	1 Hz – 20 Hz	
Elastic ring	problematic	good	10 s - 24 h	20 - 25 °C
Oscillating bubble	-	good	0.01 Hz - 500 Hz	20 - 90 °C
Oscillating drop	good	-	0.01 Hz – 10 Hz	20 - 90 °C

* For these methods, commercial instruments are available.

This paragraph will briefly present the most frequently used methods for measuring the surface and interfacial tensions as a function of time: the maximum bubble pressure, drop volume, growing bubble/drop, bubble/drop shape, and other methods.

a) The maximum bubble pressure method

About 150 years ago Simon [174] proposed the maximum bubble pressure method for measurements of surface tensions of liquids. Due to technical problems, this method was believed to be unreliable. During the last 20 years, however, more than 200 publications have been published on theoretical and experimental aspects of the bubble pressure tensiometry making this method to the most frequently used one for the very short adsorptions times from few milliseconds to some seconds. One of the advantages of this technique is the small amount of liquid required for the surface tension measurements, which is particularly important in studies of biological liquids [175].

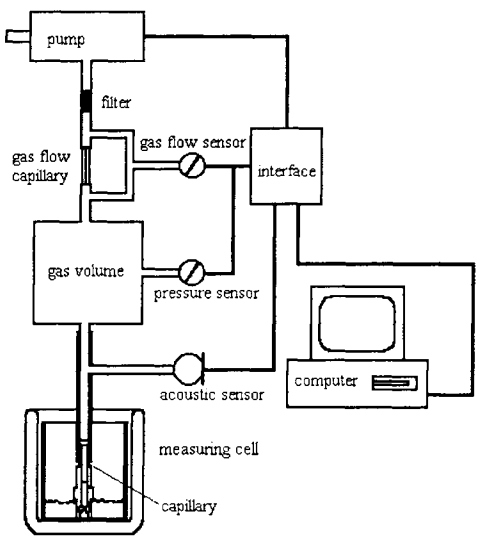

Fig. 4.12. Schematic design of the maximum bubble pressure tensiometer MPT2 from LAUDA

Since precise electrical pressure transducers are available, the progress in designing commercial instruments is tremendous. Instruments from several producers are available now. In a recent book the principles of the bubble pressure tensiometry and the theoretical backgrund have been summarised by Fainerman and Miller [176]. As an example, the tensiometer MPT2 from Lauda is shown schematically in Fig. 4.12. This device has some

peculiarities, which are of advantage for measurements in the short time range. As it was shown elsewhere, via a special design of the capillary this design allows to reach effective adsorption times of the order of 100 microseconds [46].

The functioning of the instrument, as described in detail also in the book chapter mentioned above [176], is different from most of the other instruments. Due to the large internal gas volume (about 35 cm^3) an easy procedure for determining the effective adsorption time in the moment of maximum pressure was derived (see below). The surface tension γ can be calculated from the measured maximum capillary pressure P and the known capillary radius r_{cap} using the Laplace equation in the simplified form for spherical drop/bubble shapes

$$\gamma = \frac{r_{cap} P}{2} \tag{4.119}$$

If the bubbles are larger and deviate from a spherical shape a correction factor has to added to the equation which accounts for this deviation. This correction factor f available as table or in polynomial form is needed only when capillaries with a radius $r_{cap} > 0.2$ mm are used.

The measured capillary pressure P can be expressed via the excess maximum pressure in the measuring system P_s, the hydrostatic liquid pressure $P_H = \Delta\rho g H$, and an excess pressure P_d. The excess pressure results between the measuring system and the bubble due to dynamic effects, such as aerodynamic resistance of the capillary, viscous and inertial effects in the liquid etc. ($\Delta\rho$ is the difference between the densities of liquid and gas, g the gravity and H the immersion depth of the capillary into the liquid.) Therefore, we have

$$P = P_s - P_H - P_d \tag{4.120}$$

Typically, narrow capillaries are used in the bubble pressure tensiometry ($r_{cap} < 0.01$ cm), so that no correction with respect to the sphericity of the bubble is needed and the equation for the calculation of surface tension reads

$$\gamma = \frac{r_{cap}}{2}\left(P_s - P_H - P_d\right) \tag{4.121}$$

To reach extremely short adsorption time in the millisecond and sub-millisecond range short ($l \leq 1$ cm)and wide enough ($r_{cap} \geq 0.007$ cm) capillaries have to be used so that the ratio $P_d/P \leq 0.02$, as it was shown by Kovalchuk et al. [177].

In order to calculate the effective adsorption time t_{eff}, which is necessary to compare the determined surface tension dependence with data from other methods an exact determination of the so-called deadtime is required. From some easy assumption the Poiseuille approximation results which yields [178]

$$t_d = t_b \cdot \frac{L}{k_p P}\left(1 + \frac{3}{2}\frac{r_{cap}}{r_b}\right) \qquad (4.122)$$

where k_p is the Poiseuille equation constant for a capillary not immersed into the liquid ($L = k_p P$), L the gas flow rate, $P = P_s - P_H$, t_b the time interval between two successive bubbles. A more rigorous deadtime theory developed very recently [179] had shown that corrections with respect to the non-stationarity of the gas flow through the capillary and to the effect arising at the initial section of the capillary, do not exceed a few per cent of the t_d value calculated from Eq. (4.122).

The lifetime, the time period from the moment of bubble detachment and formation of a new bubble up to the moment of maximum pressure results as the difference $t = t_b - t_d$. From this lifetime t the effective surface age t_{eff} can be calculated via the relationship

$$t_{eff} = \frac{t}{2\alpha + 1}, \qquad (4.123)$$

This equation is only of approximate character as a rigorous treatment of the problem shows that α is not a constant with a value of about 2/3 but a function of a number of parameters, such as of surface tension γ, as it was shown in [179].

b) The drop volume method

This technique is one of oldest methods for the measurement of surface and interfacial tensions between two fluids. The precursor of this method is the so-called stalagmometer method. Essentially, it consists of counting the number of drops formed from a definite amount of liquid detaching from a capillary. This drop number is then compared with values obtained for liquids of known interfacial tension. The stalagmometer method is still used in many laboratories for a first estimation of the interfacial tension of liquids.

Lohnstein founded the theoretical basis of the drop volume method already at the beginning of the last century [180, 181]. This theory is still the basis for all further refinements, which has

made the method into one of the most frequently used techniques over the years. The modern commercial devices have many advantages as compared with other commercial methods: easy handling, easy temperature control in a wide range, applicable at all liquid/fluid interfaces without any modifications, no disturbing wetting effects.

In the drop volume technique the volume of a drop formed at the tip of a given capillary has to be determined accurately which is typically realised by means of a precise dosing system. In Fig. 4.13 the principle of the drop volume apparatus TVT2 from Lauda is shown as an example.

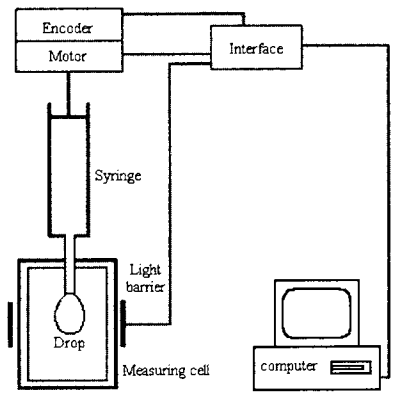

Fig. 4.13 Principle of an automated drop volume instrument, according to the TVT2 from LAUDA

The motor controller-encoder system linked with the syringe provides a constant and accurate dosing rate while the light barrier is used to detect each detaching drop. In this way, the time between the signals for two drops multiplied by the dosing rate gives the drop volume. The dosing system is linked via an interface to a computer, which controls the complete measurement. Due to the force balance between the acceleration due to gravity and interfacial tension, the critical drop volume correlates directly with the interfacial tension and the density difference $\Delta\rho$ of the two adjacent phases and is given by

$$2\pi r_{cap}\gamma \sim V\Delta\rho g. \qquad (4.124)$$

The factor $2\pi r_{cap}$ is the circumference of the drop where the interfacial tension γ acts and counterbalances the force $V\Delta\rho g$. As the drop does not detach directly at the tip of the capillary but at its neck, Eq. (4.124) needs a correction factor f, which is tabulated or exists as a polynomial [182]

$$\gamma = \frac{\Delta\rho g V}{2\pi r_{cap} f} \tag{4.125}$$

When the drop volume technique is applied with fast drop formation, i.e. less than 10 seconds per drop, additional hydrodynamic effects appear which simulate slightly higher interfacial tension values. The procedure to correct for the hydrodynamic effect is quite cumbersome however, as a good approximation the apparent value of γ can be multiplied then by the factor $\left(1 - \frac{\alpha + \beta r_{cap}}{t}\right)$ to obtain the corrected surface tension value [183].

For even shorter drop times and comparatively large capillary diameters some unexpected irregularities are observed [184]. Measurements in this short drop time range should be avoided.

The effective surface age has been determined on the basis of a diffusion controlled adsorption model. Similar to the maximum bubble pressure technique, where the bubble time is longer than t_{eff}, the drop formation time t is also significantly longer than the effective age t_{eff} and can be obtained as $t_{eff} = 3t/7$ [185]. This estimation assumes a radial flow inside and outside the growing drop and a homogeneous expansion of the drop surface.

c) The drop and bubble shape technique

An alternative approach to obtaining the liquid-vapour or liquid-liquid interfacial tension is based on the shape of a pendant drop. In essence, the shape of a drop is determined by a combination of surface tension and gravity effects. Surface forces tend to make drops spherical whereas gravity tends to elongate a pendant drop. Fig. 4.14 shows the schematic of a pendent drop set-up and an example of the images one gets (see for details [186, 187]).

The advantages of the pendent drop method is numerous: only small amounts of the liquid are required, suitable for both liquid-vapour and liquid-liquid interfaces, applicable to materials ranging from organic liquids to molten metals and from pure solvents to concentrated solutions, no limitation to the magnitude of surface or interfacial tension, accessible in a broad range of temperatures and pressures. The time interval available is of the order of part of a second up to hours and even days so that extremely slow processes can be easily followed.

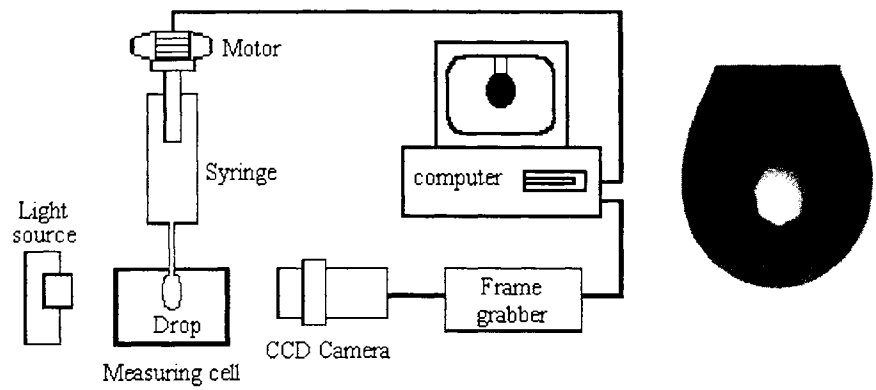

Fig. 4.14 Schematic of a pendent drop set-up and the video image of a drop

To describe a liquid meniscus and hence to obtain the interfacial tension from the drop shape the Laplace equation is used as the mechanical equilibrium condition for two homogeneous fluids separated by an interface [188]. It relates the pressure difference across a curved interface to the surface tension and the curvature of the interface

$$\gamma\left(\frac{1}{R_1}+\frac{1}{R_2}\right)=\Delta P \tag{4.126}$$

where R_1 and R_2 are the two principal radii of curvature, and ΔP is the pressure difference across the interface. In the absence of any external forces other than gravity, ΔP may be expressed as a linear function of the elevation

$$\Delta P = \Delta P_0 + (\Delta\rho) gz \tag{4.127}$$

where ΔP_0 is the pressure difference at a reference plane, $\Delta\rho$ is the density difference between the two bulk phases, g is the gravitational acceleration, and z is the vertical height of the drop measured from the reference plane. The earliest efforts in the analysis of axisymmetric drops were those of Bashforth and Adams [189]. Later Hartland and Hartley [190] used a computer program to integrate the appropriate form of the Laplace equation and the results were presented in tables. However, a significant step ahead was done by the developments of the software package called ADSA (Axisymmetric Drop Shape Analysis), which allows fitting the

Laplace equation to the shape of drops or bubbles obtained by a video camera [187, 188, 191, 192]. Today a number of commercial set-ups and respective software packages exist yielding the same quality of results.

d) Drop and bubble pressure techniques

As discussed in detail in the book [193] there is a group of methods based on static or growing drops and bubble which give access to interfacial tensions at short adsorption times, i.e. parts of a second, up to several minutes and even hours. These methods are based on the measurement of the capillary pressure, however, the entire process of the drop or bubble formation is used to study the adsorption processes at the respective interface.

All the methods are based on the Laplace equation (4.126). While the capillary pressure method works with drops or bubbles of constant size, the pressure derivative method [194] has been conceived for measuring the interfacial tension of pure liquids. To study dynamic aspects of adsorption the growing drop or bubble [25, 154] and the expanded drop [195, 196] methods have been developed.

In the applications of the capillary pressure tensiometry described, an equivalent to Eq. (4.119) is used in the two particular cases in which either the surface tension (pressure derivative method) or the drop curvature (expanded drop method) are constant. In other applications, like the expanding or growing drop methods developed respectively by Nagarajan and Wasan and McLeod and Radke, respectively [25, 154], the capillary pressure is monitored while the surface area is increasing continuously. In these methods ΔP_{cap} changes due to the variation of the drop radius and of the interfacial tension caused by the dilation of the surface which put the system in a state out of the adsorption equilibrium. The problem is that area change, flow in the bulk phases, and the adsorption kinetics of the present surface active compounds have to be considered in a model simultaneously.

Experimental set-ups as well as the corresponding theoretical models for these and other capillary pressure methods have been described in detail in a chapter by Liggieri and Ravera in the book on drops and bubble [197]. These authors also discuss very detailed the problems connected with the various experimental procedures used in the investigations with drop pressure methods. Most of all the theoretical basis of this group of experiments is well described and offers a good chance to quantitatively understand surfactant systems.

4.6.2 Interfacial relaxation studies

As mentioned above relaxation techniques are additional methods suitable to get insight into the mechanism of adsorption processes. Moreover, these methods represent the experimental tools to determine the dilational rheology of interfacial layers. The general principle of relaxation methods is the small disturbance of the interfacial layer, which has reached the equilibrium state beforehand. Particular methods are suitable to detect characteristic times of relaxations processes as they work each in a specific frequency range. This paragraph discusses briefly the most frequently used and very recently developed methods.

a) Capillary wave damping

Capillary waves can be successfully applied to investigate dynamic properties and the structure of insoluble monolayers or adsorption layers on liquid subphases. The design of the experimental set-up and the experimental procedure were described in detail elsewhere [198, 199, 200]. The dispersion equation for capillary waves

$$(\rho\omega^2 - \gamma k^3 - \rho g k)(\rho\omega^2 - mk^2\varepsilon) - \varepsilon k^3(\gamma k^3 + \rho g k) + 4i\rho\mu\omega^3 k^2 + 4\mu^2\omega^2 k^3(m-k) = 0 \qquad (4.128)$$

Here ρ and μ are the density and shear viscosity of the bulk liquid, g is the gravitational acceleration, γ is the surface tension, ω is the angular frequency, ε is the complex longitudinal dynamic surface elasticity, $k = 2\pi/\lambda + i\alpha$, λ is the wavelength, $m^2 = k^2 - i\omega\rho/\mu$ and $Re[m] > 0$.

A schematic capillary wave damping set-up is shown in Fig. 4.15.

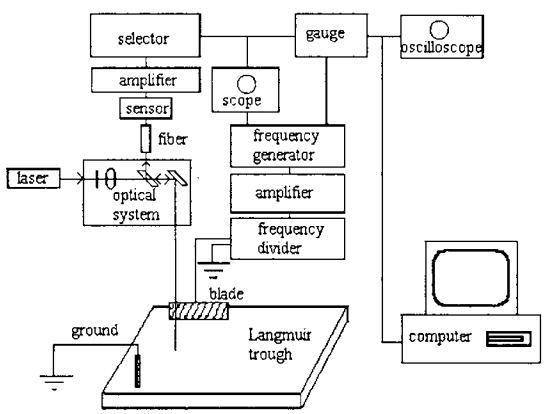

Fig. 4.15 Schematic of a capillary wave damping apparatus

The wave length λ and the damping coefficient α of capillary waves are measured by an electromechanical method based on the principle of a dynamic condenser. One part of the condenser is a thin metal plate with a thickness less than half of the wavelength while the other part is the investigated liquid surface. Waves are excited by an electromechanical vibrator fed from a low - frequency electric generator. Propagation of capillary waves causes an oscillation of the capacity of the condenser and an alternating electric current results. The amplitude and phase shift of the electric signal are measured and allow to determine the damping coefficient and the length of capillary waves. A detailed description of the experimental apparatus has been presented elsewhere [199].

b) Longitudinal wave method

While capillary waves work at comparatively high frequencies, another type of surface waves, the longitudinal waves, can be generated with rather low frequencies so that both methods complement each other. Figure 4.16 shows the schematic of a setup for measuring the characteristics of longitudinal surface waves [201, 202].

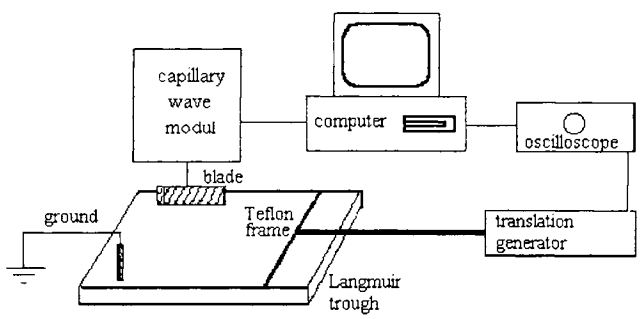

Fig. 4.16 Schematic of a longitudinal wave damping apparatus

A generator for low-frequency mechanical oscillations 1 transforms the rotation of an electro-motor to a translational motion with reversion and provides the possibility to regulate frequency and amplitude. The moving part of the generator was connected by means of a steel rod with the Teflon frame. The metal wire (0.05 mm diameter) covered by paraffin is mounted inside the frame. When the frame lay on the polished brims of the Teflon Langmuir trough the wire was wetted by the liquid and was in parallel to the liquid surface. In operation, the frame

glided back and forth along the polished brims and the oscillations of the wire excited longitudinal surface waves in the trough. The oscillation amplitudes were varied from 0.5 mm to 5 mm.

The electro-capillary method was used to create transverse surface waves. A sinusoidal voltage of a given frequency from an electric generator of high precision is applied in series to an amplifier, to a 1:2 frequency divider and after that to a metal blade. The distance between the blade and the surface of the grounded solution under investigation determined the initial amplitude of the transverse waves and was less than a millimetre. A reference platinum electrode was immersed into the solution. Under the action of the strong alternating electric field in the gap between the blade and the liquid surface transverse capillary waves were excited and propagated in the direction perpendicular to the direction of propagation of longitudinal waves. The frequency of transverse waves equals double the frequency of the voltage at the blade and is 180 Hz. Transverse surface waves were detected by an optical method. The beam of the laser passes through a focusing optical system, is reflected from the liquid surface and directed by an optical fibre to a position-sensitive photo-detector. The main part of the optical system is placed on a translation stage, which was moved by means of a micro-screw. The alternating electric current appears as result of the oscillations of the laser beam incident on the photo-detector and is amplified by a preliminary unit and a selective unit, and finally transferred to a scope. Another signal to the scope was applied from the electrical generator. A comparison of the changes of the phase difference of these two signals at simultaneous measurements of the displacements of the point where the laser beam is reflected from the liquid surface allowed us to determine the length of transverse waves.

Propagation of longitudinal waves leads to oscillations of the surface concentration of the surfactant and thereby to oscillations of the surface tension. In its turn, this induces oscillations of the length of transverse waves according to the Kelvin equation (a dispersion equation for transverse capillary waves). Moreover, this was the only observable effect connected with the propagation of longitudinal waves because the length of longitudinal waves exceeded the length of transverse waves by more than one order of magnitude and only linear waves had been used, i.e. a non-linear interaction of surface waves was avoided. The oscillations of the length of transverse waves could be observed as oscillations of the phase of the electric signal (relative to the phase of the signal from the electric generator). A phase difference gauge

converted the oscillations of the phase to a low-frequency signal with the frequency equal to that of the longitudinal surface waves and with the amplitude proportional to the amplitude of these waves. This signal was observed on the screen of an oscillograph and recorded in the memory of another one, synchronised with the motion of the Teflon frame with a thin wire.

The change of the distance between the mechanical generator of longitudinal waves 3 and the region where the laser beam is reflected from the liquid surface leads to corresponding changes of the amplitude and the phase of the signal applied to the oscillograph. This allowed us to determine the length and the damping coefficient of longitudinal waves by the same method used frequently in the measurements of transverse capillary wave characteristics. From ten to fifteen patterns of the signal in numerical form were recorded in the memory of a computer for each position of the mechanical generator and were averaged afterwards. The averaged data were used for the determination of the amplitude and phase shift by means of a non-linear regression analysis. The derivative of the dependency of the logarithm of amplitude on the distance between the oscillating wire and the region where the laser beam was reflected from the surface yields the damping coefficient of longitudinal waves and the derivative of the phase shift against this distance allowed us to determine the wavelength.

c) Oscillating drop or bubble methods

In recent years, several theoretical and experimental attempts have been performed to develop methods based on oscillations of supported drops or bubbles. For example, Tian et al. used quadrupole shape oscillations in order to estimate the equilibrium surface tension, Gibbs elasticity, and surface dilational viscosity [203]. Pratt and Thoraval [204] used a pulsed drop rheometer for measurements of the interfacial tension relaxation process of some oil soluble surfactants. The pulsed drop rheometer is based on an instantaneous expansion of a pendant water drop formed at the tip of a capillary in oil. After perturbation an interfacial relaxation sets in. The interfacial pressure decay is followed as a function of time. The oscillating bubble system uses oscillations of a bubble formed at the tip of a capillary. The amplitudes of the bubble area and pressure oscillations are measured to determine the dilational elasticity while the frequency dependence of the phase shift yields the exchange of matter mechanism at the bubble surface [205, 206].

A comprehensive analysis of oscillating drops and bubbles has been performed recently [207, 208, 209]. The apparatus shown schematically in Fig. 4.17 is designed according to the conditions analysed there. It has been shown that this type of geometries and measuring cells fulfils the requirements for stable radial drop or bubble oscillations best.

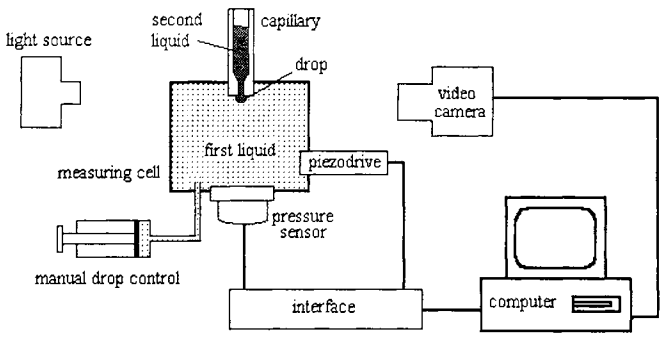

Fig. 4.17 Schematic of an oscillating drop instrument

A temperature controlled closed measuring cell is completely filled with the surfactant solution. By using a glass piston with a precision screw a small approximately hemispherical drop of a second liquid is formed at the tip of a narrow capillary immersed into the cell. Via a piezoelectric translator connected with the measuring cell, the drop volume and consequently the drop area and radius are subjected to sinusoidal oscillations. Changes in the drop radius and interfacial area produce sinusoidal changes of the pressure in the closed cell. These pressure changes are monitored by a sensitive pressure sensor which is mounted as well at the measuring cell. Its electrical signals are measured so as to obtain the pressure amplitude and the phase difference between the motion of the piezo translator and the sinusoidal changes of the pressure in the measuring cell. To observe the geometry of approximately hemispherical drops or bubbles there are two optical glass windows in the cell through which the drop can be observed over the hole measuring procedure by a video camera.

For very small sinusoidal changes of the interfacial area of hemispherical drops the pressure amplitude can be calculated from the force balance. The measured pressure amplitude can be written as the sum of a geometric (radius) component, a contribution caused by changes in the interfacial tension $\Delta\gamma$, and a hydrodynamic contribution. The dynamic pressure can be described by Eq. (4.129).

$$\Delta p = \frac{2\gamma\Delta r}{(r_0)^2} - \frac{2\Delta\gamma}{r_0} + \Delta\tilde{p}_{hydrod.} \tag{4.129}$$

with

$$r_0 \cong \frac{(r_1 + r_2)}{2} \tag{4.130}$$

The first term is a geometric component only controlled by the capillary size and the interfacial tension of the pure system. The second term is used to calculate the dilational properties. $\Delta\gamma$ as the change in interfacial tension also incorporates the elastic and viscous contributions. The third term in Eq. (4.129) is controlled by hydrodynamic effects. For example, at higher frequencies inertia effects must be considered. To maintain the experimental accuracy it is important to retain the hemispherical form of the droplet.

d) Transient drop or bubble relaxation method

These techniques measure the capillary pressure in a nearly spherical liquid drop, immersed in another immiscible fluid. The interfacial tension is related to the capillary pressure and drop radius by the Gauss-Laplace equation in its most simple form as given by Eq. (4.119). Dynamic experiments are conducted by continuously varying the drop size, thereby stressing the interface. In earlier experiments [154], oscillations of the drop shape, velocity and pressure fields have been generated after a static drop was impulsively set in motion. In continuous flow experiments by Liggieri et al. [210], Passerone et al. [194], MacLeod and Radke [152], and Zhang et al. [211] similar oscillations occur after a drop detaches from the capillary and another one starts growing after rupture of the connecting liquid bridge. The oscillations of a pendant drop arising during the detachment process create an uncertainty in the initial state of the system.

e) Stress relaxation methods

In addition to the classical harmonic or transient a group of stress relaxation experiments can be performed preferentially on a Langmuir trough. Using the barrier a pre-adsorbed surfactant layer can be expanded or compressed according to different time laws. The Fig. 4.18 shows the principal set-up of a Langmuir trough to be used for stress relaxation experiments.

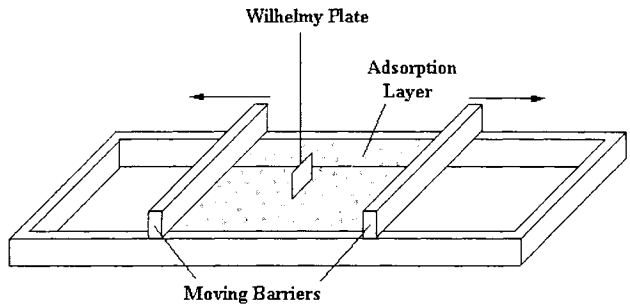

Fig. 4.18 Langmuir trough set-up designed for stress relaxation experiments

Most appropriate are experiments with constant expansion rate $dA/dt = const$ or constant relative expansion $d \ln A/dt = const$. When a constant expansion rate is used the resulting interfacial tension runs through a maximum [16]. Therefore, this experiment was called "Peak Tensiometry" by the authors. The position of the maximum (peak) depends on the expansion rate.

4.6.3 Penetration kinetics experiments

Quantitative information on penetrated layers under dynamic and equilibrium conditions require much attention in respect to the experimental technique. There are a number of penetration experiments with different advantages and drawbacks. The classical experiment is the injection technique where a soluble component is injected into the subphase below a spread monolayer. Experiments can then be performed at constant monolayer coverage [212, 213, 214] or by compression and expansion cycles [215, 216]. Another possibility is to exchange the subphase below a spread monolayer using a laminar pumping system. Other experiments were performed by using the sweeping technique as described in [217, 218].

The injection method has the disadvantage that incomplete distribution of the dissolved material in the subphase after injection can be the reason for poor reproducibility or artefacts. The subphase exchange technique requires a well adjusted pumping system to avoid monolayer gradients. Among the classical methods, the sweeping technique is superior because disturbances of the system can be largely avoided and the initial conditions can be best defined. The basic idea of this penetration technique is that in a multi-compartment trough a Langmuir monolayer, enclosed between two movable barriers and kept at a selected surface pressure, can

be swept over subphases of different composition. Thus the two components of the penetration system to be investigated can independently be characterised.

The schematic of a circular penetration apparatus and the principles of the experimental procedure are presented in Fig. 4.19.

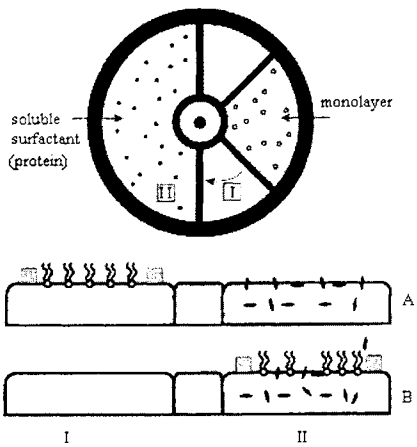

Fig. 4.19 Schematic of a penetration experiment on a multi-compartment trough, A – before monolayer manipulation, B - monolayer on the subphase containing the soluble surfactant

Such a trough can be subdivided into many compartments. For penetration experiments of a dissolved species into a Langmuir monolayer, it is useful to use three compartments. In compartment I the monolayer is spread; compartment II filled with pure water can be used for removing possible bulk components of compartment I; and finally compartment III contains the dissolved component. In many experiments however, the trough is partitioned into two semicircular regions only, as the subphase of compartment I typically consists of water. A special barrier coupling is necessary in order to move both barriers separately as well as simultaneously in a velocity range between 0.05 and 15 angular degrees per minute. A very small distance between the segment walls and the moving barriers is crucial for the functionality of the sweeping mechanism. Using a Wilhelmy plate technique the surface tension of the studied film can be measured. A penetration trough should be equipped with a Brewster angle microscope (BAM) so that the morphology of the penetration layers can be monitored [219]. A comprehensive review about this technique was given by Vollhardt recently [220].

For penetration experiments the insoluble monolayer is spread between the movable barriers at the surface of one region filled with pure buffer solution. The other region is filled by the solution of the dissolved surfactant. Afterward, the monolayer is brought to the desired state, e.g. surface pressure, molecular area, and swept onto the region containing the dissolved surfactant. Then the penetration kinetics experiments coupled with the BAM imaging were performed and the state of the penetrated monolayer in equilibrium was characterized.

The pendant drop experiments are a very new experimental technique to study penetration systems. The insoluble monolayer is spread onto the drop surface carefully by using a micro-syringe [221]. The exchange of the drop bulk phase can be easily performed by using a coaxial double-capillary as shown in Fig. 4.20.

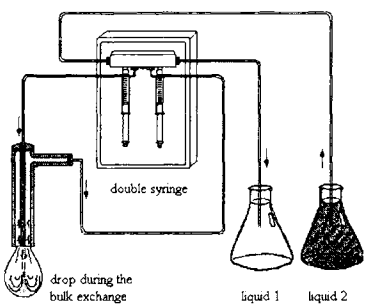

Fig. 4.20 Exchange of the drop bulk by using a double-syringe system and a co-axial double capillary; according to Wege et al. [222]

While through the inner tube the new liquid is pumped in, the bulk of the drop is pumped out via the outer tube. Due to the liquid flow the drop volume is mixed permanently. It was shown by Wege et al. [222] that the drop volume is completely exchanges when more than 250% of the drop volume has been pumped through, and that the monolayer at the drop surface is not disturbed.

4.7 Experimental results on adsorption kinetics

Most surfactants adsorb diffusion controlled at liquid interfaces. It was discussed above that exceptions observed in the literature and interpreted in terms of adsorption and desorption barriers have been understood later by the pure diffusion model when the respective experimental conditions were considered properly. One of the most important points in this respect was the systematic analysis of impurity effects on the adsorption kinetics of surfactants. This point was for example discussed in detail in the book by Dukhin et al. [2]. Another reason for the observation of an adsorption process slower than expected from diffusion is the

possibility of aggregate formation at the interface. Applying the classical diffusion model would result in a diffusion coefficient significantly smaller than physically reasonable and hence a barrier mechanism would have to be postulated. It will be shown below that a correct consideration of surface aggregation processes allow to quantitatively describe such systems in the framework of a purely diffusion controlled mechanism (cf. Fig. 4.7 and 4.8).

In contrast to surface aggregation, changes in the molar area of adsorbed molecules can lead to an apparent enhancement of the adsorption rate. Thus, observed "super-diffusion" phenomena can be understood by considering changes in the molar surface area with changing surface coverage (cf. Fig. 4.6). Again, these systems are then quantitatively understood by a purely diffusion controlled model.

In this paragraph we give examples for each of the mentioned cases, starting with a simple surfactant system that follows essentially the classical diffusion model. Then the effect of reorientation and aggregation of adsorbed molecules will be discussed by demonstrating experimental dynamic surface tension data. The adsorption dynamics of ionic surfactants has not been studied systematically so that these systems cannot be presented here extensively. Also the dynamics of adsorption at the interface between two liquids is at the beginning and we present here an impressive example.

As the theoretical models are comparatively complex, only numerical methods allow to interpret experimental data. A software package is available that allows to make model calculations for any type of the above discussed diffusion-controlled mechanism [223]. In addition to the theory for a Langmuir isotherm, where the collocation solution by Ziller and Miller can serve as analytical solution, the programme gives access also to calculations based on the Frumkin, the reorientation and aggregation isotherms.

4.7.1 Diffusion control for simple surfactants

For several non-ionic surfactants Fainerman and Miller [46] published dynamic surface tension data which can be interpreted in terms of a diffusion controlled adsorption mechanism easily. The experimental results obtained for different Triton solutions (octylphenyl poly -oxyethylene ether ($C_{14}H_{20}O(C_2H_4O)_nH$) with different numbers n of ethylene oxide groups: Triton X-100 (n=10), Triton X-114 (n=11.4), Triton X-165 (n=16.5), Triton X-305 (n=30.5) and Triton X-

405; n=40.5) are shown in Fig. 4.21 in form of a $\gamma(\sqrt{t})$ -plot. The chosen concentrations of the Tritons (X-114, X-305, X-405) were approximately the same (about 10^{-7} mol/cm³ and $5\cdot10^{-7}$ mol/cm³) in order to demonstrate the effect of the number of EO groups on the rate of surface tension decrease at short adsorption times. For all solutions we get a surface pressure $\Pi=0$ at $t=0$. This is in good agreement with Eq. (4.41). The same data restricted to the time interval $t < 5$ ms are shown in Fig. 4.22 in a $\gamma(t)$ - plot. It can be seen that quite a number of data points are obtained in the time interval 0.1 ms < t < 1 ms. Due to a comparatively small change in the design of the measuring cell of the maximum bubble pressure tensiometer MPT1 enabled the measurement of dynamic surface tensions down to 0.1 ms adsorption time [46]. The data obtained for aqueous Triton solutions agree well with the diffusion theory.

For a diffusion controlled adsorption from Eq. (4.41) and a linear relationship between Γ and γ we obtain the following equation

$$\frac{d\gamma}{d\sqrt{t}} = -2RTc_o\sqrt{\frac{D}{\pi}}\,. \tag{4.131}$$

The slope of the linear part of the curves $\gamma(\sqrt{t})$ allow to determine the diffusion coefficient. Reasonable values for D would then proof that the surfactant adsorbs diffusion controlled. In case discrepancies are observed the initial load of the bubble surface, i.e. an initial surface pressure $\lim_{\sqrt{t}\to 0}\Pi > 0$ should be taken into account in a quantitative data interpretation. Qualitatively, $\lim_{\sqrt{t}\to 0}\Pi > 0$ leads to a smaller slope of the $d\gamma/d\sqrt{t}$ -dependence and hence to smaller experimental values of $d\gamma/d\sqrt{t}$. A quantitative data analysis is possible on the basis of the model elaborated by MacLeod and Radke [25] in which the initial state of adsorption at the bubble surface has to be considered.

The dynamic surface tensions at long adsorption times were measured systematically in [224]. The results are shown as an example in the following Figs. 4.23 to 4.28. The surface activity of the various Triton compounds differs and hence the dynamic surface tensions have a different shape. While the Tritons with a large number of EO groups are less surface active and produce a surface tension change only at higher concentrations, those with the shorter EO chain adsorb strongly already at comparatively low bulk concentrations (cf. Chapter 3).

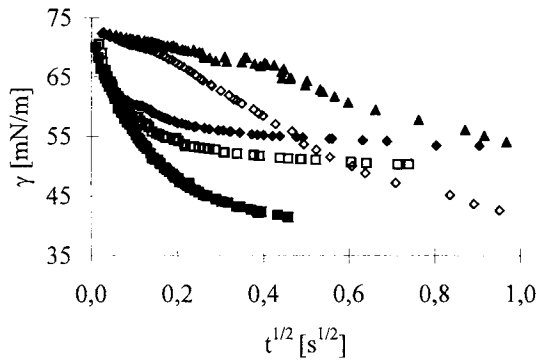

Fig. 4.21 Dynamic surface tensions of different aqueous Triton X-n solutions plotted as function of $\sqrt{t}$; n=10.0, co = $1.55 \cdot 10^{-7}$ mol/cm³ (▲); n=11.4, co = $4.23 \cdot 10^{-7}$ mol/cm³ (◇); n=16.5, co = $1.07 \cdot 10^{-6}$ mol/cm³ (◆); n=30.5, co = $4.52 \cdot 10^{-7}$ mol/cm³ (□); n=40.5, co = $5.08 \cdot 10^{-7}$ mol/cm³ (■)

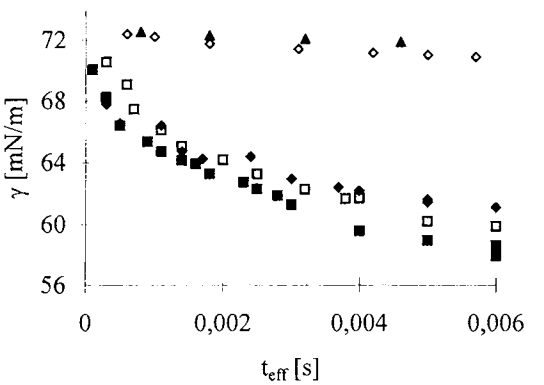

Fig. 4.22 Dynamic surface tensions of different aqueous Triton X-n solutions plotted as function of effective surface age t_{eff}; symbols are the same as in Fig. 4.21

In the range of longer adsorption times all $\gamma(1/\sqrt{t})$-dependencies are linear, as it is expected from Eq. (4.83). The data of Triton X-100 at $c_o = 1.55 \cdot 10^{-5}$ mol/cm³ (Fig. 4.27) and Triton X-405 at $c_o = 1.53 \cdot 10^{-5}$ mol/cm³ and $c_o = 2.54 \cdot 10^{-5}$ mol/cm³ (Fig. 4.23) agree very well with the data given by Van Hunsel and Joos [225] obtained by another experimental technique.

The results of $\left[\frac{d\gamma}{d(1/\sqrt{t})}\right]_{t\to\infty}$ calculated from these data are summarised in Table 4.3 together with the values of Γ_0 determined from Figs. 4.23 to 4,28 and from Eq. (4.83). The agreement is very good which means that the Tritons adsorb diffusion controlled.

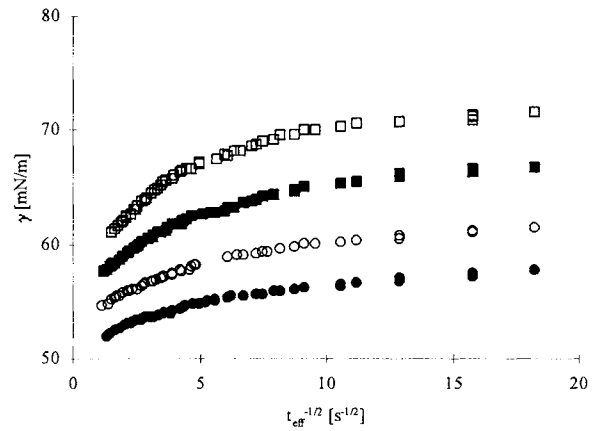

Fig. 4.23 Dynamic surface tension γ of Triton X-405 as a function of $(1/\sqrt{t})$ at different concentrations, co = 0.153 (□), 0.254 (■), 0.508 (○), 1.016 (●)10-6 mol/cm³

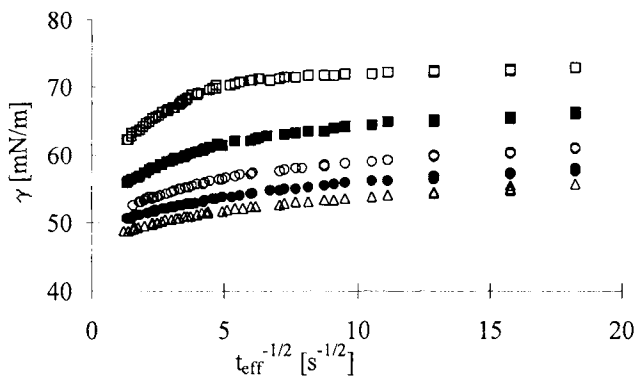

Fig. 4.24. Dynamic surface tension γ of Triton X-305 as a function of $(1/\sqrt{t})$ at different concentrations: c_o = 0.09 (□), 0.226 (■), 0.452 (○), 0.678 (●), 0.903 (Δ) 10^{-6} mol/cm³

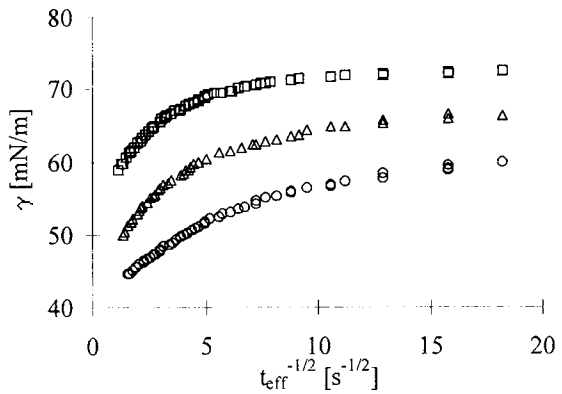

Fig. 4.25 Dynamic surface tension γ of Triton X-165 as a function of $(1/\sqrt{t})$ at different concentrations, co = 0.214 (□), 0.536 (Δ), 1.072 (O) 10-6 mol/cm³

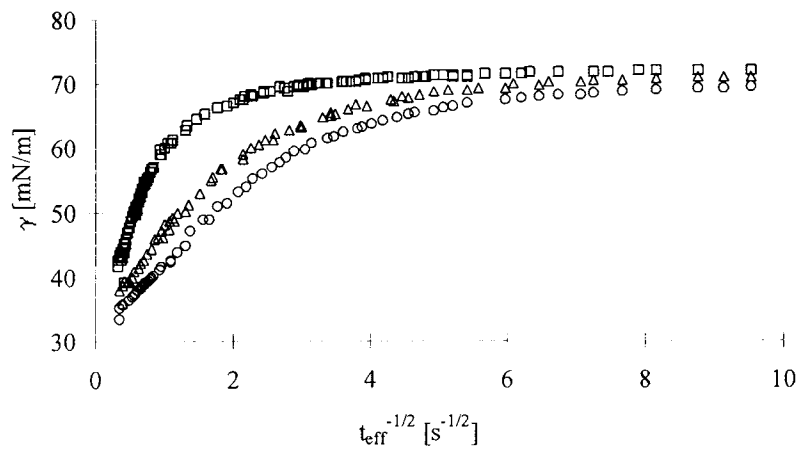

Fig. 4.26 Dynamic surface tension γ of Triton X-114 as a function of $(1/\sqrt{t})$ at different concentrations, co = 0.141 (□), 0.282 (Δ), 0.423 (O)10-6 mol/cm³

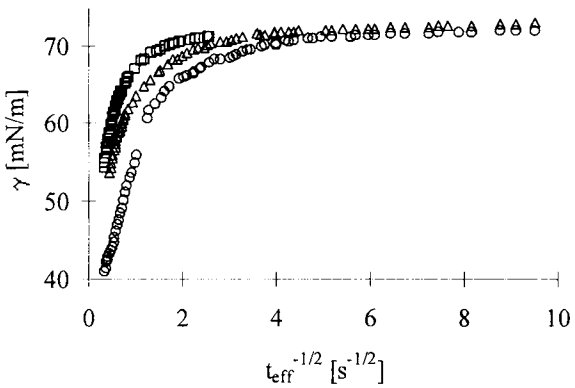

Fig. 4.27 Dynamic surface tension γ of Triton X-100 as a function of $(1/\sqrt{t})$ at different concentrations, c_o = 0.071 (□), 0.124 (Δ), 0.155 (○) 10^{-6} mol/cm³

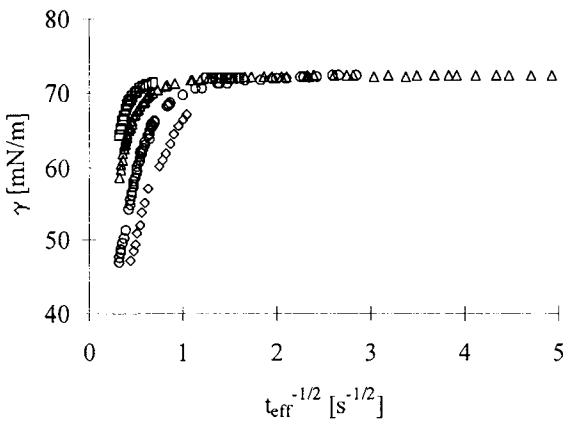

Fig. 4.28 Dynamic surface tension γ of Triton X-45 as a function of $(1/\sqrt{t})$ at different concentrations, c_o = 0.048 (□), 0.071 (Δ), 0.118 (○), 0.19 (◇) 10^{-6} mol/cm³

Table 4.3 Dynamic surface tension data for a series of Tritons, according to Fainerman and Miller [224].

Substance D [cm^2/s]	c_0 [mol/cm^3]	$\left[\frac{d\gamma}{d(1/\sqrt{t})}\right]_{t\to\infty}$ [$s^{1/2}$ mN/m]	Γ_0 (Langmuir isotherm) [10^{-10} mol/cm^2]	Γ_0 from Eq. (4.83) [10^{-10} mol/cm^2]
X-405	0.153	2.2	1.4	1.3
$7\cdot10^{-7}$	0.254	1.7	1.4	1.3
	0.508	1.0	1.4	1.4
	1.016	0.6	1.4	1.5
X-305	0.09	3.2	1.8	1.1
$7.3\cdot10^{-7}$	0.226	2.0	1.8	1.3
	0.452	1.3	1.8	1.5
	0.678	1.0	1.8	1.6
	0.903	1.0	1.8	1.9
X-165	0.214	4.4	2.7	2.0
$7.3\cdot10^{-7}$	0.536	4.0	2.8	3.0
	0.857	2.0	2.8	2.7
X-114	0.07	28	3.0	2.9
$8.6\cdot10^{-7}$	0.141	22	3.1	3.7
	0.282	14	3.1	4.1
X-100	0.047	46	3.2	3.1
$8.8\cdot10^{-7}$	0.077	38	3.2	3.6
	0.124	30	3.3	4.0
	0.155	22	3.3	3.9
X-45	0.048	90	4.6	4.5
$9.5\cdot10^{-7}$	0.071	80	4.7	5.1
	0.118	62	4.8	5.9

4.7.2 Surfactants able to change their orientation

In the literature, it is observed from time to time that adsorption processes proceed faster than expected from a diffusion mechanism. This can of course be ascribed to convection in the bulk, however, this is not a good explanation for surfactant systems, where such phenomena are observed under various experimental conditions.

For a modelling of adsorption processes the well-known integro-differential equation (4.1) derived by Ward and Tordai [3] is used. It is the most general relationship between the dynamic adsorption $\Gamma(t)$ and the subsurface concentration $c(0,t)$ for fresh non-deformed surfaces and is valid for kinetic-controlled, pure diffusion-controlled and mixed adsorption mechanisms. For a diffusion-controlled adsorption mechanism Eq. (4.1) predicts different Γ dependencies on t for different types of isotherms. For example, the Frumkin adsorption isotherm predicts a slower initial rate of surface tension decrease than the Langmuir isotherm does. In section 4.2.2. it was shown that reorientation processes in the adsorption layer can mimic adsorption processes faster than expected from diffusion. In this paragraph we will give experimental evidence, that changes in the molar area of adsorbed molecules can cause such effectively faster adsorption processes.

The Tritons have been described in the last paragraph by a diffusion controlled kinetics based on a Langmuir isotherm. As it was shown in the preceding Chapter 3, oxethylated surfactants can be usually better described by a reorientation isotherm [226]. This is however only true for high quality samples such as define compounds of the type C_nEO_m, while for technical products like the Tritons an isotherm more complicated than the Langmuir isotherm does not make sense. An analysis of dynamic surface and interfacial tensions for $C_{10}EO_8$ solutions had been performed in [227].

Let us first look into the dynamic surface tensions for $C_{10}EO_8$ at the water/air interface, as it was measured by Chang et al. [228] using the pendent bubble method. The experimental data given in Fig. 4.29 are compared with calculations for two models, based on the Langmuir and the reorientation isotherm (two-state model).

The diffusion coefficient $D = 5 \cdot 10^{-6}$ cm²/s was calculated from the equation proposed by Wilke and Chang [229]. One can see that the Langmuir equation overestimates the dynamics, i.e. the value of D required to match the experimental data would be $1.5 \cdot 10^{-5}$ cm²/s, that is 3 times

higher than the physically expected value. At the same time, the two-state model agrees well with the experimental data. Note that the equations (cf. Chapter 2) used to describe the kinetics of adsorption have been derived for a plane interface with an infinite liquid volume in absence of any convection. For a bubble immersed into the solution, sphericity and convection can lead to a more rapid adsorption than that calculated from the model used by Miller et al. [227]. This, however, is relevant only for adsorption times $t > 100$ s, as for $t < 100$ s the thickness of the diffusion boundary layer $(\pi Dt)^{1/2}$ does not exceed 20% of the bubble diameter. This allows us to conclude that the 'super-diffusion' adsorption kinetics of $C_{10}EO_8$ at the water/air interface really exist, caused by the self-regulation of the adsorbed molecules in the surface layer.

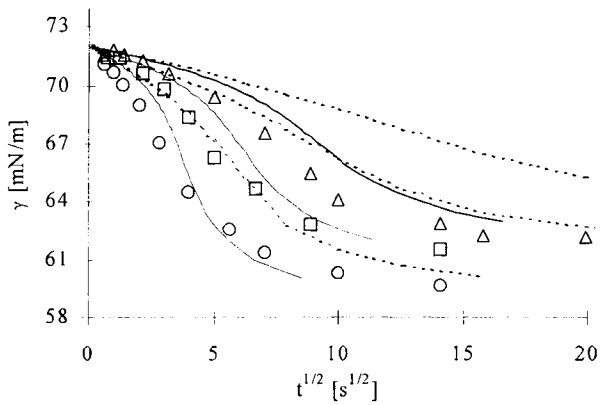

Fig. 4.29 Dynamic surface pressure for water solutions of $C_{10}EO_8$ at the air boundary for the concentrations: $c = 4 \cdot 10^{-9}$ mol/cm³ (△) $c = 6 \cdot 10^{-9}$ mol/cm³ (□), $c = 10^{-8}$ mol/cm³ (○), data from Chang et al. [228], theoretical calculations: Langmuir model (dotted lines), two-state model (solid lines).

The adsorption kinetics at liquid/liquid interfaces is a more complicated problem, as the transfer of surfactant from one phase to the other has to be taken into account. In the experiments performed by Liggieri and Ravera [197] using the expanded drop method, no preliminary saturation of the oil phase with $C_{10}EO_8$ was made. For this case, instead of Eq. (4.1), the expression (4.94) should be used, where K is the equilibrium distribution coefficient of surfactant between the oil and water phases, and D_2 is the surfactant diffusion coefficient in the oil phase. The reduced distribution coefficient defined by $K^* = K(D_2/D_1)^{1/2}$ is a parameter that reflects quantitatively the adsorption dynamics at such a liquid/liquid interface.

To estimate this coefficient K*, first the value of K can be determined experimentally, and the ratio D_2/D_1 calculated using the equation proposed by Wilke and Chang [229] . For $C_{10}EO_8$ we obtain K* = 1.8. For Tritons at the water/nonane interface the following values have been given [230]: K* = 1.5 for Triton X-45, and K* = 0.5 for Triton X-100. For decyl dimethyl phosphine oxide (C_{10}DMPO) the adsorption activity of which is close to that of $C_{10}EO_8$, a value of K* = 1.3 was found by Ferrari et al. [133].

In Fig. 4.30, experimental data for a $C_{10}EO_8$ of $c_0 = 4 \cdot 10^{-8}$ mol/cm³ are compared with calculations performed for the Langmuir model and the reorientation model using isotherm values given in the preceding chapter. As at the water/air interface, the Langmuir model overestimates the dynamic surface tensions, while the reorientation model leads to rather good agreement with the experimental data at short adsorption times t < 5 s. Similar to the water/air interface, to achieve agreement with the Langmuir model within this time range, it was necessary to increase the diffusion coefficient by a factor of three.

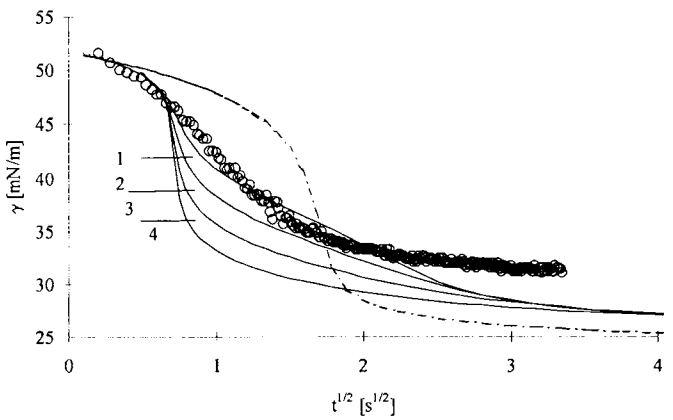

Fig. 4.30 Dynamic surface tension for water solutions of $C_{10}EO_8$ at the hexane boundary for a concentration of $c = 4 \cdot 10^{-8}$ mol/cm³ (O); theoretical calculations: reorientation quasi-equilibrium model (1-4); Langmuir model (dotted line); the parameters used were $\omega = 5.8 \cdot 10^5$ m²/mol, $\omega_{min} = 4.8 \cdot 10^5$ m²/mol, $\omega_{max} = 1.4 \cdot 10^6$ m²/mol, $D = 5 \cdot 10^{-6}$ cm²/s, K* = 1.5, and: $\alpha = 4$ (1), $\alpha = 5$ (2), $\alpha = 6$ (3), $\alpha = 7$ (4).

In the region t > 5 s, a larger difference between theory and experiment is found. The discrepancies can certainly again be ascribed to the spherical shape of the drop surface which is not taken into consideration in the used models.

We can summarise that the problem of diffusion-controlled adsorption kinetics of reorientable surfactant molecules is formulated and solved even for the case when the reorientation process within the surface layer requires some time. It was shown that this non-instantaneous reorientation can result in either acceleration or deceleration of the surface tension decrease, depending on the adsorption characteristics of the different molecular states, and on the actual surface lifetime [227]: faster (for medium Π values) or slower (large Π values) decrease of γ is caused by an oversaturation of the surface layer by the state possessing maximum molar area.

4.7.3 Surfactants undergoing 2D-aggregation

As demonstrate in the previous paragraph, interfacial reorientations can explain adsorption processes which appear as if they are faster than diffusion. However, using the correct adsorption isotherm the diffusion mechanism yield perfect agreement to the experimental data. Attempts to explain a slower surface tension decrease, a case which is often experimentally observed, were reported in literature very often. For example, Lin et al. [83, 84] assumed a phase transition in the adsorption layer to explain his data for fatty alcohols. Yousef and McCoy (1983) and Fainerman and Miller (1996b) described of data by assuming a special structure of the surface layer and a non-equilibrium surface layer, respectively. Note that the adsorption barrier concept (for example [120, 121, 122, 123, 127, 128]) is generally accepted in this case. The adsorption barrier model may, of course, be employed to explain any deviations from the diffusion controlled adsorption kinetics (for a Langmuir isotherm); however, the reasons for a slower surface tension decrease often remain obscure. Note, that even reliable experimental evidence for a slower surface tension decrease caused by aggregation within the adsorption layer does not allow the conclusion that this is an exclusive mechanism. For example, the dynamic surface tension for aqueous solutions of the slightly soluble N-Dodecyl-γ-Hydroxy-Butyric Acidamide (DHBA) exhibit a sharp decrease of the slope when the surface pressure attains a critical value which corresponds to the beginning of 2D aggregation of DHBA molecules within the adsorption layer [231].

As experimental example, the dependencies of dynamic surface tensions for 1-decanol solutions as reported by Lin et al. [83, 84] are compared in Fig. 4.31 with the results calculated from the present aggregation model.

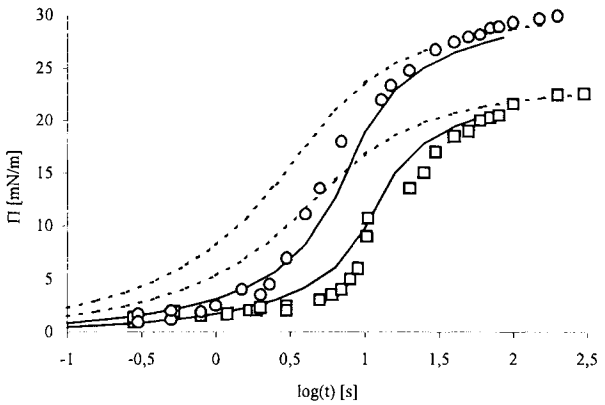

Fig. 4.31 Dynamic surface tension for 1-decanol solutions. experimental results from Lin et al. [83, 84] for $c_0 = 6.32 \cdot 10^{-5}$ mol/l (○) and $c_0 = 1.018 \cdot 10^{-4}$ mol/l (□); dotted curves calculated for a Langmuir isotherm, solid curves correspond to the aggregation model with $n = 2.5$ and $\Gamma_c \leq 10^{-9}$ mol/m², according to Aksenenko et al. [65]

In the calculations of $\gamma(t)$ the isotherm parameters for decanol at the solution/air interface were used as given Chapter 3. One can see that the aggregation model provides satisfactory agreement with experimental data, while the curves calculated from the Langmuir isotherm differ significantly within the short time range. For an aggregation number $n < 2$ or $n > 3$, the experimental data deviate much from the theory, which strongly supports the idea that decanol molecules aggregate in the adsorption layer.

Recently we studied 1-heptanol adsorption layers and found satisfactory agreement with a diffusion model for a non-equilibrium surface layer, that is, assuming the existence of concentration gradients in the subsurface [48]. It was shown by Aksenenko et al. [65] that small deviations from the diffusion model for a Langmuir isotherm for 1-heptanol solutions could be completely compensated by a dimerisation at $\Gamma_c = 5 \cdot 10^{-8}$ mol/m^2. Also for short alkanols the aggregation model describes properly the experimental data: for pentanol the optimum value was $n = 4$, while for propanol n=30 was found. So far no reasonable physical explanation can be given for this dependence of n on the alkyl chain length.

To summarise, more experimental data have to be produced to demonstrate the suitability of the aggregation model. However, the given example shows impressively, that this model can

describe experiments very well without the assumption of an adsorption barrier, i.e. within the framework of the pure diffusion- controlled adsorption.

An interesting experimental example for a diffusion-controlled adsorption process are the data for aqueous solutions of the long-chain alkanol, dodecanol, an extremely sparely soluble surfactant [232]. As one can see in Fig. 4.32, the dynamic surface pressure curves show a distinct kink point. Such points, which is shifted at lower temperatures to shorter times and disappears at higher temperatures, indicate a main phase transition of first order in the adsorption layer.

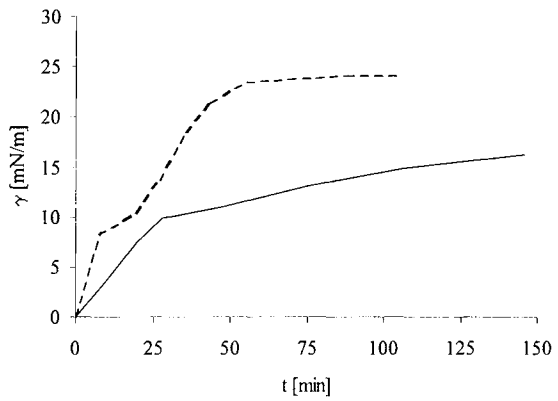

Fig. 4.32 Dynamic surface pressure for dodecanol solutions at 10°C and two concentrations: solid line – $1 \cdot 10^{-5}$mol/l, dotted line – $1.2 \cdot 10^{-5}$mol/l, according to [232]

The analysis of the adsorption kinetics shows that also the dodecanol adsorbs diffusion-controlled, however, the corresponding adsorption isotherm has to be used which allows to assume a two-dimensional aggregation at the surface (cf. paragraph 2.7).

4.7.4 Adsorption kinetics of ionic surfactants

As shown in paragraph 4.2.6. the adsorption process of ionic surfactants is much more complicated that that of a nonionic one. Although ionics are widely used in practical applications, there are not many experimental data on their adsorption dynamics. The reason maybe the lack of quantitative theories to describe the effect of the ionic charge on the adsorption process.

As an example the dynamic surface tensions of three SDS solutions are given in Fig. 4.33 measured in presence of 0.5 M NaCl. The presence of the electrolyte makes the alkyl sulphate more surface active than in pure water (cf. paragraph 2.7.2. and Chapter 3).

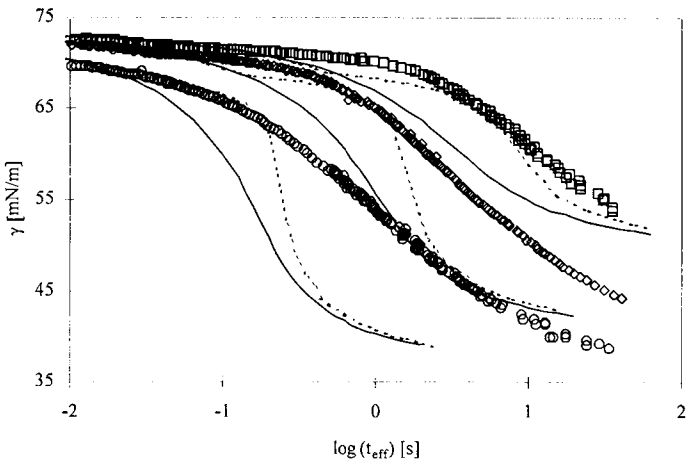

Fig. 4.33 Dynamic surface tensions for three aqueous SDS solutions in presence of 0.5 M NaCl; $c_0 = 10^{-4}$ mol/l (□), $2 \cdot 10^{-4}$ mol/l (◇), $5 \cdot 10^{-4}$ mol/l (○); calculations performed with $D = 4 \cdot 10^{-10}$ m²/s and $\omega = 2 \cdot 10^5$ m²/mol for a Langmuir isotherm (solid lines) and the aggregation model with $n > 50$ and $\Gamma_c = 1.7 \cdot 10^{-10}$ mol/cm² (dashed lines)

The analysis of the kinetic data was performed on the basis of the diffusion-controlled model, using the Langmuir and the aggregation isotherm, given by Eq. (2.16) and Eqs. (2.107) – (2.111), respectively. As one can see, the agreement with the theory is not satisfactory. The models developed mainly by the Bulgarian school [33] requires extensive numerical calculations so that its application to experimental data will be possible only after the elaboration of effective computer programmes.

4.7.5 Adsorption kinetics of surfactant mixtures

The adsorption kinetics of surfactant mixtures is a field rarely investigated. Systematic studies do not exist at all and therefore, we can give here only few information. As it was shown by the generalised model of Sutherland of Eq. (4.19) the adsorptions of the components of a mixture are independent at sufficiently low concentrations so that the dynamic surface tension $\gamma(t)$ can be calculated easily. The concentrations of the three compounds calculated for Fig. 4.34 differ

by one order of magnitude each. The surface activity (represented by the parameter b in the Langmuir isotherm) are adjusted such that the surface pressure Π reaches 5 mN/m at equilibrium.

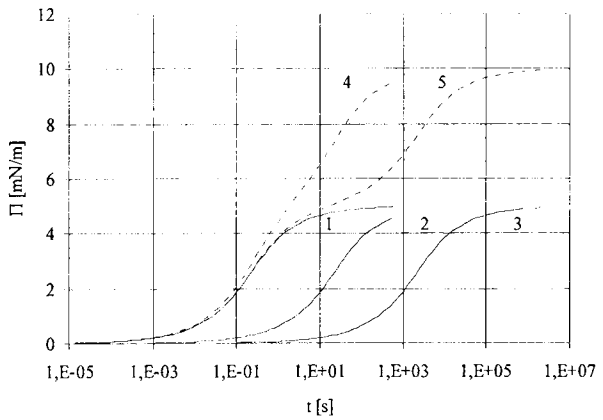

Fig. 4.34 Calculated surface pressure Π as a function of time using Eq. (4.19); $c_0 = 10^{-7}$ (1), 10^{-8}(2), 10^{-9} (3) mol/cm³, 1:1 mixtures of components 1 and 2 (4) and of components 1 and 3 (5); Π = 5 mN/m, $D = 5\ 10^{-6}$ cm²/s, $\omega = 4.8 \cdot 10^{9}$cm²/mol for both components

The mixture of components 1 and 2 yields a dependence Π(t) which looks essentially as that of a single component. For the 1:1 mixture of component 1 and 3, however, the resulting curve shows a remarkable transition region. This is caused by the characteristic time interval in which the surface pressure changes significantly. As a rough rule one can say that an increase in the bulk concentration by a factor of 10 leads to a change in the adsorption time by a factor of 100. The mixture of component 1 and 3 is characterised by a difference of 100 in the surface activity and hence by a factor of 10^4 in the adsorption time. This time difference is necessary to make such a transition region visible. The course of Π(t) is very typical for commercial surfactants which are usually mixtures of homologues or even various different compounds. A very famous example is the most frequently studied surfactant sodium dodecyl sulphate SDS, which is supplied as chemical by the homologous alcohol dodecanol [233].

The graphs shown in Fig. 4.35 are the dynamic surface tensions of three mixtures of C_{10}DMPO and C_{14}DMPO measured with the maximum bubble pressure method MPT2 (○) and ring tensiometer TE2 (◇). Although there is a general theoretical model to describe the adsorption kinetics of a surfactant mixture, model calculations are not trivial and a suitable software does not exists.

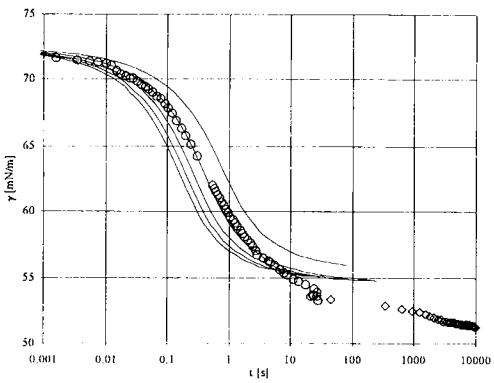

a)

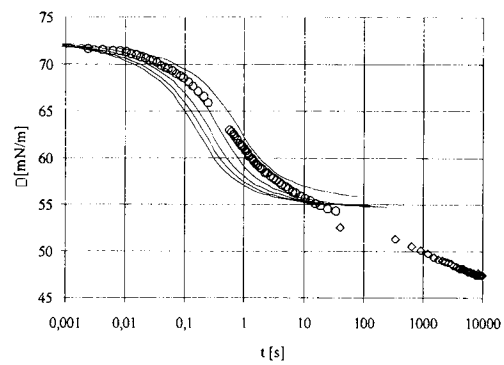

b)

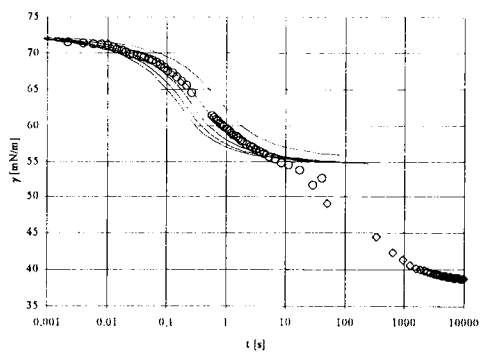

c)

Fig. 4.35 Dynamic surface tensions of a mixture of C_{10}DMPO and C_{14}DMPO; concentration ratio $c_1 | c_2 = 3 \cdot 10^{-7}$ mol/cm³ $| 10^{-9}$ mol/cm³ (a), $3 \cdot 10^{-7}$ mol/cm³ $| 3 \cdot 10^{-9}$ mol/cm³ (b), $3 \cdot 10^{-7}$ mol/cm³ $| 10^{-8}$ mol/cm³ (c); solid lines - calculated for $3 \cdot 10^{-7}$ mol/cm³ C_{10}DMPO using the parameters of the Langmuir isotherm $\omega = 2.75 \cdot 10^{9}$ cm²/mol and $b = 1.035 \cdot 10^{7}$cm³/mol and the diffusion coefficients $D = 1 \cdot 10^{-6}$, $2 \cdot 10^{-6}$, $3 \cdot 10^{-6}$, $4 \cdot 10^{-6}$, $5 \cdot 10^{-6}$ cm²/s (curves from left to right)

The graphs contain calculations for the main component of the mixture only, i.e. the shorter chain surfactant C_{10}DMPO at a concentration 300, 100 and 30 times higher as that of the second component C_{14}DMPO, respectively. Up to an adsorption time of about ten seconds the curve calculated for $D = 2 \cdot 10^{-6}$ cm²/s agrees quantitatively with the experimental points. Only at this time the second component starts to adsorb and deviations in $\gamma(t)$ are observed. With increasing C_{14}DMPO concentration the deviation increases and the total surface tension decrease becomes larger as expected for the adsorption of a mixture. The intermediate plateau is visible at the lowest C_{14}DMPO concentration but fades with further increase as the adsorption of this component sets in earlier.

The described results demonstrate very well how the adsorption kinetics allows to distinguish between the contributions of different compounds of a mixture to the measured surface tension change. Using the correct adsorption model (adsorption isotherm and equation of state) a quantitative description of the adsorption kinetics of mixtures would be possible, however, no programmes are available at present and analytical solutions do not exist.

4.7.6 Adsorption kinetics of proteins at the water/air interface

Adsorption kinetics, mainly studied by dynamic surface tension measurements, shows many features very much different from that of typical surfactants (Miller et al. 2000). The interfacial tension isotherms for standard proteins such as BSA, HSA, β-casein and β-lactoglobulin were measured at the solution/air interface by many authors using various techniques. The state of the art of the thermodynamics of adsorption was discussed in Chapter 2 while isotherm data for selected proteins were given in the preceding Chapter 3. Here we want to give few examples of the dynamic surface pressure characteristics of protein adsorption layers.

From an experimental point of view, studies with protein solutions are very difficult due to their extremely high surface activity. In many experimental techniques the adsorption at the interface, or sometimes even at the surface of the container, tubes and connectors of the dosing system, can lead to a depletion of protein in the bulk. Estimations have shown that the protein mass in the bulk of a drop and in the adsorption layer at the drop surface, are comparable for drops of a radius of 1.5 mm and a bulk concentration of $c < 20$ mg/l [234]. The use of the drop shape method however may be considerably extended to small surface pressures, usually $\Pi < 2$ mN/m and hence to low bulk concentrations when taking into account the protein mass

balance. Moreover, when using bubbles instead of drops the loss of protein due to adsorption becomes much smaller and hence the technique is suitable also for such complicated studies.

On the other hand it becomes possible to determine the protein adsorption for small Π directly from drop experiments as it was shown by Miller et al. [234] which makes this technique complementary to experiments such as radiotracer technique or ellipsometry [235, 236].

The adsorption process of proteins at liquid interface has some peculiarities. First the beginning of the adsorption process shows pronounced periods of time where for sure adsorptions proceeds but the interfacial tensions does not change. This period is called induction time. Once the interfacial tension starts to decrease due to adsorption it often exhibits extremely steep dependencies, caused by the shape of the adsorption isotherm, which is also very steep. The model equations (2.124) - (2.128) give a qualitative explanation of the nature of the induction time. In agreement with the dependencies Π on $\Gamma_\Sigma \omega$ the surface tension begins to decrease only from a certain monolayer coverage $(\Gamma_\Sigma \omega)_{min}$. For standard proteins like BSA, HSA, β-casein and β-lactoglobulin $(\Gamma_\Sigma \omega)_{min}$ is in the range between 0.1 and 0.2. This time necessary to reach the necessary minimum coverage is the above mentioned induction time. The reason for its existence is the rather small contribution of the surface layer entropy to the surface pressure. One can see from Eq. (2.122) that the contribution of entropy of mixing to the surface pressure, determined by the factor RT/ω is by two orders of magnitude lower than the factor RT/ω for surfactants. This essentially distinguishes the adsorption behaviour of proteins from that of surfactants for which no induction time exists.

Using a diffusion coefficient of 10^{-6} cm²/s for HSA the time (induction time) and the minimum adsorption Γ_{min} can be estimated at which the surface tension starts to decrease. Assuming that Γ_{min} does not depend on the protein bulk concentration for HSA of $7.25 \cdot 10^{-10}$ and $1.45 \cdot 10^{-9}$ mol/cm³ the corresponding induction times are about 20s and 5s, respectively. These results agree very well with those reported by Miller et al. [148], i.e. the process of unfolding seems to be very quick. A different situation was found for β-CS where a relaxation time of unfolding of 500 s was estimated.

The adsorption kinetics of proteins have been first systematically investigated by Graham and Phillips [73] and later by other authors, as reviewed by Wüstneck et al. [75]. The typical course

of the dynamic surface tension for some β-LG and β-CS solutions are shown in Figs. 4.36 und 4.37.

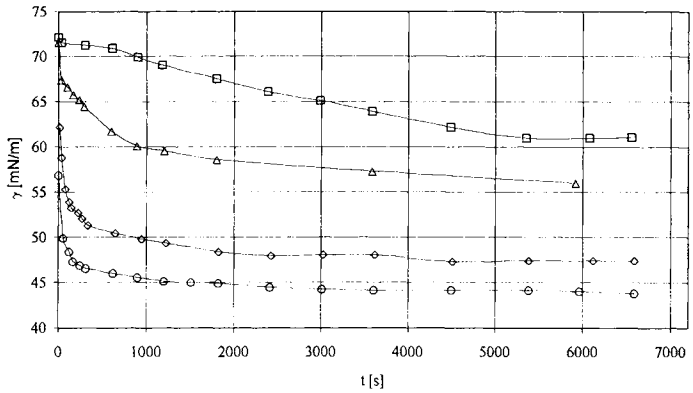

Fig. 4.36 Dynamic surface tension γ(t) of β-LG at the water/air interface, phosphate buffer at pH 5, 22°C; $c_{\beta\text{-LG}} = 10^{-10}$ (□), 10^{-9} (△), $5 \cdot 10^{-9}$ (◇), 2.10-8 (○) mol/cm³, according to Wüstneck et al. [75]

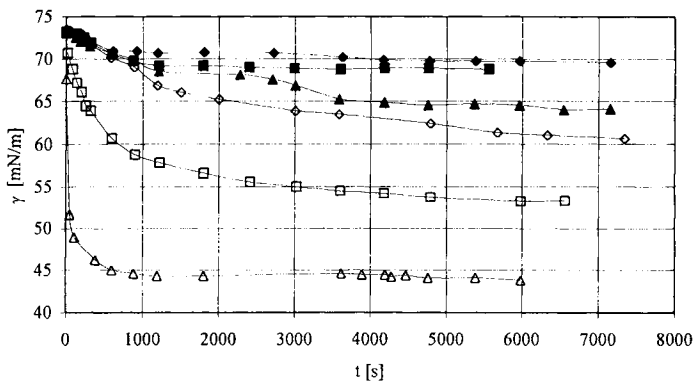

Fig. 4.37 Dynamic surface tension γ(t) of β-CS at the water/air interface, phosphate buffer at pH 7, 22°C; $c_{\beta\text{-CS}} = 10^{-11}$ (◆), $5 \cdot 10^{-11}$ (■), 10^{-10} (▲), 10^{-9} (◇), 10^{-8} (□) and $2 \cdot 10^{-8}$ (△) mol/cm³, according to Wüstneck et al. [75]

For HSA solutions the dynamics of surface tension decrease is rather different from that of surfactants. One can see from Fig. 4.38 that for HSA concentrations $c \leq 10^{-10}$ mol/cm³, almost no surface tension decrease was observed during the first 200 s and it takes more than 10 h for the equilibrium to be attained [237]. For higher concentrations the induction time as discussed above decreases quickly and the dynamic surface tension decreases in a way observed for usual surfactants.

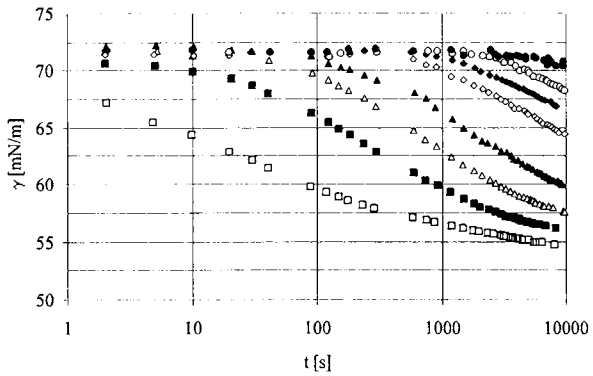

Fig. 4.38 Dynamic surface tension of HSA at the water/air interface, phosphate buffer solution at pH 5, temperature 22°C; c_{HSA} = $2 \cdot 10^{-11}$ (●), $3 \cdot 10^{-11}$ (o), $5 \cdot 10^{-11}$ (◆), $7 \cdot 10^{-11}$ (✧), 10^{-10} (▲), $5 \cdot 10^{-10}$ (Δ), 10^{-9} (■), 10^{-8} (□) mol/cm³, according to Miller et al. [238]

Different models based on effective diffusion coefficients D_{eff} have been applied for the interpretation of these data however the results show D_{eff} far from physically reasonable values. In particular with decreasing concentration the values of D_{eff} are several orders of magnitude higher than expected from the size and shape of the molecules. The reason for these discrepancies is for sure that the models have been based on a Langmuir isotherm as no other quantitative models existed at this time. Better kinetic models have to take into consideration the change in the molar area with increasing surface coverage using the new thermodynamic models and the kinetics of protein unfolding/refolding in the interfacial layers. A first attempt was made by Miller et al. [77] who discussed a model for globular proteins that allows a very good description of dynamic surface tensions for β-lactoglobulin solutions.

Figure 4.39 illustrates the comparison between the experimental values and theoretical predictions made from two models at low β-lactoglobulin concentrations. The first model assumes only a diffusional transport while the second model considers an additional time process for changes in the protein conformation in the adsorption layer. The curves for the quasi-equilibrium model overestimate the experimental data significantly, while the reorientation kinetic regime exhibits rather good agreement with the experiment. A complete agreement between the quasi-equilibrium diffusion kinetic regime and the experimental data would require the assumption of 3 to 5 times higher values of the diffusion coefficient.

Therefore, it can be concluded that the finite rate of the reorientation of β-lactoglobulin molecules in the adsorption layer, i.e. the 'oversaturation' of the interfacial layer by molecules in an extended state (maximum molar area), leads to a faster surface tension decrease at low protein concentrations. At larger concentrations the reorientation step becomes less important and at higher concentrations (higher surface coverage) the adsorption process is completely described by the diffusional transport in the solution bulk.

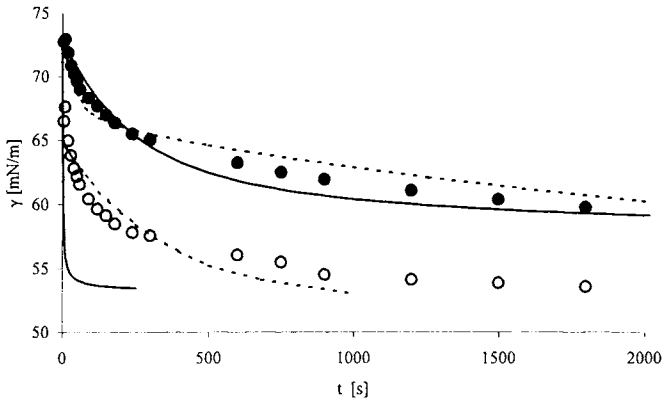

Fig. 4.39. Experimental data and theoretically calculated dynamic surface tension of β-lactoglobulin solutions for the concentrations 10^{-7} and $2 \cdot 10^{-7}$ mol/l; solid lines – quasi-equilibrium model, dotted lines – kinetic model calculated for a rate constant $k = 10^{-3}$ s^{-1}, according to [77]

The proposed theoretical model for the adsorption kinetics of globular protein at the solution/air or solution/oil interface for β-lactoglobulin agrees well with experimental data and with the general picture discussed elsewhere [77].

Further improvement of the theory can undoubtedly be obtained with an approach which accounts for the whole manifold of adsorption states (and also in the solution bulk) and the kinetics of the transitions between these states. This needs to be developed in future theoretical work.

4.7.7 Studies at liquid/liquid interfaces for finite bulk volumes

Using the above mentioned straightforward method the distribution coefficient of a surfactant can be determined by measuring the surface tension of the aqueous solution after equilibration with a definite volume of the oil phase. The following Fig. 4.40 demonstrates that the distribution coefficient K is a function of temperature T, in particular for non-ionic surfactants

such as the investigated $C_{10}EO_8$. As one can see, a temperature change from 15°C to 35°C increases the coefficient by an order of magnitude. The slope of the straight line in this figure represents the standard enthalpy of the interfacial transfer [66].

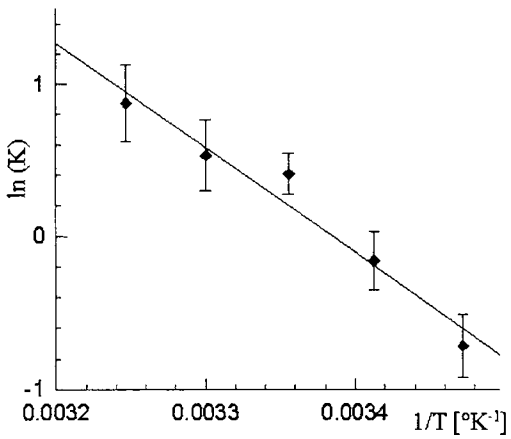

Fig. 4.40 Partition coefficients of $C_{10}E_8$ in water/hexane as a function of temperature, according to Miller et al. [142]

Typical experiments to study the adsorption of a surfactant at a water/oil interface consists in the measurement of the interfacial tension with time. An example is shown in Fig. 4.39. In this experiment, a drop of an aqueous surfactant solution is first formed in a cell filled with pure hexane. The volume ratio $Q=10^{-3}$ of the volume of the water drop (containing the surfactant) to that of the hexane bulk. The dynamic interfacial tension $\gamma(t)$ is then monitored by the pendant drop technique. The time dependence of γ for four initial concentrations of C_{13}DMPO in aqueous solution is shown in Fig. 4.41.

As the water drop provides only a limited amount of surfactant, the interfacial tension passes through a minimum when the flux of molecules adsorbing at the interface is equal to the flux of molecules desorbing into the external phase. Note that under these dynamic conditions, the interfacial tension can reach values which are well below the equilibrium values. This can be relevant for technologic processes, like the control of the droplet size in emulsions.

If we exchange the phases in the experiment completely different results are obtained. When we form a hexane drop inside a cell filled with an aqueous surfactant solution. The measured dynamic interfacial tensions for such an experiment are shown in Fig. 4.42 for three C_{13}DMPO

solutions. Now no minimum in the interfacial tension appears since the internal phase is rapidly saturated by the surfactant and a monotonic relaxation behaviour is observed.

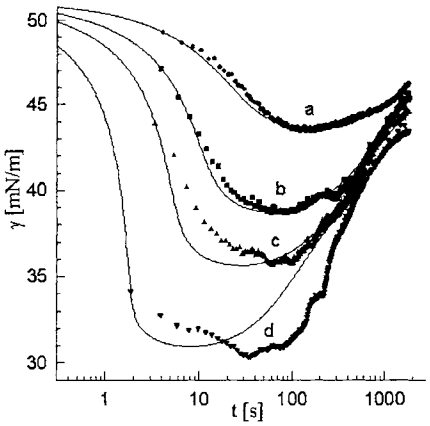

Fig. 4.41 Dynamic interfacial tension during the adsorption and transfer of C_{13}DMPO at the water/hexane interface; the hexane phase is initially free from surfactant; water/hexane volume ratio is $Q=10^{-3}$ (single water drop in a hexane environment); initial concentrations in water: $C_0=1\cdot10^{-8}$(a), $2\cdot10^{-8}$ (b), $3\cdot10^{-8}$ (c), $5\cdot10^{-8}$ mol/cm³ (d); solid curves are calculated from Eq. (4.94)

In addition to the experimental data, the dependencies γ(t) calculated from the theory of Eq. (4.94) are shown in Figs. 4.41 and 4.42. The results agree very well with the measured dynamic interfacial tension, in particular at the lower concentrations. Note that these calculations are not best fits to the experimental points but directly result from when the isotherm data for this surfactant are used (cf. Chapter 3). For larger concentrations, the deviation increases, which can possibly be caused by one of the assumptions, such a spherical symmetry for the drop and negligible deformation during the adsorption process .

Recently, the competitive adsorption dynamics of phospholipid/protein mixed system at the chloroform/water interface was investigated by using the drop volume technique. The three proteins β-Lactoglobulin, β-Casein, and Human Serum Albumin were used in this study. To investigate the influence of the phospholipid structure at concentrations close to the CAC (critic aggregation concentration) the four lipids dipalmitoyl phosphatidyl choline (DPPC), dimyristoyl phosphatidyl choline (DMPC), dimyristoyl phosphatidyl ethanolamine (DMPE)

and dipalmitoyl phosphatidyl ethanolamine (DPPE), were used as they have different chain length and/or uncharged head-groups.

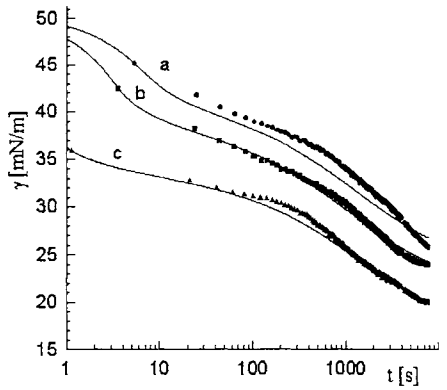

Fig. 4.42 Dynamic interfacial tension during the adsorption with transfer of surfactant of C_{13}DMPO at water/hexane interface; the hexane phase is initially free from surfactant; water/hexane volume ratio Q=1000 (single hexane drop in a water environment); initial C_{13}DMPO concentrations in water: C_0= 1.5 10^{-8} (a); 2.3 10^{-8} (b), 5.3 10^{-8} mol/cm³ (c); solid curves are calculated from Eq. (4.94)

To investigate this process of competitive adsorption of a lipid adsorbing from the chloroform phase and a protein from the aqueous phase at the joint chloroform/water interface, dynamic interfacial tensions were measured by the drop volume apparatus TVT1 from LAUDA, Germany (cf. paragraph 4.6.1). The adsorption experiments were performed such that chloroform drops containing the phospholipid were formed in the protein solution filled into the cuvette of the TVT1. At the surface of the growing drop a mixed adsorption layer is formed by adsorption of the lipid from inside the drop and by protein from outside the drop. This experimental arrangement allows studying the simultaneous competitive adsorption of both components. In contrast, most other experiments in the literature, for example performed at a Langmuir trough, are typically penetration experiments where the lipid layer is given as a spread monolayer and the protein penetrates into this layer from beneath. In this case the lipid molecules are insoluble in the adjacent liquid phase and occupy a definite place, while in the present experiment the lipid behaves like a soluble component that can be repelled from the interface due to increasing competition by adsorbing protein molecules.

Fig. 4.43 shows the dynamic interfacial tensions γ as a function of time for five different DPPC concentrations in chloroform, while the external aqueous phase contains the protein β-Casein at a bulk concentration of $5.0 \cdot 10^{-8}$ mol/l.

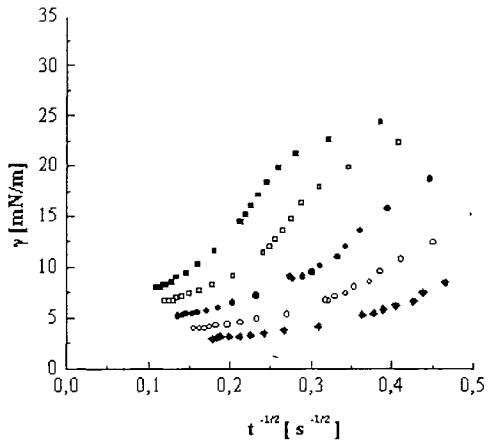

Fig. 4.43 Dependence of γ as a function of $t^{-1/2}$ for DPPC in chloroform/water systems as measured by the drop volume method at different lipid concentrations: c_0 = 2 (■), 3 (□), 4 (●), 5 (○), 6 (◆) 10^{-8} mol/cm³; external aqueous phase in the cuvette contains 5.0 10^{-8} mol/l β-Casein, according to [239]

The results demonstrate that in the time period covered by the drop volume method the lipid has reached the equilibrium adsorption before the proteins starts to adsorb significantly. This is seen from the γ-values at short times (large values of $1/\sqrt{t}$) which are significantly lower than the interfacial tension of the water/chloroform interface of 36 mN/m. Thus, the kinetics observed is the competitive adsorption or penetration of the protein into the established lipid layer. With increasing lipid concentration the absolute values get lower which supports the idea that the lipid layer is compressed by the penetrating protein molecules. A quantitative analysis of these data is impossible at present due to missing quantitative theories for such type of systems.

4.8 Experimental results on interfacial relaxations

We want to give only two examples of interfacial relaxation methods. The whole field of interfacial relaxations and rheology is so broad and of strong practical relevance that this topic deserves a whole book. At first, two examples, a harmonic and a transient experiment will be shown as example for slow relaxation experiments, while as second we will present results of experiments performed under ground and microgravity conditions, respectively, based on the principle of oscillating bubbles.

4.8.1 Slow relaxation experiments

Harmonic and transient relaxation experiments for dodecyl dimethyl phosphine oxide solutions were performed with the elastic ring method by Loglio [240]. This methods allows oscillation experiments in the frequency range from about 0.5 to 0.001 Hz and is suitable for comparatively slow relaxing systems. Slow oscillation experiments can be performed much easier now with the pendent drop apparatus [186]. Both techniques are also able to perform transient relaxation experiments. The two types of experiments have a characteristic frequency defined in the same way by Eq. (4.110).

In the drop shape technique sinusoidal area changes can be easily generated via changes of the drop volume in a very accurate way. The Fourier analysis of the surface tension response however shows that besides the main mode with the period T of the generated oscillation there are also modes with periods of 3T/2, T/2, T/4 and T/8. The origin of these modes is not yet fully understood but certainly caused by deviation of the area changes from harmonicity and surface layer compression/expansion beyond the limits of a linear theory.

A particular way of presenting harmonic relaxation data is the plot of surface tension changes versus the corresponding area changes. As one can see in Fig. 4.45 an ellipse results the tilt angle and the thickness of which contain the rheological information.

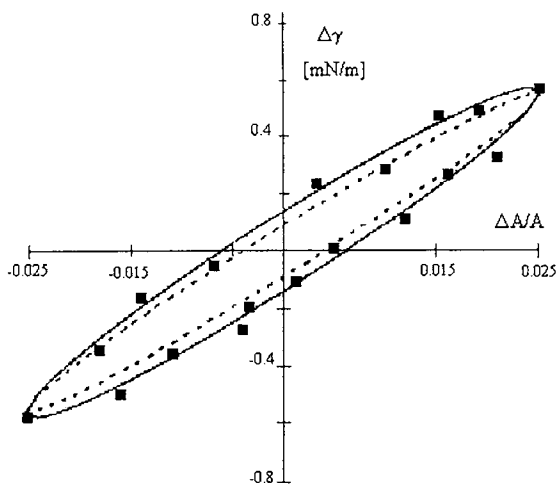

Fig. 4.44 Surface tension response for a Triton X-100 solution at $1 \cdot 10^{-5}$mol/l; a) change of surface tension with time; b) same as in (a) but plotted over the area change A(t)/A during oscillation; according to Loglio et al. [240]

While the tilt is a measure of the dilational elasticity, the thickness is proportional to the exchange of matter rate, sometimes named dilational viscosity. The ellipse thickness corresponds to the phase shift between the generated area oscillation and the surface tension response. With increasing frequencies the thickness decreases while the tilt angle increases up to a final value of representing the dilational elasticity modulus ε_0.

The general application of tensiometry was shown in [241] and it was impressively demonstrated how large the capacity of interfacial studies for medical research is. For example, selected dynamic surface tension values of serum or urine correlate with the health state of patients suffering from various diseases. In the course of a medical treatment these values then change from a pathological level back to the normal values determined as standard for a certain group of people (age and sex).

Very recently examples of rheological studies on blood were published elsewhere [242]. As an example we want to discuss some results of these investigations here. Fig. 4.45 shows the surface tension response after a step-type area change of a pendent drop area by about 10% for 6 serum samples from one and the same patient at different stages of his acute kidney insufficiency [243].

The dilational elasticity calculated from the measured jump via Eq. (4.131) are summarised in the following Table 4.4 together with the relaxation time τ calculated from the exponential function

$$\Delta\gamma(t) = \Delta\gamma_0 \exp\left[-\Delta t/\tau\right], \tag{4.131}$$

Here Δt is the time interval after the area expansion. An interpretation using the relaxation model given by Eqs. (4.115) to (4.118) is impossible as serum is a mixture of quite a number of surface active compounds of unknown concentrations. After admission to the hospital the elasticity is very low and even decreases a bit in the beginning of the therapy, while τ is maximum. After haemodialysis the elasticity goes through a maximum and levels off then at values close to the normal determined as standard for persons of this age and sex. The relaxation time decreases to less than half of the initial value. The results allow to conclude that rheological studies provide an interesting tool for medical practice and research, in particular due to the fact that very small quantities of a sample are needed.

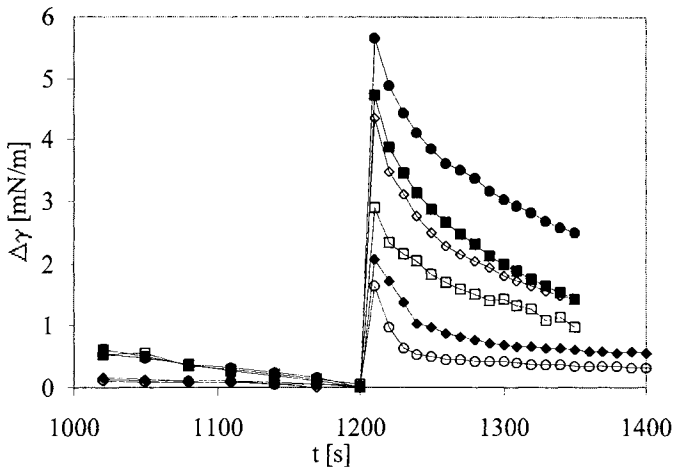

Fig. 4.45 Surface tension response of serum from a 46 years old patient admission suffering from an acute kidney insufficiency; admission to hospital (◇), therapy (○, □), after haemodialysis (●), polyuria (■), leaving the hospital (◆)

Table 4.4 Dilational elasticity ε and relaxation time τ determined from the data given in Fig. 4.45

Health state or treatment	ε [mN/m]	τ [s]
admission to hospital	12.0	273
therapy	7.7	198
therapy	26.7	180
after haemodialysis	49.1	181
polyuria	35.0	129
leaving the hospital	29.5	139

4.8.2 Oscillating bubble experiments

A set of experiments on the behaviour of oscillating bubbles were carried out recently with a device designed by Officine Galileo, Italy, designed as experimental module for the STS-95 space shuttle mission in 1999. Detailed information on the technical features was given elsewhere [244, 245]. Key point of the experiments was to compare the oscillation behaviour of bubbles under ground and microgravity conditions. The experiments were done at three temperatures 15, 25 and 35 °C, and at frequencies in the range from 0.2 to 450 Hz. A typical

measured pressure signal is shown in Fig. 4.46, together with a decomposition of the signal into the main oscillation mode and the damped oscillation of the bubble at the eigenfrequency.

As one can see the experimental set-up allows to register the initial stage of the bubble oscillation. Here a transient regime of non-established harmonic oscillations is clearly observed for larger frequencies and the measured pressure oscillation is a sum of a non-damped oscillation of the externally applied frequency and a damped oscillation with the meniscus eigenfrequency (for details cf. [208]). At larger frequencies the damped oscillation contribution as shown in Fig. 4.46c is practically absent as the damping time is sufficiently small.

From the established oscillation at times much larger than the damping time the amplitude and phase shift to the established oscillation can be obtained. Examples of the frequency dependence of the phase shift for different surfactant concentrations (C_{12}DMPO) are shown in Figs. 4.47 and 4.48, obtained under microgravity on ground, respectively, under exactly the same experimental conditions. The phase shift φ strongly increases with the surfactant concentration especially in the frequency range from 10 Hz to 150 Hz which correspond to the characteristic adsorption time of this surfactant. The largest phase shift is observed at a frequency where the surface viscosity has a maximum. The obtained results show that the phase shift measured by the oscillating bubble device with a closed cell is a very sensitive parameter of the interfacial relaxation processes.

The comparison of the two figures shows that the characteristic bubble frequency for ground conditions is two times smaller than that for microgravity conditions. The most probable reason for the decrease of the characteristic bubble frequency under ground conditions is the bubble shape deformation due to gravity on which the characteristic frequency strongly depends.

We can summarise that the oscillating bubble experiments performed during the STS-95 mission demonstrate the availability of the transient and established regimes of bubble oscillations. The transient regime provides with the damping time and the bubble eigenfrequency whereas in the established regime the amplitude- and phase-frequency dependencies can be obtained. All the above parameters depend on the relaxation processes that take place at the interface. Hence, reorientation and surface aggregation are molecular processes which can be studied by this method. The hydrodynamic theory developed in [208]

demonstrates good qualitative agreement with the measured amplitude- and phase-frequency dependencies. For a quantitative agreement between theory and experiment an adequate model of the surface layer relaxation as well as an adequate adsorption isotherm are required.

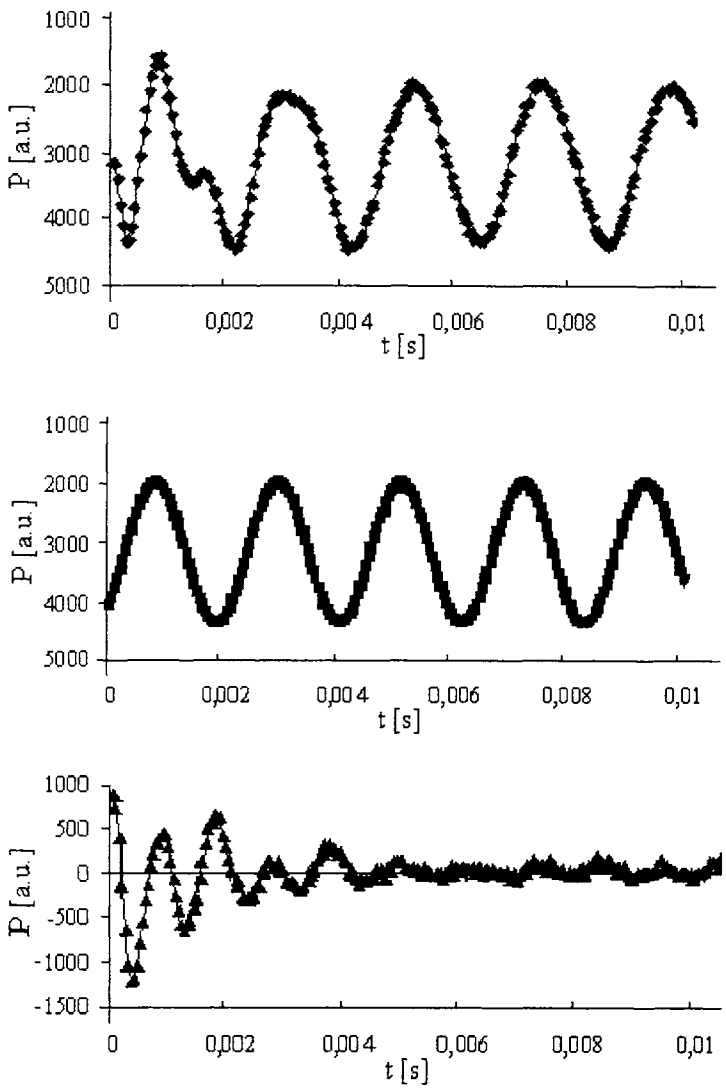

Fig. 4.46 Pressure oscillations for water at 450 Hz; a) -total signal; b) established harmonic oscillation with the externally applied frequency, c) damped oscillation with the bubble eigenfrequency

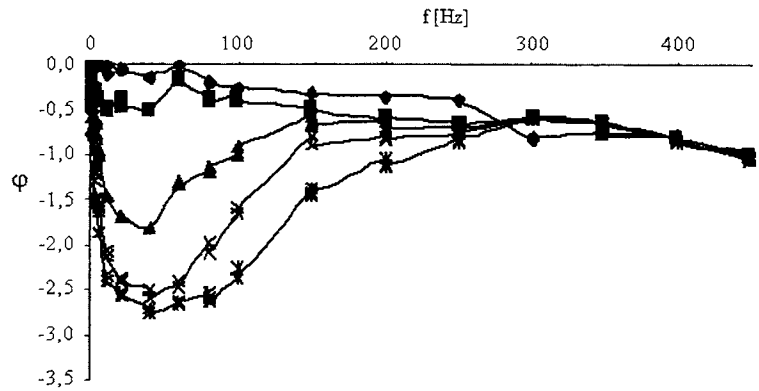

Fig. 4.47. Phase shift between the externally imposed volume variation and the measured pressure variation vs. frequency obtained microgravity conditions; C_{12}DMPO concentrations: 0 (♦) 0.005 (■), 0.01 (▲), 0.02 (×) and 0.04 (✳) mol/m^3.

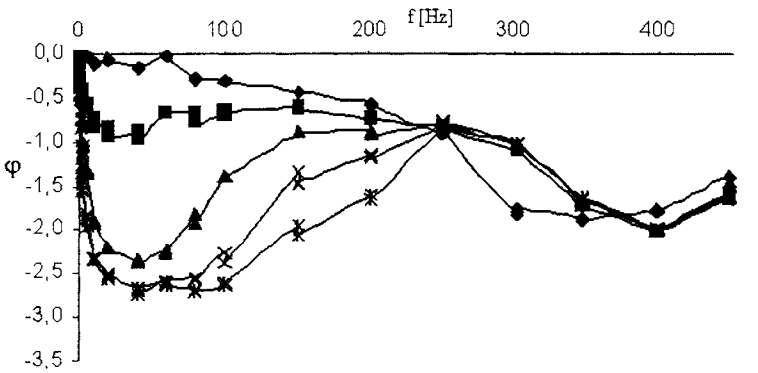

Fig. 4.48. Phase shift between the externally imposed volume variation and the measured pressure variation vs. frequency obtained under ground conditions; C_{12}DMPO concentrations: 0 (♦) 0.005 (■), 0.01 (▲), 0.02 (×) and 0.04 (✳) mol/m^3.

4.9 Penetration kinetics experiments

The easiest penetration experiments are those with a monolayer of an insoluble component spread on a subphase which contains a soluble component of the same homologous series. An example is the study by Fainerman et al. [115] of the penetration of the soluble dodecyl dimethyl phosphine oxide (C_{12}DMPO) into a monolayer of the insoluble eicosyl dimethyl phosphine oxide (C_{20}DMPO). The monolayer isotherm of C_{20}DMPO at 20 °C shows a break

point at $A \cong 0.4\ nm^2$ after which a steep increase of the surface pressure Π is observed. This behaviour suggests that 2D aggregates are formed.

The penetration of the soluble $C_{12}DMPO$ molecules into the $C_{20}DMPO$ monolayer depends significantly on the state of the $C_{20}DMPO$ monolayer. At an initial molar area of $A_0 = 0.6\ nm^2$ (state before the penetration process begins) a gaseous monolayer exists, while at $A_0 = 0.35\ nm^2$ a two-dimensional aggregation is observed. After further compression a condensed monolayer is formed with a collapse point near $A_0 = 0.22\ nm^2$. The curves in Fig. 4.49 illustrate the $C_{12}DMPO$ penetration dynamics for the two monolayer states at $A_0 = 0.6\ nm^2$ and $A_0 = 0.35\ nm^2$.

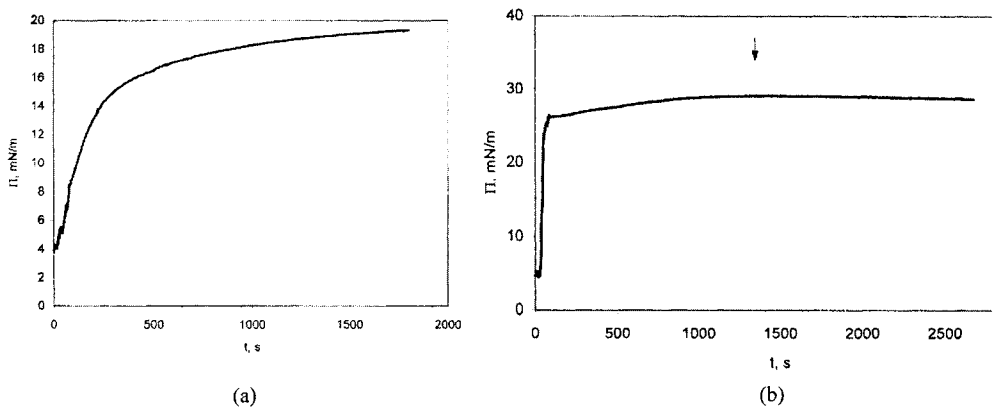

Fig. 4.49 $C_{12}DMPO$ penetration dynamics for $c = 10^{-5}$ mol/l and $A_0 = 0.6\ nm^2$ (a), $c = 10^{-4}$ mol/l and $A_0 = 0.35\ nm^2$ (b); according to Fainerman et al. [115]

The dynamic surface pressure for the lower surface coverage shows a regular behaviour. For the higher coverage, which corresponds to the coexistence region, an extremely steep increase in $\Pi(t)$ is followed by a flat region with a maximum after 1300 s at $\Pi \cong 27$ mN/m. This surface pressure value coincides with the collapse pressure of the individual $C_{20}DMPO$ monolayer. Therefore the slight decrease in the pressure of the mixed monolayer for $t > 1300$ s is certainly caused by a collapse stimulated by the adsorption of the soluble surfactant component.

A comparison of the equilibrium isotherm with the thermodynamic model of Fainerman et al. [115] suggests that mixed aggregates of the insoluble and soluble components are formed.

Further experiments have shown that penetration of the surfactant into the condensed C_{20}DMPO monolayer at $A_0 = 0.22$ nm^2 seems to be impossible. The obtained constant surface pressure demonstrates that the soluble molecules cannot penetrate into the condensed monolayer with a significant amount.

A much more complex behaviour is observed for the process of penetration of various proteins into phospholipid monolayers. This behaviour depends strongly on the protein and the solution properties although some common features are observed. Fainerman et al. [116] studied the β-lactoglobulin penetration dynamics into DPPC monolayers. For a β-lactoglobulin bulk concentration of $5 \cdot 10^{-7}$ mol/l and molar areas of the lipid larger than the critical value, $A > A_c$, first order phase transitions are observed. Thus, two-dimensional condensed phase are formed although at these molar area values the pure DPPC monolayer exists only in the fluid-like state and does not form any domains. The first-order phase transition in the DPPC monolayer becomes visible by the characteristic break point in the dynamic surface pressure curve Π(t) (see Fig. 4.50).

Beyond this phase transition point, the creation and growth of condensed phase domains is observed. The shape of these domains is very similar to those of pure DPPC domains, as one can see from the images given in Fig. 4.51. The BAM images were taken at different times after the start of the penetration experiments and the letters correspond to the respective moments in the Π(t) curve. The aggregation of DPPC into condensed phase domains is induced even if the initial surface DPPC concentration is less than 50% of the critical adsorption Γ_c.

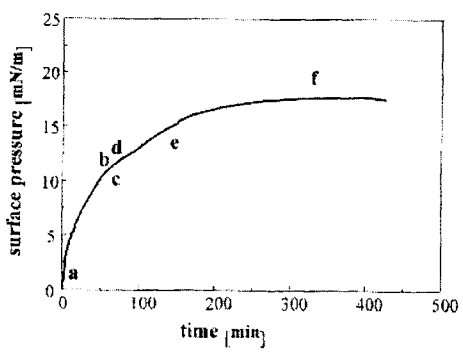

Fig. 4.50 Penetration dynamics for β-lactoglobulin penetration at A = 1.20 nm² per one DPPC molecule. The Π(t) penetration kinetics curve indicates the first order phase transition point after 29 min.

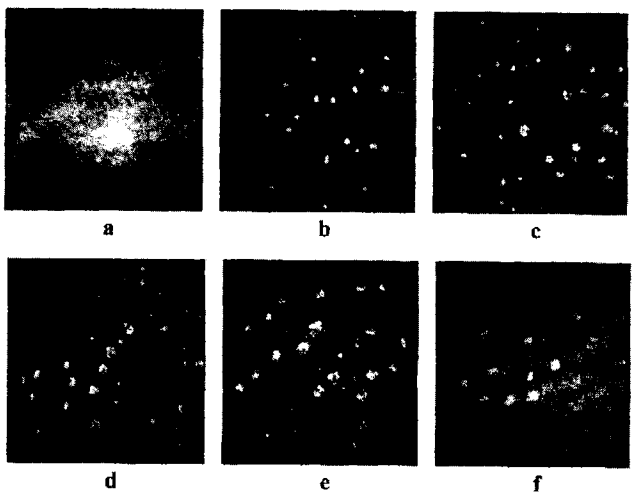

Fig. 4.51 BAM images (a) – (f) in the sequence of the letters in the Π(t) curve of Fig. 4.47; according to Fainerman et al. [116]

It is interesting to note that the surface pressure at which aggregation commences, does not remain constant but is rather a function of the initial surface coverage. The generalised Volmer model for mixed monolayers, as discussed in Chapter 2, paragraph 2.9 agrees well with this experimental finding.

The necessary time for the commencement of the DPPC aggregation can be estimated by using the simplest diffusion model of the adsorption kinetics given by Eq. (4.76). This equation, although derived for surfactants, can also be used for proteins if the surface pressure Π is not too high. This equation describes the adsorption of globular proteins, such as β-lactoglobulin, much better than of proteins with flexible chains. The comparison with experiments made by Fainerman et al. [116] for β-lactoglobulin showed good agreement (cf. Fig. 4.52).

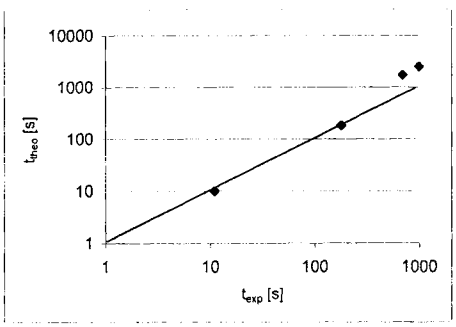

Fig. 4.52 Relation between t_{exp} and t_{theo} determined for the appearance of domains

A more quantitative description is not available at present as the state of the art of the theory does not provide better models. However, experimental support was obtained from GIXD (Grazing Incidence X-ray Diffraction) studies [246] giving evidence that indeed the condensed phase in the penetration layer consists only of DPPC. In equilibrium, the lattice structure of the penetration layer is very similar to that of pure DPPC on water. Upon additional compression, the tilt angle of the DPPC molecules deviate from that of the pure DPPC monolayers which can be understood as conformational changes of the protein in the fluid-like monolayer and succeeding squeezing out of the protein at higher surface pressures.

Further studies of general character were performed with lysozyme penetrating into DPPC monolayers [113]. Similarly to the β-lactoglobulin, the lysozyme stimulates the DPPC aggregation. Also the penetration of the flexible protein β-casein into a DPPC monolayer stimulates a 2D aggregation [247]. The penetration is quite similar to that of the globular protein β-lactoglobulin. However, some particular features are observed which cannot even qualitatively be explained on the basis of existing theories.

4.10 Summary

This chapter intended to present the state of the art of dynamic studies at liquid interfaces. It was shown that mainly dynamic surface and interfacial tensions and interfacial relaxations provide information about the processes happening when adsorption layers are formed at liquid interfaces. The first sections have demonstrated that the theories necessary to interpret experimental data are very advanced and allow a quantitative understanding. This is mainly due to the most recently developed new thermodynamic models based on molecular processes in adsorption layers, i.e. reorientations and two-dimensional aggregations. The consideration of these models in diffusion controlled adsorption kinetics models provide a general theoretical basis to a quantitative description of surfactant adsorptions. A number of experimental examples, serving as standard, is presented and the way of data interpretation demonstrated. A significant help for the user of the newly developed theories is the software package called "WardTordai". This software allows to calculate the theoretical curves $\gamma(t)$ for a given set of isotherm parameters and in a range of diffusion coefficients [223]. The following isotherms can be selected as basis for the calculations: Langmuir, Frumkin, reorientation, aggregation.

The present chapter gives also detailed introduction to a large number of experimental methods, suitable for studying dynamic interfacial tensions. The methods are discussed in terms of the available time window. There are methods which complement each other such that a time interval from less than 100 microseconds up to hours and days of adsorption time can be covered (about ten orders of magnitude). The relaxation methods, also suitable for detecting the adsorption mechanism of surfactant's adsorption provide in addition the dilational rheology of interfacial layers. It is discussed that in particular these dilational rheological studies are most informative in respect to adsorption mechanisms, as the data interpretation includes the thermodynamic model as well as the adsorption dynamics.

As conclusions from all presented experimental data one can say that all surfactants essentially follow the physical model of a diffusion control. Deviations from this general physical mechanism are usually caused by inaccuracies in the description of the equilibrium state of the adsorption layer, or by impurities in the studied samples.

4.11 References

1. G. Kretzschmar and R. Miller, Adv. Colloid Interface Sci., 36(1991)65
2. S.S. Dukhin, G. Kretzschmar and R. Miller, Dynamics of Adsorption at Liquid Interfaces: Theory, Experiment, Application, in „Studies in Interface Science", Vol. 1, D. Möbius and R. Miller (Eds.), Elsevier, Amsterdam, 1995
3. A.F.H. Ward and L. Tordai, J. Phys. Chem., 14(1946)453
4. S.R. Milner, Phil. Mag., 13(1907)96
5. K.S.G. Doss, Koll. Z., 86(1939)205
6. S. Ross, Amer. Chem. Soc., 67(1945)990
7. C.M. Blair, J. Chem. Phys., 16(1948)113
8. R.S. Hansen and T. Wallace, J. Phys. Chem., 63 (1959) 1085
9. J.F. Baret, J. Colloid Interface Sci., 30 (1969) 1
10. R. Miller and G. Kretzschmar, Colloid Polymer Sci., 258(1980)85
11. Z. Adamczyk, J. Colloid Interface Sci., 120 (1987) 477

12. F. Ravera, L. Liggieri and A. Steinchen, J. Colloid and Interface Sci., 156(1993)109

13. F. Ravera, L. Liggieri, A. Passerone and A. Steinchen, J. Colloid Interface Sci., 163(1994)309.

14. L. Liggieri, F. Ravera and A. Passerone, Colloids Surfaces A, 114 (1996) 351

15. A.V. Makievski, V.B. Fainerman, R. Miller, M. Bree, L. Liggieri and F. Ravera, Colloids Surfaces A, 122(1997)269

16. P. Joos, Dynamic Surface Phenomena, VSP, Utrecht, 1999

17. D. Möbius and R. Miller (Eds.), Drops and Bubbles in Interfacial Science, in "Studies in Interface Science", Vol. 6, Elsevier, Amsterdam, 1998

18. F.A. Veer and M. van den Tempel, J. Colloid Interface Sci., 42 (1973) 418

19. M. van den Tempel, J. Non-Newtonian Fluid Mechanics, 2 (1977) 205

20. M. van den Tempel and E.H. Lucassen-Reynders, Adv. Colloid Interface Sci., 18 (1983) 281

21. R. Haase, in "Grundzüge der physikalischen Chemie, Band II - Transportvorgänge",

22. Dr. Dietrich Steinkopff Verlag, Darmstadt 1973

23. R.S. Hansen, J. Colloid Sci., 16 (1961) 549

24. J.F. Baret, J. Chem. Phys., 65 (1968) 895

25. V.B. Fainerman, Kolloid. Zh., 39(1977)406

26. C.A. MacLeod and C.J. Radke, J. Colloid Interface Sci., 166(1994)73

27. C.H. Chang and E.I. Franses, Colloids Surfaces, 69(1992) 189

28. S.S. Dukhin, R. Miller and G. Kretzschmar, Colloid Polymer Sci., 261 (1983) 335

29. S.S. Dukhin and R. Miller, Colloid Polymer Sci., 269 (1991) 923

30. R.P. Borwankar and D.T. Wasan, Chem. Eng. Sci., 41(1986) 199

31. R. Miller, G. Kretzschmar and S.S. Dukhin, Colloid Polymer Sci., 272(1994)548

32. V.V. Kalinin and C.J. Radke, Colloids Surfaces A, 114(1997) 337

33. P.M. Vlahovska, K.D. Danov, A. Mehreteab and G. Broze, J. Colloid Interface Sci. 192(1997)194

34. K.D. Danov, P.M. Vlahovska, P.A. Kralchevsky, G. Broze and A. Mehreteab, Colloids Surfaces A, 156(1999)389

35. Yu.M. Rakita and V.B. Fainerman, Kolloid. Zh., 51(1989)714

36. C.D. Dushkin and I.B. Ivanov, Colloids Surfaces, 60 (1991) 213

37. V.B. Fainerman, Colloids Surfaces, 62 (1992) 333

38. G. Serrien, G. Geeraerts, L. Ghosh and P. Joos, Colloids Surfaces, 68(1992)219

39. K.D. Danov, P.M. Vlahovska, T. Horozov, C.D. Dushkin, P.A. Kralchevsky, A. Mehreteab and G. Broze, J. Colloid Interface Sci. 183(1996)223

40. S.Y. Lin, K. McKeigue and C. Maldarelli, Langmuir, 7 (1991) 1055

41. S.Y. Lin, T.L. Lu and W.B. Hwang, Langmuir, 11 (1995) 555

42. S.Y. Lin, W.J. Wang and C.T. Hsu, Langmuir, 13(1997) 6211

43. Q. Jiang, Y.C. Chiew and J.E. Valentini, Langmuir, 9 (1993) 273

44. R.Y. Tsay, S.Y. Lin, L.W. Lin and S.I. Chen, Langmuir, 13(1997)3191

A. Nikolov, G. Martynov and D. Exerowa, J. Colloid Interface Sci., 81(1981)116

45. R. Hirte and K. Lunkenheimer, J. Phys. Chem., 100 (1996) 13786

46. V.B. Fainerman and R. Miller, J. Colloid Interface Sci., 175 (1995) 118

47. V.B. Fainerman, R. Miller and R. Wüstneck, J. Colloid Interface Sci., 183 (1996) 25

48. V.B. Fainerman and R. Miller, Langmuir, 12 (1996) 6011

49. V.B. Fainerman, R. Miller and R. Wüstneck, J. Phys. Chem., 101 (1997) 6479

50. V.B. Fainerman, Lucassen-Reynders, E.H. and R. Miller, Colloids Surfaces A, 143(1998)141

51. V.B. Fainerman, A.V. Makievski and R. Miller, Reviews in Chemical Engineering, 14(1998)373

52. R. Miller, K. Lunkenheimer and G. Kretzschmar, Colloid Polymer Sci., 257(1979)1118

53. K. Lunkenheimer and R. Miller, Tenside, 16(1979)312

54. R. Miller and K. Lunkenheimer, Colloid Polymer Sci., 260(1982)1148

55. R. Miller and K. Lunkenheimer, Colloid Polymer Sci., 264(1986)273

56. K.L. Sutherland, Austr. J. Sci. Res., A5(1952)683

57. R. Miller, Colloids Surfaces, 46(1990)75

58. W.J. Cody, Math. Comp., 23(1968)631

59. M. Ziller and R. Miller, Colloid Polymer Sci., 264(1986)611

60. R. Miller and G. Kretzschmar, Adv. Colloid Interface Sci., 37(1991)97

A. Yousef and B.J. McCoy, J. Colloid Interface Sci., 94(1983)497

61. J.K. Ferri and K.J. Stebe, Adv. Colloid Interface Sci., 85(1999)61

62. R. Miller, Colloid Polymer Sci., 259(1981)375

63. V.B. Fainerman, R. Miller, Wüstneck, R. and A.V. Makievski, J. Phys. Chem., 100 (1996) 7669

64. E.V. Aksenenko, V.B. Fainerman and R. Miller, J. Phys. Chem., 102 (1998) 6025

65. M. Ferrari, L. Liggieri and F. Ravera, J. Phys. Chem. B, 102(1998)10521

66. L. Liggieri, M. Ferrari, A. Massa and F. Ravera, Colloids Surfaces A, 156 (1999) 455

67. R. Miller, V.B. Fainerman, E.V. Aksenenko, A.V. Makievski, J. Krägel, L. Liggieri, F. Ravera, R. Wüstneck and G. Loglio, in "Emulsions, Foams and Thin Films", P. Kumar and K.L. Mittal (Eds.), Marcel Dekker, 2000, p. 313

68. F. Ravera, L. Liggieri and R. Miller, Colloids Surfaces A, 175 (2000) 51

69. R. Miller, P. Joos and V.B. Fainerman, Adv. Colloid Interface Sci., 49(1994)249

70. S. Ghosh and H.B. Bull, Biochemistry, 2(1963) 411

71. E. Tornberg, in ACS Symposium Series, N92, Functionality and Protein Structure, Akila Pour-El (Ed.), (1972) 105

72. D.E. Graham and M.C. Phillips, J. Colloid Interface Sci., 70 (1979) 403

73. J.A. de Feijter and J. Benjamins, in E. Dickinson (Ed.) Food emulsions and foams. Special publication no. 58, Roy. Soc. Chem., 1987, p.72

74. R. Wüstneck, J. Krägel, R. Miller, V.B. Fainerman, P.J. Wilde, D.K. Sarker and D.C. Clark, Food Hydrocolloids, 10(1996)395

75. K. Kalischewski and K. Schügerl, Colloid and Polymer Sci., 257(1979) 1099

76. R. Miller, V.B. Fainerman, A.V. Makievski, R. Wüstneck, J. Krägel, D.O. Grigoriev, V.N. Kazakov and O.V. Sinyachenko, Adv. Coll. Interface Sci., 86 (2000) 39

77. R. Miller, E.V. Aksenenko, V.B. Fainerman and U. Pison, Colloids Surfaces A, (2001), in press

78. A.V. Makievski, R. Miller, V.B. Fainerman, J. Krägel and R. Wüstneck, Special Publication No. 227, "Food Emulsions and Foams: Interfaces, Interactions and Stability", E. Dickinson and J.M. Rodríguez Patino (Eds.), Royal Society of Chemistry 1999, 269

79. A.V. Makievski, V.B. Fainerman, M. Bree, R. Wüstneck, J. Krägel, R. Miller, J. Phys. Chem., 102 (1998) 417

80. V.B. Fainerman, E.V. Aksenenko and R. Miller, J. Phys. Chem., 104 (2000) 5744

81. V.B. Fainerman, D. Vollhardt and V. Melzer, J. Chem. Phys., 107 (1997) 243

82. S.-Y. Lin, T.-L. Lu and W.-B. Hwang, Langmuir, 10 (1994) 3442

83. S.-Y. Lin, W.-B. Hwang and T.-L. Lu, Colloids Surfaces A, 114 (1996) 143

84. E.V. Aksenenko, A.V. Makievski, R. Miller and V.B. Fainerman, Colloids Surfaces A, 143 (1998) 311

85. V. Melzer and D. Vollhardt, Phys. Rev. Lett., 76 (1996)3770

86. D. Vollhardt and V. Melzer, J. Chem. Phys., 101 (1997) 3370

87. P. Joos and P. Petrov, Colloids Surfaces A, 143 (1998) 273

88. M. van Uffelen and P. Joos, Colloids Surfaces A, 85(1994)119

89. T. Horozov and P. Joos, J. Colloid Interface Sci., 173 (1995) 334

90. E.A.G. Aniansson and S.N. Wall, J. Phys. Chem., 78 (1974) 1024

91. E.A.G. Aniansson and S.N. Wall,, J. Phys. Chem., 79 (1975) 857

92. E.A.G. Aniansson, S.N. Wall, M. Almgren, H. Hoffmann, I. Kielmann, W. Ulbricht, R. Zana, J. Lang and C. Tondre, J. Phys. Chem., 80 (1976) 905

93. C.D. Dushkin, Colloids Surfaces A, 143 (1998) 283

94. C.D. Dushkin, I.B. Ivanov and P.A. Kralchevsky, Colloids Surfaces, 60 (1991) 235

95. P. van den Bogaert and P. Joos, J. Phys. Chem., 83(1979)2244

96. V.B. Fainerman, Colloids Surfaces, 57 (1991) 249

97. P. Joos, J.P. Fang and G. Serrien, J. Colloid Interface Sci., 151 (1992) 144

98. V.B. Fainerman, A.V. Makievski and R. Miller, Colloids Surfaces A, 87 (1994) 61

Bonfillon, F. Sicoli and D. Langevin, J. Colloid Interface Sci., 168 (1994) 497

99. S.S. Dukhin, R. Miller and G. Kretzschmar, Colloid Polymer Sci., 263 (1985) 420.

100. R.P. Borwankar and D.T. Wasan, Chem. Eng. Sci., 43 (1988) 1323

101. S.S. Datwani and J.K. Stebe, J. Colloid Interface Sci., 219(1999)282

A. Bonfillon and D. Langevin, Langmuir 10 (1994) 2965

102. P. Joos, J. van Hunsel and B. Bleys, J. Phys. Chem., 90 (1986) 3386

103. D. Goralczyk and B. Waligora, J. Colloid Interface Sci., 88(1982) 590

104. J. Rodakiewicz-Nowak, J. Colloid Interface Sci., 85(1982), 586

105. C.A. MacLeod and C.J. Radke, Langmuir, 10 (1994) 3555

106. A.W. Adamson, Physical Chemistry of Surfaces, Wiley, New York, 1986

107. J.H. Schulman and A.H. Hughes, Biochem. J., 29(1935)1243

108. D. Vollhardt and V.B. Fainerman, Adv. Colloid Interface Sci., 86 (2000) 103

109. K. Asano, K. Miyano, H. Ui, M. Shimomura and I. Ohta, Langmuir, 9(1993)3587

110. S. Sundaram, J.K. Ferri, D. Vollhardt and K.J. Stebe, Langmuir, 14(1998)1208

111. V.B. Fainerman and D. Vollhardt, Langmuir, 15(1999)1784

112. V.B. Fainerman, A.V. Makievski, D. Vollhardt, S. Siegel and R. Miller, J. Phys. Chem. B, 103(1999)330.

113. V.B. Fainerman, J. Zhao, D. Vollhardt, A.V. Makievski and J.B. Li, J. Phys. Chem. B 103(1999)8998

114. R.S. Hansen, J. Phys. Chem., 64 (1960) 637

115. E. Rillaerts and P. Joos, J. Phys. Chem., 86(1982)3471

I. Balbaert and P. Joos, Colloids Surfaces, 23 (1987) 259

116. J.F. Baret, J. Phys. Chem., 72(1968)2755

117. F.T. Lindström, R. Haque and W.R. Coshow, J. Phys. Chem., 74 (1970) 495

118. G. Bleys and P. Joos, J. Phys. Chem., 89(1985)1027

119. C.-H. Chang and E.I. Franses, Colloids Surfaces A, 100 (1995) 1

120. V.B. Fainerman, Usp. Khim., 54(1985)161

121. V.B. Fainerman and S.V. Lylyk, Kolloid. Zh., 44(1982)598

122. P. Joos and G. Serrien, J. Colloid Interface Sci., 127(1989) 97

123. Li, B., G. Geeraerts and P. Joos, Colloids Surfaces A., 88(1994)251

124. H. Kimizuka, L.A. Abood, T. Tahara and K. Kaibara, J. Colloid Interface Sci., 40(1972)27

125. V.B. Fainerman, Kolloid. Zh., 42(1980)1143

126. R. Defay, I. Prigogine and A. Sanfeld, J. Colloid Interface Sci., 58(1977)498

127. A.I. Rusanov and V.A. Prokhorov, Interfacial Tensiometry, in "Studies in Interface Science", Vol. 3, D. Möbius and R. Miller(Editors), Elsevier, Amsterdam, 1996

128. V.B. Fainerman, S.A. Zholob, R. Miller and P. Joos, Colloids Surfaces A, 143(1998)243

129. M. Ferrari, L. Liggieri, F. Ravera, C. Amodio and R. Miller, J. Colloid Interface Sci., 186 (1997) 40

130. L. Liggieri, F. Ravera, M. Ferrari, A. Passerone and R. Miller, J Colloid Interface Sci., 186(1997) 46

131. J. Lyklema, Fundamentals of Interface and Colloid Science, Vol. I, Academic Press, London, 1993

132. E. Rubin and C.J. Radke, Chemical Eng. Sci, 35 (1980) 1129

133. R. Miller, G. Loglio and U. Tesei, Colloid Polymer Sci 270(1992) 598

134. T.S. Sørensen and M. Hennenberg, in Dynamics and Instabilities in Fluid Interfaces (T.S. Sørensen ed.), Lecture Notes in Physics, 105, Springer-Verlag, Berlin 1979

135. Hennenberg, M., Sanfeld, A. and Bish, P.M., AIChE J., 27 (1981) 1002

136. F. Ravera, M. Ferrari, L. Liggieri, R. Miller and A. Passerone, Langmuir, 13 (1997) 4817

137. F. Ravera, M. Ferrari, L. Liggieri and R. Miller, Progr. Colloid Polymer Sci., 105 (1997) 346

138. R. Miller, V.B. Fainerman, A.V. Makievski, J. Krägel, D.O. Grigoriev, F. Ravera, L. Liggieri, D.Y. Kwok and A.W. Neumann, Characterisation of water/oil interfaces, in "Encyclopaedic Handbook of Emulsion Technology", J. Sjöblom (Ed.), Marcel Dekker, New York, 2001, 1

139. G. Czichocki, M. Ferrari, L. Liggieri, F. Ravera and R. Miller, Poster on the "Surfactants in Solution Conference", Gainesville, 2000

140. G. Loglio, R. Miller, A.M. Stortini, U. Tesei, N. Degli Innocenti and R. Cini, Colloids Surfaces A, 90 (1994) 251

141. D.S. Dimitrov, I. Panaiotov, P. Richmond and L. Ter-Minassian-Saraga, J. Colloid Interface Sci., 65 (1978) 483

142. G. Loglio, U. Tesei and R. Cini, Colloid Polymer Sci. 264 (1986) 712

143. G. Loglio, U. Tesei and R. Cini, Rev. Sci. Instrum. 59 (1988) 2045

144. R. Miller, Z. Policova, R. Sedev and A.W. Neumann, Colloid Surfaces A, 76(1993)179

145. R. Miller, R. Sedev, K.-H. Schano, Ch. Ng and A.W. Neumann, Colloids Surfaces A, 69(1993) 209

146. K. Lunkenheimer and G. Kretzschmar, Z. Phys. Chem. (Leipzig), 256 (1975) 593

147. K.D. Wantke, R. Miller and K. Lunkenheimer, Z. Phys. Chem. (Leipzig), 261 (1980) 1177

148. C.A. MacLeod and C.J. Radke, J. Colloid Interface Sci., 160(1993)435

149. D.O. Johnson and K.J. Stebe, Langmuir, 4 (1994) 1179

150. R. Nagarajan and D.T. Wasan, J. Colloid Interface Sci., 159(1993)164

151. J. Lucassen and D. Giles, J. Chem. Soc. Faraday Trans.1, 71 (1975)217

152. G. Kretzschmar and K. König, J. Signalaufz.-Mater., 9 (1981) 203

153. J. Lucassen and M. van den Tempel, Chem. Eng. Sci. 27 (1972) 1283

154. P.R. Garrett and P. Joos, J. Chem. Soc. Faraday Trans.1, 69 (1975) 2161

155. R. Miller, E.V. Aksenenko and V.B. Fainerman, J. Colloid Interface Sci., 236 (2001) #

156. R. Miller, G. Loglio, U. Tesei and K.-H. Schano, Adv. Colloid Interface Sci., 37(1991)73

157. G. Loglio, U. Tesei, R. Miller, R. Cini and AW. Neumann, Colloids Surfaces, 61 (1991) 219

158. G. Loglio, U. Tesei, N. Degli Innocenti, R. Miller and R. Cini, Colloids Surfaces, 57 (1991) 335

159. K. Tajima, M. Muramatsu and T. Sasaki, Bull. Chem. Soc. Jpn., 43 (1970) 1991

160. T. Okumura, A. Nakamura, K. Tajima and T. Sasaki, Bull. Chem. Soc. Jpn. 47(1974)2986

161. M. Harke, R. Teppner, O. Schulz, H. Orendi and H. Motschmann, Rev. Sci. Instr., 68 (1997) 3130

162. R. Teppner, S. Bae, K. Haage and H. Motschmann, Langmuir, 15 (1999) 7002

163. J. Penfold, Inst. Phys. Conf. Ser. 107(1990) 213

164. T.L. Crowley, E.M. Lee, E.A. Simister, R.K. Thomas, J. Penfold and A.R. Rennie, Colloids Surfaces, 52(1991)85

165. E.A. Simister, E.M. Lee, R.K. Thomas and J. Penfold, J. Phys. Chem., 96(1992)1373

166. J. Penfold, E. Staples, L. Thompson and I. Tucker, Colloids Surfaces A, 102(1995)127

167. S.W. An, J.R. Lu and R.K. Thomas, Langmuir, 12(1996)2446

168. I.P. Purcell, J.R. Lu, R.K. Thomas, A.M. Howe and J. Penfold, Langmuir, 14(1998)1637

169. J.R. Lu, R.K. Thomas and J. Penfold, Adv. Coll. Interface Sci., 84(2000)143

170. M. Simon, Ann. Chim. Phys. 32(1851)5

171. V.N. Kazakov, O.V. Sinyachenko, V.B. Fainerman, U. Pison and R. Miller, Dynamic Surface Tensiometry in Medicine, in "Studies in Interface Science", Vol. 8, D. Möbius and R. Miller (Editors), Elsevier, Amsterdam, 1999

172. V.B. Fainerman and R. Miller, in "Drops and Bubbles in Interfacial Science", in "Studies in Interface Science", Vol. 6, D. Möbius and R. Miller (Eds.), Elsevier, Amsterdam, 1998, p. 279-326

173. V.I. Kovalchuk, S.S. Dukhin, V.B. Fainerman and R. Miller, Colloids Surfaces A, 151(1999)525

174. V.B. Fainerman, Koll. Zh. 52(1990)921

175. N.A. Mishchuk, V.B. Fainerman, V.I. Kovalchuk, R. Miller and S.S. Dukhin, Colloids Surfaces A, 175(2000) 207

176. T. Lohnstein, Ann. Physik, 20(1906)237; 20 (1906) 606; 21 (1907) 1030

177. T. Lohnstein, Z. phys. Chem., 64 (1908) 686; 84 (1913) 410

178. R. Miller and V.B. Fainerman, in "Drops and Bubbles in Interfacial Research", in "Studies in Interface Science", D. Möbius and R. Miller (Eds.), Vol. 6, Elsevier, Amsterdam, 1998, p. 139-186

179. R. Miller, M. Bree and V.B. Fainerman, Colloids Surfaces A, 142(1998)237

180. V.B. Fainerman and R. Miller, Colloids Surfaces A, 97 (1995) 255

181. R. Miller, Colloid Polymer Sci., 258(1980)179

182. G. Loglio, P. Pandolfini, R. Miller, A.V. Makievski, F. Ravera, M. Ferrari and L. Liggieri, in "Novel methods to study interfacial layers", Studies in Interface Science, Vol. 11, D. Möbius and R. Miller (Eds.), Elsevier, Amsterdam, 2001

183. P. Chen, D.Y. Kwok, R.M. Prokop, O.I. del Rio, S.S. Susnar and A.W. Neumann, in "Drops and Bubbles in Interfacial Science", in "Studies in Interface Science", Vol. 6, D. Möbius and R. Miller (Eds.), Elsevier, Amsterdam, 1998, p. 61-138

184. A.W. Neumann and J.K. Spelt, Applied Surface Thermodynamics, Marcel Dekker, New York, 1996

185. F. Bashforth and J.C. Adams, An Attempt to Test the Theory of Capillary Action, Cambridge University Press and Deighton Bell & Co., Cambridge, 1883

186. S. Hartland and R.W. Hartley, Axisymmetric Fluid-Liquid Interfaces, Elsevier Amsterdam, 1976

187. Y. Rotenberg, L. Boruvka and A.W. Neumann, J. Colloid Interface Sci. 93(1983)169

188. P. Cheng, D. Li, L. Boruvka, Y. Rotenberg and A.W. Neumann, Colloids Surfaces, 43 (1990) 151

189. D. Möbius and R. Miller (Eds.), Drops and Bubbles in Interfacial Research, in "Studies in Interface Science", Vol. 6, Elsevier, Amsterdam, 1998

A. Passerone, L. Liggieri, N. Rando, F. Ravera and E. Ricci, J. Colloid Interface Sci., 146(1991)152

190. L. Liggieri, F. Ravera and A. Passerone, Journal of Colloid and Interface Sci., 169 (1995) 226.

191. L. Liggieri, F. Ravera, A. Passerone, A. Sanfeld and A. Steinchen, Lecture Notes in Physics, 467(1996)175

192. L. Liggieri and F. Ravera, in "Drops and Bubbles in Interfacial Research", in "Studies in Interface Science", D. Möbius and R. Miller (Eds.), Vol. 6, Elsevier, Amsterdam, 1998, p. 239-278

193. B.A. Noskov and A.A. Vasyliev, Kolloidn. Zh., 50(1988)909

194. B.A. Noskov and D.O. Grigoriev, Progr. Colloid. Polym. Sci., 97(1994)1

195. B.A. Noskov and T.U. Zubkova, J. Colloid Interface Sci., 170(1995)1

196. B.A. Noskov, D.A. Alexandrov, E.V. Gumennik, V.V. Krotov and R. Miller, Colloid J. (Russ.), 60(1998)204

197. B.A. Noskov, A.V. Akentiev, G. Loglio and R. Miller, J. Phys. Chem., 104 (2000) 7923

198. Y. Tian, G. Holt and R.E. Apfel, J Colloid Interface Sci., 187(1997)1

199. G. Pratt and C. Thoraval, Proceedings of 2nd World Congress on Emulsion, Bordeaux, 1997, 2/2/125/00-2/2/125/05

200. K.-D. Wantke and H. Fruhner, in "Studies in Interface Science", Vol.6, D. Möbius and R. Miller (Eds.), Elsevier Science, Amsterdam, 1998, p.327-365

201. G. Kretzschmar and K. Lunkenheimer, Ber. Bunsenges. Phys. Chem., 74(1970)1064

202. E.K. Zholkovskij, V.I. Kovalchuk, V.B. Fainerman, G. Loglio, J. Krägel, R. Miller, S.A. Zholob and S.S. Dukhin, J. Colloid Interface Sci., 224(2000)47

203. V.I. Kovalchuk, E.K. Zholkovskij, J. Krägel, R. Miller, V.B. Fainerman, R. Wüstneck, G. Loglio and S.S. Dukhin, J. Colloid Interfaces Sci., 224 (2000) 245

204. J. Krägel, A.V. Makievski, V.I. Kovalchuk and R. Miller, in "Transport across liquid interfaces", DECHEMA Monographien, Vol. 136, E. Blaß (Ed.), Wiley-VCH, 2000, p.109-140

205. L. Liggieri, F. Ravera and A. Passerone, J. Colloid Interface Sci., 140 (1990) 436

206. X. Zhang, M.T. Harris and O.A. Basaran, J. Colloid Interface Sci., 168(1994)47

207. J.H. Schulman and E.K. Rideal, Proc. Roy. Soc. B (London), 122(1937)29

208. B.A. Pethica, Trans. Faraday Soc., 51(1955)1402

209. E.E. Eley and D.G. Hedge, Discuss. Faraday Soc., 21(1956)221

210. N.K. Adam, F.A. Askew and K.G.A. Pankhurst, Proc. Roy. Soc. A, 170(1939)485

211. M.A. McGregor and G.T. Barnes, J. Colloid Interface Sci., 54(1976)439

212. D. Vollhardt and M. Wittig, Colloids Surfaces, 47 (1990) 233

213. S. Siegel and D. Vollhardt, Colloids Surfaces A, 76 (1993) 197

214. D. Hönig and D. Möbius, J. Phys. Chem., 95(1991)4590

215. D. Vollhardt, Adv. Colloid Interface Sci., 79(1999)19

216. J.B. Li, R. Miller, R. Wüstneck, H. Möhwald and A.W. Neumann, Colloids Surfaces A, 96(1995)295

217. H.A. Wege, J.A. Holgado-Terriza, A.W. Neumann and M.A. Cabrerizo-Vilchez, Colloids Surfaces A, 156(1999)509

218. Software package "WardTordai" to calculate the dynamics of adsorption for various adsorption isotherms, available via sintech@t-online.de

219. V.B. Fainerman and R. Miller, Colloids Surfaces A, 97(1995)65

220. J. Van Hunsel and P. Joos, Colloids Surfaces, 24(1987)139

221. V.B. Fainerman, R. Miller and E.V. Aksenenko, Langmuir, 16(2000)4196

222. R. Miller, E.V. Aksenenko, L. Liggieri, F. Ravera, M. Ferrari and V.B. Fainerman, Langmuir, 15(1999)1328

223. H.C. Chang, C.T. Hsu and S.-Y. Lin, Langmuir, 14(1998) 2476

224. C.R. Wilke and P. Chang, AIChE J., 1(1955)264

225. S.A. Zholob, V.B. Fainerman and R. Miller, J. Colloid Interface Sci., 186(1997)149

226. D. Vollhardt, V.B. Fainerman and V. Melzer, J. Chem. Phys., 107 (1997) 243

227. D. Vollhardt, V.B. Fainerman and G. Emrich, J. Phys. Chem. B, 104 (2000) 8536

228. D. Vollhardt and G. Emrich, Colloids Surfaces A, 161(2000)173

229. R. Miller, V.B. Fainerman, R. Wüstneck, J. Krägel and D.V. Trukhin, Colloids Surfaces A, 131(1998)225

230. J. Benjamins, J.A. de Feijter, M.T.A. Evans, D.E. Graham and M.C. Phillips, Discuss. Faraday Soc., 59(1978)218

231. D.E. Graham and M.C. Phillips, J. Colloid Interface Sci., 70(1979)415

232. G. Gonzalez and F. MacRitchie, J. Colloid Interface Sci., 32(1970) 55

233. R. Miller, V.B. Fainerman, A.V. Makievski, J. Krägel and R. Wüstneck, Colloids Surfaces A, 161(2000) 151

234. J. Wu, J. B. Li, J. Zhao and R. Miller, Colloids Surfaces A, 175(2000) 113

235. G. Loglio, R. Miller, A.M. Stortini, U. Tesei, N. Degli Innocenti and R. Cini, Colloids Surfaces A, 95(1995)63

236. V.N. Kazakov, O.V. Sinyachenko, V.B. Fainerman, U. Pison and R. Miller, Dynamic Surface Tensiometry in Medicine, in "Studies in Interface Science", Vol. 8, D. Möbius and R. Miller (Editors), Elsevier, Amsterdam, 2000

237. A.F. Vozianov, V.N. Kazakov, O.V. Sinyachenko, V.B. Fainerman and R. Miller, Interfacial tensiometry and rheometry of biological liquids in nephrology, Izd. Donetsk. Med. Univ., Donetsk, 1999 (in Russian)

238. V.B. Fainerman, private communication

239. J. Krägel, R. Miller, A.V. Makievski, V.I. Kovalchuk, L. Liggieri, F. Ravera, M. Ferrari, A. Passerone, G. Loglio, M. Cosi and Ch. Schmidt-Harms, Proceedings of the 1st International Symposium on Microgravity Research and Applications in Physical Sciences and Biotechnology, Sorrento 2000

240. V.I. Kovalchuk, J. Krägel, E.V. Aksenenko, V.B. Fainerman, G. Loglio and L. Liggieri, in "Novel methods to study interfacial layers", Studies in Interface Science, Vol. 11, D. Möbius and R. Miller (Eds.), Elsevier, Amsterdam, 2001, p.

241. J. Zhao, D. Vollhardt, G. Brezesinski, S. Siegel, J. Wu, J.B. Li and R. Miller, Colloids Surfaces A., 171(2000) 175

242. J. Perezgil, C. Casals and D. Marsh, Biochemistry, 34 (1995) 3964

This Page Intentionally Left Blank

5. ADSORPTION FROM MICELLAR SOLUTIONS

B.A. Noskov[1] and D.O. Grigoriev[1,2]

[1] Institute of Chemistry, St. Petersburg State University, Universitetskiy pr. 2, 1989084 St. Petersburg, Petrodvoretz, Russia

[2] Max-Planck-Institut für Kolloid- und Grenzflächenforschung, Forschungscampus Golm, 14476 Potsdam/Golm, Germany

5.1. Introduction

Most of the traditional adsorption studies of surfactants correspond to dilute systems without aggregation in the bulk phase. At the same time micellar solutions are much more important from a practical point of view. To estimate the equilibrium adsorption, neglecting the effect of micelles can usually lead to reasonable results. However, the situation changes for non-equilibrium systems when the adsorption rate can increase by orders of magnitude when the of surfactant concentration is increased beyond the CMC. Current interest in the adsorption from micellar solutions is mainly caused by recent observations that the stability of foams and emulsions depends strongly on the concentration in the micellar region [1]. This effect can be explained by the influence of the micellisation rate on the adsorption kinetics.

Both problems, changes of the equilibrium adsorption with micellar concentration and the influence of micelles on the adsorption rate, are the subjects of this review. Various definitions of the CMC are represented at the outset. Nowadays the thermodynamics of micellisation is the most developed part of modern theories of micellar systems. Two main approaches ("quasichemical and "pseudophase") are discussed in the second section of this chapter. In section 3 the thermodynamic equations for the Gibbs adsorption of surfactants in the micellar region are considered together with corresponding experimental data. The subsequent sections are devoted to non-equilibrium micellar systems. First, section 4 delineates briefly the theory of

micellisation kinetics. Section 5 is devoted to the diffusion in micellar systems. This allows us to discuss the adsorption kinetics from micellar solutions in section 6. For large deviations from equilibrium the corresponding boundary problem can be solved only under rough assumptions and the interpretation of experimental results is difficult. That is why the case of small deviations from equilibrium are considered in detail in sections 7 and 8. The corresponding experimental methods are discussed briefly and it is shown that the theory can describe experimental data reasonably well.

One of the basic phenomena occurring in surfactant solutions is the aggregation of amphiphilic molecules. The formation of these aggregates, so-called *micelles* (Fig. 1), is determined by the chemical nature of amphiphilic molecules and the physico-chemical conditions of the solvent. The number of surfactant molecules composing a micelle is called *aggregation number*. This number is one of the most important characteristics of a micelle. The narrow concentration range where aggregates start to form and the physicochemical properties of the solution change abruptly has been called the *critical micelle concentration* (CMC).

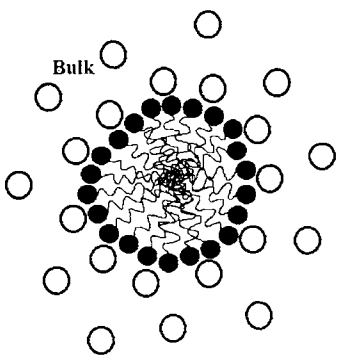

Fig. 1. Schematic presentation of a micelle of ionic surfactant in solution: the fill symbols designate the polar heads of surfactant; open symbols represent the counterions.

This definition of the CMC originates from the qualitative analysis of experimental concentration dependencies of physico-chemical properties, and is not quite strict. Indeed, the limits of the concentration range corresponding to the CMC depend on the error limits of the applied experimental method and on its sensitivity to micellar concentration. For instance, the equivalent conductivity of aqueous solutions of ionic surfactants decreases drastically just above the CMC. Sometimes other properties of surfactant solutions, for example, the intensity

of the scattered light increases rapidly at somewhat higher concentrations. As a result, the CMC values obtained from these two concentration dependencies are different and do not coincide with the values obtained from the surface tension or turbidity measurements. Numerous examples of these discrepancies can be found in the literature [2-4]. There are many attempts to specify the concept of the CMC. Hartley defined the CMC as „the more or less well defined concentration at which the transition occurred" [5]. Corrin has considered the CMC as the total surfactant concentration where a small and fixed amount of surfactant has formed aggregates [6]. According to the paper by Williams et al. [7] the CMC is a surfactant concentration where the concentration of micelles would become zero if their concentration would change according to the same dependence as it does at a little higher concentration. This means that the CMC is practically a point on the concentration axis corresponding to the intersection of two straight lines for properties of premicellar and micellar solutions. One of the most popular definition of the CMC was given by Phillips [8], who defined it using the mathematical formulation of the fact that any property (ϕ) as a function of the total surfactant concentration (c_{toti}) has an abrupt change at the CMC. Phillips considered that the most appropriate point corresponds to the maximal change of the gradient ϕ with concentration and proposed the following definition of the CMC

$$\left(\partial^3\phi/\partial c_{toti}^3\right)_{c_{tot}=CMC} = 0 \tag{5.1}$$

where

$$\phi = A \cdot c_{1i} + B \cdot c_M . \tag{5.2}$$

A and B are constant factors, and c_{1i} and c_M are the concentrations of monomers and micelles, respectively. However, it was noted later that the condition (5.1) corresponds only to the inflection point of the dependence $d\phi/dc_{toti} = f(c_{toti})$ but not to the point of maximum curvature of the function $\phi = \phi(c_{toti})$ [9]. The latter point is characterised mathematically by the following condition

$$|\phi''|/\left[1+\phi'^2\right]^{3/2} = \max \tag{5.3}$$

where $\phi'$and $\phi''$are the first and second derivatives on concentration. Nevertheless these authors proposed their own definition of the CMC as the inflection point of the curve representing the dependence $\phi(c_{toti})$

$$\left(d^2\phi/dc_{toti}^2\right)_{c_{toti}=CMC} = 0 \tag{5.4}$$

According to Hall and Pethica [10] the CMC can be identified as the total concentration where

$$\left[\partial(x_{1i} + x_M)/\partial x_d\right]_{T,p} = 0.5 \tag{5.5}$$

with

$$x_d = x_{1i} + N_m \cdot x_M \tag{5.6}$$

x_{1i} and x_M are the mole fractions of monomers and micelles, respectively, and N_m is the mean aggregation number of micelles. This definition reflects the fact that the slope of the curve representing the dependence $x_{1i}+x_M$ vs. x_d is 1 in the absence of micelles and is nearly zero just above the CMC. Israelachvili et al. [11] defined that the CMC equals to the concentration of monomers in the solution where both the monomer concentration and the concentration of micelles are the same. A comprehensive analysis of different definitions of the CMC has been given recently by Rusanov [12], who proposed a lot of various definitions. For example, the CMC can be considered to be an inflection point of the dependence $\alpha_i = \alpha_i\,(c_{toti})$ (or $\log(c_{toti})$) where α_i is the degree of micellisation of surfactant molecules of kind *i*

$$\alpha_i \equiv \sum_{n_i \geq 2} n_i \cdot c_{n_i} \Big/ c_{toti}\,, \tag{5.7}$$

where c_{ni} are the concentrations of the aggregates composed of n_i surfactant molecules of kind *i*, n_i are the corresponding aggregation numbers.

Rusanov analysed also some definitions of other authors, and used the chemical potential (the thermodynamic activity) as a property under investigation. The definitions (5.1) and (5.3), where ϕ is equal to the chemical potential, proved to be most sensitive to the presence of micelles in the solution. Another important point of this analysis is a strong dependence of this sensitivity on the aggregation number.

All the definitions of the CMC discussed above reflect a general feature of surfactant solutions, namely, a qualitative change in the concentration dependencies of their properties at the CMC. This means that the thermodynamic state of such systems must also differ from the state below the CMC and cannot be described by conventional theories proposed for non-micellar solutions. A brief review of the thermodynamics of micellisation is presented in the following section.

5.2. Theory of micellisation

The classical theories of micellisation can be divided into two classes. One approach is based on the mass action law and assumes that micelles are chemical species („quasichemical" or „chemical" approach). Then the theoretical apparatus of chemical thermodynamics is applied to the whole system containing monomers and micelles.

Another approach is the so-called „pseudophase" treatment. It uses the similarity of the first order phase transition and the micellisation process. Subsequent modifications of this approach are focused mainly on the properties of a micelle, which is considered to be a phase particle. Different theoretical models taking into account geometrical, mechanical and thermodynamic peculiarities of micelles were developed.

Both of these approaches are not free from some disadvantages related to the restrictions of the corresponding concepts. Most of the recently developed theories combine both concepts. Therefore, their predictions are in a better agreement with experimental data although some discrepancies still remain.

5.2.1. Chemical approach to the micellisation

In this approach the micellisation process is considered to be a reversible chemical reaction at which the single dispersed surfactant molecules can be regarded as reactants and the micelles as a product. The whole solution is treated as a single homogeneous phase. The aggregates play the role of chemical species and can be considered in the same manner as another component involved in the reaction. Another main assumption of this chemical treatment of micellisation is the condition of constancy of the aggregation numbers of micelles. In fact, the aggregation number depends on the thermodynamic properties of the system, for example, on the total surfactant concentration or the temperature and this assumption is not strictly correct. Nevertheless, the formalism of chemical thermodynamics may be, however, quite successfully employed to describe the micellisation phenomenon, regardless of these simplifications.

A micellar solution at constant temperature T and pressure p can be described by the following fundamental equations [12]:

$$g_v = \sum_j \mu_j \cdot c_j + \sum_i \mu_i \cdot c_i \ , \tag{5.8}$$

$$dg_v = -s_v \cdot dT + dp + \sum_j \mu_j \cdot dc_j + \sum_i \mu_i \cdot dc_i \ , \tag{5.9}$$

where g_v and s_v are the density of the Gibbs energy G and the entropy S, respectively, μ is the chemical (for ions – the electrochemical) potential, and the subscripts *i* and *j* denote the chemical species participating and not participating in micellisation, respectively.

When micelles and monomers are considered to be individual components and no other aggregates are present in the solution, equations (5.8) and (5.9) can be rewritten as follows

$$g_v = \sum_j \mu_j \cdot c_j + \mu_M \cdot c_M + \sum_i \mu_{1i} \cdot c_{1i} \ , \tag{5.10}$$

$$dg_v = -s_v \cdot dT + dp + \mu_M \cdot dc_M + \sum_j \mu_j \cdot dc_j + \sum_i \mu_{1i} \cdot dc_{1i} \ , \tag{5.11}$$

where the subscript 1 refers to monomers. The chemical potential for micelles can be determined from Eq. (5.11) as usual

$$\mu_M \equiv \left(\frac{\partial g_v}{\partial c_M} \right)_{T,p,c_j,c_{1i}} \ . \tag{5.12}$$

On the other hand the comparison of the right-hand sides of Eqs. (5.9) and (5.11) yields for the component k which participates in micellisation

$$\mu_k = \mu_M \cdot \left(\frac{\partial c_M}{\partial c_k} \right)_{T,p,c_{i\neq k},c_j} + \sum_i \mu_{1i} \cdot \left(\frac{\partial c_{1i}}{\partial c_k} \right)_{T,p,c_{i\neq k},c_j} \tag{5.13}$$

The chemical potential can be represented in the following form [12]

$$\mu_i = \mu_{is} + k_B T \cdot \ln(a_i), \tag{5.14}$$

where μ_{is} is the standard chemical potential, and $a_i = c_i f_i$ is the activity. Analogously, for the chemical potential of a micelle we have

$$\mu_M = \mu_{Ms} + k_B T \cdot \ln(a_M), \tag{5.15}$$

where $a_M = c_M f_M$ is the activity of the micelle. The generalised „chemical" equation of micellisation can be written as follows

$$\sum_i n_i S_i \Leftrightarrow M \ . \tag{5.16}$$

Here M denotes the micelle, S_i denote surfactant molecules or ions of kind *i*, and n_i are the aggregation numbers for each kind of particles. Let us rewrite the fundamental equation (5.10) for the whole system under the condition that $c_j = 0$:

$$dG = -SdT + Vdp + \mu_M dN_M + \sum_i \mu_{1i} dN_{1i}, \tag{5.17}$$

From the material balance condition one can write

$$N_{toti} = N_{1i} + n_i \cdot N_M = const\ , \tag{5.18}$$

or, for concentrations we have

$$c_{toti} = c_{1i} + n_i c_M\ . \tag{5.19}$$

Then, the simultaneous use of relations (5.17), (5.18) and the Gibbs principle of equilibrium

$$(dG)_{T,p,N_{toti}} = 0 \tag{5.20}$$

leads to the following condition of the aggregation equilibrium for micellar systems

$$\mu_M = \sum_i n_i \cdot \mu_{1i}\ . \tag{5.21}$$

Substitution of Eqs. (5.14) and (5.15) into (5.21) yields

$$a_M \Big/ \prod_i a_{1i}^{n_i} = \exp\left[\left(\sum_i n_i \cdot \mu_{is} - \mu_{iM}\right)\Big/ k_B T\right] \equiv K_a \tag{5.22}$$

This relation is the mass action law for the micellisation process. Another form of Eq. (5.22) is

$$c_M \Big/ \prod_i (c_{1i})^{n_i} = K_c\ , \tag{5.23}$$

where

$$K_c \equiv K_a \cdot \prod_i f_{1i}^{n_i} / f_M \tag{5.24}$$

depends now on the concentration because of the dependence of the activity coefficients on concentration. The only difference between K_c and K_a is the factor $\prod_i f_{1i}^{ni}/f_M$. In practice, one usually omits this coefficient in the course of calculations, which is not always correct. First, the activity coefficients of monomers in a micellar solution are a little less than unity because of the weak premicellar association. When they are raised to the high power n_i the resulting product can be significantly smaller than unity. Second, the activity coefficients of micelles can

deviate from unity because of a high micellar charge. Therefore, the simplification $f_{1i} = f_M = 1$ is not valid for micellar solutions of ionic surfactants and one has to take into account the electrostatic interaction between the particles.

For ionic micelles one of the most important properties is the charge. It is, however, not equal to the product of the aggregation number of a micelle and the charge of the surfactant ions composing the micelle because of the counterions bounded to the micelle. On the other hand, the charge of micelles is compensated only partly by counterion binding. There is a special quantity characterising this phenomena – the degree of counterion binding β defined as [12]

$$\beta \equiv -\sum_k n_k \cdot z_k \Big/ \sum_i n_i \cdot z_i > 0 . \tag{5.25}$$

Here n_i and n_k are the aggregation numbers of surface active ions and counterions, respectively, z_i and z_k are their charges which are different in sign.

The elucidation of this notion is most natural in terms of the quasichemical approach to the micellisation. Indeed, the binding of counterions depends on the state parameters and this influence is determined by the competition between electrostatic interaction counterion-micelle and the thermal motion. The energy of pair interactions of different ions in the medium with a dielectric permittivity ε is

$$u_{ik} = z_i \cdot z_k \cdot e^2 / 4\pi \cdot \varepsilon \cdot \varepsilon_0 \cdot r_m , \tag{5.26}$$

where $z_i e$ is the charge of the ion of kind *i*, e is elementary charge, ε_0 is dielectric permittivity of vacuum, and r_m is the average interionic distance. The charge of micelle in terms of Eq. (5.25) is

$$q_M = e \cdot \left(\sum_i n_i \cdot z_i + \sum_k n_k \cdot z_k \right) = (1-\beta) \cdot \sum_i n_i \cdot z_i . \tag{5.27}$$

Substituting this relation into Eq. (5.26) one obtains a sufficient condition of the absence of counterion binding by a micelle

$$(1-\beta) \cdot |z_k| \cdot e^2 \cdot \sum_i n_i \cdot z_i \Big/ 4\pi \cdot \varepsilon \cdot \varepsilon_0 \cdot r_m \cdot k_B T \le 1 \tag{5.28}$$

The counterions bounded by micelles can be very simply imaged as a layer coupled to the micellar surface like a Stern layer. Their position was evaluated from experimental

dependencies of the CMC on the counterion dimension. It was shown, for example, that the CMC values for a series of anionic surfactant with different cations decrease in the order from the smallest to the largest counterion. These results confirm that the bounded counterions retain their primary hydration shell, which increases in the opposite order. If the bounded counterions are organic compounds their binding increases also with increasing ion hydrophobicity. More information and literature sources to these phenomena is given, for instance, by Moroi [3].

The second important characteristic of ionic micellar solutions is the ionic strength. For non-micellar ionic solutions, the following well-known relation defines the ionic strength:

$$I_0 = \sum_i c_i \cdot z_i^2 / 2 . \tag{5.29}$$

In the presence of micelles we have

$$I = \left(c_M \cdot z_M^2 + \sum_i c_{1i} \cdot z_i^2 \right) \Big/ 2 . \tag{5.30}$$

The comparison of the two relations allows us to estimate the change of the ionic strength caused by the presence of micelles. Using the material balance for the case of 1:1-electrolytes we obtain [12]

$$I > I_0 \quad \text{if} \quad n_1 > (1+\beta)/(1-\beta)^2 \quad \text{and} \quad I < I_0 \quad \text{if} \quad n_1 < (1+\beta)/(1-\beta)^2 , \tag{5.31}$$

where n_1 is the aggregation number of the surface active ion. If the degree of counterion binding is about 0.5 - 0.8 and the aggregation number is of the order of ten or hundred, the condition (5.31) shows that micellisation leads to an increase in the ionic strength of the micellar solution.

The third important property of ionic micellar solutions is the activity coefficient, which is closely related to the ionic strength. The mean activity coefficient of a non-micellar solution is usually defined as

$$f_\pm = \prod_i f_i^{\nu_i/\nu} \tag{5.32}$$

where $\nu \equiv \sum_i \nu_i$ and ν_i are the stoichiometric coefficients of the dissociation reaction of a surfactant molecule S

$$S \Leftrightarrow \sum_i \nu_i S_i . \tag{5.33}$$

In a micellar solution the complicated dissociation process can be represented by the following reaction

$$S = \sum_i (c_{1i}/c_{toti}) \cdot S_i + (c_M/c_{toti}) \cdot M \ , \tag{5.34}$$

where c_{toti} is the total surfactant concentration, c_{1i} is the concentration of monomeric ions of the kind i, and c_M is the concentration of micelles. Using the material balance condition (5.19) we can reduce Eq. (5.34) to the following form

$$S = \sum_i \nu_i (1-\alpha_i) \cdot S_i + (\nu_j \alpha_j / n_j) \cdot M, \tag{5.35}$$

where $\alpha_i \equiv n_i c_M/\nu_i c$ is the degree of association (micellisation) of ions of the i^{th} species. The fractional quantities $\nu_i(1-\alpha_i)$ and $\nu_j\alpha_j/n_j$ play the role of stoichiometric coefficients in the micellisation reaction. By analogy with Eq. (5.32) the activity coefficient of the surfactant in a micellar solution can be defined as [12]

$$\ln f_{\pm}^{*} = \sum_i (\nu_i/\nu^{*})(1-\alpha_i) \cdot \ln f_{1i} + (\nu_j \alpha_j / \nu^{*} n_j) \cdot \ln f_M, \tag{5.36}$$

where $\nu^{*} \equiv \nu - \sum_i \nu_i \alpha_i + \nu_j \alpha_j / n_j$ is the total number of ions (including micelles) arising as a result of dissociation of a surfactant molecule, and f_{1i} and f_M are activity coefficients of monomeric ions and micelles, respectively.

It is noteworthy that the f_{1i} in Eq. (5.36) correspond to the real concentrations of ions $c_{toti}\nu_i(1-\alpha_i)$, whereas the experimental values are referred usually to the stoichiometric concentrations $c_{toti}\nu_i$. This results in an increase of each activity coefficient by a factor of $1-\alpha_i$. Then, neglecting the contribution of micelles in Eq. (5.36), the experimental mean activity coefficient of the surfactant ions in micellar solution can be written as

$$f_{\pm}^{e} = \prod_i [(1-\alpha_i) \cdot f_i]^{\nu_i/\nu}. \tag{5.37}$$

This equation for 1:1 electrolyte takes the form

$$f_{\pm}^{e} = [(1-\alpha)(1-\alpha\beta) f_1 f_2]^{1/2}, \tag{5.38}$$

where $\alpha \equiv \alpha_1$ and, $\beta \equiv \alpha_2/\alpha$ is the degree of counterion binding, subscripts 1 and 2 refer to the surface active ion and counterion, respectively.

As shown above, the quasichemical approach to the micellisation is based on the condition of aggregation equilibrium (5.21), which allows us to obtain the mass action law (5.22) for the micellisation process. The simplest situation arises when monodisperse micelles (only with aggregation number n_1), composed only of the non-ionic surfactant molecules (component 1), are formed. The corresponding reaction can be represented by the following equation

$$n_1 S_1 \xleftrightarrow{K_{n1}} M\,. \tag{5.39}$$

Then Eq. (5.23) becomes:

$$c_M = K_{n_1} \cdot c_1^{n_1}\,. \tag{5.40}$$

Let us suppose that K_{n1} and n_1 are constant. Then, using the material balance condition (5.19) and the degree of micellisation in the form $\alpha_1 \equiv n_1 c_M / c_{tot1}$ we obtain [12]

$$\alpha_1 (1-\alpha_1)^{-n_1} = K_{n_1} n_1 c_{tot1}^{n_1 - 1}\,. \tag{5.41}$$

The reverse function $c_{tot1}(\alpha_1)$ can be found from (5.41) in the explicit form

$$c_{tot1} = \left(K_{n_1} n_1\right)^{-1/(n_1-1)} \cdot \alpha_1^{1/(n_1-1)} \cdot (1-\alpha_1)^{-n_1/(n_1-1)}\,. \tag{5.42}$$

This function simplifies the analysis of the dependence $\alpha_1(c_{tot1})$, which has a characteristic S-shape. The inflection point in this dependence is characterised by the condition

$$\alpha_1 = \left|(n_1/2)^{1/2} - 1\right| / (n_1 - 1) \equiv \alpha_{1CMC}\,. \tag{5.43}$$

Since this point corresponds to a maximum rate of increase of the micellisation degree with the total surfactant concentration, the corresponding concentration may be taken as the CMC. This fact allows to introduce in Eq. (5.43) the degree of micellisation α_{CMC} at the CMC.

It was already mentioned above that the condition of monodispersity of micelles means that only one kind of aggregates with a fixed aggregation number n_1 is formed. From the point of view of chemical kinetics the reaction (5.39) is a reaction of n_1^{th} order. Because typical micelles consist of some tens or hundreds molecules the probability of this elementary step is zero. Therefore, Eq. (5.39) presents only the final result of n_1-1 stepwise reactions of first order. The corresponding equilibrium constant is then a product of n_1-1 constants for each step of the micellisation process. In our simplest case we can consider that all these constants are the same and we get [12]

$$K_{n_i} = K_1^{n_i - 1}. \tag{5.44}$$

When the CMC is considered to be an inflection point of the dependence $\alpha_1(\ln c_{tot1})$ the corresponding degree of micellisation at the CMC becomes

$$\alpha_{1CMC} = 1/\left(1 + n_1^{1/2}\right). \tag{5.45}$$

Substituting (5.44) into (5.41) we obtain the multiplier $(K_1 c_{tot1})^{n1-1}$ on the right-hand side. If $K_1 c_{tot1} < 1$ the whole multiplier is very small and if $K_1 c_{tot1} > 1$ the whole multiplier is very large because n_1 exceeds unity essentially. For the case $K_1 c_{tot1} = 1$, which can be used as another definition of the CMC: $(c_{tot1})_{CMC} = 1/K_1$. Equation (5.41) is transformed then into the form

$$\alpha_{1CMC}\left(1 - \alpha_{1CMC}\right)^{-n_1} = n_1. \tag{5.46}$$

Supposing that the right-hand side of Eq. (5.41) equals one, we find the equation

$$\alpha_{1CMC}\left(1 - \alpha_{1CMC}\right)^{-n_1} = 1 \tag{5.47}$$

which gives again a definition of the CMC.

Let us now consider a more general case when the solution contains a mixture of particles of a given composition. This may be a mixture of non-ionic surfactants, a mixture of non-ionic and ionic surfactants or a single ionic surfactant, which can be represented as a mixture of ions with a given stoichiometric ratio. The total concentrations of the various species in the mixture can be connected with the total concentration of the main component (denoted by subscript 1) of micelles

$$c_{toti} = b_i \cdot c_{tot1}, \tag{5.48}$$

where b_i are the coefficients for other components indicating the proportion between different components in the mixture. For example, b_i can be, for example, ratios of stoichiometric coefficients for a single electrolyte. Introducing the degree of micellisation for each component one can write

$$c_M = c_{toti} \cdot \alpha_i / n_i, \tag{5.49}$$

$$c_{1i} = c_{toti} \cdot \left(1 - \alpha_i\right). \tag{5.50}$$

and obtain

$$\alpha_i = \alpha_1 c_1 n_i / c_i n_1 = \alpha_1 n_i / b_i n_1 \equiv \beta_i \alpha_1. \tag{5.51}$$

Substitution of expressions (5.48) – (5.51) into Eq. (5.23) gives

$$c_{tot1} = (K_c n_1)^{-1/(n-1)} \cdot \alpha_1^{1/(n-1)} \cdot \prod_{i\geq 1} [b_i \cdot (1-\beta_i \alpha_1)]^{-n_i/(n-1)}, \tag{5.52}$$

where $n = \sum_i n_i$ is the total aggregation number. It is convenient to rewrite this equation in the following form

$$c_{tot1} = (K_c n_1)^{-1/(n-1)} \alpha_1^{1/(n-1)} (1-\alpha_1)^{-n_1/(n-1)} \prod_{i\geq 2} [b_i (1-\beta_i \alpha_1)]^{-n_i/(n-1)}. \tag{5.53}$$

If the mixture consists only of two kinds of particles Eq. (5.53) becomes

$$c_{tot1} = (K_c n_1)^{-1/(n-1)} b \alpha_1^{1/(n-1)} (1-\alpha_1)^{-n_1/(n-1)} (1-\beta\alpha_1)^{-n_2/(n-1)}, \tag{5.54}$$

where $b \equiv c_2/c_1$ and $\beta = c_1 n_2 / c_2 n_1$. If the CMC is defined as an inflection point of the dependence $c_{tot} = c_{tot}(\alpha)$,Eq. (5.54) yields

$$\beta^2 (n_1 + n_2 - 1)\alpha_{1CMC}^4 - 2\beta(n_1 + n_2 - 1 - \beta)\alpha_{1CMC}^3 + (n_1 + n_2\beta^2 - 1 - 4\beta - \beta^2)\alpha_{1CMC}^2 + 2(1+\beta)\alpha_{1CMC} - 1 = 0 \tag{5.55}$$

Neglecting small terms in the latter equation allows us to obtain the following estimation

$$\alpha_{1CMC} \approx (n_1 + n_2\beta^2)^{-1/2} = n_1 c_{tot2} (n_1^3 c_{tot2}^2 + n_2^3 c_{tot1}^2)^{-1/2}. \tag{5.56}$$

Note that the application of Eq. (5.40) to the micellisation of single ionic surfactant in the case of 1:1 electrolyte leads to a linear relationship between the logarithm of concentration of the surface active ion and the logarithm of counterion concentration. The absolute value of the proportionality coefficient in this relation is the degree of counterion binding introduced by Eq. (5.25). Therefore, the excess of inorganic salt with the same counterion as that of the surfactant will shift the CMC towards lower total surfactant concentrations. A more detailed discussion of this point, taking into account the mean activity coefficient of ionic surfactant was given by Rusanov [12]. An illustration of such phenomenon is presented in Fig. 5.2.

The notions of the total and standard affinity of a reaction introduced in the thermodynamics, and defined as

$$A \equiv -\sum_i \nu_i \mu_i \tag{5.57}$$

and

$$A_s \equiv -\sum \nu_i \mu_{si} = k_B T \ln K, \tag{5.58}$$

are also applicable to the micellisation considered as a chemical reaction in terms of the quasichemical approach. Than the total and standard affinity of micellisation take the form

$$A \equiv \sum_i n_i \mu_i - \mu_M , \tag{5.59}$$

$$A_s \equiv \sum_i n_i \mu_{is} - \mu_{Ms} = k_B T \ln K_a . \tag{5.60}$$

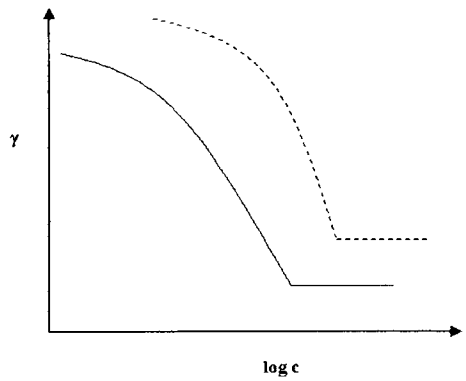

Fig. 5.2. Influence of added salt with the same ion as the counterion on the surface tension isotherm of usual surfactant. Broken line is the surface tension isotherm of salt-free surfactant solution; the solid line is the surface tension isotherm with excess of salt. The break points on the both isotherms are the CMCs of surfactant in the corresponding solutions.

To relate these quantities to measurable parameters characterising the micellisation such as the CMC and the aggregation numbers we suppose that K_a=K_c. Then, application of Eq. (5.53) at the CMC, where c_{tot1}=$(c_{tot1})_{CMC}$ and α_1=α_{1CMC}; gives [12]

$$\ln K_c = (1-n)\ln(c_{tot1})_{CMC} + \ln(\alpha_{1CMC}/n_1) - n_1 \ln(1-\alpha_{1CMC}) - \sum_{i\geq 2} n_i \ln[b_i(1-\alpha_{iCMC})]. \tag{5.61}$$

Introducing the dimensionless form of the constant K_c by

$$K_s = K_c c_{s1}^{n-1} \tag{5.62}$$

with c_{s1} as a certain standard surfactant concentration; and setting c_{s1} = 1M, we get an expression for the dimensionless affinity as follows

$$A_s^M/kT = \ln K_s^M = (1-n)\ln(c_{tot1})_{CMC} + \ln(\alpha_{1CMC}/n_1) - n_1 \ln(1-\alpha_{1CMC}) - \sum_{i\geq 2} n_i \ln[b_i(1-\alpha_{iCMC})]. \tag{5.63}$$

There are some particular cases of Eq. (5.63). For a single non-ionic surfactant it follows

$$A_s^M / k_B T = \ln K_s^M = (1 - n_1)\ln(c_{tot1})_{CMC} + \ln(\alpha_{1CMC}/n_1) - n_1 \ln(1 - \alpha_{1CMC}). \quad (5.64)$$

Neglecting small terms leads to the simple estimation

$$A_s^M = kT \ln K_s^M \approx -k_B T n_1 \ln(c_{tot1})_{CMC}. \quad (5.65)$$

In the case of a single ionic surfactant, one gets from (5.63)

$$A_s^M / k_B T = \ln K_s^M = (1 - n)\ln \nu_1 (c_{tot})_{CMC} + \ln(\alpha_{1CMC}/n_1) - \sum_{i \geq 1} n_i \ln[b_i (1 - \alpha_{iCMC})], \quad (5.66)$$

where subscript 1 denotes the surface active ion, $(c_{tot})_{CMC}$ is the CMC of this ionic surfactant, $((c_{tot1})_{CMC} = \nu_i (c_{tot})_{CMC})$, and $b_i = \nu_i/\nu_1$. An approximate form of this relation is

$$A_s^M / kT = \ln K_s^M \approx -n \ln \nu_1 (c_{tot})_{CMC} - \sum_{i \geq 2} n_i \ln[b_i (1 - \alpha_{iCMC})]. \quad (5.67)$$

If all ions are of the same valence ($b_i = 1$), we have the following approximation at small α_{iCMC}

$$A_s^M = kT \ln K_s^M \approx -k_B T n \ln \nu_1 (c_{tot})_{CMC}. \quad (5.68)$$

When only one single surface active ion is formed by dissociation of a surfactant molecule we get even a simpler form

$$A_s^M = kT \ln K_s^M \approx -k_B T n \ln (c_{tot})_{CMC} \quad (5.69)$$

The affinity of a chemical reaction is closely related to the change in the Gibbs energy of micellisation, which is considered to be an irreversible process

$$\Delta G = G_2 - G_1 = \mu_M N_M - \sum_i \mu_i N_i = N_M \left(\mu_M - \sum_i \mu_i n_i \right) = -N_M A. \quad (5.70)$$

Here A is determined by Eq. (5.59) and the material balance condition $N_i = n_i/N_M$. When the initial and final concentrations are standard, it follows from Eqs. (5.60) and (5.70)

$$\Delta G_s = -N_M A_s = -N_M k_B T \ln K_a. \quad (5.71)$$

The physical meaning and the values of ΔG_s and K_a depend on the chosen standard state. If $c_{is} = c_{iM} = 1$ mole/l, Eq. (5.71) represents the minimal work of micelle formation at the transition from an ideal molecular or ionic solution to an ideal micellar solution in an ideal system. The replacement of K_a by K_c, which is often used in practice, is not strict since the initial and final states of micellisation are not ideal solutions, but solutions with an activity corresponding to the CMC. Therefore the replacement of K_a by K_c in (5.71) defines a quantity $\Delta G_c \neq \Delta G_s$, which is not standard. However, the difference between K_a and K_c is in reality

negligible in the CMC region and one can consider that $\Delta G_c \approx \Delta G_s$. Then from Eq. (5.63) we obtain [12]

$$\Delta G_s \approx \Delta G_c = (R'T/n_1)\{(1-n)\ln(c_{tot1})_{CMC} + \ln(\alpha_{1CMC}/n_1) - n_1 \ln(1-\alpha_{1CMC})\} - (R'T/n_1)\left\{\sum_{i\geq 2} n_i \ln[b_i(1-\alpha_{iCMC})]\right\}, \tag{5.72}$$

where the standard concentration was chosen to be 1 mole/l. Taking into account that α_{1CMC} and α_{iCMC} are small small quantities which can be omitted we can rewrite Eq. (5.72) for a single non-ionic surfactant as

$$\Delta G_c^M \approx R'T \ln(c_{tot1})_{CMC}. \tag{5.73}$$

If the surfactant is a 1:1-electrolyte ($n = n_1 + n_2 = n_1(1+\beta)$ and $b_2 = 1$), Eq. (5.72) becomes

$$\Delta G_c^M \approx R'T(1+\beta)\ln(c_{tot1})_{CMC}. \tag{5.74}$$

Taking into account now the fundamental Eqs. (5.17) and Eq. (5.71) for 1 mole of the main component, one can get the standard entropy, volume and enthalpy of micellisation

$$\Delta S_s = -\partial \Delta G_s/\partial T = R'\partial(T \ln K_a/n_1)/\partial T, \tag{5.75}$$

$$\Delta V_s = \partial \Delta G_s/\partial p = -R'T\partial(\ln K_a/n_1)/\partial p, \tag{5.76}$$

$$\Delta H_s = \Delta G_s - T\partial \Delta G_s/\partial T = \partial(\Delta G_s/\partial T)/\partial(1/T) = R'T^2\partial(\ln K_a/n_1)/\partial T. \tag{5.77}$$

In the Eqs. (5.75)-(5.77) a possible dependence of the aggregation number on temperature is taken into account. However, for real systems this dependence is weak and the aggregation number n_1 can be separated as a constant factor. Similar expressions for ΔS_c, ΔV_c and ΔH_c can be easily obtained by replacing the constant K_a by K_c. Moreover, neglecting the temperature effect on the aggregation number means that the constants K_a and K_c are almost the same.

The relations (5.73) and (5.74) can be used for the elucidation of the dependencies of the CMC on the hydrocarbon chain length in homologous series of surfactants. Indeed, for each chain segment which is far enough from the polar head of a micelle the transfer energies from water into the hydrocarbon phase must be equal. Therefore, the standard Gibbs energy characterising the micellisation at constant temperature and pressure is an additive quantity with regard to the chain segment number. This fact results in a linear dependence of the logarithm of the CMC on the number of hydrocarbon chain segments. Usually this leads to constant shifts between the

individual isotherms in the diagram containing the whole set isotherms for a homologous series if the CMC is obtained from the break point in the surface tension isotherm (Fig. 5.3).

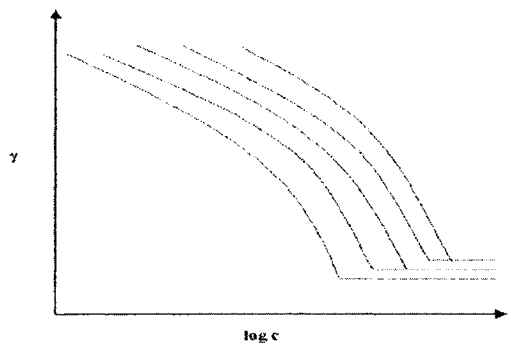

Fig. 5.3. Typical plots of surface tension isotherms for a homologous series of non-ionic surfactants.

Note that all these abovementioned expressions for the standard affinity and the standard thermodynamic functions of micellisation were based on the definition of the CMC as an inflection point in the dependence $\alpha_1(c_{tot1})$ given by Eqs. (5.53) and (5.54). If we use other definitions of the CMC, the corresponding relations will be different.

The quasichemical approach to the micellisation phenomena demonstrates the advantages of a formal application of chemical thermodynamics. In short, the main scheme of this approach can be represented as follows: aggregation equilibrium condition $\Rightarrow$ mass action law and the mass-action-law equilibrium constant $\Rightarrow$ approximate expression for this constant $\Rightarrow$ appropriate definition of the CMC $\Rightarrow$ equations relating the equilibrium constant to the measurable parameters of a micellar system $\Rightarrow$ determination of the Gibbs energy of micellisation and of other thermodynamic functions. The main assumption of the quasichemical approach is that the aggregation number is independent of other parameters like concentration of surfactant and additives, temperature and so on. In practice, however, the aggregation number is a function of these variables. The influence of some of these parameters was not studied yet. Nevertheless, the mass action model allows to give a satisfactory description of various important properties of micellar systems. This is due to the fact that, on the one hand, the dependence of the aggregation number on the total surfactant concentration in a relatively large concentration region above the CMC is usually weak and, on the other hand, the size distribution of micelles exhibits a sharp maximum and the micelles can be considered with high accuracy to be

monodisperse. Another serious restriction of the quasichemical approach consists in the formal treatment of the constant of aggregation equilibrium. This limitation is related to the consideration of micelles as ordinary chemical species. Micelles are built from many monomers and cannot strictly regarded in this way. They have also their own intrinsic structure and properties. Due to these reasons some problems remain such as the dependence of aggregation number on the concentration or the size distribution of aggregates, which cannot even be treated in the framework of this treatment. Therefore the quasichemical approach has to be complemented by another approach.

5.2.2. Pseudophase approach to micellisation

Primarily, this approach was based on the formal analogy between a first order phase transition and the micellisation. When a new phase of a pure substance is formed the chemical potential of this substance and its concentration in the initial phase do not change with the total content of this substance in the system. A similar situation is observed above the CMC, where the adsorption and the surface tension become approximately constant. In reality variations of these properties are relatively small to be observed by conventional experimental methods. The application of the Gibbs adsorption equation shows that the constancy of the surfactant activity above the CMC follows from the constancy of the surfactant adsorption Γ_2 [13]

$$-RT\Gamma_1 = \left(\frac{\partial\gamma}{\partial \ln a_1}\right)_T = \left(\frac{\partial\gamma}{\partial \ln x_1}\right)_T \left(\frac{\partial \ln x_1}{\partial \ln a_1}\right)_T . \qquad (5.78)$$

If Γ_1 is constant and $(\partial\gamma/\partial\ln x_1)_T$ is zero, the derivative $(\partial\ln a_1/\partial\ln x_1)_T$ must be zero too. Therefore, above the CMC the activity of the surfactant is also independent of x_1. This was considered as an evidence for the correctness of the phase separation model. Nevertheless it was concluded [13] that micelles cannot be considered as a true phase because of the finite aggregation number. Changes in the water structure during the separation of the new micellar phase were taken into account by Moroi et al. [14] using the condition of chemical equilibrium of the heterogeneous system (bulk phase and micellar phase) at constant temperature and pressure as

$$\left(\delta G^b\right)_{T,p} + \left(\delta G^M\right)_{T,p} = 0, \qquad (5.79)$$

where superscripts *b* and *M* refer to the bulk and micellar phases, respectively. These two contributions can be represented in the following form

$$\left(\delta G^{b}\right)_{T,p} = \mu_{w}^{b}\delta n_{w}^{b} + \mu_{w}^{st}\delta n_{w}^{st} + \mu_{l}^{b}\delta n_{l}^{b}, \tag{5.80}$$

$$\left(\delta G^{M}\right)_{T,p} = \mu_{l}^{M}\delta n_{l}^{M}, \tag{5.81}$$

where subscripts w and 1 denote the water and surfactant, respectively, and the superscript "**st**" corresponds to the structured water. Additionally, the following material balance conditions must be held for the surfactant solution of a given concentration

$$n_{w}^{b} + n_{w}^{st} = \text{const}, \tag{5.82}$$

$$n_{l}^{b} + n_{l}^{M} = \cos nt, \tag{5.83}$$

$$qn_{l}^{b} = n_{w}^{st}, \tag{5.84}$$

where the last condition denotes that a surfactant molecule has q structured water molecules around it. Then the condition (5.79) yields

$$\mu_{l}^{b} + q\mu_{w}^{st} = \mu_{l}^{M} + q\mu_{w}^{b}, \tag{5.85}$$

which describes the micelle formation in aqueous solutions. The chemical potentials of water and surfactant in the different states are [14]

$$\mu_{w}^{b} = \mu_{ws} + R'T\ln\left(1 - x_{l}\right), \tag{5.86}$$

$$\mu_{w}^{st} = \mu_{ws}^{st}, \tag{5.87}$$

$$\mu_{l}^{b} = \mu_{ls} + R'T\ln x_{l}, \tag{5.88}$$

$$\mu_{l}^{M} = \mu_{Ms}, \tag{5.89}$$

where μ_{ws} and $\mu_{ws}{}^{st}$ are the standard chemical potentials of the ordinary water in the bulk and of the structured water, and x_l is the mole fraction of surfactant in the bulk phase in equilibrium with micelles. These relations allowed Moroi et al. to obtain the following expression for the standard Gibbs free energy of micelle formation

$$R'T\ln\left(\frac{x_{l}}{\left(1-x_{l}\right)^{q}}\right) = \mu_{Ms} - \mu_{ls} + q\left(\mu_{ws} - \mu_{ws}^{st}\right) = \Delta G_{s}. \tag{5.90}$$

The calculated standard thermodynamic functions according to this equation are in a reasonable agreement with experimental data. Moreover, the authors [14] used the quasichemical approach

to the micellisation too and found that these results deviate at a greater extent from the experimental data. However, recently Moroi et al. [3, 15] have shown that the quasichemical approach is stricter from the thermodynamic point of view. This conclusion is based on the fact that the pseudophase model is not in agreement with the Gibbs phase rule [3, 12].

Some theories developed in the framework of the pseudophase approach attempt to obtain the thermodynamic properties of the whole micellar system from a detailed description of a single micelle. This is the main content of the book by Tanford [16] and this approach was developed further by Israelachvili and co-workers [11]. Let us discuss briefly some general principles of these theories. It is assumed that micelles are in equilibrium with the surrounding solution. Then the chemical potentials of both pseudophases are equal and one can write

$$\mu_{Ms} + \frac{k_B T}{n_i} \ln\left(x_{n_i}/n_i\right) = \mu_{1s} + k_B T \ln x_{1i}, \tag{5.91}$$

where the subscripts 1 and n_i denote the monomer and the micellar aggregates with the aggregation number n_i, respectively, and x_{ni} (n = 1 or n) are the corresponding mole fractions. Rearranging Eq. (5.91) gives the alternative form

$$x_{n_i} = n_i x_{1i}^{n_i} \exp\left[n_i\left(\mu_{1s} - \mu_{Ms}\right)/k_B T\right]. \tag{5.92}$$

If we assume that the surfactant solution is a binary system (surfactant + water), the total mole fraction of particles containing surfactant S becomes

$$S = \sum_{n_i=1}^{\infty} x_{n_i} . \tag{5.93}$$

The main characteristics of the size distribution of micelles are the mean aggregation number N_m and the standard deviation $\hat{\sigma}^2$:

$$N_m \equiv \sum_{n_i>1} n_i x_{n_i} \Big/ \sum_{n_i>1} x_{n_i} ; \; \hat{\sigma}^2 \equiv \left\langle n_i - N_m \right\rangle^2 = \sum_{n_i>1} n_i^2 x_{n_i} \Big/ \sum_{n_i>1} x_{n_i} - N_m^2 , \tag{5.94}$$

which can be represented as functions of x_{ni} and S [11]

$$N_m = \frac{\partial \ln\left(S - x_1\right)}{\partial \ln x_1}; \;\; \hat{\sigma}^2 = \frac{\partial N_m}{\partial \ln x_1} = N_m \frac{\partial N_m}{\partial \ln\left(S - x_1\right)}. \tag{5.95}$$

It follows from (5.92), (5.93) and (5.95) that the main parameters of polydisperse micellar systems are determined by the values of x_{ni}, and, consequently, by the difference μ_{Ms}-μ_{1s}

embodied in the exponential factor. Therefore, this difference determines the properties of a micellar system and no further investigation is possible without an estimation of this quantity.

In the simplest case μ_{Ms} has a deep minimum for a finite value of n_i, for example, for $n_i = m_i$. This situation can be the consequence of the fact that for $n_i<m_i$ μ_{Ms} is high due to a loose micellar structure allowing water penetration into the micellar core. For $n_i>m_i$ the same occurs due to head group interactions because of the electrostatic repulsion and (or) steric constraints. Then Eq. (5.92) can be represented in the more convenient form

$$\frac{x_{n_i}}{n_i} = \left(\frac{x_{m_i}}{m_i} \exp\left[m_i \left(\mu_{Ms(m_i)} - \mu_{Ms(n_i)} \right) \right] \right)^{n_i/m_i} . \qquad (5.96)$$

It follows from Israelachvili's definition of the CMC (cf. Section 5.1) and Eq. (5.96) that if the size distribution of micelles is not too large, the CMC can be calculated in the same way as in the case of monodisperse systems ($N_m = m_i$)

$$\ln(\mathrm{CMC}) = \left(\frac{m_i}{m_i - 1} \right) (\mu_{Ms} - \mu_{1s}) \Big/ k_B T - \left(\frac{1}{m_i - 1} \right) \ln m_i \approx (\mu_{Ms} - \mu_{1s}) / k_B T . \qquad (5.97)$$

Analysis of the contributions to the difference μ_{Ms}-μ_{1s} must reflect a lot of competitive factors influencing the free energy of surfactant molecules in micellar and monomer states. Israelachvili et al. [11] divided these contributions into two classes: bulk and surface terms. The bulk energy per surfactant molecule g is a function only of temperature and number of carbon atoms n_c. The surface contribution are of two kinds: those arising from the attractive hydrophobic or surface tension forces, and from repulsive forces of electrostatic origin. Since the hydrocarbon interior can be considered to be liquid-like, the surface tension contribution can be well represented by an interfacial free energy per unit area of aggregate γ, which is close to the energy characterising the liquid hydrocarbon-water interface with a value of about 50 mJ/m^2 as have been supported, for example, by Tanford [16]. On the other hand, some authors proposed significantly lower values for the interfacial tension near the micellar surface. Thus, Zana found from the analysis of the size distribution parameters of spherical micelles that for binary ionic surfactants with alkyl chains from 8 to 18 the value of γ must be close to 20 mJ/m^2 [17]. The surface area per amphiphile $\bar{a}$ is measured at the hydrocarbon-water interface and depends therefore on the choice of this interface. The van der Waals boundary is

used in [11] to define such interface. The estimation of the repulsive terms is much more difficult. Any information on the shape, size, and orientation of charged head groups, the surface charge density, the specific ionic adsorption, and the dielectric constant of the surface region is scarce. Despite of the apparent complexity of the problem, many authors suggest that all complications can be overcome by simple phenomenological expressions. Tanford [16] considered that the repulsive energy contribution could vary as a constant/$\bar{a}$. This function is a consequence of the consideration of a capacitor for the charge of the electric double layer, with the charge $e/\bar{a}$ per a unit area, and the separation d between the capacitor planes. The order of magnitude of this constant is then $2\pi e^2 d/\varepsilon$. Taking into account all contributions of the energy of a surfactant molecule in the aggregated state one can finally write

$$\mu_{Ms} = \gamma a + \frac{2\pi e^2 d}{\varepsilon a} + g . \qquad (5.98)$$

However, this expression can be applied strictly only to a plane interface. Therefore, the corresponding corrections of the curvature of the micelle surface have to be made. These corrections are small and ignored in the followed development. The monomer free energy μ_{1s} comprises two main contributions: a hydrophobic term g' due to the energy of the hydrocarbon chain in water, and the electrostatic energy associated with the charged head group. The term g' is undetermined but the quantity g'-g has the meaning of the usual hydrophobic energy required to take a hydrocarbon chain from water to a hydrocarbon bulk. This value was estimated from experimental data and amounts to about 825 cal·mol^{-1} for the CH_2-group, and about 2100 cal·mol^{-1} for the CH_3-group [16]. One has also to take into account that the head group in the aggregated state might have a different energy from that in the dispersed state due to the low dielectric constant near to the micelle surface. However, both free energies and, therefore, their difference can be expected to be much smaller than the hydrophobic free energy change. The interaction free energy of a head group in the dispersed state with the counterions and with the other head groups was also found to be negligible. The next step was the determination of the relation between a and n_i, which was determined by the shape and size of aggregates. For this purpose, geometric or packing constraints were introduced [11]. For example, the mean area per surfactant molecule in a micelle was considered close to the optimum area a_0. This assumption allows the separation of the energetic and geometric factors. The shape of the

smallest micelle consistent with the condition $a = a_0$ was called as a critical packing shape. Then the hydrocarbon core volume v and the surface area per surfactant molecule at the hydrocarbon-water interface for a spherical micelle with the radius R_m were related by

$$3v/a = R_m . \tag{5.99}$$

The radius of the spherical micelle cannot exceed a critical length l_c, roughly equal to but less than the fully extended length of the hydrocarbon chain. Therefore, once $v/a_0 l_c > 1/3$, spherical micelles will not be able to form unless $a > a_0$. This yields a critical condition for the formation of spherical micelles

$$v/a_0 l_c = 1/3 . \tag{5.100}$$

Assuming that the surface area per surfactant molecule is everywhere equal or close to the optimum area a_0 non-spherical micelles can occur alternatively when $v/a_0 l_c > 1/3$. Similar critical conditions for the formation of cylindrical micelles and planar bilayers, respectively, are

$$v/a_0 l_c = 1/2; \; v/a_0 l_c = 1 . \tag{5.101}$$

In connection with Eqs. (5.100) and (5.101) Israelachvili et al noted that regardless of the shape all aggregates must satisfy the following two criteria: No point within the structure can be farther from the hydrocarbon-water surface than l_c . The total hydrocarbon core volume of the structure V_{tot} and the total surface area $\bar{A}$ must satisfy the condition $V_{tot}/v = \bar{A}/a_0 = n_i$. The last criterion is only approximate since it assumes that the mean surface area per surfactant molecule is equal to a_0.

Note that for growing micelles in intermediate states the packing criteria formulated above are correct only at not too large deviation from a fixed form. Even then, these criteria can be invalid locally. More universal is the local packing criterion formulated in [11]

$$v/a = l\left[1 - \frac{1}{2}\left(\frac{1}{R_1} + \frac{1}{R_2}\right) + \frac{l^2}{3R_1R_2}\right], \tag{5.102}$$

where l is the length of the hydrocarbon region of the amphiphile. This equation is exact for spherical surfaces ($R_1=R_2$), cylindrical surfaces ($R_2=\infty$) or planar surfaces ($R_1=R_2=\infty$), and holds approximately for surfaces of an arbitrary shape. Further, on the basis of this packing equation different shapes were analysed that can occur at the evolution of a spherical micelle when all packing criteria are fulfilled, called an *ellipse of revolution.* These shapes can be

described in terms of criteria (5.100)-(5.102) and relations between these characteristics as *a* and n_i involved in (5.100)-(5.102) can be obtained. The corresponding expressions can be substituted into relation (5.98). The application of the developed theory shows good agreement with experimental data. For example, for spherical micelles, the authors found a reasonable semi-quantitative agreement between predicted and measured effects of changes of the hydrocarbon chain, temperature and salt concentration in the bulk even when the geometric constraints were ignored.

Better agreement can be expected only after a refinement of the theory and consideration of additional factors. These are, for example, the Stern layer, the deviations from the liquid-like behaviour of hydrocarbon chains, steric effects of the head groups. Such more sophisticated and detailed approach has been developed recently by Nagarajan [18]. Although Nagarajan's treatment in its principal points is similar to that of Israelachvili et al. [11], some essential improvements have been made. Nagarajan employed a form for the chemical potential of an aggregate slightly different from Eq. (5.91): $\mu_M = \mu_{Ms} + k_BT \ln x_{ni}$. Together with the equilibrium condition $\mu_M = \mu_1 n_i$ this leads to the following size distribution of aggregates

$$x_{n_i} = x_1^{n_i} \exp\left(-\frac{\mu_{Ms} - n_i\mu_{1s}}{k_BT}\right) = x_1^{n_i} \exp\left(-\frac{n_i\Delta\mu_{Ms}}{k_BT}\right), \qquad (5.103)$$

where $\Delta\mu_{Ms} = \mu_{Ms}/n_i - \mu_{1s}$. This quantity plays the same role in Nagarajan's theory as the difference $\mu_{Ms}-\mu_{1s}$ in the theory by Israelachvili [11]. If an expression for $\Delta\mu_{Ms}$ is available, then the aggregate size distribution can be calculated. Note that the main peculiarities of Nagarajan's theory are related to the determination of $\Delta\mu_{Ms}$. On the contrary, the geometric constraints formulated in [18] are similar to those in the treatment of Israelachvili et al. [11]. Therefore in the following we will mainly discuss various contributions to $\Delta\mu_{Ms}$. In the course of aggregation, the surfactant tail is transferred from water to the hydrophobic core of the aggregate. The corresponding contribution to the free energy can be estimated by considering that the states of the core and liquid hydrocarbon are the same. Experimental data on the solubility of hydrocarbons in water were used for this purpose. For surfactant tails made up of two hydrocarbons chains, the contribution to the transfer free energy would be smaller than that calculated under the assumption of the independence of both chains because of intermolecular interactions. For these surfactants Tanford [16] estimated that the second chain contributes to

the transfer free energy by about 60% of the contribution of an equivalent single chain molecule. Both ends of the surfactant tail have a completely different possibility to occupy a certain position inside the aggregate. The end attached to the head group is constrained to remain at the micelle-water interface. The second one, on the contrary, is free to be in any position in supposition of the core density uniformity. The positive free energy contribution resulting from this constraint is called the tail deformation free energy. Nagarajan [18] followed the method of Semenow [19] for estimation of this term. The final expression involves a lot of molecular-geometric parameters such as the volume of hydrophobic domain of the aggregate composed of n_i surfactant molecules V_{tot}, the corresponding area between the aggregate and water $\bar{A}$, the packing factor $P \cong V_{tot}/\bar{A}R_S$ (R_S is the core radius), the segment length L, and the number of the segments in the tail n_S

$$\frac{(\Delta\mu_{Ms})_{def}}{k_B T} = \frac{9P\pi^2}{80}\frac{R_S^2}{n_S L^2}. \tag{5.104}$$

The formation of an aggregate yields an interface between the hydrophobic core consisting of surfactant tails and bulk water. The free energy of formation of this interface was considered as a product of the surface area in contact with water and the macroscopic interfacial tension of this interface

$$\frac{(\Delta\mu_{Ms})_{in}}{k_B T} = \frac{\gamma_{agg}}{k_B T}(a - a_{sh}), \tag{5.105}$$

where a is the surface area of the hydrophobic core per surfactant molecule, and a_{sh} is the surface area per molecule shielded from contact with water by the polar head group. The aggregate core-water interfacial tension γ_{agg} was taken equal to the interfacial tension between water and the aliphatic hydrocarbon of the same molecular weight. The interfacial tension between water and the aliphatic hydrocarbon was calculated from the corresponding surface tension. The density of the polar head groups lying at the aggregate surface is significantly higher as compared with the infinitely dilute state of single dispersed molecules. This generates steric interactions among the head groups. For compact head groups the respective steric interactions can be estimated, for example, in the framework of the van der Waals approach

$$\frac{(\Delta\mu_{Ms})_{steric}}{k_B T} = -\ln\left(1 - \frac{a_p}{a}\right), \tag{5.106}$$

where a_p is the cross-sectional area of the polar head group near the micellar surface.

If the head groups have a permanent dipole moment they can interact at the aggregate surface. The dipoles at the surface of the micelle are oriented normal to the interface so that the poles of the dipoles are located on parallel surfaces. The dipole-dipole interaction for such orientation provides a repulsive contribution to the free energy of aggregation. The latter for the spherical micelles can be estimated by considering that the poles of the dipoles create a capacitor, which has the distance between two planes equal to the distance of charge separation or the dipole length d

$$\frac{(\Delta\mu_{Ms})_{dipole}}{k_B T} = \frac{2\pi e^2 R_S}{\varepsilon a_\delta k_B T} \frac{d}{R_S + \delta + d}, \tag{5.107}$$

where δ is the distance from the core surface to the place where the dipole is located and a_δ is the corresponding surface area per surfactant molecule.

If the surfactant has an anionic or cationic head group, then ionic interactions occur at the micellar surface. The improved approximate analytical solution of the Poisson-Boltzmann equation was used by Nagarajan for the calculations

$$\frac{(\Delta\mu_{Ms})_{ionic}}{k_B T} = 2\left[\ln\left(\frac{S}{2} + A\right) - \frac{2}{S}(A-1) - \frac{2C}{\kappa S}\ln\left(\frac{1}{2} + \frac{1}{2}A\right)\right], \tag{5.108}$$

where $A \equiv [1+(S/2)^2]^{1/2}$, $S = 4\pi e^2/\varepsilon\kappa a_\delta kT$, C is the curvature factor and κ is the reciprocal Debye length.

Equation (5.108) together with the geometric peculiarities of the micelles and with the expressions for the different contributions to the free energy of micellisation allows us to calculate all properties of a micellar system. Note that many of the above-mentioned contributions to the free energy of micellisation contain parameters related to the molecular structure of the surfactant. They can be estimated from the geometrical characteristics of molecules and molecular structure, and from experimental data on the bulk properties of individual substances.

The approach by Nagarajan leads to a reasonable agreement between predicted and measured properties of micellar systems [18]. For example, good agreement has been obtained between the measured and the predicted dependencies of CMC on the number of carbon atoms in the

tail, or of the CMC and the aggregation number on the added salt concentration, although a lot of adjusting parameters were used. The agreement between other calculated and predicted dependencies was less satisfactory, for example, for the dependencies of the weight aggregation number on the surfactant tail length or for the temperature dependence of the CMC.

Another approach has been intensively developed recently by Puvvada and Blankschtein, who considered also the formation of mixed micelles in surfactant mixtures [20-22]. For example, the free energy of formation of binary mixed surfactant micelle, containing n_A molecules of the surfactant A, n_B molecules of the surfactant B and, n_w water molecules in thermodynamic equilibrium was expressed as

$$G_f = n_W\mu_{sw} + n_A\mu_{sA} + n_B\mu_{sB} + \sum_{n\alpha} n_i N_{ni} g_{mic}(sh, n_i, y_A, l_m), \qquad (5.109)$$

where y_A is the mole fraction of component A in the mixed micelles, N_{ni} is the number of mixed micelles with the aggregation number n_i, μ_{is} are the standard-state chemical potentials, and $g_{mic}(sh, n_i, y_A, l_m)$ is the formation free energy of mixed micelles of the form *sh* and the core minor radius l_m. In contrast to the previous theoretical approaches Blankschtein and Puvvada considered some peculiarities of the surfactant structure. They assumed that the CH_2 group adjacent to the hydrophilic moiety lies within the hydration shell of this moiety, and therefore does not possess any hydrophobic properties. The hydrophilic moiety and the CH_2 group adjacent to it were considered as the head, and the rest of the surfactant molecule as the tail. The free energy of mixed micellisation $g_{mic}(sh, n_i, y_A, l_m)$ is a central element in the evaluation of the properties of micellar systems. The expressions for the micellar size and composition follow from the condition of chemical equilibrium in the system and from the respective expressions for μ_j (j =A, B or n_i) which can be easily obtained from G_f by simple differentiation

$$x_{n_i} = x_1^{n_i} \exp(-n_i g_m(y_A, \alpha_1, n_i)/k_B T - 1), \qquad (5.110)$$

where $g_m(y_A, \alpha_1)/k_BT = g_{mic}(y_A)/kT - 1 - y_A\ln\alpha_1 - (1-y_A)\ln(1-\alpha_1)$ is the modified dimensionless free energy of mixed micellisation, $x_1 = x_{1A} + x_{1B}$ is the total mole fraction of free monomers in the solution, $\alpha_1 = x_{1A}/x$, and $x = (n_A+n_B)/(n_w+n_A+n_B)$ is the total surfactant mole fraction. The order of magnitude of $g_{mic}(sh, n_i, y_A, l_m)$ is related to various free-energy terms, which include:

1). The hydrophobic free energy associated with the transfer of the hydrocarbon tail from water to the hydrocarbon mixture in the micellar core. This contribution can be obtained from available solubility data.

2). The interfacial free energy associated with the creation of the micellar core-water interface, as well as with the shielding part of that interface. This contribution is obtained from available hydrocarbon-water interfacial tension data, and the interfacial area per monomer. The effect of interfacial curvature on interfacial tension was obtained from the Tolman equation [23].

3). The configurational free energy resulting from the loss in conformational degrees of freedom was evaluated by means of the mean-field single-chain statistical mechanical approach.

4). The steric free energy associated with repulsive steric interactions between the heads. The heads at the interface were modelled as a localised monolayer, and the free energy associated with the creation of such monolayer was evaluated using Monte-Carlo simulations.

5). The electrostatic free energy was obtained by solving the Poisson-Boltzmann equation for the electric field strength and the distribution of ions around the micelle.

The total free energy of micellisation can be then composed of these contributions

$$g_{mic}(sh, n_i, y_A, l_{in}) = g_{w/hc} + g_{\sigma} + g_{hc/mic} + g_{st} + g_{elec}. \qquad (5.111)$$

In order to check this theory predictive calculations for some non-ionic and ionic surfactant system were carried out. They showed good agreement with experimental results.

All the theories described above are based on the ideal solution thermodynamics, on the one hand, and on a rather heuristic molecular treatment of micelles as a phase particle, on the other hand. Despite of their obvious successes in predicting micellar solution properties, these theories have some essential drawbacks. The number of adjusting parameters at the evaluation of different contributions to the free energy is too high, as well as the number of oversimplifications, which have been used in order to estimate these parameters. For example, the micellar core is considered as a very small fluid phase droplet surrounded by a second fluid phase and the free energy of micelle surface is estimated as the interfacial tension between these two fluid phases. In order to elucidate this problem Eriksson et al. [24] attempted to

develop a strict mechanical approach to the description of spherical micelles. They noted that the unambiguous definition of the position of the surface of tension and the corresponding value of interfacial tension in the case of micelles are extremely important in the mechanical and, consequently, thermodynamic description. The pressures in the external and interior reference phases divided by the surface of tension together with the normal component of the pressure tensor are used as the main parameters [24].

This approach, however, contains an ambiguity connected with the arbitrary choice of the pressure in the interior reference phase. This circumstance was noted by Rusanov [12]. The micelle in comparison to the bulk phase is non-uniform, even in its centre. Therefore the position of the surface of tension and the value of the interfacial tension at this surface depend on the chosen interior pressure. To avoid this ambiguity, Rusanov [12] proposed to use the product γR^2 as an invariant, independent of this choice, where γ is the interfacial tension at the surface of tension given by a sphere of radius R. The second improvement was made by Rusanov in the thermodynamic description of the so-called micellar cell, which involves not only the proper micelle but also its nearest surrounding. According to Rusanov the "surface layer" of a micelle differs in principal from the corresponding region of the two-phase system. This difference can be estimated if one takes into account the gradient of the chemical potential inside the micelles [12].

It is noteworthy that the phenomena, which are incomprehensible in the framework of the quasi-chemical approach to the micellisation, can be elucidated by the pseudophase treatment. The simplest example is the dependence of the aggregation number on the length of the hydrocarbon chain of surfactant molecules. This effect can be easily explained in the framework of Nagarajan's [18] treatment. The equilibrium area per molecule in the aggregate does not vary appreciably with the change in the tail length. Then, for a spherical or globular micelle at a given equilibrium area per molecule the aggregation number must increase with increasing tail length as a consequence of geometrical relations. A semi-quantitative explanation of this phenomenon was proposed by Rusanov [12].

Indeed, the volume of the hydrocarbon core of a spherical micelle can be roughly presented as a product of the aggregation number n_i and the volume of one hydrocarbon tail v: $V_{tot} = n_i \cdot v$. On the other hand, the same quantity can be estimated as the volume of a sphere of radius l_c, where

l_c is the length of a stretched hydrocarbon tail of the surfactant molecule as $V_{tot} = 4\pi\, l_c^3/3$. The equating of both expressions gives $n_i = 4\pi\, l_c^3/3 \cdot v$. Taking into account that l_c and v are usually linearly related to the number of carbon atoms in the tail (cf. [16]), it is clear that the aggregation number must be a strongly increasing function of the hydrocarbon tail length.

5.2.3. Mixed micelles

Most of the micellisation theories consider mixed micelles as a particular case. The general principles formulated above are obviously valid for mixed micelles too. However, the more complicated chemical nature of mixed micelles demands essential corrections. We will discuss briefly below some approaches of the thermodynamics of mixed micelles. Micellar solutions of mixed surfactants are of a paramount importance for a wide range of industrial applications. The theory of mixed micellar solutions is important not only from the fundamental point of view but also for the practical estimation of their physico-chemical properties. Theoretical studies of mixed micellar solutions are often devoted to the prediction of the CMC on the basis of physico-chemical properties of solutions of individual surfactants. Note that only few theories were developed in the framework of the quasi-chemical treatment [25-27]. Almost all existing approaches are based on the pseudo-phase model of micellisation [3, 18, 20-22, 28, 29-34]. Although micelles are not a separate phase from the point of view of a strict theory, his assumption leads to reasonable results especially for relatively large micelles with aggregation numbers n_i beyond 50 [28, 35, 36]. The limiting case of infinitively large micelles was considered, for example, by Graciaa [28]. The pseudo-phase treatment, because of its relative simplicity, is frequently used for modelling complex mixed surfactant systems of practical importance. There are different variations of the pseudo-phase approach, which can be divided into some groups [37]. The simplest theories are based on the assumption of ideal mixing of micelles [35, 36, 38-40]. In this case the activity coefficient of each component in the micellar phase is equal to unity. This approach can describe successfully the properties of micellar systems composed of homologous surfactants. Different cases of binary mixtures containing two non-ionic homologous surfactants [38], two ionic surfactants with the same surface-active ion and different mono- and bivalent counterions [29], and of multicomponent mixtures composed of homologous ionic surfactants with counterions of different valence [30] have

been investigated. However, these theories are not valid for non-homologous mixtures because one has to take into account more complex interactions between the compounds. The approaches taking into account a non-ideality of mixed micelles are most widely used. One of these models, proposed by Holland and Rubingh [31-33, 39], is based on the regular solution theory. The expressions for the chemical potential of component *i* (for both the monomer and micellar forms) containing the activity coefficient f_i and mole fraction y_i of the component i in the micelles take the form

$$\mu_{1i} = \mu_{si} + R'T \ln c_{1i}, \tag{5.112}$$

$$\mu_{Mi} = \mu_{Mis} + R'T \ln c_i^0 + R'T \ln f_i y_i. \tag{5.113}$$

Taking into account the equilibrium between micelles and the surrounding solution at the CMC ($\mu_{1i} = \mu_{Mi}$) one can write

$$c_{1i} = x_{toti} c_{CMC} = f_i y_i c_i^0, \tag{5.114}$$

where c_{1i}, x_{toti}, f_i, y_i, and c_i^0 are the monomer concentration of component *i*, its net mole fraction, its activity coefficient, its mole fraction in micellar phase and the CMCs of the pure i^{th} component, respectively. C_{CMC} is the CMC of the mixture. The material balance condition for the i^{th} component allows us to write the following relations

$$y_i = (x_{toti} c_{tot} - c_{1i})/(c_{tot} - c_{CMC}), \tag{5.115}$$

$$c_{1i} = x_{toti} y_i c_i^0 c_{tot} / (c_{tot} + y_i c_i^0 - c_{CMC}). \tag{5.116}$$

The relation between the mole fractions for two components *i* and *j* results in

$$y_i = x_{toti} c_{tot} / (f_i c_i^0 - f_j c_j^0 + x_{totj} c_{tot} / y_j). \tag{5.117}$$

The activity coefficients are taken from the regular solution theory as

$$\ln f_i = \sum_{j=1(j\neq i)}^{n} \beta_{ij} y_j^2 + \sum_{j=1,k=1}^{n} \sum_{(i\neq j\neq k)}^{j-1} (\beta_{ij} + \beta_{ik} - \beta_{jk}) y_j y_k, \tag{5.118}$$

where β_{ij} represents the pairwise interaction parameter between components *i* and *j*. To find the n activity coefficients and n mole fractions in the mixed micelles, one needs 2n equations: n equation of the type (5.117) and n equations of the type (5.118), with the additional condition that the sum of all y_i equals unity. In the general case of a multicomponent system the physical meaning of the interaction parameters β_{ij} is rather complicated. Compositions of the type non-

ionic/ionic surfactant are characterised by moderate values of β. Mixtures composed of anionic and non-ionic surfactants have slightly higher negative values of β in comparison with the cationic/non-ionic compositions. Systems of the type zwitterionic/cationic, zwitterionic/non-ionic and non-ionic/non-ionic demonstrate the lowest values of the interaction parameter. In several cases it can be even zero that means an ideal behaviour of the mixture. Negative values of β indicate that the interactions between different surfactant molecules in the mixed micelle are stronger than the interactions in a micelle containing a single surfactant. Meantime positive values of this parameter were observed too [41, 42]. When β exceeds the critical value of 2, two kinds of micelles of different composition can be observed in the solution. These systems show, consequently, two CMCs. The first one represents the total concentration when the component of higher mole fraction begins to form micellar aggregates. The second CMC appears with the micellisation of the second component, and therefore, two kinds of micelles exist above this concentration. Each type of micelles is enriched by one of the two surfactants. If the total surfactant concentration increases further, at a certain total concentration one kind of micelles can disappear because of the solubilisation into the micelles of the second kind. The corresponding total concentration beyond which only one kind of micelles exists was called by Mysels the *critical demicellisation concentration* [42].

Thus the theory of regular solutions turns out to be a useful tool to describe mixed micelle formation. However, some of the assumptions of this theory are inconsistent with a strict thermodynamic treatment. Scamehorn [43] and later Nishikido [34] presented experimental evidences of its inapplicability. Their arguments can be summarised as follows:

- The experimental findings for the heat of mixing for mixed micelles deviate from data obtained from the regular solution theory.
- The parameter β, characterising the interaction between surfactant molecules in the framework of this theory, should be independent of temperature and micellar composition. However, the experiments demonstrate a strong influence of temperature and a slighter influence of the composition on β.
- The regular solution theory predicts a symmetrical excess free energy of mixing with respect to the composition of micelles, which contradicts with experimental data.

- For non-ionic/ionic mixed micelles the degree of counterion binding must be proportional to the mole fraction of ionic component, in contrast to experimental observations.

The second discrepancy was also discussed by Graciaa [28] who found for binary surfactant mixtures that the activity coefficients, for example, in Eqs. (5.114), (5.117) and (5.118), can be expressed in the following form

$$f_i = (1 - y_i)^2 / R'T, \; i = 1, 2. \tag{5.119}$$

For the cases where f_{12} is independent of both temperature and composition, Eq. (5.119) corresponds to the regular solution model

$$f_1 = \exp\left[\beta(1-y)^2\right] \text{ and } f_2 = \exp\left[\beta y^2\right]. \tag{5.120}$$

Graciaa stated further that one of the primary sources of the nonideal behaviour of mixed micelles is the electrostatic term, in agreement with the discussion above. A similar point of view was also expressed by Nishikido [34]. All models of the charged phase presented by several authors may be classified according to Nishikido as follows:

The first group of theories includes the changes in all electrostatic effects due to mixing in the component activity coefficients. The regular solution theory and its numerous modifications belong to the group [37, 44].

In the second group the variation of the CMC of the pure ionic surfactant with the micellar composition was taken into account. However, other effects, such as changes in the micellar electrical potential, are included in the micellar activity coefficients in a manner similar to the first group of theories [45, 46].

Theories, considering changes of the micellar electrical potential and degree of counterion binding form a third group [29, 30, 47, 48].

Another modifications of the pseudo-phase treatment can be presented by Nguyen [49], Motomura et al. [50], and Osborn–Lee et al. [51]. This approach is based on the assumption that the Gibbs-Duhem equation at T, p = const is acceptable for mixed binary micellar phases

$$y_1 d \ln f_1 + y_2 d \ln f_2 = 0, \tag{5.121}$$

where all symbols have the same meaning as in Eq. (5.114). The second important assumption is the chemical equilibrium between monomers and micelles in solution so that the chemical potentials of all components are equal in the coexisting phases

$$f_i y_i CMC_i = x_i CMC_{mix}, \quad i = 1, 2. \tag{5.122}$$

Here x_i are the mole fractions of corresponding components in the monomer state. The third necessary condition is that the monomer activity coefficients in the bulk phase are equal to unity. Combination of these conditions leads to

$$d(\ln CMC_{mix})/dx_1 = (x_1 - y_1)/x_1 x_2. \tag{5.123}$$

The monomer composition is considered to be equal to the solution composition at the CMC. The right-hand part of Eq. (5.123) may be find from experimental data as the slope of the dependence of ln CMC_{mix} on x_1. Then the values of molar fractions in the micellar phase y_i can be determined. The subsequent application of Eq. (5.122) allows us to calculate the activity coefficients of both surfactants in the micelles. This approach has, however, some disadvantages. First, only binary systems can be treated. An additional condition for ionic surfactants is the presence of an indifferent electrolyte. Moreover, the application of Eq. (5.123) is quite complicated and leads to inaccurate results because of the rough estimation of the derivative. This becomes extremely difficult when the pure components have strongly different CMCs. An analogous approach was proposed in [50, 52-55] for so-called neutralised pseudophases and has approximately the same drawbacks as Nguyen's approach. Holland and Rubingh [37] noted additionally that the approaches of this kind could not predict the CMC of mixtures. These data are used there as input data for calculating other properties of micellar system. Osborn-Lee et al. [51] emphasised that the regular solution theory neglects the excess entropy of mixing at the formation of mixed aggregates. Two possible sources of the excess entropy of mixing were included in an alternative model, i.e. the non-random arrangement of two surfactants in the mixed micelle, and the conformational entropy changes in the tails of molecules.

The so-called thermodynamic-molecular models [18, 20-22] form another separate group of theories. For example, Puvvada and Blankschtein showed that the expression for the total free energy of mixed micellisation could be presented for binary surfactant mixture as follows

$$g_{mic}(sh, y_A) = y_A g^{A}_{mic}(sh) + (1 - y_A) g^{B}_{mic}(sh) + y_A(1 - y_A) g^{AB}_{mic} + k_B T[y_A \ln y_A + (1 - y_A) \ln(1 - y_A)] \quad (5.124)$$

where $g^{A}_{mic}(sh)$ and $g^{B}_{mic}(sh)$ are the free energies of micellisation of the pure surfactants A and B, respectively, given by Eq. (5.111); $g^{AB}_{mic} = g^{AB}_{hc} + g^{AB}_{elec}$ reflects the contribution due to intramicellar interactions between surfactant tails of A and B (g^{AB}_{hc}), and the corresponding electrostatic interactions (g^{AB}_{elec}). The last term on the right-hand side of Eq. (5.124) describes the free energy of mixing of two tails in a mixed micelle [21]. The first two terms on the right-hand side show that all contributions to the free energy of micellisation can be presented as a linear combination of the molar fractions of the components and the corresponding individual contributions involved in Eq. (5.111). The equation (5.110) allows us to calculate the so-called optimum composition $y_A^*(n_i)$ when the quantity x_{ni} exhibits a maximum for a given micellar aggregation number n_i [20-22].

Beyond the CMC the addition of surfactant leads mainly to the increase of the number of micelles and the total monomer concentration is practically constant. Furthermore, the first forming micelles will have a composition close to the optimum value y_A^* because the free energy of micellisation has a minimum at this composition. As it follows from Eq. (5.110) the mole fraction of these micelles x_{ni} at y_A^* is finite and becomes small only when $x_1 \approx \exp(g_m/k_BT)$. Further approximation of the CMC at this concentration and application of Eq. (5.124) for the optimum composition y_A^* allows us to get finally the relation for the CMC of the mixture as

$$1/CMC = \alpha_1 / f_A CMC_A + (1 - \alpha_1)/f_B CMC_B , \quad (5.125)$$

where $\ln f_A = g^{AB}_{mic}(1 - y_A^*)^2/kT$, $\ln f_B = g^{AB}_{mic}(y_A^*)^2/k_Bk T$, $\ln(CMC_A) = (g^{A}_{mic}-1)/ k_BT$, and $\ln(CMC_A) = (g^{B}_{mic}-1)/ k_BT$, α_1 is the same as in Eq. (5.110). The variables f_A and f_B are equivalent to the micellar activity coefficients of each surfactants, and the parameter g^{AB}_{mic}/k_BT is equal to the empirical interaction parameter used [37]. The final expression (5.125) can be applied to predict the CMC of diverse surfactant mixtures on the basis of the individual component properties (CMCs). Moreover, this approach allows us to predict with a reasonable precision the CMC from the factors g^{A}_{mic}, g^{B}_{mic} , and g^{AB}_{mic}, which can be calculated using the molecular model [20-22].

A similar approach to mixed micelles was also proposed by Nagarajan [18, 56], where most of the contributions to the standard free energy difference between the single dispersed and the aggregated states were expressed as linear functions of individual contributions. For example, the transfer free energy contribution was presented as

$$\frac{(\Delta\mu_{Ms})_{tr}}{kT} = y_A \frac{(\Delta\mu_{Ms})_{tr,A}}{kT} + y_B \frac{(\Delta\mu_{Ms})_{tr,B}}{k_B T}, \tag{5.126}$$

where $y_i = N_i/\Sigma N_i$, i = A, B. Almost all other contributions were calculated in the same manner [18]: the contribution associated with the formation of the interface between the micellar core and bulk water (Eq. (5.105)), the contribution of steric interactions of the head group (Eq. (5.106)), and the contribution arising from the deformation of the surfactant tails in micelles (Eq. (5.104)). The free energy contribution connected with the dipole interactions of the head groups were taken into account by introducing into Eq. (5.107) an additional factor that describes the fraction of surfactant molecules in the aggregate having a dipolar head group [18, 56]. The case of two oppositely charged surfactants may be regarded as the formation of ion pairs. Note that there is a contribution to the free energy of mixed micelles that is absent for single surface active components. This term accounts for the entropy and enthalpy of mixing of the surfactant tails of molecules A and B in the hydrophobic core with regard to the reference states of the micelle cores of pure A and B. This contribution was regarded in Nagarajan's theory [18, 56] by means of the Flory-Huggins expression

$$\frac{(\Delta\mu_{Ms})_{mix}}{k_B T} = \frac{(\delta_A^H - \delta_{mix}^H)^2 y_A v_{SA} + (\delta_B^H - \delta_{mix}^H)^2 y_B v_{SB}}{k_B T} + y_A \ln\eta_A + y_B \ln\eta_B, \tag{5.127}$$

where $\delta_A{}^H$ and $\delta_B{}^H$ are the Hildebrand solubility parameters of the surfactant tails of A and B, v_{SA} and v_{SB} are the molecular volumes of the surfactant tails, respectively, and $\delta_{mix}{}^H$ is the volume-fraction averaged solubility parameter of all the components within the micellar core, $\delta_{mix}{}^H = \eta_A\delta_A{}^H + \eta_B\delta_B{}^H$.

5.3. Equilibrium surface properties of micellar solutions

Measurements of the equilibrium surface tension in a broad concentration range above and below the CMC is one of the most conventional methods in the studies of surfactant solutions. The first derivative of the concentration dependence of the surface tension jumps at a certain

point, which is usually considered as the CMC. This simple definition of the CMC was already discussed at the beginning of this chapter. It has been also shown (Eqs. 5.71, 5.73-5.77) that the temperature and pressure dependencies of the CMC can be used for the evaluation of the thermodynamic functions of micellisation. On the other hand, the surface tension isotherm in the concentration range near the CMC can also be used for the determination of some properties of micellar solutions, for example, the adsorption value.

A simple attempt to estimate the composition in mixed micelles from surface tension data at the CMC was made by Funasaki and Hada using a mass balance condition [57]. Indeed the composition of micelles and the bulk solution containing two surfactants can be related to the surface tension values at the CMC. The material balance for this system takes the form

$$c_{tot} x_{tot2} = c_{CMC} x_2 + (c_{tot} - c_{CMC}) y_2 , \tag{5.128}$$

where x_{tot2}, x_2, and y_2 are the overall, bulk, and micellar mole fractions of surfactant 2 in the mixed solution, respectively, c_{tot} and c_{CMC} are the total concentration of the surfactant mixture and the CMC of the mixed solution. The mole fraction of surfactant 2 in the micelles is

$$y_2 = (c_{tot} x_{tot2} - c_{CMC} x_2)/(c_{tot} - c_{CMC}) . \tag{5.129}$$

Thus from the break point of the surface tension dependence on the total surfactant concentration one can determine c_{CMC} and x_2 (equal to x_{tot2} at the CMC) as a function of the surface tension. Furthermore, measuring the surface tension of aqueous solutions at a given concentration c_{tot} above the CMC, one can calculate the mole fraction of the surfactant 2 in micelles using Eq. (5.129). To this aim one has to substitute the values of c_{CMC} and x_2 that correspond to the measured surface tension.

Motomura et al. proposed a method of evaluation of various thermodynamic properties of micellar solutions from the surface tension data in the framework of the pseudophase treatment of micellisation [50, 52-55]. According to these authors, the micellar composition at the CMC can be found from the functional dependence of the CMC on the overall surfactant mole fraction using an analogy to the method proposed by Nguyen et al. [49]. The approach of Motomura et al. [50] gives also a possibility to determine the relation between the composition of the surface layer and the micelles. Application of the Gibbs-Duhem equation to the whole

two-phase system including the surface layer for a binary surfactant mixture leads to the following fundamental equation

$$d\gamma = -s^H dT + v^H dp - \Gamma_1^H d\mu_1 - \Gamma_2^H d\mu_2, \tag{5.130}$$

where Γ_i^H is the excess of surfactant i (i = 1, 2) per unit area when the location of the dividing surface corresponds to zero excesses of water and air, while the thermodynamic quantities are defined as follows: $\varphi^H = \varphi - (V^W\varphi^W + V^A\varphi^A)/\tilde{A}$, φ^W and φ^A are the densities of the quantity φ in the water and air phases, respectively, $\tilde{A}$ is the area of the plane surface. Substitution of the chemical potentials of both components for ideal solutions into Eq. (5.130) gives

$$d\gamma = -\Delta s dT + \Delta v dp - \frac{RT\Gamma^H}{m} dm - \frac{RT\Gamma^H}{X_1 X_2}\left(X_2^H - X_2\right) dX_2, \tag{5.131}$$

where $\Gamma^H = \Gamma_1 + \Gamma_2$, $X_2^H = \Gamma_2^H/(\Gamma_1 + \Gamma_2)$, and m is total molality of the mixture. The Gibbs-Duhem equation for the micellar phase can be represented in the form

$$s^M dT - v^M dp - N_1^M d\mu_1 - N_2^M d\mu_2 = 0, \tag{5.132}$$

φ^M is the excess molar thermodynamic quantity of a mixed micelle. Here the dividing spherical surface corresponds to the condition of zero excess of water. N_i^M is the corresponding number of molecules of the surfactant i in a single mixed micelle. At equilibrium between the coexisting pseudophases (monomer surfactant solution and micelles) the chemical potentials of the components are equal. Therefore, substitution of the chemical potentials in the form valid for ideal solutions into Eq. (5.132) and replacement of the concentration by the CMC (denoted as c_{CMC}) lead to

$$\frac{R'T}{c_{CMC}} dc_{CMC} = -\Delta_W^M s dT + \Delta_W^M v dp - \frac{R'T\Gamma^H}{m} dm - \frac{R'T}{x_1 x_2}\left(y_2 - x_2\right) dx_2, \tag{5.133}$$

where the following quantities were introduced: $\Delta_W{}^M\varphi = [\varphi^M - (N_1{}^M y_1 + N_2{}^M y_2)]/ (N_1{}^M + N_2{}^M)$ and, $(y_2 = N_2{}^M/(N_1{}^M + N_2{}^M)$. Joint application of Eqs. (5.131) and (5.133) at the CMC yields

$$x_2^{H,CMC} = y_2 - \frac{x_1 x_2}{RT\Gamma^{H,CMC}}\left(\frac{\partial\gamma^{CMC}}{\partial x_2}\right)_{T,p}, \tag{5.134}$$

The superscript CMC designates thermodynamic quantities at the CMC. This relationship between the compositions of the mixed micelles and the adsorption layer close to the CMC was successfully employed in a series of papers [58-61].

A possible interpretation of the shape of the surface tension isotherm at the CMC was given by Rusanov and Fainerman in the framework of a quasichemical approach to micellisation [62]. The general idea is as follows: the total surfactant concentration is related to the concentrations of micelles and monomers by the mass balance condition (5.18) and the mass action law in form of Eq. (5.23). From these conditions, one of two quantities can be expressed as a function of the other. For a single non-ionic surfactant this gives (see also Eq. (5.40))

$$c_{tot} = c_{1\,1} + n_1 K_{n_1} c_{1\,1}^{n_1}. \tag{5.135}$$

Application of the Gibbs equation under the assumption that the change of the surfactant activity in the monomeric form is negligible near the CMC yields

$$d\gamma/d\ln c_{tot} = -R'T\Gamma_{1(2)}\, d\ln c_{1\,1}/d\ln c_{tot}. \tag{5.136}$$

The derivative on the right-hand side of Eq. (5.136) can be evaluated from Eq. (5.135). Substitution into the Gibbs equation leads to

$$d\gamma/d\ln c_{tot} = -R'T\Gamma_{1(2)}/[1+\alpha_1(n_1-1)], \tag{5.137}$$

where α_1 is the degree of surfactant micellisation, defined above (see comments below Eq. (5.40)). The two limiting cases of this equation at $\alpha_1 = 0$ (below the CMC) and $\alpha_1 = 1$ (essentially above the CMC) take the forms

$$d\gamma/d\ln c_{tot} = -R'T\Gamma_{1(2)}, \alpha_1 = 0 \quad \text{and} \quad d\gamma/d\ln c_{tot} = -R'T\Gamma_{1(2)}/n_1, \alpha_1 = 1. \tag{5.138}$$

Comparison of the two approximations shows that the slope of the isotherm below the CMC must be essentially steeper than just at the CMC. Then the aggregation number can be estimated by means of simultaneous application of relations (5.138)

$$n_1 \approx (d\gamma/d\ln c_{tot})_{\alpha=0}/(d\gamma/d\ln c_{tot})_{\alpha=1}. \tag{5.139}$$

This method of determination of the aggregation number is, however, not very exact because the surface tension changes only slightly above the CMC. Therefore Eq. (5.139) gives usually too small values of n_1. For more precise determination of n_1 from the surface tension isotherm the denominator in Eq. (5.139) should be taken at a concentration only slightly exceeding the CMC. Then the left side of (5.139) becomes equal to $1 + \alpha_1(n_1-1)$. The value of α_1 can be immediately determined from the same isotherm according to the definition of the degree of micellisation, and, consequently, n_1 can be obtained. The more complicated case of a single

ionic surfactant was also considered in [62]. In this case, the dissociation of the surfactant molecules into ν_1 surface active ions and ν_2 counterions ($\nu = \nu_1 + \nu_2$) and the condition of electroneutrality of the surface layer ($\Gamma_{2(3)} = \Gamma_{1(3)}\nu_2/\nu_1$, where subscripts 1, 2, and 3 denote the surface active ion, counterion and solvent, respectively) must be additionally taken into account. In terms of the degree of micellisation of surface active ion α_1 and the degree of counterion binding β (Eq. 4. 25), the derivatives of the concentrations of surface active ion and counterion with respect to the total surfactant concentration have the forms [62]

$$\frac{d\ln c_{11}}{d\ln c_{tot}} \approx \frac{1-(\nu_2/\nu_1)n_1\alpha_1\beta(1-\beta)/(1-\alpha_1\beta)}{1-\alpha_1+n_1\alpha_1\left[1+(\nu_2/\nu_1)(1-\alpha_1)\beta^2/(1-\alpha_1\beta)\right]}, \tag{5.140}$$

$$\frac{d\ln c_{12}}{d\ln c_{tot}} \approx \frac{1}{1-\alpha_1\beta}\left[1-\beta+\beta(1-\alpha_1)\frac{d\ln c_{11}}{d\ln c_{tot}}\right]. \tag{5.141}$$

The analogue of Eq. (5.137) for solution of ionic surfactant takes the form

$$\frac{d\gamma}{d\ln c_{tot}} \approx -R'T\Gamma_{1(3)}\left[\frac{\nu_2}{\nu_1}\frac{1-\beta}{1-\alpha_1\beta}+\left(1+\frac{\nu_2\beta}{\nu_1}\frac{1-\alpha_1}{1-\alpha_1\beta}\right)\frac{d\ln c_{11}}{d\ln c_{tot}}\right]. \tag{5.142}$$

Note that both Eqs. (5.142) and (5.137) are derived under the same assumptions: the activity coefficients are neglected and K_c is equal to the equilibrium constant. Equation (5.142) can be rearranged further under the assumptions that $\alpha_1 = 0$ and $\alpha_1 = 1$

$$\left(\frac{d\gamma}{d\ln c}\right)_{\alpha_1=0} \approx -R'T\Gamma_{1(3)}(1+\nu_2/\nu_1); \left(\frac{d\gamma}{d\ln c}\right)_{\alpha_1=1} \approx -R'T\Gamma_{1(3)}(\nu_2/\nu_1)(1-\beta). \tag{5.143}$$

If the adsorption values are the same in both relations (5.143), an expression for the degree of counterion binding from experimental surface tensions can be easily obtained

$$(d\gamma/d\ln c_{tot})_{\alpha_1=1}/(d\gamma/d\ln c_{tot})_{\alpha_1=0} \approx (1-\beta)\nu_2/\nu. \tag{5.144}$$

A simple analysis of this equation shows that the slope of the isotherm at usual values of $\beta = 0.5$ and $\nu_2/\nu = 0.5$ should decrease drastically at the transition to the CMC. Eq. (5.144) was used later by Prokhorov and Rusanov for the evaluation of β from the surface tension of aqueous solutions of dodecyl trimethyl ammonium bromide (DTAB) [63]. The obtained value proved to be too high in comparison with the findings of independent methods. A possible reason of this discrepancy can be the assumptions used for the derivation of Eq. (5.144). Namely, the condition $\alpha_1 = 1$ can hold only at concentrations essentially exceeding the CMC. A

more sophisticated relation obtained in [63] for concentrations just above the CMC leads to more realistic values of β, but requires the micelle aggregation number as one of the input parameters. Rusanov considered an even more complicated example of two non-ionic surfactants taken at a certain ratio [12], where the Gibbs adsorption equation takes the form

$$d\gamma/R'Td\ln c = -\Gamma_{1(3)}\, d\ln c_{11}/d\ln c - \Gamma_{2(3)}\, d\ln c_{12}/d\ln c. \qquad (5.145)$$

Here c is the total concentration of the surfactants. The Eqs. (5.140) and (5.141) derived above for a single ionic surfactant can be applied if some additional parameters are introduced. Further analysis of the final expression leads to the following rule of mixed micellisation: when a mixture of two surfactants forming mixed micelles is added to a solution, the monomer concentration of the surfactant with the higher relative content in micelles than in the initial mixture passes trough a maximum whereas the monomer concentration of the second surfactant increases monotonically. This rule together with the additional condition $\Gamma_{2(3)} \gg \Gamma_{1(3)}$ allow us also to describe the behaviour of a surface active admixture participating in the micellisation. In this case the monomer concentration of the admixture will go trough a maximum with increasing total concentration. Then in the limit $\alpha_2 \to 1$ the second derivative in Eq. (5.145) will change its sign. This means that the dependence of surface tension on the total surfactant concentration (which is practically equal to the concentration of the main surfactant) can go through a minimum. Many authors observed this minimum (see, for example [64]) when the degree of purification of individual surfactants is not sufficient and small amounts of the admixture can be in the solution. Fig. 5.4 shows schematically a typical concentration dependence of the surface tension in this case.

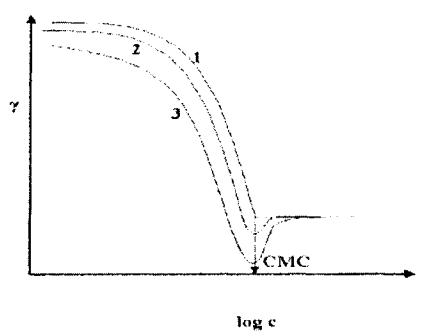

Fig. 5.4. Surface tension isotherms of a pure surfactant (1), of a mixture of the same surfactant with a small amount of a surface active impurity (2), and the same mixture with a large amount of impurity (3).

Recently it has been also shown that the surface tension of micellar solutions above the CMC can respond to the transition between spherical and rodlike micelles taking place in micellar solutions of certain surfactants in the presence of multivalent ions, such as Al^{3+}[65]. The qualitative explanation of this phenomenon is connected with the ability of Al^{3+} ion to bind three surfactant headgroups, and, consequently, to lower the area per headgroup. According to Israelachvili et al., [11] this can induce a transition from spherical to rodlike micelles. On the other hand, the new micelles adsorb additional Al^{3+} ions from the bulk. This leads also to a lower adsorption of Al^{3+} at the solution-gas interface because the competitive adsorption of the counterions follows the same tendency as their bulk concentration. The desorption of Al^{3+} causes sharp increase of the surface tension with increasing molar ratio.

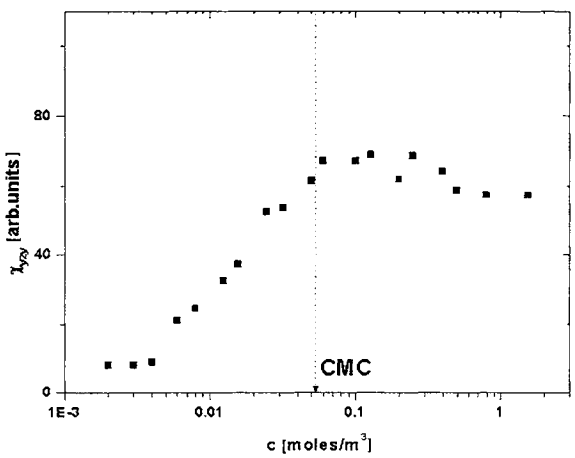

Fig. 5.5. Typical shape of the concentration dependence of the second – order susceptibility component $\chi^{(2)}_{yzy}$ measured for aqueous solutions of (*p*-nonylphenyl)decaoxyethylene glycol monoether; according to Lehmann et al. [66].

The broad spectrum of recently developed experimental techniques together with traditional measurements of the surface tension has been applied during the last decade to surface layers of micellar solutions [66-76]. For example, Lehmann et al. studied the correlation between the results of a non-linear optical technique (second-harmonic generation) and surface tension measurements [66]. The concentration dependence of the second-order susceptibility component exhibits a kink point in the vicinity of the CMC with a subsequent levelling off (Fig. 5.5). Such behaviour can be explained by the approximate constancy of the adsorption above the CMC.

The surface excess obtained by the second-harmonic generation in the concentration range below the CMC, however, changes with concentration in contradiction to the usual interpretation of surface tension data. Moreover, the absolute values of the adsorption determined by two experimental methods differ by one order of magnitude. These discrepancies were explained by means of the concept of a depth-dependent distribution of surfactant molecules [66]. Different distributions can lead to identical adsorption values. The surface excess determined by the second-harmonic generation can be attributed only to the very top layer, whereas the values obtained from surface tension techniques are apparently more sensitive to the near-surface layer.

Another powerful technique that has been successfully employed recently to investigate adsorbed layers is the neutron reflectivity [67-76]. Combination of this method with the sophisticated deuteration scheme of molecules or even their segments participating in the formation of the surface layer, gives a possibility to obtain direct information, not only on the degree of adsorption [69, 70] but also on the structure [67-72] and composition [73-76] of the surface layer. Usually, the adsorption isotherm obtained directly from neutron reflection data exhibits approximately constant values of adsorption beyond the CMC is reached [69] (cf. Fig. 5.6).

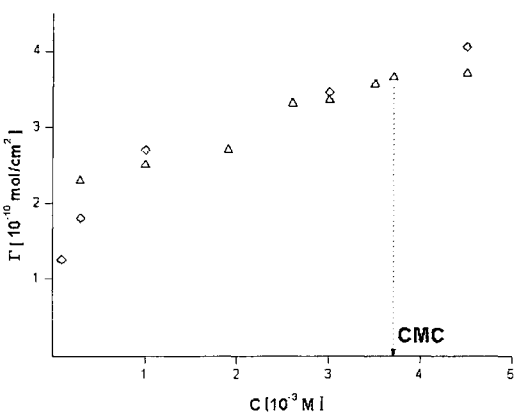

Fig. 5.6. Adsorption isotherm from neutron reflectivity data for aqueous solutions of fully deuterated (open diamonds) and chain deuterated (open triangles) tetradecyl trimethyl ammonium bromide; cf. [69].

Lu et al. studied the structure of adsorption layers for three classes of surfactants – cationic, anionic, and non-ionic in a broad concentration range up to the CMC [67]. The mean distances between the centre of distribution of the hydrophobic chain of adsorbed molecules and the mean position of the aqueous surface was calculated on the basis of neutron reflection measurement at concentrations close to the CMC. The obtained results show that in this concentration range the hydrocarbon chains are significantly immersed into the water, regardless of their chemical nature.

This approach was extended later to the homologous series of alkyl trimethyl ammonium bromides with the chain lengths from 12 to 18 carbon atoms [68-72]. A detailed investigation of the structure of adsorbed layer of tetradecyl trimethyl ammonium bromide at the concentrations below and above the CMC was carried out in [68]. The mean distances between chains and polar heads, between chains and water, and between heads and water were evaluated for concentrations just below the CMC. The thickness of the chain region depends slightly on the model but is less than the length of a fully extended chain. At a concentration about one-third of the CMC this region becomes thinner. Above the CMC the layer is closely packed and the thickness of the head-group region increases. In accordance with these findings, the adsorption values increase a little with concentration even above the CMC. This effect was analysed later and compared with the results from surface tension measurements [69]. It was shown, that the two techniques lead to the same molecular area at the CMC only if the concentration dependence of surface tension just below the CMC was described by an essentially non-linear function.

Almost the same behaviour was found for a higher homologue of this series – octadecyl trimethyl ammonium bromide [70]. A satisfactory agreement between the molecular areas at the CMC evaluated from neutron reflection and surface tension data was obtained too. Two other homologues of this series, dodecyl and hexadecyl trimethyl ammonium bromide, were investigated in [71, 72]. Labelling of blocks of two or four atoms in the surfactant molecules allowed the authors to determine the structure of the adsorbed layer at the CMC. It was shown that the inner part of the carbon chain adjacent to the head group is oriented closer to the

surface normal than the outer parts of the chain, which are progressively oriented away from the surface normal. The composition of surface layers adsorbed from the mixture of two surfactants was determined in a wide micellar concentration range by means of neutron reflection technique for various systems: sodium dodecyl sulfate / n-hexaethylen glycol monododecyl ether [73], hexadecyl trimethyl ammonium bromide / n-hexaethylen glycol monododecyl ether [74], mixture of two non-ionic surfactants [75]. These data can be considered as a direct qualitative confirmation of the formation of mixed micelles, which starts at the CMC and leads to drastic changes in the surface layer composition. The interpretation of these results in the framework of the regular solution theory is in good agreement with data obtained earlier. The shrewd labelling scheme allowed Bell et al. to determine the location of the counterions in the adsorbed layer of hexadecyl trimethyl ammonium *p*-tosylate [76].

5.4. Micellisation kinetics

5.4.1. Impact of micelles on adsorption kinetics

It is well-established now that the concentration of surfactant ions in micellar solutions changes when the total surfactant concentration c is increased. This leads to changes in the adsorption value and, consequently, to changes in the surface tension. These alterations, however, are small, even for ionic surfactants. For relatively dilute solutions, i.e. $c < 10$ CMC, as a first approximation one can consider that the monomer concentration c_1 is constant ($c_1 \approx$ CMC). Actually, for $c >$ CMC surface tension changes are usually low and in the range of accuracy of conventional methods. This fact evidences an approximate constancy of the adsorption.

The situation changes for non-equilibrium systems. The dynamic surface properties of micellar solutions depend strongly on the concentration in a broad range of surface life time and/or of the frequency of surface compression and dilation. First of all this is related to the fact that the adsorption rate of surfactants increases with concentration for both sub-micellar and micellar solutions. As an example, dynamic surface tensions of SDS in 0.1 M NaCl measured by Fainerman and Lylyk [77] are shown in Fig. 7. As one can see entirely different values of the dynamic surface tension and of the adsorption can correspond to the same surface age at $c \geq$ CMC.

Numerous data on dynamic surface tension [77-93] and dynamic surface elasticity [94-103] of aqueous micellar solutions have been published until now. These data evidence the influence of micelles on the adsorption kinetics, although they are present only in the bulk phase. This effect can surprise on a first glance because it is well-known that the surface activity of micelles is negligible and hence their adsorption is almost zero. However, the influence of micelles can be easily explained if one takes into account that the adsorption kinetics of surfactants at fluid - fluid interface is determined by the diffusional exchange between the subsurface and the bulk phase [104, 105]. It is exactly the diffusion of monomers that changes in the presence of micelles. This point of view is widely accepted and difficulties arise only if one tries to obtain quantitative estimates of the observed effects.

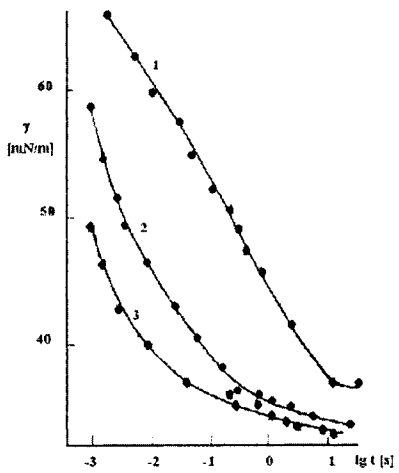

Fig. 5.7. Dynamic surface tension of SDS solutions in 0.1 M NaCl; SDS concentration: 1 mole/m^3 (1), 2 mole/m^3 (2), 4 mole/m^3 (3) [77].

The formation of a fresh interface leads to an almost instantaneous adsorption of surfactant monomers from the regions of the bulk phase close to the surface (subsurface). As a result the surfactant concentration in this regions decreases, and the diffusion of monomers from farer regions in the bulk phase begins (Fig. 5.8).

Simultaneously, the equilibrium between micelles and monomers in the subsurface layer is violated. If the diffusion rate of monomers is comparable with or less than the rate of micellisation, the deficiency of monomers can partly be compensated at the expense of micelles. In this way the concentration of micelles in the solution becomes non-uniform too,

and this leads to the diffusion of micelles. A similar situation arises also when the interface is subjected to compression. Then the diffusion of micelles and monomers proceeds in the reverse direction. Therefore, micelles act as sources or absorbers in the course of the diffusion of monomers to or from the interface.

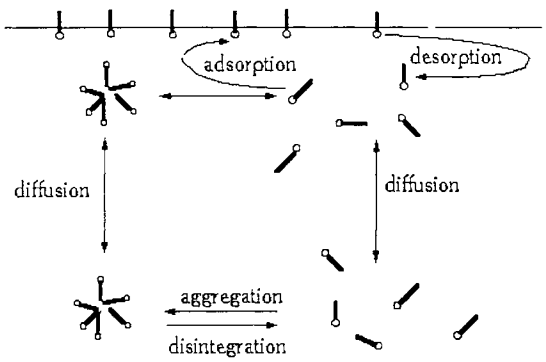

Fig. 5.8. Main processes in a micellar solution upon dilation.

It is well-known that the adsorption kinetics from non-micellar solutions can be described mathematically by a corresponding boundary problem for the diffusion equation [104, 105]. In the case of micellar solutions the diffusion equation for monomers must contain terms taking into account the influence of micelles. The single diffusion equation of monomers must be replaced by a system of two equations (for monomers and micelles). At last, it is necessary to introduce an additional boundary condition, which takes into account that micelles are not surface active. This are all alterations in the formulation of the mathematical problem. However, it will be shown below that the new problem is essentially more complex and can be solved analytically only for very particular situations and after introduction of additional simplifications.

Obviously the influence of micelles must be taken into account in the first approximation only for diffusional and mixed adsorption mechanisms. If the rate-limiting step consists in crossing the adsorption barrier by the surfactant monomers, all the relations derived for non-micellar solutions hold for $c > CMC$ too.

The main factors determining the influence of micelles on the adsorption kinetics are the rates of formation and disintegration of micelles. This leads immediately to the consequence that the treatment of the adsorption kinetics at c > CMC is impossible without preliminary investigations of the micellisation kinetics. For this reason the main results of kinetic studies of micellar systems will be presented briefly below.

5.4.2. General features of micellisation kinetics

The kinetics of formation and disintegration of micelles has been studied for about thirty years [106-130] mainly by means of special experimental methods, which have been proposed for investigation of fast chemical reaction in liquids [131]. Most of the experimental methods for micellar solutions study the relaxation of small perturbations of the aggregation equilibrium in the system. Small perturbations of the micellar concentration can be generated by either fast mixing of two solutions when one of them does not contain micelles (method of stopped flow [112]), or by a sudden shift of the equilibrium by instantaneous changes of the temperature (temperature jump method [108, 124, 129, 130]) or pressure (pressure jump method [1, 107, 116, 122, 126]). The shift of the equilibrium can be induced also by periodic compressions or expansions of a liquid element caused by ultrasound (methods of ultrasound spectrometry [109-111, 121, 125, 127]). All experimental techniques can be described by the term *relaxation spectrometry* [132] and are characterised by small deviations from equilibrium. Therefore, linearised equations can be used to describe various processes in the system.

If micelles (X_n) consist only of one kind of species (X_1 - mononers), the chemical equilibrium in the system (5.16) can be represented in the following form

$$nX_1 \Leftrightarrow X_n. \tag{5.146}$$

The reaction given by Eq. (5.146) corresponds to the following mass action law

$$K_n = c_n/c_1^n, \tag{5.147}$$

where K_n is the micellisation constant, n is the aggregation number, c_n and c_1 are the corresponding concentrations. Although it is obvious that the simple scheme (5.146) does not take into account the polydispersity of micelles, its application for modelling equilibrium properties of micellar solutions leads to reasonable results [3, 12]. At the same time the real molecular processes cannot be represented by this equation because the probability of any

elementary step in the chemical kinetics with a reaction order exceeding 2 is close to zero. However, scheme (5.146) has been used for the interpretation of kinetic studies of micellisation, probably under the influence of successive application of relation (5.147) to the description of equilibrium properties. Really, one of the first kinetic models of the micellisation process (the model of Kresheck et al. [108]) can be reduced to processes described by this equation.

The model of Kresheck et al. allows sometimes to describe the dependence of the relaxation time on surfactant concentration but cannot explain the existence of only two main relaxation processes in micellar solutions. One of the most surprising properties of rather complicated micellar systems containing aggregates of different molecular weight with different reactions of the monomer exchange is the possibility to select only two main relaxation processes. These processes were discovered by various methods in numerous experimental studies. The relaxation time of the fast process in solutions of conventional surfactants of low molecular weight usually belongs to the range of microseconds, and the slow process to the range of milliseconds. The relaxation times depend on the chemical nature of the surfactant polar head, on the electrolyte concentration and on the surfactant molecular weight. For example, for amphiphilic block copolymers with a molecular weight of about 100.000 the characteristic time of the slow process can exceed ten hours, and that of the fast process can reach ten minutes [123]. For a surfactant with a short hydrocarbon chain (heptyl ammonium chloride) the relaxation time of the fast process is less than 0.1 μs [127].

The kinetic model, which can explain the origin of these two relaxation processes and can describe the dependence of the corresponding relaxation times on the concentration, has been proposed by Aniansson and Wall [114, 115, 119]. This model allows to explain the main experimental facts and is generally accepted nowadays. At the same time, subsequent studies allowed for the determination of the application limits of this theory [116-118, 128]. Because the model of Aniansson and Wall is frequently used also for the analysis of dynamic surface properties of micellar solutions [93, 96-103, 133-138], it will be considered below in details.

Let us assume that changes of the aggregation number of different particles in the solution can take place only as result of a step by step joining or discharging of monomers. This means that instead of (5.146) the following kinetic model is considered

$$X_{j-1} + X_1 \underset{k_j^-}{\overset{k_{j-1}^+}{\Leftrightarrow}} X_j, \qquad (5.148)$$

where the subscript indicates the aggregation number, k_{j-1}^+ and k_j^- are the rate constants of the direct and the reverse reaction, respectively. Note that in their original treatment, Anniansson and Wall used k_j^+ instead k_{j-1}^+ for the constant of the direct reaction.

The second main assumption of Anniansson and Wall relates to the size distribution of aggregates. It is assumed that there is a region in the distribution curve, where the concentration of aggregates is extremely small, between the region of proper micelles described by a Gauss distribution, and the region of premicellar aggregates (dimers, trimers, etc.), where the number of particles decreases abruptly with the aggregation number (Fig. 9).

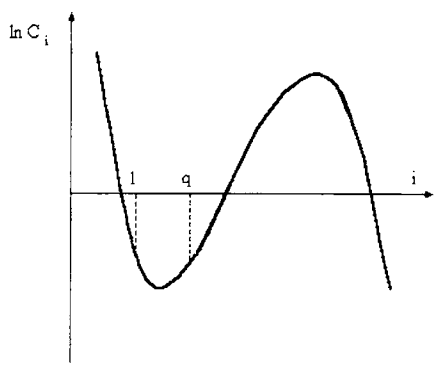

Fig. 9. Assumed size distribution of aggregates.

In this case changes in the number of aggregates in the system are really slow. Any micelle under consideration must move from the region of proper micelles through the region of the minimum of the size distribution and finally into the region of premicellar aggregates in order to be entirely dissolved. However, the reactions described by Eq. (5.148) proceed relatively slowly in the region of the distribution minimum because of the low concentration of aggregates. Therefore, the processes of formation and disintegration of micelles (motion of micelles along the distribution curve) is analogous to a diffusion through a tube of varying cross section with two wide ends connected by a narrow waist. The region of the distribution minimum plays the role of this waist.

Considerations of this kind allow us to explain the two-step nature of the micellisation process. After a quick perturbation of the aggregation equilibrium (5.148), which leads for example to an increase of the micellar concentration, the additional particles split off monomers. In this case the concentration of monomers and premicellar aggregates increases (establishment of a partial equilibrium in the region of premicellar aggregates is a fast process), and the region of the distribution corresponding to proper micelles shifts along the distribution curve in the direction of lower aggregation numbers (Fig. 10).

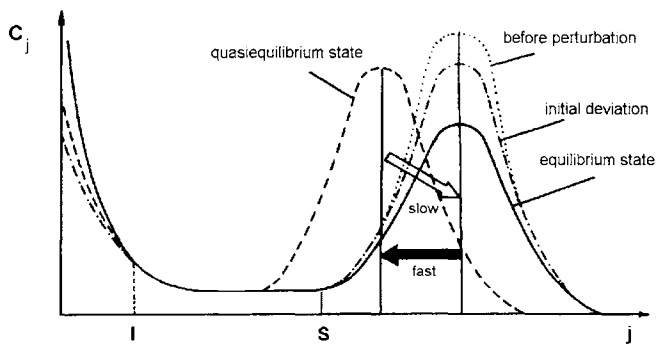

Fig. 10. Schematic of the relaxation of the size distribution of micelles.

Therefore, the fast step of the processes of formation and disintegration of micelles corresponds to the change of the mean aggregation number at a constant total number of micelles in the system. Further evolution of the system consists in a slow change of the number of micelles, and the region of micelles shifts in the opposite direction along the distribution curve at the preserved quasi-equilibrium size distributions of the aggregates in the regions of premicellar aggregates and proper micelles. These changes correspond to the slow step of the process or, in other words, to a slow diffusion in the one-dimensional space of aggregation numbers.

The following mass action law for the equilibrium concentrations c_j^0 corresponds to reactions of the type of Eq. (5.148):

$$k_{j-1}^{+} c_{j-1}^{0} c_1^{0} = k_j^{-} c_j^{0} . \qquad (5.149)$$

The corresponding kinetic equations take the following form

$$\frac{dc_j}{dt} = k_{j-1}^{+} c_1 c_{j-1} - k_j^{-} c_j + k_{j+1}^{-} c_{j+1} - k_j^{+} c_1 c_j, \; j > 1. \tag{5.150}$$

For monomers the right hand side of the kinetic equation has another form

$$\frac{dc_1}{dt} = 2k_2^{-} c_2 - k_1^{+} c_1^2 + \sum_{j>2} k_j^{-} c_j - \sum_{j>1} k_j^{+} c_1 c_j \,. \tag{5.151}$$

For small perturbations δc_j ($\delta c_j \ll c_j^0$) we can neglect the terms containing products of the type $\delta c_1 \delta c_j$ and linearise the relations (5.150) and (5.151):

$$\frac{d\delta c_j}{dt} = k_{j-1}^{+}\left(c_1^0 \delta c_{j-1} + c_{j-1}^0 c_0\right) - k_j^{-} \delta c_j + k_{j+1}^{-} \delta c_{j+1} - k_j^{+}\left(c_j^0 \delta c_1 + c_1^0 \delta c_j\right), \; j > 1 \tag{5.152}$$

$$\frac{d\delta c_1}{dt} = 2k_2^{-} \delta c_2 - 2k_1^{+} c_1^0 \delta c_1 + \sum_{j>2} k_j^{-} \delta c_j - \sum_{j>1} k_j^{+}\left(c_1^0 \delta c_j + c_j^0 \delta c_1\right). \tag{5.153}$$

We assume here that the concentration of aggregates is negligible if j exceeds a certain maximum aggregation number j_{max}.

The number of kinetic equation corresponds to the number of different aggregates in the system and is usually of the order of hundred. In the general case the same number of relaxation times corresponds to a system of ordinary linear differential equations (5.152) and (5.153). However, the assumptions made by Aniansson and Wall [114] allow us to consider the time interval corresponding to the fast and slow micellisation steps separately, and to reduce the system of Eqs. (5.152) and (5.153) to a single differential equation for each step.

5.4.3. Fast process

If the time interval under consideration is comparable with the characteristic time of the fast step of the micellisation process, aggregates in the region of the distribution minimum ($1 < j < s$) do not take part in the relaxation process. The exchange of monomers between the aggregates in the region of the minimum proceeds much slower, and it is possible to neglect the corresponding contributions to the right hand side of relations (5.150) - (5.153). Besides, the concentration of particles in the region of premicellar aggregates ($j < l$) decreases rapidly with the aggregation number, and the influence of dimers, trimers etc. is negligible. Therefore, it is sufficient to consider only monomers and proper micelles ($j > s$), and to assume that c_j takes a negligible value outside the region of micelles. Then relation (5.153) reads

$$\frac{d\delta c_1}{dt} = \sum_{j>s} k_j^- \delta c_j - \sum_{j>s} k_j^+ \left(c_1^0 \delta c_j + c_j^0 \delta c_1 \right) \tag{5.154}$$

or

$$\frac{d\delta c_1}{dt} = \sum_{j>s} \left(k_j^- - k_j^+ c_1^0 \right) \delta c_j - k^- c_m \delta c_1 \tag{5.155}$$

where the summation is only over the region of proper micelles. When writing Eq. (5.155) we took into account Eq. (5.149) and used new parameters: the total concentration of micelles c_m and the mean kinetic rate constant k^-:

$$c_m = \sum_{j>s} c_j , \tag{5.156}$$

$$k^- = \frac{\sum_{j>s} k_j^- c_j^0}{c_m} . \tag{5.157}$$

The coefficients k_j^- and $k_j^+ c_1^0$ are slow-changing functions of the aggregation number j. Aniansson and Wall assumed a linear dependence

$$k_j^+ c_1^0 - k_j^- = uj + v . \tag{5.158}$$

If one takes into account the relation

$$\delta c_1 + \sum_{j>s} j \delta c_j = 0 , \tag{5.159}$$

which follows from the conservation of mass, Eq. (5.155) takes the following form

$$\frac{d\delta c_1}{dt} = -\frac{1}{\tau_1} \delta c_1 - v \delta c_m , \tag{5.160}$$

where the new parameter

$$\frac{1}{\tau_1} = k^- c_m - u . \tag{5.161}$$

is introduced. Because δc_m is independent of time for the fast process, Eq. (5.160) represents an ordinary linear differential equation relative to δc_1. Its solution has the form

$$\delta c_1 = \left(\delta c_1^0 + v \delta c_m \tau_1 \right) e^{-t/\tau_1} - v \delta c_m \tau_1 , \tag{5.162}$$

where δc_1^0 is the initial value of the perturbation of the monomer concentration.

Thus, if all our assumptions hold, the approach to the intermediate state with essentially slow changes of the concentration (slow process) is described only by a single relaxation time. In order to determine this time it is necessary to elucidate the physical meaning of u and v.

Relation (5.158) can be represented in the form

$$k_{j+1}^{-}c_{j+1}^{0} - k_{j}^{-}c_{j}^{0} = ujc_{j}^{0} + vc_{j}^{0}. \tag{5.163}$$

If we sum up over the region of proper micelles, the left hand side disappears, and we have

$$u\bar{n}c_{m} + vc_{m} = 0, \tag{5.164}$$

where $\bar{n}$ is the mean aggregation number

$$\bar{n} = \frac{\sum_{j>s} jc_{j}}{c_{m}}. \tag{5.165}$$

Multiplication of (5.163) by j and subsequent summation yields

$$-k^{-} = u\overline{n^{2}} + v\bar{n}, \tag{5.166}$$

where

$$\overline{n^{2}} = \frac{\sum_{j>s} j^{2}c_{j}}{c_{m}}. \tag{5.167}$$

Then the expressions for u and v follow from relations (5.164) and (5.166)

$$u = -\frac{k^{-}}{\hat{\sigma}^{2}};\ v = \frac{k^{-}n}{\hat{\sigma}^{2}}, \tag{5.168}$$

where $\hat{\sigma}^{2}$ is the dispersion (second moment) of the size distribution of micelles

$$\hat{\sigma}^{2} = \overline{n^{2}} - \bar{n}^{2}. \tag{5.169}$$

Therefore we obtain the following expression for the relaxation time

$$\frac{1}{\tau_{1}} = \frac{k^{-}}{\hat{\sigma}^{2}} + \frac{k^{-}c_{m}}{c_{1}^{0}} = \frac{k^{-}}{\hat{\sigma}^{2}} + \frac{k^{-}\left(c - c_{1}^{0}\right)}{\bar{n}c_{1}^{0}}. \tag{5.170}$$

The parameters k^{-} and $\hat{\sigma}^{2}$ depend only weakly on the surfactant concentration, and as a first approximation the reverse relaxation time is a linear function of the micellar concentration and the total surfactant concentration. This conclusion is supported by experimental data. Therefore, measurements of the relaxation time at different surfactant concentrations allows us

to determine the quantities k^-/nc_1^0 and $k^-/\hat{\sigma}^2$ from the slope of the dependency of $1/\tau_1$ on $c - c_1^0$ and from the intersection point of the experimental curve with the abscissa. If the mean aggregation number is known, this method allows us to determine k^- and $\hat{\sigma}^2$. From Eq. (5.149) an estimation results for the mean kinetic constant of the reaction of monomer joining a micelle $k^+ = k^-/c_1^0$.For non-polymeric surfactants k^+ has values of the order of 10^9 l $mol^{-1}s^{-1}$ [115]. This means that the process of absorption of a monomer by a micelle is controlled by diffusion. For block copolymers, for example for poly(oxyethylene)-poly(oxypropylene)-poly(oxyethylene), the value of k^+ cannot be related to the diffusion rate of monomers. In this case the rate of the process is probably determined by the monomer transfer through the micellar corona consisting of hydrated polyoxyethylene blocks [124, 129].

5.4.4. Slow process

It has been noted above that the influence of micelles on the adsorption process is determined by their ability to be a source or sink of monomers. The capacity of this source is determined by the parameter nc_m. However, only a small part of these monomers can participate in the fast process. Therefore, at low micellar concentration, the influence of the slow process (the change of the total number of micelles in the system) on the kinetics of adsorption and desorption of surfactants will be more significant.

The analogy between the micellisation process and the diffusion through a tube with a narrow waist allows us to introduce the notion of the flow of aggregates in the space of aggregation numbers. This flow of aggregates J_j between j-1 and j can be represented in the form

$$J_j = k_{j-1}^+ c_{j-1} c_1 - k_j^- c_j . \tag{5.171}$$

This gives the following kinetic equation for the slow step of the micellisation process [119]

$$\frac{d\delta c_m}{dt} = J , \tag{5.172}$$

where J is the corresponding flow in the minimum region of the size distribution of aggregates. We can assume that in this region the flow J_j does not depend on j

$$J_j = J, \; 1 < j < s \tag{5.173}$$

The relation (5.149) holds for the current concentrations c_j in the course of the slow process in the regions of premicellar aggregates and full micelles because we assumed a quasi-equilibrium size distributions of aggregates in these regions. Then we can rewrite this relation for the concentration perturbations in the following form

$$\frac{\delta c_j}{c_j^0} - \frac{\delta c_{j-1}}{c_{j-1}^0} - \frac{\delta c_1}{c_1^0} = 0\,,\ j < l,\ j > s. \tag{5.174}$$

After summation (5.174) over the region of premicellar aggregates we find

$$\frac{\delta c_j}{c_j^0} - j\frac{\delta c_1}{c_1^0} = 0\,,\ j < l. \tag{5.175}$$

One more relation follows from (5.171) and (5.173)

$$\frac{\delta c_j}{c_j^0} - \frac{\delta c_{j-1}}{c_{j-1}^0} - \frac{\delta c_1}{c_i^0} = -\frac{J}{k_j^- c_j^0}\,,\ l < j < s. \tag{5.176}$$

Summing Eqs. (5.176) over the region of the size distribution minimum and taking into account (5.175) we find

$$\frac{\delta c_j}{c_j^0} = j\frac{\delta c_1}{c_1^0} - RJ\,,\ j = s, \tag{5.177}$$

where

$$R = \sum_{l<j<s} \frac{1}{k_j^- c_j^0} \tag{5.178}$$

is the kinetic resistance of the processes of formation and disintegration of micelles. The summation can be spread over the regions of premicellar aggregates and proper micelles because c_j^0 increases in these regions and the corresponding terms give only a negligible contribution. Application of relation (5.174) allows to extend Eq. (5.177) to the region of proper micelles.

Using the mass action law (5.156) in the following form

$$\delta c_m = \sum_{j>s} \delta c_j \tag{5.179}$$

and inserting Eq. (5.177) we find the following expression

$$\delta c_m = \left(\bar{n} \frac{\delta c_1}{c_1^0} - RJ \right) c_m . \tag{5.180}$$

Substitution of Eq. (5.177) into the mass balance (5.159) yields a relation between J and δc_1:

$$J = \frac{c_1^0 + \overline{n^2} c_m}{\bar{n} c_1^0 c_m R} \delta c_1 . \tag{5.181}$$

From Eqs. (5.180) and (5.181) we find the relation between δc_m and δc_1:

$$\delta c_m = \left(c_1^0 + \overline{\sigma^2} c_m \right) \delta c_1 / \bar{n} c_1^0 . \tag{5.178}$$

Substitution of (5.181) and (5.182) into Eq. (5.172) yields the kinetic equation for δc_1

$$\frac{d\delta c_1}{dt} = -\frac{1}{\tau_2} \delta c_1 , \tag{5.183}$$

where

$$\frac{1}{\tau_2} = \frac{1}{R c_m} \frac{c_1^0 + \overline{n^2} c_m}{c_1^0 + \hat{\sigma}^2 c_m} . \tag{5.184}$$

The first term in the numerator can be neglected for the whole concentration range with the exception of a narrow region close to the CMC. When we now consider that R depends only weakly on the concentration, Eq. (5.184) predicts a monotonous increase of τ_2 with the surfactant concentration. However, even for nonionic surfactants this prediction is not corroborated at high concentrations, thus indicating the limitations of the Aniansson and Wall model [117, 118, 130, 139].

Though this model was proposed first for nonionic surfactants, it has been applied frequently to dissociating surfactants. This can be justified if the counterions are mobile to a sufficient extent in order to arrange themselves almost instantaneously to the distribution of surface active ions or if they are in excess. There are attempts for a construction of a more general theory taking into account the surfactant dissociation. One approach is based on the consideration that counterions are a separate component and on the application of the kinetic theory of two-component micelles [119, 120]. The obtained relations for the relaxation times are essentially more cumbersome and contain a number of coefficients with uncertain concentration

dependencies. This makes a comparison with experimental data difficult. Therefore, it seems reasonable to apply the theory outlined above to ionic surfactants too, at least as approximation.

Two main relaxation times have been observed for solutions of ionic surfactants too, and the concentration dependency of the relaxation time τ_2 is in a qualitative agreement with the predictions of the Aniansson and Wall theory in the range of low and moderate micellar concentrations. It is noteworthy that the ultrasound studies of solutions of some surfactants discovered a third and fastest relaxation process with a characteristic time of the order of 1 ns [121, 127], which was connected to the exchange of monomers between premicellar aggregates and the surrounding solution [127]. For surfactants with a short hydrocarbon chain (heptyl ammonium chloride) a broad distribution of relaxation times was discovered instead of a single time τ_1, which is usually obtained in the concentration range close to the CMC [127]. This distribution was related to a change of the shape of the size distribution of micelles. When the surfactant hydrocarbon chain length decreases, the depth of the local minimum of the distribution curve (Fig. 9) decreases as well. However, in general the experimental results for ionic surfactants are in reasonable agreement with the predictions of the theory of Aniansson and Wall for low and moderate micellar concentrations.

5.4.5. Model of Kahlweit

Most of the kinetic studies of micellar systems relate to relatively low surfactant concentrations ($c \leq 10$ CMC). An extension of the concentration range to the region of higher concentrations lead to unexpected results [116-118]. After a sharp maximum the relaxation time τ_2 for solutions of ionic surfactants decrease by some orders of magnitude (Fig. 11).

In order to explain this effect it was assumed that micelles can be formed by fusion of two smaller aggregates and can disappear by fission into two small particles [116]. The aggregates formed by ionic surfactants are charged particles. At low concentrations they are stable in relation to coagulation because of repulsive electrostatic forces. When the concentration of counterions increases, the electric double layer around the aggregates shrinks, the repulsive electrostatic forces between the aggregates decrease, and the reversible fusion and fission processes can proceed

$$X_q + X_r \underset{k_{qr}^-}{\overset{k_{qr}^+}{\Leftrightarrow}} X_j,\ q + r = j, \tag{5.185}$$

where k_{qr}^+ and k_{qr}^- are the rates constants of the direct and reverse reactions respectively.

These processes are effective if q and r are outside the minimum region of the size distribution of aggregates. This means that q and r belong to the range of premicellar aggregates and j to the range of full micelles (Fig. 12). The linearised kinetic equation has the following form

$$\frac{d\delta c_j}{dt} = \sum_{q,r}\left(k_{q,r}^+ c_r^0 \delta c_q + k_{qr}^+ c_q^0 \delta c_r - k_{qr}^- \delta c_j\right),\ q, r < l, j > s,\ q + r = j. \tag{5.186}$$

Because the characteristic times of the slow and fast relaxation processes differ by orders of magnitude, the quasi-equilibrium distribution preserves outside the minimum region of the size distribution curve, and relations (5.175), (5.177) and (5.181) hold as before.

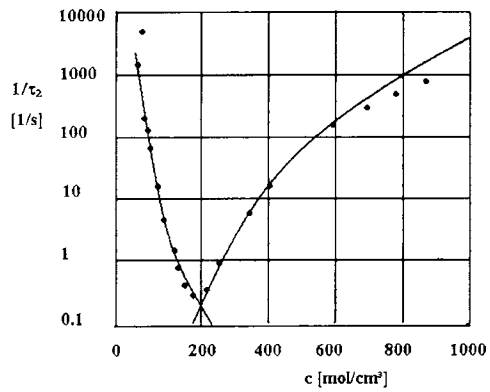

Fig. 11. Dependence of τ_2 on SDS concentration [118].

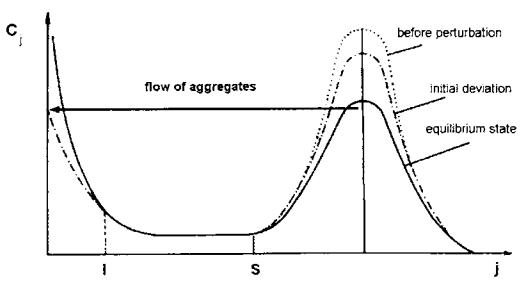

Fig. 12. Scheme of relaxation of the size distribution of micelles in the model of Kahlweit et al. [117, 118].

Substitution of (5.175) for δc_q and δc_r and (5.177), (5.181) for δc_j into relation (5.186) yields

$$\frac{d\delta c_j}{dt} = \left(\frac{c_j^0}{c_m} + \frac{\overline{n^2} c_j^0}{c_1^0} \right) \frac{f_j \delta c_1}{\overline{n} c_1^0}, \tag{5.187}$$

where

$$f_j = \sum_{q,r} k_{qr}^- . \tag{5.188}$$

Summing (5.187) up over the micellar region and using the definition

$$f = \sum_{j>s} f_j c_j^0 / c_m \tag{5.189}$$

we obtain

$$\frac{d\delta c_m}{dt} = \left(c_1^0 + \overline{n^2} c_m \right) \frac{f}{\overline{n} c_1^0} \delta c_1 . \tag{5.190}$$

Substitution of Eq. (5.182) for δc_m gives a linear differential equation for δc_1

$$\frac{d\delta c_1}{dt} = -\frac{c_1}{\tau_2}, \tag{5.191}$$

where

$$\frac{1}{\tau_2} = f \frac{c_1^0 + \overline{n^2} c_m}{c_1^0 + \hat{\sigma}^2 c_m} . \tag{5.192}$$

The concentration dependence of τ_2 is determined by the corresponding dependence of f, which increases with concentration. This result is in agreement with experimental data. The processes of formation and disintegration of micelles described by Eq. (5.148) at low and moderate concentrations and τ_2 increases with concentration. The maximum of the concentration dependence of τ_2 corresponds to a superposition of two mechanisms, given by Eqs. (5.148) and (5.185). After that, τ_2 begins to decrease rapidly in accordance with Eq. (5.192). The same dependence is also observed for anionic and cationic surfactants [117]. Recently decrease of τ_2 with concentration has been obtained also for solutions of nonionic block copolymers. This effect, according to the authors, confirms the mechanism (5.185) [129, 130]. For micelles of diblock copolymers the kinetic constants k_{qr}^+ and k_{qr}^- of fusion and fission have been recently estimated using the scaling approach [173].

The appearance of the local minimum in the concentration dependency of the relaxation time of the slow process for concentrated solutions can be connected also with formation of non-spherical micelles [140]. Actually, it is well-known that micelles change their shape with increasing concentration. The increase of the concentration of some counterions can lead to the formation of giant wormlike micelles (living polymers) [141]. In this case the equilibrium size distribution of micelles changes entirely and is described by an exponential law [141]

$$c_m(L) \sim \exp(-L/\tilde{L}); \tilde{L} \sim \eta_M^{1/2} \exp(E/2k_BT) \tag{5.193}$$

where $c_m(L)$ is the concentration of micelles of length L, $\tilde{L}$ is the mean length, η_M is the volume fraction of wormlike micelles, E is the scission energy of a polymer chain equal to the formation energy of two hemispherical ends, T is the temperature, k_B is the Boltzmann constant.

It is obvious that the kinetic theory of micellisation outlined above, cannot be applied to living polymers. For wormlike micelles one has to distinguish between several processes leading to disintegration and formation of micelles and to determine the corresponding characteristic times [141 - 145]:

1. reactions of scission or sewing together of polymeric chains

$$\tau_{break1} = (\tilde{L}k_s)^{-1}; \tag{5.194}$$

2. reactions of end interchange, when the end of one of the chains begins to interact with the middle part of another micelle, while the second micelle splits up into two parts, one of them united with the first chain

$$\tau_{break2} = \left(c_m \tilde{L} k_e\right)^{-1}; \tag{5.195}$$

3. reactions of bond interchange proceeding at the crossing of two chains, and two new polymers appear, each of them containing monomers of the two initial micelles

$$\tau_{break3} = \left(\eta_M \tilde{L} k_b\right)^{-1}; \tag{5.196}$$

4. reactions of evaporation or condensation of the ends, where monomers between the micelles and the surrounding solution exchange at the ends of the wormlike aggregates

$$\tau_{break4} = 4\tilde{L}^2 / \tilde{k}_l; \tag{5.197}$$

5. reactions of monomer interchange between the cylindrical surface of micelles and the surrounding solution, where the characteristic time is proportional to $\widetilde{L}$.

We assume here that the kinetic constants $k_s, k_e, k_b, \widetilde{k}_l$ are independent of the length of micelles and surfactant concentration. Therefore, the relaxation of concentration perturbation in solutions of wormlike micelles can be essentially more complicated. Moreover, the relaxation processes enumerated above can influence at a different extent various properties of the non-equilibrium micellar solution. This gives a general possibility to determine all these relaxation times. The first of these relaxation processes can be described by model (5.185). The fifth one corresponds obviously to the fast relaxation process in the Aniansson and Wall model. Recently Waton derived an equation for the relaxation times of fusion and fission in micellar solutions, which can be applied to an arbitrary size distribution of micelles [128]. In the limiting cases of short micelles with a narrow size distribution and wormlike micelles this theory leads to relations (5.192) and (5.194), respectively.

Concluding the discussion of micellisation kinetics it is necessary to note that a new theory based on the ideas of nucleation kinetics have been proposed recently by Kuni et al. [174, 175]. The nucleation theory allows to study in detail the size distribution of aggregates on the basis of a thermodynamic analysis and to obtain more general kinetic equations.

5.5. Diffusion in micellar solutions

The results of the preceding section allow us now to move on to describe the surfactant transport from the depth of the bulk phase to the interface or in the opposite direction. If any adsorption barriers are absent, this process determines the adsorption and desorption rates. The main step in the solution of this problem consists in the formulation of the surfactant diffusion equations for micellar solutions. The problem of surfactant diffusion to the interface was considered and solved for the first time by Lucassen for small perturbations [94]. He used the simplified model (5.146) where micelles were assumed to be monodisperse and the micellisation process was regarded as consisting of one step. Later Miller solved numerically the problem of adsorption on a fresh liquid surface using the same assumptions [146]. Joos and van Hunsel applied also the same model to the interpretation of dynamic surface tension of

micellar solutions [84]. Rillaerts and Joos tried to take into account the influence of micelles on the diffusion of monomers and used the new diffusion equation with an additional term proportional to the deviation of the monomer concentration from equilibrium [83]. It has been shown later that this approach is equivalent to the simultaneous use of the reaction model of pseudo-first order (PFOR), which is widely used in chemical kinetics, and of the assumption of equal diffusion rates of micelles and monomers [137]. In this model the rate constant is a complicated function of the rate constants of the real reactions in the system, and it can be determined only in the framework of a model of higher level.

The first attempt to take into account the two-step kinetic theory of micellisation was made by Fainerman [147]. With that end in view two pairs of diffusion equations (for micelles and monomers) were written down for two situations corresponding to the fast and slow processes. Approximate solutions of the boundary problems for these equations were used subsequently in the course of analysis of experimental data on the adsorption kinetics from micellar solutions [77, 85, 87, 88]. However, as it has been shown by Dushkin et al. [137], this approach is equivalent to the PFOR model for the slow process and probably cannot be applied to the description of the adsorption kinetics for the fast process.

A more rigorous approach to the description of the colloid surfactant diffusion to the interface was proposed by Noskov [133]. The reduced diffusion equations for micelles and monomers, which take into account the multistep nature of micellisation and the polydispersity of micelles, were derived for time intervals corresponding to the fast and slow processes using the method applied initially by Aniansson and Wall to uniform systems. Analogous equations have been derived later by Johner and Joanny [135] and also by Dushkin et al. [137]. Recently Dushkin has studied also the adsorption kinetics in the framework of a simplified model of quasi-monodisperse micelles. In this case the assumption of the existence of two kinds of micelles permits to study the main features of the surface tension relaxation in real micellar solution [138]. The main steps of the derivation of surfactant diffusion equations in micellar solutions are presented below [133, 134].

Let us restrict ourselves, as before, to small deviations from equilibrium δc_j ($\delta c_j \ll c_j^0$). Then the following diffusion equations can be written neglecting the cross diffusion fluxes:

$$\frac{\partial \delta c_j}{\partial t} = D_j \Delta \delta c_j + k_{j-1}^{+}\left(c_1^0 \delta c_{j-1} + c_{j-1}^0 \delta c_1\right) - k_j^{-} \delta c_j + k_{j+1}^{-} \delta c_{j+1} - k_{j+1}^{+}\left(c_j^0 \delta c_1 + c_1^0 \delta c_j\right); \quad j = 2,\ldots, j_{max}. \quad (5.198)$$

The D_j is the diffusion coefficient of the j^{th} aggregate, which are independent of concentration. These equations differ from the kinetic equations (5.152) only by the additional terms $D_j \Delta c_j$, which take into account the transfer of aggregates in the solution. However, the presence of the Laplace operator Δ indicates another essential difference: all variables c_j are functions not only of time but of the space coordinates too.

The equation of monomer diffusion originates from (5.153) in a similar way

$$\frac{\partial \delta c_1}{\partial t} = D_1 \delta c_1 - 2k_1^{+} \delta c_1 + 2k_2^{-} \delta c_2 + \sum_{j>2} k_j^{-} \delta c_j - \sum_{j>1} k_j^{+}\left(c_1^0 \delta c_j + c_j^0 \delta c_1\right). \quad (5.199)$$

In the general case, if the concentration perturbations are accompanied by a mechanical disturbance of the system, one has to add convection terms to the right hand side of Eqs. (5.198) and (5.199), which are proportional to the product of the liquid velocity and the concentration gradient of the corresponding aggregates. Thus these terms are of higher order for small perturbations and can be neglected for the system under consideration.

It is possible, for example, to use the method of Fourier transformations to solve the boundary problems for the system of differential equations (5.198), (5.199). In this case we have j_{max} linear differential equations of the second order. Because j_{max} is usually of the order of hundred, a further analytical investigation of Eqs. (5.198), (5.199) is senseless. However, the problem can be essentially simplified if the surfactant diffusion is treated separately for time scales comparable with the relaxation times of the fast and slow steps of micellisation, respectively.

5.5.1. Fast process

Let us at first assume that the characteristic diffusion time τ_D, which is proportional to the square of the diffusion length δ_D and inverse proportional to D ($\tau_D \sim \delta_D^2/D$), is comparable with the relaxation time of the slow micellisation step. If the diffusion proceeds in the direction of the interface, τ_D can be given in the following form [148]

$$\tau_D = \frac{1}{D_1}\left(\frac{\partial \Gamma}{\partial c_1}\right)^2. \quad (5.200)$$

Then one has to take into account on the right hand side of Eq. (5.199) only the contributions of monomers and proper micelles and obtains an analogue of Eq. (5.155) for the non-uniform system under consideration. The latter equation has to be rewritten using new variables $\tilde{c}_j$, which are the local equilibrium concentrations of the aggregates. These variables differ from the global equilibrium concentrations c_j^0 only for non-uniform systems. We have only one real equilibrium state when $c_j = c_j^0$ for any j and both non-uniform and uniform systems. However, in the former case we can consider also a local equilibrium and thus can imagine that a small element of the non-uniform system with concentrations c_j in the initial stage is isolated from the ambient medium and equilibrated. In general the final state of this imaginary process of equilibration with concentrations $\tilde{c}_j$ differs from the global equilibrium and $\tilde{c}_j \neq c_j^0$. The concentrations $\tilde{c}_j$ are entirely determined by the local concentrations c_j, which depend on time and space coordinates for a non-equilibrium non-uniform system. Therefore, the local equilibrium concentrations will be functions of time and space coordinates too. At the same time they will meet all equilibrium equations, for example relation (5.149). This condition allows us to rewrite relation (5.199) in the following form

$$\frac{\partial \delta c_1}{\partial t} = D_1 \Delta \delta c_1 - \sum_{j>s} k_j^+ c_j^0 \delta \tilde{c}_1 + \sum_{j>s} \left(k_j^- - k_j^+ c_1^0\right) \delta \tilde{c}_j , \qquad (5.201)$$

where $\delta \tilde{c}_j \equiv c_j - \tilde{c}_j$. Multiplying Eq. (5.198) by j, summing up from j = s to j = n^0 and neglecting the small terms corresponding to the transition of micelles to the region of the minimum in the size distribution of aggregates we find the second differential equation

$$\frac{\partial n c_m}{\partial t} = D_m \Delta \bar{n} c_m + \sum_{j>s} k_j^+ \left(c_j^0 \delta \tilde{c}_1 + c_1^0 \delta \tilde{c}_j\right) - \sum_{j>s} k_j^- \delta \tilde{c}_j , \qquad (5.202)$$

where D_m is the mean diffusion coefficient of micelles. Note that the mean aggregation number n and the total number of micelles in Eq. (5.202) now depend on space coordinates and time. In the subsequent transformations we will use the following relation

$$\delta \tilde{c}_1 = -\sum_{j>s} j \delta \tilde{c}_j , \qquad (5.203)$$

which follows from the approximate local equation of the surfactant mass balance

$$c_1 + \sum_{j>s} jc_j = \tilde{c}_1 + \sum_{j=s} j\tilde{c}_j . \tag{5.204}$$

If we introduce the mean rate constant k^- and use the assumption (5.158), Eqs. (5.201) and (5.202) can be presented in a simple form

$$\frac{\partial \delta c_1}{\partial t} = D_1 \Delta \delta c_1 - \left(\frac{k^- c_m^0}{c_1^0} - u \right) \delta \tilde{c}_1 - v \delta \tilde{c}_m , \tag{5.205}$$

$$\frac{\partial n c_m}{\partial t} = D_m \Delta n c_m - \left(\frac{k^- c_m^0}{c_1^0} - u \right) \delta \tilde{c}_1 - v \delta \tilde{c}_m . \tag{5.206}$$

The subsequent transformations are connected with the transition from variables nc_m and $\tilde{c}_1$ to c_1 and $\tilde{c}_m$. Now we will use the mass action law (5.147) for equilibrium concentrations

$$\left(c_1^0\right)^{n_0} = K_n c_m^0 ; \quad \left(\tilde{c}_1\right)^{n_0} = K_n \tilde{c}_m , \tag{5.207}$$

where n^0 is the equilibrium aggregation number, which is independent of concentration. Then using relation (5.203) we obtain

$$\delta \tilde{c}_1 = \delta c_1 + \frac{c_1^0}{n^0 c_m^0} \delta \tilde{c}_m - \frac{c_1^0}{n^0 c_m^0} \delta c_m , \tag{5.208}$$

$$\delta(nc_m) = -\delta c_1 - \left(n^0 + \frac{c_1^0}{n^0 c_m^0} \right) \delta \tilde{c}_m + \left(n^0 + \frac{c_1^0}{n^0 c_m} \right) \delta c_m . \tag{5.209}$$

Substitution of Eqs. (5.208) and (5.209) and expressions for u and v into Eqs. (5.205) and (5.206) and summing (5.198) up from j = s to j = j_{max} under the condition of a constant total number of micelles in the system we finally obtain a system of differential equations in partial derivatives, which describes the surfactant diffusion for $t \ll \tau_2$ [134]

$$\frac{\partial \delta c_1}{\partial t} = D_1 \Delta \delta c_1 - \frac{\delta c_1}{\tau_1} - \frac{\left[\left(c_1^0\right)^2 + \overline{n^2} c_1^0 c_m^0 \right] \delta \tilde{c}_m}{n^0 c_m^0 \left[c_1^0 + c_m^0 \hat{\sigma}^2 \right] \tau_1} + \frac{c_1^0 \delta c_m}{c_m^o n^0 \tau_1} , \tag{5.210}$$

$$\frac{\partial \delta c_m}{\partial t} = D_m \Delta \delta c_m , \tag{5.211}$$

$$\frac{\partial \delta \tilde{c}_m}{\partial t} = \left(D_m - D_1 \right) \left(n^0 + \frac{c_1^0}{n^0 c_m^0} \right)^{-1} \Delta \delta c_1 + D_m \Delta \delta \tilde{c}_m . \tag{5.212}$$

If the concentration distribution in the system is uniform, the kinetic equation for the first relaxation process (5.160) follows from equation (5.210).

The Eqs. (5.210) and (5.211) describe the diffusion of monomers and micelles as before. The physical meaning of Eq. (5.212) is not so obvious. It can be regarded as the equation of the local balance of surfactants in micelles. If the initial distribution of micelles is homogeneous and only the monomer concentration is perturbed, the first relaxation process can lead to the dependence of the aggregation numbers on space coordinates and time even in absence of a concentration gradient of the total number of micelles. Surfactants can be transferred not only as a result of the monomer diffusion but due to the diffusion of aggregates of different aggregation numbers. This effect is described by equation (5.212).

If the initial micellar concentration in the system c_m is uniform, it follows from Eq. (5.211) that the homogeneous distribution of this variable will persist during the whole process. At the same time particles with different aggregation numbers can diffuse leading to changes of $\widetilde{c}_m$ in time and space. This is realised in particular during compression and expansion of the surface.

5.5.2. Slow process

If the surfactant concentration is not too high, the second step of micellisation is the quasi-equilibrium process of the change of the total number of micelles. The characteristic time of the transition to this quasi-equilibrium state is of the order of τ_1. The possibility of investigation of the diffusion process in the framework of these ideas is connected with the more rigid requirement of a local quasi-equilibrium. This means that all concentration changes in the system have to be negligible during the time τ_1. It follows from Eq. (5.210) that this condition must hold if any noticeable alterations of the total surfactant concentration proceed for a time interval essentially exceeding τ_1. Because $\tau_2 \gg \tau_1$, the latter condition is not too rigid and it is possible to study the influence of the second step of micellisation on diffusion in terms of the concept of a quasi-equilibrium process leading to a real equilibrium of the total number of micelles in the system.

Let us assume that the condition for the aggregation equilibrium (5.149) holds for the local concentrations c_j of aggregates, which belong to the regions of premicellar aggregates and full micelles ($j < l$, $s < j$) in an arbitrary point of the system. Then Eq. (5.174) holds also locally for the perturbations $\delta \widetilde{c}_j$:

$$\frac{\delta\tilde{c}_j}{c_j^0} - \frac{\delta\tilde{c}_{j-1}}{c_j^0} - \frac{\delta\tilde{c}_1}{c_1^0} \approx 0, \quad j < l; \quad j > s. \tag{5.213}$$

Then we obtain as before the diffusion equation of micelles by the summation of Eq. (5.198) from $j = s$ to $j = j_{max}$

$$\frac{\partial \delta c_m}{\partial t} = D_m \Delta \delta c_m - J_m, \tag{5.214}$$

where J_m is the quasi-stationary flow of aggregates which pass from the micellar region ($j > s$) to the region of the minimum of the size distribution of aggregates ($1 < j < s$). The corresponding equation for monomers takes the form

$$\frac{\partial \delta c_1}{\partial t} = D_1 \Delta \delta c_1 + J_1, \tag{5.215}$$

where J_1 is the quasi-stationary flow of monomers. The fluxes J_1 and J_m can be determined by the method given in the preceding section.

The terminus quasi-stationary flow means that the flow of particles J_j changing their aggregation number from j to j-1 does not depend on j in the minimum region ($J_j = J = -J_m$ at $1 < j < s$). Then in analogy to Eq. (5.176) we get for the region of the minimum

$$\frac{\delta\tilde{c}_j}{c_j^0} - \frac{\delta\tilde{c}_{j-1}}{c_{j-1}^0} = \frac{\delta\tilde{c}_1}{c_1^0} - \frac{J}{k_j^- c_j^0}. \tag{5.216}$$

Summation of relation (5.213) for $j < l$ yields

$$\delta\tilde{c}_j / c_j^0 = j\delta\tilde{c}_1 / c_1^0. \tag{5.217}$$

Summation of relation (5.216) for $j > s$, use of Eq. (5.212) and the condition of equilibrium (5.149) allow us to express the concentration of aggregates of aggregation number j in the micellar region as function of the monomer concentration:

$$\frac{\partial\tilde{c}_j}{c_j^0} = j\frac{\delta\tilde{c}_1}{c_1^0} - RJ. \tag{5.218}$$

Substitution of Eq. (5.218) into the local surfactant mass balance (5.204) yields an expression for J, which coincides with Eq. (5.181) and is justified for any small volume of the system

$$J = \frac{c_1^0 + \overline{n^2 c_m}}{n^0 c_1^0 c_m R}\delta\tilde{c}_1. \tag{5.219}$$

Using the same procedure it is possible to obtain an expression for J_1

$$J_1 = \frac{c_1^0 + \overline{n^2} c_m}{\left(c_1^0 + \hat{\sigma}^2 c_m\right) c_m R} \delta\tilde{c}_1 . \tag{5.220}$$

In order to express the deviation of the monomer concentration from the local equilibrium $\delta\tilde{c}_1$ as a function of the perturbations relative to the initial concentrations $\delta c_1, \delta c_m$ we use Eq. (5.209) and the following relationship

$$\delta\tilde{c}_m = -\frac{c_1^0 + \hat{\sigma}^2 c_m}{c_1^0 n^0} \delta\tilde{c}_1 , \tag{5.221}$$

which follows from Eqs. (5.218) and (5.219) and the definition of the total number of micelles. Then we get

$$\delta\tilde{c}_1 = \frac{\left(n^0\right)^2 c_m}{c_1^0 + \overline{n^2} c_m} \delta c_1 - \frac{c_1^0 n^0}{c_1^0 + \overline{n^2} c_m} \delta c_m . \tag{5.222}$$

Substituting relations (5.219), (5.220), and (5.222) into Eqs. (5.214) and (5.215) we obtain the following system of equations, which describes the diffusion of monomers and micelles [133, 134]:

$$\frac{\partial \delta c_1}{\partial t} = D_1 \Delta \delta c_1 - \frac{\left(n^0\right)^2 \delta c_1}{R\left(c_1^0 + \hat{\sigma}^2 c_m\right)} + \frac{c_1^0 n^0 \delta c_m}{R c_m \left(c_1^0 + \hat{\sigma}^2 c_m\right)}, \tag{5.223}$$

$$\frac{\partial \delta c_m}{\partial t} = D_m \Delta \delta c_m - \frac{\delta c_m}{c_m R} + \frac{n^0 \delta c_1}{c_1^0 R} . \tag{5.224}$$

Eq. (5.223) coincides with the monomer diffusion equation proposed by Evans et al. [149] if the rate constant R_b in [149] is replaced by $c_1^0\left[R c_m \left(c_1^0 + \hat{\sigma}^2 c_m\right)\right]^{-1}$. However, the obtained result is not restricted to the interpretation of the coefficients only, which have been used before. Eq. (5.224) does not coincide with the corresponding diffusion equation in [149] even if we replace R_b by this expression. Unlike the equations derived in the preceding works, the system (5.223) and (5.224) takes into account the polydispersity of micelles and the two-step nature of the micellisation. Actually, the release or incorporation of monomers in the second step of disintegration or formation of micelles is determined not only by their transition from the micellar to the premicellar region and their subsequent disintegration (as characterised by the parameter J) but also by the alteration of the size distribution of micelles. The latter change

leads also to the release or incorporation of monomers. Therefore, the assumption $n^0|J_m| = |J_1|$, which is equivalent to the approach given in [149], is too inaccurate.

In conclusion of this section let us consider the surfactant diffusion in a concentrated solution, where the micellisation kinetics is described by the model of Kahlweit et al. (5.185). If we neglect all other routes of the micellisation process, the following diffusion equation corresponds to the mechanism (5.185):

$$\frac{\partial \delta c_j}{\partial t} = D_j \Delta \delta c_j + \sum_{p,r} \left(k_{pr}^{+} c_r^0 \delta \tilde{c}_p + k_{pr}^{+} c_p^0 \delta \tilde{c}_r - k_{pr}^{-} \delta \tilde{c}_j \right). \tag{5.225}$$

When we consider again the time interval essentially exceeding τ_1, the condition of the quasi-stationary flow of monomers in the minimum region of the size distribution of aggregates is justified and the relations (5.216) to (5.220) hold. Then, substituting expressions (5.217) for $\delta \tilde{c}_r$, $\delta \tilde{c}_p$, and (5.218) for $\delta \tilde{c}_j$ into equation (5.225), summing up from j = s to j = j_{max} and using relations (5.221), (5.222) we get

$$\frac{\partial \delta c_m}{\partial t} = D_m \Delta \delta c_m - f \delta c_m + \frac{n^0 c_m}{c_1^0} f \delta c_1 , \tag{5.226}$$

where f is determined by Eq. (5.189). Using the relationship

$$J_1 = -f \frac{c_1^0 + \overline{n^2} c_m}{c_1^0 + \hat{\sigma}^2 c_m} \delta \tilde{c}_1 , \tag{5.227}$$

which follows from the condition of a quasi-stationary flow, the monomer diffusion equation (5.215) is reduced to the following form

$$\frac{\partial \delta c_1}{\partial t} = D_1 \Delta \delta c_1 - f \frac{(n^0)^2 c_m}{c_1^0 + \hat{\sigma}^2 c_m} \delta c_1 + f \frac{c_1^0 n^0}{c_1^0 + \hat{\sigma}^2 c_m} \delta c_m . \tag{5.228}$$

5.6. Dynamic surface tension of micellar solutions

The diffusion equations of micelles and monomers obtained in the preceding sections allow us to formulate a mathematical problem of surfactant diffusion to the interface. Investigation of the adsorption kinetics is reduced then to the solution of this problem. It is noteworthy that the diffusion equations (5.210) - (5.211), (5.223), (5.224), (5.226), (5.228) and the results given in the preceding sections on the relaxation kinetics of the concentration perturbations in the

initially homogeneous micellar system were derived only for small deviations from equilibrium. This restriction relates not only to the theory delineated in this work but also to the PFOR model, where the release and incorporation of monomers is described by a term proportional to the deviation of the monomer concentration from equilibrium [83, 85, 87 - 90, 93]. Moreover, to the best of our knowledge, all surfactant diffusion equations, which have been derived by now for micellar solutions, cannot be applied at finite deviations from equilibrium. At the same time, most of the experimental results on adsorption kinetics from micellar solutions were obtained by methods based on measurements of the dynamic surface tension [77 - 93]. In the latter case creation of a fresh interface leads to significant deviations from equilibrium, and consequently to non-linear processes in the system. These processes cannot be entirely accounted for in a mathematical description of the system. Hence comparison of calculations based on the linearised diffusion equations with experimental data cannot lead to perfectly correct physical conclusions.

Another difficulty arising from this comparison is connected with the mathematical complexity of the corresponding boundary problems even if only linear diffusion equations are used. The mathematical description of the adsorption kinetics from micellar solutions is essentially more complicated in comparison with the case of the adsorption process from sub-micellar solutions. Analytical solutions of the corresponding boundary problems using rather poor approximations have been obtained only for a small number of situations. A sufficiently general solution cannot be obtained analytically and the deficiency of the rather well elaborated numerical methods often compel experimentalists to apply approximate solutions. Therefore, it seems important to consider the main equations proposed for the description of kinetic dependencies of the surface tension and adsorption, and to elucidate the limits of their application before the discussion of experimental results.

Studies of the adsorption kinetics for a surface age comparable with the characteristic time τ_2 seem to be most interesting. For many surfactants the fast process is usually beyond the time interval accessible to dynamic surface tension methods. Besides, the fast process leads to a release or incorporation of only a small part of monomers in comparison to the slow process, and one can expect a noticeable influence on the adsorption only at high concentrations. If we assume that the micellar concentration is not too high and the size distribution of micelles is

sufficiently narrow ($c_1^0 \gg \hat{\sigma}^2 c_m$), the two pairs of diffusion equations (5.223) and (5.224), or (5.226) and (5.228) can be reduced to the same form

$$\frac{\partial \delta c_1}{\partial t} = D_1 \Delta \delta c_1 - k_1 \delta c_1 + n^0 k_2 \delta c_m , \tag{5.229}$$

$$\frac{\partial \delta c_m}{\partial t} = D_m \Delta \delta c_m - k_2 \delta c_m + \frac{k_1}{n^0} \delta c_1 , \tag{5.230}$$

where the interrelation of the coefficients k_1 and k_2 with the kinetic constants R and f can be easily found by comparison of these equations with relations (5.223) and (5.224) or (5.226) and (5.228), respectively.

According to the Stokes - Einstein equation, the diffusion coefficient of an aggregate is inverse proportional to its radius. Consequently, we have [78, 150]

$$\frac{D_m}{D_1} \equiv \tilde{\gamma}^2 \cong \left(n^0\right)^{-1/3} . \tag{5.231}$$

Multiplying relation (5.230) by n^0, adding it to relation (5.229) and taking into account equation (5.231) we obtain

$$\frac{\partial \left(c_1 + n^0 c_m\right)}{\partial t} = D_1 \Delta \left(c_1 + n^0 \tilde{\gamma}^2 c_m\right). \tag{5.232}$$

If the relationship between c_1 and c_m is known, the set of Eqs. (5.229), (5.230) can be reduced to a single diffusion equation. Joos and Van Hunsel assumed that the diffusion proceeds essentially slower than the second (slow) step of micellisation so that there is equilibrium between micelles and monomers at any moment [84]

$$k_1 c_1 = k_2 n^0 c_m . \tag{5.233}$$

Using the total surfactant concentration $c_T = c_1 + n^0 c_m$, the diffusion equation for c_T reads

$$\frac{\partial c_T}{\partial t} = \frac{D_1 \left(1 + \tilde{\beta} \tilde{\gamma}^2\right)}{1 + \tilde{\beta}} \Delta c_T , \tag{5.234}$$

where

$$\tilde{\beta} \equiv n^0 c_m / c_1^0 . \tag{5.235}$$

If we consider adsorption to a plane surface, we can deal only with a one-dimensional diffusion and the Laplace operator in Eq. (5.234) can be replaced by the second derivative $\partial^2/\partial z^2$, where

z is the distance from the surface. The boundary conditions for the monomer concentration are the same as for non-micellar solutions

$$c_1 \to c_1^0 \quad \text{at } z \to \infty, \tag{5.236}$$

$$\frac{\partial \Gamma}{\partial t} = D_1 \left(\frac{\partial c_1}{\partial z} \right)_{z=0}. \tag{5.237}$$

The perturbations of the micellar concentration also fade away at a distance from the surface

$$c_m \to c_m^0 \quad \text{at } z \to \infty. \tag{5.238}$$

Another boundary condition follows from the assumption that micelles are not surface active:

$$\left(\frac{\partial c_m}{\partial z} \right)_{z=0} = 0. \tag{5.239}$$

Relations (5.236) and (5.238) mean that the perturbations of the total surfactant concentration also tend to zero far away from the surface

$$c_T \to c_T^0 \quad \text{at } z \to \infty. \tag{5.240}$$

Combination of Eqs. (5.237) and (5.239) together with (5.231) and (5.235) leads to the following boundary condition for c_T

$$\frac{\partial \Gamma}{\partial t} = \frac{D_1 \left(1 + \tilde{\gamma}^2 \tilde{\beta}\right)}{1 + \tilde{\beta}} \left(\frac{\partial c_T}{\partial z} \right)_{z=0}. \tag{5.241}$$

Therefore, the boundary problem (5.234), (5.240), (5.241) is formally reduced to the classical problem of adsorption of non-aggregated surfactant to a plane surface, which has been solved about half a century ago by Ward and Tordai [151]. If the standard initial condition of zero adsorption $\Gamma = 0$ at $t = 0$ is used, this problem has the solution

$$\Gamma = 2 \left[\frac{D_1 \left(1 + \tilde{\gamma}^2 \tilde{\beta}\right)}{\pi \left(1 + \tilde{\beta}\right)} \right]^{1/2} \int_0^{\sqrt{t}} \left[c_T^0 - c_T^s (t - \lambda) \right] d\sqrt{\lambda}, \tag{5.242}$$

where $c^s{}_T$ is the subsurface surfactant concentration.

The concentrations $c^s{}_T$ and $c^0{}_T$ can be expressed as functions of the monomer concentration by means of Eq. (5.235). Then we obtain

$$\Gamma = 2\left[\frac{D_1\left(1+\tilde{\beta}\right)\left(1+\tilde{\gamma}^2\tilde{\beta}\right)}{\pi}\right]^{1/2}\int_0^{\sqrt{t}}\left[c_1^0 - c_1^s\left(t-\lambda\right)\right]d\sqrt{\lambda} \quad . \tag{5.243}$$

If we introduce the effective diffusion coefficient

$$D^* \equiv D\left(1+\tilde{\beta}\right)\left(1+\tilde{\beta}\tilde{\gamma}^2\right), \tag{5.244}$$

Eq. (5.243) fully coincides with the Ward and Tordai equation. Hence it follows immediately that the presence of micelles in the solution leads to an acceleration of the adsorption and desorption processes if equilibrium between monomers and micelles can be assumed. All the relations obtained for non-micellar solutions can be used in this case too if the diffusion coefficient of monomers is replaced by the effective coefficient D*.

However, the condition of local equilibrium between monomers and micelles (5.233), which is equivalent to inequality $\tau_D \gg \tau_2$, is too rigorous and holds only in exceptional cases. The characteristic times τ_2 and τ_D are not entirely independent quantities. Both times increase with the increase of the surface activity. Condition (5.233) can be approximately fulfilled only for surfactants of high surface activity and for a limited concentration range. Joos and van Hunsel demonstrated the applicability of Eq. (5.243) for solutions of Brij-58 at $c_T < 75\ c_1^0$ [84].

If the PFOR model is used, an analytical solution of the surfactant diffusion problem in a micellar solution can be obtained. For this model only the monomer diffusion has to be considered, which is described by the equation [78, 83, 85, 87-89, 93, 137, 138, 147]

$$\frac{\partial \delta c_1}{\partial t} = D_1 \Delta \delta c_1 - \frac{1}{\tau_2}\delta c_1 . \tag{5.245}$$

As has been shown by Dushkin et al. [137] this equation can be obtained from the equation system (5.223), (5.224) if we assume that the diffusion coefficients of the all aggregates coincide with the diffusion coefficient of monomers. Eq. (5.245) can be also derived for $nc_m \gg c_1^0$ and $D_m \ll D_1$ [78].

A solution of the problem (5.236), (5.237), (5.245) can be obtained by means of general methods of mathematical physics. Petkova and Dushkin have shown recently that the method of the Green functions is most suitable for this purpose [152]. They presented the analytical kinetic dependencies of $\Gamma(t)$ for flat and spherical surfaces, and also for the more general

boundary condition including an adsorption barrier. For the interpretation of experimental dynamic surface tension data only the simplest relation was used [83]

$$\Gamma(t) = c_1^0\sqrt{D_1\tau_2}\left[\left(\frac{1}{2}+\frac{1}{\tau_2}\right)\mathrm{erf}\left(\sqrt{\frac{t}{\tau_2}}\right)+\sqrt{\frac{t}{\pi\tau_2}}e^{-t/\tau_2}\right]-\sqrt{\frac{D_1}{\tau_2}}\int_0^t c_{1s}(t')\mathrm{erf}\left(\sqrt{\frac{t-t'}{\tau_2}}\right)dt''-\sqrt{\frac{D_1}{\pi}}\int_0^t\frac{c_{1s}(t')}{\sqrt{t-t'}}e^{(t-t')/\tau_2}dt', \tag{5.246}$$

where c_{1s} is the subsurface concentration, and erf(z) is the error function. This equation corresponds to the case of adsorption on a flat surface when the rate of the process is determined by diffusion in the bulk and the initial adsorption is zero. If a small and fast compression or expansion of the liquid surface is considered, the deviation of the dynamic surface tension from equilibrium $\Delta\gamma$ can be represented in the form

$$\Delta\gamma = \Delta\gamma_0\frac{\Delta\Gamma}{\Delta\Gamma_0}, \tag{5.247}$$

where the subscript zero indicates the initial perturbation. Substitution of $\Delta\Gamma/\Delta\Gamma_0$ obtained from the boundary value problem of Eqs. (5.236), (5.237), (5.245) into Eq. (5.247) yields the dynamic surface tension change

$$\Delta\gamma = \frac{\Delta\gamma}{2G}e^{-t/\tau_2}\left\{(1+G)E\left[\frac{1+G}{2}\left(\frac{t}{\tau_D}\right)^{1/2}\right]-(1-G)E\left[\frac{1-G}{2}\left(\frac{t}{\tau_D}\right)^{1/2}\right]\right\}, \tag{5.248}$$

where $E(z) = \exp(z^2)\,\mathrm{erfc}(z)$, $\mathrm{erfc}(z) = 1 - \mathrm{erf}(z)$, $G = (1+4\tau_D/\tau_2)^{1/2}$.

Eq. (5.248) has been obtained for the first time by Dushkin et al [138] and is a generalisation of the well-known Sutherland equation [153] for the case of micellar solutions. However, Eq. (5.248) is obtained on the basis of rather rough assumptions for the diffusion of micelles and can be used only as approximation. Note that Dushkin at al. have recently obtained a generalisation of Eq. (5.248) for slow surface dilation with a constant rate [154].

Eq. (5.248) and its modification for a deformed surface [154], together with the corresponding equations for $\Delta\Gamma$ [152] and Eq. (5.243) are the only analytical results obtained as solution of the boundary value problem for the diffusion equations of micelles and monomers. An approximate relation for $\Delta\gamma$ can be also obtained without integration of the diffusion equations with the help of the penetration theory [155]. In this case the derivative on the right hand side of Eq. (5.237) is replaced by the ratio of finite differences

$$\frac{\partial \Gamma}{\partial t} = D_l \left(\frac{\partial c_l}{\partial z} \right)_{z=0} \approx D_l \frac{c_l^0 - c_{ls}}{\hat{\delta}}, \tag{5.249}$$

where $\hat{\delta}$ is the diffusion penetration depth. The following universal relationship has been obtained for this parameter in the case of diffusion with a chemical reaction [155]

$$\hat{\delta} = \frac{\sqrt{\pi D_l t}}{\sqrt{\pi\, kt}\, \mathrm{erf}\sqrt{kt} + e^{-kt}}, \tag{5.250}$$

where k is the kinetic coefficient equal to $1/\tau_2$ for the slow step of micellisation.

Substitution of Eq. (5.250) into (5.249) and subsequent integration of the obtained ordinary differential equation lead to a relationship similar to Eq. (5.248) [89]. This shows on the one hand side that the "penetration theory" yields a useful approximation, on the other hand it indicates that Eq. (5.248) cannot be accurate.

Application of numerical methods have been rather seldom in studies of adsorption kinetics from micellar solutions. The main difficulties are probably connected with the large number of independent parameters. The first work belongs to Miller [146]. Fainerman and Rakita also published numerical results of the solution of the boundary value problem (5.236), (5.237), (5.245) [85]. Recently Danov et al. proposed an original method for solving the boundary value problem for the diffusion of micelles and monomers [92]. The system of equations was reduced to a system of ordinary differential equations by using a model concentration profile in the bulk phase. The obtained results agree better with dynamic surface tensions of micellar solutions than equation (5.248).

It has been already indicated (Fig. 7) that micelles can lead to an essential acceleration of the adsorption process. Therefore, special experimental techniques are necessary for its investigation, allowing measurements of the dynamic surface tension in a time interval of milliseconds. The maximum bubble pressure method [78, 81, 83, 89, 90, 93] and the oscillating jet method [77, 82, 86, 87, 88, 90, 92, 93, 156] are most frequently used for these purposes. The inclined plate method [83, 89, 90, 93], the method of constant surface dilation [85] and the drop volume method [84] have been used also for slow adsorbing surfactants.

Solutions of Triton X-100 were investigated most frequently probably because sufficient information on the equilibrium surface properties and adsorption kinetics from non-micellar

solutions are given in literature [83, 88 - 90, 93]. The dynamic surface tension was also measured for micellar solutions of sodium alkyl sulphates including the solutions with additions of electrolytes [77, 79, 83, 85, 87, 88, 92], and for micellar solutions of some cationic surfactants [83]. For most of these systems it was assumed that the adsorption kinetics was controlled by diffusion and, consequently, relations of the type (5.243), (5.247) can be applied. Fainerman considered that the observed weak concentration dependence of the dynamic surface tension could be caused by the presence of an adsorption barrier ([77, 87], Fig. 13). Moreover, if one takes into account that the adsorption process can be fast enough in the system under investigation, the effect can be also explained by the weak influence of micelles on the dynamic surface tension at surface lifetimes accessible by maximum bubble pressure tensiometry.

Some authors compared the dynamic surface tensions with calculations for the final stage of the adsorption close to equilibrium (at $t \to \infty$) when a simple limiting relation following from equation (5.245) can be applied [83, 88, 90]. When $t \to \infty$ the following equality follows from the Ward and Tordai equation [83]

$$\frac{d\gamma}{dt^{-1/2}} = \frac{RT\Gamma^2}{c_0}\sqrt{\frac{\pi}{4D_1}}, \qquad (5.251)$$

where R is the gas constant, T is the temperature, c_0 is the bulk concentration.

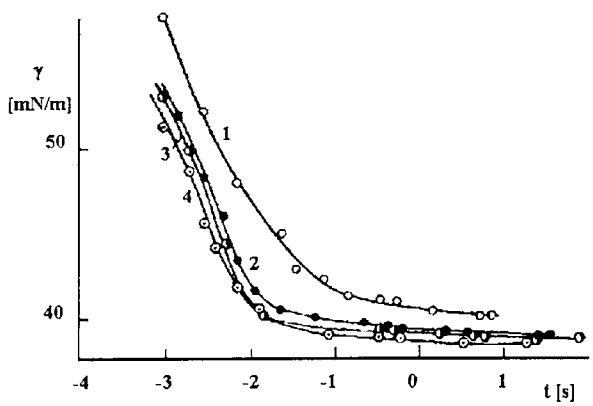

Fig. 13. Dynamic surface tension of SDS solutions at concentrations $8 \cdot 10^{-6}$ mol/cm^3 (1), 10^{-5} mol/cm^3 (2), $1.4 \cdot 10^{-5}$ mol/cm^3 (3), $2 \cdot 10^{-5}$ mol/cm^3 (4), according to [77].

Another relation follows from Eq. (5.246) under the same condition [83, 90]

$$\frac{d\gamma}{dt^{-1}} = \frac{RT\Gamma^2}{c_1^0}\sqrt{\frac{\tau_2}{D_1}} \quad (5.252)$$

Eqs. (5.251) and (5.252) allow us to find τ_2 from $d\sigma/dt^{-1/2}$ at the CMC and above

$$\frac{\left(d\gamma/dt^{-1/2}\right)_{c_T=CMC}}{\left(d\gamma/dt^{-1}\right)_{c_T>CMC}} = \sqrt{\frac{\pi}{4\tau_2}}. \quad (5.253)$$

The values of τ_2 obtained by this method are of the same order of magnitude as those from relaxation spectrometry of the bulk phase [83, 88, 90]. These results according to the authors indicate the possibility to use Eq. (5.253) to estimate the characteristic time of the slow step of micellisation. Note that in general, in most works only agreement in the order of magnitude was obtained for two independent ways of the determination of τ_2 based on measurements of the dynamic surface tension using relations of the type (5.243), (5.246), (5.248), (5.253), and from relaxations in the bulk phase [77, 83, 85, 88 - 91, 93]. However, better agreement cannot be expected if one takes into account that all relations for the kinetics of adsorption and surface tension for micellar solutions are derived on the basis of numerous rough approximations.

A method based on the comparison of experimental and calculated kinetic dependencies of the dynamic surface tension can be more precise in comparison with the use of Eq. (5.253) [77, 85, 89, 92, 93]. Mitrancheva et al. presented the most detailed data and compared calculated dynamic surface tension with results obtained for solutions of TRITON X-100 using three different experimental methods: the inclined plate, the oscillating jet and the maximum bubble pressure methods [93]. The inclined plate method yielded values of τ_2 different from the results of the two other techniques. This discrepancy is probably connected with the differences in the attainable surface age. Thus the inclined plate method can be used only at relatively high surface life times when the surface tension tends asymptotically to equilibrium, and when the accuracy of determination of τ_2 decreases. In addition the insufficiently investigated peculiarities of the liquid flow along the inclined plane can be another source of experimental errors [93].

The characteristic times of the slow step of micellisation determined by the maximum bubble pressure and oscillating jet methods have the same orders of magnitude at low concentrations and agree with results of investigation of the bulk phase [139, 157] (Fig. 5.14). At higher

concentrations even the orders of magnitude are in disagreement. Any attempt to explain these discrepancies should take into account that data of different relaxation spectrometry methods for the bulk neither agree to a sufficient extent [129, 154], as various methods of monitoring relaxation processes are unequally sensitive to concentration changes of micelles and monomers. At the same time, the situation is entirely different when one measures surface properties because they are only sensitive to the monomer concentration.

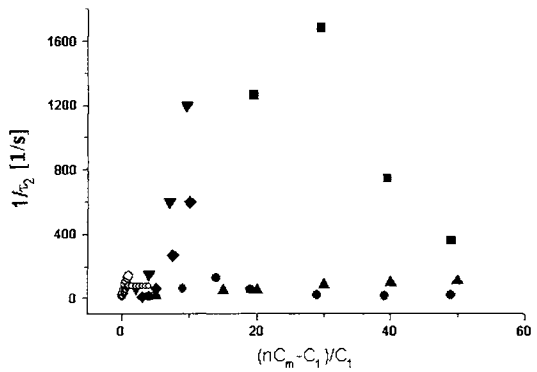

Fig. 5.14. Dependence of τ_2 on the relative amount of Triton X-100 aggregated in micelles obtained by different methods of the dynamic surface tension: oscillating jet [93] (■), maximum bubble pressure [93] (▲), [89] (●), [90] (▼), inclined plate [83] (◆);open symbols refer to results of relaxation methods for the bulk phase [166, 167]; according to [93].

One of the reasons of the insufficient reliability of micellisation kinetics data determined from dynamic surface tensions, consists in the insufficient precision of the calculation methods for the adsorption kinetics from micellar solutions. It has been already noted that the assumption of a small deviation from equilibrium used at the derivation of Eq. (5.248) is not fulfilled by experiments. The assumptions of aggregation equilibrium or equal diffusion rates of micelles and monomers allow to obtain only rough estimates of the dynamic surface tension. An additional cause of these difficulties consists in the lack of reliable methods for surface tension measurements at small surface ages. The recent hydrodynamic analysis of the theoretical foundations of the oscillating jet and maximum bubble pressure methods has shown that using these techniques for measurements in the millisecond time scale requires to account for numerous hydrodynamic effects [105, 158, 159]. These effects are usually not taken into account by experimentalists, in particular in studies of micellar solutions. A detailed analysis of

the theoretical foundations of dynamic surface tension methods is beyond the scope of this chapter. However, in brief one can say the determination of dynamic surface tensions by the oscillating jet method requires corrections in respect to the inhomogeneous velocity profile in the jet, the surface tension gradient along the jet surface, and the influence of the dynamic surface tension on hydrodynamic oscillations. All these effects have never been taken into account simultaneously until now. Moreover, the influence of the surface elasticity has never been taken into account when calculating the dynamic surface tension from the Bohr equation. This means that all the results obtained by the oscillating jet method are only more or less good estimates.

An analysis of the maximum bubble pressure method including all known theoretical approaches was given only recently so that data from literature are only of approximate character [160]. Therefore, the current level of kinetic theories of adsorption from micellar solutions and the corresponding experimental technique is still insufficient for investigations of the micellisation kinetics with a precision comparable to that of bulk relaxation methods. This pessimistic conclusion, however, relates to a less extent to methods based on small (mainly periodic) perturbations of the adsorption equilibrium.

5.7. Dynamic surface elasticity of micellar solutions

If external perturbations are small, the evolution of all characteristics of the system is described by linear equations. In particular the linear diffusion equations (5.210) - (5.212), (5.223), (5.224), (5.226), (5.228) can be applied. However, if one uses modern experimental techniques, the limitation to low perturbations is not too strict especially for periodic processes. Many experimental methods are based on the registration of the system response (mainly of the surface tension relaxation) to a small surface compression or expansion, mainly covering the range of low frequencies (≤ 0.1 Hz). The oscillating barrier method as a typical example [95] uses a Langmuir trough where the surface area is changed periodically with a given amplitude and frequency. The induced surface tension oscillations are measured then. At frequencies > 0.1 Hz the surface deformations in the Langmuir trough become non-uniform, and it is necessary to use high-frequency experimental techniques, such as the methods of transverse

[96 - 101, 105] and longitudinal [102, 103] surface waves, and also the oscillating bubble or drop method [161].

The measurements of the characteristics of transverse surface waves are possible when the ratio of oscillation amplitude to wavelength is less than 0.1 % and all perturbations are really small [105]. The potential of relaxation methods was appreciated already by Lucassen (1975) who used the oscillating barrier method [94, 95]. However, for most surfactants the characteristic adsorption times correspond to frequencies, which are inaccessible for this method. The application of surface wave techniques to micellar solutions relates to later time [96 - 105].

The dynamic surface elasticity ε determines the response of the system (the perturbation of surface tension $\delta\gamma$) to a small change of the area of a surface element $\delta\widetilde{S}$

$$\varepsilon = \frac{\delta\gamma}{\delta \ln\widetilde{S}}. \qquad (5.254)$$

In the general case the phase of oscillations of the surface tension and the phase of periodical alterations of the surface area do not coincide. Then it is convenient to use complex numbers in order to describe the oscillations, and to consider two components of the surface elasticity, *the surface storage modulus* ε_r and *the surface loss modulus* ε_i

$$\varepsilon = \varepsilon_r + i\varepsilon_i. \qquad (5.255)$$

For surface waves the surface elasticity is connected with the complex wave number $k = 2\pi/\lambda + i\alpha$ via the dispersion equation

$$(\rho\omega^2 - \gamma k^3 - \rho g k)(\rho\omega^2 - m k^2\varepsilon) - \varepsilon k^3(\gamma k^3 + \rho g k) + 4i\rho\mu\omega^3 k^2 + 4\mu^2\omega^2 k^3(m - k) = 0, \qquad (5.256)$$

where $m^2 = k^2 - i\omega\rho/\mu$ ($Re[m] > 0$), λ is the wavelength, α is the damping coefficient, ω is the angular frequency, μ is the liquid viscosity, ρ is the liquid density, and g is the gravitational acceleration.

The measurement of the wave characteristics and application of Eq. (5.256) to experimental results allow to determine the surface parameters γ and ε. The dynamic surface elasticity is the most interesting property because it is connected with the kinetic coefficients of the relaxation processes in the system. The observed correlations between τ_2 and the efficiency of numerous processes of technological implication (foam formation [122], solubilisation of impurities [163], bubble formation [1], liquid spreading [163], emulsification [165]) are determined first

of all by the influence of the characteristic time of the slow step of micellisation on the dynamic surface elasticity. The elasticity determines, in turn, the hydrodynamics of liquids with a free surface. The foundations of the surface viscoelasticity theory of non-micellar surfactant solutions have been delineated recently in [162].

The main relations between the complex dynamic surface elasticity and the kinetic characteristics of micellisation are presented below [103, 133, 134]. Let a small surface element of the area $\widetilde{S}$ be subjected to a small periodic surface dilation $\delta\widetilde{S}$

$$\widetilde{S} = \widetilde{S}_0 + \delta\widetilde{S} = \widetilde{S}_0 + \left(\delta\widetilde{S}\right)_0 e^{-i\omega t}. \tag{5.257}$$

Then the surface tension, the adsorption, the concentrations of monomers and micelles will be also changed according to the harmonic law

$$\gamma = \gamma_0 + \delta\gamma = \gamma_0 + (\delta\gamma)_0 e^{-i\omega t}, \tag{5.258}$$

$$\Gamma = \Gamma_0 + \delta\Gamma == \Gamma_0 + (\delta\Gamma)_0 e^{-i\omega t}, \tag{5.259}$$

$$c_1 = c_1^0 + \delta c_1 = c_1^0 + (\delta c_1)_0 e^{-i\omega t}, \tag{5.260}$$

$$c_m = c_m^0 + \delta c_m = c_m^0 + (\delta c_m)_0 e^{-i\omega t}. \tag{5.261}$$

If these relations are used, the time differentiation can be replaced by the multiplication by the factor -iωt. Then, for a diffusion to a flat surface the diffusion equations in partial derivatives (5.210) - (5.212), (5.223), (5.224), (5.226), (5.228) are reduced to ordinary second order differential equations. Besides, because of the condition c_m = const, which follows from Eq. (5.211) and the boundary condition (5.239) for the slow relaxation process, the micellar concentration is uniform and one has to solve only the boundary value problem for Eqs. (5.210), (5.212). Therefore, for any step of micellisation and for different relaxation mechanisms we always obtain a system of two ordinary linear differential equations. For the slow process of micellisation (5.148) the characteristic equation has the form

$$\left[i\omega + D_1\left(t_j^2 - k^2\right) - \frac{\left(n^0\right)^2}{R\left(c_1^0 + \hat{\sigma}^2 c_m^0\right)}\right] \times \left[i\omega + D_m\left(t_j^2 - k^2\right) - \frac{1}{c_m^0 R}\right] - \frac{\left(n^0\right)^2}{R c_m^0\left(c_1^0 + \hat{\sigma}^2 c_m^0\right)} = 0. \tag{5.262}$$

If the micellar concentration is sufficiently high $\left(n^0\right)^2\left(c_1^0 + \hat{\sigma}^2 c_m^0\right)^{-1} c_m^0 \gg 1$ (excluding the concentration range close to the CMC), we find the following roots of this equation

$$t_{1,3}^2 = k^2 - i\omega D_m^{-1},\ t_{2,4}^2 = k^2 - D_1^{-1}\left(i\omega - \tau_2^{-1}\right). \tag{5.263}$$

In the opposite case $\left(n^0\right)^2\left(c_1^0 + \hat{\sigma}^2 c_m^0\right)^{-1} c_m^0 \ll 1$ (concentration range close to the CMC), when the micellar concentration is essentially less than the monomer concentration we obtain

$$t_{1,3}^2 = k^2 - i\omega D_m^{-1} + \left(2c_m^0 R D_m\right)^{-1},\ t_{2,4}^2 = k^2 - i\omega D_1^{-1}. \tag{5.264}$$

Note that among the four roots of equation (5.262) only two have a positive real component and thus yield a solution of the problem. If we discard the other roots and take into account condition (5.239), the solution of Eqs. (5.223) and (5.224) read

$$\left(\delta c_1\right)_0 = C_{11}e^{-t_1 z} + C_{12}e^{-t_2 z},\ \left(\delta c_m\right)_0 = C_m\left(e^{-t_1 z} - \frac{t_1}{t_2}e^{-t_2 z}\right). \tag{5.265}$$

Substitution of Eqs. (5.260), (5.261) and (5.265) into Eq. (5.223) gives the ratio C_{11}/C_{12}:

$$\frac{C_{11}}{C_{12}} = -\frac{t_2}{t_1}\frac{i\omega + D_1 t_2^2 - \tau_2^{-1}}{i\omega + D_1 t_1^2 - \tau_2^{-1}}. \tag{5.266}$$

For small harmonic deformations the dynamic surface elasticity has the form

$$\varepsilon = \frac{d\gamma}{d\ln\tilde{S}} = \frac{d\gamma}{d\ln\Gamma}\frac{d\ln\Gamma}{d\ln\tilde{S}}. \tag{5.267}$$

To determine the second derivative on the right hand side of Eq. (5.267) we can use the mass balance at the surface

$$\frac{1}{\tilde{S}}\frac{d\left(\Gamma\tilde{S}\right)}{dt} = q, \tag{5.268}$$

where q is the adsorption flux of surfactant from the bulk to the surface (at equilibrium q = 0). The surface diffusion of the surfactant is neglected here. The flux q can be represented as a diffusion flux from the bulk to the subsurface

$$q = D_1\left(\frac{dc_1}{dz}\right)_{z=0} \tag{5.269}$$

and a flux from the subsurface to the surface layer (adsorption flux itself)

$$q = \hat{\beta}c_1\big|_{z=0}\left(1 - \frac{\Gamma}{\Gamma_\infty}\right) - \hat{\alpha}\Gamma, \tag{5.270}$$

where Γ_∞ is the maximum adsorption, $\hat{\beta}$ and $\hat{\alpha}$ are the kinetic coefficients of adsorption und desorption, respectively. Substitution of Eqs. (5.259) - (5.261) and (5.265) into Eqs. (5.268) - (5.270) and neglecting terms of higher orders, we obtain

$$\frac{d\ln\Gamma}{d\ln\tilde{S}} = -i\omega\left[i\omega - \frac{D_1\left(\hat{\alpha}+\hat{\beta}c_1^0/\Gamma_\infty\right)\left(1+\frac{t_2C_{12}}{t_1C_{11}}\right)}{D_1\left(1+\frac{t_2C_{12}}{t_1C_{11}}\right)-\frac{\hat{\beta}}{t_1}\left(1-\frac{\Gamma}{\Gamma_\infty}\right)\left(1+\frac{C_{12}}{C_{11}}\right)}\right]^{-1}. \qquad (5.271)$$

A final substitution of Eq. (5.271) into relation (5.267) and taking into account Eq. (5.266) we find the dynamic dilational surface elasticity of micellar solutions

$$\varepsilon = -\frac{\partial\gamma}{\partial\ln\Gamma}\left\{1-\frac{iD_1\left(\hat{\alpha}+\frac{\hat{\beta}c_1}{\Gamma_\infty}\right)\left(t_{21}^2-t_{11}^2\right)}{-\omega D_1\left(t_{21}^2-t_{11}^2\right)+ \atop +\frac{\omega\hat{\beta}}{D_1}\left(1-\frac{\Gamma}{\Gamma_\infty}\right)\left[\frac{i\omega+D_1\left(t_{21}^2-k^2\right)-\tau_{21}^1}{t_{11}}-\frac{i\omega+D_1\left(t_{11}^2-k^2\right)-\tau_{21}^{-1}}{t_{21}}\right]}\right\}^{-1}. \qquad (5.272)$$

This relation describes not only periodic deformations of a liquid surface. Using methods of integral transformations it is possible to show that the dynamic surface elasticity is a fundamental surface property and its value determines the system response to a small arbitrary surface dilation [161]. With this method it is also possible to determine the dynamic elasticity of liquid-liquid interfaces where the surfactant is soluble in both adjacent phases [133]. Moreover, similar transformations lead to an expression for the dynamic surface elasticity for the case when the mechanism of the slow step of micellisation is determined by scheme (5.185) or for frequencies corresponding to the fast step of micellisation [133, 134]. However, as stated above, it is the slow process which mainly influences the adsorption kinetics from micellar solutions.

Let us consider different particular forms of relation (5.272). If the surfactant in the solution exists mainly in form of micelles, and using the approximation (5.263) for the roots of characteristic equation (5.262), we obtain

$$\varepsilon = -\frac{\partial\gamma}{\partial \ln\Gamma}\left[1+\frac{iD_1\left(\alpha+\frac{\hat{\beta}c_1^0}{\Gamma_\infty}\right)\left(-\frac{i\omega}{D_1}+\frac{1}{D_1\tau_2}\right)^{1/2}}{\omega\hat{\beta}\left(1-\frac{\Gamma}{\Gamma_\infty}\right)+\omega D_1\left(-\frac{i\omega}{D_1}+\frac{1}{D_1\tau_2}\right)^{1/2}}\right]^{-1} \tag{5.273}$$

Note that the diffusion of micelles does not influence the dynamic surface elasticity. This fact can be easily explained if we take into account that any increase of the total micellar concentration is accompanied by a decrease of the relative changes of c_m. Hence, changes of the local monomer concentration are partly compensated at the expense of micelles, when the adsorption and desorption processes are determined by diffusion of monomers normal to the interface. However, the corresponding local relative changes of the micellar concentrations are negligible when c_m is sufficiently large.

If $\omega \gg \tau_2^{-1}$ and micelles are not involved in the relaxation process, Eq. (5.273) is reduced to the expression for the dynamic surface elasticity of surfactant solutions below the CMC [162, 165].

With the characteristic time of surfactant diffusion and of the relaxation time τ of the adsorption process itself [165],

$$\tau = \left(\hat{\alpha}+\frac{\hat{\beta}c_1^0}{\Gamma_\infty}\right)^{-1}, \tag{5.274}$$

the Eq. (5.273) can be split into the real and imaginary parts of the surface elasticity

$$\varepsilon_r = -\frac{\partial\gamma}{\partial \ln\Gamma}\left\{1-\frac{\omega\tau_d^{1/2}\tau_2^{1/2}\left(d(\omega\tau_2)-1\right)^{1/2}+2^{1/2}d(\omega\tau_2)}{2\omega\tau_d^{1/2}\tau_2^{1/2}\left[\omega\tau\left(d(\omega\tau_2)+1\right)^{1/2}+\left(d(\omega\tau_2)-1\right)^{1/2}\right]+2^{1/2}\omega^2\tau_d\tau_2+2^{1/2}d(\omega\tau_2)\left(1+\omega^2\tau^2\right)}\right\} \tag{5.275}$$

$$\varepsilon_i = \frac{\partial\gamma}{\partial \ln\Gamma}\frac{\omega\tau_d^{1/2}\tau_2^{1/2}\left(d(\omega\tau_2)+1\right)^{1/2}+2^{1/2}\omega\tau d(\omega\tau_2)}{2\omega\tau_d^{1/2}\tau_2^{1/2}\left[\omega\tau\left(d(\omega\tau_2)+1\right)^{1/2}+\left(d(\omega\tau_2)-1\right)^{1/2}\right]+2^{1/2}\omega^2\tau_d\tau_2+2^{1/2}d(\omega\tau_2)\left(1+\omega^2\tau^2\right)} \tag{5.276}$$

where $d(\omega\tau_2) \equiv \left(1+\omega^2\tau_2^2\right)^{1/2}$.

Relations (5.275), (5.276) can be used for the interpretation of experimental results obtained by surface relaxation spectrometry methods, for example, by the capillary wave method.

At sufficiently high frequencies ($\omega \gg \hat{\beta}^2 D_1^{-1}$ independent of the relationship between ω and τ_2^{-1}) the diffusion in the bulk, and consequently the micellisation, does not influence the surface elasticity. In the opposite case of low frequencies $\left(\tau_2^{-1}, \omega \ll \hat{\beta}^2 D_1^{-1}\right)$ the micellisation kinetics does not influence the dynamic surface elasticity only when $\omega \gg \tau_2^{-1}$. In a more general case the dynamic surface elasticity can be represented at low frequencies in the following form

$$\varepsilon = -\frac{\partial \gamma}{\partial \ln \Gamma}\left\{1 - \frac{iD_1 t_2}{\omega}\left(\frac{\partial \Gamma}{\partial c}\right)^{-1}\right\}^{-1} . \qquad (5.277)$$

Here t_2^{-1} is the diffusion layer thickness determined by relation (5.263) which contains a term related to the micellisation. At high micellisation rates $\left(\omega \ll \tau_2^{-1}\right)$ we obtain

$$\varepsilon = -\frac{\partial \gamma}{\partial \ln \Gamma}\left\{1 + \frac{i\sqrt{D_1/\tau_2}\left(\hat{\alpha} + \hat{\beta} c_1^0/\Gamma_\infty\right)}{\omega\hat{\beta}\left(1 - \Gamma/\Gamma_\infty\right) + \omega\sqrt{D_1/\tau_2}}\right\}^{-1} . \qquad (5.278)$$

If we assume also that $\hat{\beta}^2 \ll D_1\tau_2^{-1}$, then the dynamic surface elasticity is independent of the bulk diffusion coefficient as in the case of high frequencies. This means that if the micellisation rate is high enough, the diffusion layer becomes so thin that the surfactant exchange between the surface layer and the bulk is determined by the adsorption process only. We have to take into account here that the processes of micellisation and adsorption are not entirely independent. It is quite possible that the parameters τ_2 and $\hat{\beta}$ are interconnected, although the present knowledge does not permit evidence. Thus, at high frequencies the dynamic surface elasticity does not change when the total surfactant concentration exceeds the CMC. As all changes of the main surface properties (γ, Γ) are insignificant beyond the CMC, the value of ε will also remain almost constant for higher concentrations. For low frequencies, however, the dependency $\varepsilon(\omega)$ can differ for concentrations below and above the CMC, and, hence, measurements of the dynamic surface elasticity can yield the kinetics of micellisation.

The calculations of the real and imaginary parts of the complex dynamic surface elasticity via Eqs. (5.275) and (5.276) (at τ = 0) illustrate these conclusions. Figure 15 shows the dependencies of the non-dimensional quantities $\varepsilon_r' = -\varepsilon_r\left(\partial\gamma/\partial \ln \Gamma\right)^{-1}$ (1) and

$\varepsilon_i' = -\varepsilon_i(\partial\gamma/\partial \ln \Gamma)^{-1}$ (2) on the frequency when $2D_i^{-1}\partial\Gamma/\partial c = 1\,s^{-1}$. The two pairs of curves correspond to the cases $\tau_2 = 0$ (solid line) and $\tau_2 = 0.1$ ñ$^{-1}$ (dashed line).

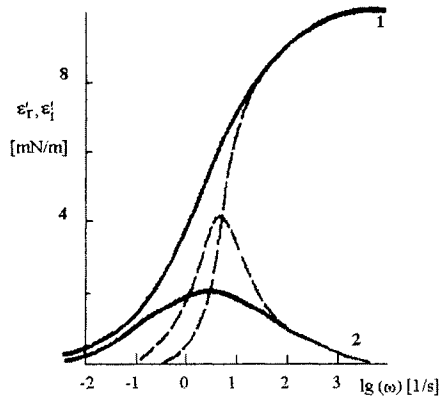

Fig. 5.15. Real and imaginary parts of the dynamic surface elasticity as a function of frequency; further explanations are given in the text.

The extended frequency range of the diffusion relaxation spans about five orders of magnitude. The influence of micellisation leads to faster changes of the surface elasticity with frequency. If the adsorption kinetics is determined by diffusion and $\omega \sim \tau_2^{-1}$, the micellisation influences also the concentration dependence of the surface elasticity. The transition through the CMC has to lead to an abrupt drop according to Eqs. (5.275) and (5.276). Then it follows from the dispersion relation (5.256) that the damping coefficient of transverse capillary waves goes through a local maximum at concentrations close to the CMC.

The region of the CMC $\left(n^2\left(c_1^0 + \hat{\sigma}^2 c_m\right)^{-1} c_m \ll 1\right)$ requires special consideration. Substitution of of t_2 and t_1 from Eq. (5.264) into (5.272), and the transition to the limit $c_m \to 0$ leads to the dynamic surface elasticity of sub-micellar solutions [165] and thus to a rather obvious conclusion: if a solution contains mainly monomers, micelles do not influence the dynamic surface properties. Therefore, even for low frequencies (diffusion controlled adsorption kinetics) there is a concentration range close to the CMC where the surface elasticity is almost constant and begins to increase gradually only at further increasing concentration. Finally the surface elasticity takes values given by relations (5.275) - (5.278). This concentration dependence was observed in experiments with nonionic surfactants [95]. The oscillating barrier

method employed in that study, allowed a qualitative conclusion about the influence of micellisation on the dynamic surface elasticity.

New experimental methods created during the last two decades allow to investigate the concentration and frequency dependence of the dynamic surface elasticity more systematically. That is why the dynamic surface elasticity behaviour in the region of the CMC deserves special attention. Relations (5.264) in the first approximation take the form

$$t_1 \approx \frac{1}{\sqrt{c_m R D_m}};\ t_2 \approx (1-i)\sqrt{\frac{\omega}{2D_1}} \tag{5.279}$$

Then Eq. (5.272) for the liquid - gas interface becomes

$$\varepsilon = -\frac{\partial \gamma}{\partial \ln \Gamma}\left\{1+\left[i\omega\tau + (1-i)\sqrt{\frac{\omega}{2D_1}}\frac{\partial \Gamma}{\partial c_1}\times\left[1-\frac{(1-i)\sqrt{c_m R\omega\frac{D_m}{2D_1}}-1}{\frac{1}{c_m R D_m}-i\omega\left(\frac{1}{D_m}-\frac{1}{D_1}\right)}\tau_2^{-1}D_1^{-1}\right]\right]^{-1}\right\}^{-1} \tag{5.280}$$

If only frequencies $< \tau_2^{-1}$ are considered, the approximation for the dynamic surface elasticity is

$$\varepsilon = -\frac{\partial \gamma}{\partial \ln \Gamma}\left\{1+\frac{1}{i\omega+(1-i)\sqrt{\frac{\omega}{2D_1}}\frac{\partial \Gamma}{\partial c_1}\left(1-n^2\frac{c_m D_m}{c_1^0 D_1}\right)}\right\}^{-1} \tag{5.281}$$

Note that relation (5.281) does not contain any kinetic characteristics of micellisation. If the micellar concentration is low and the formation (disintegration) of micelles is sufficiently fast ($\tau_2^{-1} \geq \omega$), the adsorption rate and, consequently, the dynamic surface elasticity depend only on the efficiency of the surfactant transfer by micelles from the bulk to the surface, and, therefore, on the diffusion coefficient of micelles and the mean aggregation number. This means that the micellar size can be determined from dynamic surface properties. Really, if approximation (5.231) for the diffusion coefficient of micelles is used, it follows from Eq. (5.281)

$$\varepsilon = -\frac{\partial \gamma}{\partial \ln \Gamma}\left[1 + \frac{1}{i\omega\tau + (1-i)\sqrt{\frac{\omega}{2D_1}}\frac{\partial \Gamma}{\partial c_1}\left(1 - n^{7/3}\frac{c_m}{c_1^0}\right)}\right]^{-1}, \qquad (5.282)$$

and therefore, the measurement of the dynamic surface elasticity in the concentration range close to the CMC allows to determine the mean aggregation number. Note that the transition from mechanism (5.148) to mechanism (5.185) does not change the form of the obtained expressions for ε and, consequently, the main conclusions hold.

5.8. Capillary wave studies of micellar solutions

Among various relaxation spectrometry methods of liquid surface layers the transverse capillary waves has been used most frequently for micellar solutions [96 - 101]. The shape of the concentration dependence of the wavelength is the same for all investigated cationic, anionic and nonionic surfactants and resembles the corresponding dependence of surface tension. Figure 16 shows as an example the experimental results for solutions of SDS [96].

The wavelength drops abruptly at the CMC, and in the micellar region any changes do not exceed the limits of experimental accuracy. The similarity between the surface tension isotherm and the wavelength can be deduced from the dispersion relation (5.256). Actually the wavelength is determined first of all by the static surface tension, which is practically constant above the CMC, while the dynamic surface elasticity influences the wavelength only slightly. At the same time, as it follows from the dispersion relation (5.256), the dynamic surface elasticity influences the damping coefficient of capillary waves much stronger. However, the damping coefficient is also almost constant for micellar solutions of some of the investigated surfactants such as cetyl trimethyl ammonium chloride (CTACh)) [168], dodecyl ammonium chloride (DACh) (Fig. 5.17) [168], dodecyl dimethyl phosphine oxide (DPO) [101]).

A special situation appears for solutions of SDS where the damping coefficient starts to increase at concentrations several times greater than the CMC (Fig. 5.18) [96]. The latter effect can be explained if one takes into account that the shear viscosity of the bulk phase of micellar solutions increases with concentration too. The dashed line in Fig. 5.17 at c > CMC shows the calculations

from the dispersion Eq. (5.256). The calculated damping coefficients increase with concentration too and the deviation from the experiment was within the experimental error.

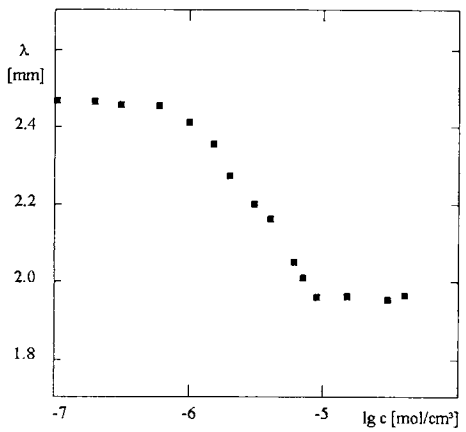

Fig. 5.16. Dependence of the wavelength on SDS concentration at a frequency of 180 Hz [96].

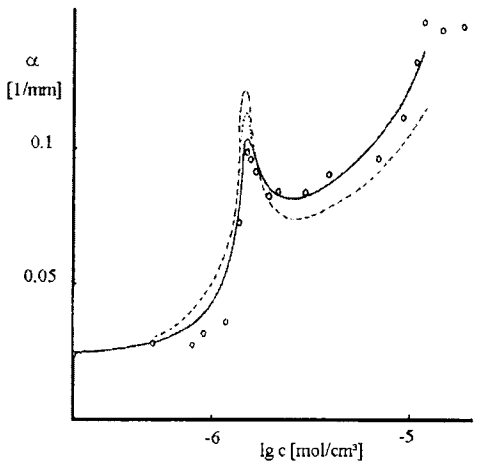

Fig. 5.17. Dependence of the damping coefficient of capillary waves on DACh concentration at the frequency of 200 Hz [168]; curves are calculated according to Eq. (5.256) for the diffusion - controlled adsorption mechanism (solid line), for the mixed adsorption mechanism (dotted line), and for the barrier - controlled adsorption mechanism (dashed line).

The constancy of the damping coefficient beyond the CMC in the systems under consideration corresponds to the approximate constancy of the dynamic surface elasticity. This means that micelles do not take part in the exchange of surfactant molecules between the surface layer and the bulk phase. According to the results of the preceding section this situation is possible when

the characteristic time of the slow step of micellisation exceeds essentially the period of capillary waves. Therefore, the rate of formation and disintegration of aggregates in solutions of SDS, DACh, CTACh and DPO is so low that the sizes of aggregates (aggregation numbers) are practically frozen and do not follow the fast changes of the subsurface concentration.

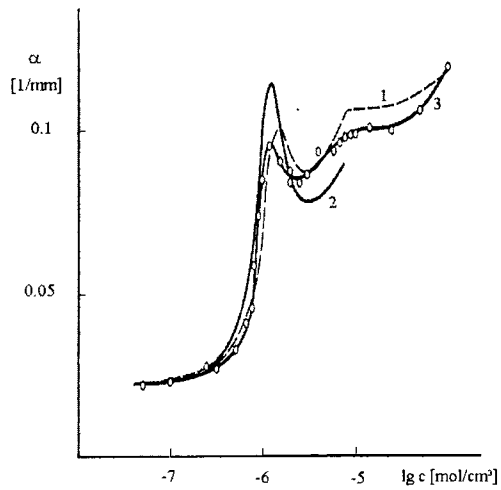

Fig. 5.18. Dependence of the damping coefficient of capillary waves on SDS concentration at a frequency of 200 Hz [96]; curves 1 and 2 are calculated according to Eq. (5.256) for a diffusion - controlled adsorption mechanism (1) and for the barrier -controlled adsorption mechanism (2), 3 corresponds to the experimental data.

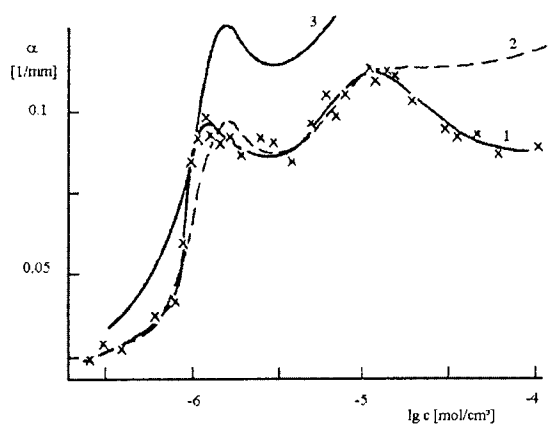

Fig. 5.19. Dependency of the damping coefficient of capillary waves on the DPB concentration at a frequency of 200 Hz [97]; curves 2 and 3 are calculated according to Eq. (5.256) for the diffusion - controlled adsorption mechanism (2), barrier -controlled adsorption mechanism (3), 1 - experimental data.

This means that the following estimate can be used for these systems

$$\tau_2 \gg 0.001\,\mathrm{s} \tag{5.283}$$

This inequality agrees with the results of direct measurements of the formation and disintegration rate of micelles for solutions of DSN, DACh and CTACh [115]. To the best of our knowledge the micellisation kinetics in solutions of DPO has not been studied so far by relaxation spectrometry of the bulk phase.

In the opposite case, when the characteristic time of the slow step of micellisation is comparable with or less than the period of capillary waves the theory given in section 5.4 predicts a decrease of the dynamic surface elasticity modulus with concentration above the CMC, and consequently the appearance of a local maximum of the damping coefficient at the CMC. This maximum has been actually discovered for the fist time for solutions of dodecyl piridinium bromide (DPB) [97] (Fig. 5.19), decyl piridinium bromide (DePB) [97] (Fig. 5.20), sodium decyl sulphate (SDeS) [100], and decyl dimethyl phosphine oxide (DePO) [101]. For all these systems the concentration corresponding to the local maximum coincides with the CMC, and a further decrease of the damping coefficient exceeds the error limits several times. For solutions of DPB and DePO the maximum at the CMC can be observed simultaneously with a local maximum for diluted solutions. As it follows from the numerical analysis of the dispersion equation (5.256), the latter maximum appears when the dynamic surface elasticity modulus increases with concentration and exceeds approximately 0.15γ [105]. This condition does not hold for solutions of SDeS and DePB, so the second maximum is absent for these systems. The rate of decrease of α above the CMC increases at the transition from solutions of DPB to solutions of DePB and SDeS, and takes intermediate values for solutions of DePO. If the values of the surface properties (γ and ε) at the CMC are used for the calculations of the damping coefficient via Eq. (5.256) and only the concentration changes of the bulk viscosity are taken into account, the calculations disagree with the experimental dependencies, as shown in Figs. 5.19 and 5.20 by the dashed lines.

While passing the CMC the damping coefficient decreases for DPB solutions (Fig. 5.19). For DePB solutions the damping coefficient begins to increase again at concentrations more than two times the CMC, and a local minimum appears on the dependence $\alpha(\lg c)$ (cf. Fig. 5.20).

This effect is connected with the fast increase of the bulk shear viscosity for relatively concentrated surfactant solutions. The increase of the viscosity and the decrease of the surface elasticity have opposite effects on the wave damping, but for solutions of DePB the former influence is prevailing. Note also that the CMC for DePB solutions exceeds that for DPB.

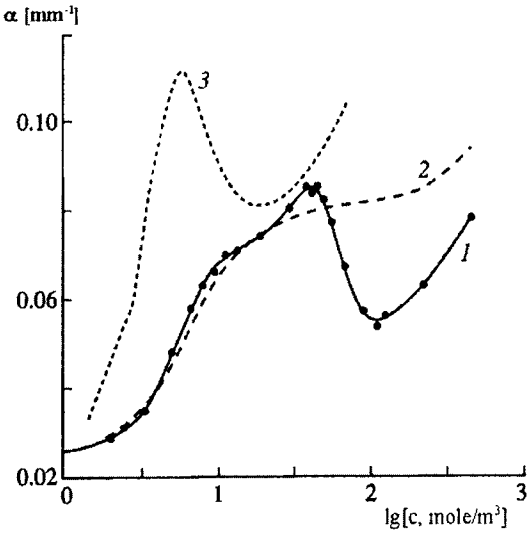

Fig. 5.20. Dependence of the damping coefficient of capillary waves on DePB concentration at a frequency of 200 Hz [98]; curves 1 and 2 are calculated according to Eq. (5.256) for the diffusion - controlled adsorption mechanism (2), barrier - controlled adsorption mechanism (3), 1 - experimental data.

The obtained experimental data can be used for calculations of the characteristic time of the slow step of micellisation according to the equations given in the section 5.4 if the adsorption mechanism of monomers is known. This mechanism can be determined by means of capillary waves for concentrations below the CMC. The curves in Figs. 17 - 20 in this concentration range show the results of calculations of the damping coefficient according to dispersion equation (5.256) for different adsorption mechanisms. It follows from the comparison of the calculated and the measured dependencies for all the investigated systems that the adsorption rate is determined by the surfactant diffusion. It is natural to assume that the actual adsorption mechanism of monomers does not change with the transition to micellar solutions. In this case it is possible to simplify the general expressions (5.275) and (5.276) for the components of the dynamic surface elasticity. If we neglect the effect of an adsorption barrier and use $\tau = 0$, we get

$$\varepsilon_r = -\frac{\partial\gamma}{\partial \ln\Gamma}\frac{1+\left(\frac{\partial\Gamma}{\partial c_1}\right)^{-1}\sqrt{\frac{D_1}{2\omega^2\tau_2}}\sqrt{\sqrt{1+\omega^2\tau_2^2}-1}}{\left[1+\left(\frac{\partial\Gamma}{\partial c_1}\right)^{-1}\sqrt{\frac{D_1}{2\omega^2\tau_2}}\sqrt{\sqrt{1+\omega^2\tau_2^2}-1}\right]^2+\left(\frac{\partial\Gamma}{\partial c_1}\right)^{-2}\frac{D_1}{2\omega^2\tau_2}\left(\sqrt{1+\omega^2\tau_2^2}+1\right)}, \quad (5.284)$$

$$\varepsilon_i = \frac{\partial\gamma}{\partial \ln\Gamma}\frac{\left(\frac{\partial\Gamma}{\partial c_1}\right)^{-1}\sqrt{\frac{D_1}{2\omega^2\tau_2}}\sqrt{\sqrt{1+\omega^2\tau_2^2}+1}}{\left[1+\left(\frac{\partial\Gamma}{\partial c_1}\right)^{-1}\sqrt{\frac{D_1}{2\omega^2\tau_2}}\sqrt{\sqrt{1+\omega^2\tau_2^2}-1}\right]^2+\left(\frac{\partial\Gamma}{\partial c_1}\right)^{-2}\frac{D_1}{2\omega^2\tau_2}\left(\sqrt{1+\omega^2\tau_2^2}+1\right)}. \quad (5.285)$$

As a first approximation the equilibrium surface properties above the CMC can be regarded as independent of concentration. Then the parameters $\partial\gamma/\partial\ln\Gamma, \partial\Gamma/\partial c_1, D_1$ on the right hand side are constant and equal to their values at the CMC. Thus, the components of the dynamic surface elasticity are functions only of the parameter τ_2. For a given value of τ_2 the dispersion relation (5.256) together with Eqs. (5.284) and (5.285) allow to calculate the damping coefficient of capillary waves for micellar surfactant solutions. Then, choosing values of τ_2 at given concentrations and fitting α to the measured value one can determine τ_2. The consecutive application of this procedure to different points of the experimental curve α(lg c) allows to obtain the concentration dependence of the characteristic time of the slow step of micellisation process τ_2(c). The results of these calculations for micellar solutions of DPB, DePB, SDeS and DePO are shown in Table 1. The same table contains experimental data obtained by the bulk relaxation spectrometry [169 - 172] (temperature jump and stopped flow methods). We can consider that the agreement between the values of τ_2 for DPB solutions calculated from capillary waves and those obtained from relaxations in the bulk is satisfactory if we take into account the principal difference between the applied experimental methods and the real accuracy of the determination of the relaxation time (Table 1). For DPB solutions the deviations of the experimental data from the course calculated under the assumption that the micellisation kinetics does not influence the dynamic surface elasticity are not large (Fig. 5.19), and the corresponding precision of the τ_2 values probably does not permit a detailed analysis of

the dependence τ_2(lg c). It is noteworthy that the dependencies τ_2^{-1}(c) obtained in [169, 170] by means of the temperature jump and stopped flow methods are also not in perfect agreement.

To the best of our knowledge the micellisation kinetics in DePB solutions have not been studied yet by means of relaxation spectrometry of the bulk phase. That is why we compare the results obtained from capillary waves with values of τ_2 for solutions of decyl piridinium iodide (DPI) [169] (Table 1). The orders of magnitude of τ_2 obtained by different methods are in reasonable agreement. Note that the absolute values of the damping coefficient for micellar solutions of DePB are lower in comparison with the corresponding values for DPB. Therefore, the sensitivity of the damping coefficient to the kinetic coefficients is higher, and the concentration dependence of τ_2 can be studied with higher precision in the former case. In general this dependence has a shape, which is typical to solutions of ionic surfactants [115]. After a narrow concentration range where τ_2 fast decreases this parameter increases again with concentration in accordance with Eq. (5.184). However, the rate of changes of τ_2 is greater than predicted by this equation. This fact is probably a consequence of the neglection of surfactant dissociation. Besides, the assumption of a small monomer concentration in comparison with the total surfactant concentration is also not accurate enough for the given concentration range. Therefore, at the transition from DPB to DePB the characteristic times of micellisation decrease, and this leads to a faster decrease of the damping coefficient of capillary waves in the concentration range above the CMC. Although the surface activity of SDeS is comparable with that of DePB, the relaxation times for SDeS solutions are greater, on the average, and comparable with the corresponding times for DPB solutions. The data obtained by means of the relaxation studies of the bulk phase confirm this conclusion (Table 1) [171, 172].

The values of τ_2 obtained by the capillary wave method are in satisfactory agreement with the results given in [171, 172]. However, the shapes of the two concentration dependencies of τ_2 are different in the region close to the CMC. This is probably a consequence of the difficulties of the theoretical description of the dynamic surface elasticity. The values of τ_2 for SDeS solutions are greater than the corresponding results for DePB solutions and this leads to smaller changes of the damping coefficient in the range of micellar solutions. The processes of formation and disintegration of micelles are slower for SDS than for SDeS and do not influence the damping coefficient for SDS in the frequency range under investigation (Fig. 5.17).

Table 1 Characteristic times of the slow step of the micellisation process at 293 K

Surfactant	Results of calculations on the basis of experimental data on the damping coefficient of capillary waves		Results of relaxation methods of the bulk phase	
	c, 10^{-6} mol/cm^3	τ_2, ms	c, 10^{-6} mol/cm^3	τ_2, ms
DPB	20	1.3	[169]	
	30	0.53	12	0.60
	35	0.45	13	0.50
	45	0.35	14	0.47
	60	0.30	16	0.68
	100	0.24	18	0.90
			[170]	
			24	0.40
			28	0.49
			40	0.83
			70	1.64
			84	1.43
			100	1.23
			118	0.91
DePB	55	0.75	DePI	
	68	0.24	[169]	
	98	0.045	23	0.20
	110	0.005	24	0.14
	124	0.010	26	0.07
	224	0.045	30	0.05
	448	0.10		
SDeS	60	0.60	[171]	
	80	0.40	33.8	0.20
	100	0.47	[172]	
	120	0.60	39	0.30
	160	1.0	45	0.24
			53	0.27
			69	0.36
			84	0.55
			106	0.95
			125	1.25
			150	2.20
			200	3.70
DePO	10	0.120		
	15	0.022		
	20	0.011		
	25	0.010		

The influence of micellisation on the propagation of capillary waves has been discovered only for solutions of the nonionic surfactant - DePO. The determined values of τ_2 are comparable with the results for solutions of DePB but they decrease monotonously with concentration. Therefore, the obtained results evidence that relations (5.284) and (5.285) describe the concentration dependence of the dynamic surface elasticity well. Hence, the method of transverse capillary waves can be used for studies of micellisation kinetics of surfactants with relatively low surface activity. For surfactants with higher surface activity where the formation and disintegration of micelles proceed slower the method of longitudinal surface waves can be used [102, 103]. The characteristics of longitudinal waves are more sensitive to the dynamic surface elasticity, and this allows one to study the micellisation kinetics under the condition $n^2\left(c_1^0+\hat{\sigma}^2 c_m\right)^{-1} c_m \ll 1$. In this concentration range Eq. (5.282) can be applied, and thus the mean aggregation number can be determined from the wave characteristics [103].

5.9. Main Notations

A	affinity of a reaction
A_s	standard affinity of a reaction
$\bar{A}$	total surface area of a spherical micelle
$\tilde{A}$	area of the dividing surface corresponding to zero surface excess of water and air
$\bar{a}$	surface area per surfactant molecule in a micelle
a_0	optimum area per surfactant molecule in a micelle
a_p	cross-sectional area of the polar head group near the micelle surface
a_{sh}	surface area per molecule shielded from contact with water by the polar head group
a_i	activity of chemical species participating in micellisation
a_M	activity of a micelle
a_δ	surface area per surfactant molecule at distance δ
C	curvature factor of a micelle surface
c_{1i}	concentration of monomers of kind i
c	total surfactant concentration

c_0	bulk concentration
c_1	monomer concentration
c_j	concentration of aggregates with the aggregation number j
c_m	total micellar concentration
c_i^0	CMC of the pure i^{th} component of mixed micelle
c_{CMC}	CMC of the mixture
c_{ni}	concentrations of aggregates composed of *n* surfactant molecules of kind *i*
c_{tot}	total concentration of surfactant in a mixed micellar solution
c_{toti}	total concentration of surfactant of kind *i*
$\tilde{c}_j$	local equilibrium concentration of aggregates
c^s_T	subsurface surfactant concentration
D_j	diffusion coefficient of the j^{th} aggregate
D_m	mean diffusion coefficient of micelles
D*	effective diffusion coefficient
E	energy of scission of a polymeric chain
f_i	activity coefficient
f_M	activity coefficient of micelles
$f_\pm$	mean activity coefficient of a non-micellar solution
$f_\pm^*$	activity coefficient of the surfactant in a micellar solution
$f_\pm^e$	experimental mean activity coefficient of the surfactant in a micellar solution
g	bulk energy per surfactant molecule
g′	term reflecting the energy of the hydrocarbon chain in water
g_v	density of the Gibbs energy G
$g^i_{mic}(sh)$	free energy of micellisation of the pure surfactant *i*
g^{AB}_{mic}	contribution in the free energy of mixed micellisation due intramicellar interactions
g^{AB}_{hc}	term reflecting intramicellar interactions between tails of surfactants A and B
g^{AB}_{elec}	term reflecting the electrostatic part of intramicellar interactions between surfactants A and B
I	ionic strength of micellar ionic solution
I_0	ionic strength of non-micellar ionic solution
J	flux of aggregates in the region of the minimum of the size distribution
J_j	flux of aggregates between j-1 and j

J_m quasi-stationary flux of aggregates passing from the micellar region to the minimum of the size distribution of aggregates

J_1 quasi-stationary flux of forming or consumed monomers

K_a, K_n, K_c various forms of the micellisation constant

K_s dimensionless form of the constant K_c

k^+, k^- mean kinetic coefficients

k complex wave number

k_{j-1}^+ rate constant of the monomer joining to a micelle

k_j^- rate constant of the monomer splitting off

k_B Boltzmann constant

L length of micelles

$\tilde{L}$ mean length of micelles

l_c critical length of the radius of a spherical micelle

l_m minor radius of the core of a spherical micelle

N_{toti} total number of molecules of surfactant *i* participating in the micellisation

N_{1i} number of molecules of the type *i* in the monomer state participating in the micellisation

N_M number of micelles as separate particles

N_i^M number of molecules of the surfactant *i* in a mixed micelle

n aggregation number

$\bar{n}$ mean aggregation number

n^0 equilibrium aggregation number

n_c number of carbon atoms in surfactant molecule

n_i aggregation number of the aggregates composed of *n* surfactant molecules of kind *i*

n_k aggregation number of counterion in micelle

P packing factor in a spherical micelle

p pressure

q adsorption flow of surfactant from the bulk phase to the surface

q_M charge of micelle

R kinetic resistance of formation and disintegration of micelles

R′ gas constant

R_m radius of a spherical micelle

R_S	core radius of a spherical micelle
r_m	average interionic distance
$\widetilde{S}$	surface area
s_v	density of the entropy S
T	temperature
t	time
V_{tot}	total hydrocarbon core volume of a spherical micelle
x_i	mole fraction of component *i*
x_{1i}	mole fractions of monomers of kind *i* in micellar solution
x_{ni}	mole fraction of the aggregates composed of *n* surfactant molecules of kind *i*
x_M	mole fractions of micelles in micellar solution
x_{toti}	overall mole fractions of the surfactant *i* in mixed micellar solution
y_i	mole fraction of the component *i* in the mixed micelle
z_i	charge of a surface active ion
z_k	charge of a counterion
α	damping coefficient
$\hat{\alpha}$	kinetic coefficient of desorption
α_i	degree of micellisation of molecules of kind *i*
α_{CMC}	degree of micellisation at the CMC
β	degree of counterion binding
β_{ij}	pairwise interaction parameter between components *i* and *j* in mixed micelles
$\hat{\beta}$	kinetic coefficient of adsorption,
Γ	adsorption
Γ_∞	maximum adsorption
$\Gamma_{i(j)}$	adsorption of component *i* at zero adsorption of component *j*
γ	surface tension
δ	distance from the core surface to the place where the dipole is located
$\hat{\delta}$	diffusion penetration depth
δ_i^H	Hildebrand solubility parameters of the tails of surfactants *i*
ε	dynamic surface elasticity
λ	wavelength
η_i	corresponding volume fraction of surfactant *i*

η_M	volume fraction of wormlike micelles
μ	liquid viscosity
μ_i	chemical (for ions – the electrochemical) potential
μ_M	chemical potential of a micelle
ν	hydrocarbon core volume per a surfactant molecule in a spherical micelle
ν_i	stoichiometric coefficients of the dissociation reaction of a surfactant molecule
ν^*	total number of ions (including micelles) arising as a result of dissociation of a surfactant molecule
ν_{Si}	molecular volume of surfactant tail of surfactant *i* in a mixed micelle
ρ	liquid density
$\hat{\sigma}^2$	standard deviation of micellar size distribution
$\hat{\sigma}^2$	dispersion (second moment) of the size distribution of micelles
τ	relaxation time of adsorption
τ_1	relaxation time of the fast step of the micellisation process
τ_2	relaxation time of the slow step of the micellisation process
τ_d	characteristic time of the diffusion to the surface
ω	angular frequency
ϕ	generalised colligative property
ΔG	change in the Gibbs energy in the course of micellisation
ΔG_s	change in the standard Gibbs energy in the course of micellisation
ΔH_s	standard enthalpy of micellisation
ΔS_s	standard entropy of micellisation
ΔV_s	standard volume of micellisation

5.10. References

1. P.D.T. Huibers, S.G. Oh, and D.O. Shah, in: *Surfactants in Solution*, A. K. Chattopadhyay, K. L. Mittal (Eds.), M. Dekker, New York, 1996, p. 105.
2. N.M. van Os, J.R. Haak, L. A. M. Rupert, *Physico-chemical properties of selected anionic, cationic and nonionic surfactants*, Elsevier, Amsterdam-L-NY-Tokyo, 1993.
3. Y. Moroi, *Micelles. Theoretical and applied aspects*, Plenum Press, NY-L, 1992.
4. G.C. Kresheck, *Water: A comprehensive Treatise,* Vol. 4, *Aqueous solutions of Amphiphiles and Macromolecules*, Plenum Press, NY, 1975.

5. G.S. Hartley, *Aqueous solutions of Paraffin-Chain Salts*, Hermann, Paris, 1936.
6. M.L. Corrin, J. Colloid Sci., 3(1948)333.
7. R.J. Williams, J.N. Phillips, and K.J. Mysels, Trans. Faraday Soc., 51(1955)728.
8. J.N. Phillips, Trans. Faraday Soc., 51(1955)561.
9. H.S. Chung and I.J. Heilweil, J. Phys. Chem., 74(1970)488.
10. D.G. Hall and B.A. Pethica, *Nonionic Surfactants*, Chapt. 16, Dekker, NY, 1967.
11. J.N. Israelachvili, D.J. Mitchell, and B.W. Ninham, J. Chem. Soc. Faraday Trans. 2, 72(1976)1525.
12. A.I. Rusanov, *Micellisation in Surfactant Solutions*, Chemistry Reviews, Vol. 22, Part 1, Harwood Academic Publishers, Amsterdam, 1997.
13. K. Shinoda and E. Hutchinson, J. Phys. Chem., 66(1962)577.
14. Y. Moroi, N. Nishikido, H. Uehara, and R. Matuura, J. Colloid Interface Sci., 50(1975)254.
15. N. Yoshida, K. Matsuoka, and Y. Moroi, J. Colloid Interface Sci., 187(1997)388.
16. C. Tanford, *The Hydrophobic Effect: Formation of micelles and Biological Membranes*, Wiley, NY, 1973.
17. R. Zana, Langmuir, 11(1995)2314.
18. R. Nagarajan, *Theory of Micelle formation: quantitative approach to predicting micellar propeties from surfactant molecular structure, in: Structure-performance relationships in surfactants*, Eds.: K. Esumi and M. Ueno, Surfactant science series, Vol. 70, Marcel Dekker, NY 1997, pp. 1-81.
19. A.N. Semenov, Soviet. Phys. JETP, 61(1985)733.
20. S. Puvvada and D. Blankschtein, J. Chem. Phys., 92(1990)3710.
21. S. Puvvada and D. Blankschtein, J. Phys. Chem., 96(1992)5567.
22. S. Puvvada and D. Blankschtein, *Molecular thermodynamic Theory of mixed micellar solution*, in: *Mixed surfactant systems* ACS symposium Series Vol. 501, Eds. : P.M. Holland and D.N. Rubingh, Am. Chem. Soc., Washington, DC 1992, pp. 96-113.
23. R.C. Tolman, J. Chem. Phys., 16(1948)758.
24. J.C. Eriksson, S. Ljunggren and U. Henriksson, J. Chem. Soc. Faraday Trans. 2, 81(1985)833.

25. R.F. Kamrath, E.I. Franses, in: *Phenomena in Mixed Surfactant Systems,* J.F. Scamehorn –Ed., ACS Symposium Series 311, ACS, Washington, DC, 1986, pp. 44-60.
26. R.F. Kamrath, E.I. Franses, J. Phys. Chem., 88(1984)1642.
27. S. Wall and S. Elvingson, J. Phys. Chem., 89(1985)2695.
28. A.P. Graciaa, J. Lachaise and R.S. Schechter, *The thermodynamics of mixed micelle formation*, in: *Mixed Surfactant Systems*, Eds. : K. Ogino and M. Abe; Surfactant science series, V. 46, Marcel Dekker, NY 1993, pp. 63-97.
29. Y. Moroi, K. Motomura and R. Matuura, J. Colloid Interface Sci., 46(1974)111.
30. Y. Moroi, N. Nishikido, and R. Matuura, J. Colloid Interface Sci., 50(1975)344.
31. D.N. Rubingh, in: *Solution Chemistry of Surfactants*, K.L. Mittal – Ed., Vol. 1, Plenum Press, NY, 1979.
32. P.M. Holland and D.N. Rubingh, J. Phys. Chem., 87(1983)1984.
33. P.M. Holland, Advances in Colloid and Int. Sci., 26(1986)111.
34. N. Nishikido, *Thermodynamic models for mixed micellisation*, in: *Mixed Surfactant Systems*, Eds.: K. Ogino and M. Abe, Surfactant science series, V. 46, Marcel Dekker, NY 1993, pp. 23-61.
35. L. Benjamin, J. Phys. Chem., 68(1964)3575.
36. R.F. Kamrath and E.I. Franses, Ind. Eng. Chem. Fundam., 22(1983)230.
37. P.M. Holland and D.N. Rubingh, in: *Mixed Surfactant Systems*, P.M. Holland and D.N. Rubingh -Eds., ACS Symposium Series 501, ACS, Washington, DC, 1992, p. 2-31.
38. J.H. Clint, J. Chem. Soc., 71(1975)1327.
39. P.M. Holland, in: *Structure/Performance Relationships in Surfactants*, M. J. Rosen-Ed., ACS Symposium Series 253, ACS, Washington, DC, 1984, pp. 141-151.
40. G.G. Warr, F. Griese, and T.W. Healy, J. Phys. Chem., 87(1983)1220.
41. P. Mukerjee and A.Y.S. Yang, J. Phys. Chem., 80(1976)1388.
42. K.J. Mysels, J. Colloid Interface Sci., 66(1978)331.
43. J.F. Scamehorn, in: *Phenomena in Mixed Surfactant Systems*, J.F. Scamehorn–Ed., ACS Symposium Series 311, ACS, Washington, DC, 1986, p. 1.
44. M.J. Rosen, in: *Surfactant and Interfacial Phenomena*, Wiley, NY, 1989, Chapt. 11.

45. J.F. Scamehorn, R.S. Schechter and W.H. Wade, J. Dispersion Sci. Technol., 3(1982)261.

46. A.P. Graciaa, M. BenGhoulan, G. Marion and J. Lachaise, J. Phys. Chem., 93(1989)4167.

47. N. Nishikido, J. Colloid Int. Sci., 60(1977)242.

48. J. F. Rathman and J.F. Scamehorn, Langmuir, 2(1986)354.

49. G.M. Nguyen, J.F. Rathman and J.F. Scamehorn, J. Colloid Interface Sci., 112(1986)439.

50. K. Motomura and M. Aratono, in: *Mixed Surfactant Systems*, K. Ogino and M. Abe (Eds.), Surfactant Science Series, V. 46, Marcel Dekker, NY 1993, pp. 99-144.

51. I.W. Osborn-Lee, R.S. Schechter, W.H. Wade, and Y. Barakat, J. Colloid Interface Sci., 108(1985)61.

52. K. Motomura, S. -I. Iwanaga, Y. Hayami, S. Uryu, and R. Matuura, J. Colloid Interface Sci., 80(1981)33.

53. K. Motomura, S. -I. Iwanaga, M. Yamanaka, M. Aratono, and R. Matuura, J. Colloid Interface Sci., 86(1982)151.

54. K. Motomura, M. Yamanaka, and M. Aratono, Colloid Polym. Sci., 262(1984)949.

55. K. Motomura, S. -I. Iwanaga, S. Uryu, H. Matsukiyo, M. Yamanaka, and R. Matuura, Colloids and Surfaces, 9(1984)19.

56. R. Nagarajan, *Micellisation of Binary Surfactant Mixtures: Theory*, in: Mixed Surfactant Systems, P.M. Holland and D.N. Rubingh (Eds.), ACS Symposium Series 501, ACS, Washington, DC, 1992, pp. 54-95.

57. N. Funasaki and S. Hada, J. Phys. Chem., 83(1979)2471.

58. H. Iyota, N. Todoroki, N. Ikeda, K. Motomura, and M. Aratono, J. Colloid Interface Sci., 208(1998)203.

59. M. Aratono, M. Villeneuve, T. Takiue, N. Ikeda, and H. Iyota, J. Colloid Interface Sci., 200(1998)161.

60. H. Iyota, T. Tomimitsu, K. Motomura, and M. Aratono, Langmuir, 19(1998)5347.

61. M. Aratono, M. Ikeguchi, T. Takiue, N. Ikeda, and K. Motomura, J. Colloid Interface Sci., 174(1995)156.

62. A.I. Rusanov and V.B. Fainerman, Dokl. Akad. Nauk SSSR, 308(1989)651, (in Russian).
63. V.A. Prokhorov and A.I. Rusanov, Kolloidn. Zh., 52(1990)1109 (in Russian).
64. G.D. Miles and L. Shedlovsky, J. Phys. Chem., 48(1944)57.
65. R.G. Alargova, K.D. Danov, J.T. Petkov, P.A. Kralchevsky, G. Broze, and A. Mehreteab, Langmuir, 13(1997)5544.
66. S. Lehmann, G. Busse, M. Kahlweit, R. Stolle, F. Simon, and G. Marowsky, Langmuir, 11(1995)1174.
67. J.R. Lu, E.A. Simister, E.M. Lee, R.K. Thomas, A.R. Rennie, J. Penfold, Langmuir, 8(1992)1837.
68. E.A. Simister, E.M. Lee, R.K. Thomas and J. Penfold, J. Phys. Chem., 96(1992)1373.
69. E.A. Simister, R.K. Thomas, J. Penfold, R. Aveyard, B.P. Binks, P. Cooper, P.D.I. Fletcher, J.R. Lu, and A. Sokolowski, J. Phys. Chem., 96(1992)1383.
70. J.R. Lu, E.A. Simister, R.K. Thomas and J. Penfold, J. Phys. Chem., 97(1993)6024,
71. J.R. Lu, Z.X. Li, J. Smallwood, R.K. Thomas and J. Penfold, J. Phys. Chem., 99(1995)8233.
72. J.R. Lu, Z.X. Li, R.K. Thomas and J. Penfold, J. Chem. Soc., Faraday Trans., 92(1996)403.
73. J. Penfold, E. Staples, L. Thompson, I. Tucker, J. Hines, R. K. Thomas, and J. R. Lu, Langmuir, 11(1995)2496.
74. J. Penfold, E. Staples, P. Cummins, I. Tucker, L. Thompson, R.K. Thomas, E.A. Simister and J.R. Lu, J. Chem. Soc., Faraday Trans., 92(1996)1773.
75. J. Penfold, E. Staples, L. Thompson and I. Tucker, Colloids Surfaces A, 102(1995)127.
76. G.R. Bell, C.D. Bain, Z.X. Li, R.K. Thomas, D.C. Duffy and J. Penfold, J. Am. Chem. Soc., 119(1997)10227.
77. V.B. Fainerman and S.V. Lylyk, Zh. Prikladnoj Chimii., 56(1983)2217, (in Russian).
78. P. Joos, *Dynamic Surface Phenomena*, VSP, Utrecht, 1999.
79. D.K. Owens, J. Colloid Interface Sci., 29(1969)436.
80. K. Tajima, M. Iwahashi and T. Sasaki, Bull. Chem. Soc. Japan, 44(1971)3251.
81. V.I. Kofanov, S.V. Rudenko and C.M. Levi, Kolloidn. Zh., 37(1975)172, (in Russian).

82. Z.N. Markina, N.M. Zadymova and N.N. Cikurina, Kolloidn. Zh., 40(1978)876, (in Russian).
83. E. Rillaerts, P. Joos, J. Phys. Chem., 86(1982)3471.
84. P. Joos, and J. Van Hunsel, Colloids Surfaces, 33(1988)99.
85. V.B. Fainerman and Yu.M. Rakita, Kolloidn. Zh., 52(1990)106, (in Russian).
86. Tz.H. Iliev and C.D. Dushkin, Colloid Polym. Sci., 270(1992)370.
87. V.B. Fainerman, Colloids Surfaces A, 62(1992)333.
88. V.B. Fainerman and A.V. Makievski, Colloids Surfaces A, 69(1993)249.
89. G. Geeraets, and P. Joos, Colloids Surfaces A, 90(1994)149.
90. A.V. Makievski, V.B. Fainerman and P. Joos, J. Colloid Interface Sci., 166(1994)6.
91. P. Petrov, and P. Joos, J. Colloid Interface Sci., 181(1996)530.
92. K.D. Danov, P.M. Vlahovska, T. Horozov, C.D. Dushkin, P.A. Kralchevsky, A. Mehretab, and G. Broze, J. Colloid Interface Sci., 183(1996)223.
93. J.V. Mitrancheva, C.D. Dushkin and P. Joos, Colloid Polym. Sci., 274(1996)356.
94. J. Lucassen, Faraday Discuss. Chem. Soc., 59(1975)76.
95. J. Lucassen and D. Giles, J. Chem. Soc. Faraday Trans. I, 71(1975)217.
96. B.A. Noskov, O.A. Anikeeva and N.V. Makarova, Kolloidn. Zh., 52(1990)1091 (in Russian).
97. D.O. Grigoriev, B.A. Noskov and S.I. Semchenko, Kolloidn. Zh., 55(1993)45 (in Russian).
98. D.O. Grigoriev, V.V. Krotov and B.A. Noskov, Kolloidn. Zh., 56(1994)637 (in Russian).
99. B.A. Noskov and D.O. Grigoriev, Progr. Colloid Polymer Sci., 97(1994)1.
100. B.A. Noskov and D.O. Grigoriev, Langmuir, 12(1996)3399.
101. B.A. Noskov, D.O. Grigoriev and R. Miller, J. Colloid Interface Sci., 188(1997)9.
102. B.A. Noskov, D.A. Alexandrov, V.V. Krotov and R. Miller, Kolloidn. Zh., 60(1998)204.
103. B.A. Noskov, D.A. Alexandrov and R. Miller, J. Colloid Interface Sci., 219(1999)250.
104. S.S. Dukhin, G. Kretzschmar and R. Miller, in: *Studies of Interface Science*, Vol. 1, D. Möbius and R. Miller (Eds), Elsevier, Amsterdam, 1995, 475 p.
105. B.A. Noskov, Adv. Colloid Interface Sci., 69(1996)63.

106. J.F. McKellar and J.H. Andreae, Nature, 195(1962)778; 195(1962)865.
107. S.D. Hamann, J. Phys. Chem., 66(1962)1359.
108. G.C. Kresheck, E. Hamori, G. Davenport and H.A. Scheraga, J. Am. Chem. Soc., 88(1964)246.
109. T. Yasunaga, H. Oguri, and M. Miura, J. Colloid Interface Sci., 23(1967)352.
110. R. Zana, J. Lang and C.R. Acad. Sci., Ser. C, 266(1968)893.
111. P.J. Sams, E. Wyn-Jones and Rassing, Chem. Phys. Lett., 13(1972)233.
112. T. Yasunaga, K. Takeda and S. Harada, J. Colloid Interface Sci., 42(1973)457.
113. R. Folger, H. Hoffmann and W. Ulbricht, Ber. Bunsenges Phys. Chem., 78(1974)986.
114. E.A.G. Aniansson and S.N. Wall, J. Phys. Chem., 78(1974)1024; 79(1975)857.
115. E.A.G. Aniansson, S.N. Wall, M. Almgren, H. Hoffmann, I. Kielmann, W. Ulbricht, R. Zana, J. Lang and C. Tondre, J. Phys. Chem., 80(1976)905.
116. E. Lessner, M. Teubner and M. Kahlweit, J. Phys. Chem., 85(1981)3167.
117. M. Kahlweit, Pure Appl. Chem., 53(1981)2069.
118. M. Kahlweit, J. Colloid Interface Sci., 90(1982)92.
119. E.A.G. Aniansson, in: *Aggregation Processes in Solution*, E. Wyn-Jones and J. Gormally (Eds.), Vol. 26, Elsevier, Amsterdam, 1983, p. 70.
120. Ch. Elvingsson and S. Wall, J. Phys. Chem., 90(1986)5250.
121. U. Kaatze, W. Berger and K. Lautscham, Ber. Bunsenges. Phys. Chem., 92(1988)872.
122. S.G. Oh. and D.O. Shah, Langmuir, 7(1991)1316.
123. Ch. Honda, Y. Hasegawa, R. Hirunuma and T. Nose, Macromolecules, 27(1994)7660.
124. E. Hecht and H. Hoffmann, Colloids Surfaces A, 96(1995)181.
125. W.A. Wan-Badhi, T. Lukas, D. M. Bloor and E. Wyn-Jones, J. Colloid Interface Sci., 169(1995)462.
126. R. Leung and D.O. Shah, J. Colloid Int. Sci., 113(1986)484.
127. T. Telgmann and U. Kaatze, J. Phys. Chem. B, 101(1997)7758; (1997)7766.
128. G. Waton, J. Phys. Chem. B, 101(1997)9727.
129. I. Goldmints, J.F. Holzwarth, K.A. Smith and T.A. Hatton, Langmuir, 13(1997)6130.
130. G. Waton, B. Michels and R. Zana, J. Colloid Interface Sci., 212(1999)593.

131. *Investigation of Rates and Mechanisms of Reactions*, G.G. Hammes (Ed.), John Wiley, New York, 1974, 716 p.
132. M. Eigen, in: *Investigation of Rates and Mechanisms of Reactions*, G. G. Hammes (Ed.), John Wiley, New York, 1974, p 79.
133. B.A. Noskov, Izv. AN SSSR, Ser. Fluid dynamics, N. 2(1989)105.
134. B.A. Noskov, Kolloid Zh., 52(1990)509; 52(1990)796.
135. A. Johner and J. F. Joanny, Macromolecules, 23(1990)5299.
136. C.D. Dushkin and I. B. Ivanov, Colloids Surfaces, 60(1991)213.
137. C.D. Dushkin, I.B. Ivanov and P.A. Kralchevsky, Colloids Surfaces, 60(1991)235.
138. C.D. Dushkin, Colloids Surfaces A, 143(1998)283.
139. C.-U. Herrmann and M. Kahlweit, J. Phys. Chem., 84(1980)1536.
140. S.G. Oh, S.P. Klein and D.O. Shah, AIChE J., 38(1992)149.
141. M.E. Cates and S.J. Candau, J. Phys.: Condens. Matter., 2(1990)6869.
142. M.S. Turner and M.E. Cates, J. Phys. France, 51(1990)307.
143. C.M. Marques, M.S. Turner and M.E. Cates, J. Chem. Phys., 99(1993)7260.
144. M.S. Turner, C.M. Marques and M.E. Cates, Langmuir, 9(1993)695.
145. B.A. Noskov, in: *Thermodynamic of Heterogeneous Systems and Theory of Surface Phenomena*, N. P. Markusin (Ed.), Publishing house of St. Petersburg State University, 1996, N10, P. 178.
146. R. Miller, Colloid Polym. Sci., 259(1981)1124.
147. V.B. Fainerman, Kolloidn. Zh., 43(1981)94.
148. V.V. Krotov, Kolloidn. Zh., 39(1977)48.
149. D.J. Evans, S. Mukherjee, D. J. Mitchell and B.W. Ninham, J. Colloid Interface Sci., 93(1983)184.
150. D.H.McQueen and J.J. Hermans, J. Colloid Interface Sci., 39(1972)389.
151. A.F.H. Ward and L. Tordai, J. Chem. Phys., 14(1946)453.
152. A. Petkova and C.D. Dushkin, Colloid Polym. Sci., 274(1996)952.
153. K.L. Sutherland, Austral. J. Sci. Res. A, 5(1952)683.
154. C.D. Dushkin, Tz.H. Iliev and Y.S. Radkov, Colloid Polym. Sci, 273(1995)379.
155. P.V. Danckwerts, Trans. Faraday Soc., 46(1950)300, 701(1950); 47(1951)1014.
156. C.D. Dushkin and Tz.H. Iliev, Colloid Polym. Sci, 272(1994)1157.

157. S-K. Chan, U. Herrman, W. Ostner and M. Kahlweit, Ber. Bunsenges. Phys. Chem., 81(1977)396.

158. S.S. Dukhin, V.B. Fainerman and R. Miller, Colloids Surfaces A, 114(1996)61.

159. V.I. Kovalchuk, S.S. Dukhin, A.V. Makievski, V.B. Fainerman and R. Miller, J. Colloid Interface Sci., 198(1998)191.

160. V.I. Kovalchuk and S.S. Dukhin, Colloids Surfaces A, (2001), in press

161. K.-D. Wantke, H. Fruhner, J. Fang and K. Lunkenheimer, J. Colloid Interface Sci., 208(1998)34.

162. B.A. Noskov and J. Loglio, Colloids Surfaces A., 143(1998)167.

163. S.G. Oh and D.O. Shah, J. Am. Oil Soc., 70(1993)673; Langmuir, 8(1992)1232.

164. S.G. Oh, M. Jobalia and D.O. Shah, J. Colloid Interface Sci., 155(1993)511.

165. B.A. Noskov, Kolloidn. Zh., 44(1982)492.

166. S.-K. Chan, U. Herrmann, W. Ostner and M. Kahlweit, Ber. Bunsenges. Phys. Chem. 81(1977)396.

167. U. Hermann and M. Kahlweit, J. Phys. Chem., 84(1980)1546.

168. B.A. Noskov, Colloids Surfaces A, 71(1993)99.

169. H. Hoffman, R. Nagel and G. Platz, Colloid Polym. Sci., 254(1976)812.

170. C. Tondre and R. Zana, J. Colloid Interface Sci., 66(1978)544.

171. T. Inoue, Y. Shibuya and R. Shimozava, J. Colloid Interface Sci., 65(1978)370.

172. St. Diekman, Ber. Bunsenges. Phys. Chem., 83(1979)528.

173. E.E. Dormidontova, Macromolecules 32 (1999) 7630.

174. A.I. Rusanov, F.M. Kuni, A. K. Schekin, Kolloidn. Zh., 62(2000)167.

175. F.M. Kuni, A.K. Schekin A.P. Grinin and A.I. Rusanov, Kolloidn. Zh., 62(2000)172.

This Page Intentionally Left Blank

6. THEORY AND PRACTICAL APPLICATION ASPECTS OF SURFACTANTS

B.E. Chistyakov

Scientific and production company 'SintezPAV', Rzhevskoe Chaussee 16,
309250 Shebekino - Belgorod Region, Russia

This first part of this chapter deals with the physicochemical basis of surfactant application, i.e. the effect of type and concentration of surfactants and their mixtures on the change of the interfacial nature, and the stability control of dispersed systems. Here, the stability of dispersed systems is discussed in two aspects. Aggregative stability means maintenance of the mean particle size of the dispersed phase. Disturbance of the aggregative stability of foams occurs as a result of coalescence and diffusive transfer processes. Simultaneously, disturbance of the hydrostatic stability of foams takes place, which consists in a redistribution of the liquid phase through the height of the foam column. The disturbance of aggregative stability of foams is due to flocculation, coalescence and diffusive transfer processes. Examples of stability control of dispersed systems under real application conditions are given. Main principles of surfactant action have also been formulated, e.g. in the flotation process and in detergency.

The second part of the chapter deals with the effects that are achieved when using surfactants to increase the standard of living of an individual - body care, enhancement of the action of pharmaceuticals, improvement of food quality (natural surfactants). Examples of the stability control of foams and emulsions using surfactant formulations as well as of the flow properties control of finished preparations are given.

The third part demonstrates the rapid expansion of surfactant applications in the process of the development of human civilisation starting from more than hundred years of experience of using surfactants in traditional fields (ore dressing, manufacture of textiles, fabrics, paints etc.) to novel applications (intensification of oil, gas and coal recovery) up to high-technology products (microelectronics, biotechnology etc.). In conclusion, ecological problems connected with the manufacture of surfactants and, simultaneously, the use of surfactants for liquidation of technologically induced catastrophes and natural disasters are analysed in brief.

6.1. INTRODUCTION

Historical information about the use of surface–active agents dates back to the pre–Christian time of the development of human civilisation [1, 2]. During several centuries natural surfactants were mainly used, i.e. fatty acid soaps prepared from vegetable oils (olive oil, coconut oil etc.) or vegetable extracts (e.g. liquorice root extract). Synthetic surfactants appeared in Germany in the twenties (ethoxylated surfactants) and thirties (alkyl benzene sulfonates) of our century. The application field of surfactants expanded rapidly and already in the late eighties surfactants were applied in households and more than 100 technical branches [3]. With the beginning of the trial production of so-called biosurfactants [4] a new boom of the expansion of surfactant application fields began. By now, surfactants are known to be used, according to some estimations, to solve more than 300 problems in household, science and technology. Hence, it is very difficult to completely present surfactants' application for which several principles are known. In the edition of the monographs "Surfactant Science Series" many authors have been presented their views to the scheme "manufacture—properties—use" both for conventional types of surfactants like anionics, cationics, nonionics, amphoterics, and special new types of surfactants [4, 5]. Such an approach cannot give a full idea of the application of surfactants or their mixtures. There is another approach, the consideration of formation and destruction conditions of one of the types of dispersed systems, for example foams, using different types of surfactants [6]. In this case, however, additional research on properties of surfactant properties is required. This chapter is an attempt of a complex approach to the description of surfactants' applications on the basis of their features. The material presents the physicochemical basis of surfactant application, the importance in foam, emulsion and disperse systems, their to meet the household needs of man, their role in the development of human civilisation, and finally the relationship of surfactants and ecology.

6.2. PHYSICOCHEMICAL BASES OF SURFACTANT APPLICATION

Versatility and application range of surfactants is due to their unique structure which distinguishes these substances in the big world of organic products. In general, the surfactant molecule is presented as a "match" or a "tadpole" — a rather long tail is connected to a big "head". However, such geometrical asymmetry reflects only to a very little degree the special features of the structure of surfactant molecules. In fact, the mean diameter of the "head" of

conventional surfactants, determined, in particular, by the area per molecule in the adsorption layer, is of the order of 1 nm which is much larger than the mean diameter of the hydrocarbon chain [7]. The difference between polarities of "head" and "tail" is more substantial, and Rehbinder was the first to draw attention to this fact [8]. This feature was further reflected in the development of the school on the hydrophilic–lipophilic balance (HLB), the essence of which is discussed in Section 6.4.

The physicochemical basis of surfactant applications are based on a number of rules which are well described in detail many times in the literature, for example in Moscow University publication [9].

6.2.1. Adsorption of surfactants and change of the interfacial nature

The means of determining the adsorption properties of surfactants depends strongly on the nature of the interface to be studied. This paragraph aims at a very brief summary of how the three general types of interfaces are modified by surfactants.

6.2.2. Liquid–gas interface

The general principles of the adsorption of surfactants at liquid/gas interfaces and the structure of adsorption layers are well described in detail for example in [10] as well as in Chapter 2. The main effect of adsorption is the substantial change of the interfacial pressure Π of a given interface. This property is described in a first approximation by the Langmuir- von Szyszkowski equation (2.16)

$$\Pi = \gamma_0 - \gamma = \frac{RT}{\omega_1} \ln(1 + b_1 c_1) \qquad (6.1)$$

The constant b_1 increases by a certain factor (essentially between 3 to 3.5) when the hydrophobic chain increases by one CH_2 group, which corresponds to the Traube rule.

The presence of ionic or nonionic hydrocarbon surfactants in the solution allows to lower the surface tension of water to 30—35 dynes/cm. These values are achieved at different bulk concentrations depending on the surfactant chain length. The ionic strength of the solutions has a substantial influence on the concentration at which micellisation sets in and a minimum interfacial tension is achieved. Principally lower values (to even below 20 dynes/cm) are achieved when using fluoro- hydrocarbon based surfactants. Micelle formation in surfactant

solutions is described in detail in [17]. The effect of micelles on the properties of interfacial layers is extensively discussed in Chapter 5. The effect of surfactants on l/g interfaces is of particular importance in the processes of foam formation, wetting, washing–off of dirt and flotation.

6.2.3. Liquid–liquid interface

The structure of surfactants determines considerably their behaviour at the interface between two immiscible liquids which differ considerably in their polarity. In practice, water or an aqueous electrolyte solution are most frequently considered as a polar phase, and hydrocarbons or their mixtures, e.g. oil fractions, as an apolar phase. In this connection, substances practically completely soluble in water are ascribed to the so–called water–soluble surfactants[i]. Typical anionics are, depending on the polar group type, alkali metal salts, with a hydrocarbon tail of a length of C_{12}—C_{18}. Magnesium salts of alkyl ethoxysulphates are also partly soluble. Bivalent and trivalent metal derivatives of the same anionics are typically ascribed to oil–soluble surfactants.

Nonionics like alcohol ethoxylates, alkylphenols and alkylolamides having an average hydrocarbon radical length of C_{12}—C_{16}, products containing up to 4 EO moles are ascribed to oil–soluble, those containing over 10 moles as water–soluble and those with 4 to 10 EO moles to water–oil–soluble. In this case, the surfactant is distributed between aqueous and oil phases. A quantitative characteristic of this process is the distribution coefficient $K = c_w / c_o$ where c_w is the surfactant concentration in the aqueous phase and c_o is the surfactant concentration in the oil phase. The value of K is considerably influenced by temperature, oil–phase polarity and electrolyte content in water [13, 14]. The basic rules are observed when water–soluble surfactants adsorb at a water/hydrocarbon interface (Szyszkowski equation, Traube rule etc.) similarly to the processes taking place at liquid–gas interfaces. The kinetics of adsorption can however change totally, as it was demonstrated theoretically and by experimental examples in Section 4.4. Note, that the adsorption of oil–soluble surfactants at the surface of hydrocarbons is weak and changes only slightly with the chain length in a homologous series.

---

[i] Not only aqueous surfactant solutions of low concentration are meant, but also micellar solutions at c » CMC.

One of the principal distinction between the liquid–liquid and liquid–gas interface is the possibility to achieve very low interfacial tensions down close to zero. This possibility is realised provided the surfactant is soluble both in the aqueous and hydrocarbon phase, as well as using binary mixtures of water–soluble and oil–soluble surfactants. This phenomenon is of special importance for the formation of emulsions and microemulsions, in the removal of dirt and in the enhanced oil recovery.

6.2.4. Liquid–solid interface - wetting phenomena

The nature of surfactant adsorption on solid surfaces depends on the polarity and solubility of the surfactant. Thus, when an aqueous surfactant solution is in contact with non-polar coal particles, adsorption layers are formed which have polar groups oriented towards the aqueous phase. In contrast, surfactant solutions in oils (hydrocarbons, vegetable oil oxidation products etc.) in contact with polar materials or powders (carbonates, silicates) the polar groups are on the solid phase surface.

These general concepts of colloid chemistry have an important exception connected with chemisorption processes. Thus, when carboxylic acid soaps (e.g. sodium oleate) are incorporated into an aqueous chalk suspension, adsorption layers are formed on the chalk particles, in which the hydrocarbon chains are oriented to the aqueous phase.

Adsorption (as well as chemisorption) processes can lead to a drastic change of the surface nature, i.e. its hydrophilisation or hydrophobisation (oleophilisation). A criterion of the surface nature is the wetting contact angle θ. When a drop of a liquid is applied on a solid surface, then three different interfaces are formed (Fig. 6.1) with the corresponding tensions γ_{sg}, γ_{lg} and γ_{sl}.

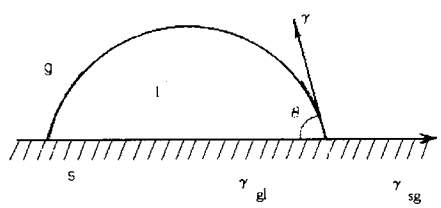

Fig.6.1 Equilibrium of surface tension forces on wetting perimeter

The angle θ between the liquid–gas (lg) and solid–liquid (sl) interfaces is called contact angle. The equilibrium condition of the interfacial tension forces is expressed by the Young equation

$$\gamma_{sg} = \gamma_{sl} + \gamma_{gl} \cos \theta \qquad (6.2)$$

The following three main variants can be observed here:

1. Wetting (or partial wetting) of the interface by the liquid at $\theta < 90$ deg.; $\cos\theta > 0$; the surface is regarded as hydrophilic (oleophobic);
2. Non–wetting ("bad" wetting) at $\theta > 90$ deg; $\cos\theta < 0$; the surface is regarded as hydrophobic (oleophilic);
3. "Complete wetting", or spreading, where the contact angle approaches zero (or no contact angle exists), and the liquid spreads into a thin film.

A more detailed description of wetting and spreading mechanisms is given in [10, 15], and peculiarities of wetting for water–imbibing surfaces are shown in [16]. In all cases, the dynamic nature of the processes is emphasized here. The contact angle is rather the cause than the effect of wetting which consists in displacement of s/g surfaces by s/l surfaces. In practice, experimental values of contact angles formed by a water droplet on a given surface in air are used to determine the nature of the surface.

The modern assortment of commercial surfactants allows to regulate very effectively the nature of a solid surface. This is important practically for all fields of surfactants' application, especially in washing and flotation processes, oil recovery, preparation of filled polymers and paints.

6.3. SURFACTANTS IN FOAM FORMATION AND FOAM DESTRUCTION PROCESSES

Foam is a disperse system in which the dispersed phase is a gas (most commonly air) and the dispersion medium is a liquid (for aqueous foams, it is water). Foam structure and foam properties have been a subject of a number of comprehensive reviews [6, 17, 18]. From the viewpoint of practical applications, aqueous foams can be, provisionally, divided into two big classes: dynamic (bubble) foams which are stable only when gas is constantly being dispersed in the liquid; 2) medium and high–expansion foams capable of maintaining the volume during several hours or even days. In general, the basic surface science rules are established in foam models: foam films, monodisperse foams in which the dispersed phase is in the form of spheres (bubble foams) or polyhedral (high–expansion foams). Meanwhile, "real" foams are considerably different from these models. First of all, the main foam structure parameters (dispersity, expansion, foam film thickness, pressure in the Plateau–Gibbs boarders) depend

considerably on the dispersion medium parameters (surfactant and electrolyte contents, viscosity, etc.) as well as on the conditions of gas dispersion in the medium. In particular, real foams exhibit a considerable polydispersity. Therefore, main attention is paid here to the effect of the concentration of surfactants and other components on the formation and stability of real forms. Non–aqueous foams which are described in quite detail in [6] exhibit special properties.

6.3.1. Foam formation

As a measure of foam stability, the rate of foam formation W_p^0 was proposed when a foam is produced [19]. This parameter can be determined experimentally on the basis of consideration of the balance of air volumes used to obtain the foam.

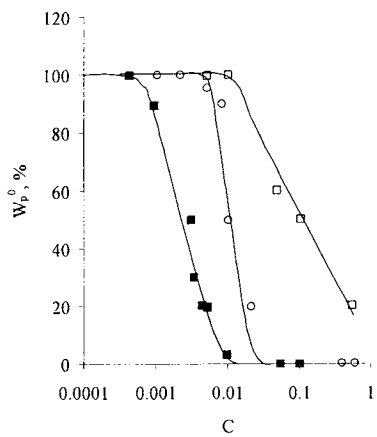

Fig. 6.2 Foam formation isotherms of aqueous surfactant solutions, foam formation rate W_o = 0.83 cm²/s; ■ – C_{10}-C_{13} sodium alkyl ethoxy sulphate, O - sodium lauryl sulphate, □ – lauryl ethoxy sulphate

Under condition of a small liquid contents in the foam, within the period of time t under air supply into a volume V_1, where a volume V_2 of foam was produced, and the volume V_3 of foam was collapsed:

$$V_1/t = V_2/t + V_3/t. \tag{6.3}$$

Then, V_3/t is the velocity of collapse in the process of foam formation, and V_1/t is the rate of foaming. Thus, V_3/t is the rate of foam decay in the process of its formation W_p^0. Hence we can write

$$W_p^0 = W_o - V_2/t. \tag{6.4}$$

It follows that if the foam does not decay during foam formation ($W_p^0 = 0$), then $W_o = V_2/t$, and the volume of the foam formed is determined by the volume of air blown in. A constant build-up of the foam volume is observed in the course of the experiment. When no formation of an appreciable foam volume is observed, $W_p^0 = W_o$.

Investigations have shown that, at a constant foaming rate, the foam volume measured within a fixed period of time depends on the surfactant concentration. At low concentrations, the foam volume is low due to high W_p^0 values. With increasing surfactant concentration $W_p^0 \rightarrow 0$, the foam volume increases during the whole period of time proportionally to the volume of air introduced. For low surfactant concentrations, at the change of the foaming rate (W_o), the angle of slope of the linear relationship W_p^0 (W_o) is determined by the surfactant concentration in the foaming solution. At some minimum surfactant concentration, $W_p^0 = W_o$ is reached, and no measurable foam volume is formed in the experiment.

With the increase of the foaming rate W_o, the foam cell size increases which is especially appreciable at low surfactant concentrations. In a foam obtained from a highly concentrated solutions, for which under experiment conditions, $W_p^0 = 0$ throughout the entire range of the W_o change, the cell size changes little (diameter 3 to 4 mm) increasing with the W_o growth. As the concentration diminishes, this difference becomes more and more significant. It should be noted that at low foaming rates ($W_o = 0.65$ cm^3/s) there is practically no change of cell sizes with diminishing solution concentration.

The foam collapse rate W_p^0 as a function of surfactant concentration can be called foam formation isotherm (Fig. 6.2). As it is seen from Fig. 6.2, that W_p^0 sharply increases in a narrow concentration range below adsorption layer saturation. The W_p^0 value can thus be a characteristic of the aggregation stability of foams during the formation process.

For the evaluation of the foamability of a surfactant the bulk concentration is used at which the relative rate of foam collapse is equal to 50% of its formation (c_W^{50}). The c_W^{50} values determined from foam formation isotherms of a number of products are given in Table 6.1. As it is seen, typical representatives of anionics (sodium dodecyl sulphate), cationics (cetyl trimethyl ammonium bromide) and nonionics (ethoxylated alkylphenols) give bubble foams at very low concentrations, and the foam stability of ionic surfactants does not differ much from that of nonionics. For anionics, the highest concentrations are required for soaps of higher carboxylic acids.

Table 6.1 c_W^{50} values of some selected surfactants

Surfactant	c_W^{50} [wt.%]
Sodium oleate	0.1
Sodium dodecyl sulphate	0.044
Cetyl trimethyl ammonium bromide	0.005
C_{10}—C_{13} sodium alkyl ethoxysulphates	0.003
Na ABS	0.01
Ethoxylated Alkylphenols (Neonol AP—15)	0.004

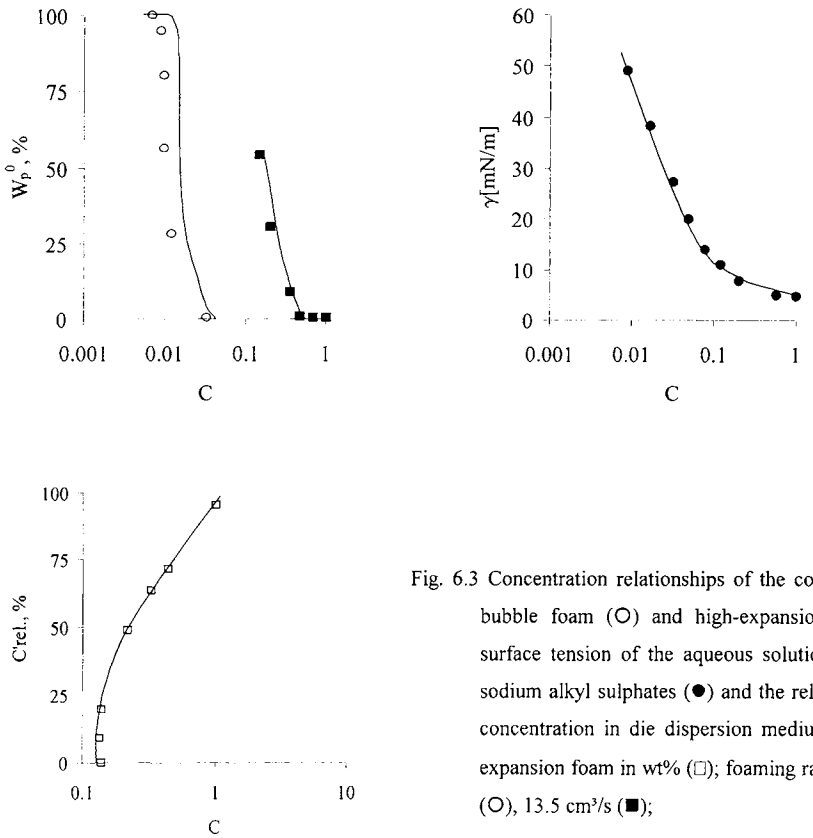

Fig. 6.3 Concentration relationships of the collapse rate of bubble foam (○) and high-expansion foam (■); surface tension of the aqueous solution of C_{10}-C_{13} sodium alkyl sulphates (●) and the relative residual concentration in die dispersion medium of a high-expansion foam in wt% (□); foaming rate 0.83 cm³/s (○), 13.5 cm³/s (■);

It is interesting to compare the concentration regions of the formation of bubble and high–expansion foams (Fig. 6.3). As noted above, bubble foams are formed at surfactant bulk concentrations lower than the concentration of the adsorption layer saturation (Curve 1). At the same time, high–expansion foams are formed at concentrations much higher than the CMC. Thus, for example, for foams with a foam–expansion value of 140, an appreciable decay in the process of formation begins already in the region of $c \approx$ CMC (Curves 2 and 3), and a stable formation ($W_p^0 = 0$) is observed at concentrations of the studied sodium alkyl sulphate 1.5 times higher than the CMC.

The study of electrolyte effects on the surfactant behaviour in aqueous solutions has shown that even for industrial surfactants which are mixtures of homologues the electrolyte effect on c and CMC is significant. At a sodium chloride concentration of 100 g/l the CMC of sodium alkyl sulphates decreases by more than one order of magnitude. Relatively small electrolyte additives (up to 10 g/l) increase the stability of foams, i.e. an increase of W_p^0 is observed at lower bulk surfactant concentrations. However, a subsequent increase in electrolyte concentration produces practically no influence on W_p^0. As noted above, an appreciable volume of bubble foam is produced not only at $W_p^0 = 0$, but also in the entire interval $0 < W_p^0 < 100$. Throughout the whole concentration range, the addition of electrolyte lowers the W_p^0 value by 20—30 %. For example, while there is practically no foaming ($W_p^0 = 95$ %) at 0.0045 wt% of C_{10}—C_{13} sodium alkylsulphates in distilled water, the W_p^0 value falls to 60 % with the addition of sodium chloride up to the concentration of 10 g/l and the formation of an appreciable amount of foam is observed in the experiment.

Investigations of the electrolyte effect on the formation of high–expansion foams from sodium alkylsulphate solutions shows (Fig. 6.4) that the W_p^0 value decreases when 10 g/l of sodium chloride is added. While a stable foaming is observed up to the foam expansion of 200 at foamer concentrations of 0.3 weight % in absence of sodium chloride, the foams show $W_p^0=0$ up to a foam ratio of 350 in the presence of 10 g/l electrolyte. However, in contrast with the bubble foams, further addition of electrolyte causes a sharp increase in W_p^0. At 120 g/l NaCl, the formation of foams having a foam expansion higher than 150 becomes impossible at all.

The addition of electrolyte into a foamer solution reduces its molecular solubility and leads, as a result, to a sharp increase in the W_p^0 value. On the other hand, in the concentration range studied, there is a transition of foam films from a higher thickness to common black films, and then to Newton black films [17]. Such a transition corresponds to an increase of the lifetime of the films as investigated by the Scheludko technique.

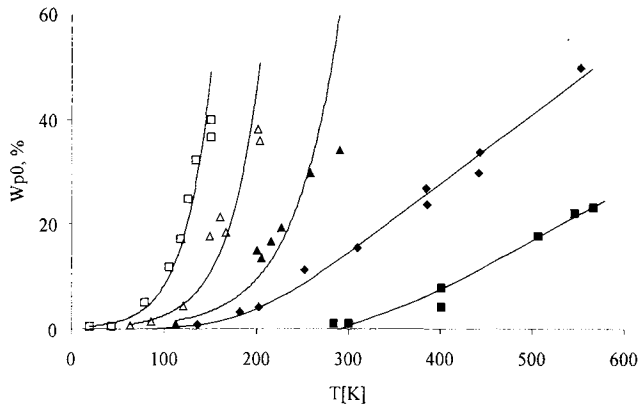

Fig. 6.4 Effect of NaCl on the formation of high-expansion foams from 0.3% sodium alkyl sulphate solution of; foaming rate W_0=12.8 cm³/s, c_{NaCl} = 0 (◆), 10 (■), 30 (σ), 50 (Δ), 120 (□) g/l

Thin films are highly susceptible to outer influences which, under the conditions of a dynamic structure of high–expansion foams, leads to an increase in the rate of foam decay as the electrolyte concentration increases. This is obviously due to the determining contribution of the foam rupture to the stability of the foam structure at its formation which is confirmed by a typical "crack" observed when foam is generated from solutions having a high electrolyte content. This phenomenon is not observed in absence of electrolyte.

6.3.2. Surfactants and foam stability control

A number of fundamental works are dedicated to the investigation of foam stability [6, 17] but the interest of the investigators in this problem is persistent, which is evidenced by recent review papers, e.g. [20]. In this section data are given which can be of interest for the practical application of foams. First of all, several processes take place simultaneously in real foams, which lead to foam collapse. The main processes are redistribution of the disperse medium in differently high foam column layers and the change of the mean radius of the foam cells [12].

The result of these processes is a gradual decrease in the foam column height (H) in a "layer–wise" foam collapse or a "avalanche –like" decay of the foam volume when reaching a critical size of the polyhedral foam cells.

Under hydrostatic foam stability the redistribution of the dispersion medium in foams is meant with a simultaneous consideration of gravitation and capillary forces. The ideas of hydrostatic foam stability were for the first time formulated, independently of each other, by three Russian (at the end of the 70–ties of the 20th century) and further developed by Krotov (cf. [11]). For a foam in a gravitational field, the behaviour of the liquid is determined by a relationship between the liquid pressure gradient in the Gibbs–Plateau channel P_G and ρg, where ρ is the density of the liquid; g is gravitational acceleration. For $\rho g > dP_G/dH$, a drainage of the liquid takes place, with a drainage rate proportional to the difference of $\rho g - dP_G/dH$. For $\rho g < dP_G/dH$, the liquid moves against the gravity force – suction of liquid. In the hydrostatic equilibrium between capillary forces and gravity, the corresponding condition is

$$dP_G/dH + \rho g = 0. \qquad (6.5)$$

When this condition is met, the liquid in the foam is redistributed due to its drainage from the films and disappearance of a part of the Gibbs–Plateau channels.

The redistribution of the liquid between the films and the Gibbs– Plateau channels ("microsyneresis" of a foam) occurs rather rapidly. Estimations show that, for bubble and high–expansion foams, 90 % of liquid flows from the films into the channels within the first few minutes after formation. The film thickness (h) decreases as result of the microsyneresis, which leads to the disturbance of the aggregative foam stability. It should be noted that the microsyneresis can be much slower for high–dispersion (R=0.1—0.5) "spumoid" foams. "Macrosyneresis", or "drainage", i.e. flow of liquid out of the foam due to gravitational forces is described in [6, 11] in detail. Additives inhibiting syneresis are described in [24] in detail, and they can be, provisionally, divided into two groups. The first group is formed by water–soluble polymers, biopolymers, high–concentration surfactant solutions ($c \gg CMC$), liquid crystals, whose use leads to an increase in the viscosity of the dispersion medium. The second group involves additives enhancing physico-mechanical properties of the foam films – amine oxides, higher alcohols, alkylolamides of higher aliphatic acids and others. These additives substantially increase the aggregative foam stability.

The aggregative foam stability is manifested in changes of the foam dispersity. There are two main causes of aggregative foam stability disturbances: a) coalescence of foam cells due to the rupture of bilateral films separating them; b) disappearance of foam cells due to gas penetration from small cells into larger ones (Ostwald ripening).

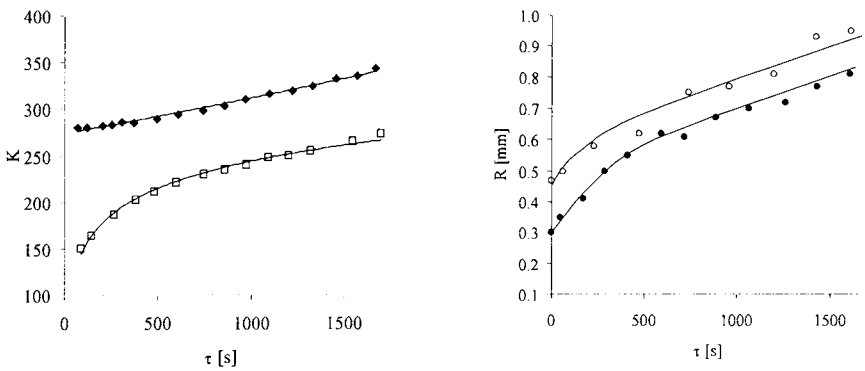

a) b)

Fig. 6.5 Comparison of local expansion and dispersity kinetics in foams; Surfactant : C_{10}-c_{13} sodium alkylsulphates; a) mean initial foam expansion K = 260 (◆), 90 (□) , b) mean equivalent foam cell radius R = 0.48 mm (○), 0.22 mm (●)

Real foams differ from models in their remarkable polydispersity as we noted above. Another feature of real foams is the considerable changes in their structural parameters (film thickness, Plateau—Gibbs channel radii etc.) typical of the first temporal stages after formation. In this connection, we further use, rather provisionally, the terms "rapid" or "slow" coalescence, although there is a high probability that the change of dispersity occurs as a result of diffusion as well. Fig. 6.6 represents typical relationships between foam cell number n_s and time for high–expansion foams produced from 1 % aqueous C_{10}—C_{13} sodium alkylsulphate solutions (Curves 1—3). Similar kinetic curves have also been obtained for foams from solutions of other foaming agents in the expansion range between 50—600. As it is seen from Fig. 6.6, the kinetic curves are composed of two portions. The first portion depends of the foam expansion, so that their values decrease with the increasing expansion. It should be noted that similar kinetic curves (see Fig. 6.5, Curve 4) are described in [25] for low–expansion foams having an

mean cell radius of 100 μm, produced by whipping from 1.5 % aqueous dodecyl benzene sulfonate solution. The slope determined from $dn_s/dt(n_s)$ can be referred to rapid and slow coalescence constants k_1 and k_2, respectively, and considered as measure of the aggregative foam stability [26].

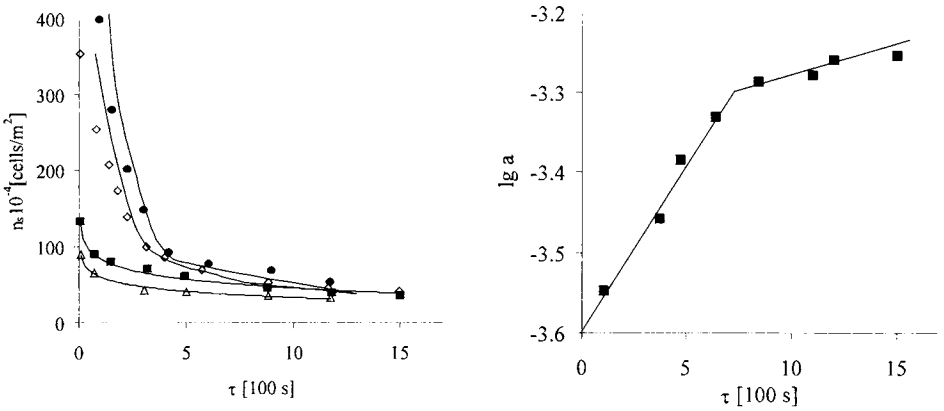

a) b)

Fig. 6.6 Kinetics of the change of cell number n (a) and dispersity parameter in foams (b); mean initial expansion K of the foams: 90 (Γ), 230 (■), 420 (Δ), data from [25] (●), b) – data from [17]

The study of changes in the foam dispersity with time has shown that the linear function $\lg \overline{R}(t)$ describes experimental data well. The relationship $\lg \overline{R}(t)$ is composed of an initial range of rapid growth of the mean equivalent cell radius and an extended range of slow growth (Fig. 6.6, Curves 3 and 4). The plot of data [20] in the co–ordinates of $\lg \overline{R}$ — t has shown that the same rule describes the change of low–expansion foams. A similar relationship [17] corresponds to the change of the length of the foam column with time for the foams collapsing under the conditions of increased pressure in the Plateau — Gibbs boarders (see Fig. 6.6, Curve 5). Hence, the value τ_R as the period of stable foam dispersity, calculated from the slope of the $\lg \overline{R}(t)$ relationship can also be proposed as an aggregative stability criterion.

The change of foam expansion with time depends on the initial expansion of the foam obtained (Fig. 6.5, Curves 1 and 2). The foams of initially higher expansion than the equilibrium expansion are characterized by the presence of a horizontal initial area on the lg K(t) curves, while those of lower expansion than the equilibrium expansion exhibit an initial range

characterized by a steeper slope. The exponential form of K(t) allows to estimate the τ_K value, i.e. the period of the foam stability by expansion, as an aggregative stability characteristic, which is determined in a similar way as τ_R.

The rapid coalescence can proceed differently, depending on the foam structure parameters (see Fig. 6.5). For foams whose initial expansion is higher than the equilibrium expansion, the decrease in dispersity does not lead to a local expansion change. Those foams the expansion of which is lower than the equilibrium expansion are characterized by a simultaneous sharp increase in the mean equivalent cell radius and the local expansion. For foams whose expansion is higher than the equilibrium expansion obtained experimental data indicate that the rapid decrease in foam dispersity corresponds to the time before the establishment of hydrostatic equilibrium when there is a rapid outflow of the dispersion medium from a low–expansion foams and its redistribution through the foam column height.

Experimental values of aggregative foam stability characteristics are presented in Table 6.1. The rate constants of rapid and slow coalescence can be assigned, in accordance with the above considerations, to hydrostatically non–equilibrium and equilibrium conditions, respectively.

Table 6.1 Aggregative foam stability characteristics

Foaming agent *	Mean expansion $\bar{K}$	Coalescence rate constants $10^{-3}s^{-1}$		Stability periods 10^2 s	
		rapid k_1	slow k_2	dispersity τ_R	expansion τ_K
C_{10}—C_{13} sodium alkylsulphates	100	4.7	0.83	36	32
	200	3.2	0.80	34	32
	300	3.8	0.7	34	43
	400	4.8	0.44	—	46
AS + 0.1 wt.% of C_{10}—C_{14} higher alcohols	100	1.7	0.43	74.5	—
	200	1.1	0.37	108	91
AS + 0.1 wt.% of carboxymethyl cellulose	100	1.4	0.38	35	23
	200	6.4	0.4	42	34
	400	5.6	0.5	49	44
C_{10}—C_{13} sodium alkyl ethoxy sulphates; 1 wt.% in aqueous solution	100	1.9	0.7	28	33
	300	1.9	0.6	30	—
	400	1.8	0.3	22.6	—

For slow coalescence, the proximity of τ_R and τ_K indicates that the main part of the dispersion medium separates from the local volume on account of the cell growth due to rupture of the foam films. The introduction of stabilisers like higher aliphatic alcohols reduces k_1 and k_2 values almost double. The higher alcohols stabilise the foams in a wide expansion range while water–soluble polymers are effective only for low–expansion foams. The type of foaming agent also produces a considerable influence on the aggregative foam stability. For example, sodium alkyl ethoxysulphates give more stable foams as compared with sodium alkylsulphates in the expansion range studied, which is especially seen from the values of k_1.

Under practice conditions, the foam stability depends on the nature of the surface in contact with the foam. Foam–hydrocarbon liquid interactions are best studied [27], and it has been shown that hydrocarbons should be dispersed in an aqueous phase to prevent a foam collapse, i.e. it is necessary, in parallel with the foam formation, to produce stable oil–in–water emulsions (or microemulsions) in order to avoid any contact of the foam films with the hydrocarbon droplets.

There is less information available about the effect of air humidity on the foam stability. The experimental data obtained in [28] clearly show that even a slight undersaturation of air leads to a sharp acceleration of foam collapse (see Fig 6.6). The relationship of lg H — τ is linear, and the slope depends on the air humidity. Note that creation of relative humidity of about 100% leads to a foam column which practically does not fall, while the foam dispersity decreases. For a considerably decreased humidity (~ 40%), the foam column collapsed within a short period of time.

The study of aggregative foam stability has shown that the change of the mean equivalent radius in the foam volume is

$$d\overline{R}/d\tau \sim \overline{R}. \qquad (6.6.)$$

The introduction of the probability of rupture of bulk as well as surface films J_s, the foam column height decrease rate $dH/d\tau$ can be compared with the foam dispersity change rate.

The rate of foam column height change is determined by the product of the number of surface films (i.e. films in contact with the outer medium) $n_s \approx 1/\pi R^2$ multiplied by the average change of the column volume ($4/3\ \pi \overline{R}^3$) and the probability of the rupture J_s

$$\frac{dH}{d\tau} = \frac{4}{3}\overline{R}^3 \frac{1}{\pi \overline{R}^2} J_s \sim \overline{R} J_s . \qquad (6.7)$$

On the other hand, $d\overline{R}/d\tau \sim \overline{R}\ J_v$. Hence we get

$$\frac{dH/d\tau}{dR/d\tau} \sim \frac{J_s}{Jv} . \qquad (6.8)$$

Thus, the relationships of rate of foam column height change and rate of dispersity change depend on the probability of the rupture of surface films and bulk films. If $J_s \approx J_v$, then the change of the column height occurs together with the change of the foam cell size. In this case, there is little change of the foam column height, while the foam dispersity can change drastically. It is just this what occurs when foam is collapsed in a closed volume or in the atmosphere having the air humidity close to 100 %. But if there is an intensive collapse of the foam column with time without any appreciable change of the foam cell size, then $J_s \gg J_v$, i.e. the probability of the rupture of outer surface films in contact with the medium is much higher than that of the rupture of films in the foam bulk.

It is important, from a practical point of view, that extremely thin black films are ruptured under the condition of reduced humidity, since evaporation of the dispersion medium leads to their ultimate thinning and appearance of high de– wedging pressures. Here are two possibilities to produce stable (under the conditions of dry air) foams. On the one hand, this is reduction of permeability of adsorption layers for water vapours and thus inhibition of the evaporation rate. On the other hand, it is the use of surfactants for foam stabilisation leading to the formation of a structure–mechanical barrier, i.e. gel–like interlayer.

Such low–permeable layers can be formed not only on account of high–molecular surfactants. It has been shown in [29] that the adsorption layer permeability of proteins (bovine serum albumin, gamma–globulin) and lauryl sulphate, determined by loss in weight of the evaporating film, is practically the same. Addition of higher alcohols to alkyl sulphates enhances the foam stability under dry air conditions. When lauryl alcohol was added to dodecyl sulphate, it turned out that the life time of the foam increased by 10 to 20 % at reduced air humidity. Note that this effect is more pronounced at maximum undersaturation of air by water vapours.

A foam stability control is also possible by using so–called "antifoamers" which are added when foam is produced, or "defoamers" which are used to destroy the produced foam. These phenomena are described in [17, 30] in more detail, and we shall describe them in the corresponding sections dealing with the application of surfactants.

6.4. *SURFACTANTS AND CONTROL OF EMULSION PROPERTIES*

During the last 30 years, the application spectrum of emulsions has become considerably broader. To avoid detailed enumeration of their applications, it is enough to say that without emulsions it is impossible today to imagine such areas as pharmaceutical industry, oil recovery, polymer production and a large number of other fields which will be discussed in the subsequent chapters in more detail. At the same time, our knowledge of emulsion properties has become broader and deeper, too. Following the classical studies by Becher [31] and Sherman [26] in the sixties, broad reviews have been published in the recent years, dealing with emulsion application theory and practice [33—35]. Detailed analyses have been carried out on the use of emulsions in food industry [36] and in oil recovery and oil refinery [37, 38]. Special properties and efficient application conditions for microemulsions were subject of reviews [39—41]. Considering all this, it seems important to outline the concepts of structure and principles of emulsion stability control using surfactants, which will facilitate the further discussion of surfactant applications.

6.4.1. Emulsion structure and stability

Emulsions are disperse systems which are formed by two condensed immiscible liquid phases differing in polarity. Depending on which liquid is the disperse phase, real emulsions are divided into two big groups—type I, o/w emulsions, and type II, w/o emulsions. Except the pair of liquids water –oil, considerably differing in their polarity values (ε_1) and (ε_2), emulsions can form from other liquids, but in all cases to type I belong the emulsions in which the low–polar phase forms the disperse phase in the polar dispersion medium. Finally, in some cases, so–called multiple emulsions of two types, namely o/w/o or w/o/w, can be produced. In addition to the polarity differences of the dispersion medium (DM) and disperse phase (DP), the emulsion structure and properties are considerably influenced by density and viscosity of the liquids as well as by the volume fraction V_2 of DP in DM. The quantitative value of V_2 is a criterion to sort out three emulsion types which belong to w/o and o/w types. Emulsions having

V_2 = 0.01—0.3 are commonly regarded as dilute systems and the DP droplets have a spherical form. In the following range of V_2 = 0.2—0.74 [42—44], a mutual contact of the emulsion droplets is observed provided they maintain their spherical forms, but the bulk packing of the spheres undergoes changes ranging from a cubic to a dense cubic one, like a honeycomb. For real emulsions exhibiting considerable polydispersity, "contraction" of the emulsion droplets and formation of polyhedral structures instead of a dense packing of spheres is observed for $V_2 \geq 0.9$ and each droplet comes into a close contact with the others and cannot move because of room limitation.

Another important emulsion structure parameter is the mean diameter of the droplets ($\bar{d}$) which determines their dispersity. It is common to call disperse systems having $\bar{d} \geq 0.1$ μm among the so–called "macroemulsions'. Microemulsions are thermodynamically stable disperse systems; many investigators name them homogeneous, others consider them "microheterogeneous" [39—41]. Achievement of extremely low (γ < 0.1 mN/m) interfacial tensions is a prerequisite to obtain microemulsions.

Aggregative stability of emulsions consists in maintaining their dispersity, i.e. constancy of $\bar{d}$. Loss of aggregative stability leads to a change in the sedimentation stability. Disturbance of "aggregative stability" may result in a total decay of the system into two layers or formation of "cream" (for w/o emulsions) as well as sedimentation with an elevated disperse phase content (for o/w emulsions). In either of the cases, the emulsions become unusable for practical application. According to modern concepts [34—45], the aggregative emulsion stability is destroyed as a result of coalescence processes (coagulation), flocculation and diffusive transfer (Ostwald ripening).

The coalescence rate, i.e. formation of larger droplets after collision of two droplets, depends on the number of collisions and on the properties of the adsorption layers. For dilute emulsions, as well as emulsions having V_2 = 0.3—0.74, coalescence is the main process leading to the disturbance of their aggregative stability. Hence, prerequisite for the production of appreciable volumes of any type of emulsions suitable for practical application is provision of their coalescence stability. In case of o/w emulsions, maximum stability against coalescence is achieved through the formation, on the surface of the disperse phase particles, of structured adsorption layers, a structure–mechanical barrier defined by Rehbinder [8]. Such layers are

formed when using water–soluble, natural and synthetic, polymers and—in some cases—typical amphiphilic surfactants. For w/o emulsions, of which water–crude oil emulsions can serve as typical examples, ultimate coalescence stability is provided due to the formation of fast layers of natural crude–oil surfactants, solid emulsifiers, as well as the joint presence of the two components.

In case of a constant contact of emulsion droplets, which is typical of highly concentrated systems, diffusive transfer (isothermal distillation, recondensation, Ostwald ripening) is of great importance, along with coalescence. This phenomenon has been extensively studied in [46—47].

At every given moment of time, there are particles of critical radius (R_{cr}) in the emulsion, the other particles decreasing in size at $R_1 < R_{cr}$, while the particles $R_2 > R_{cr}$ are growing. On the other hand, the recondensation rate depends on the content of impurities in the disperse phase and its solubility in the dispersion medium. It has been established in an investigation of emulsions of hydrocarbons (hexane, octane, decane, and others) and perfluorodecalin ($V_2 = 0.1$), stabilized by dodecyl sulphate and EO/PO block-copolymer Proxanol P–26R, that the growth rate is proportional to the mean radius $\overline{R}^3$ which is in agreement with the Lifshits–Slezov theory. It turned out that even at small solubilities (10^{-5}—10^{-8} vol. %) of the disperse phase in water, there is isothermal distillation in highly disperse emulsions. Since the diffusion processes are characterized by a long duration (up to hundreds of hours) due to the peculiarities described above, it should be recognized that their most substantial contribution to the general process of reduction of the dispersity of the system will be observed during the ultimate coalescence stability and high dispersity.

The flocculation process is less investigated with respect to emulsions, especially water–in–oil emulsions. According to the DLVO theory [48] the aggregation stability of a disperse system is determined by the sum of energy of ion–electrostatic repulsion (U_i) and Van–der–Waals attraction (U_m)

$$U = U_m - U_i . \qquad (6.9)$$

The terms of this sum depend on the distance (h) between the particles, U_m falling proportionally (h^{-2}) with increasing distance, while U_i decreases exponentially. There are, as a rule, two minima in the energetic curves reflecting the interaction between two particles as a

function of the distance: a near (primary) and a far (secondary) minimum, as well as an energy barrier. Three forms of U(h) relationships reflecting the possibility of coexistence of three states of the system are possible [49]. The first, unstable, state is observed if at all distances the attractive forces dominate over the repulsive forces, or if the energy barrier is comparable with the thermal energy of the particle movement kT. In this case, there is a rapid aggregation of particles in the primary minimum, two cases being possible as to the emulsions. When approaching, two droplets come into contact with each other under formation of a film whose rupture leads to coalescence and complete stratification of the system. In the other case, if the emulsion droplets are stabilized against coalescence by fast interfacial layers and there is an interlayer of the dispersion medium left between them, then sufficiently large aggregates, floccules, can be formed when the droplets are approaching each other.

The second, unstable, state can be realized if the secondary energy minimum is deep enough, and the repulsion barrier is well above kT (usually $\geq$ 15 kT).

The aggregative stability of w/o emulsions, as it has been stated until recently, is related first of all to the presence of a structure–mechanical barrier as well as a steric factor. This is mainly due to a low dielectric permeability of hydrocarbons and, as a result of it, to their small ionisation. It is shown in an investigation by Bedenko [50], that the main process disturbing their aggregative stability is flocculation, i.e. the formation of floccules—large compact aggregates whose sizes are one order of magnitude larger than the droplet size of the initial emulsion. This results in a loss of sedimentation stability due to a rapid sedimentation of the floccules in the gravitational field. In the following section, two ways of prevention of flocculation of w/o emulsions will be shown: a) using additives ionising in a hydrocarbon medium; b) using surfactant mixtures whose optimum ratio leads to a maximum lyophilisation of the droplet surface. At the same time, analysing the recent experimental and theoretical works [51], it can be concluded that the classical DLVO theory reveals a low predicting power for emulsions.

6.4.2. Peculiarities of surfactants selection for emulsion stabilisation

The problem of selecting a surfactant for an effective emulsion stabilisation has already been intensively discussed for more than 80 years after the publication of the classic work by Bancroft [33]. This rule which in some papers [52] is referred to as a "thumb rule" gives a

rather simple recommendation: to produce o/w emulsions, one has to use surfactants preferably soluble in the water phase, and, to produce w/o emulsions, surfactants soluble in the non-polar hydrocarbon phase. Further [52, 53], the HLB theory has received wide application. According to Griffin's concept, an optimum surfactant structure or an optimum ratio of two surfactant types for a given emulsion type can be determined from the table values both for surfactants' HLB and for the "required" HLB (HLB_r) for a given disperse phase. This approach is widely used for the selection of emulsifiers in pharmaceutical and other industries. However, as it was noted in [52], the temperature effect on the surfactant properties is not taken into consideration. A further development of Shinoda's concept by Davies [52] is based on the distribution of surfactants between the phases as a function of the Phase Inversion Temperature PIT and the micellar behaviour of surfactants in solution. At temperatures below TIP, nonionics, most commonly used in practice, are distributed preferably in the aqueous phase, primarily in the form of micelles solubilising a considerable amount of oil. At temperatures above TIP, nonionics in micellar form are in the non-polar (oil) phase with an appreciable amount of water solubilised. From this the emulsion type and stability can be determined. Not only the temperature, but also the electrolyte content in the aqueous phase, as well as the polarity of the oil phase controlled by organic additives (e.g. aliphatic alcohols), produce a certain influence on the distribution of nonionics between the phases. It was shown for example in [53] that the emulsion stability of xylene is influenced by the charge of the droplets.

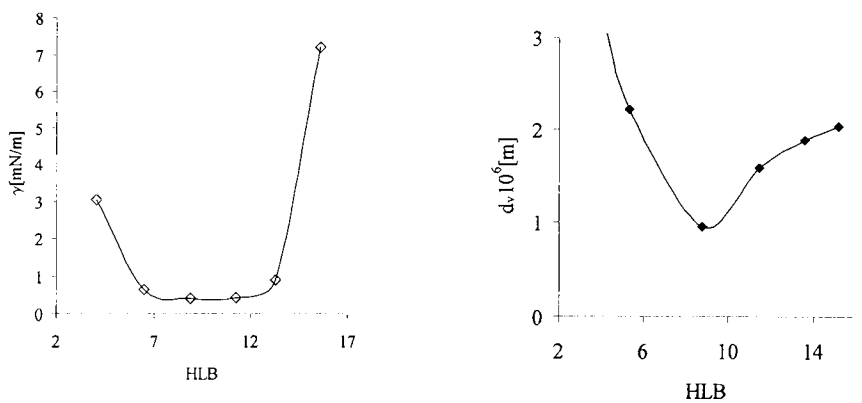

Fig. 6.7 Interfacial tension γ (a) and mean droplet diameter $\bar{d}$ (b), of a decane in water emulsions as a function of the HLB of the emulsifier mixture Span 80/Tween 80 (total 0.5 wt%)

Using the HLB system for the characterisation of surfactants, a minimum interfacial tension is observed when the HLB_r is reached. Fig. 6.7 shows, as an example, the interfacial tension and the droplet size in emulsions of decane and sunflower oil, respectively, as a function of the HLB. For decane, the minimum γ value and the minimum size of emulsion droplets are observed in the region of HLB ~ 9; and for sunflower oil around 11, which corresponds to the required HLB values. Apparently, one of the reasons leading to an increase in emulsion stability when reaching HLB_{tp} is the increase of emulsion dispersity under conditions of the maximum decrease in interfacial energy.

Two processes take place simultaneously in the emulsion formation: a) dispersion of one liquid in another; b) coalescence, i.e. irreversible fusion of two or more droplets and formation of a larger one. The coalescence proceeds in several subsequent stages [54]: formation of a thin film as result of droplet contact, "thinning" of the film, and its rupture when achieving a critical thickness. The role of the surfactant concentration in the formation of emulsions can be demonstrated using as an example sunflower oil emulsions stabilized by potassium monododecyl phosphate (see Fig. 6.8).

The emulsions were prepared on an ultrasonic disperser, coalescence stability was determined from the volume of the separated oil phase after 24 hours. As it is seen from Fig. 6.8, a complete coalescence stability of the emulsions is achieved at surfactant concentrations beyond the CMC. At the same time, the concentration at which the maximum coalescence stability is achieved is not sufficient to provide sedimentation stability of the emulsions.

The maximum sedimentation stability is achieved at C > CMC. After the CMC, the emulsion droplet size decreases in accordance with the rate of interfacial tension decrease. Increase in sedimentation stability is observed in accordance with increasing degree of dispersity.

These data proof the need of using surfactants at C » CMC. The "excessive" bulk concentration of surfactants is required not only for an effective decrease of γ but also for the formation of a protective adsorption layer after the abrupt increase in interfacial area caused by the growing number of small size droplets. Thus, emulsions formed with typical surfactants behave towards sedimentation stability similar to those stabilized by natural surfactants. In this respect the advantage becomes better understandable of the so–called "true", i.e. micelle–forming, surfactants as compared to the surfactants unable to form aggregate. "True" surfactants not

only do form gel–like protective layers but they also provide for some "reserve" of surfactants due to the presence of micelles in the dispersion medium. This "reserve" allows to reduce the interfacial tension and to form a protective layer while the degree of dispersity of an emulsion increases. In absence of such a surfactant "reserve", i.e. of non-colloidal surfactants dissolved in the dispersion medium, stable emulsions cannot be obtained.

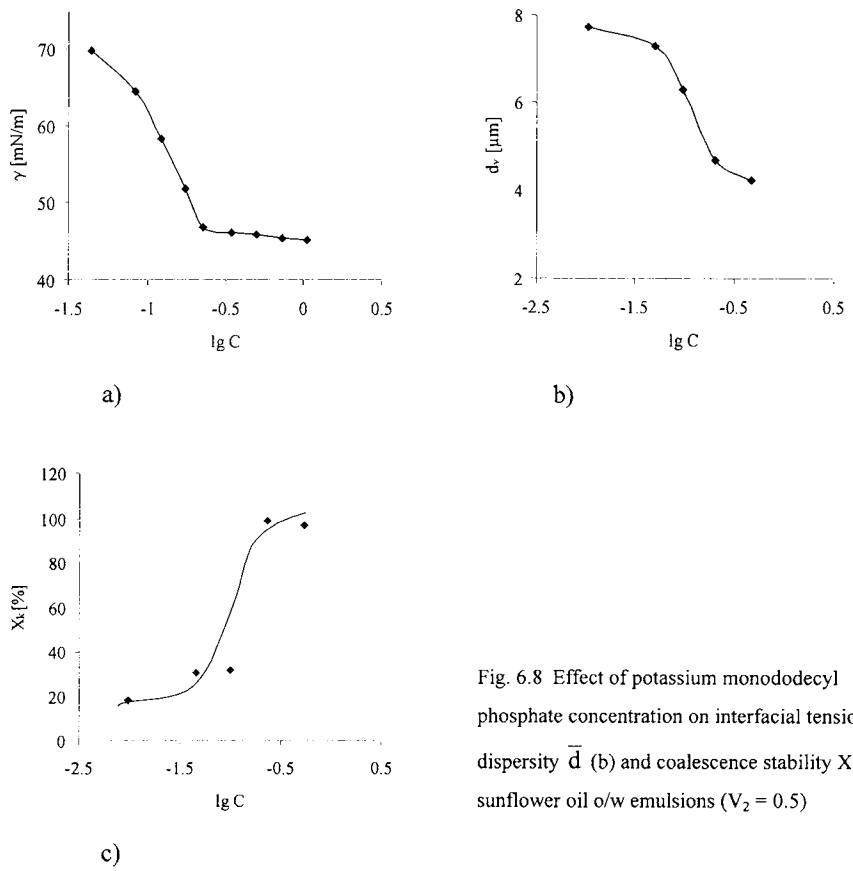

Fig. 6.8 Effect of potassium monododecyl phosphate concentration on interfacial tension γ (a), dispersity $\bar{d}$ (b) and coalescence stability X_K (c) of sunflower oil o/w emulsions (V_2 = 0.5)

Another technique to increase sedimentation stability of emulsions is viscosity control of the disperse phase. It is noted in [31—32, 35] that the viscosity of the disperse phase influences the stability of o/w emulsions. The effect of the disperse phase viscosity of various nature on the mean size $\bar{d}$ of the emulsion droplets is clearly seen from Fig. 6.9. The change of the nature of high–viscosity hydrocarbon component (decane, toluene, MS–20 oil) has no substantial effect

on the emulsion dispersity. At the same time, for all phases, the emulsion droplet size shows a linear increase with increasing viscosity.

The surfactant concentration has a great effect on the decrease in the dispersity degree of the emulsions. An abrupt decrease in the droplet size becomes appreciable with addition of even small surfactant amounts—0.25% of ethoxylated alkylphenol. This dispersity increase unequivocally leads to an increase in sedimentation stability.

The appreciable influence of the viscosity decrease on the droplet size decrease at small additives of a surfactant stabiliser is caused not only by the increased dispersion degree due to the decreasing interfacial tension, but prevents also coalescence of droplets. The increase of the surfactant concentration, after a certain limit, practically without influencing the coalescence, leads to an increase of dispersity due to a reduced interfacial tension.

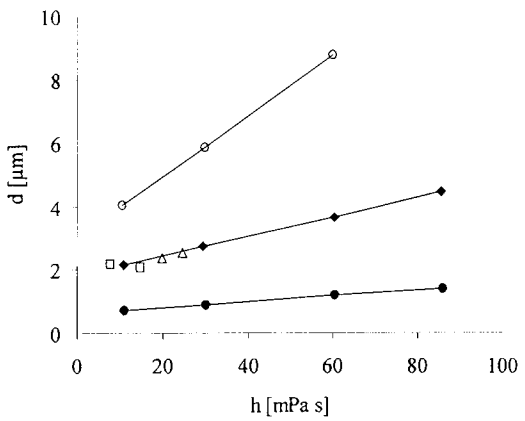

Fig. 6.9 Average size $\bar{d}$ of the emulsion droplets (V_2=0.4) as a function of the hydrocarbon phase viscosity; Neonol AF–12 concentration: 0.25 wt.% (○); 0.5 wt.% (◆); 1.0 wt.% (●), oil phase composition: MC-20 oil + spindle oil (○, ◆, ●); MC–20 oil + decane (Δ); MC–20 oil + toluene (□)

The increase of the Neonol concentration from 0.5% to 1% in the system aqueous AF–12 Neonol emulsifier solution–decane leads to an interfacial tension decrease from 3.2 to 2.3 mN/m. Thus, the viscosity decrease of the disperse phase due to the introduction of low–viscosity components leads, under equal dispersion conditions, to a linear droplet size reduction which is especially appreciable for low surfactant concentrations. After the emulsion

is stabilized against coalescence, the decrease in dispersity is determined by the interfacial tension reduction.

Preparation of diluted o/w emulsions for high–viscosity oils is connected with substantial difficulties. The following procedure is suggested in [56]. At high concentrations of nonionics or their mixtures with anionics, a storage–stable w/o emulsion is prepared. For direct use, this emulsion undergoes phase–inversion by adding water. This technique was used to emulsify silicon oils, however, it can also be used for hydrocarbon oils to prepare cutting oils, plant protection compositions and others.

There are other methods to control the stability of emulsions during formation. The effects of temperature, dispersion rate, phase introduction period on the emulsion stability are studied in [51]. It has been shown that the way of cooling influences the emulsion stability, which is first of all connected with structural changes in the surfactant solutions.

The main process disturbing the aggregative stability of w/o emulsions is flocculation, i.e. formation of large compact aggregates which rapidly sediment in the gravity field [50, 58]. Two variants are proposed to increase the aggregative stability of w/o emulsions: a) use of oil–soluble surfactants and their mixtures with water–soluble surfactants; b) introduction of stabilizing additives which are able to enhance the electrostatic repulsion of the droplets.

Water–in–heptane emulsions ($V_2 = 0.1$) produced by means of an ultrasonic disperser and stabilized by this type of surfactants exhibited an extremely high coalescence stability. No aqueous phase separation in form of large droplets within a long period of time (several months) was observed.

Considering that flocculation parameters were measured within 30 minutes, conditions were created where there was practically no change in the number or size of the particles. The aggregative emulsion stability changed in this case only due to the flocculation of single droplets whose size was practically constant.

The change of the flocculation degree is particularly considerable with increasing concentration of oil–soluble surfactants, such as Span–80 (see Fig. 6.10). While at a Span–80 concentration of 0.4 wt% the emulsion is practically completely flocculated, increasing concentration to 1.15 wt% leads to a flocculation degree less than 0.1%. The same rule of the change of the flocculation degree is observed for emulsions stabilized by pentol. At 0.3 wt%

pentol the flocculation degree is 0.93, while at 2 wt% the emulsion obtained is practically non–flocculated ($F \approx 0.03$).

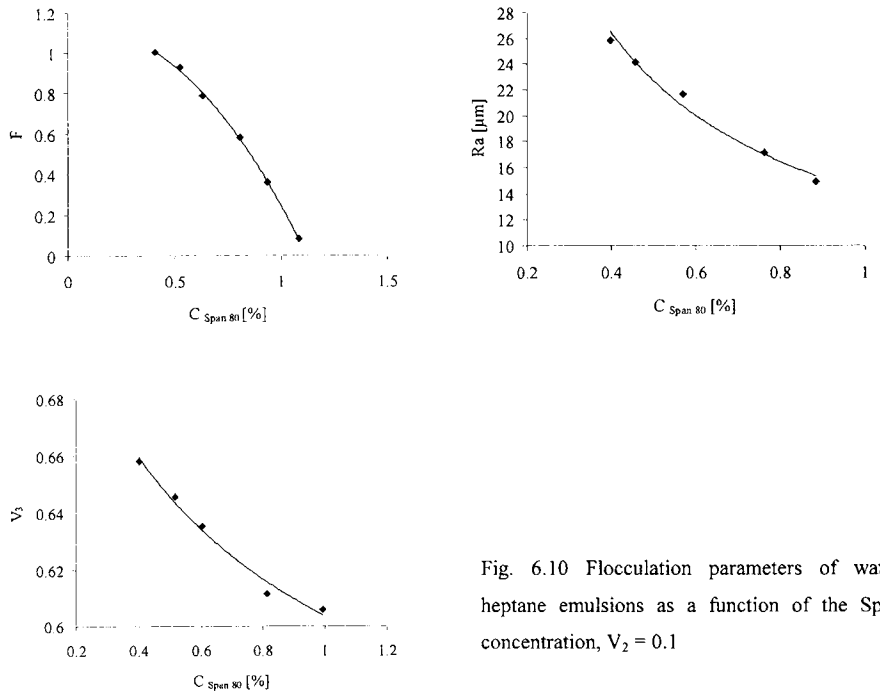

Fig. 6.10 Flocculation parameters of water-in-heptane emulsions as a function of the Span-80 concentration, $V_2 = 0.1$

It is important to note that flocculation develops at practically the same emulsion dispersity for all water–in–heptane emulsions stabilized by an oil–soluble nonionic and the resulting droplet radius is about 0.35 μm.

It is common to use mixtures of two surfactants for emulsion stabilisation. The rules of emulsion flocculation with binary mixtures of water–soluble and oil–soluble surfactants have been investigated at constant total surfactant concentration. The water–soluble component was introduced into the bidistilled water, and the oil–soluble component was introduced into the hydrocarbon phase. When using binary mixtures pentol–Tween–80 to stabilise water–heptane emulsions ($V_2 = 0.1$) (cf. Fig. 6.11), the minimum flocculation degree (F=0.05) is achieved at a pentol : Tween ratio of 6:4 (total surfactant concentration is 1 wt%). Note that, at the given surfactant ratio, the emulsion droplet radius is 0.27 μm as compared with R=0.37 μm for

emulsions stabilized with pentol alone. In this case, the radius of the floccules decreases from R_a=13 μm (for 1% pentol) to 7 μm for the optimum pentol–Tween ratio.

Note that the minimum flocculation degree value is observed at the same surfactant ratios at which the minimum interfacial tension value is achieved. This makes clear the previously known facts about the increase of the emulsion stability at low γ. This occurs, first of all, due to an appreciable decrease in the flocculation degree up to its complete suppression. These phenomena result in an increase in the sedimentation stability both for non–flocculated emulsions (dispersity increase) and partly flocculated emulsions (decrease in flock size and flocculation degree).

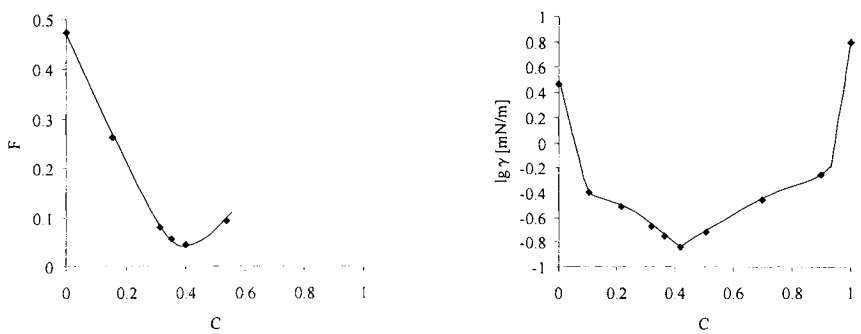

a) b)

Fig. 6.11 Flocculation degree (a) for emulsions with V_2 = 0.1 and interfacial tension γ (b) as a function of the emulsion composition

The flocculation inhibition in the presence of oil–soluble surfactants accounts for the electrokinetic repulsion of water droplets in hydrocarbons due to the presence of the ζ-potential. This potential, according to Bedenko, can acquire positive values up to 30 mV at Span–80 concentration increasing up to 1%, and, when chromium stearate is added to the oil-soluble surfactants, even up to ~ 50 mV. The diffusion layer in hydrocarbon media is characterised by a considerable amorphousness and the Debye length $æ^{-1}$ is around 1 nm, thus comparable with the distance between the emulsion droplets.

Table 6.2 presents data on the sedimentation stability of emulsions stabilised by some typical nonionics as an example of efficiency of flocculation inhibition using chromium stearate additives as antiflocculant.

Table 6.2. Effect of antiflocculation additive ($CrSt_3$) on sedimentation stability of water–Diesel fuel emulsions stabilised by nonionics

Nonionic and its concentration, wt.%	Sedimentation stability (hours)	
	No additive	$CrSt_3$ (0.05 %)
Sorbitane monooleate, 1.0 %	0.1	10 5
Pentol, 1.0	0.1	
Pentol P–12–15–6 1.0	0.05	5
Pentol P–12–15–6 0.6.	0.1	30

One can see that surfactants like esters of monobasic alcohols and higher acids give water–in–hydrocarbon emulsions the sedimentation stability of which is 3—5 minutes. Application of an antiflocculation additive leads to a significant increase in sedimentation stability of up to 10 hours. Note that emulsions stabilised by a nonionic like Span have a high coalescence stability: there is no aqueous serum separated as a continuous layer within several months.

From this point of view, polyethylene glycol ethers of higher alcohols or alkylphenols like Neonol P1215–6 (oxo synthesis of higher alcohols C_{12}—C_{15} with 6 EO) have a broader industrial basis. In addition to the oxo synthesis of higher alcohols C_{12}—C_{18} obtained by other methods can be used to obtain this type of surfactants. However, this type of products forms emulsions having a low coalescence stability and an aqueous serum is formed within few days.

Satisfactory emulsion stability results are observed when using a three–component emulsifier: B1215–6 (0.7 wt.%) + sorbitane oleate (0.3 wt.%) + chromium salts of C_{17}—C_{20} synthetic fatty acids (0.1 wt.%). Such emulsions do not cream within 10 to 30 days, and their sedimentation stability is 30—50 hours.

6.5. SURFACTANTS IN MULTIPHASE DISPERSED SYSTEMS

The previous sections dealt with physicochemical basis of properties control in dispersed systems such as foams (g/l system) and emulsions (l1/l2). Under real conditions, one has to do with multiphase systems, in which the dispersed system is characterised not only by the presence of three phases (l, s, g), but also by a multicomponent composition. From our

viewpoint, the most frequently investigated system are the flotation process and the detergency of surfactants. Physicochemical aspects of other applications will be also discussed below.

6.5.1. Surfactants in flotation

From a technological and economical point of view, the final goal of a flotation process is the separation of useful components from the initial mineral raw materials. Such useful components are minerals containing ferrous and non-ferrous metals, the so–called "ore–free" fossils (fluorite, apatite etc.) as well as graphite and coal. The flotation separation technology comprises the following main stages: a) grinding of initial raw materials and preparation of ore pulp; b) froth flotation producing a concentrate; c) concentrate condensation. Surfactants are used at different concentrations in all process stages.

The key stage of the entire process is a selective wetting of one of the components of the ore pulp with its subsequent concentration in the foam layer ("direct" flotation) or in the chamber product ("inverse" flotation). The physicochemical basis of flotation were formulated in the thirties–fifties of the last century [59—60] and further subjected to more specific investigations. Plenty of chemical and colloid-chemical processes take place simultaneously in the flotation pulp during a rather short period of time (usually several minutes), the main of which are:

1) adsorption of surfactants at l/g and l/s_1, l/s_2 and l/s_3 interfaces, meaning that solid phase particles (s_1, s_2, s_3, and so on) having a dispersity from 5 to 500 μm differ substantially in their nature.

2) Dispersion of air and solid particles as a result of simultaneous mechanical and interfacial tension forces at l/g and l/s interfaces.

3) Interaction of surfactants with ions present in the flotation pulp.

4) Contact of a hydrophobic solid particle with an air bubble, sticking to the bubble and transportation of mineral particles into the foam layer.

5) Aggregation (flocculation) of solid particles, formation of large (flock–like) aggregates, contact of these aggregates with air bubbles and formation of a three–phase flotation foam.

Selectivity of the flotation process is determined by both selective hydrophobisation of mineral particles and conditions of their aggregation, stability and conditions of destruction of three–phase flotation foams.

The conditions of air dispersion during flotation followed by the formation of two–phase and three–phase foams have been investigated by Aleinikov [61] and Ershkovskij [62] more in detail. It has been shown [61] that at certain concentrations of a low–molecular (non-micelle–forming) surfactant, e.g. isoamyl alcohol, air bubbles of minimum size are formed under comparable conditions of mechanical action. The minimum (at a constant total air volume fed into the flotation chamber) bubble size produces, first of all, an influence on their volume fraction in the flotation pulp and, therefore, also on the probability of bubble–mineral particle contacts. In [62], the effect of organic (thiourea, terpineol, phenol etc.) and inorganic compounds on the stability of the flotation foams were investigated. Both aliphatic polybasic alcohols (n–propanol, i–propanol, n–butanol), dibasic alcohols (ethylene glycol) and cyclic alcohols (phenol, terpineol and others) give sufficiently stable foams, the foam stability being increased, independent of the alcohol structure, as the liquid/gas interfacial tension value decreases. A special attention was paid to both the so–called "catalysts" and "poisons" of the foams. Thus, thiourea added at 0.003–0.008 wt. % to 2 % n–propyl alcohol solution increased the foam stability from 20 s to several minutes. Finely dispersed suspensions of sulphide minerals, e.g. molybdenum sulphide and others, sharply increase the foam stability which is very important in their selective flotation.

As a result of these works, the so–called "frothers", i.e. surfactants which preferably adsorb at l/g interfaces and practically do not influence the nature of l/s surfaces, were sorted out from the class of flotation agents.

However, more than 50 years later, some of the details of the formation of flotation foams continue to be investigated. In a recent review [63], two types of frothers were compared: Dowfroth MIBC (lower ketones with admixed alcohols and aldehydes) and Triton X–100. The rising velocity of bubbles in flotation columns depended on the frother type to the extent to which their inhibition factor rose which is due to the difference of the type of adsorption layers at the l/g interfaces. In [64], the effect of similar frothers on the bubble rise velocity (from 0.9 to 2.7 mm in size) was investigated in flotation columns as a function of the frother

concentration and the height of the bubble rise. The achievement of a constant (final) velocity independent of the frother concentration was a special feature of dynamic foam formation in the presence of frothers.

The bubble size has a substantial effect on the flotation rate of small particles [65]. A computer analysis of the relationship of the flotation rate of micron and submicron size particle has shown that this relationship does not depend on density and viscosity of the medium but is determined by the relationship of the sizes of bubble and floated particle.

Not less complicated processes are observed in the interaction of flotation agents with finely dispersed solid particles. A special class of the so–called collecting agents is singled out which selectively adsorb on the particles flotated. Classically, three main adsorption mechanisms are pointed out here: 1) the so–called "physical" adsorption occurring due to the opposite electrokinetic potential values of the solid particle and the nature of the surfactant ion; 2) "chemical" adsorption occurring due to the chemical reactions of surfactant ions with the surface ions of the particles flotated; 3) formation of complex compounds on the surface.

There was a lively discussion during many years between supporters and opponents of the first two theories, but the analysis of recent time literature shows that, depending on the conditions, both processes and their combinations are possible in real flotation processes.

Most common is the theory of chemisorption of collectors at the surface of solid particles. However, it is, as a rule, at the same time noted that simultaneously concurrent processes take place, which are connected both with adsorption of surfactants at l/g interfaces and with their interaction with ions in the flotation pulp. Thus, it is shown in [66] that saturated C_{12}—C_{14} fatty acids are selectively "chemisorbed" on calcium carbonate surfaces which provides them with an effective hydrophobisation. At the same time, C_5—C_6 acids are adsorbed mainly at l/g interfaces which produces a substantial influence on the stability of the flotation foams. Free and Miller [67] have thoroughly investigated the behaviour of sodium oleate in the flotation of a calcium mineral, fluorite. It has been established that calcium dioleates are formed both in the bulk and at l/s interfaces. In this case, an effective hydrophobisation of the surface of fluorite particles takes place both due to the interaction of oleate with calcium ions on the "active" sites and by adsorption of calcium dioleates formed in the solution. It has been once more confirmed [68] that classical collecting agents, xanthogenates, e.g. ethyl xanthogenate, form on the

surface of sulphide minerals (chalcopyrite etc.) copper xanthogenides which are further oxidised to dixanthogenides, thus providing a high degree of hydrophobicity to the mineral particles which contributes to the increase in flotation selectivity.

In case of using mixtures of two and more collectors, the selective hydrophobisation is accomplished simultaneously both due to chemisorption and physical adsorption. It is shown in [69] that the simultaneous use of fatty acids and hydrocarbon oils for calcium phosphate flotation from quartz different processes are observed. Fatty acid soaps form chemical compounds on the surface of the material floated, after which the hydrocarbon oil physically adsorbs. It has been experimentally established that hydrocarbon oil is transferred from quartz particles to the surface of floated phosphate. When using mixtures of anionics and nonionics, hydrophobisation of particle surfaces is also accomplished both due to the formation of chemical compounds and physical adsorption which is confirmed by measurements of the zeta–potential of the particles floated [70].

In the second half of the sixties, a new "paradigm" was formed, which says that collecting agents form "complex" structures on individual areas of l/s interfaces. In this aspect, the selectivity of the surface ion–aqueous solution ion interaction was based on the ideas of the classical analytical chemistry of solutions.

For this reason, we consider it hardly possible to cite all of the publications. Let us focus only on the following examples. Hydroxamic acids have already been for a long time subject of the classical analytical chemistry. In [71], the possibility of using these compounds in flotation of rare–earth minerals is shown. It has been concluded that on a mineral surface cerium chelates are formed. Besides, chemisorption is accompanied by a physical multilayer adsorption of hydroxamic acid derivatives formed by reaction with cations in the water phase. A number of chelate–forming compounds including hydroxamic acids has been tested in flotation of niobium ores [72]. The best results are obtained when using alkyl phosphonic acids. Chemisorption mechanism and the structure of the surface compounds are established by spectroscopic methods.

Physical adsorption of collectors at the surface of floated particles is very rarely observed in a "pure form". This phenomenon is especially typical of cationics which form positively charged ions in aqueous solutions. Therefore, cationics are used in the so–called "inverse" flotation of a

number of minerals when the polar component remains in the "chamber" product and quartz or other silicium oxides are extracted into the foam product.

A relatively new field is the use of flotation in wet textile processes [73]. The ζ–potential of cotton fibres in aqueous solutions is negative, therefore they are effectively floated by cationics like quaternary ammonium salts, e.g. dodecyl trimethyl ammonium chloride. Sysilia et al. [74] have established, by measuring the electrokinetic potential, a clear rule between the positive surface charge of chromite and flotation efficiency. At low pH, chromite was effectively floated by fatty acid soaps, the ions of which are negatively charged under these conditions. The surfactant adsorption is reversible which is indicative of its physical nature.

This section describes only the influence produced on the flotation process by two main surfactant types—foamers and collectors. Meanwhile, there is a complex of compounds used in real processes: pH adjustment, hydrophilisation of surfaces, water "softeners", high–molecular compounds (flocculating as well as deflocculating agents), and others. The choice of flotation modes and "bouquets" of reagents is determined in every particular case depending on mineral composition of raw materials (nature of solids), water quality, aeration intensity and other factors.

6.5.2. Detergency of surfactants

As noted earlier, mankind has used washing products for more than 4000 years, including synthetic ones starting from the twenties of the 20th century [1]. The general physicochemical principles of surfactant detergency were formulated for the first time by Rehbinder [75]. Later on, the role of individual washing actions was discussed in [76, 77] in more detail. An attempt was made in a popular–scientific edition by Abramzon to generalize in short the existing views [78]. The washing action mechanism in non–aqueous surfactant solutions used in the so–called dry cleaning are discussed in [79]. Despite the great progress made in the field of investigation of surfactant solutions, formation and properties of adsorption layers, role of surfactants in stabilisation of dispersed systems, all investigators recognize that there is up to now no strict theory of surfactant detergency. Nevertheless, the following elementary actions in the process of soil removal are generally accepted: 1) surface wetting by the washing solution and displacement of the dirt from the surface; 2) dispersion (in case of liquid impurities—

emulsification and solubilisation) of soils and their transfer into the solution bulk; 3) retention of dirt in the solution and prevention of re-deposition on fabrics.

The role of the individual acts depends, as a rule, on the surface polarity and its "porosity", and the nature of the surface. In view of the wide use of washing processes, surfaces to be washed can be glass, metals (both as starting materials and after coating with paints), porcelain, artificial and synthetic fabrics, human skin and hair.

Peculiarities of using detergents for cosmetic and personal care purposes are in detail discussed by Pletnev [80]. It is noted, in particular, that in case of using detergents for these purposes a complete removal of soils from the human skin can result in its dryness and dermatitis.

Wetting is generally accepted to be in all cases the primary action for the detergency to be accomplished. In general, this process consists in displacement of soils from the surface with the change of solid/soil interface to solid/washing solution interface. Rehbinder [75] underlined the special importance to the formation of surfactant adsorption layers close to saturation both on the surface to be washed and on the soil particles. This leads to a gradual increase in the wetting contact angle (see Fig. 6.1) followed by tearing of liquid soil from the surface. When reaching ultra–low interfacial tensions at solution/soil interfaces the respective surface is ultimately modified.

Views similar to those given above were formulated later by Adam [81] who suggested the so–called roll–up mechanism. According to this theory further developed later by Thompson [82], the balance of surface forces is changed on the contact line "oil (i.e. soil)–surface–water" on adding surfactants which leads to an increase in the contact angle in the oil phase and tearing of the droplet from the surface when stirring in the washing bath. Thus, attention was paid in [82] to the role of hydraulic forces in washing off soils. However, in some cases, part of the soil remains on the surface which requires additional mechanical energy [83].

The nature of the surface produces a substantial influence on washing. Kissa [16] analysed in detail the phenomena of wetting and capillary "suction", i.e. impregnation of fabrics. On this basis, it is possible to assume the degree of complication of the mechanism of washing–off impurities which have to be removed not only from the "surface" of the fabric but also from its inner parts. It was also shown that effective washing depends on the nature of soil adsorption on fabrics [84]. For example, in the sequence polyester–cotton–nylon the affinity of coffee

stains to fabric increases, and formation of chemisorption compounds is observed on nylon. In this case, the use of conventional detergent compositions will have no success, and chemical processes must be used, e.g. "bleaching", i.e. oxidation of soils using perborates. By the way, note that bleaching agents are necessary components of practice for all detergents.

Emulsification is the most important act of the washing process. To prevent secondary soil deposition, formation of a coalescence–stable low–concentration emulsion is needed. As it is shown above (see section 6.4), the formation of such an emulsion is possible under real conditions considering the surfactant concentration in the washing solution and hydrodynamic conditions of the soil deposition process. As far as solid soils are concerned, the process of dispersion of particles is important here. To prevent their re-deposition on the surface washed, water–soluble polymers are used, e.g. carboxymethyl cellulose. Effective dispersion agents are also inorganic salts, e.g. alkali metal silicates.

The most frequently discussed topic in washing is the role of solubilisation processes. Many investigators [76] attract attention to the fact that the surfactant concentration in a washing solution is much lower than CMC, and in this connection, solubilisation of oils is principally excluded due to absence of surfactant micelles. At the same time, the review of recent works [85, 86] show that solubilisation can play a dominant role both in washing fabrics and in the removal of soils from solid surfaces. These views are based on the following mechanisms. Surfactants adsorb at w/o interfaces under formation of densely packed adsorption layers which leads to a high "local" surfactant concentration as compared with the rather low concentration in the washing solution. After that, noticeable "penetration" of water into the oily soil is possible, under formation of liquid–crystal phases. Then, mesomorphic phases are swelled and destroyed under the formation of emulsion droplets.

When non–aqueous surfactant solutions are used to remove soils from fabrics, furs, leathers (so–called "dry–cleaning" process), solubilisation is a quite necessary and sufficient condition for the soil removal considering sufficiently low CMC values. The same also applies to washing of metal surfaces where surfactant additives are often added both to polar (alcohols, ketones, etc.) and non–polar media (aliphatic or aromatic hydrocarbons and their mixtures).

The surfactant structure also produces a substantial influence on their action mechanism in the washing process. It is shown in [87] that alkyl polyglycosides are not only emulsifiers but also

efficient dispersion agents which is the result of their adsorption at l/s interfaces. These surfactants are successfully used as components of detergents and cleaners.

Foam formation also plays a certain role in the washing process. The persistent conviction of consumers expressed as "no foaming, no washing" compels the producers to manufacture a wide spectrum of detergents with an obligatory possibility of foam formation in the washing solution. As a result, tests on determination of volume and stability of foams in the solution (e.g. Ross–Miles test) are included in many standards for efficacy characterisation of detergents [6].

On the other hand, the functional role of foam in personal care products (shampoos, creams, tooth pastes etc.) is rather disputable, yet producers are compelled to manufacture preparations allowing to obtain stable foams [88]. Foam properties and, therefore, component composition of the solution depend on the final use. For one range of products (soap bars, shampoos, tooth pastes, foam baths etc.), the foam is formed by stirring. For another group (e.g. aerosol preparations: for shaving, for carpet cleaning, for cleaning hard surfaces etc.) application is possible only when a stable foam is formed initially. It is emphasised in [88] that preparations of the first group must provide a considerable volume of foam maintaining its stability during the application (generally from 2 to 20 minutes) after which the foam must collapse in the process of dilution due to rinsing with water.

Aerosol foams exhibit, as a rule, high dispersity and viscosity. Hence, aggregative stability of such foams is important. Loss of aggregative stability means drainage of liquid from the foam and it becomes unsuitable for use. Note that the possibility of preparing "liquid–absorbing" foams and their subsequent use for soil removal was established for the first time in the early nineties [20].

As detergents are nowadays used in machine washing, the problem of foam stability control has gained a special actuality. The way typical defoamers let the foam collapse is the so–called heterogeneous mechanism [17, 30]. The use of a number of surfactants which control the volume and stability of foams both during its formation and in the process of use is investigated in [89] in detail. These surfactants are either practically completely dissolved in water (fatty acid soaps, mono– and dialkyl phosphates and others) or dispersed in the presence of other surfactants (higher acid mono– and diamides). The use of surfactants exhibiting a high

wetting and emulsifying power (alkylbenzene sulfonates, alkylsulphates, ethoxylated alcohols and alkylphenols) in a composition with the above additives controlling foam stability allow to obtain detergents which can be used in modern washing machines.

Based on the material given above, a typical "finished" or commercial detergent composition must contain the following components: 1) surfactants (wetting, dispersion, emulsification, foaming); 2) high–molecular surfactants preventing re-deposition of soils; 3) inorganic salts controlling pH and ionic composition of the washing solution (silicates, carbonates, phosphates). Depending on the functional purpose, these compositions contain bleaching agents, perfumes and other components. For pasty or liquid laundry detergents as well as personal care products, their viscoelastic properties are of great importance. It is shown in [90] that polymers, ethoxy alcohol carboxylates and alkyl polyglycosides can be efficient viscosity controllers. Detergent compositions are discussed in more detail in the subsequent section.

6.6. THE USE OF SURFACTANTS TO MEET THE NEEDS OF MAN

In the course of the development of civilisation, the increase of lifetime of an individual is one of the important objectives to maintain the human society. This is considerably influenced by the sanitary conditions of man's home, clothes and body care. From this standpoint, many analysts place the consumption level of surfactants (in form of detergents and other preparations) per head among the main criteria of the development levels of state and society. A huge stream of information about the use of surfactants in this area does not allow to discuss, within the framework of a short review, the whole variety of effects obtainable under the action of surfactants. Therefore, the following themes will be discussed in this section only: 1) surfactants in detergents and cleaners and personal care products; 2) surfactants in foodstuffs; 3) surfactants in pharmaceuticals. Such a construction of the section is due to the influence of by-effects which are possible at long or "momentary" contacts between surfactant and man's organism. "Secondary" effects are possible in using surfactants in agricultural chemistry, but we do not consider it expedient to elucidate these problems within the framework of this section, considering vast reviews by Tadros [91, 92].

6.6.1. Surfactants in the manufacture of detergents and cleaners

A wide use of synthetic detergents (SD) began in the forties of the 20th century, after mastering the commercial production of anionics (alkyl sulfonates – Germany; alkylbenzene sulfonates – USA, United Kingdom) and nonionics (ethoxylated alkyl benzenes – Germany).

Conventional formulations of cleaners and detergents obligatorily include, independent of their trade form (powders, pastes, gels, liquids), the following components: 1) active matter (i.e. a surfactant or surfactant mixtures); 2) substances activating the washing effect; 3) auxiliaries: perfumes, fillers, viscosity controllers etc. Formulators have to solve the following tasks here:

1) the preparation must provide the removal of soils differing in their physicochemical properties (fats, solid particles, proteins, dyeing pigments etc.) In addition, the washing process must take place within the shortest possible time intervals -- a few minutes maximum;

2) versatility of the preparation which must be manifested in consideration of the value of soil adhesion to the surface to be washed, which can be: a) absorbing (fabrics, wood, ceramics etc.) but differing in its degree of hydrophilicity from maximum (cotton) to minimum (polyamide fibres); b) non-absorbing (glass, metals, plastics etc.), which also differs in its degree of hydrophilicity;

3) the degree in which surfactants affect the human organism and the environment.

Since this seems to be the most important factor at present, it is necessary to characterise the tendency of surfactant choice briefly. For anionics, detailed descriptions of surfactant effect on human skin, respiratory tract and gastrointestinal tract functions are given in a review by Gloxhuber and Künstler [93]. Systematic studies of the effect of structure of surfactants on their dermatological action have shown that there is a direct relationship between their adsorption on the skin and irritating effect [94]. As a result of complex investigations, it has been shown that maximum adsorption is observed for sodium alkylsulphates and linear alkylbenzene sulfonates. Then, in descending degree, follow α-olefine sulfonates and alkyl ethoxysulphates. C_{14}-C_{16} fatty acid soaps and alkyl phosphates exhibit the lowest adsorption and minimum irritating effect. These data confirm the experience of many years of using soaps as the best means for washing soils off the human body.

At the same time, surfactants like alkylbenzene sulfonates remain the most widely used basis for laundry detergents. Anionics remain the main products for making detergent compositions. Some of the application aspects of relatively new types of anionics (α-olefin sulfonates, sulfocarboxylic acids, alkyl phosphates etc.), whose commercial manufacture began in the 60-ties – 70-ties of the 20th century, are described by Stache [95]. The application of conventional types of nonionics like ethoxylated alcohols or alkyl phenols is presented in [13 –14]. Alkyl polyglycosides were widely used in the last 5 – 8 years [96]. However, the main tendency in the development of new generation detergents is the use of surfactant mixtures in their optimum composition [97, 98].

The development of detergent compositions containing surfactant mixtures allows to ensure a high detergency of preparations irrespective of the conditions of their application, e.g. temperature of water or containing hardness salts. This is due both to the change of molecular solubility of surfactants and to the micellar solubility due to the increase (or decrease) of the Krafft point. Surfactant mixtures also allow to control foam formation in washing solutions which is very important for modern washing machines.

Let us mention only a few typical examples for using surfactant mixtures. It is shown in [95] that, using alkyl sulphates mixed with alkyl benzene sulfonates (ABS), it is possible to obtain maximum detergency due to the improved emulsifying power of ABS in washing oily soils. A detailed description of anionic-nonionic mixtures is given in [97, 98]. The main advantages of these compositions consists in that various types of soils can be washed off in water of a higher hardness including sea water. Besides, it is possible to wash at relatively low temperatures (25 - 30 °C).

A second qualitative jump connected with the development of detergent compositions is based on the investigation of mixed surfactant-polymer solutions. It has been shown in [99] that aqueous solutions of water-soluble cellulose esters (a conventional component of detergent compositions) give mixed micelles in mixtures with ionics, and this is a convincing evidence of that the presence of cellulose esters and other polymers in detergent compositions not only prevents re-deposition (secondary deposition of soils on fabrics) but also enhances the detergency of surfactants.

Finally, in the last 10 or 15 years enzymes are, as a rule, detergent components [100], which allows to enhance the effect of microbiological processes along with the physicochemical factors influencing soil removal.

6.6.2. Trade forms of detergents and features of compositions

Conventional detergents are manufactured in two main trade forms – as powders [101] and liquids [102], while the term "liquid" is interpreted rather broadly. Usually, these are not only viscous liquids but also concentrated suspensions and flowing pastes, as well as gel-like products. Powdered detergents usually contain 8 to 15 wt% surfactants, the rest is fillers and auxiliaries. Liquid detergents can contain between 15 and 30 wt% surfactants. In the last 5 – 10 years, there was a clear tendency to develop and establish productions of so-called "compact" and "overcompact" detergents containing more than 40 wt% of active matter [103].

Although powdered detergents account for no less than 80 per cent of sales of all detergents in Europe and no less than 65 – 70 per cent in the USA, in view of the traditions established on the consumer market, liquid detergents have a number of advantages. First of all, they do not form aerosols when dosed and dissolve rapidly in water. Besides, the volume dosage is very attractive for rank and file consumers.

The choice of an active base for making a detergent composition is determined in addition to enhanced efficiency by two main factors: 1) compatibility with builders and complex-forming additives; 2) foam control in a broad sense from "high" foam in manual washing (common consumer's approach – if there is much foam, there is a good washing) to minimum foam formation in up-to-date automatic washing machines.

In the 60ties – 70ties of the 20^{th} century formulators of detergent compositions were intensively working on the problem of substitution of sodium tripolyphosphate (TPP) by other kinds of builders which could perform the role of binding (sequestering) of calcium ions and enhancing detergency at this expense. Two main research directions to replace TPP can be pointed out: a) use of finely-dispersed alumosilicate powders, e.g zeolites; b) use of complexation agents like citrates, polycarboxylates, polyamines. It should be noted that this problem has not been solved up to now despite the "abundance" of patents on phosphate-free detergents. This, in turn, is determined by two circumstances: the trade forms of powdered detergents using water-insoluble zeolites give suspensions in washing solutions and are

deposited on fabrics or on the parts of washing machines and pipings. The use of complexation agents both in powdered and especially in liquid detergents becomes inconvenient for economic reasons.

Due to different requirements of ecological legislations both in different countries of the world and in different regions of individual countries (legislations of States in the USA and those of the federal lands in Germany), tripolyphosphate contents in formulations may vary considerably but this product is up to now an essential component of the main preparations both of powder and liquid forms. The use of phosphorus-containing surfactants [104] could be very promising in this direction. Diethanolamine salts of alkyl phosphates based on higher C_{10} to C_{14} alcohols are not only an active base for detergent compositions but they take also part in binding (sequestering) the calcium ions. Ammonium and alkali salts of alkyl phosphates play an active role in the process of binding calcium ions with alumosilicates, thus contributing to their transfer from the water bulk to the surface of the latter. New data on the role of borates in the washing process have been published in [105]. It was noted earlier that perborates were classical bleaching agents in detergent compositions. However, borates can effectively bind calcium ions along with silicates, phosphates and carbonates.

The control of foam formation is of great importance, especially in connection with the wide use of modern activator-type washing machines. A comprehensive patent review of detergent formulations for various types of washing machines is given in [106]. Formulators (most from Colgate-Palmolive and Procter & Gamble) focussed their attention on a maximum detergency at an optimum ratio of surfactant : defoamer : enzymes, with special attention to the effect of water hardness on foam formation. Along with traditional defoamers the so-called antifoams are discussed in [107], i.e. substances which prevent foam formation. The most attractive seems to be the use of fatty acid soaps or anionic/nonionic mixtures at an optimum ratio. Light-duty liquid detergents are designed for dishwashing, for the washing of kitchen utensils, automobiles and manual washing of delicate fabrics. A typical formulation of this kind includes surfactants, a foam stabilizer, hydrotropes and an antistatic [108]]. Liquid heavy-duty detergents are third-generation products and compete, to a certain degree, with powders. As a rule, they includes anionic/nonionic blends with an obligatory inclusion of enzymes and preservatives [109].

6.6.3. Surfactants for the manufacture of personal care products

The range of personal care products is rather wide, such as shampoos, foam baths, shaving products, creams, tooth pastes. An almost complete review of the use of surfactants for cosmetic and personal care purposes was given in [80]. We see it necessary to focus on two aspects of the effect of surfactants on the stability of dispersed systems under different application conditions.

For shampoos, shaving foams and tooth pastes, high stability and definite foam structure is one of the main factors determining the commercial value of the product. In this connection, conventional shampoos include anionics (ammonium or triethanolamine salts of alkylsulphates mixed with alkylolamides of natural fatty acids, e.g. coconut oil acids, as well as amphoteric surfactants and hydrolysed proteins. Detailed patent data on the formulations are given in [80, 110] and other reviews.

For cosmetic preparations, the stability of emulsions and suspensions is of special importance since typical storage times range from one year to three years – during such long periods no breaking of the product must happen. During the 80^{th} or 90^{th}, nonionics produced on the basis of natural fatty acids – mono- and polyglycerides, sucrose esters as well as phospholipids were used to stabilise high-concentration emulsions. In the mid-eighties, biosurfactants having a similar structure are preferred [111]. Both for synthetic and biosurfactants whose structure includes a hydrophobic radical and a rather clearly identifiable hydrophilic group, HLB technique is widely used to develop formulations. Problems come up when choosing silicone surfactants which are widely used as emulsifiers in cosmetics [112]. These surfactants are, as a rule, oligomers of different molecular weights, designed to stabilise w/o or multiple w/o/w emulsions. Emulsifiers are chosen empirically but a large experimental material has been gathered which allows formulators not only to achieve the required emulsion stability but also to provide required technological properties (viscosity, stickiness to skin, spreading etc.). Ethoxylated phytostyrol derivatives are a new type of emulsifiers, which not only provide a high emulsion stability but also a favourable effect on skin and hair. Owing to this fact, they are often included in lotions, hair rinsers and sun-cream products [113].

6.6.4. Surfactants and pharmaceuticals

The use of surfactants in the manufacture of ointments, emulsions and suspensions has been known already in the time when chemistry was in the period of "alchemy". By now, the common term "external preparations" is in use in pharmacy, and the choice of surfactants is focussed on the stabilisation of dispersed systems (foams, emulsions, suspensions).

Intensive study of the effect of surfactants on biological processes in living organisms began in the second half of the 20th century. The ideas of that the human organism is a "living colloid" were common in the scientific world of physico-chemists since the times of classics, e.g. Thomas Graham (1864). These ideas were many times given reasons for by the fact that the main organism functions – first of all, breathing and digestion – are accomplished by a "cascade" of l/g, l_1/l_2, s/l interfaces. In [114], the notion "biological surfaces" was for the first time formulated, which differ considerably from model systems (e.g. membranes) studied within the framework of the classical colloid chemistry. A detailed analysis was given of the effect of natural surfactants such as proteins, dextrins, nucleic acids etc. on the mass transport through "living" biomembranes and of their effect on interfacial phenomena and mass transport processes both on "external" surfaces (skin, mucous membranes etc.) and in biomembranes at the level of bacterial cells, blood plasma and other "biological objects" in "living" organisms (plants, insects, warm-blooded animals, humans). These papers give a key to the use of both natural and synthetic surfactants in pharmacy and veterinary medicine.

Among general studies in nature, investigations on the so-called "pulmonary surfactant" should be, first of all, pointed out [115 - 116]. Reviews by Pison et al describe in detail the eventual composition of the lung surfactant and its main functions. The important role of pulmonary surfactants is emphasized in [115] since the l/g interface in the lung tissue is over 150 m^2. On the one hand side, the surfactant film decreases the l/g interfacial tension thus preventing alveolar collapse and keeping the gas exchange surface available. On the other hand, this surface "modified" by the pulmonary surfactant protects the organism from infectious agents and irritants which may be present in air or blood. Components of the pulmonary surfactant and its biophysical functions are described in [116] in detail. It has been shown possible to achieve very low surface tensions of the l/g interface (< 10 mN/m) using a captive-bubble

surfactometer, which is practically unachievable under normal conditions and with standard synthetic surfactants.

The role of dynamic surface tension is studied in the paper by Fainerman et al [117] using a number of biological objects as an example (blood, urine, amniotic fluids etc.), and the possibility is shown of using this test for primary diagnostics of a number of diseases. However, it is not the task of this chapter to discuss this phenomenon in detail here.

Administration of drugs in form of aerosols is used widely. There is a large number of literature sources dealing with the effect of surfactants on the droplet size of aqueous aerosols. Note the systematic study [118] which shows the effect of a number of surfactants (sodium lauryl sulphate Tween 20, Tween 80) in concentrations ranging from 0.001 to 1 wt % on the droplet size of a number of drugs. The mean mass diameter of aerosol droplets (over 90%) did not exceed 0.05 μm, the droplets having minimum polydispersity which had a positive effect on the pharmacological action of drugs administered.

It is emphasized in [119] that the surfactant administration is day-to-day practice in the cure of babies with inborn respiratory distress syndromes and, as a rule, is accompanied by an improvement of the lung function. For adults, this effect is manifested weaker. The role of surfactant antifoams for pharmaceuticals is shown in [120, 121]. A complex of an antifoam (e.g. Span 65 0.025% and cetyl alcohol 0.05%) with alpha-protease contributes to protein diffusion to the lung tissue and enhances the pharmaceutical effect.

The role of antifoams is discussed in Berger's review [121] in more detail. First of all, the nature of intestinal gases has been determined, which may produce foam and, therefore, result in gastrointestinal malfunction and, finally, in dyspepsia. In this case, silicone antifoam materials are effective. Many years of experiments on animals have shown the absence of their toxicity towards warm-blooded animals and humans, and they are rather widely used in pharmaceutical practice [121, 122]. Anionics are used in pharmaceutics as emulsifiers in the manufacture of creams, ointments, lotions and other products for external use, and their action on skin, mucous membranes, eyes and other surfaces of the human body have been investigated well enough [123]. Besides, they are also used for the internal administration to promote the action of antimicrobial drugs, laxatives and other drugs coming into the organism through the gastrointestinal tract.

Lauryl sulphate enhances the paracellular transport of hydrophilic preparations, e.g. bisphosphonates, tiludronates etc [124], but also that of hydrophobic components such as dodecanamide derivatives [125]. In the latter case, mixtures of lauryl sulphate with the anionic Triton X-100 are used. Ethylene oxide-propylene oxide block copolymers have found wide-spread application in pharmaceutical practice [126], the properties of which can be controlled depending on the length and relative position of hydrophobic (polyoxypropylene) and hydrophilic (polyoxyethylene) chains. They are used as emulsifiers, dispersing and wetting agents. New kinds of highly purified block copolymers are incorporated as vaccine adjuvants for the treatment of bacterial and viral infections.

New surfactants produced both by biosynthesis [4] and by synthesis are now being tested along with conventional synthetic surfactants. In this respect, cationics on the basis of arginine, which show a high inhibiting power to staphylococci, streptococci and other bacteria, are of special interest as bactericidal compositions [127].

The use of pharmaceuticals in form of emulsions is of special interest. Thus, for example, o/w emulsions stabilised by surfactants, such as mono- and diglycerides, are successfully used as pseuo-doxime-proxetil protection from intestinal lumen hydrolysis through oral administration [128]. Multiple w/o/w emulsions stabilised by Tween 20/Span 20 or Tween 80/Span 80 mixtures contributed to a prolonged "retention" of cytarabine in one of the phases, and its gradual "release" ensured a prolonged action of the drug [129].

The action of multiple emulsions stabilised by ethoxylated sorbitane monooleate and triglyceride after oral administration of insulin has been studied in [130]. The example of test animals has clearly shown that encapsulated insulin obtains prolonged protection from the proteolytic action of the digestive enzymes.

Microemulsions are also widely used in pharmaceutical practice [131, 132]. Thus, when comparing the permeation of tetracycline applied in the form of cream, gel and microemulsion through skin membranes, it has been shown that the diffusion time of the drug is three to four times lower, and the amount of the drug "absorbed" is also three to five times higher [131].

In view of considerable concentrations of surfactants and co-surfactants used to stabilise microemulsions, special attention is paid to the choice of low-toxic surfactants [132]. Such

microemulsion compositions have been rather widely tested for the solubilisation of local anaesthetics, steroids, anxiolytics and some other drugs [132].

Vast investigations in the field of microemulsions for pharmaceutical use have been carried out by Riess [133 – 134]. He has demonstrated that lipid emulsions are used for parenteral nutrition and also as "trade forms" to deliver vitamins, prostaglandins and sedative drugs to the "hearth" of disease. Lipid-based emulsions are used as external antifungals and drugs for the treatment of joint diseases. It has been shown that it is important to achieve a high coalescence stability of emulsions during storage and their subsequent destruction when delivered to the hearth of disease to release the active drug component.

Special attention of the investigators – both physicians and colloid chemists – was attracted to fluorohydrocarbons in water [134 – 136]. In this case, fluorohydrocarbons are oxygen carriers and can serve as blood substitutes. Clinical tests have been successfully passed and, in part, have already been tested in surgery. These are, by their structure, highly dispersed emulsions having a very narrow distribution by composition, bluish-coloured, hence the term "blue blood". On the first stage, various fluorine-containing surfactants, including fluorinated lipoproteides, semifluorinated phospholipids etc, were used to stabilise fluorohydrocarbon emulsions. However, the attempts to achieve emulsion stability needed for the practical use had no success. The studies by Pertsov and Kabalnov [47, 55] have shown that, for fluorinated emulsions, diffusion transport is one of the mechanisms of their destruction. Most successful was the use of block copolymers with a determined structure, which prevent the aggregation of red blood cells in the whole blood [136]. The same surfactants have been widely used as stabilisers for fluorohydrocarbon emulsions.

6.6.5. Surfactants in the manufacture of foods

A rather complete analysis of sanitary and legal aspects of using surfactants in the manufacture of foods is given in the vast monograph [36] by Schuster. The same source gives information on laws in the USA, Germany and European countries, requirements to "food additives" comprising surfactants. Our task is only to concisely elucidate the colloid-chemical aspects of this problem. According to [36], surfactants are used in making bakery and confectionery goods, margarine, ice-cream, chocolate, sausages etc. A detailed description is given for preparation, purification and application methods of the main types of food surfactants:

lecithins from various sources; mono- and diglycerides based on both saturated and unsaturated natural fatty acids; calcium and magnesium salts of fatty acids; citrates and phosphates of mono- and diglycerides; as well as conventional surfactants of Span and Tween series.

However, consumers in some countries are sometimes distrustful towards chemical additives obtained by chemical methods, although from natural raw materials (acids, glycerides, sugars, citric acids etc.). For this reason, intensive work was carried out during the last 15 to 20 years to produce biosurfactants [137]. Glycolipids and their derivatives (sucrose lipids, fructose lipids) as well as polysaccharides, proteins, amine derivatives of peptides and lipids have been tested as effective emulsifiers for a number of purposes. Arabic gums which are water-soluble polysaccharides are new types of emulsifiers for citric oil, foamers for alcohol-free beverages and preparation of both fat-soluble and water-soluble vitamins. The study by Thevenet [138] deals with structure, preparation methods and emulsifying properties of these products. Dickinson and Wasan [139] paid special attention to some other differences. First, these are high-molecular compounds the structure of which is not studied in detail (lipids, proteins, polysaccharides) and hence their use is very limited by corresponding laws. Second, which is the main point, it is very difficult to determine their behaviour in compositions with other surfactants, e.g. lecithins, which require careful investigations on model systems. Finally, it is necessary to study the influence of these systems on the storage of the finished food products, such as ice-cream, process cheese, mayonnaise.

In [140], attention is paid to the fact that experiments on the adsorption layer structure of proteins, e.g. milk protein, based on the investigation of adsorption on flat oil-water interfaces do not always adequately reflect the real processes under conditions of emulsion preparation since adsorption proceeds at a higher rate there. At the same time, these investigations predetermine, in many aspects, the choice of compositions for the preparation of emulsions. However, the properties of an emulsifier, such as β-casein, which are studied well enough, cannot be mechanistically transferred to other protein types, e.g. soya. Each protein requires extensive additional studies.

Dickinson [141] has shown that physical emulsion properties are highly dependent on the structure of the adsorption layers at the surface of dispersed droplets. The structure of the adsorption layers of caseins, e.g. β-casein, considerably differs from the structure of "globular"

serum proteins, e.g. β-lactoglobulin. All this considerably influences the stability and flow properties of emulsions.

One of the main goals which can be achieved using emulsions both in food industry and in pharmaceutical industry is the controlled emulsion stability of the active component at the moment of its transport to the biological object and a high emulsion stability during storage. This goal is achieved using multiple ("double") w/o/w or o/w/o emulsions which are flowing, low-viscous liquids [142]. W/o/w emulsions can be formed using an oil-soluble emulsifier (Span) stabilising the inner phase, and a second water-soluble (Tween) used at 1:10 ratio. The emulsions contain rather large droplets (5 – 10 μm), show a satisfactory stability, but the rate of "release", i.e. migration of the oil phase is retarded during application. Two variants of the preparation of multiple emulsions are considered [142]. The first is the use of the hydrophobic emulsifier Span 80 in combination with globular protein, bovine serum albumin (BSA) in the amount of 0.1/100 g, and the second is the use of the same protein with a hydrophilic emulsifier (Tween 80). In both cases, a synergistic effect is manifested as far as the emulsion stability is concerned. The diffusion coefficient of the ionic compounds, such as NaCl is decreased in the presence of BSA, and a more controllable transport of both molecules and water is achieved. It is recommended to use this technique in food industry when ionic components are entrapped in a liquid composition and are released, when needed, at a controlled rate. Results similar to [142] were obtained with a soybean oil/water emulsion at 90:1 ratio Tween 60:sodium caseinate [143].

The structure of adsorption layers is of great importance during preparation of food foams and emulsions. These problems have been studied in [144] for protein adsorption at the liquid/gas interfaces and in [145] for liquid/liquid interfaces. Due attention is also paid to the interaction of typical emulsifiers and proteins during preparation of food emulsions [146 – 147]. Addition of an oil-soluble emulsifier to proteins during preparation of w/o emulsions [146] increased the emulsification rate, but at high concentrations decreased it due to the increase in oil viscosity. In this case, the emulsifier displaced β-casein from the surface easier than β-lactoglobulin. However, there was no complete displacement into the aqueous phase since multiple emulsions were formed, as mentioned above [142 –143]. Hence, the choice of the surfactant/protein ratio is important.

It has been shown in [147] that "aerated" model emulsions of palm kernel oil, coconut oil, as well as butter, which are used in making ice-cream can be obtained at an optimum surfactant/protein ratio. A combination of Tween 60 and skimmed milk powder provided a higher stability than using mono- and diglycerides. In particular, this can be due to the fact that Tween 60, at the same time, effectively inhibited the coalescence of gas bubbles.

Not only emulsifier composition but also the preparation process of the emulsions influence on the stability of food emulsions. It has been shown in [148] that the "mode of cooling" is a dominating factor. The progressive cooling at room temperature gives a better stability than the "brutal" cooling with a water bath.

Of great importance are methods of preparation of food emulsions which is discussed in detail in a report by Schubert [149]. The size of emulsion droplets is determined by the energy density in a dispersing machine and by the nature of the emulsifier. Jet dispersing systems are more efficient. But after jet disruption, it is necessary to employ "rapid" emulsifiers, i.e. emulsifiers having a higher interfacial adsorption rate. Besides, the droplet coalescence rate sharply decreases sufficiently low concentrations. Preparation of high oil content emulsions using a "slow" emulsifier, e.g. egg yolk, requires rather long residence in a zone of high force density. Emulsion break-up is often observed in toothed disc dispersing machines. This can be avoided by addition of a stabilisation zone after the dispersion zone.

Microemulsions play a special role in the incorporation of food additives in finished products [150]. Aromas and some food dyes are typically oil-soluble compounds. It has been shown experimentally that microemulsions formed with Tween 20 are able to solubilise quite large quantities of flavours. Up to 3 moles of flavour could be solubilised per mole of Tween 20. Incorporation of vitamins in foods, e.g. vitamin E, and β-carotene turned out to be also effective. In this case, the solubilisation of vitamin E in nonionic micelles protects it from oxidation decomposition. Finally, the solubilisation of ascorbic acid in sardine oil microemulsion droplets prevents lipid oxidation. The effect is enhanced on adding tocopherol into the oil phase.

6.7. SURFACTANTS AND CIVILISATION DEVELOPMENT

We have already noted [3, 151] that surfactants are, to a higher or lower extent, used in over 100 various fields. It is neither possible nor necessary to describe all these fields within the

framework of this chapter. Therefore, we shall only focus on the following sub-sections: 1. traditional surfactant applications (flotation, textile industry, paper industry, paints etc.); 2. surfactants and the problems of fuels and energy sources (oil, coal, gas); 3. surfactants and new applications (including surfactants and removal of natural and technological disaster effects).

6.7.1. Surfactants in flotation

Flotation has been used for more than 100 years to separate sulphides, oxides and other salts from ores, as well as to obtain phosphates, barite, chromite and other materials. Up to 90% of copper, lead, nickel, zinc are extracted using flotation in the USA [152 – 153]. In Russia, flotation is widely used to additionally obtain apatite, barite and phosphates. Flotation of iron oxides is not used in practise yet, but the number of experiments carried out in this direction is rather large. The main physicochemical principles of flotation have been discussed above [59 – 74]. Here, only some practical problems will be discussed. In [153], requirements are pointed out which apply to three-phase flotation foams, and the main components of the process are defined, i.e. surfactant – collector; surfactant – frother; activator, depressants, colligend, gangue. The peculiarities of flotation and foam separation in batch and continuous modes are outlined as well as the structure and properties of the main types of flotation agents described. As surfaces of the majority of mineral particles are hydrophilic in nature, hydrophobisation of particles is necessary for a selective separation.

The conditions of copper separation from mixed copper/zinc ores of various compositions are different [154]. While the optimum potential for mineral separation from the "difficult" ore chalcopyrite was +50 to + 150 mV, the separation of the copper mineral sphalerite from mixed ores required a negative potential of about –150 mV. In all cases, xanthogenates and dithiophosphates were used as agents.

Separation of minerals is rather difficult when they contain cations similar in their properties, for example, barite and calcium carbonate. In the presence of the collector sodium oleate, non-specific particle agglomeration is observed, which can be overcome using the modifier sodium lignosulfonate [155]. Under these conditions, selective agglomeration of barite particles was observed and satisfactory process parameters were achieved.

Quartz is a "barren" material when separating a number of minerals. In [156], different flotation rates of quartz particles were investigated using the cationic surfactant n-dodecyl

trimethyl ammonium bromide. It was shown that a fraction of the quartz particles lifted up in the froth returns to the slurry to be flotated again. Numerical simulations of the gas flow rate optimisation were compared with experimental data of particle content profiles through the height of the column, and showed quantitative agreement with the particles flotated "secondarily" within an average error of 18.4%.

An original technological solution for phosphate separation has been proposed in [157]. The typical flow-sheet requires rather high consumptions of anionic collectors, e.g. fatty acid soaps. The authors have proposed a two-step flow-sheet in which fine particles are first floated with a minimum aminoacid consumption. The concentrate from prefloat is then floatated with a fatty acid/fuel oil emulsion. As a result, a phosphorite concentrate is produced which contains about 30 % P_2O_5, and the P_2O_5 recovery is over 93%.

Cationic agents are rather often used in flotation processes. In [158], surfactants were synthesised on the basis of 1-chlorododecane and mono-, di- or triethanol amine, which contained different numbers of hydrophilic groups at one radical. The effect of their structure on surface-active and flotation properties have been studied in detail.

The so-called chelating collectors, such as hydroxamic acids, continue to be studied by flotation specialists. The flotation selectivity of minerals partly soluble in the flotation pulp has been studied, at bench scale, in [159]. It has been shown that optimum results are achieved, when the mineral to be floated is the most soluble in the system and the chelate formed with the cation on the surface is most stable.

The problem of magnesite and serpentine separation has been studied in [160] using IR-spectroscopic methods and direct flotation experiments. The carboxylate ion is chemically adsorbed on the surface of magnesite, by which its high hydrophobisation is achieved. In contrast, at the surface of serpentine it is physically adsorbed. Cationic collectors are adsorbed physically on both minerals. On this basis, it is possible to separate the minerals in two ways. In the direct flotation, magnesite is concentrated in the foam using an anionic; in the reverse flotation, using a cationic, with addition of a number of depressants, serpentine is transferred into the foam fraction, and magnesite remains in the "tails".

Dewatering and filtration are the most important processes in flotation. It is shown in [161] that the settling rate of iron ore fines can be enhanced 25 to 30-fold at optimum concentrations of

certain high-molecular flocculants. The residual filter cake moisture content is 18.2% without surfactants, and with suitable surfactants added, e.g. petroleum sulfonates, this moisture content is reduced to 12.6%. It is very important that the specific cake resistance to filtration can be reduced 6 to 8-fold by using a surfactant, e.g. sodium petroleum sulfonate, at a concentration of about 1.5 g/t. Similar results were obtained under laboratory conditions on filtration of iron ore sludge flocculated when ethylene oxide-based nonionics mixed with flocculants were used [162].

6.7.2. Surfactants in textile, paper and leather industries

The use of surfactants for the production of textiles and leathers has a lot in common. Surfactants have been used for more than 150 years in the textile industry. Before the term "surfactants" was introduced, substances of similar structure, for example, sulfonated oils of various nature, were referred to as textile auxiliaries up to the mid-twenties of the 20th century. Its use begins with the initial step of raw material preparation, e.g. crude wool washing, crude skin soaking with subsequent defatting. In the pulp and paper industry, surfactants are used for "degumming" of cellulose. Surfactants are effective in dying of articles. It is not necessary to elucidate individual aspects of the effect of surfactants on technological processes, since corresponding reviews have been published. Thus, the multi-volume editions by Lindher on the use of surfactants in the production of fabric fibres and the structure of the main types of surfactants [163] have not lost their importance. The assortment and the trade names of surfactants manufactured in the seventies of the 20th century are in detail discussed in the guide-book by McCutcheons [164] and data concerning the use of surfactants are given in [165, 166] for the textile industry and in [167] for the pulp and paper industry. Outdated is the review on surfactants in the leather industry [168], but the main effects have remained unchanged, although the surfactant range has been widened considerably.

In recent time, main attention was focused on the treatment of fiber surfaces, wetting control, and the penetration rate of fabrics by corresponding process solutions. According to [169], the imbibition of fabrics takes place as result of two processes: a) a "bulk" imbibition, since the strands of yarn behave as an assembly of capillaries; b) a surface rise due to the formation of surfactant adsorption layers.

Wetting and wicking are discussed in [16] more in detail. Wetting is the displacement of a fibre-air interface by a fibre-liquid interface which is influenced by surfactants solely. Wicking is the flow of a liquid, driven by capillary forces. The wicking process can proceed in 4 variants: 1) capillary penetration only (usually in the absence of surfactants); 2) capillary penetration with simultaneous diffusion of the liquid into the interior of the fibres; 3) adsorption of surfactant on the fibres with simultaneous capillary penetration; 4) adsorption of surfactant on the fibres with simultaneous imbibition and capillary penetration. In all cases, the effect of penetration increases in the presence of surfactants.

It has been shown in [170] that the impregnation of a highly hydrophobic non-woven material – high-density polyethylene – in a CO_2 solution is due to the wetting of the fibres with a nonionic surfactant N, N-dimethyl dodecyl amine N-oxide. Impurities contained in surfactants have a certain effect on the wetting of surfactants. [171] describes the action of a new surfactant - decyl galacturonat derived from decanol and sugar. The industrial preparation may contain up to 13% of decanol. It has been shown that the presence of decanol in a certain amount accelerates the time of complete wetting on a cotton fabric, which is related to the adsorption of surface-active molecules at the advancing liquid front/fabric contact line.

The so-called synthetic fibres, e.g. nylon, show their peculiarities of wetting in the presence of surfactants of various nature. Capillary wetting rates of nylon fibrous assemblies were studied in [172] using conductivity measurements as well as contact angle measurements by the Wilhelmy method. For sodium dodecyl sulphate and dodecyl trimethyl ammonium chloride a minimum wetting rate was observed near pH 4, which coincided with the isoelectric point of the nylon fibre. When the surface charge increased, the wetting rate increased.

The wettability of various wood fibres was studied in [173], including bleached and unbleached, and alkyl ketene dimer sized and non-sized fibres. An improvement of the wettability with an increase of the surfactant concentration, except nonionics, was observed for all types of fibres. It has been noted in [174] that the electrokinetic potential of fibres determines considerably the efficiency of their washing and dying. Alkali mercerisation of cotton influences not only the fine structure, morphology and conformation of cellulose molecules, but also the negative electrokinetic potential of the cotton fibres. Based on this, the selection of mercerisation conditions due to changes in the NaOH concentration will allow to

obtain an optimum electrokinetic potential and to achieve an effective use of cationic surfactants, e.g. dodecyl trimethyl ammonium chloride.

For the synthetic fibre poly(ethylene terephthalate) it is very important to impart antistatic properties to it [175]. Studies on the effect of the structure of cationic surfactants on the half-life time of static charge decay and surface resistivity (R_s) of PET fibres show best results with a methylated quarternary ammonium salt of a stearyl amine-ethylene oxide adduct or hydrochloride of a lauryl amine-EO adduct with 10 EO.

To reduce the consumption of surfactants and improve the ecological aspects of new methods of surface modification of viscose and glass fibres, polyelectrolytes were investigated [176]. Optimum results were obtained for a mixture of a polycation (polydiallyl dimethyl ammonium chloride) and polyanion (maleic acid-co-alpha-methyl styrene). Fluorine-containing surfactants can be used to modify surfaces of polyamide fibers [177]. A bimolecular adsorption layer is formed on the fibre surface at a surfactant concentration equal to CMC. The decrease in the zeta-potential of fibres during the formation of the first layer is much larger than its increase during the formation of the second layer due to the reversed surface charge.

Soil removal from blend fabrics is a rather difficult task. It is shown that polyoxyethylene alcohols with a broader polymer homologue distribution are more effective soil removers [178]. The effect of molar mass distribution on the properties of nonionic surfactants is discussed above [13, 14].

Dying of fabrics is one of the final operations. Solubilisation of dyes in micelles of nonionic surfactants enhances the penetration into the fibre [179]. This method can be used for dying wool, silk, nylon and polyacetate fibres. For cationic dyes, a surfactant is chosen which dissolves in the fibre and acts to mordant the dye in the fibre and to increase light-fastness.

A detailed description of various machines for applying foams to fabrics for finishing, dying and printing is given in [180]. These methods depend on the foam properties. For high-stability low-expansion foams, controllable slots are needed for the foam layer to be uniform through the whole area of the fabric. In other cases, semi-stable foams are applied which collapse when injected through slots, and the liquid formed at foam collapse varies from 5 to 100 %. Information concerning specific foamer compositions for mercerisation and dying are only of

general nature. Typical anionic foamers, such as alkyl sulphates and alkyl ethoxysulphates are mentioned.

Using the theory of hydrostatic foam stability [21, 26], the behaviour of foams in contact with fabrics was studied [181]. Under these conditions, the drainage of liquid from the foam occurs under the influence of the following processes: 1) suction of liquid due to capillarity of high-dispersion foams; 2) imbibition of foam by the capillary structure of fabrics. The production of foams with a controlled structure allows to achieve a more uniform application of a dye to a fabric. Foamer formulations were developed containing surfactants and a water-soluble polymer, which allow to achieve a minimum initial syneresis rate up to 10^{-6} m/s^2 [182].

In spite of the obvious advantages of foam dying, especially in terms of the reduction of effluent and drying costs, dying in the bath volume is more widely used for a number of reasons. The problem of a strong reduction of the dying bath volume arises, which, in turn, leads to an increase in surfactant concentrations and, therefore, to an increased foaming in dying baths. Sawicki [183] gives various antifoam formulations which are compatible with surfactants and dyes and do not adversely affect the quality of dying.

Similar defoaming problems arise in the pulp and paper industry, especially in cooking and washing Kraft pulp. Patent data on antifoam formulations are given in [184], but the majority of these include hydrocarbons (kerosene, mineral oils etc). At the same time, advantages of antifoams based on amide waxes and hydrophobic silicone or their mixtures are emphasised. [185] gives comparative characteristics of practically all main types of defoamers and shows the advantage of introducing defoamers in form of emulsions.

The use of microemulsions in the dying process [186] is relatively new and little practiced. The major part of patents and other references are dedicated to the solubilisation of various dyes in surfactant micelles, and microemulsion compositions are given, which consist of a classical triad: surfactant, co-surfactant, solubilisable substance (dye). In some cases, o/w emulsions were added, in which xylene or hexadecane were used as oil phase. Only few examples are

---

[2] The minimum initial syneresis rate W_0 was calculated by the formula $W_0 = \frac{H}{y\overline{K}_{in} * \chi_0}$, where H is the foam height, $\overline{K}_{in}$ is the initial foam expansion rate, y is the coordinate $\frac{\tau}{\chi_0 - \gamma_\tau} \Big| \tau \to 0$.

given for the specific use of microemulsions. It is quite probable that the data given in the first section will help to extend the use of this method.

6.7.3. Surfactants in the manufacture of paint materials

Usual paints can be considered in general as concentrated suspensions in polar and non-polar media. Typical paint formulations include the following components: a film forming agent (aqueous dispersion of latexes, varnishes, lacquers); a pigment (most commonly, titanium dioxide as well as iron oxides and non-organic pigments); fillers (chalk, kaolin, talc etc.) and additives controlling the physicochemical paint characteristics, which include surfactants ensuring stability and flow properties of the suspensions [187, 188]. Our further attention will be focused mainly on the use of water-based paints, to which an overwhelming number of publications was dedicated during the last 10 years.

The influence of the blends of two latexes on the drying rate and film properties is discussed in [189]. Butylmethacrylate-butylacrylate copolymer [P(BMA-co-BA)] was used as a soft latex with a glass transition temperature of T_g=17°C, and poly(methyl methacrylate) [PMMA] was used as a hard latex with T_g=48°C. The latexes had equal particle dispersity (103 nm and 111 nm, respectively) and were practically monodisperse. The goal of the study was to obtain transparent films possessing a higher hardness. The soft latex dries slower (about 180 min) than the hard latex (about 200 min.). The water loss of 90% using the blends at the optimum ratio of 60% for "soft" and 40% for "hard" is achieved within 270 min. The authors give a model of water transport from the films proved by optical methods. Addition of a surfactant (SDS) in an amount of up to 6% practically did not effect the drying rate, however, the films formed have good transparency, higher hardness and temperature stability: the films containing 50% of hard latex were thermically stable up to 110 °C instead of 23 °C. The high T_g component imparts a high mechanical strength to the film, and both components must have similar refractive indices to ensure transparency, and the hard latex must be highly dispersed.

Very important is the study of the influence of the critical pigment volume concentration (CPVC) on the gloss of the coating and the nature of the paint formulation itself (white/blue tinted) [190]. Emulsion and pigment particles form a closely packed array that forms as the water evaporates and the film forming agent coalesces. The CPVC belongs to the ultimate pigment volume concentrations where all particles are dispersed, and no pigment agglomerates

are present because of a sufficiently high surfactant concentration. Vinyl acetate/n-butyl acrylate copolymer latexes 85/15 wt.% with a particle sizes ranging from 200 to 1200 nm were used as a film forming agent. The coating properties were studied using a standard formulation consisting of a white base composed of 69.4 wt.% of TiO_2, 22 wt.% of deionised water, propylene glycol (5.05) and surfactant (Tamol 731 1.61% + 0.3% of Triton GR7M), as well as an antifoam (0.4%), a tripolyphosphate (0.5%), and a film forming agent. The paint itself contained 37.5% of the "white base" and 62.5% of latex. 2.5% of hydroxyethyl cellulose was used to control lightness. According to the data published earlier, latex particle size vs. CPVC is a linear relationship (the CPVC increases with the decreasing particle size) at 0.3 – 0.7 μm, which is close to a logarithmic dependence at lower values. It was established in the study that the CPVC as reached under the condition $X=1.44Y^{2.65}$ where

$$X = \frac{\text{number of latex particles}}{\text{number of pigment particles}}, \tag{6.10}$$

$$Y = \frac{\text{diameter of pigment particles}}{\text{diameter of latex particles}}. \tag{6.11}$$

This formula was proved both for a white and a phthalo blue pigment-tinted paint. According to the authors, this formula allows to predict the effect of the latex particle size on the CPVC. Calcium carbonate (chalk, marble etc.) is widely used as filler in water-based paints. The effect of the polymer surfactant, polyethylene oxide, and sulfonated Kraft lignin on the stability of two $CaCO_3$ types – natural HYDROCARB 65 (OMYA) with a mean particle diameter of 0.7 μm, and chemically precipitated M-60 (Mississippi Lime) with a mean particle diameter of 0.95 μm) was studied in [191]. The natural chalk suspension remains stable in absence of $CaCl_2$, whereas chemically precipitated chalk aggregates even in the absence of salt. Destabilisation of $CaCO_3$ suspensions takes place in the presence of 0.01 M $CaCl_2$, but remains stable even in the presence of 0.002 M $CaCl_2$ when 5 mg PEO per gram $CaCO_3$ is added. At the same time, the measurements of the electrophoretic mobility of M-60 particles have shown that the addition of both anionic and cationic surfactant allows to increase the suspension stability. Thus, a simultaneous action of two factors is observed – electrostatic repulsion of particles according to the DLVO-theory, and a steric factor – polymer latex formation.

It was shown earlier in [192] that liquid suspensions of natural chalk with a mean particle size of about 50 μm at a content of 70 – 75% in water can be obtained using additives of nonionic and ionic surfactants of a certain structure. Without surfactant additives, the suspension becomes non-liquid at a chalk content of 50–55%. The experimental data on the effect of surfactants on the electrokinetic potential of chalk particles in suspension indicate a substantial role of the electrostatic factor in securing the liquefying action of anionic additives.

Kaolin and alumina suspensions are also, in some cases, included in water paint formulations. It has been shown in [193] that a maximum shear yield stress is observed with AKP-30 alumina suspensions of a mean primary particle diameter of ca. 0.3 μm at pH 9, independent of the particle volume fraction between 0.2 – 0.3. For kaolin suspensions, the maximum shear yield stress is observed at pH 6 independent of the solid volume fraction. A direct correlation with the electrokinetic potential is observed. Thus, the pair-wise particle interaction is due to the electrostatic interaction which allows to control the stability of these suspensions.

The ζ-potential and the surface charge of pigment particles in a polymer solution has a direct effect on the suspension stability [194]. Ultra-fine pigment particles (< 0.05 μm) were formed during dispersion, which both adsorb on larger pigment particles and are included in the latex structure. Here, a steric factor increases the sedimentation stability of the suspensions additionally.

The adsorption of sodium dodecyl sulphate and a cationic surfactant on alumina particle surfaces was investigated in [195]. The adsorption of anionics decreased with the dielectric constant of the medium and the particles acquire a hydrophobic nature. Addition of sufficient anionic did not lead to a hydrophilisation of the particles, which indicates the absence of a second adsorption layer. The cationic surfactant displaced the anionic from the surface and increased the positive surface charge. Aluminium pigment dispersions are also used in the manufacture of paints. However, as it is shown in [196], an intensive corrosion takes place in alkaline medium, which can be measured gas-volumetrically by evolution of hydrogen. The corrosion can be considerably inhibited using aqueous alkyd dispersions at pH 8. It was shown by photometric methods, that TiO_2 surface treatment substantially influences the gloss of coatings [197]. The properties of a coating, such as colour change, loss of gloss, chalking etc, undergo substantial changes under weathering trials depending on the TiO_2 type.

The advantages of using two-component silicone-acrylic dispersions to improve the quality of coatings from water-based paints are shown in [198]. For this purpose acrylic resin was modified by tert.-amino groups, and silicone resin used for curing contains epoxy and alkoxysilyl groups. In this way, resistance to water and alkali is enhanced, and the film is formed under ambient conditions. In [199] it is demonstrated that acrylic coatings, when exposed to UV radiation, undergo ageing processes which are identified by CO_2 and O_2 release from the film. Investigation methods of UV stability of coatings have been proposed for optimum selection of dispersions and surfactants.

The effect of the surface tension on the quality of coatings is studied in [200]. When a coating is applied to a curved substrate, surface tension gradients are produced in the corners as result of diffusion of water-soluble surfactants. Hence, the coating thickness reduces at the circumference and increases in the centre. It is shown that an optimum surfactant concentration as well as an optimum method of coating application are important.

The dispersion stability can be increased due to thickeners added, e.g. ethoxylated urethanes, which are able to form associates with the film forming latex [201]. At the same time, the dispersion contains a certain amount of surfactants: these is "free" surfactant present in the latex, and added surfactant to disperse pigments and fillers. Stability is achieved by varying interaction with the two dispersed phases – latex particles associated with the thickener, and pigment particles.

The use of antifoams is of special importance for the preparation of water-based paints [202]. Although foam problems also occur in textile and paper industries, there are some special features for paints. First, foam is formed in machines with high and medium shear rates, such as high-speed mills. The presence of a considerable foam volume inhibits the process and considerably reduces the useful load volume of the machine. Besides, foam inhibits the operation of the filling equipment. Problems also occur when paints are applied to a surface, especially using effective sprays, dipping methods and foam-curtain devices. The main reason of foam formation are surfactants used to stabilize aqueous latex dispersions. Thus, nonionic surfactants, instead of anionics, are preferred as they form less foam of low stability.

On the first step of the broad production of water-based paints, silicone antifoams have the highest efficiency. However, when they are used, surface coating defects are observed, which

can be described as "pinholes", "wrinkles", "craters" etc. These defects are connected with surface wetting problems in view of the hydrophobic nature of polysiloxane compounds. Attempts are made to overcome these defects by varying the structure of siloxanes, their joint emulsification with other antifoams, and so on. In this aspect, the patent literature lists hundreds of patents, and the choice of the required silicone antifoam is made on the basis of paint formulation, surface to be painted and mode of paint application to the surface. Antifoams based on wax and hydrocarbon emulsions are most widely used together with low-foaming emulsifiers. Two examples of typical antifoam formulations are:

Formulation I:

	Parts by weight
Scale wax	20
Candelilla wax	2
Glyceryl monostearate	15
Ricinoleic acid	5
23.5% sodium hydroxide	2.3
Water	55.5

Formulation II:

	Parts by weight
Scale wax	5
Paraffin oil	5
Glyceryl monostearate	5
Methyl ricinoleate	10
Monostearate	10
Water	64
40% aq. Formaldehyde	0.4

Mineral oils, Diesel oil and other hydrocarbon liquids can be used as oils, while acids, ethoxylated alcohols and alkylphenols (6 –10 EO) serve as surfactants. A finely dispersed silica (aerosil) is often added to enhance the defoaming effect. However, excess amounts of the so-called emulsion antifoams may negatively act, such as loss of gloss in the manufacture of new semi-gloss paints. When using paints containing two pigments, loss of colour may occur due to redistribution of surfactant adsorption on different pigments. However, this is a long process, and the sample to be dyed should be observed for at least 48 h.

Despite the positive ecological properties of water-based paints, they also cause some problems. It has been shown in [203] that the average total organic content in the booth water

of car assembly plants, in terms of COD measurements, spans from 3,300 to 16,400 ppm which, according to the authors, represents non-volatile organics as fine particles (<0.45 μm).

The use of surfactants for the manufacture of printing paints deserves an individual discussion. Surfactants and their mixtures with high-molecular compounds are used in preparation of thickening agents which are indispensable components of all printing paints [204].

A further progress perspective in the field of water-based paints could be their use for painting ships [205]. However, these studies are only in the beginning. The main difficulty is corrosion prevention. Maximum protection from stress corrosion cracking is ensured by alkyd paints combined with phenolic epoxy paints during a 6.5-year exposure [206]. These data were obtained on pre-contaminated steel plates. In Russia now water-based dispersion primers with anticorrosive properties have been developed and manufactured [207]. This was possible after incorporation of corrosion inhibitors combined with surfactants into the formulations.

The stability improvement of TiO_2 suspensions is important not only for water-based paints, but also for paints based on non-polar or low-polar solvents. It is shown in [208] that TiO_2 powders modified with an anionic surfactant, e.g. sodium dodecyl sulphate, are dispersed to smaller sizes, and their sedimentation stability increases. The production of water-alkyd emulsions is inhibited due to low mechanical stability. These emulsions can easily break when exposed to shear forces such as those produced by pumps, and when intensively agitated during dispersion. [209] demonstrates that most stable emulsions can be obtained with alkyds showing high acid numbers, as well as with highly polymerised alkyds of low viscosities.

Östberg et al. [210] have investigated in detail the influence of the emulsifier type and alkyd properties on droplet size and stability of alkyd emulsions. Alkyd S-68 (Bergvik Kemi AB, Sweden) was mainly used as an alkyd resin, containing 67.8% of oil, acid value=10.6, viscosity=680 mPa s. Other oils were also used, with acid values 8 – 9 and viscosities from 180 to 970 mPa s. The surfactants used were:

nonionic - ethoxylated (7-18 EO groups) fatty acid monoethanolamides, ethoxylated nonylphenols (20 EO groups);

anionic - dodecyl benzene sulfonate, hexadecyl sulphates, ethoxylated (2-3 EO groups) sulphates of $C_{12} - C_{14}$ and $C_{16} - C_{18}$ higher alcohols.

When preparing emulsions containing 50% alkyd in water, in the range from about 60°C to about 80°C temperature had little effect on the droplet size remaining in the range from 0.7 to 0.8 μm. For nonionic surfactants, the droplet size decreased up to 70 – 80°C, depending on the degree of ethoxylation, after which it sharply rose from 0.8 – 0.9 to 8 – 9 μm. This is probably due to the cloud temperature of the nonionics and the corresponding change of their HLB.

For anionics, when preparing 50% emulsions of alkyd S-68 at 70°C, the minimum droplet size was achieved at 4 – 6% surfactants in alkyd, the estimated adsorption layer thickness being about 50 – 60 Å. For nonionics, 8 – 10% was the optimum surfactant concentration in alkyd to obtain a minimum droplet size, while the adsorption layer thickness was between 100 Å and 400 Å. The authors concluded that at low concentrations the packing density of anionic surfactants at the droplet surface is rather low. For ethoxylated nonionics, there is some critical concentration corresponding to a close packing at the droplet surface, below which the droplet size sharply increases, and the emulsion stability decreases.

Data on the preparation of alkyd emulsions by the phase inversion technique were presented in [211]. This technique is accomplished by adding water to an alkyd/surfactant mixture under formation of a stable emulsion. The determination of surfactant's solubility in water and alkyd phases allows to calculate the quantity of water required for phase inversion. Effective emulsifiers are ethoxylated sulphates (2-3 EO groups) of $C_{12} - C_{14}$ and $C_{16} - C_{18}$ higher alcohols. With these surfactants, the emulsification becomes less dependent on the temperature than with nonionic surfactants.

The properties of alkyds have a substantial effect on the weather resistance of coatings. Graft-copolymers of castor oil alkyd with methyl and butyl methacrylate substantially reduce the drying rate, improve the weather resistance and mechanical properties of coatings [112].

6.7.4. Use of surfactants in building technology and metallurgy

The role of surfactants for the manufacture of foamed concrete and foamed gypsum is described in corresponding publications and is very limited by nature. Anionic surfactants or their mixtures with nonionic surfactants are, as a rule, used as foamers. Much attention is paid to the function of surfactants for road asphalts. Foamed asphalts are used under certain conditions [213] prepared with both natural surfactants contained in asphalts and synthesised

water-soluble anionic surfactants as foamers. Theory and practice of asphalt emulsions were in the focus of interest of the Second World Congress on Emulsions [214].

Both anionic and cationic asphalt emulsifiers can be obtained on the basis of tall oil acids, the oil containing blends of higher unsaturated acids and resin acids [215]. Anionic emulsifiers provide stable emulsions, especially with addition of small amounts of lignin or a nonionic co-emulsifier. Cationic emulsifiers are produced by condensation of tall oil fatty acids with polyamines such as diethylene triamine, triethylene tetramine and so on, as well as with complex mixtures of polyamines, including piperazines and other admixtures. By chemical structure, these products are mixtures of imidazolines and amidoamines. The emulsions exhibit a high curing rate due to the interaction of negatively charged aggregate surfaces and a good asphalt-to-aggregate adhesion. Owing to this, they are superior to anionic emulsions.

The causes of breaking of asphalt emulsions in contact with mineral particles of various nature are analysed in [216]. When mineral particles are in contact with water, the pH value of the medium changes and the emulsions stabilised by cationic surfactants are stable between pH 1.3 to pH 6.3. Emulsions stabilized with anionic surfactants break at pH < 10. In Japan [217], special cement-asphalt emulsions have been developed for low-traffic roads.

In metallurgy, surfactants are used in the production of cutting oils used for cutting, sizing etc, as well as in drawing metals, and for other purposes. Typical formulations differ only in the type of surfactant and mineral oil quality. In [218], the following example formulation is given:

Mineral oil	20 – 60
Fatty ester	10 – 30
Sulphated fats, sulfited fats, sulfonates	5 – 15
Fatty acid soaps and alkanolamines	0 – 5
Nonionic emulsifiers	5 – 10
Corrosion inhibitors	0 – 1
Biocides	0.5 – 2
Antioxidant agents	0.5 – 2
Antifoam agents	0 – 1
Water	0 – 10

In practice, these high-concentration emulsions are diluted to 4 – 5% by oil content.

6.7.5. The role of surfactants in enhanced oil recovery

Some aspects of surfactant's application in oil recovery go back to the beginning of the 20th century. These are stabilisation of clay drilling muds in wells with natural surfactants. Another application – demulsification of crude oils – began to develop in the thirties after synthetic anionic and nonionic surfactants had appeared on the market. A real boom for surfactants in the petroleum industry began in the sixties and still continues now. To master the pressure drop as a feature of oil reservoir structure, methods of injecting water and gas into the reservoir began to be widely used. Even these methods, called "secondary oil recovery", left 50-70% of the original oil in place. Therefore, experiments and practical trials were started on the development of tertiary or enhanced oil recovery methods (EOR), a term of worldwide recognition.

A number of reviews appeared on the use of surfactants and their mixtures, as well as surfactant-polymer mixtures in EOR during the sixties to eighties [219 –223]. Schramm published monographs on the use of emulsions [37] and foams [224] in oil recovery processes. In Russia, a small guidebook on agents used in the petroleum industry was issued 15 years ago [225]. All this facilitates the discussion of this problem in the present chapter where we make efforts to demonstrate the main results obtained earlier and to attract attention to new work.

First of all, there are systematic studies by Milter and Austad concerning the displacement of oil from low-permeable chalk material [226 – 228]. Different mechanisms are observed when a 1.0 wt.% wetting solution of a surfactant such as alkyl propoxyethoxy sulphate was used to displace heptane [226]. At the start, a countercurrent flow in the presence of surfactant sets in, but later, heptane is displaced from the horizontal surface under gravity forces. As a result of long-time experiments (ca. 200 days), no difference was observed between the displacement of hydrocarbons in presence or absence of a surfactant. The same authors [227] conducted their experiments both with heptane (a model) and with crude oil. In the presence of the same surfactant concentrations, low interfacial tension values were achieved (0.2 – 0.004 mN/m). The increase in oil production was from 5% to 10% depending on the experimental (model) core length in the range of 5 – 55 cm. Cationic surfactants were tested on the same material in [228]. The extra oil value depended on the surfactant delivery method: a) after a water flood; b) surfactant delivered along with water. Positive results were obtained in the second method.

These experiments show that it is possible to achieve positive results using EOR after a thorough investigation of the nature of mineral rock constituents of the oil reservoir and the choice of the surfactant delivery method. The dynamic interfacial tension is crucial in EOR. Using a model acidic oil, alkali solutions and surfactants at an optimum ratio, ionised water and surfactant adsorb simultaneous onto the interface, resulting in low dynamic interfacial tension [229]. Combined adsorption of surfactant (alkyl propoxyethoxy sulphate) and polymer (xanthan) was studied in [230].

In some cases, for example in a clay material, the use of surfactants in EOR does not allow to achieve either technological or economical results [234], where the following technique was used: first, alkali was injected whereby calcium ions fixed on the clays and contained in the connate water were removed, then surfactants and polymer were injected, both with the same alkali. The oil production was boosted from 50% of the original oil in place (without an alkali added previously) to 70% when using surfactant/polymer mixtures with a preliminary washing (with an alkali). The benefits of using surfactant mixtures in EOR processes are shown in a general form in [98]. The so-called non-ideal mixtures of surfactants, e.g. anionic-nonionic; cationic-nonionic; anionic-cationic give the best effects. The use of nonionics in these mixtures allows to effectively use ionic surfactants in brines and positively influences the wetting and dispersion of oil in water.

Positive results for high-temperature oil deposits are obtained when using a complex mixture consisting of surfactants, metal salts and carbamide. This composition was used in Noyabrsk field trials [232]. Water composition and injection rate also substantially influence the EOR efficiency [233]. At low flow rates, surfactant-containing connate water injected into the reservoir substantially enhances the oil recovery, while at high flow rates it has practically no effect on the efficiency.

6.7.6. Emulsions in EOR processes and refining

The enhanced oil recovery using solutions of surfactants or their mixtures has attained relatively little application. This is, first of all, due to the fact that surfactants adsorb from the solution on porous media of the reservoir, the specific surface of which may range from 150 to 3000 cm^2/cm^3, therefore, the use of emulsions, microemulsions and the so-called micellar-polymer flooding turned out to be more effective. In all of these processes, the flow

characteristics of the dispersions used are the controlling factors. The general principles of the rheology of emulsions have been formulated by Tadros [234]. The main parameters of the emulsion viscosity are the emulsion type (o/w or w/o), the volume fraction of the dispersed phase, droplet size and flocculation degree of the droplets, as well as the nature of the dispersion medium (viscosity, pH value, electrolyte content).

The emulsion behaviour in porous media is discussed in [235]. O/w emulsions with volume fractions of up to 50% show Newtonian behaviour, whereas those with more than 50% are non-Newtonian liquids, the apparent viscosity of which depends on the shear rate. The viscosities of such emulsions are more than 20 times that of water and sometimes can be even comparable with that of oil. When the emulsion is moving, a temporary permeability reduction of the reservoir may occur due to the capture of small droplets by the surface of the porous medium. In this case, stable o/w emulsions may flow not as a continuous liquid, i.e. the emulsion flow largely depends on the nature of the porous medium. Therefore, it is necessary to know about the structure and physicochemical characteristics of the oil reservoir (porous medium): porosity, the mean pore diameter, the mean pore size and pore size distribution, chemical composition of the minerals ("acidic", "basic", "neutral"), the nature of the pore surface, first of all wettability, for a successful application of the emulsion flooding method.

General principles of micellar-polymer flooding are discussed in [236]. A surfactant solution having a concentration much higher than CMC is injected into the well, which allows to achieve ultra-low oil/water interfacial tension values of the order of 10^{-3} mN/m. A polymer is used to raise the water viscosity. Such a combination of reagents allows to extract oil from thin capillaries. Model trials as well as field trials have shown that it is possible to achieve 60 – 80% oil recovery. However, the method had not attained widespread application for economic reasons in view of high surfactant consumption and expensiveness. In view of the fact that oil is the main raw material for the surfactant production, there is so far no answer to the question whether it is possible to obtain, from the additionally recovered oil, the quantity of surfactants required to accomplish this method. In this connection, proposals concerning the combined alkali-surfactant-polymer (ASP) flooding are very promising. When an alkali is injected, surfactants may form at its contact with oil components, and intensive studies are carried out in this direction.

Several micellar-polymer flooding models as applied to the EOR are discussed in [237]. It is noted that the co-solvent ordinarily used in this process considerably influences not only the microemulsion stabilisation, but also the removal of "impurities" in the pores of the medium. The idea of using an alkali in micellar-polymer flooding is discussed in [238] in detail. The alkali effect on the main oil components was studied: aromatic hydrocarbons, saturated and unsaturated compounds, "light" and "heavy resin" compounds and asphaltenes. It is demonstrated that at pH 12 surfactants formed from resins allow to achieve an interfacial tension value close to zero. For asphaltenes, such results are achieved at pH 14. In the system alkali solution (concentration between 1300 to 9000 ppm)/crude oil at 1:1 volume ratio a zone of spontaneous emulsification appears, which is only possible at ultra-low interfacial tensions.

Optimum parameters for a successful accomplishment of the EOR process are defined in [239]. First, they can be realized in reservoirs consisting of sandstones, sands, carbonates or mixtures of these materials with a layer thickness of under 25 m and permeability of over 20 mD, containing crude oil with a viscosity of <60 mPa s. In this case, a formulation containing, along with alkali, 20 – 30 g/l salts, ethoxysulphates and alkyl sulfonates, used for injection at a temperature below 80 °C. The authors are optimistic about the wide commercial use of EOR, since oil will remain the main energy source up to the second half of the 21st century. Surfactants can also be used to recover oil containing gas for the purpose of gas hydrate formation control [240].

One of the most important steps of oil refining is demulsification of oil emulsions both of o/w and w/o types. O/w emulsions may contain up to 40% water, and their breaking is, as a rule, accomplished under field conditions at special stations where the field oil arrives. W/o emulsions of 4 – 5% water content are subjected to demulsification directly at refineries. General approaches to the problem and theories of the process are given in [37, 38].

In practice considerable difficulties are encountered in selecting both demulsifiers and demulsification methods. Thermal, electric and chemical demulsification methods are listed in [241]. The latter is discussed very briefly and includes commonly known conditions: 1) choice of demulsifier and its optimum concentration; 2) effective stirring at a certain temperature; 3) optimum period of time to allow the phases to separate and to obtain a clear-cut boundary between the phases. Besides, 2 examples of rather well-known formulations are given, which

include ethoxylated resins, EO/PO block-copolymers and isopropyl alcohol. In a study by Pozdnyshev [242], well-known in the East, main attention was paid to the effect of natural surfactants on the emulsion stability. About 25 oil samples from different fields in Russia were analysed on their content of natural stabilizers (asphaltenes, porphyrins, "mixed"), as well as mechanical impurities. Using demulsifiers "disolvan" and "oksifos" as examples, demulsifier consumption as a function of natural stabilizer adsorption was determined. The obtained relationship is almost linear. Synergistic effects are manifested in cationic-nonionic mixtures at a certain ratio. The effect of water-soluble polymers with typical nonionic and ionic surfactant demulsifiers was studied and the causes of emulsion "ageing" and features of emulsion breaking were analysed. Satisfactory results are obtained when low-boiling hydrocarbons are introduced into the oil followed by heat treatment, and the low-boiling hydrocarbons evolving during heating ("deaeration" of oil) contribute to the breaking of emulsion aggregates. Special attention was paid to the breaking of emulsions containing so-called mechanical impurities which are fine particles of both hydrophobic and hydrophilic nature. These particles form stable aggregates with natural stabilizers and resin compounds in oil, and they also form "armored" layers at the interface. To break such emulsions, one has to sharply increase the consumption of demulsifiers from 80 g/t to 2 kg/t, to increase the process temperature and, in some cases, to use centrifuges.

Interesting results on emulsifier-natural stabiliser interactions were described in [243]. Ethoxylated phenol-formaldehyde resins were used as emulsifiers, e.g. polyalkylphenols-polyalkylene-polyamines-formaldehyde ethoxylates (PAPAFE). PAPAFE containing more amino groups are able to solubilise asphaltenes. This leads to desorption of these natural surfactants from the interface, thus increasing the demulsifying effect.

Interesting results are obtained not only on nonionic-natural surfactant stabiliser interactions, but also as for the modus of demulsifier delivery [244]. It was established experimentally, that when delivering a water-soluble demulsifier into the oil containing a w/o emulsion, and an oil-soluble demulsifier into the flushing water, the emulsion breaking efficiency sharply increases, and it was established that the water-soluble demulsifier must have a HLB > 10, and the oil-soluble a HLB < 6. It is assumed that an interphase diffusion of the emulsifiers takes place, which leads to a complete breaking of the "armoring" shells on the water droplet surfaces with subsequent coalescence of the droplets.

Rather interesting demulsification methods were proposed recently [245]: the use of membranes both of hydrophilic and hydrophobic nature to break down w/o emulsions and w/o/s mixtures. Hydrophobic membranes had pore sizes from 0.02 to 0.2 μm, and the dispersed aqueous phase droplet sizes ranged from 1 to 5 μm. The effect of water droplet retention is present even though the molecular weight of the water molecule (18) is much smaller than that of tetradecane (198) which was used as a model.

An air flotation method was proposed for breaking o/w emulsions after its treatment with a cationic, high molecular weight flocculent. It has been found that in the presence of the flocculent the emulsion film is less stable than the starting pseudo-emulsion film, which determines the efficiency of the process [246]. The flocculent improves oil spreading on the water-air surface, thereby enhancing separation efficiency.

Emulsions can be used in pipeline transportation of heavy crude oils [247]. This is a cost-effective alternative to heated pipelines. O/w emulsions are composed of 30% aqueous phase and 70% crude oil and have a viscosity range from 50 to 200 cP. A mixture of ethoxylated alkylphenols was used for the emulsion stabilisation. Emulsion stability is provided in a solution containing 1.7% NaCl at total consumption of the mixture of 1500 ppm. The emulsion is prepared at 50 – 70 °C. For the subsequent demulsification, it is necessary to raise the temperature up to 100 °C and to add a demulsifier.

A new development is the use of emulsions as fuels for vehicles. The following studies have been selected from the numerous patent sources on this topic. The possibility of making stable water-diesel emulsions containing 10% of water and 0.75% of an emulsifier whose composition is not specified is shown in [248]. When the water content increases, the emulsions break.

Emulsification of two marine fuel oil types was compared in [249]. When using residual fuel oil, a higher stability was obtained in comparison with the distillate fuel oil. Rather stable w/o emulsions were obtained using the emulsifier Span 20 at concentrations of 1.5 – 2%. At higher emulsifier concentration, the emulsion properties (droplet size, stability, viscosity) deteriorated.

Investigations on water-fuel emulsions using different types of fuels such as gasoline, diesel fuel, fuel oil are discussed in [250], based on results on emulsion droplet stabilisation against flocculation and coalescence [50 – 58]. Water-gasoline fuels containing up to 10% of water

were obtained, and they were tested on engines. Although improvement of the exhaust gas composition was achieved, this method was not used for economic reasons: to obtain emulsions stable within 24 hours, more than 1.5% of a complex emulsifier mixture is needed.

Fuel emulsions for diesel engines, stable within a period of over 6 months and containing 10% to 30% water at relatively low emulsifier amounts have been comprehensively tested on a stand scale, as well as on vehicles (heavy trucks, marine vessels). However, commercialisation of these fuels as for car engines requires changes to be made in the design of their fuel systems. At the same time, this problem has been successfully solved for the river vessels [251].

6.7.7. Foams in EOR processes and refining

The features of foam application in petroleum industry were summarised by Schramm [224]. Thereafter only very few publications appeared on this subject, so that we mainly describe Schramm's concepts. First of all, these are foams which contribute to an enhanced efficiency of oil recovery: foam drilling fluids, foam fracturing fluids, gas mobility control foams, and foam acidising fluids.

Foams can also be used to treat zones near bottom holes to remove solid impurities and for oil and gas well drilling. Stable foams are used in all of the above cases. In other cases, defoaming is necessary to provide a normal course of the processes. First of all, these are foaming in distillation and fractionation towers, producing oil well and well-head foams, fuel oil tank foams.

It is pointed out in [252] that more than 10% of the world oil recovery is accomplished by injecting steam or CO_2 for the production of oil by EOR. Here, the foam bubble size is comparable or slightly more than the pore diameter. To increase oil production, highly disperse steam foam is required, which "pushes" the oil out of the reservoir while moving both as a continuous and discontinuous flow. It has to be emphasized that the choice of surfactant is important to accomplish the process. Typically, the surfactant concentration is much higher than CMC, which predetermines the expensiveness of the process. The foam is destroyed when coming in contact with oil and rock, which requires its increased consumption. Three mechanisms of foam formation under reservoir conditions are proposed in [253], determined by the liquid flow rate and the throat radius between the pores. When the foam flows in a reservoir, its aggregative stability is disturbed due to coalescence. Hence, the choice of

surfactants for the formation of foams stable under reservoir conditions can be accomplished by measuring the capillary pressure in the lamellae. The influence of the capillary pressure in the lamellae and Plateau-Gibbs boarders on foam stability is described in detail in [17]. The influence of the gas (nitrogen) flow rate and surfactant concentration on the pressure drop along the model cores filled with pore media and the displaced liquid volume was investigated and optimum relationships can be established between the relevant parameters.

Under certain conditions, a stable aqueous foam can be formed in a water-hydrocarbon system [255], where the foam stability is determined by the stability of the "pseudo-emulsion" film, i.e. the aqueous film between an emulsified water droplet and the gas phase. This effect was detected in earlier investigations on the gas flow rate for water-hydrocarbon mixtures where the hydrocarbon ratio was between 10 and 90% [256]. The formation of a noticeable foam volume was observed in the emulsification of a hydrocarbon, i.e. when the system was transformed from a two-phase (heterogeneous) system into a microheterogeneous phase, i.e. a highly disperse o/w emulsion. The foam formation, at the same surfactant concentration, depends on the gas delivery rate. In the presence of a hydrocarbons the gas supply rate required for foam formation is usually 2 – 10 times higher than in absence of hydrocarbons. The higher the hydrocarbon ratio, the higher the "critical" air consumption at which emulsification and subsequent foam formation take place. Thus, at 1:1 ratio, the critical consumption is ca. $8 \cdot 10^{-6}$ m^3/s, and for 1:19 ratio, it is $20 \cdot 10^{-6}$ m^3/s. These data have been obtained for low-viscosity hydrocarbons. For high-viscosity hydrocarbons, corrections are necessary, however, the main principle remains valid: the formation of aqueous foam in the presence of a hydrocarbon is only possible in the transition from a two-phase gas-water system to a three-phase "gas-o/w emulsion" system, i.e. in a transition from a heterogeneous system to a micro-heterogeneous system.

Schramm [257] considers it a big problem that foams are sensitive to the contact with oil under porous medium in oil recovery. While proposing a several foam breaking mechanisms under reservoir conditions, the author believes the emulsification process of oil in water is the most important step. In emulsification, the contact area of pseudo-emulsion films increases with the oil contents. In case the pseudo-emulsion films are stable, the foam stability and thus the process efficiency increases. Thinning of pseudo-emulsion films leads to its rupture when gas is continuously injected into the media, flooded with a surfactant solution at residual oil

saturation. Thus, it has again to be emphasised that, for a successful application of a method, it is necessary to adjust the surfactant formulations to a specific oil reservoir.

Surfactant adsorption on the reservoir surface is another important factor to be considered when using foams in EOR processes is discussed in [258]. Adsorption experiments with surfactants of different structures were performed on cores of a number of materials (quartz, sandstones, kaolin, calcite and others), both "clean" and modified (impregnated) with hydrocarbons of various structure ("light" oil, "high-viscosity" oil, asphaltenes). Minimum adsorption, as well as maximum oil recovery based was observed when using amphoteric surfactants as well as surfactant mixtures, e.g. diphenyl ether disulfonate – α-olefin sulfonate (DPES-AOS).

In [259] results are obtained when using foams for EOR in oil fields in China. Many oil fields in China contain up to 80% water as result of water flooding, and the oil recovery does not exceed 20%. The main reason of the low reservoir recovery is a strong heterogeneity of the reservoir which causes the injected water to channel through only the high-permeability zones. Injection of foams in the water-oil front can improve the profiles of injected liquids in view of a drastic difference in flow properties between foam and water, so that the efficiency of oil production can be increased. Anionic surfactants (petroleum sulfonates, α-olefin sulfonates, alkylsulphates) as well as their mixtures with nonionic surfactant and polyacrylamide were tested under laboratory conditions. Data are presented concerning one of the projects accomplished in one of the oil fields in China. Within the period from May 1971 to June 1973 (26.6 months) 933 m^3 of 1% solution of surfactant mixture and 8082 m^3 air has been injected which is equivalent to about 5% of the reservoir volume. The water cut decreased by 27.7% while the recovery factor increased by 6%-8%.

In [260], preparation conditions of gas-blocking foams were studied. Experiments were performed on cores filled with 100-μm glass beads with a permeability of 8.5 D. In absence of surfactants, the gas passed easily as a jet through the core filled with water. With the surfactant sodium alkyl ethoxysulphate increased from 0.1 to 0.5 wt.%, a "foam piston" was formed which pushed the surfactant solution. To achieve a gas blockage, the porous medium must exceed a certain minimum length greater than the length of travel for the displacement front to

become a piston. The surfactant concentration must exceed the CMC, and combinations of surfactants resistant to the oil action are preferred (cf. [257, 258]).

A review on field applications of steam foams is given in [261]. It is shown that experiments on injection of aqueous steam foam surfactant solutions, conducted earlier gave a relatively low increase in oil recovery, but remained profitable nevertheless. To achieve better results, the reservoir structure must be taken into consideration for the choice of an optimum foam injection regime.

Features of using steam foams for EOR as applied to heavy oil and bitumen are shown in [262]. Foam-forming components which are injected with the steam stabilise the lamellae and form the so-called steam-foam. This results in an increase in the pressure gradient in the steam-swept region, the steam flows to the unheated area, and the displacement efficiency of the heated oil increases. The application efficiency of this method depends on the thermal stability of the surfactants. Thus, a petroleum sulfonate was only about 10% decomposed after 28 days at pH 9 and 205 °C. C_{16}-C_{18} alkylaryl sulfonate lost activity by 2 – 3% after 10 days at 299°C and pH 11, and the surfactant concentration decreases more than 3-fold at pH 4. In general, the surfactant degradation increases with increasing temperature and hydrophobic chain length.

Field trial results on the use of CO_2 foams for EOR in Texas and Utah are given in [263]. 161,000 lb of active surfactant was injected in four field trials within 18 months. In all cases, increased oil production was observed. The surfactants Rhodapex CD-128 and Chaser CB-1045 were used.

It has been mentioned above that foams can unfavourably affect the refining processes. Formation processes of non-aqueous foams are not well enough studied. In a vast review [264], comparison between aqueous and non-aqueous foams has been made. The stabilisation of non-aqueous foams (e.g. on a hydrocarbon basis) seems to be impossible with usual hydrocarbon surfactants because of the weak liquid-gas interfacial tension lowering gradients. Fluorinated or silicone-type surfactants can be used as eventually better stabilisers. These recommendations are, in our opinion, only applicable to the production of the so-called hardening foams (polystyrene foams, polyurethane foams etc.).

Foam formation in oils and their processing products depend primarily on the contents of natural surfactants, oil viscosity and stirring intensity during pumping, especially in contact with air, as well as evolution of low-boiling hydrocarbons from oil (halogenic foaming).

It was shown that in the presence of oil-soluble surfactants, stable foams are formed at a certain water content in diesel fuel, and maximum stability is achieved at a relatively low aqueous phase concentration (1% – 2%) corresponding to the transition of the solubilised solution to an inverted emulsion [265]: with increasing viscosity of the surfactant solutions in the diesel fuel, the foam stability increases substantially. These ideas can be used when considering foam formation in other petroleum products containing small amounts of water and natural surfactants.

Detailed recommendations on the use of antifoams in oil refining are given by Callaghan [266]. There is no need to repeat the detailed tables there, but note that polydimethyl siloxanes of high and low viscosity, as well as their mixtures with highly dispersed SiO_2, fluorosilicones, silicone glycols as well as alkyl polyacrylates are the main antifoams for many applications. Non-polar liquids (white spirit, kerosene, diesel fuel, toluene etc.) as well as polar substances (methyl-ethyl ketone, acetone, amyl acetate etc.) are used as diluents. Compositions are not given in [266] so that oil engineers have to adjust the recipes both to the process conditions (such as fractionating column operation conditions) and to the properties of the oil processed.

6.7.8. Surfactants – coal extraction and processing

Some decades ago, the problem of low-grade high-ash coal flotation was very acute. Hydrocarbon liquids (e.g. kerosene), $C_6 – C_8$ alcohols and their mixtures as well as anionic surfactants, such as petroleum sulfonates (trade name DS PAS) were used as flotation agents [267]. Later, the coal flotation problem lost its actuality, though a certain interest continues to exist for some regions. The possibility of using o/w emulsions for the flotation of high-ash coals was shown in [268]. Emulsions of kerosene fraction 200-300°C were used which contained aromatic, naphthalenic and paraffinic hydrocarbons (FDF agent) and mixtures of aliphatic alcohols, aldehydes and ethers with hydroxyl numbers of 220-230 (VRBS). FDF emulsions (10 vol%) contained 10 μm particles and VRBS emulsions of 5 μm particles. In flotation of intermediate particles (0.5 mm) the ash content in the concentrate was 4.7%, and

the tailings contained up to 73% of ash, i.e. essential separation of the starting material was achieved.

Dewatering processes are of great importance for fine clean coals [269]. Surfactants (e.g. sodium dodecyl sulphate) reduce the moisture content of filter cake in the dewatering of suspensions. A direct correlation has been established between the surface tension reduction in the coal system and the moisture content in the filter cake. Improvement of final product properties owing to the change of coal particle wettability can be achieved only in the presence of effective dewatering additives. In the mid-eighties, due to the observed periodical changes of world oil prices, a new type of alternative fuel – high-concentration water-coal suspensions (HWCS) gained interest. Such suspensions must fulfil a number of indispensable requirements: the concentration of coal must be 62-66 wt.%, the effective viscosity at deformation rates of 10 s^{-1} at the level of 1 Pa s, sedimentation storage stability no less than 15 days, high stability under dynamic conditions.

In Russia, a so-called "Interdisciplinary Group" was established which was in charge to develop HWCS suspensions and their hydro-transportation at distances over 200 km [270, 271]. The investigations developed in two main directions: 1) stabilisation mechanism of the suspensions and control of their flow properties; 2) the choice of additives – surfactants, polymers, inorganic substances which control the suspension properties.

The main laws of the flow properties of disperse HWCS systems are well described in [272, 273]. The main conclusions of this study consist in that the process of degradation of HWCS structures is described by an exponential equation which is determined by the depth and the rate constant of the degradation. Then, it is proposed to consider, along with the steady-mode suspension flow curve, an initial-moment flow curve, which provides additional information on the flow behaviour of the suspension in transition regimes.

Bedenko et al [275 – 276] have, to a certain extent, developed the ideas by Rehbinder and Urjev, of the effect of disperse phase particle size on the strength of the structure and viscosity η using HWCS as an example. In mixtures of fine (e.g. d_f =21.8 μm) and coarse coal fraction (e.g. d_c = 180 μm), the finely divided fraction as a continuous medium can completely fill out the entire void volume between the particles of the coarse fraction. Experimental data have shown that at $d_c/d_f > 4$, a synergistic effect of the packing density of particles in the mixture is

observed, whereas at $d_c/d_f > 8$, an optimum composition of the mixture is provided, which is in good agreement with the model. Thus, at a 60:40 ratio of coarse fraction to finely divided fraction, a minimum viscosity for a 50% coal suspension is achieved. When anionic surfactants (e.g. naphtalene sulfonic acid condensation products) adsorb on coal particles, the ζ-potential of the particles rises sharply (to -100÷-120 mV), which leads to an increase in the electrostatic repulsion and thus, to a decrease in the strength of the structure and suspension viscosity. Natural surfactants, e.g. humates (CAA – carbon alkali agent) and lignosulfonates contain polar groups (hydroxyl groups, carboxyl groups, sulfo groups), and it has been established that the ion-electrostatic factor controls their effect on the suspension viscosity.

The plasticising activity of ethoxylated alkylphenols and EO/PO block-copolymers depends on the number (m) of the EO units in a surfactant molecule. Ethoxylated alkylphenols with m>40 have a substantial effect on the viscosity reduction of HWCS. It may be connected with the fact that they can form rather thick hydrated layers when adsorbing on the particles, which play the role of a structure-mechanical barrier. The addition of ethoxylated alkylphenols with m<40 produce a thickening effect on the suspensions which may be connected with the features of coal particle wetting by aqueous surfactant solutions.

A correlation was found between sedimentation stability and structuring of HWCS. It has been shown [275, 276] that independent of the type of surfactant added, the stabilisation begins when the strength of 0.1-0.5 Pa is reached. For HWCS stabilisation, low additions (0.05 to 0.5 wt.%) of high-molecular water-soluble polymers, such as carboxy methyl cellulose, can be used. This may be connected with "bridging" due to the adsorption at the particles of the two different ends of the molecule. Tadros et al. [277] investigated the influence of a polyelectrolyte and nonionic surfactants on the rheology of HWCS. Sodium sulfonate was used as a polyelectrolyte surfactant (Ufoxane 3A). When more than 0.1% Ufoxane 3A was added, an appreciable deflocculation of the suspension was observed, accompanying the decrease in the sedimentation volume. At the same time, a noticeable increase in the negative ζ-potential of the coal particle surface was observed, which is in agreement with data obtained with other types of surfactants [276]. PEO-PPO-PEO copolymers containing from 4 to 174 EO units per 55 moles PO were studied simultaneously. At a chain length of < 37 EO moles, the effect of viscosity reduction is small. With increasing PEO chain length, the deflocculation degree increased, and the suspension viscosity decreased. Some maximum concentration was

observed, at which the flocculation increased again. The author considers the combination of nonionic surfactants and polyelectrolyte surfactants as a promising development to obtain stable HWCS.

Also the effect of block-copolymer surfactants (Synperonic NPE) on the viscosity and stability of suspensions as a function of the PEO chain length is studied [278]. The critical volume fraction of coal in suspension and maximum stability were observed for a surfactant with 48 PEO units. At 27 PEO units, flocculation appeared. In the interval from 79 to 174 PEO, desorption resulted leding to an increase in suspension flocculation. Thus, the choice of an optimum PEO content is very important to obtain liquid and stable suspensions, considering the features of the coal nature.

A combination of two surfactants was studied in [279]: ethoxylated nonylphenol of 150 moles EO (DNP 150) and adsorbing on the coal particle surface, and a water-soluble polymer polyethylene oxide (POE) the adsorption of which on the particles was not fixed. At a closely packed adsorption layers of DNP 150 on the surface of the coal particles and a minimum POE addition, a suspension was obtained which did not settle for 2 weeks. After this time, the suspension exhibited minimum settling without large increases in suspension viscosity.

In [280], dynamic surface tension and CMC values were determined for one nonionic surfactant NP-100 and four anionic surfactants containing sulfo-groups. The measurements were made in suspensions containing between 40 to 50% coal particles with a mean size of 55μm. These data may be useful in developing surfactant formulations for HWCS stabilisation.

The effect of temperature and surfactants on the viscosity of coal-water mixtures is shown in [281]. It has been shown that the volume content of coal in suspension can be increased while preserving its flowability at a certain surfactant content. Stable and pseudo-plastic suspensions were obtained both with anionic surfactants containing electrolyte, and with ethoxylated alkylphenols with a high content of oxyethylene groups. But the rate of reduction of the apparent viscosity begins to decrease with increasing temperature which seems to be connected with the change of the surfactant structure in solution and adsorption layers.

A composition was proposed consisting of sodium humates – plastisising component – and stabilizing components (Na_2CO_3, CaO), carboxymethyl cellulose [282]. At a total consumption of 1 wt.% per tonne of coal, 600 tonnes of suspensions was obtained containing 60-61 wt% of

coal, used at the Belovskaja power station. A dispersing agent was proposed with the trade name NF (naphtalene sulphonic acid and formaldehyde condensation product) combined with pyrolysis products of high-viscosity oils for the preparation of HWCS suspensions [283]. The principles of stabilisation and control of the flow properties of HWCS have been determined as a function of the additives used. Commercialisation depends on the economic efficiency of HWCS, which can differ for different regions and extraction methods of coal (e.g. hydroextraction) as well as on its ash content and grinding costs.

6.8. SURFACTANTS IN NOVEL TECHNOLOGIES

In the late eighties, the new field of nano-technology, began to develop [284]. Considering the data presented in [284 – 287] and [41, pp. 227 – 265], the following main conclusions can be made. Nano-particles are small atomic clusters of 10 – 1000 atoms, which exhibit properties between the molecular and micro-heterogeneous size limits, and may contain crystalline, amorphous and quasi-crystalline phases. The microemulsion method is one of the novel techniques for the synthesis of nano-particles due to the ability of microemulsions to solubilise substances which are insoluble in both polar and apolar media [284].

Compared with coarse-grained materials, nano-particles can possess unique electronic, magnetic and optical properties. The main principle of producing nano-particles with microemulsions consists in mixing two types of microemulsions, i.e. o/w and w/o microemulsions. In this way, for example, ultra-fine particles are obtained, whose core and external shells consist of Fe salts, and in the intermediate layer copper is contained. To produce microemulsions, anionic surfactants such as Aerosol OT (AOT) are used, one mole of which can solubilise up to 8 moles of the aqueous phase.

The self-organization of the parent surfactant phases allows, due to structure changes, to control the final size of the particles and, in some cases, their shape [285]. Using microemulsions, it is possible to obtain semiconductor, metallic, and superconductor particles as well porous ceramic materials. Conductive films can be obtained using Langmuir-Blodgett (LB) films. The high stability of LB technology against external influences is due to the "dead zone" under each deposited layer [286]. It was shown that defects with sizes up to 5 nm can be created in a conductive film.

A method to obtain nano-particles at air/water interfaces has been described in [287]. Spreading of surfactant-coated metallic, semi-conducting, magnetic and ferroelectric nano-particles on water surfaces results in the formation of monoparticulate thick films which then can be transferred, layer by layer, to solid substrates. These films can find potential applications in advanced electronic and electro-optical devices. Here and further, we give only typical examples of using surfactants in novel technologies. A more detailed description can be found in a new edition of "Surfactants Science Series" [288].

Interesting features were also revealed for the "photo-surfactant" 4-ethylazobenzene 4'-(oxyethyl) trimethyl ammonium bromide (EZTABr) in comparison with the typical cationic surfactant dodecyl trimethyl ammonium bromide (DTABr) [289]. A trans/cis transition takes place in EZTABr on UV irradiation. The CMC of the "photo surfactant" increases depending on the cis-form content. As for the surface activity, it decreases in the sequence DTABr > trans-EZTABr > cis-EZTABr. These data must be taken into consideration, in practice, when using this kind of surfactants. Information on the use of surfactants for the preparation of photo-resists necessary for advanced magnetic recording devices is given in [290]. The system used can be applied on various surfaces, such as copper, gold, alumina. The surface treatment with surfactant solutions plays a key role in the increase of the resolution. Depending on the surfactant structure, solution concentration, period of application, and order of processing steps, under proper conditions, significant enhancement of photo-resist contrast is achieved which is accompanied by improvement of photo-resist image profile and resolution. The above method is particularly useful in electroplating applications.

The recovery of metal ions from rinse solutions is important in electroplating. It has been shown in [291] that nickel ions can be recovered using a liquid surfactant membrane (LSM) obtained on the basis of di(2-ethylhexyl) phosphoric acid. The LMS permeation by nickel ions (external phase) is affected by the membrane viscosity which depends on the surfactant concentration.

Surfactants improve the effectiveness of using conducting silver powders for screen printing [292]. Caprylic acid and triethanolamine were used as surfactants. The pastes obtained after the treatment with surfactants demonstrate a good effectiveness which increase with the surface

area from $5 \cdot 10^3$ mg/kg to $10 \cdot 10^3$ mg/kg, the pastes remaining pseudo-plastic. At the same time, the increase in the paste density had practically no influence on its rheology.

Many composite materials can also be obtained only using surfactants. Thus, formulations including TiO_2, polyethylene and calcium carbonate were only obtained by dispersing TiO_2 and $CaCO_3$ powders in polyethylene after dispersing particle aggregates with the corresponding surfactants [293].

Sub-micron $PbTiO_3$ can be obtained with w/o emulsions which is advantageous to the conventional reaction route [294]. The powders were prepared by first emulsifying the Pb and Ti salts at appropriate ratios in an n-octane solution. The powder morphology and, first of all, uniform particle size distribution was affected by surfactant concentration and agitation time. During the subsequent heating, tetragonal $PbTiO_3$ began to form from above 560 °C, and heating at 900 °C yielded pure $PbTiO_3$ particles of sub-micron sizes.

Quite original is the attempt to obtain porous materials, for example, from crystalline calcium carbonate (aragonite) similar to the natural material chalk of a certain porosity [192]. Another attempt was made to synthesize macro-porous aragonite with a structure similar to the cocco-spheres of certain marine algae [295]. For this purpose, oil-water-surfactant microemulsions supersaturated with calcium bicarbonate were obtained. The pore size was determined by the water and oil concentration ratio. Microemulsions were applied on the substrate of micrometer-sized polystyrene beads. Hollow spherical shells of finished structure were produced as a result of a rapid mineralisation. The authors suggest that such materials could gain widespread use in materials chemistry.

Highly disperse silicas of various nature (hydrophobic and hydrophilic) have gained widespread use in technology, e.g. as antifoam additives [38]. But the technology of their manufacture requires a high energy consumption, and the costs are also high. An emulsion-gel technique for the preparation of highly disperse silica has been proposed where from tetraethyl orthosilicate-ethanol-aqueous ammonia, 70 – 640-nm particles were obtained by precipitation from homogeneous solutions [296]. The emulsion-gel method (water content ca. 15 wt.% and surfactant content less than 0.5%), yields best results, although the particle size can increase to some hundred nanometers.

Many modern composite materials are prepared by microemulsion methods. Polyaniline was prepared by one-step micellar chemical polymerisation of aniline with dodecyl benzene sulfonic acid via complex formation [297]. A transparent polyaniline suspension was made by dispersing polyaniline in m-cresol. Polyaniline composites blended with polymethyl methacrylate (PMMA) exhibits relatively high conductivity at low polyaniline volume fractions and keeps good mechanical properties equivalent to those of PMMA. It should be noted that most methods proposed for the preparation of new materials are at a laboratory level, however, a widespread commercial use can be predicted for the next decade.

Let us now discuss some applications of microemulsions in catalytic processes. It has been shown in [298] that the use of microemulsions instead of organic solvents for electrochemical reactions is advantageous from both economical and ecological reasons. The electrode/fluid interface in microemulsions probably consists of a dynamic layer of surfactant molecules packed more loosely on the electrode than in aqueous solutions. Microemulsions provide good yields of carbon-carbon addition products in reactions catalysed by cobalt complexes when preparing vitamin B_{12}. Excellent stereo-selective control in microemulsions made with the cationic surfactant cetyl trimethyl ammonium bromide was demonstrated for the catalytic cyclisation of 2-(4-bromobutyl)-2-cyclohexene-1-one to 1-decalone. Electrochemical synthesis may be a viable future approach to environmentally friendly chemical methods.

Microcapsules containing polymer and pigment were prepared in [299] by dispersing a viscous suspension of pigment and oil-soluble shell monomer forming o/w emulsions. Subsequently, a water-soluble shell monomer was added to the emulsion droplets, encapsulating them via interfacial polycondensation. These microcapsules were then heated for free radical polymerisation of the core monomers. It has been shown that polyvinyl alcohol (PVOH) used as stabiliser reacts with the oil-soluble shell monomers. The decrease of PVOH concentration as result of this interaction leads to coalescence of the particles and to the increase of their equilibrium particle size, however, methods are proposed to prevent the depletion of PVOH.

The effect of emulsions formation stabilised with CTAB in presence or absence of catalysts ($CuSO_4$, $CuBr_2$) was studied in [300]. It was shown that the high rates and selectivity of oxidation are achieved at a high stirring efficiency of the system when the entire micellar phase

is distributed over the interface, and when radical are initiated in the interfacial layer of the lyotropic surfactant liquid crystal, which stabilises the emulsion.

The oxidation rate of emulsions of ethyl linoleate (EL) diluted with n-tetradecane in the presence of Tween 20 was studied in [301]. The emulsions had an initial droplet diameter of 0.3 μm and total oil contents of 5 wt.% (EL-tetradecane). At 1% EL in oil, oxidation proceeds at a slow rate. At 20% EL in oil, the oxidation rate was rapid initially and then slowed down with time. In the absence of tetradecane, the oxidation rate was slow at first, and then increased with time. In all cases, the oxidation remained high in the presence of emulsifier.

The use of two types of liquid membranes is described in [302]: liquid emulsion membranes (LEMs), and supported liquid membranes (SLMs), where isoparaffin or kerosene and their mixtures were used as organic phases. A surfactant of the type of Span 80 served as emulsifier. LEMs are used, for example, for selective separation of L-phenylalanine from a racemic mixture of L-leucine biosynthesis as well as conversion of penicillins to 6-APA (6-aminopenicillanic acid). SLMs have a higher stability. A number of their commercial applications have been studied, e.g. in separation of penicillin from fermentation broth, as well as in the recovery of citric acid, lactic acid and some aminoacids. Compared with other separation methods (ultrafiltration, ultracentrifugation and ion exchange), LEMs and SLMs are advantageous in the separation of stereospecific isomers in racemic mixtures.

Interesting data on the application of microemulsions in analytical chemistry are given in [303]. In recent time, aprotic solvents, such as acetonitrile, have been widely used in titrimetric methods. However, these solvents are toxic, flammable and have a number of merely technical disadvantages such as high dielectric constant which narrows the number of substances determined. The titration of "week" acids, such as *o*-chlorophenol, *p*-nitrophenol, decanoic acid, with amines in the form of o/w emulsions containing CTAB and butanol is possible. This section deals only with some aspects of surfactant application in novel technologies, but these applications demonstrate a continuous further development.

6.9. SURFACTANTS AND ENVIRONMENT

Some years ago, a monograph was published [304] in which this problem was elucidated in detail. At the same time, some of the questions remain disputable, such as methods of determination of biodegradation of surfactants, their objective assessment, influence on the

environment. In our opinion, not enough attention is paid to the methods of using surfactants and surfactant-stabilised disperse systems (foams, microemulsions, flotation processes) for decontamination of the environment, first of all water, soil, and air. This section includes examples for using surfactants to control technological catastrophes (oil spills, fires etc.). In our opinion, this section could be complementary to the above review, even more as it contains results from the Russian literature, which are not so widely known to experts in the West.

Let us first discuss the main flow-sheets of surfactants' impact on environmental pollution. First of all, the so-called "open" schemes of using surfactants are predominant: aqueous surfactant solution is fed into the process, after which a portion of it comes, along with pollutants, into waters and soils. Soil removal from the surfaces of various nature, flotation, use of surfactants in the textile industry can be considered as belonging to these processes. On the other hand, there are "closed" schemes, where a surfactant is completely adsorbed in the product after use and does not get into the environment (productions of foamed concrete, asphalt emulsions, and others). Preparation of highly concentrated water-coal suspensions can also be assigned to the closed schemes since the surfactants are burnt together with the fuel while improving the composition of the exhaust gases (see above). Finally, there are "semi-closed" schemes where considerable surfactant amounts adsorb on natural sorbents at a sufficient depth, i.e. the use of surfactants in EOR. But in the perspective, development of closed circuits is possible where part of the surfactant is recycled to the initial process, for example, the use of the so-called return waters in the flotation.

In the study by Bocharov and Krasovskij [305], the concentration c_m for maximum surfactant adsorption at the water/air interface and the maximum permissible concentration (MPC) of surfactants present in household waters are compared and a large table of data given. For example, for sodium alkyl sulfates, the MPC and c_m values, respectively, are 0.5 and 0.6±0.1; for dodecyl benzene sulfonate 0.5 and 0.4±0.1. For nonionics $R(OC_2H_4)OH$, where R=aliphatic radical and n = ethoxy groups number, these values are: for $R=C_{10}$- $C_{13}/n=7$: 0.1 and 0.12±0.3; for $R=C_{10}$- $C_{18}/n=10$: 0.1 and 0.10±0.02. Thus, adsorption isotherm studies are very promising for the determination of MPC in comparison with the frequently applied foaming method where the MPC is determined at a concentration where dynamic foam bubbles appear in the waste water.

Another important point in this study is the comparative determination of surfactant degradation in tests with basin models and in aerotanks [305]. The relationship $\ln c(t)/c_0 = f(c)$, (c_0 is the initial surfactant concentration and c(t) the concentration at time t) shows two portions:

- the first time period of about 8 days when sludge adaptation reaches equilibrium while the surfactant concentration practically does not change,
- the second period of usually 3 – 4 days, where the concentration is sharply reduced due to surfactant degradation by the adapted microflora.

In an aerotank system, more periods are observed in the relationship $c_0/c(t)$:

- surfactant adsorption on activated sludge (1 day);
- adaptation and degradation of surfactant on non-adapted activated sludge (2-4 days)
- reaching an equilibrium state and surfactant degradation by adapted microflora.

It is proposed to characterise the biodegradation degree by the rate constant K_{st} in a stationary mode, which is determined by the expression

$$(c_0\text{-}c(t))/c_0 = \frac{K_{st}}{K(t) - K_{st}} . \qquad (6.12)$$

The basic factor for a surfactant to be classified as biologically "hard" substance is its low adsorptive capacity due to which the required sludge adaptation and the stationary state are reached only after 15 – 20 and more days. Biologically "soft" surfactants easily adsorb on activated sludge, and their adaptation is reached in a shorter period of time (2 to 4 days).

The important problem of measuring surfactant concentrations in sewerage systems from the moment they get into municipal treatment plants is studied in [306]. Observations of virtually untreated sewage waters confirmed laboratory data which show that surfactants such as alcohol ethoxylates (nonionic surfactants), alcohol ethoxysulphates (anionic surfactants) degrade to more than a half during several hours of the residence in the sewerage system. This half-life time turned out to be still shorter for glucose amides. These tests show that the ecological load of treatment plants can be considerably reduced in the sewerage systems.

More attention is paid to sea pollution. Some aspects of ecological danger of aquatic pollution by nonionic surfactants, Triton X-100 (TX) as an example, were studied in [307]. In the presence of 1 mg/l TX, the cell density of the diatom Thalassiosira pseudonana decreases by 50%. The decrease in the specific growth rate was about 10% in presence of 0.1 mg/l TX. The diatom sensitivity to TX was higher than that of some red and green algae. The negative effect of surfactants present in the sea water on coastal vegetation is shown in [308, 309]. Pines were dipped for a short time in distilled sea water as well as in a saline solution of dodecyl benzene sulfonate [308]. The surfactant accumulated mainly in the epicuticular wax which suggests the possibility of pollution for coastal trees. In [309], "in vivo" tests along the Tyrrhenian coast in Italy are shown. The decline of coastal vegetation is a phenomenon affecting some areas of the Mediterranean region and Australia, which is due to the presence of surfactants in marine aerosols. The impact of surfactants on vegetation is local and occurs only in association with strong sea winds or when considerable surfactant concentrations are present in the coastal zone. Much attention is paid to the determination of the pollution degree of the sea surface using different methods. Thus, the effect of surfactant on the growth of wind waves was investigated in [310] by simultaneous observations with optical and microwave sensors. The suppression of ripples by surface slicks was most significant at low winds up to a wind-friction velocity of 15 cm/s.

The impact of a surfactant on a turbulent shear layer near the air-sea interface was studied by direct numerical simulations [311] which show that the inviscid blocking effect of a clean interface, the attenuation of vertical fluctuating velocities and the increase in horizontal turbulence intensities is significantly reduced by surfactant contamination. If the surface is covered by a surfactant, concentration gradients are formed by the impinging turbulent eddies which diminish the renewal of near-surface fluids and reduce the scalar transfer rate.

To control the sea surface pollution, essentially by urban sewage, a simple indicator obtained by counting the colonies of luminescent and non-luminescent bacteria developing on filters, a solid culture medium, was applied [312]. Results from a reference area and polluted sites, and their variations during the year are reported. This method allows to assess the pollution degree and the area of the polluted sites to give recommendations on cleaning.

The cleaning of the sea surface from oil has become very important during the last 20 years. Among the numerous studies on the negative effect of oil films on marine organisms note, for example, the work by Lyons and Harvey [313], who assessed the consequences of an oil spill near the British Isles. It has been shown that the oil spill resulted in elevated levels of DNA adducts in specimens of L. pholis which could potentially cause genetic damage in this native marine species. Further studies are required to assess the full extent of the genotoxic impact of oil spills on this area's native marine life.

About 5 years ago, the world community started creating a satellite system for oil spill monitoring [314]. The main goals of such systems are: the early detection of accidental oil spills, progress of oil spills to support containment and clean-up intervention, identification of culprits in the case of intentional discharges, and for law enforcement purposes. The main oil spill control methods are:

- collection of thick oil slicks using special means,
- dissipation of a thin oil slick followed by its dispersion and biodegradation using natural microorganisms or incorporation of dispersing agents;
- enlargement of the area occupied by the thin oil film followed by its collection;
- application of special oil adsorbents agents followed by the utilization of the oil-adsorbent mixture.

An oil dispersing agent OM-6 was developed in [315] which is a mixture of low-ethoxylated higher alcohols (C_{10}-$C_{13}(OEt)_3$) and liquid paraffins. A lot of 400 tons of OM-6 was manufactured and tested under Black Sea conditions. "In vivo" trials showed that, by that moment of time, OM-r was superior to Correxite 9527 and Correxite 8664 of Esso.

The achievements of biologists have confirmed the vitality of using dispersing agents to liquidate oil contamination. First, a number of natural marine organisms has been established, which decompose oil hydrocarbons to biogas CO_2+CH_4 [316, p. 350-351]. These microorganisms are able to decompose 100 g/l of oil slicks at sea per year. Second, a number of companies (Polyban Corp., Natural Hydrocarbon Elimination Corp., LECA SA, and others) have developed special biological additives to enhance the biodegradation of oil products at sea. These additives are available under various trademarks. To decompose oils special

effective additives have been developed containing nonionic surfactants, fatty acids, phosphorus-based compounds which are nontoxic to marine organisms and fish [316].

A cleaning method of the sea from thin oil films was tested on a laboratory scale in [317]. At first, an oil flick is treated, along the perimeter, with a dispersion of a magnetic material in kerosene having a magnetization degree of 0.5 to 5.0 Gauss. Then, along the perimeter, a solution of low-ethoxylated surfactants is applied, which leads to a considerable reduction of the oil slick, the system being able to orient itself in the magnetic force field. Further, the oil products thus treated can be collected using electromagnetic devices or delivered to their collection site.

A number of sorbents have been proposed to clean water surfaces from oil [318]. The use of hydrophobic aerosil was proposed for this purpose, which, however, can hardly be accomplished for economic reasons. More promising seems to be the proposal to use natural materials for oil absorption, such as turf, diatomite, vermiculite, swelled perlite. A method has been proposed for the modification of perlite by a consequent treatment with cationic surfactants and higher carboxylic acid salts. Such modification of swelled perlite increases its "oil capacity" up to 600%, the water absorption decreases 10 –100-fold, and the "sinkability" decreases considerably. The degree of oil removal from the water surface is, according to "in vitro" tests data, 98 – 99%. Methods have been found to use oil-saturated sorbents.

Besides, the possibility of soil contamination by surfactants is investigated, as well as methods to locate and eliminate these contaminations. Adsorption of linear alkylbenzene sulfonate (LAS) on soils has been studied in [319]. At low LAS concentrations (< 90 μg/ml), the adsorption isotherm was linear in nature, and when exceeding this concentration, the LAS adsorption on soil had an exponential nature, and in all cases, the adsorption capacity depends substantially on the content of clay. Under real conditions, at low surfactant concentrations, the adsorption capacity of soil is rather low and leads to an ecological contamination of soil.

Adsorption of anionic and nonionic surfactants on sorbents of various nature, such as coal, microporous silica gel, aluminium oxide, has been studied in detail by Klimenko et al. [320]. It has been shown that, at c>CMC, the adsorption is polymolecular in nature which can be an explanation for the data obtained in [319].

The problem of an eventual negative effect on soil when sludge with linear alkylbenzene sulfonate (LAS) adsorbed on it in the form of Ca/Mg salts is discussed in [321]. The aerobic degradation of LAS entering the soil with sludge as a fertilizer is the most important mechanism of decreasing the LAS concentration in soil. Based on literature data and field trial data, it was concluded that no human health risk exists with indirect exposure to LAS through either food or drinking water. Current LAS use does not pose a risk to terrestrial organisms such as plants and invertebrates.

A complex problem is removal of soils in pump and treat technology of aquifers [322]. It was noted that field tests show a formation of emulsions of surfactants with liquid contaminants which increased the system viscosity and led to negative results. Laboratory experiments were performed with columns packed with 0.2-mm glass beads at various concentrations of m-xylene and 1% alcohol ethoxylate surfactant solution (Witconol® SN90). Emulsions were formed "in situ" when the aqueous surfactant solution was passed through the column containing m-xylene. As m-xylene concentration increases, emulsion viscosity increases which, in turn, caused a decrease in the relative permeability within the soil column and an increase in the gradient required to maintain a constant flow rate. To achieve positive results under field conditions, a preliminary detailed examination of the degree and nature of soil contamination is necessary, after which a suitable emulsifier can be chosen.

The removal of mineral oils from sea sand was studied in [323] in presence of aqueous solutions of nonionic surfactants (Triton X-100, Triton X-114, Alconox) with and without solid additives, such as granular activated carbon, powder activated carbon. The process was conducted in a scrubber by froth flotation. Contaminants and fine sand particles were transferred, together with sorbents, into the water-froth stream, whereas clean sand remained in the "tails". Without addition of sorbent, the content of contaminants (total oil and grease - TOG) was 4000 ppm, while the additives reduced the TOG content to less than 1000 ppm.

Surfactants are often used for cleaning objects as well as for industrial waste water treatment. Thus, high-molecular fluorocarbon surfactants in a perfluorinated carrier liquid were used as liquid rinses for the decontamination of model electronic circuit boards [324]. A three log reduction in contamination was obtained in 1 hour, and the circuit boards were still functional

after cleaning. Radioactive particles removed were captured by filters, and the liquids were used repeatedly.

The removal of oily and other soils from metal surfaces is rather often performed using flammable liquids (gasoline, kerosene, C_2-C_4 alcohols, and so on) which affects both the environment and the sanitary condition of industrial shops. So-called "industrial detergents" are based on aqueous or water-emulsion surfactant solutions for the removal of soils in the machine-building industry (washing of parts during the assembly), in metallurgy (rolling, e.g. aluminum bands), in radio engineering, etc. These preparations contain typically surfactant mixtures, corrosion inhibitors and pH adjusters and are manufactured in the form of powders or concentrated liquids [325, 326].

Ion flotation in the presence of surfactants for the treatment of rinses and separation of metal ions is of interest since the sixties [327, 328]. Here, we take only a few examples. The recovery of silver ions from highly diluted solutions is possible by forming a silver-thiourea complex in form of a colloidal precipitate (sublate) followed by sublate flotation with sodium dodecyl benzene sulfonate [329]. Skrylev [330] has developed methods for the removal of non-ferrous metal salts from waste waters. Subject of the investigations were 0.01 – 0.001% solutions of ferrous metal salts. Typical anionic surfactants (alkyl sulfates, alkyl phosphates, alkyl xanthogenates of potassium) or cationic surfactants (quaternary ammonium salts) were used as collectors in ion flotation from diluted solutions. At certain pH, a sublate containing a non-ferrous metal ion was formed, followed by a sublate film formation at the surface due to the rise of the complexes with air bubbles stabilised by the surfactants.

The removal of perchloroethylene solvents such as the very toxic trichloroethylene (TCE) from soil and water is a rather difficult problem [331]. A bench-scale study was conducted in TCE-contaminated sand columns. The following operation was tested. Foam obtained using the anionic surfactant Steol CS-330 was injected in a pulsed operation, after which artificial groundwater followed, and then foam again. The result was 75% of the initial TCE content. After the TCE-degrading bacterial strain ENV 435 had been added with the second pulse of foam, the result of the treatment was 95-99%.

Bonkhoff and Schwuger performed laboratory experiments on decontamination of soils using microemulsions [332]. Pyrene was used as a model contaminant. Repeated washing with water

gave only 0.0001 g/l solubilisation of pyrene, and the solubilisation result with the addition of the surfactant C_{12}-C_{14} (EO_7) was 2.7 mg/l. The best results were obtained with a microemulsion containing 10% C_{12}-C_{14} (EO_7) + 3% rape-oil methyl ester at a 1:2 ratio of extraction solution/soil.

Large-scale fires can be regarded as technological catastrophes, that is why the development of foam forming formulations as fire extinguishers was started in the forties. General data on the mechanisms of foam destruction and behaviour features of foam structures in contact with fire depending on the foam expansion ratio are listed in [333]. In particular, high-expansion foams (K>800) are recommended for use when fighting fires in "closed" rooms such as cellars, ship holds, etc.). Also, methods of testing foams for their suitability in firefighting are given. However, detailed data on foamer formulations were presented in [334] which was published a relatively long time ago. In contrast with foamers based on protein hydrolysates giving foams with expansion ratios of 5 – 6 which are not suitable for firefighting of oil products, the up-to-date formulations are able to form medium- and high-expansion foams. Synthetic foamers manufactured in different countries under the trade names of "Meteor" (Sweden), "Expandiol" (UK), "Stauecke" and "Karate" (Germany) contain surfactant mixtures of alkyl sulphates and alkyl ethoxysulphates, as well as C_{12}-C_{14} primary higher fatty alcohols and/or fatty acid diethanolamides.

Firefighting formulations for oil products usually contain a synergistic mixture of two fluorohydrocarbon surfactants (amphoteric + nonionic, amphoteric + cationic, anionic + cationic). The most important condition for the effectiveness of fluorohydrocarbon foamers (aqueous film-forming foaming agents – AFFF), consisting in their rapid defoaming and elimination of re-ignition, is a positive value of the spreading coefficient $S_{w/o}$ of their aqueous solutions on the oil surface.

$$S_{w/o} = \gamma_0 - \gamma_w - \gamma_{w/o} > 0 \qquad (6.13)$$

or

$$\gamma_w + \gamma_{w/o} < \gamma_0, \qquad (6.14)$$

i.e. the sum of the surface tension (γ_w) of the foamer solution and its interfacial tension at the liquid interface ($\gamma_{w/0}$) must be lower than the surface tension of the solvent.

For fire-fighting on polar organic liquids (alcohol, acetone, etc), sodium alginate, protein condensation products and some biosurfactants are incorporated into the foamer formulations. These additives, including polysaccharides, give a gel-like "float" inhibiting the penetration of the polar liquid into the foam and preventing its collapse.

The foam application for cleaning the atmosphere from dust in mining is discussed in [334].

ACKNOWLEDGEMENT

The results of joint investigations with A.V. Pertsov, V.N. Chernin and V.G. Bedenko have been used in this chapter reflected by a respective referencing. Special thanks are given to A.S. Philippov who has charged himself with the labour of translation and preparation of the manuscript for publication.

6.10. REFERENCES

1. H. Jan and E.E. Van, in "Historical Overview on Enzymes in Detergency", H. Jan, E.E. Van and O. Misset (Eds.), Surfactant Sci. Ser., Vol. 69, Marcel Dekker, New York, 1997.
2. D. Myers, Surfactant Science and Technology, 2nd Ed., VCH Publishers, Inc., 1992.
3. B.E. Chistjakov, Osnovnye oblasti primenenija PAV, in: Poverkhnostnoaktivnye veshchestva: spravochnik, Khimija, Leningrad, 1979, 8 (rus.); D.R. Karsa, Industrial Applications of Surfactants II, Royal Society of Chemistry, Cambridge CB4 4WF, 1980.
4. Biosurfactants: Production-Properties-Applications, B. Dobiaš (Ed.), Surfactant Sci. Ser., Vol. 48, Marcel Dekker, New York, 1993.
5. Novel Surfactants. Preparation, Applications and Biodegradability. K. Holmberg (Ed.), Surfactant Sci. Ser., Vol. 74, Marcel Dekker, New York, 1998.
6. Foams: Theory, Measurements, and Applications, R.K. Prud'homme and S.A. Khan (Eds.), Surfactant Sci. Ser., Vol. 57, Marcel Dekker, New York, 1995.
7. Poverkhnostnye javlenija i poverkhnostnoaktivnye veshchestva: spravochnik. A.A.Abramzon and E.D. Shchukin (Eds.), Khimiya, Leningrad, 1984 (rus.)
8. P.A. Rehbinder, Izbrannye trudy, Poverkhnostnye javlenija v dispersnykh sistemakh, Nauka, Moscow, Vol. 1, 1978 (rus.).
9. E.D. Shchukin, A.V. Pertsov and E.A. Amelina, Kolloidnaja Khimija, Moskovskii gosud. Universitet, Moscow, 1992 (rus.).

10. A.W. Adamson, Physical Chemistry of Surfactants, 5th ed., John Wiley, New York, 1990.
11. A.I. Rusanov, Fazovye ravnovesija i poverkhnostnye javlenija, Khimija, Moscow, 1967 (rus.).
12. Micellisation, Solubilisation and Microemulsions, K. Mittal (Ed.), Plenum Press, New York, 1977.
13. W. Schönfeldt, Grenzflächenaktive Äthylenoxyd-Addukte - ihre Herstellung, Eigenschaften, Anwendung und Analyse, Wissenschafts Verlag mbH, Stuttgart, 1976.
14. Nonionic Surfactant: Organic Chemistry, N.M. Van Os (Ed.), Surfactant Sci. Ser., Vol. 72, Marcel Dekker, New York, 1997.
15. B.D. Summ and Ju.V. Gorjunov, Fiziko-khimicheskie osnovy smachivanija i rastekanija. Moscow, Khimija, 1976 (rus.).
16. E. Kissa, Textile Res. J., 10 (1996) 660.
17. D. Exerowa and P.M. Kruglyakov, Foam and Foam Films, in "Studies in Interface Science", Vol. 5, D. Möbius and R. Miller (Eds.), Elsevier, Amsterdam, 1997.
18. J.J. Bikerman, Foams, Springer-Verlag, New York, 1973.
19. B.E. Chistjakov and V.N. Chernin, Kolloidn. Zh., 50 (1988) 187.
20. R.J. Pugh, Adv. Colloid Interface Sci., 64 (1996) 67.
21. A.V. Pertsov, V.N. Chernin, B.E. Chistjakov, E.D. Shchukin, Dokl. Akademii Nauk SSSR, 238 (1978) 1395 (rus.).
22. K.B. Kann, Kolloidn. Zh., 40 (1978) 858.
23. V.V. Krotov, Doklady Akademii Nauk SSSR, 254 (1978) 402.
24. K.-Y. Lai and N. Dixit, Additives for Foams, in [6], pp. 316.
25. G.E. New, Proc. IVth Inter. Congr. Surf. Active, Academic Press, London, 2 (1964) 1169.
26. B.E. Chistjakov and V.N. Chernin, In: Obrazovanie i ustoichivost' pen, in: "Uspekhi Kolloidn. Khimii", Khimija, Leningrad, 1991, pp. 306 (rus.).
27. D.T. Wasan and K. Koczo, In: "Foams: Fundamentals and Applications in the Petroleum Industry", L. Schramm (Ed.), Am. Chem. Soc., Washington, DC, 1992.
28. A.V. Pertsov, V.F. Boratshuk, B.E. Chistjakov, E.D. Shchukin, DAN SSSR, 250 (1980) 906 (rus.).
29. M. Blank and I. Musselwhite, J. Colloid Interface Sci., 27 (1968) 188.
30. Defoaming: Theory and Industrial Applications, P.R. Garrett (Ed.), Surfactant Sci. Ser., Vol. 45, Marcel Dekker, New York, 1992.

31. P. Becher, Emulsions: Theory and Practice, 2nd ed. Rein. Publ. Corp, New York, 1965.

32. P. Sherman, Emulsion Science, Academic Press, London, 1968.

33. Encyclopedia of Emulsion Technology, P. Becher (Ed.), Vol. 1 - Basic Theory, 1983; Vol. 2 - Applications, 1985, Vol. 3 - Theory, Measurement and Applications, 1987, Vol. 4 - Emulsification, Stability and Rheology, M. Dekker, New York, 1996.

34. Emulsions and Emulsions Stability, J. Sjöblom (Ed.), Surface Sci. Ser., Vol. 61, Marcel Dekker, New York, 1996.

35. Drops and Bubbles in Interfacial Research, D. Möbius and R. Miller (Eds.), Studies in Interface Science, Vol. 6, Elsevier, Amsterdam, 1998.

36. Emulgatoren für Lebensmittel, G. Schuster (Ed.), Springer-Verlag, Berlin, Heidelberg, 1985.

37. Emulsions in Petroleum Industry, L. Schramm (Ed.), Marcel Dekker, Washington, DC, 1992.

38. Demulsification: Industrial Applications, K. Lissant (Ed.), Surfactant Sci. Ser., Vol. 13, Marcel Dekker, New York, 1983.

39. Microemulsions: Theory and Practice, L.M. Prince (Ed.), Acad. Press, New York, 1977.

40. Surfactants in Solution, A.K. Chattopadpyaay and K.L. Mittal (Eds.), Surfactant Sci. Ser., Vol. 64, Marcel Dekker, New York, 1996.

41. Industrial Applications of Microemulsions, C. Solans and H. Kunieda (Eds.), Surfactant Sci. Ser., Vol. 66, Marcel Dekker, New York, 1997.

42. B. Dobiaš, Tenside Detergents, 15 (1978) 225.

43. H.M. Princen, J. Colloid Interface Sci., 71 (1979) 55.

44. H. Kunieda, A.C. Johns, R. Pons and C. Solans, Highly Concentrated Emulsions -Gel Emulsions: Macro-Self-Organizing Structures, in: [41], pp. 359.

45. Coagulation and Flocculation Theory: Theory and Applications, B. Dobiaš (Ed.), Surfactants Science Ser., Vol. 47, Marcel Dekker, New York, 1993.

46. A.E. Kabalnov, A.V. Pertsov, E.D. Shchukin, Kolloidn. Zh., 46 (1984) 1108 (rus.).

47. A.E. Kabalnov and A.V. Pertsov, J. Colloid Interface Sci., 118 (1987) 590.

48. B.V. Derjaguin, Uspekhi khimii, 46 (1979) 675.

49. H. Sonntag and K. Strenge, Coagulation and Stability of disperse Systems, Holsted Press, New York, 1972.

50. V.G. Bedenko and A.V. Pertsov, Vlijanie PAV na agregativnuju ustoichivost' emulsii i suspenzii s uglevodorodnoi dispersionnoi sredoi, Khimija, Leningrad, 1991, p. 306 (rus.).

51. A.E. Kabalnov, Current Opinion in Colloid Interface Sci., 30 (1998) 270.

52. H.T. Davis, Colloids and Surfaces A, 91 (1994) 9.

53. A.R. Mahadeshwar and S.G. Dixit, J. Dispersion Sci. Technology, 19 (1998) 43.

54. P.D.J. Fletcher, Interactions of Emulsion Drops, in: [35], pp. 563.

55. V.G. Bedenko, T.I. Nichikova and B.E. Chistjakov, Kolloidn. Zh., 48 (1986) 528.

56. G.A. Gilles, Practical Problem Concerning Specialty Chemicals: Emulsification of Viscous Oils, in "Proc. of II World Congress on Emulsions", Bordeaux, France, 4 (1997) 337.

57. F. Nelloud, G. Mortimesters and J.F. Laget, Drug Development and Industrial Pharmacy, 22 (1996) 159.

58. V.G. Bedenko, V.N. Chernin and B.E. Chistjakov, Kolloidn. Zh., 45 (1983) 542.

59. P.A. Rehbinder, K fizikokhimii flotatsionnykh protsessov, in: [8], pp. 300.

60. K. Sutherland and J. Work, Printsipy flotatsii, Moscow, Metallurgizdat, 1958.

61. N.A. Alejnikoff, Kolloid Beihefte, 36 (1932) 86.

62. G.O. Ershkovski, Obrazovanie flotatsionnoj peny, Moscow, GONTI, 1938.

63. M.T. Ityokumbul, A.I.A. Salama and A.M. Altawell, Minerals Engineering, 8 (1995) 77.

64. A. Sam and C.O. Gomez, Intern. J. Mineral Processing, 47 (1996) 177.

65. M. Loewenberg and R.H. Davis, Chem. Eng. Sci., 49 (1994) 3923.

66. L. Evans, B.P. Thadloy, J.D. Morgan, S.K. Nicol, D.H. Napper and G.G. Warr, Colloids Surfaces A, 102 (1995) 80.

67. M.L. Free and J.D. Miller, Int. J. Mineral Processing, 48 (1996) 197.

68. J.A. Mielczarski, J.M. Cases and O. Barres, J. Colloid Interface Sci., 178 (1996) 740.

69. Y. Lu, J. Drelich and J.D. Miller, Minerals Engineering, 10 (1997) 1219

70. K.H. Roo and K.S.E. Fossberg, Int. J. Mineral Processing, 51 (1997) 67.

71. J. Ren, S. Lu, S. Song and J.A. Win, Minerals Engineering, 10 (1997) 1395.

72. X.P. Zheng, M. Misre, R.W. Smith, J.K. Qiao, Minerals Engineering, 9(1996) 331.

73. A.M. Grancaric, T. Pusic, I. Solijacic and R. Rilitsen, Text. Chemist and Colorist, 29 (1997) 33.

74. S. Sysilia and H. Laapas, Minerals Engineering, 9 (1996) 519.

75. Fizikokhimija mojushchego deistvija, P.A. Rehbinder (Ed.), Pishchepromizdat, Leningrad - Moscow, 1935, pp. 162 (rus.).

76. Detergency: Theory and Test Methods, W.G. Cutler and R.C. Davis (Eds.). Surfactant Science Ser., Vol. 5, Marcel Dekker, New York, 1972.

77. Detergency: Theory and Technology, W.G. Cutler and E. Kissa (Eds.), Surfactant Science Ser., Vol. 20, Marcel Dekker, New York, 1972.

78. A.A. Abramzon, Chto nuzhno znat' o mojushchikh sredstvakh, Khimizdat, St. - Petersburg, 1999, pp. 42 (rus.).

79. V.A. Volkov, Poverkhnostno-aktivnye veshchestva v mojushchikh sredstvakh i usiliteljakh khimicheskoi chistki. Legprombytizdat, Moscow, 1985, pp. 200 (rus.).

80. M.Ju. Pletnev, Kosmetiko - gigienicheskie mojushchie sredstva, Khimija, Moscow, 1990 (rus.).

81. W.K. Adam, J. Soc. Dyers Color., 53 (1937) 121.

82. L. Thompson, J. Colloid Interface Sci., 162 (1994) 61.

83. A.F. Koretskij and V.A. Kolosanova, in "Fiziko – khimicheskie osnovy primenenija PAV", RAN, Tashkent, 1977, pp. 238.

84. E. Kissa, J. Am. Oil Chem. Soc., 72 (1985) 793.

85. C. Broze, Solubilisation and Detergency in Solubilisation in Surfactant Aggregates, Su.D. Cheiston and J.F. Scamehorn (Eds.), Surfactant Science Ser., Vol. 55, Marcel Dekker, New York, 1995, pp. 493.

86. A. Nuria, The role of Microemulsions in Detergency Process, in "Industrial Applications of Microemulsions", C. Solans and H. Kunieda (Eds.), Surf. Science Ser., Vol. 66, Marcel Dekker, 1997, pp. 377.

87. D. Nickel, W. von Rybinski, E.M. Kutschmann, C. Stubenrauch and G.H. Findenegg, Fett - Wissenschaft - Technologie, 98 (1996) 363.

88. M. Rieger, Foams in Personal Care Products, in "Foams: Theory, Measurements, and Applications", R.K. Prud'homme and S.A. Khan (Eds.), Surfactant Science Ser., Vol. 57, Marcel Dekker, New York, 1995, pp. 381.

89. H. Ferch and W. Leonhardt, Foam Control in Detergent Products. in: [30], pp. 221.

90. D. Balzer and S. Varwig, Colloids Surfaces A, 99 (1995) 233.

91. Surfactants in Agrochemicals, Th.F. Tadros (Ed.), Surfactant Science Ser., Vol. 54, Marcel Dekker, New York, 1996.

92. Th.F. Tadros, Microemulsions in Agrochemicals, in: [41], pp. 199.

93. Anionic surfactants: biochemistry, toxicology, dermatology, Ch. Gloxhuber and K. Künstler (Eds.), 2nd ed., Surfactant Science Ser., Vol. 43, Marcel Dekker, New York, 1992.

94. L.D. Rhein and F.C. Simion, Surfactant Interactions with Skin, in: Interfacial Phenomena in Biological Systems, Surfactant Science Ser., Vol. 39, Marcel Dekker, New York, 1991.

95. Anionic Surfactants. Organic Chemistry, H.W. Stache (Ed.), Surfactant Science Ser., Vol. 56, Marcel Dekker, New York, 1995.

96. W.V. Rybinski and K. Hill, Alkyl Polyglycosides, in: [5], pp. 32.

97. Mixed Surfactant Systems, K. Ogino and M. Abe (Eds.), Surfactant Science Ser., Vol. 46, Marcel Dekker, New York, 1993.

98. R.M. Hill. Application of Surfactant Mixtures in: [95], p. 317.

99. P. Hannson and B. Lindman, Current Opinion Colloid Interface Sci., 1 (1996) 604.

100. Enzymes in Detergency, J.H. Van El, O. Misset and E.J. Baas (Eds.), Surfactant Science Ser., Vol. 69, New York, Marcel Dekker, 1997.

101. Powdered Surfactant, M.S. Showell(Ed.), Surfactant Science Ser., Vol. 71, Marcel Dekker, New York, 1998.

102. Liquid Detergents, K.-Y. Lai (Ed.), Surfactant Science Ser., Vol. 67, Marcel Dekker, New York, 1997.

103. E. Smulders, P. Krings and H. Verbeek, Tenside Surfactants Detergents, 34 (1997) 386.

104. G. Wasow, Phosphorus-containing anionic surfactants, in: [95], pp. 580.

105. M.J. Greenhillhooper, Tenside Surfactants Detergents, 33 (1996) 363.

106. P.A. Gozlin, W. Dixit and L. Kuo-Yan, Liquid Automatic Dishwasher Detergents, in: [102], pp. 226.

107. H. Ferez and W. Leonhardt, Foam Control in Detergent Products, in: [6], pp. 221.

108. L. Kuo-Yann and A.H. McGandlish, Light-Duty Liquid Detergents, in: [102], pp. 208.

109. A. Sachdov and S. Krishnan, Heavy-Duty Liquid Detergents, in: [102], pp. 252.

110. M. Rieger, Foams in Personal Care Products, in: [6], pp. 382.

111. V. Kekner and N. Kosaric, Biosurfactants for Cosmetics, in: [4], pp. 373.

112. I. Schlachter, G. Feldmann-Krane, Silicone Surfactants, in: [5], pp. 202.

113. M. Svensson, Surfactants Based on Styrols and Other Alicyclic Compounds, in: [5], pp. 180.

114. Interfacial Phenomena in Biological Systems, M. Bender (Ed.), Surfactant Sci. Ser., Vol. 39 New York, Marcel Dekker, 1991.

115. U. Pison, R. Herold and S. Schürch, Colloids Surfaces A, 114 (1996) 165.

116. R. Herold, R. Dewitz, S. Schürch and U. Pison, Pulmonary Surfactant and Biophysical Function, in: [35], pp. 434.

117. V.N. Kazakov, O.V. Sinjachenko, V.B. Fainerman, U. Pison and R. Miller, Dynamic surface tensiometry in medicine, Studies in Interface Science, D. Möbius and R. Miller (Eds.), Vol. 8, Elsevier, Amsterdam, 2000

118. O.N.M. McCallion, K.M.G. Taylor, M. Thomas and A.J. Taylor, Int. J. Pharmaceutics, 129 (1996) 123.

119. J. Lewis and R.A.W. Veldhuizen, J. Aerosol Medicine, 9 (1996) 143.

120. N.P. Flament, P. Leterme, T. Burnouf and A.T. Gayot, Int. J. Pharmaceutics, 156 (1997) 211.

121. R. Berger, Application of Antifoams in Pharmaceuticals, in: [30], pp. 177.

122. V. Bergeron, P. Cooper, C. Fischer, J. Giermanskakahn, D. Langevin, A Pouchelon, Colloids Surfaces A, 122 (1997) 103.

123. W. Kästner, Pharmacological Properties, in: Anionic Surfactants: Biochemistry, Toxicology, Dermatology, Ch. Gloxhuber and K. Künstler (Eds.), 2nd ed., Surfactant Science Ser., Vol. 43, Marcel Dekker, New York, 1992.

124. X. Boulenc, T. Breul, J.C. Gautier, V. Berger, P. Saudemon, H. Joyeux, C. Rougues, Int. J. Pharmaceutics 123 (1995) 71.

125. P.E. Luner, S.R. Babu and S.C. Mehta, Int. J. Pharmaceutics, 128 (1996) 29.

126. M.J. Newman, J.K. Actor, M. Balusubramanian and C. Jagannath C., Therapeutic Drug Carrier Systems, 15 (1998) 89.

127. R. Infante, L. Pérez and A. Pinazo, Novel Cationic Surfactants from Arginine. in: [5], pp. 87.

128. S. Craustemanciet, D. Brossard, M.O. Decroix, R. Farinotti, J.C. Chaumeil, Int. J. Pharmaceutics, 165 (1998) 97.

129. C.K. Kim, S.C. Kim, H.J. Shin, K.M. Kim, K.H. Oh, Y.B. Lee, I.J. Oh, Int. J. Pharmaceutics, 124 (1995) 61.

130. A. Silva-Cunha, J.-L. Grossiord and M. Seiller, 2nd World Congress on Emulsions, Congress Proceedings, Vol. 4. 4.-216-01 – 4.216-06.

131. M.R. Gasco, Microemulsions in the Pharmaceutical Field: Perspectives and Applications, in: [41], pp. 97.

132. M.J. Garcia-Celma, Solubilisation of Drugs in Microemulsions, in: [45], pp. 123.

133. J.G. Riess, 2nd World Congress on Emulsion, Congress Proceedings, Vol. 4, 1997, pp. 305.

134. J.G. Riess. New J. Chem., 19 (1995) 891.

135. Fluorinated Surfactants: Synthesis - Properties - Applications, E. Kissa (ed.), Surfactant Sci. Ser., Vol. 50, Marcel Dekker, New York, 1994.

136. J.K. Armstrong, H.J. Meiselman and T.C. Fisher, Thrombosis Research, 79 (1995) 437.

137. J. Velikonja and N. Kosaric. Biosurfactants in Food Applications, in: [4], p. 419.

138. F. Thevenet. 2nd World Congress on Emulsion, Congress Proceedings, Vol. 4. 4.-2-017 11 – 4-2-017-06. Bordeaux - France, 1997.

139. E. Dickinson and D.T. Wasan, Current Opinion Colloid Interface Sci. 2 (1997) 565.

140. D. Douglas and D.G. Dalgleish, Current Opinion Colloid Interface Sci. 2 (1997) 573.

141. E. Dickinson, J. Chem. Soc., Faraday Tr., 94 (1998) 1657.

142. N. Garti, Food Science & Technology, 30 (1997) 222.

143. D.G. Dalgleish, M. Srinivasan and H. Singh, J. Agr. Food Chem., 43 (1995) 2351.

144. A.V. Makievski, V.B. Fainerman, M. Bree, R. Wüstneck, J. Krägel and R. Miller, J. Phys. Chem. 102 (1998) 417.

145. Proteins at Liquid Interfaces, in "Studies in Interface Science", Vol. 7, D. Möbius and R. Miller (Eds.), Elsevier, 1998.

146. P.A. Gunning, A.R. Mackie, F.A. Husband, M.L. Parker, D.C. Clark J. Food Sci., 63 (1998) 39.

147. B.M.C. Pelan, K.M. Watts, I.J. Campbell and A. Lips, J. Dairy Sci., 80 (1997) 2631.

148. F. Nielloud, G. Martimestres, J.P. Laget, C. Fernandes and H. Maillols, Drug Dev. & Ind. Pharmacy, 22 (1996) 159.

149. H. Schubert, New Developments in the Production of Food Emulsions, Proceedings of the 2nd World Congress on Emulsion, Vol. 4, 1997, pp. 327.

150. S.R. Dungun, Microemulsion in Foods: Properties and Applications, in: [41], pp.147.

151. B.E. Chistjakov, V.G. Pravdin and A.I. Dernovaja, Poverkhnostno-aktivnye veshchestva v narodnom khozjaistve, Khimija, Moscow, 1989 (rus.).

152. D.W. Fuerstenau and R. Herra-Urbina, in: Surfactant Based Separation Process, J. Scameron and J. Harwell (Eds.), Surfactant Sci. Ser., Vol. 33, Marcel Dekker, New York, 1989.

153. K.R. Prud'homme and G.G. Warr, Foams in Mineral Flotation and Separation Processes, in: [6], p 511.

154. J.O. Leppinen, V.V. Hintikka and R.P. Kalapudas, Minerals Engineering, 11 (1998) 39.

155. Z. Sadowski, Colloids Surfaces A, 96 (995) 277.

156. K. Kubota, T. Nishikawa, S. Hayashi and H. Imakoma, J. Chem. Eng. Japan, 31 (1998) 187.

157. P. Zhang, Y. Yu and M. Bogan, Minerals Engineering, 10 (1997) 983.

158. A.M.A. Omar and N.A. Abdel-Khalek, Tenside Surfactants Detergents, 34 (1997) 3.

159. S.M. Assis, L.C.M. Montenegro and A.E.C. Peres, Minerals Engineering, 9 (1996) 103.

160. N. Gence and H. Ozdag, Int. J. Mineral Processing, 43 (1995) 37.

161. B.P. Singh and L. Besra, Separation Science & Technology, 32 (1997) 2201.

162. L. Besra, B.P. Singh and D.K. Sengupta, Powder Technology, 96 (1998) 240.

163. K. Lindner, Tenside - Textilhilfsmittel, Bd. I - III, Stuttgart Verlagsgesellschaft, 1964-1971, pp. 3159.

164. Mc Cutcheons, Detergents and Emulsifiers. North American Edition, All. Publ. Corp, New Jersey, 1974, pp. 247.

165. R.H. Peters, Textile Chemistry, Vol. 3, Elsevier, Amsterdam, 1975.

166. E.R. Trotman, Dying and Chemical Technology of Textile Fibres, 6th ed, Gribbin, High Wycombe, 1984, pp. 350.

167. Corpus Information Services, Market Study: Chemicals for Pulp and Paper in Canada, Southam Communications, Ltd, 1985.

168. P.I. Levenko, Poverkhnostno-aktivnye veshchestva v kozhevennoi i mekhovoi promyshlennosti, Legkaja industria, Moscow, 1974.

169. I. Pezron, G. Bourgain and D. Quere, J. Colloid Interface Sci., 173 (1995) 319.

170. X. Ma, Ind. Eng. Chem. Res., 35 (1997) 1586.

171. I. Pezron, G. Bourgain and D. Clausse, Colloid Polymer Sci., 274 (1996) 166.

172. Y. Okamura, K. Gotoh, M. Kosaka and N. Tagawa, J. Adhesion Science Technology, 12 (1998) 639.

173. J.L. Deng and M. Abazeri, Wood Fiber Sci., 30 (1998) 155.

174. A.M. Grancaric, T. Pusic, I. Soljacic and V. Ribitsch, Textile Chemist & Colorist, 29 (1997) 33.

175. Y. Sano, M. Konda, C.W. Lee, Y. Kimura and T. Saegusa, Angewandte Makromolekulare Chemie, 251 (1997) 81.

176. S. Schmidt, H.M. Buchhammer and K. Lunkwitz, Tenside Surfactants Detergents, 34 (1997) 267.

177. A.N. Zhironkin, V.A. Volkov and A.S. Gordeev, Kolloidny Zh., 59 (1997) 442.

178. I. Rusznak, P. Sallay, A. Vig and L. Farkas, Tenside Surfactants Detergents, 35 (1998) 123.

179. R.L. Gamblin, Textile Chemist & Colorist, 28 (1996) 12.

180. Th.F. Cooke and D.E. Hirt, Foam Wet Processing in the Textile Industry, in: [6], p. 339.

181. T.V. Ivanova, V.N. Chernin and B.E. Chistjakov, Kolloidn. Zh., 53 (1991) 714.

182. T.V. Ivanova, V.N. Chernin, B.E. Chistjakov - Razrabotka energosberegajushchikh tekhnologij otdelki tekstilnykh materialov, TsNIITELegprom (1992), Moscow, p. 40.

183. G.C. Sawicki, High-Performance Antifoams for the Textile Dying Industry, in: [30], p. 193.

184. S.L. Allen, L.H. Allen and T.H. Flaherty, Defoaming in the Pulp and Paper Industry, in: [30], p. 151.

185. B.E. Chistjakov, L.A. Melnik and V.N. Chernin, Khimicheskie penogasiteli. - TsNIITENeftekhim, Moscow, 1989.

186. E. Barni, P. Savarino and G. Viscardi, Microemulsions in Dying Processes, in: [30], p. 209.

187. S.I. Tolstaja and S.A. Shabanova, Primenenie poverkhnostnoaktivnykh veshchestv v lakokrasochnoi promyshlennosti, Moscow, 1976 (rus.)

188. R. Lambourne, Paint and Surface Coatings: Theory and Practice. Ellis Harward Limited, John Wiley and Sons, New York, Chichester, Brisbane, Toronto, 1987.

189. M.A. Winnik and J.R. Feng, J. Coatings Technology, 68 (1996) 39.

190. G. Del Rio and A. Rudin, Progr. Organic Coatings, 28 (1996) 259.

191. M. Cechova, B. Alince and T.G.M. van de Ven, Colloids Surfaces A, 141 (1998) 153.

192. V.G. Bedenko, B.E. Chistjakov and S.P. Ternovskaja, Regulirovanie reologicheskikh svoistv vodnykh i nevodnykh suspenzij mela. - Simposium Stroiprogress-2000. Tezisy dokladov, BTISM, 1991, pp. 44.

193. S.B. Johnon, A.S. Russel and P.J. Scales, Colloids Surfaces A, 141 (1998) 119.

194. T. Fujitani, Progr. Organic Coatings, 29 (1996) 97.

195. M. Colic and D.W. Fuerstenau, Langmuir, 13 (1997) 6644.

196. B. Muller and A. Holland, JOCCA-Surface Coatings International, 80 (1997) 321.

197. R. Gaumet, N. Siampiringue, J. Lemaire and B. Pacaud, JOCCA-Surface Coatings International, 80 (1997) 367.

198. N. Harui and T. Agawa, J. Coatings Technology, 70 (1998) 73.

199. P. Vink, T.P.M. Koster, H.F.N. Fontijn and A. Mackor, Polymer Degradation & Stability. 48 (1995) 155.

200. D.E. Weidner, L.W. Schwartz and R.R. Eley, J. Colloid Interface Sci., 179 (1996) 66.

201. M. Chen, W.H. Wetzel, Z.J. Ma and J.E. Glass, J. Coatings Technology, 69 (1997) 73.

202. M.R. Porter, Antifoams for Paints, in: [30], p. 269.

203. S.F. Kia, D.N. Rai and R.L. Williams, J. Coatings Technology, 68 (1996) 87.

204. A.V. Senakhov, V.V. Koval, F.I. Sadov, Zagustki, ikh teorija i primenenie. Legkaja industrija, Moscow, 1972 (rus.).

205. L.H. Townsend, JOCCA-Surface Coatings International, 80 (1997) 479.

206. S.J. Allan, R. May, M.F. Taylor and J. Walters, GEC J. Research, 12 (1995) 86.

207. I.A. Tolmachev, Lakokrasochnye materialy, 11 (1997) 27.

208. M. Arellano, I. Michelhaciski, D.I. Feke and I. Manaszloczower, J. Coatings Technology, 68 (1996) 103.

209. G. Ostberg and B. Bergenstahl, J. Coatings Technology, 66 (1994) 37.

210. G. Östberg, B. Bergenstahl and M. Hulden, Colloids Surfaces A, 94 (1995) 161.

211. G. Ostberg and B. Bergenstahl, J. Coatings Technology, 68 (1996) 39.

212. S. Majamdar, D. Kumar and Y.P.S. Nirvan, J. Coatings Technology, 70 (1998) 27.

213. M.N. Pershin, E.N. Barinov and G.V. Korenevskij, Vspenennye bitumy i ikh primenenie v dorozhnom stroitelstve. Moscow, Transport, 1989, pp. 78.

214. 2nd World Congress on Emulsions, Congress Proceedings, Vol. 1-4, Bordeaux - France, 1997.

215. P. Schilling, Anionic and Cationic Asphalt Emulsions Prepared with Modified Tall Oil, in: [214], Vol. 4, 4-1a-023/0.1-0.8.

216. M. Bourrel, Controlling Asphalt Emulsion Breaking for Road Paving, in: [214], Vol. 4, p. 295.

217. K. Shoji, A. Ryusuke and S. Katsutoshi, Application of Cement-Asphalt Emulsion mortar for Construction of Natural Stone Pavement, in: [214], Vol. 4, 1-1b-0.63.

218. F. Gusi, A.C. Auguet and F.X. Gaillard, Emulsions and Microemulsions in Metalworking Processes, in: [41], p. 389.

219. B.C. Craft and M.F. Hawkins, Applied Petroleum Reservoir Engineering; Prentice Hall, Engelwood Cliffs, NJ, 1959, pp. 259.

220. D.O. Shah and R.S. Schechter, Improved Oil Recovery by Surfactant and Polymer Flooding, Academic Press, New York, 1977.

221. J.J. Taber, Surface Phenomena in Enhanced Oil Recovery, D.O. Shah (Ed.), Plenum Press, New York, 1981.

222. L.W. Lake, Enhanced Oil Recovery, Prentice Hall, Engelwood Cliffs, NJ, 1959, pp. 259.

223. M. Baviere, Basic Concepts in Enhanced Oil Recovery Processes, Elsevier, London, 1991.

224. L.L. Schramm, Foams: Fundamentals and Applications in the Petroleum Industry, American Chemical Society, Washington D.C., 1994.

225. D.L. Rakhmankulov, S.S. Zlotskij, V.I. Markhasin, O.V. Peshkin, V. Ja. Shchekaturova, B.N. Mastobaev, Khimicheskie reagenty v dobyche i transporte nefti, Khimija, Moscow, 1987 (rus.).

226. J. Milter and T. Austad, Colloids Surfaces A, 113 (1996) 269.

227. J. Milter and T. Austad, Colloids Surfaces A, 117 (1996) 109.

228. T. Austad, B. Matre, J. Milter, A. Sevareid and L. Oyno, Colloids Surfaces A, 137 (1998) 117.

229. Y. Touhami, V. Homof and G.H. Neale, Colloids Surfaces A, 132 (1998) 61.

230. T. Austad, S. Erkann, J. Fjelde and K. Taugbol, Colloids Surfaces A, 127 (1997) 69.

231. M. Baviere, P. Glenat, V. Plazanet and J. Labrid, Spe Reservoir Engineering, 10 (1995) 187.

232. R.N. Mukhametzyanov, S.G. Safin, R.R. Ganiyev, M.A. Kuchma and M.G. Gafiullin, Neftyanoe Khozyaistvo, 7 (1994) 21.

233. L. Thibodeau and G.H. Neale, J. Petroleum Sci. & Engineering, 19 (1998) 159.

234. T.F. Tadros, Colloids & Surfaces A, 91 (1994) 39.

235. S.L. Kokal, B.B. Maini and R. Woo, Flow of Emulsions in Porous Media, in: [37], p. 219.

236. K.C. Taylor and B.F. Hawkins, Emulsions in Enhanced Oil Recovery, in: [37], pp. 263.

237. S.A. Khan, G.A. Pope and J.A. Trangenstein, Transport in Porous Media, 24 (1996) 35.

238. H. Rivas, X. Gutierrez and J.L. Ziritt, Microemulsion and Optimal Formulation Ocurrence in pH-Dependent Systems as Found in Alkaline-Enhanced Oil Recovery, in: [41], pp. 305.

239. M. Baviére and J.P. Canselier, Microemulsions in the Chemical EOR Process, in: [41], p. 332.

240. A.A. Sonin, T. Palermo and A. Lubek, Chem. Eng. J., 69 (1998) 93.

241. R. Grace, Commercial Emulsion Breaking, in: [37], p. 313.

242. G.N. Pozdnyshev, Stabilizatsija i razrushenie neftjanykh emulsij, Nauka, Moscow,1982 (rus.).

243. N. Zaki, and A. Algabagh, Tenside Surfactants Detergents, 34 (1999) 12

244. V.V. Makovkin and N.M. Nikolaeva, TsNIITENeftekhim, 57 (1989) 120.

245. N.P. Tirmizi, B. Raghuraman and J. Wiencek, AIChE J., 42 (1996) 1263.

246. A.D. Nikolov, M. Randie, C.S. Shetty and D.T. Wasan, Chem. Eng. Comm., 153 (1996) 337.

247. D.P. Rimmer, A.A. Gregoli, J.A. Hamshar and E. Yildirim, Pipeline Emulsion Transportation for Heavy Oils, in: [37], p. 295.

248. E. Zayas, J.J. Llovera, D.M. Castro, C. Oyeyipo, E. Fonseca and F. Tellez, Evaluation of Water-Diesel Emulsions, in: [214], Vol. 4, 4-3-333/04.

249. C.Y. Lin and C.M. Lin, J. Ship Research, 39(1995) 86.

250. B.E. Chistjakov and V.G. Bedenko, Khimija i tekhnologija topliv i masel, Moscow, Khimija, (1982) 22 (rus.).

251. O.A. Gladkov and E.Ju. Lerman, Sozdanie malotoksichnykh dizelej rechnykh sudov, Leningrad, Sudostroenie, 1990.

252. W.R. Rossen, Foams in Enhanced Oil Recovery, in: [6], p. 414.

253. R.R. Kovscek and C.J. Radke, Fundamentals of Foam Transport in Porous Media, in: [224], pp.125.

254. O. Fergui, H. Bertin and M. Quintard, J. Petroleum Sci. Eng., 20 (1998) 9.

255. D.T. Wasan, K. Koczo and A.D. Nikolov, Mechanisms of Aqueous Foam Stability and Antifoaming Action with and without Oil, in: [224], pp. 70.

256. B.E. Chistjakov and V.N. Chernin, Osobennosti penoobrazovanija v smesjakh voda-uglevodorodnaja zhidkost, Gasovaja promyshlennost, Moscow, 1997, pp. 30.

257. L.L. Schramm, Foam Sensitivity to Crude Oil in Porous Media, in: [224], pp. 165.

258. K. Mannhardt and J.J. Novosad, Adsorption of Foam-Forming Surfactants for Hydrocarbon-Miscible Flooding at High Salinities, in: [224], pp. 263.

259. C.-Z. Yang, Y.-G. Li and Z.-J. Dai, Enhanced Oil Recovery by Foam Flooding, Proceedings Eurofoam 2000, p. 239-246, Verlag MIT Publishing, Bremen, 2000.

260. J.E. Hannsen and M. Dalland, Gas-Blocking Foams, in: [224], pp. 321.

261. T.N. Patzek, Spe Reservoir Engineering, 11 (1996) 79.

262. E.E. Isaaks, J. Ivory and M.K. Green, Steam-Foams for Heavy Oil and Bitumen Recovery, in: [224], 233.

263. M.L. Hoefner and E.M. Evans, Spe Reservoir Engineering. 10 (1995) 273.

264. D.L. Schmidt, Nonaqueous Foams, in: [6], p. 287.

265. V.G. Bedenko, V.N. Chernin and B.E. Chistjakov, Kolloidn. Zh., 47 (1985) 948.

266. I.C. Callaghan, Antifoams for Nonaqueous System in the Oil Industry, in: [30], pp. 119.

267. N.S. Vlasova, V.I. Klassen and I.N. Plaksin, Issledovanie deistvija reagentov pri flotatsii kamennykh uglej, Izd. AN SSSR, Moscow, 1972, pp. 170.

268. A. Baichenko and S. Barany, in: [214], Vol. 4, pp. 4-4, 229/01.

269. B.P. Singh, Filtration and Separation, 34 (1997) 159.

270. Issledovanie tekhnologii i oborudovanija terminal'nykh kompleksov magistral'nogo gidrotransporta. Sb. Trudov, Gidrotransport, Moscow, 1986, pp. 115 (rus.).

271. Metody regulirovanija strukturno-reologicheskikh svoistv i korrozionnoj aktivnosti vysokokontsentrirovannykh dispersnykh sistem, VNIPIgidrotruboprovod, sbornik nauchnykh trudov, Moscow, 1987, (rus.).

272. E.E. Babik, Reologija dispersnykh sistem. - Izd-vo Leningradskogo Universiteta, Leningrad, 1981 (rus).

273. N.B. Urjev and A.A. Potanin, Tekuchest' suspenzij i poroshkov, Khimija, Moscow, 1992, pp. 256 (rus.).

274. N.B. Urjev, V.M. Tarakanov, I.A. Bogonin and V.E. Chernomaz, Reologicheskie kharakteristiki vysokokontsentrirovannykh vodougol'nykh suspenzij v uslovijakh nestatsionarnogo potoka, in: [271], pp. 3 (rus).

275. V.G. Bedenko, Vlijanie poljarnosti sredy i dispersnosti chastits na reologicheskie svoistva i agregativnuju ustoichivost' suspenzij kamennogo uglja. in: [271], pp. 28 (rus).

276. V.G. Bedenko and T.N. Nichikova, Khimija tverdogo topliva, (1988) 122 (rus.).

277. T.F. Tadros, P. Taylor and G. Bognolo, Langmuir, 11 (1995) 4678.

278. L. Trochetmignard, P. Taylor, G. Bognolo and T.F. Tadros, Colloids Surfaces A, 95 (1995) 37.

279. P.R. Tudor, D. Atkinson, R.J. Crawford and D.E. Mainwaring, Fuel, 75 (1996) 443.

280. K.D. Kihm and P. Geignan, Fuel, 74 (1995) 295.

281. N.S. Roh, D.H. Shin, D.C. Kim and J.D. Kim, Fuel, 74 (1995) 1313.

282. V.G. Bedenko, B.E. Chistjakov, V.A. Minkov and T.S. Gubanova, Izmenenie reologicheskikh svoistv VVUS v zavisimosti ot dobavok razlichnoi prirody, in: [271], pp. 15 (rus).

283. N.B. Urev, V.V. Saskovets, S.V. Choi, L.I. Peregudova, A.P. Izhik, L.G. Vinogradova and N.P. Krutko, Colloid J. Russian Academy Sci., 57 (1995) 77.

284. V. Chhabra, M.L. Free, P.K. Kang, S.E. Truesdail and D.O. Shah, Tenside Surfactants Detergents, 34 (1997) 156.

285. J. Eastoe and B. Warne, Current Opinion in Colloid Interface Sci., 1 (1996) 800.

286. V.A. Bykov, Biosensors & Bioelectronics, 11 (1996) 923.

287. J.H. Fendler, Current Opinion Colloid Interface Sci., 1 (1996) 202.

288. Surfaces of Nanoparticles and Porous Materials, J.H. Schwarz and Ch. Contesku (Eds.), Surfactant Sci. Ser., Vol. 78, Marcel Dekker, New York, 1999

289. L. Yang, N. Takisawa, T. Hayashita and K. Shirahama, J. Phys. Chem., 99 (1995) 8799.

290. D.R. Mckean, T.P. Russel, W.D. Hinsberg, D. Hofer, A.F. Renaldo and C.G. Willson, J. Vacuum Science & Technology B, 13 (1995) 3000.

291. R.S. Juang and J.D. Jiang, J. Membrane Sci., 100 (1995)163.

292. J.C. Lin and C.Y. Wang, Materials Chemistry & Physics, 45 (1996) 136.

293. M. Arellano, I. Manaszloczower and D.L. Feke, Polymer Composites, 16 (1995) 489.

294. C.H. Lu and J.P. Wu, Materials Letters, 27 (1996) 13.

295. D. Walsh and S. Mann, Nature, 377 (1995) 320.

296. R. Lindberg, J. Sjöblom and G. Sundholm, Colloids & Surfaces A, 99 (1995) 79.

297. N. Kuramoto and K. Terama, Polymers for Advanced Technologies, 93 (1998) 222.

298. J. F. Rusling and D.L. Zhou, J. Electroanalytical Chem., 439 (1997) 89.

299. H.K. Mahabadi, T.H. Ng and H.S. Tan, J. Microencapsulation, 13 (1996) 559.

300. L.P. Panicheva, S.A. Panichev, E.A. Turnaeva, V.A. Turnaev and A.V. Yuffa, Kinetics Catalysis, 37 (1996) 377.

301. J.N. Coupland, Z. Zhu, H. Wan, D.J. Mcclements, W.W. Nawar and P. Chinachoti, J. Am. Oil Chemists' Society, 73 (1996) 795.

302. P.R. Patnaik, Biotechnology Advances, 13 (1995) 175.

303. A. Shukla, The Applications of Microemulsions for Analytical Determinations, in: [41], p. 48.

304. Detergent in the Environment, M.J. Schwuger (Ed.), Surfactant Sci. Ser. Vol. 65, Marcel Dekker, New York, 1987.

305. V.V. Bocharov and G.N. Krasovskij, Kolloidno-khimicheskie i gigienicheskie osnovy normirovanija PAV v vode vodojomov, v sb. Uspekhi kolloidnoj khimii, Khimija, Leningrad, 1991, p. 377 (rus.)

306. D.G. Matthijs, N. Itrich, P. Masscheleyn, A. Rottiers, M. Stalmans and T. Federle, Water Sci. Technol., 31 (1995) 321.

307. N. Fisher, M. Maertzwernte and S.A. Ostroumov, Izvestiia Akademii Nauk SSSR. Ser. Biol., 1 (1996) 91.

308. B. Richard, P. Grieu, P.M. Badot and J.P. Garrec, Annales Sci. Forestieres, 53 (1996) 921.

309. F. Bussotti, P. Grossoni and F. Pantani, Annales Sci. Forestieres, 52 (1995) 251.

310. A. Savtchenko, S. Tang and J. Wu, J. Marine Systems, 13 (1997) 273.

311. W.T. Tsai, J. Geophysical Research-Oceans, 101 (1996) 28557.

312. G. Sbrilli, M. Cruscanti, M. Bucci, C. Gaggi and E. Bacci, Environmental Toxicology & Chem., 16 (1997) 135.

313. B.P. Lyons, J.S. Harvey and J.M. Parry, Mutation Research-Genetic Toxicology & Environmental Mutogenesis, 390 (1997) 263.

314. G. Perrotta and P. Xefteris, Spill Sci. Technol. Bulletin, 3 (1996) 73.

315. N.A. Melnik, B.E. Chistjakov, G.N. Semanov, A.K. Goldenfon and F.V. Linchevskij, Avtor. Svid-vo SSSR № 947275, Bull. Otkrytija i izobretenija, 28 (1982) 135.

316. R. Müller-Hurtig and F. Wagner, Biosurfactants for Environmental Control, in: [4], pp. 448.

317. B.E. Chistjakov, N.A. Melnik, V.G. Germashev, F.V. Linchevskij and E.E. Bibik, Bull. Otkrytija i izobretenija, 35 (1981) 130.

318. Kolloidno-khimicheskie problemy ekologii. - Tezisy dokladov Vsesojuzhoj konferentsii, Minsk, Akademija Nauk Belorussii, 1990, pp. 218.

319. Z.Q. Ou, A. Yediler, Y.W. He, L.Q. Jia, A. Kettrup and T.H. Sun, Chemosphere, 32 (1996) 827.

320. A.M. Kochanovski, N.A. Klimenko, G.M. Levchenko and I.G. Roda, Adsorbtsija organicheskikh veshchestv iz vody. Khimija, Leningrad, 1990, pp. 256.

321. W. Dewolf and T. Feijtel, Chemosphere, 36 (1998) 1319.

322. S.C. Crawford, C.J. Bruell, D.K. Ryan and J.W. Duggan, J. Soil Contamination, 6 (1997) 355.

323. Y.M. Elshoubary and D.E. Woodmansee, Environmental Progress, 15 (1996) 173.

324. C.S. Yam, O.K. Harling and R. Kaiser, J. Adhesion, 60 (1997) 163.

325. Poverkhnostno-aktivnye veshchestva i mojushchie sredstva, Spravochnik, Khimija, Moscow, 1993, pp. 270.

326. I.K. Getmanskij, A.I. Shchegol-Alimova, Pozharobezopasnye tekhnicheskie mojushchie sredstva, spravochnik, Mashinostroenie, Moscow, 1982, pp. 32.

327. F. Sebba, Ion Flotation, Elsevier, Amsterdam - London – New York, 1962.

328. S.F. Kuzkin and A.M. Golman, Flotatsija ionov i molekul, Nedra, Moscow, 1978, pp. 133.

329. X.C. He, Separation Sci. Technol., 33 (1998) 141.

330. L.D. Skrylev, V.F. Sazonova, S.V. Perlova and V.V. Menchuk, Kolloidno-khimicheskie osnovy flotatsionnykh metodov ochistki stochnykh vod promyshlennykh predprijatij ot ionov tsvetnykh metallov, in: [317], pp. 49.

331. R.K. Rothmel, R.W. Peters, E. Stmartin and M.F. Deflaun, Environmental Sci. Technol., 32 (1998) 1667.

332. K. Bonkhoff, M.J. Schwuger and G. Subklew, Use of Microemulsions for the Extraction of Contaminated Solids, in: [41], pp. 355.

333. T. Briggs, Foams for Fire-Fighting, in: [6], pp. 465.

334. M.Ju. Pletnev, B.E. Chistjakov and I.G. Vlasenko, Sovremennye penoobrazujushchie sostavy, svoistva i oblasti primenenija, TsNIITENeftekhim, Moscow, 1984, pp. 38.

7. SOFTWARE TOOLS TO INTERPRET THE THERMODYNAMICS AND KINETICS OF SURFACTANT ADSORPTION

E.V. Aksenenko

Institute of Colloid Chemistry and Chemistry of Water, Ukrainian National Academy of Sciences, 42 Vernadsky avenue, Kyiv (Kiev) 03680, Ukraine

In the present stage of interfacial science, there exists a number of models which give a more or less rigorous explanation of the phenomena observed at interfaces on a molecular level. These models inevitably involve mathematics which is more complicated than that used earlier; and the related calculations, in general, cannot be performed even using quite advanced computational software available now, e.g. MatCad or MatLab packages.

At the same time, a scientist needs not only the mathematical tool which could help him to calculate the isotherm or kinetic curve determined by a particular model. It is much more important to have a tool which helps in the analysis of experimental data: how far can phenomena taking place in the experimental system can be explained in the framework of a particular model? Moreover, with automated and computerised experimental devices currently available, one should naturally expect to have also the software, which is designed so as to provide him with the option of interactive and easily understandable way to analyse the results.

In this chapter, four independent software modules are described:

- IsoFit, which implements the search for the best fit between an experimental isotherm and the isotherms calculated for Langmuir, Frumkin, Two-State Reorientation and Aggregation models.
- IonMix, which implements the search for the best fit between an experimental isotherm and the isotherms calculated for the model describing mixtures of 1:1 ionic surfactants.

- NonIonMix, which implements the search for the best fit between an experimental isotherm and those calculated for models describing the mixture of two non-ionic surfactants, or a non-ionic with an ionic surfactant.
- WardTordai, which implements the solution of the Ward-Tordai equation for Langmuir, Frumkin, Two-State Reorientation Quasiequilibrium, Two-State Reorientation Kinetics and Aggregation models. Using this module, the user can compare (both visually and numerically) his experimental data with the kinetic curves calculated from any of these models.

When designing the software, the following considerations were taken into account: the attempt was made to make the software easy-to-use for any person who is familiar with ordinary MS Windows application software. The windows, buttons and other fields involved in the program interface bear self-explanatory labels. The programs are accompanied by manuals where detailed instructions are given on how to manipulate with the program; also the calculation methods and models are presented. Also, we tried to make the programs as compatible with other software common to the target users as possible. On the other hand, it was considered most appropriate to implement only 'Scientific English' as the interface language. The characters from other languages (encodings) could be used only in the comment sections of input/output files, as explained in the User's Manual which accompanies the programs.

In this Chapter, we present first features common to all the programs, namely the fitting strategy and the input/output data organisation. Then, each particular program is described with reference to the underlying mathematics. For each program, examples are given which explain its application to the systems considered. It is assumed that the reader, when studying these examples, uses the corresponding software supplied with the book.

7.1. Features common to all programs

7.1.1. Evaluation of model parameters

In this book, some models were proposed to describe the adsorption process at the interface. These models involve several parameters. Some of these parameters are quite obvious: e.g. the area occupied by a surfactant molecule at the interface can be approximately calculated from

geometric considerations. However, the values of other parameters should be estimated in a more sophisticated way. For example, it seems impossible to calculate the exact value of, say, Frumkin's model parameter a (which reflects the intermolecular interaction) for any system of practical interest, because such calculation would involve the solution of a multiparticle quantum mechanical problem and subsequent averaging over the characteristic relaxation times. Also, the theory involves other model parameters which are determined by physical processes still more difficult to analyse. In this situation, an inverse approach to the problem seems to be natural: one can try to determine the parameters relevant to the particular model from the requirement that the theoretical values of physical observables calculated from the model equations should exhibit the best possible agreement with the values observed in the experiment.

Fitting of particular theoretical model to experimental data to reach adequate description of the system studied, raises two main questions should be answered:

(i) which target function (i.e., the quantity whose minimum determines the set of parameters corresponding to the best fit between theoretical model and experimental data) should be chosen. Here a number of possible options were tried; for the IonMix, NonIonMix and WardTordai programs, the mean square deviation between the experimental and calculated values was implemented, while for the IsoFit program we have found a more sophisticated form of the target function to be appropriate, see Section 7.2.1.

(ii) how should the fitting procedure be organised, i.e., what algorithm should be used to minimise the target function over the set of model parameters. Here it would seem to be more straightforward to implement an automated search for the set of model parameters which leads to the target function minimum. However, it was found impossible for two reasons.

First, it can be rigorously shown, see e.g. [1] that, while for the search for a global minimum in the one-dimensional parameter space (i.e., for a single optimised parameter) a finite algorithm can be constructed, for a multidimensional problem any of such algorithm, in general, converges at the zero measure manifold only. It means that it is impossible to construct a procedure which ensures the convergence to the global minimum of the target function hypersurface in the multidimensional parameter space.

Second, as the experimental data involved in the calculation of target function always contain measurement errors, the target function hypersurface is generally 'folded'. This is illustrated by Fig. 7.1, where the target function profile is shown by contour lines of the values calculated in the nodes of a grid, which covers the range of parameters in the neighbourhood of the minimum sought for. In this Figure, the target function values which are lower than all the values calculated in the nearest neighbouring nodes, correspond to the 'local' and 'edge' minima, depending on whether they are located inside the scanned region or at its boundary.

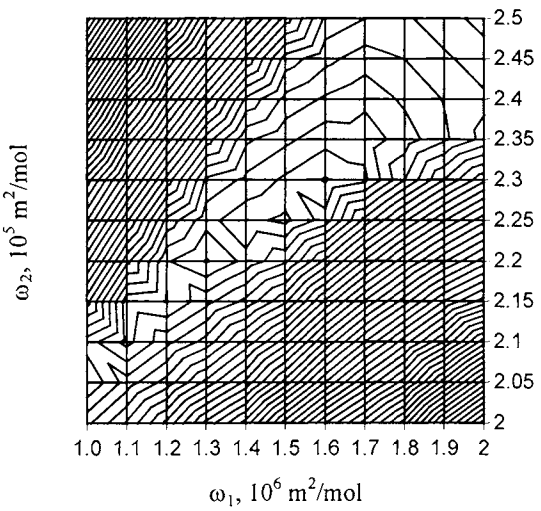

Figure 7.1. Target function contour lines corresponding to the scanning of C_{14}DMPO data with the IsoFit program for the reorientation model over the range of $\omega_1 = (1.0 \div 2.0) \cdot 10^6$ m^2/mol and $\omega_2 = (2.0 \div 2.5) \cdot 10^5$ m^2/mol; $\alpha = 0$.

It is clearly seen that there is a 'valley' of the target function profile, stretched in the SW-NE direction across the region scanned through. A closer examination of the data shows that in this valley at least four local 'depressions' exist. This is just the situation in which the automated minimisation procedure becomes deficient, failing to perform the global minimum search. Therefore, the procedures implemented in the fitting programs provide for a scanning over the grid in the predefined region of one- or multidimensional parameters (hyper)space, and the enumeration of all the local and edge minima of target function found in the nodes of the grid.

These minima are then listed by the program in an ascending order. Then the user has options to define the scanning regions more precisely.

7.1.2. Input/output file format

The format of input/output files used by the programs implements the data encapsulation feature to the extent that the initial (experimental) data are stored also as part of the output information. This avoids the multiplication of files: one can open the initial file by the program, make the calculations, and store the resulting file under the same filename. Next time when the user returns to the problem, opens the file and continues the calculations with the same file.

The type of the input/output files is the ordinary MS DOS or Windows text filetype, corresponding to the *.txt extension. This enables one to edit the files using familiar editors. Also, this feature makes it easy to produce initial files of experimental data automatically, via any suitable analogue-to-digital data converter.

7.2. IsoFit

The IsoFit program was developed to fit a particular adsorption model to experimental data obtained for single surfactant solution at equilibrium. The results obtained by this program are extensively discussed in Chapter 3. Here the relevant mathematics is presented in more detail as compared to the initial publication [2]. Also examples are given which illustrate the features of the software.

7.2.1. Backgrounds of fitting procedure

For any thermodynamic model of the adsorbed layer implemented in this package, the equation of state can be expressed in a dimensionless form:

$$-\frac{\Pi\omega}{RT} = F(\Gamma\omega;\alpha_1,\alpha_2,\ldots\alpha_n) \tag{7.1}$$

and the adsorption isotherm can also be represented in a dimensionless form:

$$bc = G(\Gamma\omega, \omega; \alpha_1, \alpha_2, \ldots \alpha_n) \tag{7.2}$$

Here Π is the surface pressure, Γ is the adsorption, c is the concentration, b is the adsorption equilibrium constant, ω is the area per molecule in the surface layer, and F and G are some functions dependent on Γ, ω and other model parameters denoted here as $\alpha_1, \alpha_2, \ldots \alpha_n$. For the simplest models considered, namely Langmuir and Frumkin models, ω is the model parameter, while for more advanced models this is a property which is defined via model equations. It is essential that in each case Γ enters the equations via the surface coverage coefficient, $\theta = \Gamma\omega$. Also, for each model there exists a parameter, say ω', which has the dimension of the area per molecule, and, being introduced into Eq. (7.1), enables one to reduce this equation to a dimensionless form

$$- p = (\omega'/\omega)F(\theta; \alpha_1, \alpha_2, \ldots \alpha_n), \tag{7.3}$$

where

$$p = \Pi\omega'/RT \tag{7.4}$$

and ω' is a combination of the parameter(s) $\alpha_1, \alpha_2, \ldots \alpha_n$, while the adsorption isotherm expressed in these variables is

$$bc = G(\theta, \omega; \alpha_1, \alpha_2, \ldots \alpha_n). \tag{7.5}$$

In most cases the dependence shown here as Eq. (7.5) is defined in an implicit form, i.e., involves a set of (transcendental) equations which should be solved numerically to represent Eq. (7.5).

Eliminating the θ and ω between Eqs. (7.3) and (7.5) – this is possible due to special forms of the equations – one obtains the dependence

$$bc = P(\Pi; \alpha_1, \alpha_2, \ldots \alpha_n), \tag{7.6}$$

which is used in the fitting procedure organised as follows.

For each particular set of $\alpha_1, \alpha_2, \ldots \alpha_n$ the value of b_i in each of the m experimental points (c_i, Π_i), $(i = 1, 2, \ldots, m)$ is calculated from Eq. (7.6). A mean value of b is calculated as the weighted average over all n values:

$$b = \sum_{i=1}^{m} b_i \frac{\Delta\Pi_i}{\Pi_n - \Pi_1}. \tag{7.7}$$

Here $\Delta\Pi_i = (\Pi_{i+1} - \Pi_{i-1})/2$ is the pressure range corresponding to the i^{th} point. The set of parameters $\alpha_1, \alpha_2, \ldots \alpha_n$ is considered optimum when the difference ΔS is minimal,

$$\Delta S = \sum_{i=1}^{m} \left|\log c_{ex,i} - \log c_{cal,i}\right| \Delta\Pi_i = \min. \tag{7.8}$$

Here the subscripts 'ex' and 'cal' refer to the experimental and calculated (for the same Π_i) surfactant concentrations, respectively. As the values of $\Delta c_i = \left|c_{ex,i} - c_{cal,i}\right|$ are small as compared to $c_{ex,i}$, one can transform the minimisation condition, Eq. (7.8), into a dimensionless form:

$$\varepsilon = \sum_{i=1}^{m} \frac{\Delta c_i}{c_{ex,i}} \frac{\Delta\Pi_i}{\Pi_m - \Pi_1} = \min \tag{7.9}$$

where the *target function* ε is the weighted (over Π) average of the relative deviations between the experimental and calculated c_i values.

In the package, in addition to the averaging with respect to the difference modulus, described by Eqs. (7.8) and (7.9), another form was also implemented, namely the ordinary mean square averaging. The results obtained using both averaging forms were in many cases identical.

7.2.2. Models implemented in the program

For a quick reference we repeat the most important equations here, used in the fitting routines of the software package.

Frumkin model [3] is defined by Eqs. (3.1)-(3.2):

$$-\frac{\Pi\omega}{RT} = \ln(1-\theta) + a\theta^2 \qquad \text{Equation of state (7.10)}$$

$$bc = \frac{\theta}{1-\theta}\exp(-2a\theta) \qquad \text{Adsorption isotherm (7.11)}$$

where a is the model parameter, $\theta = \Gamma\omega$. Then, the dependence (7.6) is determined by Eq. (7.10) and the numerical solution $\theta = \theta(\Pi)$ of Eq. (7.11.). The solution procedure is explained in the Manual in details.

The **Langmuir** model is a special case of the Frumkin model, with a = 0.

Reorientation model [4] is defined by Eqs. (2.84)-(2.88) or (3.3)-(3.7):

$$-\frac{\Pi\omega}{RT} = \ln(1-\Gamma\omega) \qquad \text{Equation of state (7.12)}$$

$$bc = \frac{\Gamma_2\omega}{(1-\Gamma\omega)^{\omega_2/\omega}} \qquad \text{Adsorption isotherm (7.13)}$$

Here ω is no longer a model parameter, but should be calculated from the equations:

$$\Gamma = \Gamma_1 + \Gamma_2\,, \qquad (7.14)$$

$$\omega\Gamma = \omega_1\Gamma_1 + \omega_2\Gamma_2\,, \qquad (7.15)$$

$$\frac{\Gamma_1}{\Gamma_2} = \exp\left(\frac{\omega_1-\omega_2}{\omega}\right)\left(\frac{\omega_1}{\omega_2}\right)^{\alpha}\exp\left[-\frac{\Pi(\omega_1-\omega_2)}{RT}\right]. \qquad (7.16)$$

For this model, the parameters are ω_1, ω_2 (molar areas of molecules in states 1 and 2 in the adsorbed layer. It is assumed that $\omega_1 > \omega_2$), and α. Γ_1 and Γ_2 are the partial adsorptions of the molecules in states 1 and 2, which should be eliminated via Eqs. (7.14) – (7.16). The solution procedure is discussed in detail in the Manual, so that we present it here only in brief.

Namely, introducing the quantities:

$$\Omega = \omega/\omega_2, \qquad \Omega_1 = \omega_1/\omega_2 = \text{const}, \qquad p = \Pi\omega_2/RT \qquad (7.17)$$

one can reduce Eqs. (7.14) – (7.16) to a single transcendental equation in Ω:

$$\frac{\Omega-1}{\Omega_1-\Omega} = \exp\left(\frac{\Omega_1-1}{\Omega}\right)\cdot\Omega_1^{\alpha}\exp[-p(\Omega_1-1)]. \qquad (7.18)$$

It can be easily shown that a single root of this equation $\Omega = \Omega(p)$ always exists in the interval $1 < \Omega < \Omega_1$, and, with this root calculated numerically, one can calculate the quantities

$$\Gamma\omega = \theta = 1 - \exp(-p\Omega) \tag{7.19}$$

$$bc = \frac{\Omega_1 - \Omega}{\Omega_1 - 1} \cdot \frac{\theta}{(1-\theta)^{1/\Omega}} \tag{7.20}$$

which determines the dependence (7.6).

Aggregation model [5] is defined by Eqs. (3.8)-(3.10):

$$-\frac{\Pi\omega}{RT} = \ln\left\{1 - \Gamma_1\omega\left[1 + (\Gamma_1/\Gamma_c)^{n-1}\right]\right\} \qquad \text{Equation of state (7.21)}$$

$$bc = \frac{\Gamma_1\omega}{\left\{1 - \Gamma_1\omega\left[1 + (\Gamma_1/\Gamma_c)^{n-1}\right]\right\}^{\omega_1/\omega}} \qquad \text{Adsorption isotherm (7.22)}$$

where Γ_1 is the partial adsorption of monomers, Γ_c is the critical adsorption of monomers, n is the aggregation number, ω_1 is the area per one monomer. The average molar area ω is expressed via the equation:

$$\frac{\omega}{\omega_1} = \frac{1 + n(\Gamma_1/\Gamma_c)^{n-1}}{1 + (\Gamma_1/\Gamma_c)^{n-1}}. \tag{7.23}$$

Then, introducing

$$p = \Pi\omega_1/RT, \qquad \kappa = \Gamma_1/\Gamma_c \tag{7.24}$$

one obtains the equation for κ,

$$-p = \frac{1 + \kappa^{n-1}}{1 + n\kappa^{n-1}} \cdot \ln\left[1 - (\Gamma_c\omega_1)\kappa\left(1 + n\kappa^{n-1}\right)\right]. \tag{7.25}$$

The solution of this equation is explained in detail in the Manual, and only the final result is presented here. Namely, the surface coverage is expressed via the root κ of Eq. (7.25) as

$$\theta = (\Gamma_c\omega_1)\kappa\left(1 + n\kappa^{n-1}\right) \tag{7.26}$$

and for bc one obtains the expression

$$bc = \frac{\theta}{1+\kappa^{n-1}}(1-\theta)^{-(1+\kappa^{n-1})/(1+n\kappa^{n-1})}, \tag{7.27}$$

which determines the dependence (7.6).

7.2.3. Examples

(1) **Normal octyl alcohol C_8OH**. This system is discussed in Section 3.3.1.

Starting the IsoFit program located in the IsoFit folder on your CD, and opening the C8OHf.txt file, you will immediately see the final result of the optimisation, however, it is instructive to repeat the procedure step-by-step.

To start with this system, the initial guesses for the Frumkin model parameters should be chosen. The van der Waalsian cross-section of the alkyl chain is 0.42 nm × 0.45 nm = 0.19 nm^2, which gives the lower estimate of the area per mole of $\omega = 1.15 \cdot 10^5$ m^2/mol. The a value is expected to be in the range between 0 and 2.

Pressing the buttons labelled by the parameter name in the Model parameters area toggles the Fix/Scan regime for this parameter. Set the initial guess for ω as indicated above ($\omega = 1.15 \cdot 10^5$ m^2/mol), and the scanning range 0 to 2 for a, set the value 5 for the number of nodes in a, then press Calculate button. When the calculation run is complete, the plots in the target and isotherm windows are displayed similar to what is shown in Figures 7.2 and 7.3, respectively.

In the target window the values of target function ε for different a are displayed, see Fig. 7.2; that corresponding to the minimum deviation is marked by different colour. The curves in the isotherm window correspond to these a values; the curve which correspond to the current a value is displayed in the actual program window in the magenta colour (in Fig. 7.3 this curve is thick). The user can switch between current values by clicking the corresponding point in the target window; the current point is indicated by small triangle.

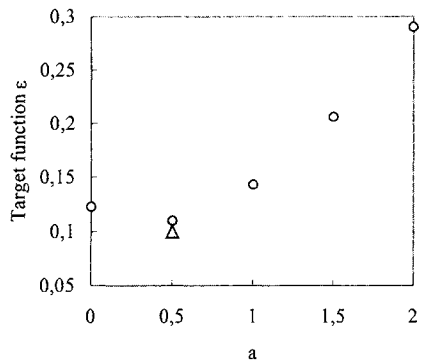

Figure 7.2. Values of target function ε as scanned in the a range 0 to 2 for $\omega = 1.15 \cdot 10^5$ m²/mol; experimental data are for normal octyl alcohol C_8OH as given in Fig. 7.3

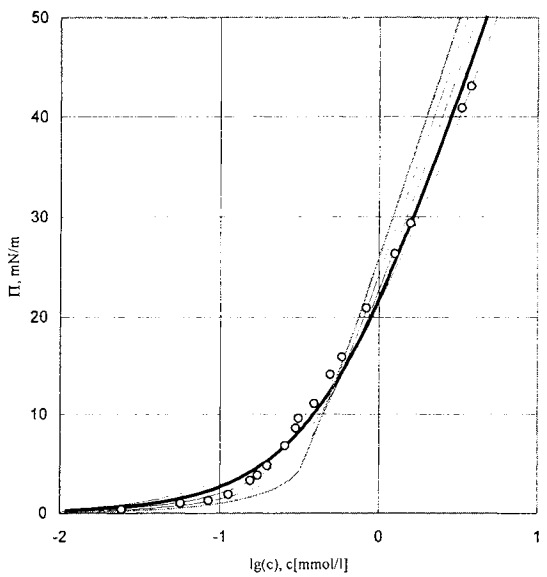

Figure 7.3. Experimental (circles) and calculated surface pressure in the a range 0 to 2 for $\omega = 1.15 \cdot 10^5$ m²/mol; the experimental data for normal octyl alcohol C_8OH.

Next, the scanning can be performed over the two model parameters. Choosing the ranges for the parameters as: $(1.0 \div 2.0) \cdot 10^5$ m²/mol for ω, and (1÷3) for a, setting the nodes number to 11, and pressing Calculate button, the user starts the calculation process. When the calculation run

is completed, the user will be informed that one local and one edge minimum exist in the region covered by the scanning. Clicking at the corresponding Local or Edge label in the minima list displays the b, target function and model parameters for this particular minimum in the Target data area. The lowest value of the target function corresponds to $\omega = 1.7 \cdot 10^5$ m^2/mol and a = 1.4, the values shown in the initial C8OHf.txt file.

To calculate the optimum values of model parameters more precisely, the user can repeat the calculations within a narrower range of parameters variation. In this particular case, choosing the scanning ranges $(1.6 \div 1.7) \cdot 10^5$ m^2/mol for ω, and (1.3÷1.4) for a, one obtains for the lowest local minimum the values shown in Table 3.1 for C_8OH (cf. Chapter 2).

(2) **Oxyethylated alcohol $C_{14}EO_8$**. This system is discussed in Section 3.3.7.

For this system, the C14EO8.txt file contains the initial experimental data only and are displayed when the file is loaded into the program. Choose Reorientation from the Model isotherm menu. For the reorientation model, the estimates for the maximum (ω_1) and minimum (ω_2) area per $C_{14}EO_8$ molecule are of the order of 2 and 0.5 nm^2, respectively. Then, the IsoFit program can be used to vary the values within rather wide ranges: $\omega_1 = (0.5 \div 5.0) \cdot 10^6$ m^2/mol, $\omega_2 = (0.5 \div 5.0) \cdot 10^5$ m^2/mol, $\alpha = (0 \div 5)$; the default number (11) of the scanning nodes could be accepted. The fitting procedure in this range shows that a number of local minima exists, among which the lowest is that corresponding to the values: $\omega_1 = 1.4 \cdot 10^6$ m^2/mol, $\omega_2 = 3.2 \cdot 10^5$ m^2/mol and $\alpha = 2.5$. In the report window the message is displayed which tells that 11 points were out of physical domain. This is because of the fact that in these points the values of ω_1 and ω_2 were both equal to $5.0 \cdot 10^5$ m^2/mol, while the model implies $\omega_1 > \omega_2$, cf. Eqs. (7.16)-(7.20). Repeating next the search in a more narrow range, i.e. $\omega_1 = (1.2 \div 1.6) \cdot 10^6$ m^2/mol, $\omega_2 = (2.8 \div 3.4) \cdot 10^5$ m^2/mol, $\alpha = (2.3 \div 2.9)$, one obtains the lower local minimum values quite close to those shown in Table 3.13.

7.3. NonIonMix

7.3.1 Model description and equations

For the mixture of two non-ionic surfactants, or the mixture of a non-ionic with an ionic surfactant, assuming that the behaviour of each surfactant is governed by the Frumkin model, the system was shown in Section 2.4 to obey the equation of state (2.35):

$$\Pi = -\frac{RT}{\omega}\left[\ln(1-\theta_1-\theta_2)+a_1\theta_1^2+a_2\theta_2^2+2a_{12}\theta_1\theta_2\right], \tag{7.28}$$

where the average area per molecule is

$$\omega = \frac{\omega_1\Gamma_1+\omega_2\Gamma_1}{\Gamma_1+\Gamma_2}. \tag{7.29}$$

Here the subscript i (i = 1, 2) refers to the surfactant molecular species, $\theta_i = \Gamma_i\omega_i$ is the surface layer coverage by i^{th} surfactant, Γ_i is the adsorption of i^{th} surfactant, $\Pi = \gamma_0 - \gamma$ is the surface pressure, γ_0 is the surface tension of solvent. In the program, two forms of the isotherm equations are implemented:

model A -

$$\left.\begin{aligned} b_1c_1 &= \frac{\theta_1}{(1-\theta_1-\theta_2)^{n_1}}\exp(-2a_1\theta_1-2a_{12}\theta_2) \\ b_2c_2 &= \frac{\theta_2}{(1-\theta_1-\theta_2)^{n_2}}\exp(-2a_2\theta_2-2a_{12}\theta_1) \end{aligned}\right\}, \tag{7.30-A}$$

and **model B** (cf. Eqs. (2.36)) -

$$\left.\begin{aligned} b_1c_1 &= \frac{\theta_1}{(1-\theta_1-\theta_2)^{n_1}}\exp(-2a_1\theta_1-2a_{12}\theta_2)\exp\left[(1-n_1)(a_1\theta_1^2+a_2\theta_2^2+2a_{12}\theta_1\theta_2)\right] \\ b_2c_2 &= \frac{\theta_2}{(1-\theta_1-\theta_2)^{n_2}}\exp(-2a_2\theta_2-2a_{12}\theta_1)\exp\left[(1-n_2)(a_1\theta_1^2+a_2\theta_2^2+2a_{12}\theta_1\theta_2)\right] \end{aligned}\right\}. \tag{7.30-B}$$

Here c_i (i = 1,2) is the concentration of i^{th} surfactant, $n_1 = \omega_1/\omega$, $n_2 = \omega_2/\omega$. Then, with known parameters characteristic for the individual isotherms (b_i, a_i and ω_i, i = 1, 2) the set of equations (7.30-A) or (7.30-B) can be solved for any trial value of a_{12}. A reasonable initial guess for the

parameter a_{12} that corresponds to the case when the system exhibits no synergy is $a_{12} = (a_1 + a_2)/2$.

In the experimental data, the inorganic electrolyte concentration is usually kept fixed. For any system studied, the experimental runs are performed either for fixed molar fractions x_1 and x_2, i.e. $c_1 = c \cdot x_1/(x_1 + x_2)$, $c_2 = c \cdot x_2/(x_1 + x_2)$, or for fixed concentration of, say, the second component. These experimental conditions were accounted for in the procedure implemented to obtain the numerical solution.

The concentration value $c = c_1 + c_2$ is scanned through the relevant range. The numerical procedure used for the solution of the set (7.30) is described in the Manual. For each c, Eq. (7.28) is used to calculate the surface pressure or surface tension. The target function is calculated as the mean square deviation between the experimental data and the theoretical values calculated over the same set of c values. Similarly to other programs (IsoFit and IonMix), the scanning through the a_{12} range was implemented rather than an automated search for the optimum a_{12} value.

7.3.2 Example

Mixture of oxyethylated decyl alcohol and sodium dodecyl sulphate in 0.01 M NaCl.

This system is discussed in Section 3.6. The initial data for this system are stored in the C12SO4Na-C10EO5.txt file. The values of model parameters defined in this file were calculated from the Frumkin model. When the data are loaded into the NonIonMix program, the experimental values are displayed. Next, choosing the interval for $a_{12} = (0.8 \div 1.2)$, selecting 5 for the scanning nodes number and pressing Run button one starts the calculations. When the calculations are done, the results are reported in the target window and isotherm window, which is shown schematically in Figs. 7.4 and 7.5, respectively.

It is seen from the target window that the value which corresponds to the minimum deviation between experimental and theoretical values is $a_{12} \approx 1.1$. Clicking at this point (marked green) in the target window and choosing (for example) the $x_1{:}x_2 = 1{:}100$ experimental series, one obtains the plots in the target and isotherm windows similar to what is shown in Figs. 7.4 and 7.5. The magenta curve (shown as thick line in Fig. 7.5) corresponds to the experimental series

and a_{12} value chosen by the program control; thin black lines correspond to other experimental series for the a_{12} value chosen, and gray lines show the isotherms for the experimental series chosen and different a_{12} values.

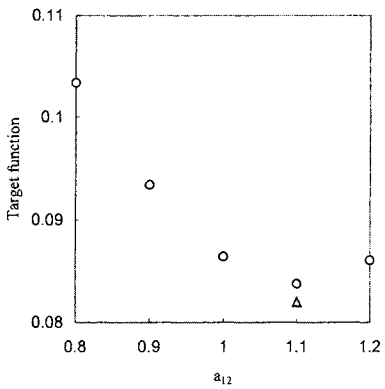

Figure 7.4. Values of target function for scanning the data for mixtures of $C_{10}EO_5$ and $C_{12}SO_4Na$ in 0.01 M NaCl with ratios 1:1, 1:10, 1:100 and 1:500 through the a_{12} range 0.8 to 1.2.

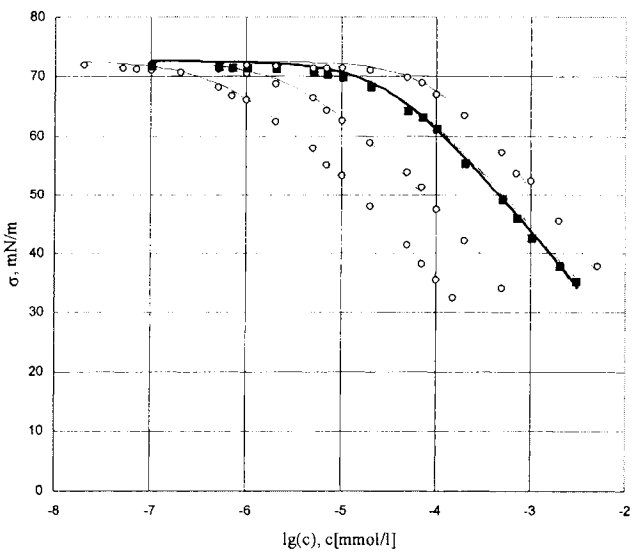

Figure 7.5. Experimental (points) and theoretical (lines) values of surface tension for mixtures of $C_{10}EO_5$ and $C_{12}SO_4Na$ solutions in 0.01 M NaCl with ratios 1:1, 1:10, 1:100 and 1:500, calculated for $a_{12} = 1.1$.

7.4. IonMix

7.4.1. Model description and equations

For the most simple case, a mixture of ionic homologues, the system was shown in Section 2.5.1 to obey the set of equations (2.49), (2.50):

$$\Pi = -\frac{RT}{\omega}\left[\ln(1-\theta_1-\theta_2)+a_1\theta_1^2+a_2\theta_2^2+2a_{12}\theta_1\theta_2\right], \tag{7.31}$$

$$\left.\begin{aligned} b_1(c_1(c_1+c_2+c_3))^{1/2} f &= \frac{[\theta_1(\theta_1+\theta_2)]^{1/2}}{(1-\theta_1-\theta_2)}\exp(-2a_1\theta_1-2a_{12}\theta_2) \\ b_2(c_2(c_1+c_2+c_3))^{1/2} f &= \frac{[\theta_2(\theta_1+\theta_2)]^{1/2}}{(1-\theta_1-\theta_2)}\exp(-2a_2\theta_2-2a_{12}\theta_1) \end{aligned}\right\} \tag{7.32}$$

where c_i (i = 1,2) is the concentration of i^{th} surfactant, c_3 is the concentration of inorganic electrolyte with common counter-ion, and the coverage-related dimensionless values $\theta_1 = 2\Gamma_1\omega$, $\theta_2 = 2\Gamma_2\omega$ are introduced, where Γ_i is the partial adsorption of the i^{th} species; for the mean area per molecule ω the expression $\omega = (\theta_1 + \theta_2)/(\theta_1/\omega_1 + \theta_2/\omega_2)$ was assumed. The surfactant activity coefficient in the solution is given by the Debye-Hückel-type equation

$$\log f = -\frac{0.0162 c_0^{1/2}}{1+0.0416 c_0^{1/2}} + 0.000055 c_0 . \tag{7.33}$$

Here $c_0 = c_1 + c_2 + c_3$, and the concentrations are expressed in 10^{-3} mol/l. Then, with known parameters characteristic for the individual isotherms (b_i, a_i and ω_i, i = 1, 2) the set of equations (7.31) and (7.32) can be solved for any trial a_{12} value, with a reasonable initial guess for the parameter a_{12} that corresponds to the case when the system exhibits no synergy, i.e. $a_{12} = (a_1 + a_2)/2$.

In the experimental data, the inorganic electrolyte concentration is usually kept fixed. For any system studied, the experimental runs are performed either for fixed molar fractions x_1 and x_2, i.e. $c_1 = c \cdot x_1/(x_1 + x_2)$, $c_2 = c \cdot x_2/(x_1 + x_2)$, or for fixed concentration of, say, the second component. These experimental conditions were accounted for in the procedure implemented to obtain the numerical solution.

The concentration value $c = c_1 + c_2$ is scanned through the relevant range. The numerical procedure used for the solution of the set (7.32) is described in the Manual. For each c value, Eq. (7.31) is used to calculate the surface pressure or surface tension. The target function is calculated as the mean square deviation between the experimental data and the theoretical values calculated over the same set of c values. Similarly to other programs (IsoFit and NonIonMix), the scanning through the a_{12} range was implemented rather than an automated search for the optimum a_{12} value.

7.4.2. Example

Mixture of decyl ammonium chloride and dodecyl ammonium chloride in 5 mmol/l solution of NaCl. This system is discussed in Section 3.7.1.

The model implemented by this program is quite similar to the NonIonMix problem described above in Section 7.4, and also the interface and controls in IonMix are much like that used in NonIonMix.

The initial data for this system are stored in the C10ACl-C12ACl.txt file. The values of model parameters defined in this file were calculated from the Frumkin model. When the data from this file are loaded into the IonMix program, the experimental values are displayed. Next, choosing the interval for $a_{12} = (1.25 \div 1.75)$, selecting 5 for the scanning nodes number and pressing Run button one starts the calculations. When the calculations are over, the results are reported in the target and isotherm windows, shown schematically in Figs. 7.6 and 7.7, respectively.

It is seen from the target window that the value which corresponds to the minimum deviation between the experimental and theoretical values is $a_{12} \approx 1.5$. Clicking at this point (marked green) in the target window and choosing (for example) the $x_1:x_2 = 15:1$ experimental series, one obtains the plots in the target and isotherm windows similar to what is shown in Figs. 7.6 and 7.7. The magenta curve (shown as thick line in Fig. 7.7) corresponds to the experimental series and a_{12} value chosen by the program controls; thin black lines correspond to other experimental series for the a_{12} value chosen, and gray lines show the isotherms for the experimental series chosen and different a_{12} values.

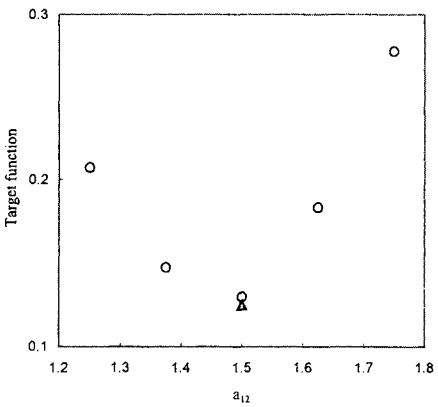

Figure 7.6. Values of target function for scanning the data for mixtures of decyl ammonium chloride and dodecyl ammonium chloride in 5 10^{-3} mol/l solution of NaCl through the a_{12} range 1.25 to 1.75.

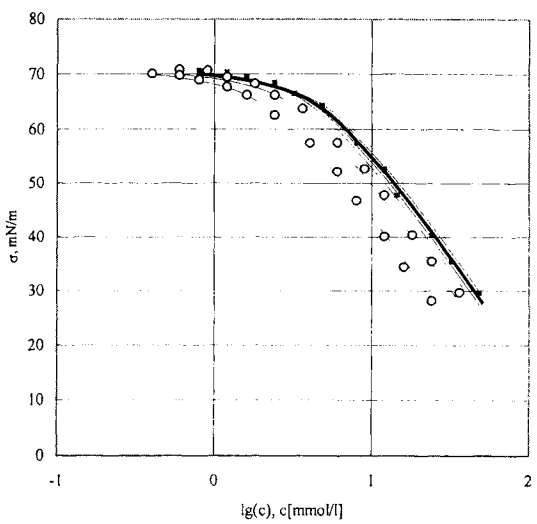

Figure 7.7. Experimental (points) and theoretical (lines) values of surface tension for mixtures of decyl ammonium chloride and dodecyl ammonium chloride solutions in 0.01 M NaCl with ratios 15:1, 5:1 and 5:3, calculated for $a_{12} = 1.5$.

7.5. WardTordai

7.5.1. Numerical solution of the Ward-Tordai equation

The equation which is implemented in the software is somewhat more general than the ordinary Ward-Tordai equation (4.3) first proposed in [6], and accounts also for the existence of an adjacent second liquid phase,

$$\Gamma(t) = 2\sqrt{\frac{D}{\pi}}\left[c_0\sqrt{t} - \left(1 + K\sqrt{\frac{D_a}{D}}\right)\int_0^{\sqrt{t}} c(0, t - t')\,d\sqrt{t'}\right], \tag{7.34}$$

where t is the time, D is the surfactant diffusion coefficient in the solution, D_a is the diffusion coefficient in the adjacent phase, K is the surfactant distribution coefficient. Here c_0 is the bulk concentration of the surfactant, and c(0, t) is the surfactant concentration in the surface layer.

For any particular adsorption model, the adsorption isotherm

$$c = c(\Gamma) \tag{7.35}$$

enters the integrand. Introducing the dimensionless variables

$$\gamma(t) = \Gamma(t)/\Gamma_\infty, \quad \tau = D\left(\frac{c_0}{\Gamma_\infty}\right)^2 t, \quad C \equiv C(\tau - \tau') = c(0, t - t')/c_0, \quad \lambda = 1 + K\sqrt{D_a/D} \tag{7.36}$$

one transforms Eq. (7.34) into the form

$$\gamma(\Theta^2) = \frac{2}{\sqrt{\pi}}\left[\Theta - \lambda\int_0^{\Theta} C(\Theta^2 - \vartheta^2)\,d\vartheta\right] \tag{7.37}$$

where the variable $\Theta = \sqrt{\tau}$ was introduced. In the program, the solution of Eq. (7.37) is obtained using a finite difference procedure mapped onto the Θ axis, with equidistant nodes $\Theta i = i\cdot\delta$ at which the values of $C(\Theta_i^2) \equiv C_i$ are calculated. For the n^{th} node, the relation holds

$$\gamma(\Theta_n^2) = \frac{2}{\sqrt{\pi}}\left[\Theta_n - \lambda\int_0^{\Theta_n} C(\Theta_n^2 - \vartheta^2)\,d\vartheta\right], \tag{7.38}$$

and, as the value of $C(0) = C_0 \equiv 0$ is known, the recursion procedure is closed. To calculate the integral on the right hand side of Eq. (7.38) numerically, at each n^{th} step one has to integrate over the set $\{\Theta_{n,i}\}$ of non-equidistant nodes, defined for any $i = 1, \ldots, n-1$ via the relation

$$\Theta_n^2 - \Theta_{n,i}^2 = \left\{\Theta_0^2, \Theta_1^2, \ldots, \Theta_i^2, \ldots, \Theta_{n-1}^2\right\}. \tag{7.39}$$

Then, Eq. (7.38) becomes

$$\gamma\left(\Theta_n^2\right) = \frac{2}{\sqrt{\pi}}\delta\left[n - \lambda I_k^{(n)}\left(\Theta_{n,0}, \ldots, \Theta_{n,n-i}, \ldots, \Theta_{n,n}; C_n, \ldots, C_i, \ldots, C_0\right)\right] \tag{7.40}$$

where $I_k^{(n)}$ is the integral calculated using the appropriate k^{th} order quadrature scheme. Treating separately the term which contains the unknown value C_n, one can represent $I_k^{(n)}$ in the form

$$I_k^{(n)} = A_k^{(n)}\left(\Theta_{n,0}, \ldots, \Theta_{n,n}\right)C_n + B_k^{(n)}\left(\Theta_{n,1}, \ldots, \Theta_{n,n}; C_{n-1}, \ldots, C_0\right), \tag{7.41}$$

which, combined with Eq. (7.40), yields

$$\gamma_n = \frac{2}{\sqrt{\pi}}\delta\left[n - \lambda B_k^{(n)} - \lambda A_k^{(n)} C_n\right]. \tag{7.42}$$

Here $\gamma_n = \gamma\left(\Theta_n^2\right)$. As γ_n is related to C_n via the isotherm $C = C(\gamma)$, cf. Eq. (7.35), then Eq. (7.42) can be numerically solved at each n^{th} node.

The procedure described above was implemented in the WardTordai program. The first-order quadrature scheme was found to be accurate enough, see [7].

7.5.2. Models implemented in the program

As mentioned above, a complete set of equation involves and equation of the type of Eq. (7.35), otherwise a numerical solution of the Ward-Tordai equation is not available. The software package includes all adsorption models described in Chapter 3, i.e. the classical Langmuir and Frumkin model as well as the reorientation and 2D-aggregation models.

Frumkin's model, Eqs. (7.10), (7.11) above, for the purpose of this subsection can be presented in a more convenient form:

$$bc(0,t) = \frac{\Gamma\omega}{1-\Gamma\omega}\exp(-2a\Gamma\omega), \qquad \text{Adsorption isotherm (7.43)}$$

$$\Pi = -\frac{RT}{\omega}\left[\ln(1-\Gamma\omega) + a(\Gamma\omega)^2\right]. \qquad \text{Equation of state (7.44)}$$

Introducing the dimensionless parameters

$$bc_0 = B, \qquad w = \omega\Gamma_\infty \qquad (7.45)$$

with γ and C defined as in Eqs. (7.36), one transforms the equations into

$$BC = \frac{\gamma w}{1-\gamma w}\exp(-2a\gamma w), \qquad (7.46)$$

$$-\frac{\Pi\omega}{RT} = \ln(1-\gamma w) + a(\gamma w)^2. \qquad (7.47)$$

Then, **boundary condition** are needed. As for $t \to \infty$ the relations:

$$\Pi(t \to \infty) = \Pi_0, \qquad C(t \to \infty) = 1, \qquad \gamma(t \to \infty) = 1, \qquad (7.47)$$

are valid, and one can transform Eq. (7.47) into

$$-\frac{\Pi_0\omega}{RT} = \ln(1-w) + aw^2. \qquad (7.48)$$

For any physical value of Π_0, this equation can be solved numerically with respect to w. Once the w value is known, one can calculate the values

$$\Gamma_\infty = w/\omega, \qquad (7.49)$$

$$B = \frac{w}{1-w}\exp(-2aw). \qquad (7.50)$$

With this B value, for each γ one can calculate the C value as

$$C = \frac{1}{B}\frac{\gamma w}{1-\gamma w}\exp(-2a\gamma w). \qquad (7.51)$$

Thus closing the finite difference procedure defined in Section 7.6.1; for each θ (and, hence, t) the values γ, C, and also Π from Eq. (7.47) can be calculated.

The **Langmuir** model is a special case of the Frumkin model, with a = 0.

Two-state reorientation model in the kinetic case (cf. Section 4.2.2) is defined by the equations

$$bc_1(0,t)\beta = \frac{\Gamma_1\omega}{(1-\Gamma\omega)^{\omega_1/\omega}}, \qquad \text{Adsorption isotherm for molecules in state 1} \tag{7.52}$$

$$bc_2(0,t) = \frac{\Gamma_2\omega}{(1-\Gamma\omega)^{\omega_2/\omega}}, \qquad \text{Adsorption isotherm for molecules in state 2} \tag{7.53}$$

where it is assumed that $\omega_1 > \omega_2$, and

$$\beta = \left(\frac{\omega_1}{\omega_2}\right)^{\alpha} \exp\left(\frac{\omega_1-\omega_2}{\omega}\right) \tag{7.54}$$

with ω defined by

$$\Gamma = \Gamma_1 + \Gamma_2, \qquad \omega\Gamma = \omega_1\Gamma_1 + \omega_2\Gamma_2, \tag{7.55}$$

and the partial concentrations related to the total concentration c(0,t) by the relation

$$c(0,t) = \frac{c_1(0,t)\left(\frac{\Gamma_1}{\Gamma_1^0}\right) + c_2(0,t)\left(\frac{\Gamma_2}{\Gamma_2^0}\right)}{\left(\frac{\Gamma_1}{\Gamma_1^0}\right) + \left(\frac{\Gamma_2}{\Gamma_2^0}\right)}, \tag{7.56}$$

with

$$\frac{\Gamma_1^0}{\Gamma_2^0} = \beta\exp\left[-\frac{\Pi(\omega_1-\omega_2)}{RT}\right], \tag{7.57}$$

$$\Pi = -\frac{RT}{\omega}\left[\ln(1-\Gamma\omega) - a(\Gamma\omega)^2\right]. \qquad \text{Equation of state} \tag{7.58}$$

Here two cases can be distinguished:

***Two-state reorientation model* – quasi-equilibrium:**

$$\Gamma_1 - \beta\Gamma_2 \exp\left[-\frac{\Pi(\omega_1 - \omega_2)}{RT}\right] = 0 \tag{7.59}$$

***Two-state reorientation model* – kinetics:**

$$\frac{1}{2}\frac{d\Gamma}{dt} - \frac{d\Gamma_1}{dt} = k\left\{\Gamma_1 - \beta\Gamma_2 \exp\left[-\frac{\Pi(\omega_1 - \omega_2)}{RT}\right]\right\} \tag{7.60}$$

Introducing the dimensionless parameters similar to Eq. (7.45),

$$bc_0 = B, \qquad w = \omega\Gamma_\infty \tag{7.61}$$

$$\Gamma_1 = \gamma_1\Gamma_\infty, \qquad \Gamma_2 = \gamma_2\Gamma_\infty \tag{7.62}$$

$$w_1 = \omega_1\Gamma_\infty, \qquad w_2 = \omega_2\Gamma_\infty \tag{7.63}$$

$$\Omega = \omega/\omega_2 = w/w_2 \tag{7.64}$$

$$\Omega_1 = \omega_1/\omega_2 = w_1/w_2 = \text{const} > 1 \quad \text{(note that, as } \omega_1 > \omega_2\text{)} \tag{7.65}$$

$$1 < \Omega < \Omega_1 \tag{7.66}$$

with γ and C defined as in Eqs. (7.36), respectively, one transforms Eqs. (7.55) and (7.58) into

$$\gamma_1 = \frac{\Omega - 1}{\Omega_1 - 1}\gamma, \qquad \gamma_2 = \frac{\Omega_1 - \Omega}{\Omega_1 - 1}\gamma \tag{7.67}$$

$$-\frac{\Pi\Omega\omega_2}{RT} = \ln(1 - \gamma w) - a(\gamma w)^2 \tag{7.68}$$

Boundary condition solution

Assuming that at $t \to \infty$, the derivatives $d/dt \to 0$, one can see that the two cases defined above (quasi-equilibrium and kinetic) are described by the same boundary condition (7.47), common for all adsorption models. Then, from either Eq. (7.59) or Eq. (7.60) one obtains:

$$\frac{\Omega_\infty - 1}{\Omega_1 - \Omega_\infty} = \Omega_1^\alpha \exp\left[-\frac{\Pi_\infty(\omega_1 - \omega_2)}{RT}\right]\exp\left(\frac{\Omega_1 - 1}{\Omega_\infty}\right). \tag{7.69}$$

This expression should be considered as the equation with respect to Ω_∞, which is the value of Ω at $t \to \infty$. It is easily seen that, as within the relevant interval $1 < \Omega < \Omega_1$, the left hand side of this equation is a monotonously increasing function from 0 to infinity, while the right hand side of this equation is a monotonously decreasing positive function, a single root of this equation always exists,

$$\Omega_\infty = \Omega_\infty(\Pi_\infty), \tag{7.70}$$

which, being calculated numerically, and introduced into Eq. (7.68), yields

$$-\frac{\Pi_\infty \Omega_\infty \omega_2}{RT} = \ln(1 - w_\infty) - a(w_\infty)^2. \tag{7.71}$$

This equation, solved numerically, yields the dependence

$$w_\infty = w_\infty(\Pi_\infty), \tag{7.72}$$

from which the values

$$w_2 = w_\infty/\Omega_\infty \tag{7.73}$$

$$\Gamma_\infty = w_\infty/\Omega_\infty\omega_2 \tag{7.74}$$

$$\gamma_1^{(\infty)} = \frac{\Omega_\infty - 1}{\Omega_1 - 1}, \qquad \gamma_2^{(\infty)} = \frac{\Omega_1 - \Omega_\infty}{\Omega_1 - 1} \tag{7.75}$$

can be calculated. Then, from Eqs. (7.56), (7.57) one obtains the expression for B,

$$B = w_\infty \frac{\left(\frac{\gamma_1^{(\infty)}}{\beta_\infty}\right)^2 (1 - w_\infty)^{-\Omega_1/\Omega_\infty} + \left(\gamma_2^{(\infty)}\right)^2 (1 - w_\infty)^{-1/\Omega_\infty} \exp\left[-\frac{\Pi_\infty(\omega_1 - \omega_2)}{RT}\right]}{\frac{\gamma_1^{(\infty)}}{\beta_\infty} + \gamma_2^{(\infty)} \exp\left[-\frac{\Pi_\infty(\omega_1 - \omega_2)}{RT}\right]}, \tag{7.76}$$

where

$$\beta_\infty = \left(\frac{\omega_1}{\omega_2}\right)^\alpha \exp\left(\frac{\omega_1 - \omega_2}{\omega_\infty}\right) = \Omega_1^\alpha \exp\left(\frac{\omega_1 - \omega_2}{\Omega_\infty \omega_2}\right) \tag{7.77}$$

For the **quasi-equilibrium** case, with the variables introduced above, Eq. (7.59) becomes

$$\frac{\Omega - 1}{\Omega_1 - \Omega} = \Omega_1^\alpha \exp\left\{\left(\frac{\Omega_1 - 1}{\Omega}\right)\left[1 + \ln(1 - \gamma\Omega w_2) - a(\gamma\Omega w_2)^2\right]\right\}. \tag{7.78}$$

For the **kinetic** case, with the variables introduced above, and

$$\psi = \frac{D}{k}\left(\frac{c_0}{\Gamma_\infty}\right) \tag{7.79}$$

Eq. (7.60) becomes

$$\psi\left[\frac{1}{2}\frac{d\gamma}{d\tau} - \frac{d\gamma_1}{d\tau}\right] = \gamma\left\{\frac{\Omega - 1}{\Omega_1 - 1} - \frac{\Omega_1 - \Omega}{\Omega_1 - 1}\Omega_1^\alpha \exp\left\{\left(\frac{\Omega_1 - 1}{\Omega}\right)\left[1 + \ln(1 - \gamma\Omega w_2) - a(\gamma\Omega w_2)^2\right]\right\}\right\}, \tag{7.80}$$

and, keeping in mind our first-order finite difference scheme for the solution of the Ward-Tordai equation, with $\theta = \sqrt{\tau}$, one transforms Eq. (7.80) into the form

$$\begin{aligned}\frac{\psi}{2\theta \cdot \Delta\theta}\left[\left(\frac{1}{2} - \frac{\Omega - 1}{\Omega_1 - 1}\right)\gamma - \left(\frac{1}{2}\gamma^{(n-1)} - \gamma_1^{(n-1)}\right)\right] = \\ \gamma\left\{\frac{\Omega - 1}{\Omega_1 - 1} - \frac{\Omega_1 - \Omega}{\Omega_1 - 1}\Omega_1^\alpha \exp\left\{\left(\frac{\Omega_1 - 1}{\Omega}\right)\left[1 + \ln(1 - \gamma\Omega w_2) - a(\gamma\Omega w_2)^2\right]\right\}\right\}\end{aligned} \tag{7.81}$$

where the derivatives were expressed approximately as

$$\frac{d\gamma}{d\tau} = \frac{1}{2\theta}\frac{d\gamma}{d\theta} \cong \frac{1}{2\theta}\frac{\gamma - \gamma^{(n-1)}}{\Delta\theta}, \tag{7.82}$$

$$\frac{d\gamma_1}{d\tau} = \frac{1}{2\theta}\frac{d\gamma_1}{d\theta} \cong \frac{1}{2\theta}\frac{\gamma_1 - \gamma_1^{(n-1)}}{\Delta\theta} = \frac{1}{2\theta \cdot \Delta\theta}\left(\frac{\Omega - 1}{\Omega_1 - 1}\gamma - \gamma_1^{(n-1)}\right), \tag{7.83}$$

and $\gamma^{(n-1)}$ and $\gamma_1^{(n-1)}$ are the values of γ and γ_1, calculated in the previous $(n-1)^{th}$ step of the finite difference procedure corresponding to θ_n. As the values of $\gamma(\theta = 0)$ and $\gamma_1(\theta = 0)$ are obviously zero, the procedure is unambiguously defined.

Equations (7.78) or (7.80) can be solved numerically in the relevant interval $1 < \Omega < \min\{\Omega_1, 1/\gamma w_2\}$. Once the root $\Omega = \Omega(\gamma)$ of the corresponding equation is calculated, one can calculate the values $w = \Omega \cdot w_2$, the surface pressure Π from Eq. (7.68), the partial adsorption values γ_1, γ_2 from Eqs. (7.67), and hence the isotherm

$$C = \frac{w}{B}\frac{\left(\frac{\gamma_1}{\beta}\right)^2 (1-\gamma w)^{-\Omega_1/\Omega} + (\gamma_2)^2 (1-\gamma w)^{-1/\Omega} \exp\left[-\frac{\Pi(\omega_1-\omega_2)}{RT}\right]}{\frac{\gamma_1}{\beta} + \gamma_2 \exp\left[-\frac{\Pi(\omega_1-\omega_2)}{RT}\right]}. \tag{7.84}$$

Aggregation model, cf. Section 4.2.3, is defined by the equations

$$bc(0,t) = \frac{\Gamma_1 \omega}{(1-\Gamma\omega)^{\omega_1/\omega}} \qquad \text{Adsorption isotherm (7.85)}$$

with Γ, Γ_1 and ω being interrelated by

$$\Gamma = \Gamma_1 + \Gamma_n = \Gamma_1 + \Gamma_1 \cdot (\Gamma_1/\Gamma_c)^{n-1}, \tag{7.86}$$

$$\omega = \omega_1 \frac{1 + n(\Gamma_1/\Gamma_c)^{n-1}}{1 + (\Gamma_1/\Gamma_c)^{n-1}}, \tag{7.87}$$

$$\Pi = -\frac{RT}{\omega}\ln(1-\Gamma\omega). \qquad \text{Equation of state (7.88)}$$

Introducing the dimensionless parameters (7.45) and

$$w_1 = \omega_1\Gamma_\infty, \qquad \Gamma = \gamma\Gamma_\infty, \qquad \Gamma_1 = \gamma_1\Gamma_\infty, \qquad \Gamma_c = \gamma_c\Gamma_\infty \tag{7.89}$$

$$\Omega = \omega/\omega_1 = w/w_1, \qquad \kappa = \Gamma_1/\Gamma_c = \gamma_1/\gamma_c, \tag{7.90}$$

after some algebraic transformations one finally obtains the equation

$$\gamma = \gamma_c \kappa \, (1 + n \cdot \kappa^{n-1}). \tag{7.91}$$

From the numerical solution of this equation $\kappa = \kappa(\gamma)$, if γ_c is known, all variables can be determined:

$$\Omega = \frac{1 + n\kappa^{n-1}}{1 + \kappa^{n-1}}, \qquad \gamma_1 = \kappa \cdot \gamma_c \tag{7.92}$$

$$BC = \frac{(\Gamma_c \omega_1)\kappa\Omega}{\left[1 - (\Gamma_c \omega_1)\kappa\left(1 + \kappa^{n-1}\right)\Omega\right]^{1/\Omega}} \tag{7.93}$$

$$-\frac{\Pi\omega_1}{RT} = \frac{1}{\Omega}\ln(1 - \gamma w) \tag{7.94}$$

where the dimensionless value $\Gamma_c\omega_1$ is clearly seen to be the model parameter. Following the procedure similar to that described in previous paragraphs, one obtains for the **boundary condition**

$$-\frac{\Pi_\infty \omega_1}{RT} = \frac{1 + \kappa_\infty^{n-1}}{1 + n\kappa_\infty^{n-1}} \ln\left[1 - (\Gamma_c \omega_1)\kappa_\infty\left(1 + n\kappa_\infty^{n-1}\right)\right]. \tag{7.95}$$

The solution of this equation κ_∞ is seen to be located in the range $0 < \kappa_\infty < \kappa_m$, where κ_m is the only positive root of the equation

$$1 - (\Gamma_c \omega_1)\kappa_m\left(1 + n\kappa_m^{n-1}\right) = 0. \tag{7.96}$$

It is readily seen that, in the interval $0 < \kappa_\infty < \kappa_m$, the right hand side of Eq. (7.95) is an increasing function, while its left hand side for any set of given system and model parameters is constant. Therefore, from the single solution κ_∞ of Eq. (7.95) one can calculate

$$\gamma_c = 1/\left[\kappa_\infty\left(1 + n\kappa_\infty^{n-1}\right)\right], \tag{7.97}$$

and hence, all values of the variables at $t \rightarrow \infty$. Next, the B value can be determined similarly to the procedures described for other models above. Then, with the κ value calculated from the numerical solution of Eq. (7.91), the Π and C values can be determined for each γ.

7.5.3. Examples

(1) Solution of 1-dodecanol in water at 5°C; surfactant concentration $1.2 \cdot 10^{-5}$ mol/l. This system was discussed in [8]. In particular, it was shown in the experiments with spread monolayers that for low surface pressures ($\Pi < 5$ mN/m) mostly dimers are present in the monolayer, while for higher surface pressures the Brewster angular microscopy suggests the formation of large clusters. The experimental data for this system are contained in the file C12OH-5r.txt.

The procedure of data loading and starting the program is extensively described in the WardTordai manual. Figure 7.8 illustrates the results obtained for this system by the calculations using the program. The aggregation model was assumed, with the partial molar surface area $\omega_1 = 1.3 \cdot 10^5$ m^2/mol.

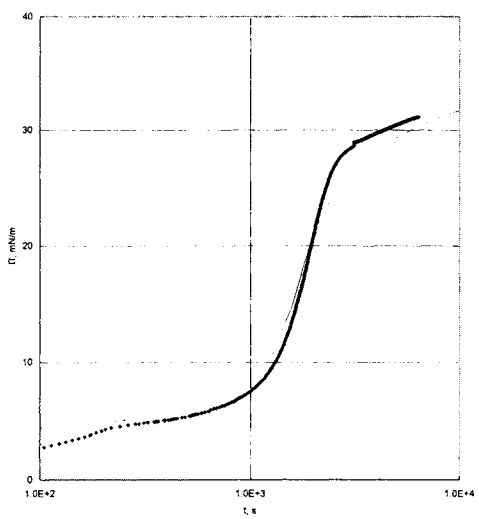

Figure 7.8. Solution of 1-dodecanol in water at 5°C; surfactant concentration $1.2 \cdot 10^{-5}$ mol/l. Points, experimental data [8]; results calculated from the aggregation model: dashed line, n = 2, $\Gamma_c = 1 \cdot 10^{-10}$ mol/m^2; solid line, n = 100, $\Gamma_c = 1.7 \cdot 10^{-6}$ mol/m^2.

For the low-pressure branch, the value $n = 2$ (dimers) was chosen. It follows from the calculations that for $\Gamma_c < 1 \cdot 10^{-10}$ mol/m^2 the kinetic curve remains virtually the same as shown in Fig. 7.8 by the dashed line. The high-pressure branch of the experimental curve is described quite agreeably assuming that the monolayer consists of large clusters (for any $n > 50$ the results appear to be virtually the same), see solid line in Fig. 7.8.

(2) Decyl dimethyl phosphine oxide solution in water at 25°C [9]. The experimental data Π *vs* t for this system measured at bulk concentrations 0.1 mol/m^3, 0.3 mol/m^3 and 1.0 mol/m^3 using MPT, TE and TVT methods are contained in the files C10DMPO-01R.txt, C10DMPO-03R.txt and C10DMPO-10R.txt, respectively. Figure 7.9 illustrates the results obtained for the system by calculations with WardTordai program. It is clearly seen that the experimental data obtained by various methods can be adequately approximated by the Frumkin model.

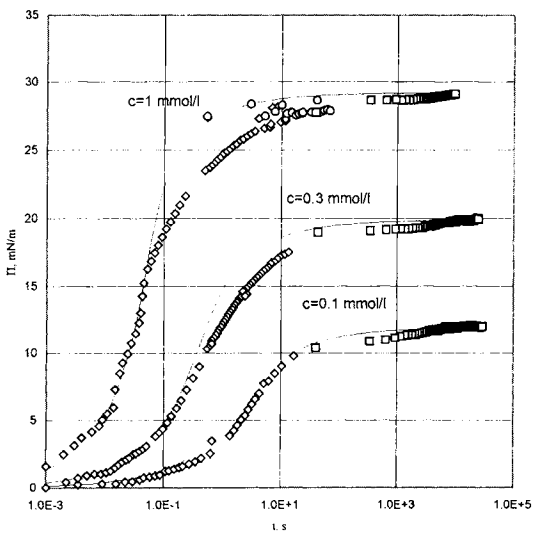

Figure 7.9. Aqueous solutions of C_{10}DMPO at 25°C [9], experimental data obtained by ◊ - MPT; □ - TE; and ○ - TVT methods, lines represent the results calculated for Frumkin's model with $\omega = 2.52\ 10^5$ m²/mol, $a = -0.25$.

Acknowledgement

The authors of this chapter is very grateful for the many fruitful and inspiring discussions with Valentin B. Fainerman during the development of the software, suggestions for routines and careful critical testing.

References

1. P.E. Gill, W. Murray and M.H. Wright, *Practical Optimization*, Academic Press, 1981
2. V.B. Fainerman, R. Miller, E.V. Aksenenko, J. Phys. Chem. B, 104(2000)5744.
3. A.N. Frumkin, Z. Phys. Chem. (Leipzig), 116(1925)466.
4. V.B. Fainerman, R. Miller, R. Wüstneck, J. Phys. Chem., 101(1997)6479.
5. V.B. Fainerman, R. Miller, Langmuir, 12(1996)6011.
6. A.F.H. Ward and L. Tordai, J. Phys. Chem., 14(1946)453]
7. E.V. Aksenenko, A.V. Makievski, R. Miller and V.B. Fainerman, Colloids Surfaces A, 143 (1998) 311
8. D. Vollhardt, V.B. Fainerman and G. Emrich, J. Phys. Chem B, 104(2000)8536
9. A.V. Makievski and D. Grigoriev, Colloid Surfaces A, 143(1998)233.

Subject Index

This Page Intentionally Left Blank